

AD-A023 513

ENGINEERING DESIGN HANDBOOK: RECOILLESS RIFLE
WEAPON SYSTEMS

Army Materiel Command
Alexandria, Virginia

15 January 1976

DISTRIBUTED BY:

NTIS

National Technical Information Service
U. S. DEPARTMENT OF COMMERCE

119184

AMC PAMPHLET

AMCP 706-238

AD A023 513

ENGINEERING DESIGN HANDBOOK

RECOILLESS RIFLE WEAPON SYSTEMS

HEADQUARTERS, US ARMY MATERIEL COMMAND

JANUARY 1976

REPRODUCED BY
NATIONAL TECHNICAL
INFORMATION SERVICE
U. S. DEPARTMENT OF COMMERCE
SPRINGFIELD, VA. 22161

APR 7 1976

**DEPARTMENT OF THE ARMY
HEADQUARTERS UNITED STATES ARMY MATERIEL COMMAND
5001 Eisenhower Ave, Alexandria, VA 22333**

**AMC PAMPHLET
No. 706-238**

15 January 1976

**ENGINEERING DESIGN HANDBOOK
RECOILLESS RIFLE WEAPON SYSTEMS**

TABLE OF CONTENTS

<i>Paragraph</i>		<i>Page</i>
	LIST OF ILLUSTRATIONS	xix
	LIST OF TABLES	xxvii
	PREFACE	xxix
 PART ONE INTRODUCTION 		
CHAPTER I BACKGROUND INFORMATION		
	SECTION I SCOPE	1-1
	SECTION II HISTORY	
1-1	General	1-3
1-2	History to End of World War II	1-3
1-2.1	Development Prior to 1943	1-3
1-2.2	Development of 57 mm Rifle, M18	1-3
1-2.3	Development of 75 mm Rifle, T21 (M20)	1-9
1-2.4	Development of 105 mm Rifle to End of World War II	1-11
1-3	History Post-World War II	1-11
1-3.1	Development of 105 mm Rifle, T19 (M27)	1-11
1-3.2	Development of 106 mm BAT Weapon System	1-12
1-3.2.1	Development at Frankford Arsenal	1-12
1-3.2.2	Development at Firestone	1-14
1-3.2.3	Development of 106 mm Rifle, M40	1-14
1-3.2.4	Development at Frigidaire	1-15
1-3.2.5	Spotting Rifle Development	1-16
1-4	Other Recoilless Weapons of Caliber 105 mm or Smaller	1-17
1-4.1	37 mm Rifle, T62	1-17
1-4.2	57 mm Rifle, T66	1-17

TABLE OF CONTENTS (Cont'd)

<i>Paragraph</i>		<i>Page</i>
1-4.3	2.75-in. Rifle, T190	1-18
1-4.4	90 mm Rifle and Ammunition	1-19
1-4.5	Development of Repeating Rifles 105 mm, T189 and T237	1-22
1-4.6	Development of 105 mm Rifle, T136	1-26
1-4.7	Development of Weapon System T165 and T166, Self- propelled (ONTOS) Using 106 mm, T170 Recoilless Rifle	1-26
1-5	Other Large Caliber Weapons (Larger than 105 mm) ..	1-30
1-5.1	Development of 120 mm HAW	1-30
1-5.2	DAVY CROCKETT 120 mm, XM63 (XM28) and 155 mm, XM64 (XM29)	1-32
1-5.3	Development of 8-in. Cannon (EIK)	1-35
1-5.4	Development of Self-ejecting Breech	1-37
1-6	Research Programs	1-37
1-6.1	Introduction	1-37
1-6.2	Midwest Research Institute	1-38
1-6.2.1	Gun Temperature	1-38
1-6.2.2	Sheet Propellant Studies	1-38
1-6.2.3	Gun Dynamics	1-39
1-6.2.4	Ignition Studies	1-39
1-6.2.5	Flash Characteristics	1-39
1-6.3	Armour Research Foundation	1-40
1-6.3.1	Interior Ballistic Theory	1-40
1-6.3.2	Propellants	1-41
1-6.3.3	Expendable Cartridge Case	1-41
1-6.3.4	Nozzle Studies	1-42
1-6.3.5	Stress Analysis	1-43
1-6.4	Firestone Tire and Rubber Company	1-44
1-6.4.1	Aerodynamics	1-44
1-6.4.2	Fuze Studies	1-44
1-6.5	Universal Winding Company	1-44
1-6.6	A. D. Little, Inc.	1-45
1-6.7	Harvey Aluminum (Harvey Machine Co.)	1-45
1-6.8	CARDE	1-46
1-6.9	Franklin Institute	1-46
	References	1-47

CHAPTER 2 SYSTEM DESIGN AND INTEGRATION

2-0	List of Symbols	2-1
-----	-----------------------	-----

TABLE OF CONTENTS (Cont'd)

<i>Paragraph</i>		<i>Page</i>
SECTION I INTRODUCTION		
2-1	Scope	2-3
2-2	Definition of Terms	2-3
2-3	General Principles of Operation	2-4
SECTION II SYSTEM REQUIREMENTS		
2-4	General	2-9
2-5	Required Muzzle Energy	2-9
2-5.1	Kill Probability	2-9
2-5.2	Hit Probability	2-9
2-5.3	Vulnerable Area	2-11
2-6	Weapon System Weight	2-11
SECTION III DETERMINATION OF BALLISTIC PARAMETERS		
2-7	Determine Throat Area	2-13
2-8	Determine Gun and Propellant Requirements	2-13
2-9	Verify Calculations With Test Weapon	2-15
2-10	Complete Design of Gun, Round, and Ancillary Equipment	2-16
SECTION IV NUMERICAL EXAMPLE		
	References	2-21
PART TWO THEORETICAL ANALYSIS CHAPTER 3 TERMINAL BALLISTICS		
3-0	List of Symbols	3-1
SECTION I INTRODUCTION		
3-1	Scope	3-3
3-2	Background	3-3
3-3	Typical Recoilless Warheads	3-3
SECTION II HEAT WARHEAD		
3-4	Qualitative Description	3-7
3-5	Factors Affecting Performance	3-7
3-5.1	Introduction	3-7
3-5.2	Projectile Spin	3-8
3-5.3	Physical Properties of Liner	3-9

TABLE OF CONTENTS (Cont'd)

<i>Paragraph</i>		<i>Page</i>
3-5.4	Standoff	3-10
3-5.5	Cone Angle	3-11
3-5.6	Liner Wall Thickness	3-12
3-5.7	Liner Shape	3-12
3-5.8	Alignment of Cone and Charge	3-12
3-5.9	Confinement	3-13

SECTION III HE WARHEAD

3-6	Qualitative Description	3-15
3-7	Determination of Fragmentation Characteristics	3-15
3-7.1	Fragment Size Distribution	3-15
3-7.2	Initial Fragment Speed	3-16
3-7.3	Fragment Slow Down	3-18
3-7.4	Fragmentation Patterns	3-18
3-7.5	Controlled Fragmentation	3-20
3-7.5.1	Preformed Fragment	3-20
3-7.5.2	Notched or Grooved Rings	3-21
3-7.5.3	Notched or Grooved Wire	3-21
3-7.5.4	Notched Casings	3-22
3-7.5.5	Multiple Walls	3-22
3-7.5.6	Metallurgically Modified Material	3-22

SECTION IV OTHER TYPES OF WARHEADS

3-8	HEP Warhead	3-23
3-8.1	Introduction	3-23
3-8.2	Advantages and Disadvantages	3-23
3-8.3	Theory of Performance	3-24
3-8.4	General Conclusions	3-24
3-9	Other Types of Warheads	3-25
	References	3-25

CHAPTER 4 EXTERIOR BALLISTICS

4-0	List of Symbols	4-1
-----	-----------------------	-----

SECTION I INTRODUCTION

4-1	Scope	4-5
4-2	Weapon System Interaction	4-5
4-3	Qualitative Description	4-5

TABLE OF CONTENTS (Cont'd)

<i>Paragraph</i>		<i>Page</i>
SECTION II AERODYNAMIC FORCES AND MOMENTS		
4-4	General	4-7
4-5	Aerodynamic Forces	4-7
4-5.1	Normal, Lift, and Drag Forces	4-7
4-5.2	Magnus Force	4-7
4-6	Aerodynamic Moments	4-7
4-6.1	Static Moment	4-7
4-6.2	Damping Moment	4-8
4-6.3	Magnus Moment	4-8
4-6.4	Roll Damping Moment	4-8
4-7	Force and Moment Coefficients	4-9
4-7.1	Aerodynamic Force Coefficients	4-9
4-7.2	Moment Coefficients and Moments	4-10
4-8	Determination of Aerodynamic Coefficients	4-11
SECTION III PROJECTILE STABILITY		
4-9	Introduction	4-13
4-10	Basic Stability Considerations	4-13
4-11	Spin Stabilization	4-13
4-11.1	Gyroscopic Stability	4-13
4-11.2	Yaw of Repose	4-14
4-11.3	Dynamic Stability	4-15
4-11.4	Aerodynamic Jump of Spin-stabilized Projectiles	4-15
4-i2	Fin Stabilization	4-17
4-12.1	Introduction	4-17
4-12.2	Fin Types	4-17
4-12.3	Dynamic Stability	4-18
4-12.4	Aerodynamic Jump of Fin-stabilized Projectiles	4-18
4-12.5	Magnus Stability	4-19
4-12.6	Resonance Instability	4-19
SECTION IV AERODYNAMIC DRAG		
4-13	General	4-21
4-14	Subsonic Velocities	4-22
4-15	Transonic	4-23
4-16	Supersonic	4-23
4-17	Typical Values of Drag	4-23

TABLE OF CONTENTS (Cont'd)

<i>Paragraph</i>		<i>Page</i>
SECTION V PARTICLE TRAJECTORY CALCULATIONS		
4-18	Trajectory Problem	4-27
4-19	Trajectory Equations	4-27
4-20	Solutions of the Equations	4-27
4-20.1	Semiempirical Equations for Flat Trajectories	4-28
4-20.2	Digital Computer Solutions	4-29
4-20.3	Other Methods	4-30
4-20.3.1	Numerical Integration	4-30
4-20.3.2	Siacci Tables	4-30
	References	4-34
CHAPTER 5 INTERIOR BALLISTICS		
5-0	List of Symbols	5-1
SECTION I INTRODUCTION		
5-1	Scope	5-7
5-2	Qualitative Description of the Interior Ballistic Problem	5-7
5-3	Use of Existing References on Interior Ballistic Theory ..	5-9
5-4	Design Data for Several Recoilless Rifles and Ammuni- tion	5-9
SECTION II EMPIRICAL AND GRAPHICAL METHODS FOR QUICK APPROXIMATIONS		
5-5	Solutions Based on Efficiency Considerations	5-11
5-5.1	Introduction	5-11
5-5.2	Thermodynamic Efficiency	5-11
5-5.3	Piezometric Efficiency	5-12
5-5.4	Efficiency Tables and Graphs	5-12
5-5.5	Numerical Example	5-13
5-6	Tabulated Design Data	5-14
5-6.1	Method	5-14
5-6.2	Example	5-18
5-7	Graphical Solutions	5-19
5-7.1	Introduction	5-19
5-7.2	Procedure for Using Graphs	5-25
5-7.3	Numerical Example	5-29
5-8	Similitude Relations	5-29
5-8.1	Introduction	5-29

TABLE OF CONTENTS (Cont'd)

<i>Paragraph</i>		<i>Page</i>
5-8.2	Characteristic Similitude Relations	5-31
5-9	Effect of Ballistic Variations	5-31
5-9.1	Introduction	5-31
5-9.2	Effect of Quickness Factor B/W_0	5-32
5-9.3	Effect of Impetus F	5-32
5-9.4	Effect of Propellant Regressiveness W/L	5-33
5-9.5	Effect of Flow Factor Γ	5-33
SECTION III BASIC INTERIOR BALLISTIC EQUATIONS		
5-10	Equations for Projectile Acceleration	5-35
5-11	Equation of State for Propellant Gas	5-35
5-12	Equation for Rate of Propellant Burning	5-37
5-13	Equation for Discharge of Propellant Gas Through Nozzle	5-41
5-14	Equation for Accumulation of Gas in Gun	5-41
5-15	Energy Equation	5-41
5-16	Summary of Equations	5-42
SECTION IV DISCUSSION OF SOLUTION TO EQUATIONS		
		5 45
SECTION V SIMPLE SOLUTION BASED ON CONSTANT AVERAGE TEMPERATURE		
5-17	Introduction	5-47
5-18	Method	5-47
5-19	Example	5-48
SECTION VI ANALYTIC EQUATIONS FOR OPTIMIZING CERTAIN GUN PARAMETERS		
5-20	The Lightest Gun for a Specified Muzzle Energy	5-51
5-21	The Shortest Gun for a Specified Muzzle Velocity	5-55
5-22	Numerical Example	5-55
SECTION VII INTERIOR BALLISTIC SOLUTION USING DIGITAL COMPUTER		
		5-57
SECTION VIII SOLUTION FOR AFTER "ALL-BURNT" CONDITION		
5-23	Introduction	5-59
5-24	Modification of Equations for "All-Burnt" Condition ..	5-59

TABLE OF CONTENTS (Cont'd)

<i>Paragraph</i>		<i>Page</i>
5-25	Solution of Equations for "All-Burnt" Condition	5-59
5-26	Example	5-60

SECTION IX HEAT TRANSFER

5-27	Introduction	5-61
5-28	Basic Equations	5-61
5-29	Solution of the Equations	5-62
5-30	Temperature Distribution Data	5-64
5-30.1	Theoretical Calculation	5-64
5-30.1.1	Single Shot Analysis	5-64
5-30.1.2	Determination of Temperature as a Function of Round Number and Rate of Fire	5-64
5-30.2	Experimental Phase	5-78

SECTION X SPECIAL TOPICS

5-31	Loss of Unburnt Propellant	5-81
5-32	Pressure Gradient in Gun	5-83
5-33	Form Factor for Propellant Burning	5-83
5-34	Muzzle Flash	5-85
5-34.1	Basic Theory	5-85
5-34.2	Flash Suppression	5-85
5-35	Calculation of "Bare" Gun Weight	5-86
5-36	List of Numerical Constants Used in Interior Ballistic Calculations	5-87
	References	5-87
	Bibliography	5-88

CHAPTER 6 CANCELLATION OF RECOIL

6-0	List of Symbols	6-1
-----	---------------------------	-----

SECTION I INTRODUCTION

6-1	Conservation of Momentum	6-5
6-2	The Supersonic Nozzle	6-5
6-3	Effect on Interior Ballistics	6-6

**SECTION II THEORY OF THE DE LAVAL
(CONVERGENT-DIVERGENT) NOZZLE**

6-4	Assumptions	6-9
6-5	Definitions	6-9

TABLE OF CONTENTS (Cont'd)

<i>Paragraph</i>		<i>Page</i>
6-6	Basic Equations	6-10
6-6.1	Rate of Flow	6-10
6-6.2	Mass Flow	6-12
6-6.3	Thrust Generated by Nozzle	6-13
6-7	Design Considerations	6-15
SECTION III THEORY OF RECOIL CANCELLATION		
6-8	Definition of Momentum Ratio Parameter	6-21
6-9	Equation for Momentum Ratio as a Function of Gun and Nozzle Parameters	6-22
6-10	Equations for Ratio of Chamber Pressure to Ideal Reservoir Pressure	6-22
6-11	Graphical Solution of the Equations	6-23
6-12	Nozzle Performance Factors	6-24
6-12.1	Variation of Nozzle Thrust With Nozzle Expansion Angle	6-24
6-12.2	Variation of Nozzle Thrust With Expansion Ratio ...	6-25
6-12.3	Effect of Nozzle Approach Area and Chamber Con- figuration on Rifle Performance	6-27
SECTION IV NOZZLE EROSION		
6-13	General Discussion	6-31
6-14	Theory	6-31
6-15	Erosion Resistance of Various Metals	6-32
6-16	Similitude Relationships	6-36
6-17	Other Factors That Affect Erosion Rate	6-37
SECTION V BORE-SIZE NOZZLE		6-39
SECTION VI RECOIL COMPENSATORS		6-41
SECTION VII BLAST EFFECTS		
6-18	Introduction	6-43
6-19	Various Damage Mechanisms	6-43
6-20	Blast and Flash Patterns	6-44
6-21	Experimental Data	6-49
6-21.1	Pressure Contours	6-49
6-21.2	Danger Areas	6-51
6-21.3	Ducting	6-51
	References	6-53
	Bibliography	6-55

TABLE OF CONTENTS (Cont'd)

<i>Paragraph</i>		<i>Page</i>
CHAPTER 7 SYSTEM EFFECTIVENESS		
7-0	List of Symbols	7-1
	SECTION I INTRODUCTION	7-3
	SECTION II HIT PROBABILITY	
7-1	General	7-5
7-2	Sources of Error	7-5
7-3	Calculation of Hit Probability	7-6
7-3.1	General	7-6
7-3.2	Errors Associated With Type of Fire Control System ..	7-7
7-3.3	Lateral and Vertical Single Shot Hit Probabilities	7-8
7-4	Use of Spotting Round	7-9
7-4.1	General	7-9
7-4.2	Magnitude of Mismatch	7-10
7-5	Probability of Hit With Recoilless Rifles	7-11
7-5.1	Comparison of Simple Sight and Spotting Round	7-11
7-5.2	Probability of Hit for Standard Weapons	7-11
7-5.3	Probability of Hit as a Function of Various Conditions	7-18
7-5.4	Probability of Hit as a Function of Muzzle Velocity ..	7-18
	SECTION III KILL PROBABILITY	
7-6	Introduction	7-23
7-7	Hard Target	7-23
7-7.1	Introduction	7-23
7-7.2	Types of Kill	7-23
7-7.3	Vulnerable Area	7-23
7-7.4	Calculation of Kill Probability	7-24
7-7.5	Typical Values of Kill Probability	7-25
7-8	Area Target	7-25
7-8.1	Introduction	7-25
7-8.2	Lethal Area	7-25
	References	7-27
	Bibliography	7-27
CHAPTER 8 MEASUREMENT TECHNIQUES		
8-0	List of Symbols	8-1
	SECTION I INTRODUCTION	8-3

TABLE OF CONTENTS (Cont'd)

<i>Paragraph</i>		<i>Page</i>
SECTION II MEASUREMENT OF VELOCITY		
8-1	General	8-5
8-2	Detecting Devices	8-6
8-2.1	Breakwire System	8-7
8-2.2	Make System	8-8
8-2.3	Solenoid Coil Detectors	8-10
8-2.4	Sky Screen	8-11
8-2.5	Radar Velocity Measurements	8-11
8-2.6	Photographic Methods	8-13
SECTION III PRESSURE MEASUREMENTS		
8-3	General	8-17
8-4	Copper Crusher Gage	8-17
8-5	Piezoelectric Gage	8-18
8-6	Strain Gages	8-18
SECTION IV OTHER MEASUREMENT TECHNIQUES		
8-7	Strain Measurements	8-21
8-7.1	General	8-21
8-7.2	The Gage	8-21
8-7.3	Other Uses of Strain Gages	8-21
8-8	Acceleration Measurement	8-22
8-8.1	General	8-22
8-8.2	Accelerometers	8-22
8-9	Recoil Measurements	8-23
8-9.1	General	8-23
8-9.2	Measurement of Recoil Impulse	8-24
8-9.3	Measurement of Recoil Forces	8-24
8-10	Measurement of Temperature	8-24
8-10.1	General	8-24
8-10.2	Techniques	8-24
8-11	Projectile Motion	8-24
8-11.1	Yaw	8-24
8-11.2	Spin	8-25
8-12	Blast	8-26
8-12.1	General	8-26
8-12.2	Blast Gages	8-26
8-13	Recording Equipment	8-28
8-13.1	Oscilloscope	8-28
8-13.2	Magnetic Tape	8-28
SECTION V GENERAL CONSIDERATIONS		
	References	8-31

TABLE OF CONTENTS (Cont'd)

<i>Paragraph</i>		<i>Page</i>
PART THREE DESIGN		
CHAPTER 9 BASIC DESIGN CONSIDERATIONS		
SECTION I INTRODUCTION TO DESIGN CONSIDERATIONS		
9-1	Advantages of Recoilless Rifles	9-1
9-2	Importance of System Design Approach	9-1
9-3	Description of Various Weapon Configurations	9-2
9-3.1	Basic Principle	9-2
9-3.2	The Davis Gun	9-2
9-3.3	Russian and German Designs	9-3
9-3.4	The Burney Gun	9-5
9-3.5	The Hybrid Weapon	9-7
9-3.6	Side-loading Configuration	9-5
9-3.7	Configuration With Perforated Cartridge Case	9-10
9-3.8	Special Configurations	9-15
9-4	Disadvantages	9-15
SECTION II HUMAN ENGINEERING		
9-5	Introduction	9-37
9-6	Primary Factors	9-37
9-6.1	The Man Using the Weapon	9-37
9-6.2	Field Servicing	9-39
9-6.3	Manufacturing Personnel	9-39
9-7	Human Factors Engineering Evaluation	9-40
9-8	Areas of Application	9-40
9-9	Specific Responsibilities	9-40
SECTION III RELIABILITY		
9-10	Basic Principles	9-43
9-11	Materials	9-44
9-12	Environmental Deterioration	9-45
SECTION IV MAINTAINABILITY		
9-13	Basic Principles	9-49
9-14	Accessibility	9-49
9-15	Standardization	9-50
	References	9-50

TABLE OF CONTENTS (Cont'd)

<i>Paragraph</i>		<i>Page</i>
CHAPTER 10 RIFLE AND RIFLE COMPONENTS		
10-0	List of Symbols	10-1
SECTION I OVERALL DESIGN CONSIDERATIONS		
10-1	General	10-3
10-2	Hammer Blow	10-3
10-3	Firing Pin	10-3
10-4	Primer	10-4
10-5	Booster	10-4
10-6	Propellant	10-4
10-7	Cartridge Case	10-5
10-8	Projectile	10-5
10-9	Breech-Cartridge Relation	10-6
10-10	Chamber-Cartridge Relation	10-6
10-11	Tube-Cartridge Relation	10-6
10-12	Chamber	10-6
10-13	Nozzles	10-7
10-14	Tube	10-7
10-15	Summary	10-8
SECTION II NOZZLE		
10-16	General	10-9
10-17	Nozzle Erosion	10-9
10-18	Various Types of Nozzles	10-10
10-18.1	Central Nozzle	10-10
10-18.2	Central Nozzle With Bar	10-12
10-18.3	Central Expanding Nozzle	10-13
10-18.4	Multiple Nozzle and Front Orifice	10-13
10-18.5	Annular Nozzle	10-14
10-18.6	Interrupted Annular Nozzle	10-16
10-18.7	Kidney-shaped Nozzle	10-16
SECTION III BREECH		
10-19	General	10-19
10-20	Characteristics	10-19
10-21	Sealing Propellant Gases	10-20
10-22	Breech Types	10-20
10-23	Breech Actuator	10-22

TABLE OF CONTENTS (Cont'd)

<i>Paragraph</i>		<i>Page</i>
SECTION IV CHAMBER		
10-24	General	10-23
10-25	Significance of Chamber Volume	10-23
10-26	Ejection of Propellant	10-23
SECTION V TUBE		
10-27	General	10-25
10-28	Design Considerations	10-25
10-29	Other Subjects To Be Considered in Design	10-26
SECTION VI FIRING MECHANISM		
10-30	Design Characteristics	10-29
10-31	Examples	10-29
10-32	Safety Devices	10-31
	References	10-37
	Bibliography	10-38
CHAPTER 11 AMMUNITION		
11-0	List of Symbols	11-1
SECTION I GENERAL		
11-1	Introduction	11-3
11-2	Overall Design Considerations	11-3
11-3	List of Existing Cartridges With Characteristics	11-5
SECTION II PROJECTILE		
11-4	Introduction	11-7
11-5	Projectile Types	11-7
11-6	Design Considerations	11-10
11-6.1	Envelope	11-10
11-6.2	Required Information	11-10
11-6.3	Method of Stabilization	11-11
11-7	Metal Parts Security—Structural Integrity Within the Ballistic Environment	11-11
11-7.1	General	11-11
11-7.2	Stress Analysis	11-12
11-8	Aerodynamic Design	11-13
11-9	Other Design Considerations	11-13

TABLE OF CONTENTS (Cont'd)

<i>Paragraph</i>		<i>Page</i>
11-10	Warhead Design	11-15
11-11	Rotating Band	11-15
11-12	Obturator	11-15
11-13	Strain Compensation	11-16
11-14	Shot Start	11-16
11-15	Spigots	11-16

SECTION III CARTRIDGE CASE

11-16	Introduction	11-17
11-17	The Perforated Cartridge Case	11-17
11-17.1	General	11-17
11-17.2	Effect on Interior Ballistics	11-19
11-17.3	Effect of Perforation Hole Diameter	11-19
11-17.4	Pressure Differential Across Cartridge Case	11-23
11-17.5	Stress Analysis	11-24
11-17.6	Liners for the Perforated Cartridge Case	11-28
11-17.7	Materials for Liners	11-29
11-17.8	Applications of Liners	11-30
11-18	The Frangible Cartridge Case	11-31
11-18.1	General	11-31
11-18.2	Requirements	11-31
11-18.3	Materials for Frangible Case	11-32
11-18.4	The DAVY CROCKETT Cartridge Case	11-32
11-19	The Unperforated Cartridge Case	11-33

SECTION IV IGNITER

11-20	Introduction	11-35
11-20.1	Scope	11-35
11-20.2	Background	11-35
11-21	Igniter Configuration	11-36
11-21.1	General	11-36
11-21.2	Secondary Igniter Charge	11-36
11-21.3	Main Igniter Charge	11-36
11-21.4	Primer Adapter and Ignition Tube	11-36
11-21.5	Primer	11-39
11-21.5.1	Small Arms Percussion Primers	11-39
11-21.5.2	Artillery-type Primers	11-40
11-22	Basic Design Information	11-40
11-23	Development Procedure	11-41
11-23.1	General	11-41
11-23.2	Determination of Hole Size and Pattern	11-41
11-23.3	Sample Calculations	11-43
11-23.4	Selection of Hole Pattern	11-44

TABLE OF CONTENTS (Cont'd)

<i>Paragraph</i>		<i>Page</i>
11-23.5	Preliminary Ballistic Testing	11-44
11-23.6	Final Engineering Testing	11-45
SECTION V THE FUZE		
11-24	General	11-49
11-25	Type of Fuzing	11-49
11-26	Safe-Arm Separation	11-49
SECTION VI PROPELLANT		
11-27	Introduction	11-51
11-28	History	11-52
11-29	Basic Characteristics	11-52
11-29.1	Propellant Compositions	11-52
11-29.2	Impetus	11-53
11-29.3	Flame Temperature	11-53
11-29.4	Web Thickness	11-53
11-29.5	Burning Rate	11-53
11-29.6	Propellant Shape ..	11-54
11-30	Chemical and Physical Characteristics	11-54
11-31	Progressive and Regressive Burning	11-56
	References	11-56
	Bibliography	11-57
CHAPTER 12 MOUNTS		
SECTION I INTRODUCTION		
12-1	General	12-1
12-2	Specific Examples	12-3
12-2.1	M79 Mount	12-3
12-2.2	T173 Mount	12-4
12-2.3	XM124 Mount	12-5
12-2.4	T234 Mount	12-5
SECTION II ACCESSORY MOUNTING EQUIPMENT		
12-3	General	12-9
12-4	Mounting Methods	12-9
12-4.1	Moderately Stressed Weapons	12-9
12-4.2	Highly Stressed Weapons	12-10
12-5	Mounting Requirements	12-10

TABLE OF CONTENTS (Cont'd)

<i>Paragraph</i>		<i>Page</i>
12-5.1	Ground and Vehicular Mounts	12-10
12-5.2	Telescope Mount	12-13
12-5.3	Spotting Rifle Mount	12-13
	References	12-17

CHAPTER 13 FIRE CONTROL

13-1	General	13-1
13-2	Typical Designs	13-2
13-2.1	106 mm Rifle, M40 With Cal .50 Spotting Rifle, M8C .	13-2
13-2.2	120 mm Rifle, XM105 With Spotting Rifle, XM90E1 .	13-3
13-3	Types of Spotter-Tracer Rounds	13-3
13-4	Evaluation of Target Display	13-4
13-5	Compositions	13-4
13-6	Ignition	13-5
	References	13-9
	Bibliography	13-9
	Index	I-1

LIST OF ILLUSTRATIONS

<i>Figure</i>	<i>Title</i>	<i>Page</i>
1-1	Rifle, Recoilless, 57 mm, M18	1-8
1-2	Rifle, Recoilless, 75 mm, M20	1-10
1-3	Rifle, Recoilless, 105 mm, M27; Jeep and Towed Mounts	1-2
1-4	Rifle, Recoilless, 106 mm, M40, on the Ground Mount .	1-15
1-5	Rifle, Recoilless, 90 mm, M67, With Cartridge, HEAT, M371 (Sectioned)	1-21
1-6	Rifle, Recoilless, 90 mm, T234	1-23
1-7	Rear View of Recoilless Rifle, Repeating, 105 mm, T189, Breech Open	1-24
1-8	Sketch of T189 Rifle Modified for Gas Operation	1-25
1-9	Revolver Type, Repeating Recoilless Rifle, T237, Sectional Views	1-27
1-10	105 mm Rifle, T136; 105 mm Mount, T149; Cal .50 Rifle, T43 and the Interim Sight	1-28
1-11	106 mm Self-propelled T165 (ONTOS Vehicle)	1-29
1-12	120 mm Rifle, XM105	1-31
1-13	Recoilless Weapons—Conventional and Spigot Type ...	1-33
1-14	DAVY CROCKETT System, XM28, Man-portable, 2000-m Infantry Atomic Weapon	1-34
1-15	DAVY CROCKETT XM29 Weapon System, 4000-m Range	1-35
2-1	Schematic Functional Diagram Showing a Gun Back- to-back With a Rocket Motor To Achieve Recoilless- ness	2-5
2-2	Schematic Recoilless Gun	2-6
2-3	Gas Flow in the Chamber and Nozzle	2-7
2-4	Rear Blast Danger Area of Rifle, 120 mm, XM105	2-8
2-5	System Requirements	2-10
2-6	Weight of Weapon vs Initial Energy of Projectiles for Recoilless Systems	2-11
2-7	Weight of Bare Rifle vs Energy, Momentum of Pro- jectile, for Recoilless Systems	2-12
2-8	Pressure vs Travel 120 mm HAW Recoilless Rifle	2-14
2-9	Bare Weapon Weight vs Peak Pressure	2-20
3-1	Typical HEAT Recoilless Warhead Cross Section	3-4
3-2	Typical HE Recoilless Warhead Cross Section	3-5
3-3	Penetration as a Function of Projectile Spin Rate	3-8
3-4	Penetration for 30-deg Electroformed Copper Cones into Mild Steel Targets	3-10
3-5	Maximum Penetration into Mild Steel Targets at Optimum Standoff vs Cone Angle for Electroformed Cones	3-11
3-6	Cone Thickness vs Penetration for 45-deg Copper Cones	3-13

LIST OF ILLUSTRATIONS (Cont'd)

<i>Figure</i>	<i>Title</i>	<i>Page</i>
3-7	Fragment Mass Distribution	3-17
3-8	Graphs for Determining the Initial Fragment Velocity V_0	3-19
3-9	Typical Angular Fragment Distribution	3-20
4-1	Coordinate System	4-8
4-2	Graph of $1/s_g$ vs s_d	4-16
4-3	Projectile Shapes	4-24
4-4	Drag Coefficient vs Mach Number	4-25
4-5	Coordinate System for Trajectory Calculations	4-28
4-6	Angle of Elevation Nomogram	4-31
5-1	Schematic of Gun Showing Interior Ballistic Parameters	5-8
5-2	Weight of Propellant C_i per Unit Projectile Weight M as a Function of Muzzle Velocity V_m for Ballistic Efficiencies ($e_b = 0.4$ and 0.5)	5-14
5-3	(A) Chamber Volume as a Function of Propellant Weight for Loading Densities 0.4, 0.5, and 0.6 g-cm^{-3}	5-15
	(B) Chamber Volume as a Function of Barrel Volume (Bore Area Times Travel) for Expansion Ratios 2, 3, 4, and 5	5-15
5-4	Muzzle Velocity as a Function of Projectile Travel in the Barrel for Peak Projectile Acceleration 2,500, 5,000, 7,500, and 10,000 g's	5-16
5-5	Charge to Projectile Weight Ratio as a Function of Reduced Muzzle Velocity ($V_b/(A/A_r)$) for Values of λ from 0.3 to 0.6	5-20
5-6	$\psi'_b (A/A_r)$ as a Function of $V_b/(A/A_r)$ and λ	5-21
5-7	$\psi'_o/(A/A_r)$ as a Function of Factor λ	5-22
5-8	ψ'_p as a Function of ψ'_o and $(\psi'_b - \psi'_o)/V_b$	5-23
5-9	Bore Area Times Projectile Travel AL as a Function of AY and $\psi'_p V_b$	5-24
5-10	Bore Area Times Projectile Travel AL as a Function of AY and $\psi'_b V_b$	5-25
5-11	Effective Mass to Peak Pressure Ratio m'/P_p as a Function of AY for Values of $\psi'_p \times 10^{-4}$ from 1 to 12	5-26
5-12	Effective Mass to Peak Pressure Ratio m'/P_p as a Function of AY for Values of $\psi'_p \times 10^{-4}$ from 1 to 20	5-27
5-13	Charge to Projectile Weight Ratio C_i/M as a Function of Effective Projectile Mass to Projectile Weight Ratio m'/M for Values of λ from 0.3 to 0.6	5-28
5-14	Ballistic Parameters as a Function of Factor λ	5-30
5-15	The Parameter δ as a Function of the Projectile Weight to Charge Weight Ratio L/C_i	5-36
5-16	Burning Rate as a Function of Average Pressure for M10 Composition Propellant, Lot FDAP81	5-38

LIST OF ILLUSTRATIONS (Cont'd)

<i>Figure</i>	<i>Title</i>	<i>Page</i>
5-17	"Effective" Burning Rate Constant B as a Function of Maximum Pressure P_p	5-40
5-18	$f(V_m, \lambda)$ as a Function of λ	5-53
5-19	ψ_p' as a Function of ψ_m'	5-54
5-20	Equilibrium Temperature as a Function of Initial Temperature Rise and Decay	5-65
5-21	Number of Rounds To Achieve Given Fraction of Equilibrium Temperature	5-66
5-22	Reduced Temperature vs Round Number for Given Rate of Fire ($h' = 0.02 \text{ min}^{-1}$)	5-68
5-23	Reduced Temperature vs Round Number for Given Rate of Fire ($h' = 0.04 \text{ min}^{-1}$)	5-69
5-24	Reduced Temperature vs Round Number for Given Rate of Fire ($h' = 0.06 \text{ min}^{-1}$)	5-70
5-25	Reduced Temperature vs Round Number for Given Rate of Fire ($h' = 0.08 \text{ min}^{-1}$)	5-71
5-26	Reduced Temperature vs Round Number for Given Rate of Fire ($h' = 0.10 \text{ min}^{-1}$)	5-72
5-27	Reduced Temperature vs Round Number for Given Rate of Fire ($h' = 0.12 \text{ min}^{-1}$)	5-73
5-28	Reduced Temperature vs Round Number for Given Rate of Fire ($h' = 0.14 \text{ min}^{-1}$)	5-74
5-29	Reduced Temperature vs Round Number for Given Rate of Fire ($h' = 0.16 \text{ min}^{-1}$)	5-75
5-30	Reduced Temperature vs Round Number for Given Rate of Fire ($h' = 0.18 \text{ min}^{-1}$)	5-76
5-31	Reduced Temperature vs Round Number for Given Rate of Fire ($h' = 0.20 \text{ min}^{-1}$)	5-77
5-32	Experimental Temperature Distribution in Rifle	5-79
5-33	Multiplying Factor F_7 for Converting 7-perforated Webs (W_7) of M10 Propellant to Equivalent Single-perforated Webs (W)	5-84
6-1	Schematic of Nozzle Showing Design Parameters	6-10
6-2	Distribution of Forces Acting on Nozzle	6-13
6-3	Thrust Coefficient C_F as a Function of Pressure Ratio p_o/p_e	6-14
6-4	Calculated Optimum Thrust Coefficient C_F as a Function of Expansion Ratio ϵ ($\gamma = 1.3$)	6-15
6-5	Calculated Optimum Thrust Coefficient C_F as a Function of Expansion Ratio ϵ ($\gamma = 1.2$)	6-16
6-6	Chamber Pressure/Ideal Reservoir Pressure as a Function of Chamber Area/Nozzle Throat Area ($\gamma = 1.25$)	6-24
6-7	Lines of Constant Dimensionless Recoil ω	6-25

LIST OF ILLUSTRATIONS (Cont'd)

<i>Figure</i>	<i>Title</i>	<i>Page</i>
6-8	Percent Recoil Force Imbalance as a Function of Nozzle Throat Area	6-28
6-9	Effect of Approach Area A_i on Recoil Imbalance of the 57 mm Recoilless Rifle, M18	6-29
6-10	Theoretical Classification of Metals on the Basis of Heat Transfer Properties	6-36
6-11	Jet Boundaries for Jet Pressure Ratios from 1 to 10 ($\alpha = 5$ deg, $\gamma = 1.2$, $M_e = 2.0$)	6-46
6-12	Jet Boundaries for Jet Pressure Ratios from 1 to 10 ($\alpha = 10$ deg, $\gamma = 1.2$, $M_e = 2.0$)	6-46
6-13	Jet Boundary Patterns for Various Parameters	6-47
6-14	Peak Pressure Contours for Backblast of the 105 mm Recoilless Rifle, M27	6-50
6-15	Typical Ducting Configurations	6-52
7-1	Comparison of Total Hit Probability p_H for Different Fire Control Systems as a Function of Range	7-13
7-2	Probability of Hit-57 mm M18 Rifle; M306A1 HE Projectile	7-13
7-3	Probability of Hit-57 mm M18 Rifle; M307 HEAT Projectile	7-14
7-4	Probability of Hit-75 mm M20 Rifle; M309 HE Pro- jectile	7-14
7-5	Probability of Hit-75 mm M20 Rifle; M310 HEAT Projectile	7-15
7-6	Probability of Hit-105 mm M27 Rifle; M323 HE Pro- jectile	7-15
7-7	Probability of Hit-105 mm M27 Rifle; M324 HEAT Projectile	7-16
7-8	Probability of Hit-90 mm M67 Rifle; M371 HEAT Projectile	7-16
7-9	Probability of Hit-106 mm M40 Rifle; M344 HEAT Projectile	7-19
7-10	Effect of Muzzle Velocity on Single Shot Hit Prob- ability	7-20
7-11	Effect of Muzzle Velocity on Probability of One Hit Out of Two Shots	7-21
7-12	Effect of Muzzle Velocity on Probability of One Hit Out of Three Shots	7-22
7-13	Variation of Expected Number of Kills With Range, Caliber, and Muzzle Velocity	7-26
8-1	Velocity Measurement Schematic	8-6
8-2	Velocity Measurement With Staggered Array of Detec- tors	8-6
8-3	Circuit for Breakwire System	8-7
8-4	Measuring the Projectile Speed	8-9

LIST OF ILLUSTRATIONS (Cont'd)

<i>Figure</i>	<i>Title</i>	<i>Page</i>
8-5	Make System Circuit	8-9
8-6	Solenoid Output Waveform	8-10
8-7	Series Wiring of Coils	8-11
8-8	Radar Velocity Measurement Schematic	8-13
8-9	Radar Velocity and Displacement Schematic	8-13
8-10	Radar Velocity and Displacement Schematic Using a Reflector	8-14
8-11	Simple X-band Interferometer	8-14
8-12	Photographic Method for Velocity Measurement	8-15
8-13	Copper Crusher Gage	8-17
8-14	Input Circuit	8-19
8-15	Strain Gage	8-20
8-16	Divider Circuit for Strain Gage	8-22
8-17	Portable Pendulum	8-23
8-18	Photoelectric Recoil Measuring Device	8-24
8-19	Bore-surface Thermocouple	8-25
8-20	Typical Blast Waveform	8-27
8-21	Typical Pressure-Time Curve	8-29
9-1	The Davis Gun Mounted on WW I Martin Bomber	9-3
9-2	28 cm German Recoilless Gun	9-4
9-3	Burney 95 mm R.C.L. Twin Jet Gun and Carriage	9-6
9-4	60 mm Recoilless Mortar	9-7
9-5	81 mm Recoilless Mortar	9-8
9-6	4.2 in. Recoilless Chemical Mortar	9-9
9-7	T135 Front Nozzle Rifle	9-10
9-8	Side-loading Configuration	9-11
9-9	Rifle, Repeating, 105 mm, T237, Assembly Drawing	9-12
9-10	Rifle, Repeating, 105 mm, T237, Installation Drawing	9-13
9-11	Rifle, Repeating, 105 mm, T237, on Assembly Mount	9-14
9-12	Configuration of Recoilless Rifle With Perforated Car- tridge Case	9-16
9-13	M40 Rifle With Recoil Compensating Ring in Place	9-17
9-14	Sketch of Perforated Cartridge Case With Blow-out Disc	9-18
9-15	Fin-stabilized Projectile With Propellant Attached, Quarter Section—Ammunition, HEAT, 90 mm, T249E6	9-19
9-16	Hybrid Rocket-gun	9-20
9-17	Configuration to Fire Over-caliber Projectile, DAVY CROCKETT System, XM28	9-21
9-18	XM29 Weapon System Installed on M38A1 Vehicle	9-22
9-19	Rifle, Multiple, 106 mm, Self-propelled, M50	9-24
9-20	M56, Type A, M40, Recoilless Rifle	9-25
9-21	T114, Type B, Dual, M40 Recoilless Rifle	9-26

LIST OF ILLUSTRATIONS (Cont'd)

<i>Figure</i>	<i>Title</i>	<i>Page</i>
9-22	M50, Type A, Dual T237, Repeating Recoilless Rifle, Revolver Type	9-27
9-23	T114, Type B, Modified T237, Repeating Recoilless Rifle, Revolver Type	9-28
9-24	BB-1, (Mechanical Ram), Repeating Recoilless Rifle, Magazine Type	9-29
9-25	Ballistic Ram, Repeating Recoilless Rifle, Mounted on Lightweight Vehicle	9-30
9-26	M50, Type A, BB-1 (Mechanical Ram), Repeating Recoilless Rifle, Magazine Type	9-31
9-27	M56, Type B, BB-1 (Mechanical Ram), Repeating Recoilless Rifle, Magazine Type	9-32
9-28	T114, Type B, BB-1 (Mechanical Ram), Repeating Recoilless Rifle, Magazine Type	9-33
9-29	T114, Type A, Ballistic Ram, Repeating Recoilless Rifle, Magazine Type	9-34
9-30	T114, Type B, Ballistic Ram, Repeating Recoilless Rifle, Magazine Type	9-35
9-31	T114, Type B, Side-loading, Repeating Recoilless Rifle, Magazine Type	9-36
10-1	Central Nozzle	10-11
10-2	Central Nozzle With Bar	10-12
10-3	Central Expanding Nozzle	10-14
10-4	Multiple Nozzle and Front Orifice	10-15
10-5	Annular Nozzle	10-16
10-6	Interrupted Annular Nozzle	10-16
10-7	Nozzle With Kidney-shaped Orifices	10-17
10-8	Rotating Cam Ring Breach Mechanism	10-21
10-9	Firing Mechanism	10-30
10-10	Trigger Firing Mechanism, 120 mm Recoilless Rifle, XM105	10-32
10-11	Major Level of Actuation for Firing Mechanism, 120 mm Recoilless Rifle, XM105	10-33
10-12	Minor Level of Actuation for Firing Mechanism, 120 mm Recoilless Rifle, XM105	10-34
10-13	Trigger Mechanism, 120 mm Recoilless Rifle, XM105 ..	10-35
10-14	Trigger Mechanism Components, 120 mm Recoilless Rifle, XM105	10-36
11-1	106 mm Cartridge, HEAT, M344A1	11-4
11-2	Folding Fin HEAT Projectile	11-8
11-3	Fixed Fin HEAT Projectile	11-8
11-4	HE Projectile	11-8
11-5	HEP Projectile	11-8
11-6	WP Projectile	11-9
11-7	Canister Projectile	11-9

LIST OF ILLUSTRATIONS (Cont'd)

<i>Figure</i>	<i>Title</i>	<i>Page</i>
11-8	Breech Loading—Forward Orifice	11-18
11-9	Breech Loading—Rear Orifice, Perforated Case	11-18
11-10	Axial Nozzle—Combustible Case	11-18
11-11	Various Ballistic Parameters as a Function of a Percent Perforation of Cartridge Case, M30A1B1	11-20
11-12	Various Ballistic Parameters as a Function of Cartridge Case Hole Diameter	11-21
11-13	Gas Flow Through Cartridge Case	11-25
11-14	Pressure Differential Across 57 mm Cartridge Case, M30	11-26
11-15	Perforation Array	11-27
11-16	Perforated Case Force Diagram—Fixed Fins Conditions.	11-29
11-17	Conventional Ignition System	11-37
11-18	Linear (PYROCORE) Ignition System	11-38
11-19	P-T Curves for Good and Poor Ignition	11-46
12-1	Prone Firing Position (Rifle, 57 mm, T66)	12-2
12-2	106 mm Rifle Mount, M79	12-3
12-3	106 mm Rifle Mount, T173 Removed from Tripod, T26	12-4
12-4	Mount, XM124	12-6
12-5	Two-hand Control (Tracking Handle and Trigger Handle) Vehicle Mounted	12-7
12-6	Integral Accessory Package for 90 mm Recoilless Rifle, T234	12-8
12-7	Accessory Sleeve (Mounting Bracket) for HAW 120 mm Rifle, XM105	12-11
12-8	Ground and Vehicular Mount for 120 mm Recoilless Rifle System, XM105—HAW Jeep Mounted—Traveling Position	12-12
12-9	Exploded View of Telescope Mount, M110	12-14
12-10	Rifle, Recoilless, 90 mm, M67 With 10 mm Pistol, Spotting, XM14 and Telescope	12-15
12-11	Spotting Pistol, XM14 Mounted on 90 mm Rifle, M67 .	12-16
13-1	Bullet, Spotter-tracer, Cal .50, M48A2	13-6
13-2	Design of Cal .50 Bullet, T140E12	13-8

LIST OF TABLES

<i>Table No.</i>	<i>Title</i>	<i>Page</i>
1-1	Data on Existing US Recoilless Rifles	1-4
3-1	Gurney Constant for Various Explosives	3-18
4-1	Recoilless Ammunition Characteristics	4-22
5-1	Ballistic Parameters for Several Guns and Rounds	5-9
5-2	Piezometric, Ballistic, and Thermodynamic Efficiencies of Some Existing Recoilless Rifles	5-13
5-3(A)	General Ballistic Design Data Based on Simplified Theory	5-17
5-3(B)	Table of Parameters Based on Simplified Theory	5-19
5-4	Comparison of Theoretical and Observed Temperature Data	5-67
5-5	Numerical Constants Used in Interior Ballistic Calcula- tions	5-87
6-1	Velocity Ratio and Expansion Ratio as Functions of Pressure Ratio ($\gamma = 1.23$)	6-13
6-2	Variation of Nozzle Thrust With Nozzle Expansion Angle 2α	6-27
6-3	Variation of Recoil Force Imbalance With Nozzle Ex- pansion Ratio	6-27
6-4	Ballistic Data for the 57 mm Recoilless Rifle, M18, Fired With Various Chamber Configurations	6-30
6-5	Estimated Erosion of Gun Nozzles as a Function of Bore Diameter	6-38
6-6	Increase in Charge and Ammunition Weights--Y-duct Compared With Case of Zero Included Angle	6-53
7-1	Magnitude of Errors for Calculating Hit Probability ...	7-8
7-2	Magnitude of Mismatch System 1	7-10
7-3	Magnitude of Mismatch System 2	7-11
7-4	Magnitude of Mismatch System 3	7-12
7-5	Single Shot Hit Probability--Visual Range Estimation ..	7-17
7-6	Single Shot Hit Probability--Crude Range Finder	7-17
7-7	Single Shot Hit Probability--Spotting Rifle	7-18
7-8	Independent and Normally Distributed Quasi-combat Errors Assumed To Cause Impact Errors	7-19
9-1	Comparison of 75 mm Recoilless and Closed Breech Weapon Systems	9-2
11-1	Data for Some Recoilless Rifle Projectiles	11-6
11-2	Cartridge Case Data for M30A1B1	11-23
11-3	Composition of Several Propellants	11-55

PREFACE

The Engineering Design Handbook Series of the US Army Materiel Command is a coordinated series of authoritative handbooks containing basic information and fundamental data useful in the design and development of Army materiel and systems so as to meet the tactical and the technical needs of the Armed Forces.

This handbook, one of the Engineering Design Handbook Series, covers the basic principles of operation of recoilless weapon systems, and provides the fundamental design methods and procedures employed as a basis for future design and development of such systems. Technologies and the associated supporting scientific disciplines that are unique in application to recoilless weapon systems are presented in sufficient detail to provide the design engineer with the system development rationale together with specific subsystem design methodologies. Included in the presentation are highlights of early developments; system design and operation procedures; terminal, exterior, and interior ballistics; recoil cancellation, system effectiveness, and measurement techniques; basic design considerations; rifle and rifle components; ammunition; mounts; and fire control. The extension and adaptation of the basic technology to newer generation weapons—e.g., the TOW System and DRAGON—are not covered.

This handbook was prepared by OEA, Inc., Des Plaines, Illinois—for the Engineering Handbook Office, Research Triangle Institute, Research Triangle Park, NC—under the general supervision of Mr. A. D. Kafadar; the principal authors were Dr. Nuri Y. Olcer and Mr. Sam Levin. Technical coordination was provided by an Ad Hoc Working Group—chaired by Mr. John J. Donnelly, Frankford Arsenal—with representatives from the US Army Tank-Automotive Command, Picatinny Arsenal, Rock Island Arsenal, and Watervliet Arsenal.

The Engineering Design Handbooks fall into two basic categories—those approved for release and sale, and those classified for security reasons. The US Army Materiel Command policy is to release these Engineering Design Handbooks in accordance with current DOD Directive 7230.7, dated 18 September 1973. All unclassified Handbooks can be obtained from the National Technical Information Service (NTIS). Procedures for acquiring these Handbooks follow:

a. All Department of Army activities having need for the Handbooks must submit their request on an official requisition form (DA Form 17, dated Jan 70) directly to:

Commander
Letterkenny Army Depot
ATTN: AMXLE-ATD
Chambersburg, PA 17201

(Requests for classified documents must be submitted, with appropriate "Need to Know" justification, to Letterkenny Army Depot.) DA activities will not requisition Handbooks for further free distribution

b. All other requestors—DOD, Navy, Air Force, Marine Corps, nonmilitary Government agencies, contractors, private industry, individuals, universities, and others—must purchase these Handbooks from:

National Technical Information Service
Department of Commerce
Springfield, VA 22151

Classified documents may be released on a "Need to Know" basis verified by an official Department of Army representative and processed from Defense Documentation Center (DDC), ATTN: DDC-TSR, Cameron Station, Alexandria, VA 22314.

Comments and suggestions on this Handbook are welcome and should be addressed to:

Commander
US Army Materiel Development
and Readiness Command
ATTN: DRCRD-TT
Alexandria, VA 22333

(DA Forms 2028, Recommended Changes to Publications, which are available through normal publications supply channels, may be used for comments/suggestions.)

PART ONE**INTRODUCTION****CHAPTER 1****BACKGROUND INFORMATION****SECTION I****SCOPE**

This handbook is an exposition of proven methods and materials for the engineering design of recoilless weapon systems. Its purpose is to guide the engineer—the mature practitioner as well as the novice—past known pitfalls and more directly to his project goals. By providing this comprehensive summary of the available relevant technology and the system engineering rationale, it is intended to aid the technical manager, the project engineer, and the component designer to carry out his responsibilities with maximum efficiency.

While the purpose of this handbook is to give the engineer all the information he needs to develop a complete system, greater stress is laid on those principles and design features unique to the recoilless weapon and ammuni-

tion, avoiding unnecessary repetition of material available in other Engineering Design Handbooks and common texts. For example, information that is obviously common to other weapon subsystems—such as warhead design, fuze design, optical sight design, and ballistic measurements—are covered here only in a general way to enable the engineer to comprehend the interrelationships of the various subsystems in the context of the integrated whole. References are given for the detailed treatments of these areas that are contained in the Engineering Design Handbook Series and other pertinent documents. This allows for more detailed and exhaustive coverage of those aspects that are peculiar to recoilless systems without excessive bulkiness of the text. It is intended in this way to maximize the utility of the handbook.

SECTION II

HISTORY

1-1 GENERAL

The purpose of this section on history is to summarize the work that has been accomplished during recoilless weapon development. This summary, while describing past achievements, is intended to serve as a guide for future work in this area. As a detailed history would require several volumes, only the major events in the program outlined in Table 1-1 are highlighted herein. In order for the reader to obtain a more detailed description of these programs, Refs. 26 and 27 provide an index of the published recoilless rifle information.

1-2 HISTORY TO END OF WORLD WAR II

1-2.1 DEVELOPMENT PRIOR TO 1943

The idea of eliminating recoil from weapon systems is not new. Leonardo da Vinci (1452-1519), among the prodigious number and variety of mechanical concepts and artistic works he endowed to mankind, left a sketch of a recoilless gun concept showing two projectiles fired simultaneously in opposite directions from a straight tube.

Work on the development of minimizing recoil in guns has covered a little over one hundred years, starting with the use of pre-engraved, rotating bands as a means of decreasing recoil being patented in 1857. However, the modern history of recoilless weapons does not begin until the beginning of the twentieth century. In 1914, US Navy Commander Cleland Davis developed the concept of combining two guns back-to-back, one firing the projectile forward and the other firing a wad of grease and birdshot rearward to yield net recoillessness. Commander Davis obtained patents for this invention which he reduced to practice and mounted experimentally on an airplane (Ref. 1).

In 1921, a British patent was issued to

Charles J. Cooke on a recoilless gun using the vented propellant gas jet to balance the recoil. However, the first recoilless guns developed using this nozzle principle is accredited to the Russians. A Russian weapon of 76.2 mm caliber was first introduced in 1936 and used in combat in 1941 against the Finns. Its design and construction were based on the general principles of a patent issued in 1917, to the Russian mathematician, Riabouchinsky (Ref. 1).

The Germans developed a recoilless gun of the two-projectile type in 1939 to equip aircraft with large caliber (88 mm) armament to attack surface targets. The recoil momentum imparted by firing its 7-kg projectile was balanced by accelerating the cartridge case (of equal weight) in the opposite direction. It was mounted under the aircraft fuselage intended for dive attack against battleships and other important and difficult surface targets (Ref. 1).

Another German recoilless weapon, this one constructed with a nozzle to use the gas jet balancing principle, was issued to its field forces in the early 1940's for land combat. It was the 75 mm L.G. 40. Also, in the early 1940's, the British actively were investigating recoilless guns with Sir Dennis Burney making significant contributions to the advancement of the technology.

1-2.2 DEVELOPMENT OF 57 mm RIFLE, M18

US Army interest was aroused by the knowledge of some of the foreign development and was stimulated by the prospect of equipping the infantry with a lightweight cannon capable of defeating armor. In early 1943, the US Army Chief of Ordnance instructed one of its research and development elements, the Pitman-Dunn Laboratory at Frankford Arsenal in Philadelphia, to

TABLE 1-1
DATA ON EXISTING US RECOILLESS RIFLES

Designation	Caliber, mm	Weight, lb	Length, in.	Type of Mount	Projectile			Program Start Date	Description	Status	Design Agency
					Weight, lb	Velocity, fps	Pressure, psi				
T62	37		49	Caliber .30 MG	1.61	1000	6,060	1946	Infantry shoulder weapon	Shelved	Frankford Arsenal
T15 (M18)	37	30	62	Caliber .30 MG	2.75	1200	6,500	1943	Infantry shoulder or tripod weapon	Standardized	Frankford Arsenal, Frigidaire Division, General Motors Corp.
T66	57	27	48	Integral	2.75	1200	7,100	1947	Improved shoulder or tripod weapon	Evaluation	Frankford Arsenal
T190	65								High-Performance Aircraft Rifle	Shelved	Armour Research Foundation
T116	75	67	65	Caliber .30 MG	6.75	1000	9,000	1943	Lightweight launcher for air-to-air	Development	Armour Research Foundation
T17	75	250	86	Caliber .30 MG	14.00	1500	25,000	1944			Frankford Arsenal
T21 (M20)	75	104	82	Caliber .30 MG	14.00	1000	9,000	1944	Infantry tripod weapon	Standardized	National Forge & Ord Frankford Arsenal
T192	75	35	66		5.50	1000	5,550	1953	Scale model BAT studies	Development	Frankford Arsenal

TABLE 1-1
DATA ON EXISTING US RECOILLESS RIFLES (Continued)

Designation	Caliber, mm	Weight, lb	Length, in.	Type of Mount	Projectile			Program Start Date	Description	Status	Design Agency
					Weight, lb	Velocity, fps	Pressure, psi				
T41 (ARF)	75	75	68.75	Caliber .30 MG	-	-	-	1950	Lightweight semi-automatic shoulder tripod	Develop- ment	National Forge & Ord, Armour Research Foundation
T184	90	33	43.50	Integral	-	-	-	-	Platoon antitank rocket launcher (shoulder or tri- pod)	Develop- ment	Midwest Re- search Insti- tute
T149	90	47	60	Integral	9.00	900	5,500	1948	Platoon antitank rifle (shoulder or tripod)	Develop- ment	A. D. Little, Inc.
T219E4 (M67)	90	35	53	Integral	6.80	700	7,780	1955	Platoon antitank rifle (shoulder or tripod)	Standardized	Midwest Re- search Insti- tute
T234E	90	30.5	60	Integral	7.00	900	5,400	1955	Super-platoon antitank rifle (shoulder or tri- pod)	Shelved	United Shoe Machinery
T18	105	120	97	Caliber .30 MG	12.00	1000	9,000	1945			Frankford Ar- senal
T19 (M27)	105	330	134	M22-M75	29.00	1250	10,000	1945	Jeep-mounted rifle	Standardized	Frankford Ar- senal
T135-7	105	307	-	T151	17.50	1660	16,600	1953	Front nozzle, battalion antitank rifle, mountable on ground, tri- pod, jeep, light- armor vehicle	Develop- ment	Frigidaire Divi- sion, General Motors Corp., Armour Re- search Foundation

TABLE 1-1
DATA ON EXISTING US RECOILLESS RIFLES (Continued)

Designation	Caliber, mm	Weight, lb	Length, in.	Type of Mount	Projectile		Program Start Date	Description	Status	Design Agency
					Weight, lb	Velocity, fps				
T135	105							Semi-automatic antitank rifle	Develop- ment	Harvey Ma- chine Company
T136E2	105	240	134	T149	17.00	1700	1950	Battalion antitank rifle, mountable on ground, tri- pod, jeep	Shelved	Frankford Ar- senal
T137	105							Battalion antitank rifle, mountable on ground, tripod, jeep, light-armor vehicle	Develop- ment	Firestone Tire & Rubber Co.
T170E3 (M40A1)	106	281	134	T149E3 (M79)	17.00	1650	1952	Battalion antitank rifle, mountable on ground, tripod, jeep, light-armor vehicle	Standardized	Frankford Arsenal
T237	105	820	144	--	17.00	--	1952	Repeating antitank rifle	Shelved	United Shoe Machinery Co.
XM105E1	120	391	141.25	XM124	18.10	1810	1959	Heavy antitank weapon, mount- able on ground, jeep	Shelved	Frankford Arsenal
XM63 (M28)	120	--	--	--	--	--	--	2,000-m range	Standardized	
XM64 (M29)	155	--	--	M121	--	--	--	4,000-m range	Standardized	
E1K (or 8 in.)	350	--	--	--	--	--	1954	Long-range artillery rifle	Shelved	Parish Pressed Steel Co.

explore the feasibility of "... applying the recoilless principle to the development of a man-portable, infantry-type weapon for defeat of armor". A program was established on recoilless rifles under the general coordination of Colonel René R. Studler, Assistant Chief of Ordnance for Small Arms Research and Development, and his staff, especially Dr. Lafayette Boyd Hedge. Execution and the technical direction of the program was assigned to Frankford Arsenal. By mid-year, Dr. William J. Kroeger, a physicist employed in that laboratory, had evolved mathematical expressions of the essential thermodynamic relationships governing the ballistic operation of recoilless guns. Concurrently, teaming up with Mr. C. Walton Musser and a small group of scientists and engineers, these principles were reduced to practice in the form of an experimental recoilless gun consisting of a smooth-bore 2.75-in. caliber tube, a propellant combustion chamber, and a breechblock perforated with many small nozzles. This first laboratory "test gun" was fired on 27 July 1943 (Ref. 2).

At a meeting held at the Office, Chief of Ordnance, on 10 September 1943, it was decided to center the first recoilless rifle design about a caliber 57 mm shoulder-fired rifle firing a 2.75-lb pre-engraved projectile. Test Gun No. 2 was designed, but even before test data from Gun No. 2 were available, the demand for a lightweight weapon prompted the start of the final design of the 57 mm weapon. By October 1943, a firm practical design of the 57 mm Rifle, T15 (M18) was achieved.

The T15 Rifle proceeded through development test firings, beginning in October 1943 at Frankford Arsenal and ending with a final demonstration before War and Navy Department representatives on 26 September 1944 at Aberdeen Proving Ground. In early 1945, limited production of the 57 mm rifle was begun and in March 1945, a shipment of fifty rifles was made for use in European Theater. During April and May 1945, changes in design, dictated by observation of weapons in combat conditions, were initiated. The design

of the weapon then was felt to be adequate for service use and at the request of the Army Ground Forces, the 57 mm rifle was standardized in June 1945 (Ref. 2). In less than two years from the beginning of development, the first standardized US recoilless weapon system was issued to combat troops. This was the Rifle, Recoilless, 57 mm, M18 shown in Fig. 1-1. In 1945, General Somervell, Commanding General of the Army Service Forces, reporting to the Congress on the development of new weapons, stated: "Together with the V-T fuze, the recoilless gun was the most startling development of the War until the moment the atomic bomb exploded" (Ref. 2).

The design goal of this system was one-man portability and operability, with a second man to resupply ammunition and load subsequent rounds in a series. It was to be fired from the shoulder standing or kneeling and from the ground supported on a light integral mount. Its role was to give the infantry heavy weapons platoon organic fire support capability, complementing the mortar and machine gun with flat trajectory high explosive firepower. The 57 mm M18 System, weighing 44 lb, and designed to fire a 2.75-lb projectile at 1200 fps, was used with striking success in the European and Pacific Theaters in WW II.

The unique design features that contributed principally to the successful culmination of this project in a practical field weapon were:

1. Pre-engraved Rotating Band. This eliminated the engraving loads on the rifling and the induced stresses in the gun tube, permitting a thin-walled, lightweight tube structure. Also, it eliminated the engraving force irreproducibility and the resulting feedback effects into the interior ballistics and recoil balance.

2. Perforated Cartridge Case. The cartridge case was designed to perform the traditional functions of containing the propellant, projectile, and primer integrating the ammuni-

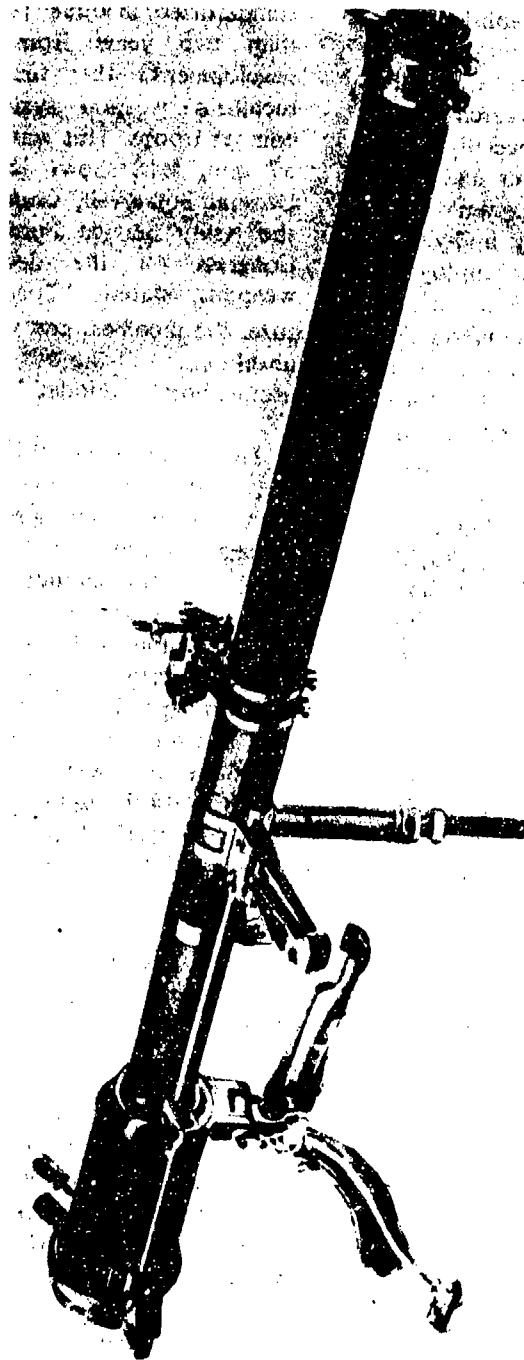


Figure 1-1. Rifle, Recoilless, 57 mm, M18

tion as a package, and interfacing mechanically with the gun structure. In addition, however, the cartridge case served as a cage, supporting the propellant during ignition and venting the recoil-balancing gases through the case liner and then through the perforations in its sidewall, allowing the gases to stream rearward along the chamber and to exit through the nozzles.

3. Nozzle Design. The nozzle was designed with helical cant to balance projectile spin torque reaction and with simple nozzle "blocks" to enable field adjustment of the effective flow characteristics to restore recoil balance after erosion of the nozzle had progressed to an unacceptable level of recoil imbalance.

4. Pressure Joints. The threaded joint connecting the chamber and tube was designed so that internal pressure tended to force the mating parts more tightly together due to elastic deformation during the ballistic cycle. This has become a basic design tenet in recoilless weapon engineering as well as in other pressure vessel design. It is more important in the thin wall sections found in recoilless systems than in conventional guns which have much thicker sections.

1-2.3 DEVELOPMENT OF 75 mm RIFLE, T21 (M20)

Following a demonstration of the Rifle, 57 mm, T15, to the US Army Infantry Board in February 1944, it was recommended by Headquarters, Army Ground Forces that weapons of the 75 mm and 105 mm size be developed in addition to the 57 mm recoilless rifle. Design requirements called for a 75 mm size rifle that fired a projectile weighing approximately 5 lb with a muzzle velocity of 1000 fps. Chamber pressure was to be approximately 4000 psi. The design of the 75 mm size rifle was performed at Frankford Arsenal and was given the nomenclature "Rifle, 75 mm, T16". The design of the Rifle, 75 mm, T16, was based on the principles which contributed to the success of the initial

Rifle, 57 mm, T15. However, the design exceeded the original Ordnance Office directives and it was recommended that the T16 design project be closed, but that further consideration be given to a 75 mm size rifle (Ref. 3).

A change in requirements to a 75 mm size rifle firing a conventional 75 mm artillery projectile at a velocity of 1500 fps at a chamber pressure of 25,000 psi prompted the design of a rifle designated as Rifle, Recoilless, 75 mm, T17. The gun was designed to be fired electrically and use a nonperforated cartridge case. The case fitted the contour of the chamber and had its own venturi. "Consequently", as stated in Ref. 3, "there were no erosion problems such as would have been encountered in a recoilless rifle having the venturi as part of the breech and firing at these pressures". Changing tactical requirements prompted the discontinuance of work on the T17 Rifle in favor of a lightweight weapon that would fire a standard HEAT projectile at a muzzle velocity of 2150 fps and a chamber pressure of approximately 7000 psi (Rifle, Recoilless, 75 mm, T21).

The final design configuration of the T21 Rifle was designated as Rifle, 75 mm, T21E4. The T21E4 Rifle fired a 75 mm HEAT projectile with a muzzle velocity of 1000 fps at a chamber pressure of 6500 psi. The complete weight of the rifle was 110 lb with design features basically similar to those of the Rifle, 57 mm, M18. A notable difference was the interrupted thread breechblock, annular nozzle, and tapered chamber of the T21E4 Rifle. With respect to the pre-engraved rotating band, cartridge case with perforated sidewall, helically canted nozzle, and self-sealing joints, the T21E4 Rifle carried out the basic design principles of the M18 incorporating refinements based on the additional experience gained. The T21E4 Rifle was furnished to troops in the European Theater in March 1945. Approximately three months later, the T21E4 Rifle was standardized along with Rifle, 57 mm, M18 and designated as Rifle, 75 mm, M20 as shown in Fig. 1-2.

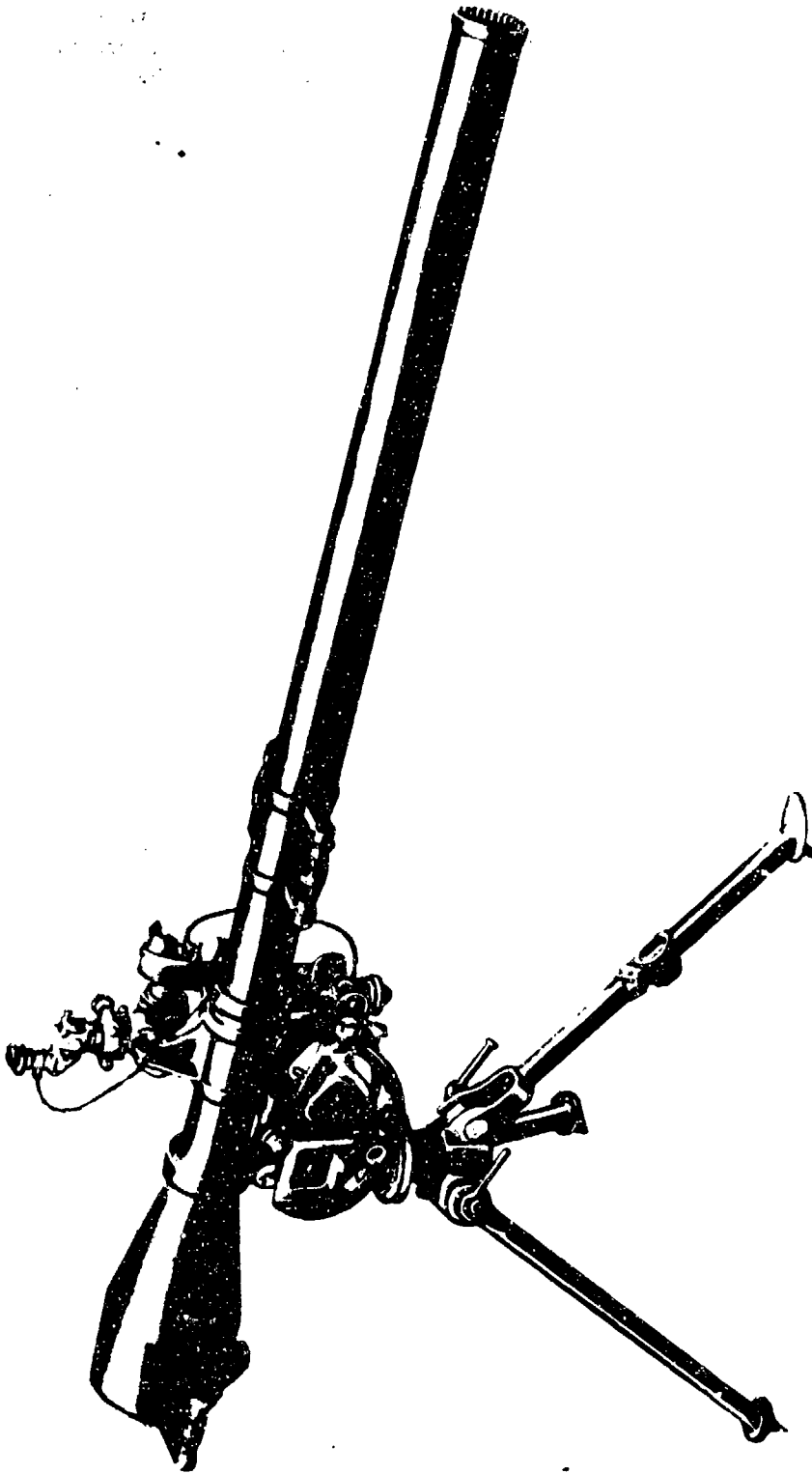


Figure 1-2. Rifle, Recoilless, 75 mm, M20

1-2.4 DEVELOPMENT OF 105 mm RIFLE TO END OF WORLD WAR II

As stated in par. 1-2.3, the desire to have a lightweight rifle in the 105 mm class also was expressed after the successful demonstration of the Rifle, 57 mm, T15. The task of designing this weapon was assigned to Frankford Arsenal. Performance requirements were scaled from the T15 Rifle and indicated that a lightweight projectile weighing approximately 10 lb could be fired at a muzzle velocity of 1000 fps at a rated maximum chamber pressure of approximately 8000 psi. Other requirements included the use of a perforated cartridge case and the use of a pre-engraved projectile in order to utilize best the principles established during ballistic experience with the T15 Rifle. Designated as the T18 configuration, the initial 105 mm rifle design was abandoned since it was felt the time necessary to develop and manufacture the lightweight projectile was excessive. This design, therefore, was superseded by the Rifle, 105 mm, T19, which fired a standard projectile already being manufactured (Ref. 3).

The Rifle, 105 mm, T19 was designed to fire a standard HEAT 105 mm projectile at a velocity of 1250 fps at a chamber pressure of 8500 psi. The rifle weighed approximately 352 lb and was comparable in performance to the Howitzer, 105 mm, M2A1 with HEAT Projectile, M67.

The designs of the firing and breech mechanisms of the T18 and T19 Rifles are similar to those of the Rifle, 75 mm, M20. The only major difference is that the interrupted thread lugs retaining the breechblock in place are integral with the chamber in the Rifle T18; whereas, in the M20 Rifle and T19 Rifle, the lugs holding the breechblock are contained in a bushing that is in turn threaded into the chamber.

By April, 1944, just 6 months after program inception, Frankford Arsenal had completed the first of the T19 models. In May 1944, this T19 rifle was demonstrated

successfully before representatives from the War Department General Staff, Headquarters Army Ground Forces, and Service Boards. However, active development of the 105 mm rifle was suspended by Ordnance Committee action in June 1947.

1-3 HISTORY POST-WORLD WAR II

1-3.1 DEVELOPMENT OF 105 mm RIFLE, T19 (M27)

In February 1950, the 105 mm recoilless rifle program was reactivated. Firing tests of the T19 Rifle were continued and led to the standardization of the T19 Rifle. Designated as the Rifle, 105 mm, M27 (Fig. 1-3), the T19 Rifle became the interim standard 105 mm recoilless rifle. It was used extensively and with great success in the Korean action. In addition, a program was initiated for the development of a 105 mm battalion antitank (BAT) weapon that would meet field requirements more completely.

During the BAT program, a fixed fin-stabilized 105 mm HEAT round, capable of defeating any known tank at a range of 1000 yd was being developed. Concurrently, it was felt that a similar round should be developed for the interim standard Rifle, 105 mm, M27. The complete family of lightweight projectiles for the M27 Rifle then would include the fixed fin-stabilized 105 mm HEAT projectile designated as the T184 along with the spin-stabilized T268 HE (high explosive), T269 WP (white phosphorus), and T139 HEP (high explosive plastic) Projectiles.

With the development of a fixed fin-stabilized round, it was necessary to counterbore the M27 Rifle in order for it to accept the 2 in. longer cartridge case. In addition to this modification of the existing M27 Rifle and the standardization of the 105 mm, T184 round, considerable work was performed in trying to improve the long range flight characteristics of the spin-stabilized HE and WP projectiles. This work mainly was concerned with substituting different types of

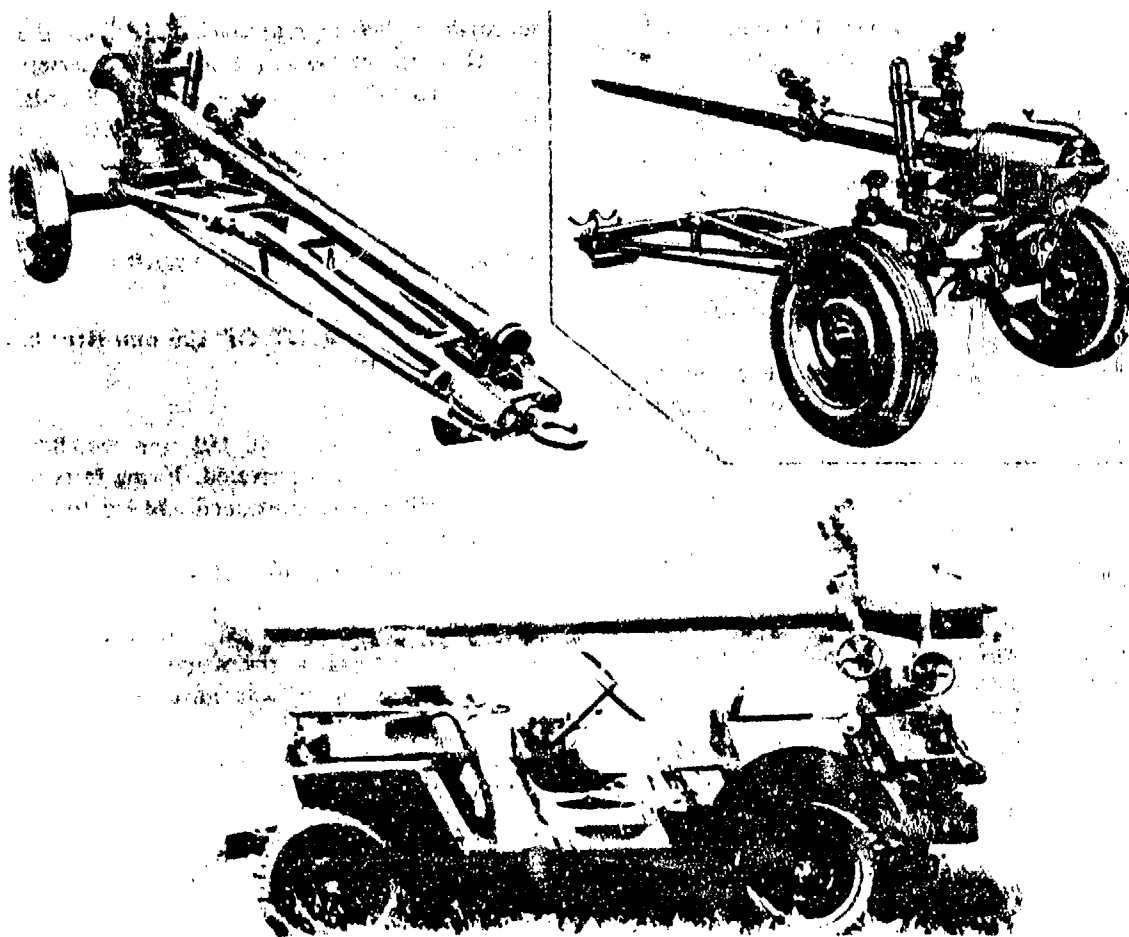


Figure 1-3. Rifle, Recoilless, 105 mm, M27; Jeep and Towed Mounts

boattail bases for the existing round base.

1-3.2 DEVELOPMENT OF 106 mm BAT WEAPON SYSTEM

1-3.2.1 Development at Frankford Arsenal

In April 1950, Frankford Arsenal was assigned to supervise the initial development studies of a 105 mm battalion antitank (BAT) weapon. By August 1950, Frankford Arsenal was given the overall technical supervisory role in the total BAT development project. Besides this supervisory role, Frankford

Arsenal was to develop a long chamber 105 mm recoilless weapon (and mount) using the rear nozzle principle and a smooth bore tube to launch a long boom, fixed-fin projectile. The rifle was designated as the T136 (Ref. 2).

Design of the barrel and chamber of the T136 Rifle was completed by October 1950. The first prototype barrel was assembled with a chamber made at Frankford Arsenal and a modified nozzle-breech assembly from a Rifle, 105 mm, M27. The decision to use a modified M27 breech was dictated largely by the urgency of the development program.

This first T136 Rifle was proof-fired satisfactorily in February 1951. The second and third T136 Rifles were assembled during the spring of 1951 and were equipped with mounts and cal .50 spotting rifles. By completion of development test firings with the T136 Rifles, the following chief features had been achieved (Ref. 2):

1. At 195 lb, the rifle weighed 135 lb less than the weight of the Rifle, 105 mm, M27.

2. The rifle had a smooth bore for use with fin-stabilized projectiles.

3. The barrel incorporated the principle of "strain compensation", developed in connection with the Rifle, 57 mm, T66. Calculations showed, in the case of a thin-walled rifle, that the increase in the bore during firing combined with the barrel and projectile tolerances and the projectile clearance might easily account for the yawing and consequent observed inaccuracy. Performance was improved significantly by the use of oversize projectiles which fit the barrel *during* rather than *before* firing.

4. The breech opened from right to left to permit easier loading when the loader stands in his normal position on the right side of the weapon. Moreover, the breech operating handle could be placed either above or below the chamber.

In October, 1951, certain design changes were made. The resulting T136E1 Rifle differed from the T136 model in the following respects (Ref. 2):

1. Portions of the chamber and barrel were increased in diameter in order to provide clearance for cases fabricated from sheet.

2. The barrel was machined to accept the plastic rotating band immediately ahead of the oversized bourrelet of the 105 mm T118E10 Projectile.

3. The barrel was provided with shallow groove rifling (0.006 in. deep) with 1 turn in 360 calibers.

4. Both spotting rifle brackets were improved. The rear bracket was designed to serve also as a mounting for the sights. (A spotting rifle is a subcaliber weapon that fires a projectile whose trajectory matches the major caliber projectile (see par. 1-3.2.5).)

Soon after the T136E1 model was designed, the need arose for more rapid firing, up to 6 rounds per minute, which is about the limit for manual operation. At this rate of fire, the gun temperature soon rises to a point where there is significant degradation in the yield strength of the steel. These considerations led, in early 1952, to a 105 mm Rifle, T136E2, which provided adequate strength up to 600°F. The weight of this rifle was 214 lb as compared with the 197 lb of the T136E1 model.

Development of major caliber ammunition at Frankford Arsenal centered chiefly around the T118 and the T184 designs. The T118 round was intended to supply a fin-stabilized projectile for use in the smooth bore T136 Rifle. It originally was scaled up from the 90 mm T108 round, which had a projectile with a long boom and fixed-fins. The first design had four fins that were shrouded, i.e., enclosed to an open end cylinder. Since this shroud often was damaged during launching, the design was changed to six longer and unshrouded fins. This remained as the basic design throughout the entire series of E numbers, which differed chiefly in modifications of the case and the liner. The only other change in the projectile (T118E10) consisted of increasing the bourrelet diameter from 4.133 to 4.145 in. This increase was made in order to take advantage of the principle of strain compensation. The bourrelet, whose diameter was 0.011 in. more than that of the static bore, fit the strained bore. This improved the obturation (prevention of gas

escape between bore and bourrelet) and insured against excessive weapon wear and erratic launching of the projectile from the muzzle (Ref. 2).

The T184 round development was begun in February 1951, and was intended to furnish an improved HEAT round for interim use in the M27 Rifle. It was fin-stabilized and incorporated the latest fuze and shaped charge design. It was almost identical with the T118, but it did not have the oversize bourrelet and it did have canted fins (4 deg) in order to maintain a modest spin (approximately 10 rev per sec) that appeared adequate during flight and did not degrade terminal penetration significantly. This was considered necessary to smooth out the effects of small aerodynamic asymmetries imparted by friction in traversing the launcher. This round was fired satisfactorily for accuracy in the summer of 1951 (Ref. 2).

1-3.2.2 Development at Firestone

In August 1950, the Firestone Tire and Rubber Company was awarded a contract for the design and development of a short chamber, 105 mm recoilless rifle (and mount). This rifle was to have the rear nozzle principle and be able to use either a slow spin projectile fired from a rifled tube or a fin- or drag-stabilized projectile launched from a smooth bore tube. This gun was designated as the T137. Firestone was also requested to investigate a slow-spin round, conceived at the Ballistic Research Laboratories and designated as the T138 round; a folding-fin type round (similar to a 75 mm round developed by Armour Research Foundation) designated as the T119; and a drag-stabilized or short-fixed fin round, known as "Moby-Dick" and designated as the T171 (Ref. 2).

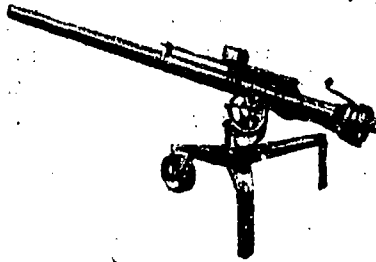
In a three year period, 1950-1953, Firestone developed the "short chamber" (500 in³ chamber volume) Recoilless Rifle and Mount designated as the T137 and T152, respectively. Beginning with interior ballistic

calculations in September 1950, the first prototype T137 Rifle was assembled and proof tested by June 1951. The greatest number of test firings were conducted with the slow spin-stabilized T138 Projectile and by the end of 1952, the round was developed to the point of satisfactory accuracy at ranges up to 1500 yd.

The folding-fin Projectile HEAT, T119 was developed by mid-1953 (preferential treatment was given to the T138 Projectile as requested) to the point of satisfactory accuracy at 1000 yd from a smooth bore tube. When the requirement from the ONTOS (see par. 1-4.7) development specified a rifled tube, Firestone altered the T119 Projectile and secured a "better-than-required" accuracy at ranges up to 2000 yd. In July 1953, the T119E11 Projectile was approved as the standard ammunition for the BAT Rifle and Ammunition System and was designated as "Shell, HEAT, 106 mm, M344" (Ref. 2).

1-3.2.3 Development of 106 mm Rifle, M40

The 105 mm, T136 Rifle System was developed to a high degree of compliance with the military characteristics desired by the Army Field Forces; prototypes of weapon and ammunition successfully passing engineering tests at Aberdeen Proving Ground. However, the ammunition design was based on the concept of a family of homogeneous fin-stabilized projectiles. During 1952, the decision was made by the Ordnance Office to include only one fin-stabilized projectile (the HEAT) in the family; the balance being spin-stabilized projectiles. In view of this decision, the Arsenal project was re-oriented; the development of the T136 system was suspended and major attention concentrated on the development of the T170 Rifle, which had been initiated in the fall of 1951. It was to have conventional deep rifling so that it would be capable of firing spin- as well as fin-stabilized projectiles. This rifle, whose design was completed late in 1951, used standard breech components of the M27



SHOWN:
 RIFLE, 106 MILLIMETER, M40A1
 W/RIFLE, CALIBER 50,
 SPOTTING, M8C
 MOUNT, RIFLE, 106-MM, M79

*Figure 1-4. Rifle, Recoilless, 106 mm, M40,
 on the Ground Mount*

Rifle, that were altered slightly to prevent firing of similar but unsuitable ammunition. It was similar in external appearance to the T136 Rifle and incorporated the various improvements that gradually had been added to the design of the T136—such as high yield strength material, strain compensation, spotting rifle mounting brackets, firing mechanism, and breech opening mechanism. Prototypes of the T170 barrel were made at Frankford and Watervliet arsenals. This rifle was later standardized as the Rifle, Recoilless, 106 mm, M40 shown in Fig. 1-4 and became the major caliber weapon of the BAT System (Ref. 2). The M40 Rifle actually has a bore diameter of 105 mm, but is called 106 mm for logistical reasons.

In July 1952, the Office, Chief of Ordnance decided that the Frankford Arsenal T170 and Firestone T137 Systems would remain as possible choices for the BAT Rifle System. At this time, the following combinations of packages of projectiles were selected for use in the BAT System:

1. T138E57 HEAT, T263 HE, T261 WP fired from a tube with a twist of 1 turn in 200 calibers
2. T119 HEAT, M323 HE, M325 WP, M326 (T139E36) HEP fired from a tube with a rifling twist of 1 turn in 20 calibers

3. T184 HEAT, M323 HE, M325 WP, M326 (T139E36) HEP fired from a tube with a rifling twist of 1 turn in 20 calibers.

Combined engineering and field service tests were performed at the Aberdeen Proving Ground during September and October, 1952, to evaluate the rifles and ammunition still under consideration for the BAT System. As a result of these tests, the T138 slow-spin projectile was eliminated from further consideration because its performance at an extended range of 2000 yd was inferior to that of the finned HEAT rounds. As a result of subsequent Service Board Tests at Fort Benning, Georgia, and further comparison tests at Aberdeen Proving Ground, the Frankford Arsenal T170 Rifle and the Firestone Tire and Rubber Company Cartridge T119E11 were selected for the interim BAT System. Upon standardization, the HEAT folding-fin-stabilized cartridge was designated as M344, and the T170 Rifle designated as the Rifle, 106 mm, M40.

1-3.2.4 Development at Frigidaire

The Frigidaire Division of the General Motors Corporation was assigned the task of developing a front-orifice type 105 mm recoilless rifle for the battalion antitank (BAT) Weapon System. This rifle was to be capable of firing the projectiles developed under the other BAT programs. Designated as T135, the front-orifice rifle used a solid-wall cartridge case instead of a perforated case. The exit of the recoil neutralizing propellant gases took place at the mouth of the cartridge case, expanding radially into a small chamber and then rearward through the nozzle.

Specifications called for the BAT Rifle to fire a 17.5-lb projectile 1000 yd with a 0.25 mil accuracy. The maximum chamber pressure was to be about 12,500 psi with a muzzle velocity of 1750 fps. The desired weight of the rifle was to be as near 200 lb as possible. Interior ballistics were performed by the Armour Research Foundation in order to

establish the chamber, barrel length, and nozzle characteristics of the first prototype rifle. The design of the T135 Rifle evolved through seven prototype and engineering models with firing tests of the various models performed at Fort Sheridan, Illinois, by Armour Research Foundation. Although the final models of the T135 weapon were found to be mechanically and ballistically successful, the lightest model weighed over 300 lb. With studies indicating that the minimum possible weight for a front-orifice rifle would be 250-275 lb, it was decided that the front-orifice rifle was too heavy to be carried by hand. As a result, the program was terminated with the manufacture of the last engineering model.

1-3.2.5 Spotting Rifle Development

During the formulation of the BAT program, the concept of the subcaliber spotting rifle was introduced. The subcaliber rifle is mounted on the major caliber rifle with its bore approximately parallel to that of the major caliber rifle in order for the spotting projectile to match the trajectory of the major caliber round. In May 1950, Frankford Arsenal was advised by the Office, Chief of Ordnance that it should initiate work on the design of a cal .50 spotting bullet having as high a ballistic coefficient as possible. By July 1950, the development of a cal .50 spotting rifle was begun at both Springfield Armory and the Remington Arms Company.

The development of the cal .50 spotting rifle at Springfield Armory resulted in four distinct rifle models. These four models were designated as the T43, T46, T46E1, and T46E2. The first of these models, designated as the T43, used the standard cal .50 machine gun cartridge loaded with a reduced powder charge. Weighing 661 grains, the projectile attained a muzzle velocity of 1800 fps in a 36-in. length barrel. The T43 Rifle was semiautomatic, gas-operated, and used a conventional double column box magazine.

Due to the urgency of the spotting rifle development, detailed component drawings of the T43 model were prepared in haste, the first component drawings being released for fabrication just nine weeks after program initiation. The first test T43 model was fired at Springfield Armory 17 weeks after the program start. Since the drawings were hurriedly prepared, they did not guarantee 100 percent interchangeability of parts for assembly and function, and because the service life of the component parts left much to be desired, only limited test firings were conducted with the T43 Rifle (Ref. 4).

The second step in spotting rifle development was undertaken to correct deficiencies existing in the previous T43 model and to accommodate a shortened cal .50 round. The length of the round was reduced because of the reduced powder charge required. The major design change in the T46 Rifle was a change in the slide and receiver design from a rectangular to cylindrical construction while retaining the rectangular bolt construction of the T43 Rifle. While better than the T43 design, the T46 Rifle was plagued with the following types of malfunctions: (1) operating power was marginal, (2) ammunition was not properly fed, (3) spent cartridge cases were not always ejected, and (4) firing mechanism failed to remain in the cocked or ready-to-fire position.

In order to eliminate these malfunctions and reduce the firing error of the T46 model, a second redesign of the cal .50 spotting rifle was made. Designated as the T46E1, the new model had a reduced barrel length, from 36 to 32 in., in order to reduce the projectile travel from gas port to muzzle exit. This change causes an earlier venting of the bore gas pressure, resulting in a lower chamber pressure at the instant of breech unlock. An increase in the initial volume of the gas system retarded the early acceleration of the piston and, because of the resulting longer gas system time, the maximum piston velocity is reduced.

While these design changes led to improvements in the weapon accuracy and a reduction in the number of malfunctions, it was felt that a better design was still in order. In the next redesign of the spotting rifle, designated as the T46E2, three major improvements were made:

1. The cable pull load required to fire the rifle was reduced.

2. The rebound of the operating slide from battery was reduced.

3. The operating power in the rifle was controlled by incorporation of a needle-valve type gas-regulator. The improvement of the spring forces acting on the firing cable was a matter of refinement and adjustment of the existing design with the reduction of the slide rebound, malfunctions caused by the hammer impacting the firing pin when it is in the locked, out-of-battery position were prevented. Differences in the effective rigidity of the rifle mounts in addition to variation in the magnitude and operating power given by different lots of spotting rifle ammunition made the incorporation of a power regulating device imperative.

As a result of these design changes and numerous refinements throughout the spotting rifle design, function was improved to a substantially satisfactory status. The firing error of the T46E2 was almost one-half the error obtained with the T46 design; at a range of 100 yd the mean target radius was 1.50 in. for the T46E2 Rifle as compared to 2.82 in. for the T46 model.

1-4 OTHER RECOILLESS WEAPONS OF CALIBER 106 mm OR SMALLER

1-4.1 37 mm RIFLE, T62

In July, 1945, the Office, Chief of Ordnance requested Frankford Arsenal Ordnance Laboratory to design and develop a 37 mm single shot recoilless rifle. Designated as

the Rifle, 37 mm. T62, this rifle was to fire Projectiles M54 and M63 at velocities of 1250 and 1200 fps, respectively. This 37 mm recoilless rifle was to be shoulder-fired for use as an antipersonnel type weapon. The first design of the T62 Rifle was proof-fired in May 1946. After firing of the tenth round, the lugs that locked the breech into the chamber showed evidence of failure by bending and firing was discontinued. In addition to the breech design failure, the first eight rounds fired resulted in ignition failures (Ref. 3).

The breech locking mechanism and the firing mechanism were redesigned and the new rifle model designated as T62E1. This rifle functioned satisfactorily in subsequent proof-firings. However, the change development to give the required ballistic performance was never completed since the project was shelved.

1-4.2 57 mm RIFLE, T66

In 1951, a replacement of the original 57 mm recoilless rifle (the M18) was proposed. Technological advances from those crude models of relatively early days offered improvements in practically all areas: interior ballistics, flight dynamics, HEAT penetration performance, and structural and mechanical design of the rifle. The new rifle, designated as the T66, was to match the performance of the M18 Rifle (1200 fps) at a considerably lower maximum chamber pressure. One of the first considerations in the T66 barrel design was the use of steel with a higher yield strength. As such, the barrel walls could be of relatively thin cross section as compared to that of the M18 Rifle. By use of better propellants, the first T66 Rifle design was 14 in. shorter than the M18 Rifle and weighed 28 lb including all accessories, as compared to a weight of 44 lb for the M18.

All development activity proceeded smoothly until firing tests were performed on the initial T66 designs. Considerable inaccuracy was encountered and the basic cause

was not known. After considerable investigation into such possible causative areas as the method of mounting and nozzle symmetry, it was found that the projectiles were yawing excessively. Upon further studies, it was hypothesized that the yaw in exterior flight was related to the yaw and balloting of the projectile during bore travel. Further calculations showed that the expansion of the highly stressed barrel during firing could be great enough so that if the projectile was crowded to one side of the bore, it could become disengaged completely from the rifling on the other side. The use of high-speed X-ray equipment verified this hypothesis by indicating that significant yaw did occur within the barrel (Ref. 6).

As a result of these studies, it was found that for any weapon which uses a barrel that is strained highly by firing, the projectile should be designed to fit the barrel during the firing rather than prior to firing. The use of this strain compensation principle was first made in the T66 Rifle and has been used on many of the subsequent recoilless rifle programs.

In late 1954, a requirement that the T66 Rifle be capable of firing the same mixed family of fin- and spin-stabilized projectiles as used in the M18 Rifle was added. The projectiles developed during the T66 program were the spin-stabilized HE, T115 and the fixed fin-stabilized HEAT, T188. Complete prototype systems were designed, built, and successfully demonstrated. However, the project was terminated due to lack of sufficient user interest in 1958, after completion of User Tests by the US Army Infantry Board. More information on the T66 development program is found in Refs. 6, 7, 8, and 9.

1-4.3 2.75-in. RIFLE, T190

Among the programs conducted at the Armour Research Foundation was the development of a single shot and repeating recoilless rifle to fire the 2.75 in. boosted

rocket used in the T121 ammunition. These weapons were intended for air-to-air use and, accordingly, carried restrictions of light-weight, simplicity, and ease of loading. Requirements for the single shot 2.75-in. recoilless rifle, designated as the T190, were (Ref. 4):

1. Fire a 2.75-in. spin-stabilized boosted rocket with a nominal weight of 5.5 lb
2. A muzzle velocity of 1200 fps
3. Peak chamber pressure under 6000 psi if possible
4. Recoil balance such that the transmitted force to airframe is less than 1000 lb
5. Rifle front profile as small as possible for purpose of parallel stacking of rifle
6. Use of muzzle and nozzle blast tubes to shield adjacent portions of assembly and aircraft
7. Weight of loaded cluster to be 300 lb maximum.

The repeating version, designated as the T191, has essentially the same requirements except that the boosted rocket was to be fired in automatic operation at a minimum rate of fire of 600 rounds per minute.

The principal technical problems of interest concerned design for minimum system weight, interior ballistic uniformity at the low operating pressure of 6000 psi and over the extreme ambient temperature range for aircraft, automatic feed mechanism design, effects of nozzle erosion, gun heating, and blast effects on the aircraft structure. Compromise solutions to the trunnion reaction problem were examined, considering partial recoillessness coupled with soft mounting. Pre-engraved vs self-engraving rotating bands in the uniform twist and increasing twist were investigated with respect to ballistic reproducibility. The pre-engraved

band with uniform twist solution was found to be superior. Perhaps the most striking event in the program, from a technical history standpoint, was the construction and testing of a glass fiber reinforced plastic gun. In collaboration with the US Naval Ordnance Laboratory at White Oak, Maryland, a test gun was designed, built, and fired (1956). The tube survived several shots at full pressure and velocity, and showed acceptable ballistic uniformity and projectile accuracy. This was an early indication (perhaps the first) of the potential for this material for construction of guns. The project was terminated in 1957 with the suspension of the user requirement. For more information regarding the 2.75-in. recoilless rifle, the reader is directed to the material found in Refs. 4 and 5.

1-4.4 90 mm RIFLE AND AMMUNITION

Various evaluation studies of multipurpose shoulder weapons conducted in the late 1940's indicated the need for a 90 mm recoilless rifle. As a result of these studies, Arthur D. Little, Inc. and Midwest Research Institute (MRI) were given Ordnance Contracts to develop 90 mm platoon antitank (PAT) recoilless rifles. The objectives of these programs were to develop a rifle weighing less than 30 lb, capable of being either shoulder- or ground-fired. The rifle was to have very good accuracy at 500 yd and capable of defeating tank armor up to 6 in. thick at a maximum obliquity of 60 deg (Ref. 4).

The Arthur D. Little rifle, designated as the T149, differed from the more conventional rifles developed before 1951, being very light for its caliber and using a novel breech mechanism. The annular two-lobe nozzle breech is basically a rotating cam ring which locks the round in place, cocks the firing mechanism, and actuates the extractor. Recoil compensation is provided as the discharging propellant gases pass through the annular nozzle. The nozzle contours are formed by the inner surfaces of the chamber and cam ring, and by the outer surface of the cartridge

case base. Another unique feature of the T149 Rifle was a firing mechanism in the lower rear of the chamber which caused a firing pin to be driven radially into a side-fire percussion cap in the cartridge case base (Ref. 10).

The PAT program at Arthur D. Little also included the development of fin-stabilized HEAT, HE, and WP projectiles for use with the T149 Rifle. Weighing 9 lb, the Projectile, HEAT, T249 was the only projectile carried through complete development. The design of the HEAT projectile was based largely on the configuration of the 105 mm, T118 configuration. One of the interesting and unique design aspects of the T249 Projectile concerned the application of the rotating bands to the projectile. Prior to PAT development, rotating bands, whether plastic or metal, were fabricated from sheet stock and then cemented or brazed to the projectile, or machined integrally from the projectile. In the Projectile, HEAT, T249, a plastic rotating band is injection-molded directly to the projectile.

In February, 1952, the Office, Chief of Ordnance, set priorities on the development of a suitable PAT rifle-ammunition system. Since the T149 Rifle was given last priority, the T149 Rifle and ammunition were never presented for user tests (Ref. 11).

Midwest Research Institute received its PAT weapon contract in December 1951. The objectives of the PAT program were very similar to those given to Arthur D. Little. The MRI 90 mm recoilless rifle design was designated as the T184. The T184 Rifle design also achieved a very low weight due to the employment of two unconventional features not previously used in recoilless rifle design. The first unique aspect was the use of a reverse tapered cartridge case (smaller in diameter at the base than at the mouth). The cartridge case has a 57 mm base which permits the use of a reduced diameter and thus lighter breechblock. Secondly, the

breechblock was a two part assembly composed of a steel breechblock and an aluminum venturi expansion cone which further contributed to weight reduction (Ref. 4).

Initial analytical studies in the PAT program indicated that a conventional 6-lb projectile and a recoilless rifle having a bare weight of 25 lb could not meet the required first round hit probability at the specified range and muzzle velocity. Further studies indicated the need for using rocket-assisted (RA) projectiles. Two RA projectiles were designed for use in the T184 Rifle. The first projectile, designated as the T273 HEP RA, was designed on the basis of a scaleup of the 2.75-in. T131 Rocket, and contained a solid cast grain rocket motor and an HEP warhead. The second projectile, designated as the T274 HEAT RA, employed the same rocket motor as the T273 round but contained a shaped charge warhead. The warhead was separated from the rocket motor by a bearing section that permitted the rocket motor to rotate at the high speed required for round stability while the warhead was maintained at the low spin rate necessary for maximum terminal effectiveness (Ref. 4).

As a result of the HEP round not being able to meet the armor defeating requirements and because of the wide dispersions encountered during range firings, the T184 program was terminated in 1955 in favor of the T219 program which was to be conducted at Midwest Research Institute. The T219 PAT Rifle requirements permitted an increase in rifle weight to 30 lb so that the peak chamber pressure could be increased in order to eliminate the need for a rocket-assisted projectile.

The 90 mm T219E4 model, as shown in Fig. 1-5, is a 35-lb bore-sized, shoulder-fired, recoilless rifle. The T219E4 PAT Rifle incorporates a central-orifice, bar breech, and may be loaded and fired by one man, although it was designed for a two-man team.

Firing the Cartridge, 90 mm, HEAT, T249E6 at a muzzle velocity of 700 fps, the T219E4 Rifle attained a first round hit probability of 50 percent at 500 yd (unaided visual ranging) and was capable of defeating any armor likely to be encountered in the battle area. Primarily designed as an antitank weapon, it was also highly effective against emplacements and grouped personnel.

By August 1959, the T219E4 Rifle, T249E6 Cartridge, and auxiliary items were standardized and designated as Rifle MAW (medium antitank weapon), 90 mm, M67; Cartridge, 90 mm, HEAT, M371; Telescope, M103; and Telescope Mount, M110. This standardization was given conditionally on the basis that certain design corrections would be made. The deficiency to be corrected was the low temperature firing performance. During arctic firing tests, the CARDE (see par. 1-6.10) T31 sheet Propellant used in the T249 Cartridge revealed an apparent tendency toward high velocity levels and dispersions, accompanied by potentially unsafe high pressures. As a result, emphasis was placed in establishing the suitability of a granular propellant. On the basis of the best uniform performance, M5 Propellant was selected for use in the M371 Cartridge. Other improvements made in the 90 mm MAW Weapon System were the simplification of the breech design, by reducing the number of components from 28 to 14 parts, and the strengthening of the projectile spike-to-body assembly in order to prevent separation of the spike from the body.

During studies of the various designs for the ultimate battalion antitank (U-BAT) weapon, it became evident that one of the designs offered greater promise in obtaining a very lightweight rifle, and that a rifle of this nature would find tremendous application in the 90 mm PAT Rifle program. Designated as the T234, this rifle design had several unique features. One feature was the absence of a breech that must be opened and closed by the operator. As described in Ref. 12, the nozzle

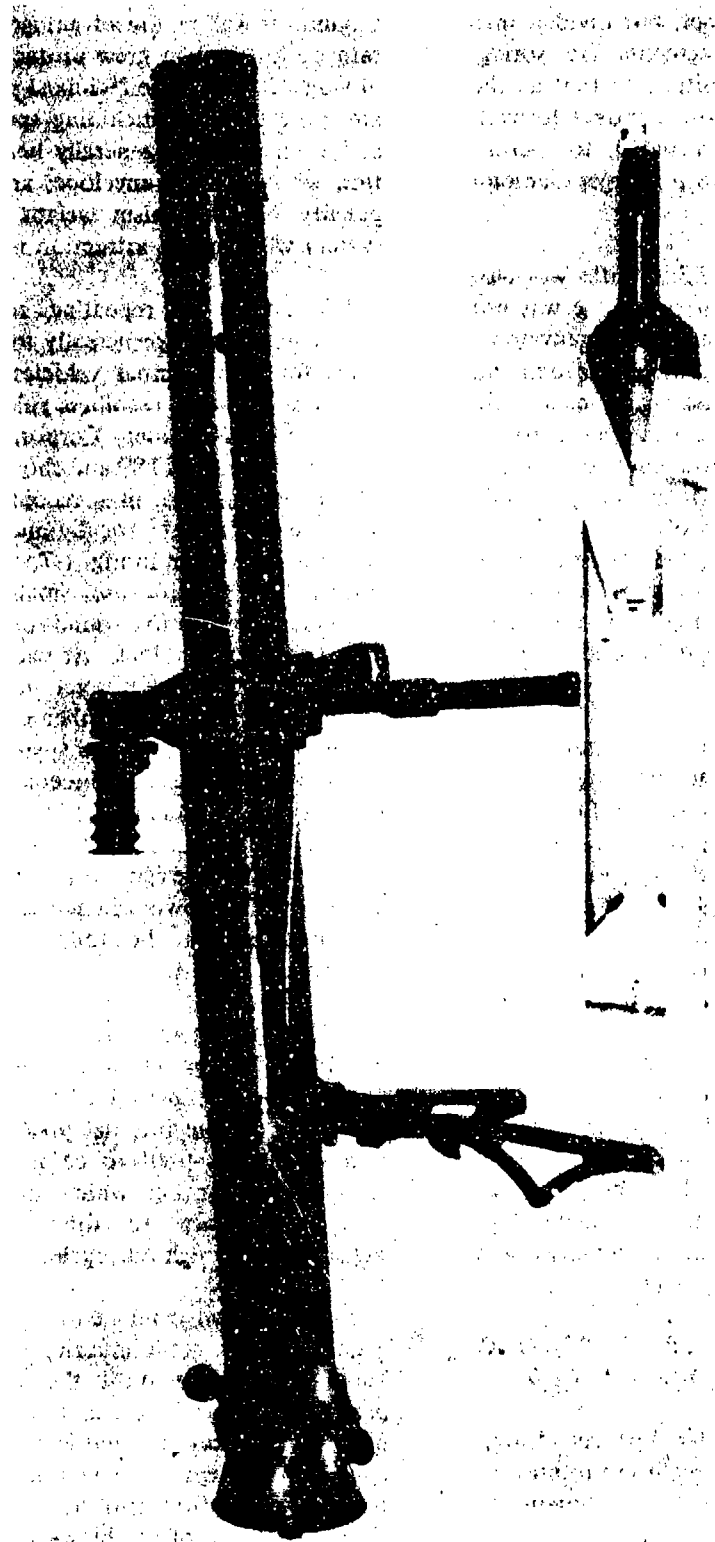


Figure 1-5. Rifle, Recoilless, 90 mm, M67, With Cartridge, HEAT, M371 (Sectioned)

is of central-orifice design, but divided into eight segments. The segments are spring-loaded to the closed position so that as the round is inserted, the nozzle moves forward and expands radially outward to permit chambering of a round with a larger diameter than the nozzle throat.

Ammunition for the T234 Rifle was also unique in that a metal cartridge case was not used. Instead, a thin, plastic powder envelope, which is consumed during firing, was used and the need for expended case extraction eliminated. Firing of the chambered round was accomplished by attaching an ignition transmission line (pigtail) to the projectile boom. After chambering of the round, the end of the pigtail is inserted into the firing mechanism contained in the rear part of the rifle mount. Shown in Fig. 1-6, the T234 Rifle weighs 34.5 lb with the round weighing 8.5 lb.

In early 1957, several original requirements were changed under the heading of the Super-PAT program. The 90 mm Super-PAT Rifle was to be essentially the same design as the 1st configuration of the T234 Rifle. However, it was to employ a high strength steel barrel-chamber (200k to 205k psi yield strength as compared to normal yield strengths of 160k to 175k psi). Internal, external, and terminal ballistic conditions were to remain the same, although with the addition of cal .405 spotting pistol, the weapon system was to be capable of a 90 percent first round hit probability at 500 yd. In June 1958, the Super-PAT program was terminated before completion of the development program as the major emphasis was shifted to the T219 PAT program.

1-4.5 DEVELOPMENT OF REPEATING RIFLES 105 mm, T189 AND T237

Beginning with German efforts during World War II, there was a recurrent interest in recoilless weapons capable of automatic or semiautomatic fire. For combat vehicles (air,

ground, or water), the advantages of increased rate of fire and in crew protection are quite obvious. Some of the technical problems, too, are quite obvious, including space limitation at breech location, generally heavier ammunition with a longer envelope, and the greater penalty of mechanism weight in a weapon system whose great attraction is light weight.

US efforts in repeating recoilless rifle design were aimed principally toward applications for land combat vehicles. Design of a repeating 105 mm recoilless rifle began at the United Shoe Machinery Corporation in 1953. Designated as the T189 and shown in Fig. 1-7, this repeating 105 mm recoilless rifle was designed in both electrically and gas-operated versions. As shown in Fig. 1-7, the electrically operated T189 Rifle uses small electric gear motors to rotate a five-round reel between the barrel and breechblock. At each position of the reel assembly, the barrel and breechblock are coupled with a chamber containing one round. The electrical drive system extends or retracts and rotates the breechblock to open or close and lock the round in place.

One of the designs for the gas-operated T189 Rifle is shown schematically in Fig. 1-8 and operated in the following manner as described in Ref. 13:

1. Energy obtained by bleeding propellant gas from the barrel during the blow-down period (i.e., the period after projectile exit during which the internal pressure decays to atmospheric) is used to compress a pair of nested driving springs which then provide the energy necessary to drive the indexing mechanism through one cycle.

2. Gas is bled from a barrel port (shown in Fig. 1-8) close to the muzzle, which does not become operative until the projectile has passed. Upon projectile exit, the gas turning into the port expands and is conveyed to the cylinder through a telescoping length of tubing. The gas flow into the cylinder lasts for about 0.012 sec of the blow-down period. At

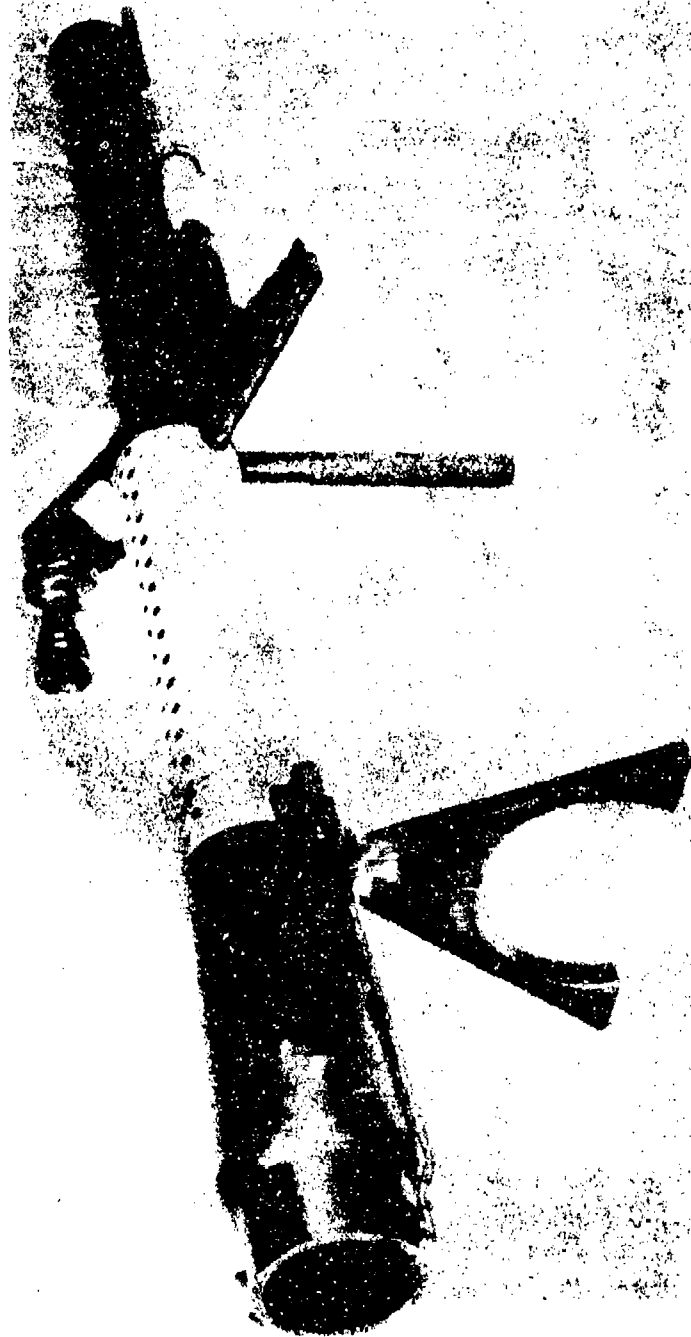


Figure 1-6. Rifle, Recoilless, 90 mm, T234

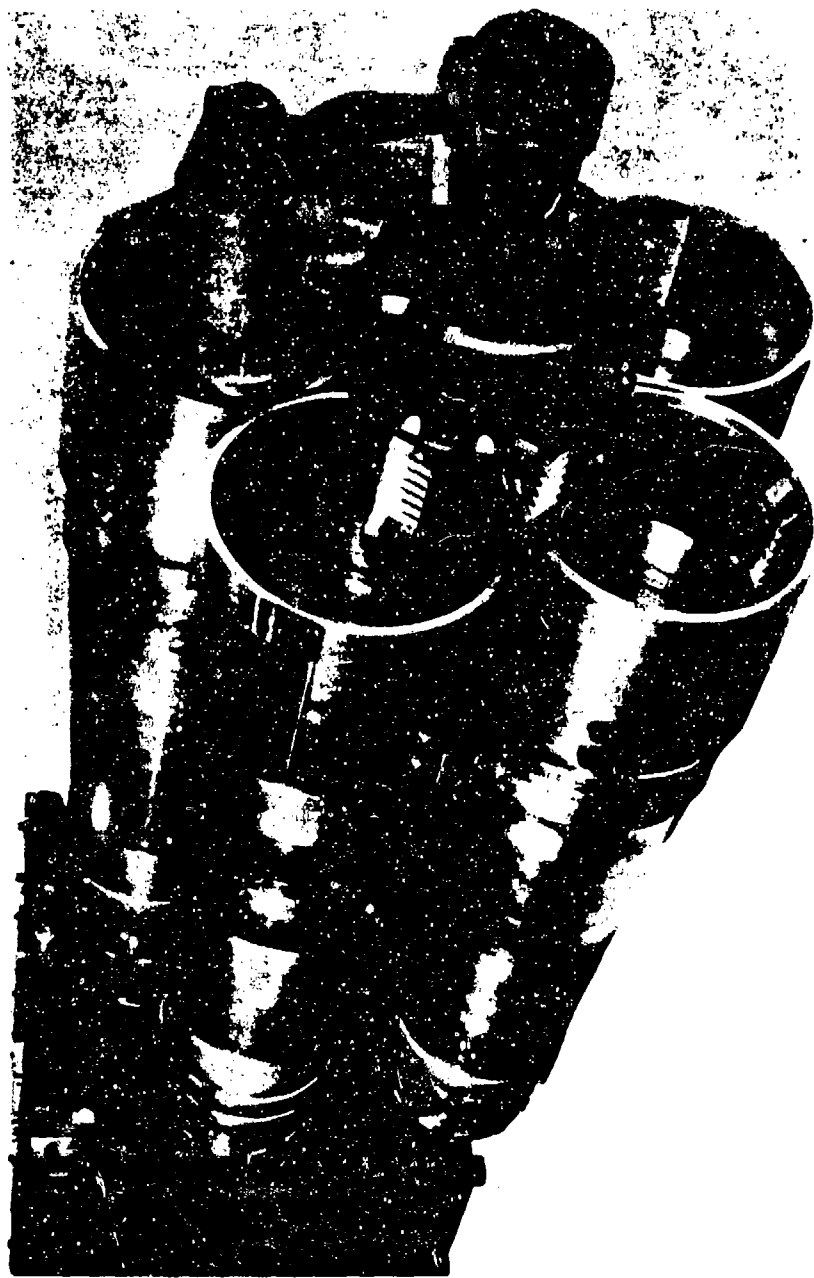


Figure 1-7. Rear View of Recoilless Rifle, Repeating, 105 mm, T189, Breech Open

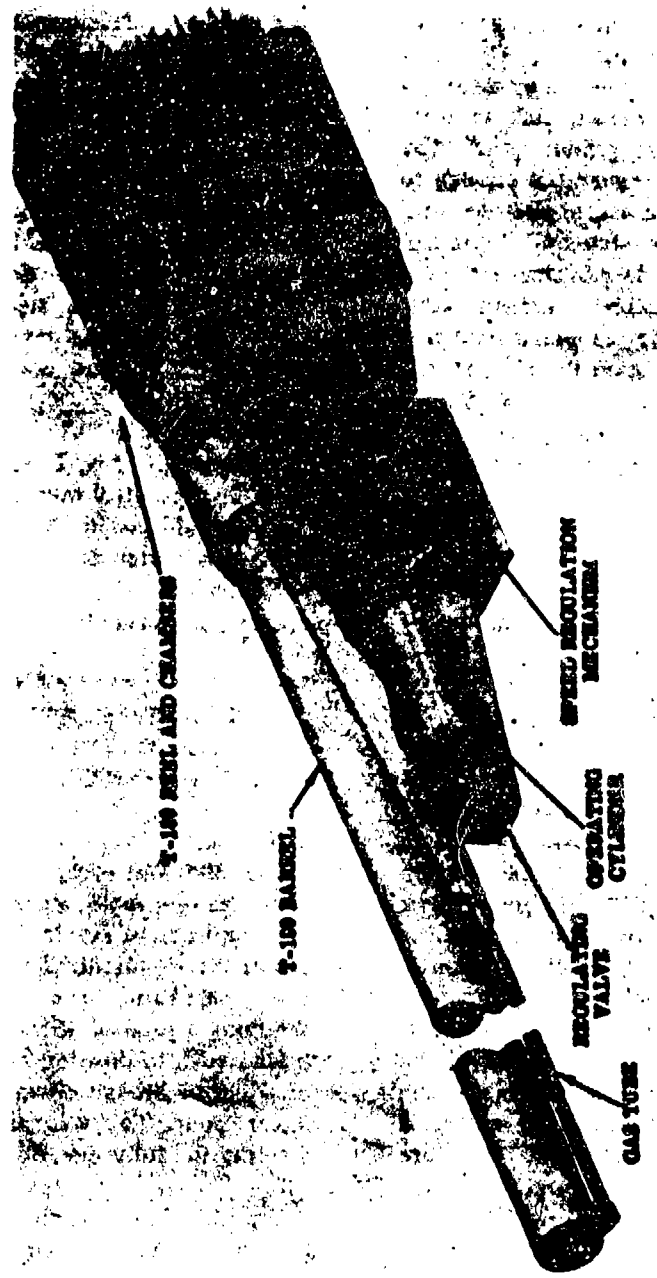


Figure 1-8. Sketch of T189 Rifle Modified for Gas Operation

the end of this time, the blow-down pressure and the pressure in the cylinder will reach equilibrium. The quick acting check valve then closes and retains the cylinder charge.

3. During the cylinder charging stroke, the drive springs are compressed. The gear segment, connected to the piston by means of an operating link, is rotated and, in turn, causes rotation of a pinion gear. The movement of the gear segment is enough to rotate the pinion gear backward just one turn. The gun indexing cycle occurs on the return stroke of the piston. The gas charge then is allowed to escape through an exhaust valve that is separate from the gas feed duct. When the back pressure (acting on the piston) falls below the driving spring pressure, the return stroke begins. On the return stroke, the pinion gear, now engaged to the gun camshaft by the pawl, is rotated one turn forward, indexing the gun through its cycle.

During efforts to simplify the operation and design of the T189 Rifle, an entirely new design was accomplished. It was decided that the new design should replace the T189 design and was given the T237 designation.

The repeating T237 Rifle design incorporated several design features. As shown in Fig. 1-9, a drive motor was geared down to a "lead screw" type drive shaft. Partial rotation of this screw unlocked both the breechblock and the barrel, and proceeded to translate the breechblock axially a predetermined distance. During breechblock travel, the reel containing the five chambers also was moved rearward at a slower rate so as to clear the end of the barrel. A drum then revolves the reel into the next position. When the electric motor is reversed, the breechblock and reel are returned to the closed position and rotationally locked. The T237 repeating recoilless rifle program proceeded through the manufacture of one test rifle. However, the program terminated in mid-1956 by the Office, Chief of Ordnance before any extensive testing of the system was performed.

1-4.6 DEVELOPMENT OF 105 mm RIFLE, T136

The 105 mm Recoilless Rifle, T136 was one of the three original weapon concepts selected for development and evaluation under Ordnance Project TS4-4024. Fig. 1-10 shows this weapon with T149 Mount and with the cal .50 Rifle, T43 installed. In October 1951, changes were incorporated altering the configuration to the T136E1. In November 1951, the design again was changed where provision was included for the expected 21 percent degradation in yield strength of the gun steel when heated to 600°F. T136E2 was the designation assigned to this temperature compensated recoilless rifle.

Portions of this T136 system ultimately were incorporated in the standardized BAT Weapon, M40. The chamber design of the T136 was united with the barrel of the M27 to form the T170 configuration, which ultimately became the standardized M40.

1-4.7 DEVELOPMENT OF WEAPON SYSTEM T165 AND T166, SELF-PROPELLED (ONTOS) USING 106 mm, T170 RECOILLESS RIFLE

The initial long range military characteristics of the BAT weapon system called for a fully man-portable weapon weighing in the neighborhood of 200 lb. The weapon that was eventually standardized for the BAT program was the Rifle, 106 mm, T170 (M40). Weighing a total of 485 lb, the weapon could be moved into position by a crew of two men or could be broken down for hand carry by a larger group. This was still a long way from meeting the fully man-portable requirements.

As the best interim carrier, the Jeep Carrier, M38A1 provided:

1. A low silhouette
2. Good road and cross speed

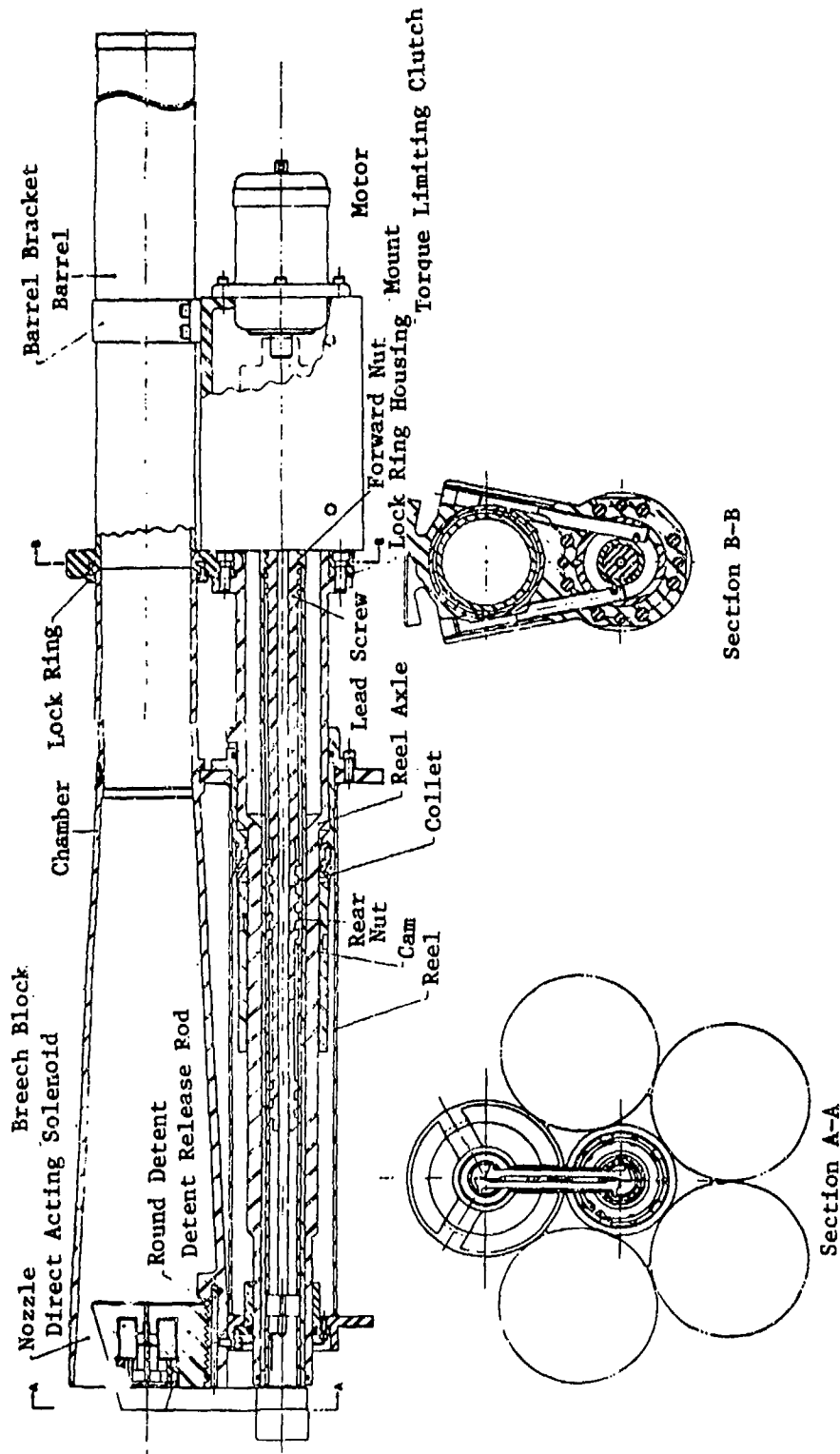


Figure 1-9. Revolver Type, Repeating Recoilless Rifle, T237, Sectional Views

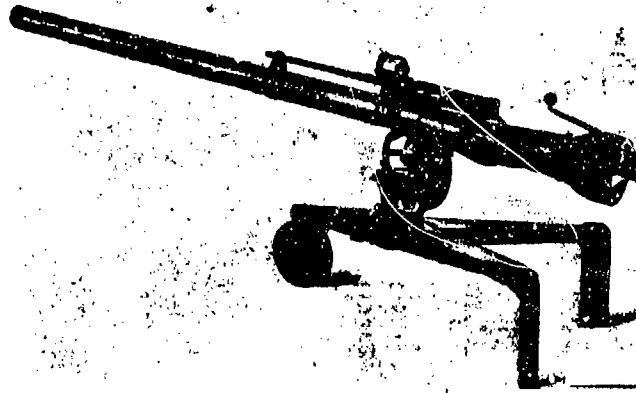


Figure 1-10. 105 mm Rifle, T136; 105 mm Mount, T149; Cal .50 Rifle, T43 and the Interim Sight

3. Ruggedness and reliability
4. Standardized simple operation and maintenance
5. Good cruising ranges
6. Relatively low cost and ease of production.

However, it lacked:

1. Armor protection
2. Adequate load capacity
3. Cross-country mobility of a tracked vehicle.

As a result, studies and searches were made into the development of a lightweight fully-tracked system that would be sufficiently durable and easily maintained for use in the infantry regiment. Two systems were developed around the (ONTOS) vehicle. A six-rifle, ONTOS vehicle designated as the T166 shown in Fig. 1-11 and a one-rifle ONTOS vehicle designated as the T165 were developed using

Rifles, 106 mm, T170 similar to the standardized M40 Rifle. This T165 system was designed to go into combat with the six BAT systems loaded and operable by the crew within the protected compartment. It could be fired in salvo, ripple, or single shot. After firing, the breeches could be opened mechanically from within the vehicle, but subsequent rounds were chambered by the crew reaching out through the open doors. Two of the six rifles were designed to be dismounted quickly from the vehicle and operated from a compact folding ground tripod when the tactical situation required it. In service tests of these weapon systems in late 1952, the vehicles were found to be unsuitable for use as BAT weapons carriers within an infantry battalion. While the ONTOS vehicle provided the necessary armor protection and fully-tracked cross-country mobility, it had the disadvantages of mechanical unreliability, reduced accuracy, increased weight, inadequate space for crew and ammunition, and limited protection afforded by armor when recoilless rifles were reloaded from outside the vehicle (Ref. 4). As such, the M38A1 Jeep Carrier was maintained as the interim carrier for the Rifle, 106 mm, M40.

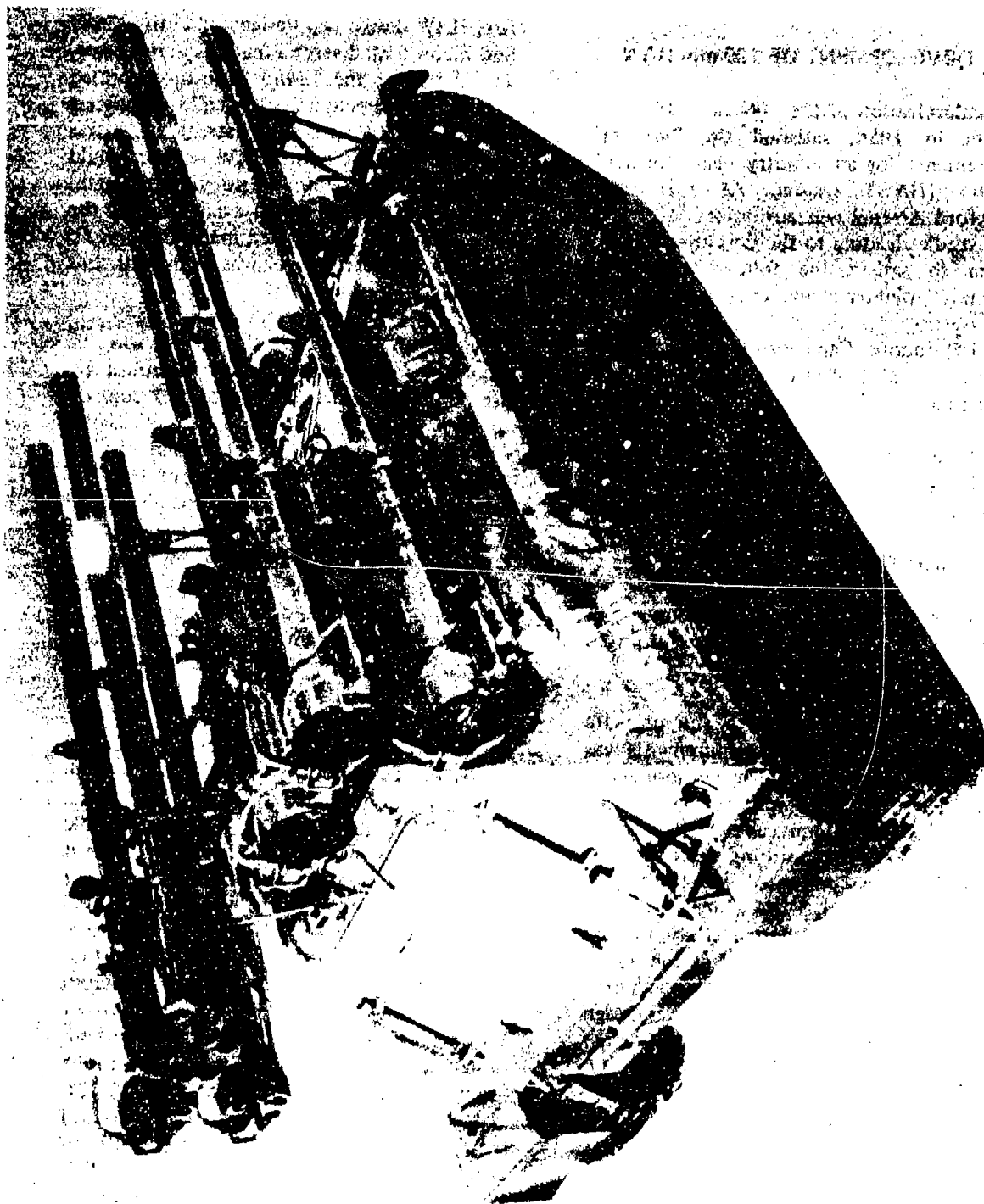


Figure 1-11. 106 mm Self-propelled T165 (ONTOS Vehicle)

1-5 OTHER LARGE CALIBER WEAPONS (LARGER THAN 105 mm)

1-5.1 DEVELOPMENT OF 120 mm HAW

Standardization of the 106 mm, M40 BAT System in 1954, satisfied the "interim" requirements for an infantry heavy antitank weapon (HAW) system. At this time, Frankford Arsenal was authorized to initiate R&D studies leading to the development of a system to satisfy the following principal "ultimate" military characteristics:

1. Destructive Capacity. Defeat 6 in. of heavy armor at 64-deg obliquity, 90 percent of the time.
2. Range and Accuracy. First round hit probability of 0.75 at 2000 yd and 0.90 at 1000 yd.
3. System Weight. 200 lb desired.
4. Rate of Fire. 10 aimed rounds per minute (not sustained). Go into action in 30 sec.

The first work specific to the ultimate battalion antitank (U-BAT) requirements was initiated in 1955 with caliber and lethability studies. These activities were the basis for the selection of a 120 mm caliber rifle for the U-BAT weapon. The resulting design for the 120 mm rifle was patterned after the design of the Rifle, 90 mm, T234 which was, in its original conception, a design study for the U-BAT application. Designated as the T246, the 120 mm Rifle incorporated the segmented nozzle and central orifice type breech design used in the T234 Rifle. Development of the T246 Rifle was suspended in December 1957.

In early 1959, the work begun under the U-BAT program was reactivated under the heavy antitank weapon (HAW) program. The HAW program, however, was committed to the development of a 2000-yd system which would provide greater lethality, improved

range and accuracy, reduced system weight, and improved simplicity and accuracy. The first HAW design was designated as the XM89 and incorporated several features in its design. The barrel of the XM89 Rifle incorporated the strain compensation principle using steel with a 160,000-psi yield strength. It was expected that the entire HAW weapon would use steel with a 200,000 psi yield strength, but because of its limited availability at the time, high cost and limited machinability, no complete HAW rifle ever was made with this material.

A second feature of the XM89 was the incorporation of a variable control mount. By use of a down range pointing joystick control, the rifle could be moved in free traverse and elevation for use against close and moving target with a direct control ratio of 1:1. The joystick control also provided variable control ranging between a ratio of 9:1 and 36:1 for laying the rifle on distant fixed targets. Other unique features of the 120 mm, XM89 were the use of a 15 mm spotting rifle and a trigger firing mechanism from which both major and spotting rifles could be fired with the same trigger (Ref. 14).

During the second quarter of calendar year 1961, the development of the XM89 system was divided into two directions. The first direction being development with a frangible cartridge case and the second, development with a steel cartridge case. Development of the frangible cartridge case system, designated as the XM89E1, proceeded through initial firing tests in a satisfactory manner. At that point, the XM89E1 system was removed from the development program. Development of the perforated steel cartridge case system, designated as the XM89E2 and later to be known as the XM105 (shown in Fig. 1-12), was slowed by minor strength problems and mechanical difficulties, but finished with an accelerated testing program in mid-1972. While it was felt that, with small improvements, the XM105 system could be standardized, its excessive system weight (398 lb

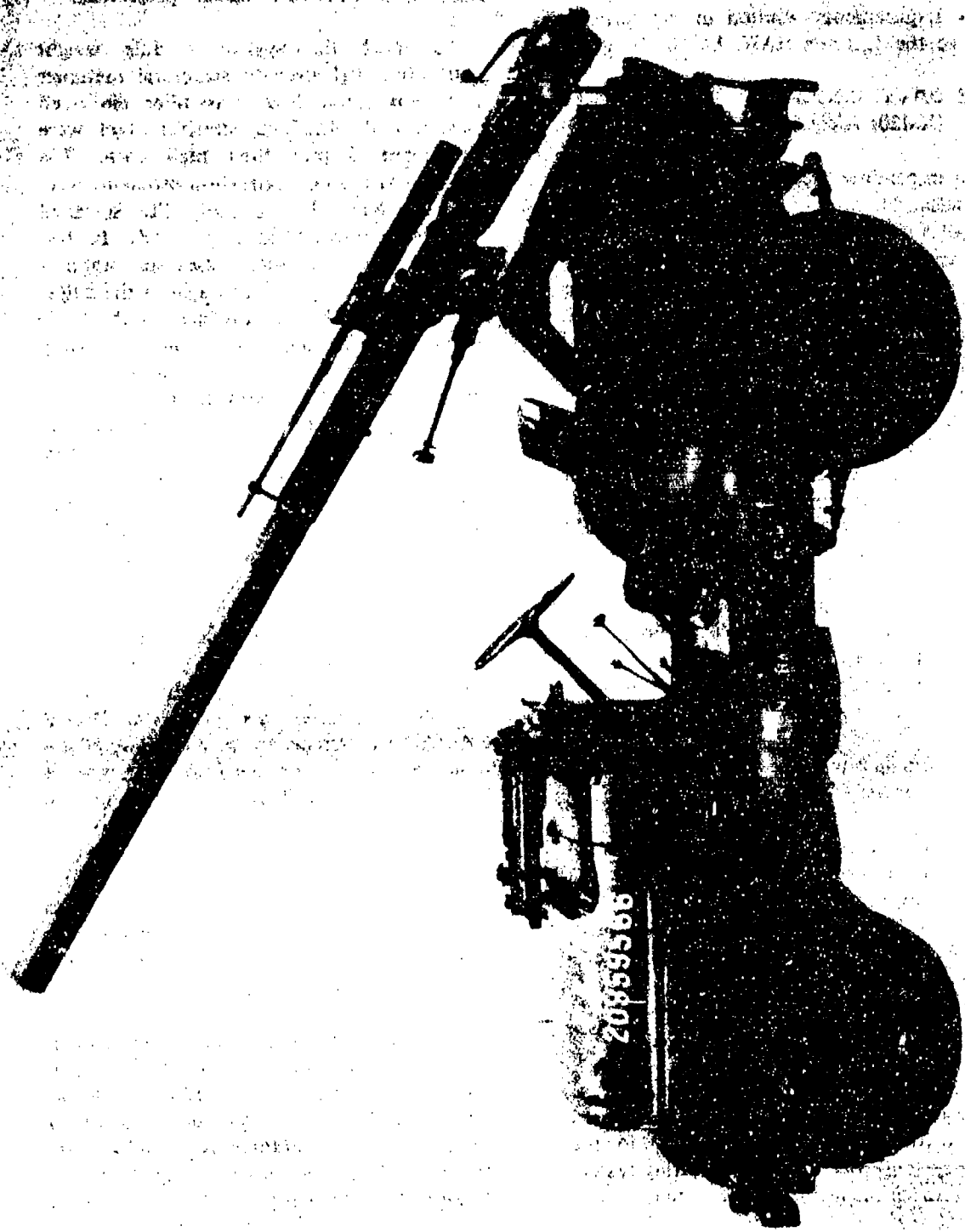


Figure 1-12. 120 mm Rifle, XM105

instead of the desired 200 lb) and the selection of the TOW missile to satisfy the HAW requirements resulted in the termination of the 120 mm HAW, XM105 program.

1-5.2 DAVY CROCKETT 120 mm, XM63 (XM28) AND 155 mm, XM64 (XM29)

An impending break-through in the design of nuclear devices in the mid-1950's led to the idea of a tactical nuclear weapon system—perhaps capable of man-portability over limited distances in difficult terrain. There was growing confidence in the feasibility of developing subkiloton devices lighter in weight, structurally more resistant to acceleration stresses, and more efficient in the use of critical nuclear materials than had been available previously. Based on the estimates available, a lightweight recoilless weapon system concept was synthesized. It was envisioned that such a system capability could have important effects on the structure and deployment of ground forces. The availability of such huge elements of firepower in the hands of foot troops capable of immediate reaction to rich targets of opportunity could provide an advantage of significant proportions.

The principal problems facing the designer were as follows:

1. Design a breakdown system in which each module can be carried over limited distances by an individual soldier.
2. Accommodate the roughly 12-in. diameter warhead.
3. Limit maximum acceleration.
4. Insure high reliability and precision of delivery. The problems that were encountered resulted from the long range (4000 m for the XM29 system) over which the spotting system was to match the major caliber system.
5. Minimize system action time (i.e., the

time required to set up the weapon and mount, insert the cartridge and projectile).

To meet the system module weight limitation, high-strength structural materials such as titanium alloys, glass fiber reinforced plastic, and ultra-high strength steel were considered despite their high costs. The warhead size and acceleration problems were accommodated by adopting the so-called "spigot" configuration (Fig. 1-13). In this scheme, the propulsion gases act upon a "pusher" tube (spigot) throughout the ballistic stroke and the oversize warhead is accelerated via this tube from a starting position in front of the gun muzzle. This avoids the structural problems of a large low pressure gun tube and the interior ballistic reproducibility problems associated with very low operating pressures. High precision of delivery was demanded by the need to insure against injury to friendly troops as well as the requirement to employ the extremely high cost warhead effectively.

The projectile weight, size, velocity, and acceleration limits along with the use of the spigot configuration, allow the use of a smooth bore barrel. Also, since the DAVY CROCKETT systems are very low rate of fire weapons, there is no need for any type of breech mechanism. This leads to the muzzle loading and simple nozzle end configurations of the DAVY CROCKETT weapons. Another unique feature of the DAVY CROCKETT were the lightweight mounts. Weighing less than 20 lb, the mounts had adjustable rear lugs, fine and coarse elevation, and quick collapse for stowage.

The operational requirements for a man-portable system were met with two weapon systems. The 120 mm, XM28 System as shown in Fig. 1-14, was designed for a maximum range of 2000 m. A second system, 155 mm, XM29, as shown in Fig. 1-15, was developed concurrently to provide a 4000-m system capable of field maneuver on a jeep or other light vehicle. The XM29 System is

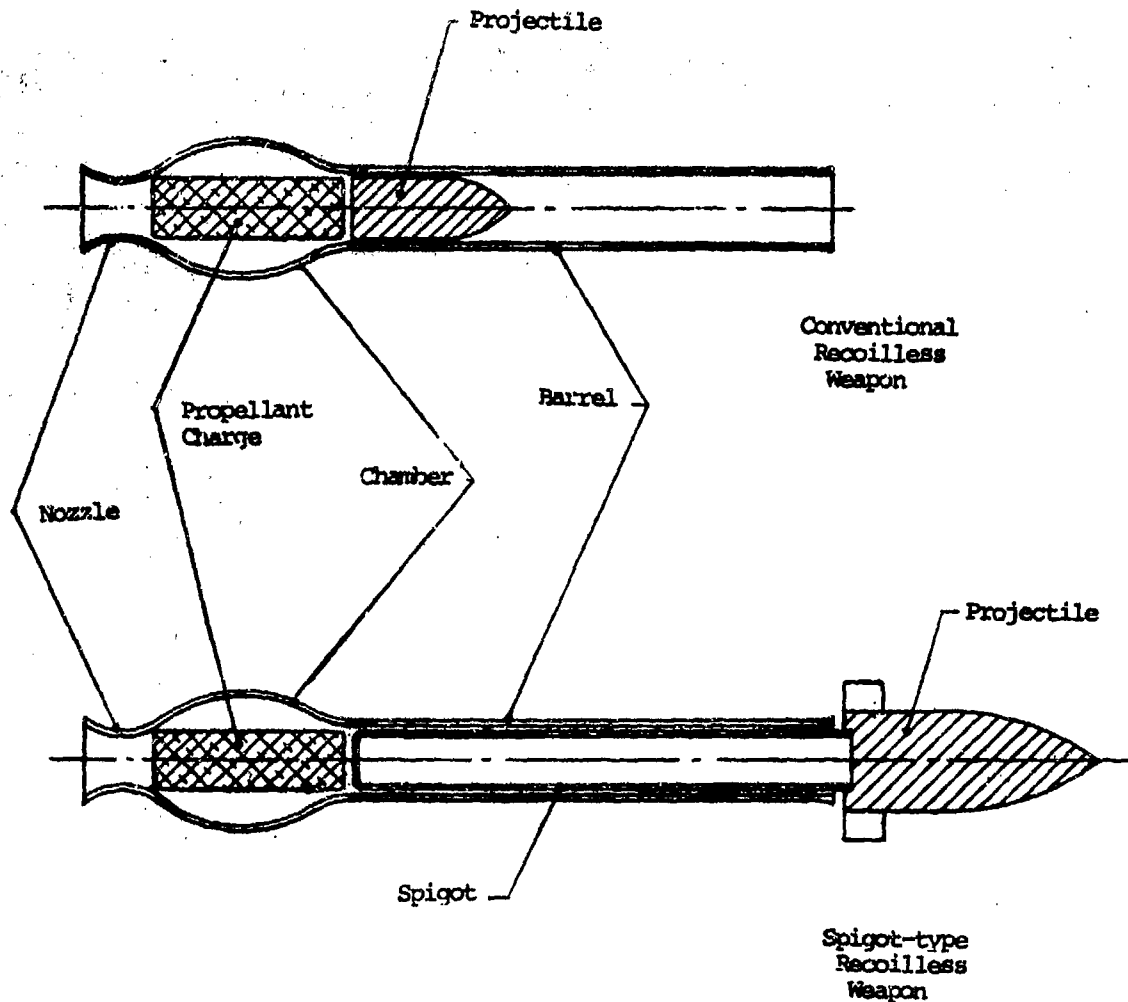


Figure 1-13. Recoilless Weapons—Conventional and Spigot Type

capable of firing from a jeep carrier or it can be displaced by troops and fired from a ground mount.

In the official press release of the DAVY CROCKETT systems by the Army on 4 May 1960, the Secretary of the Army described these systems as a development which "...dwarfs in firepower anything we have ever known in the immediate area of the battle line". He stated that "DAVY CROCKETT will significantly enhance the military posture of the U.S. ground forces. With this

weapon, small combat units will have organic atomic power that they will be able to take with them to any trouble spot in the world in a matter of hours. On the battlefield, the small unit will have within its own ranks, firepower that formerly could be obtained only from heavy artillery". Among the engineering advances achieved were:

1. First titanium gun in US Army
2. Hi-Low spotter cartridge—unprecedented velocity uniformity

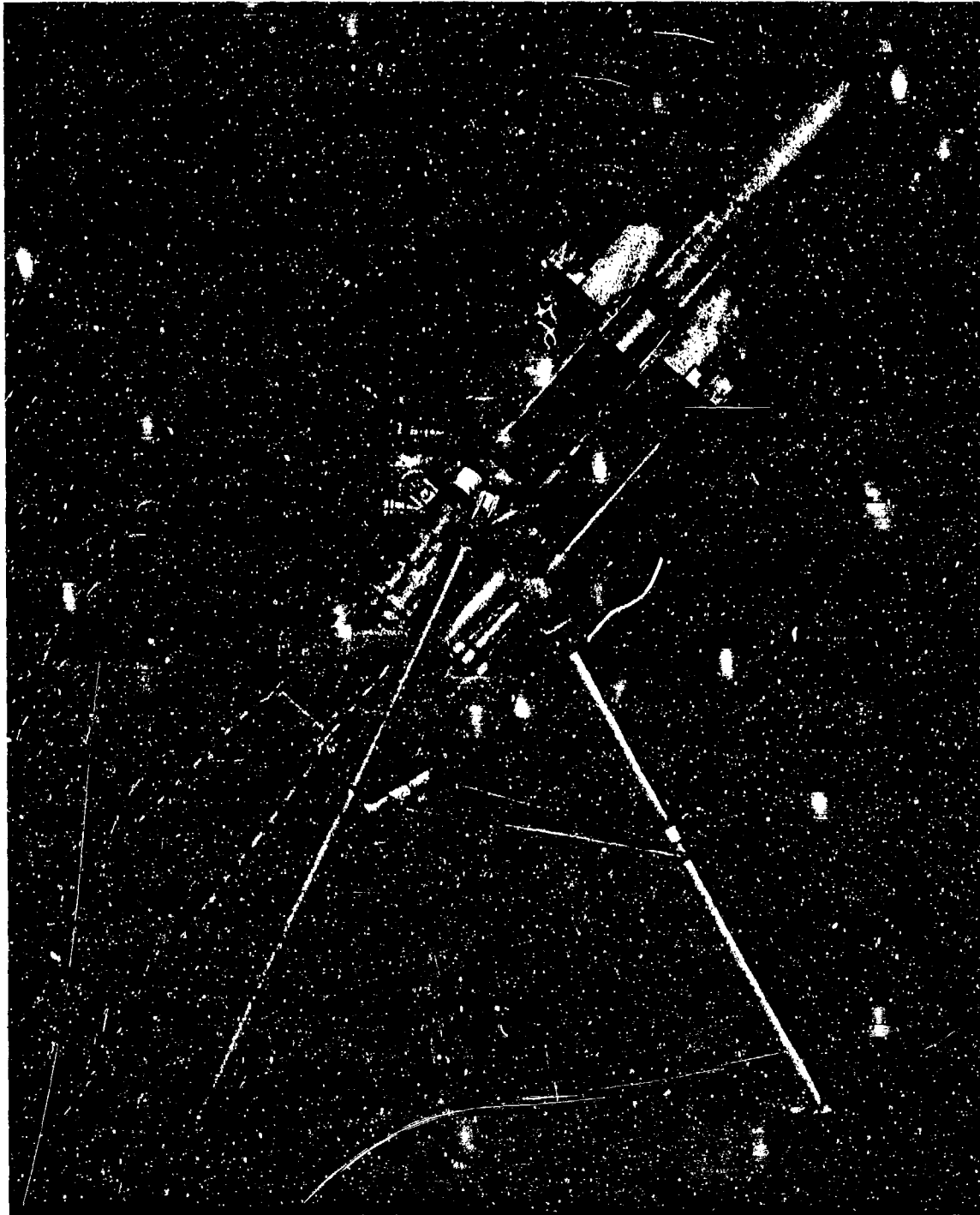


Figure 1-14. DAVY CROCKETT System, XM28, Man-portable, 2000-m Infantry Atomic Weapon



Figure 1-15. DAVY CROCKETT XM29 Weapon System, 4000-m Range

3. PYROCORE primer—improved velocity uniformity

4. Unique spigot delivery—minimum system weight and size

5. First use of D38 (reactor byproduct) in spotter projectile

6. First multizone recoilless system.

The reason which made many of these advances possible was that cost was not as critical a factor, comparatively speaking, as it was in most other recoilless rifle programs. This was true because of the need for the accurate delivery of the rather expensive warhead. As such, the use of high cost materials such as titanium was warranted in the DAVY CROCKETT system and not in others, even though experimental work on titanium, Fiberglas, Fiberglas wound, and glass-metal structures had given good results in PAT, Super-PAT, and other recoilless programs.

1-5.3 DEVELOPMENT OF 8-in. CANNON (EIK)

In 1954-55, the Office, Chief of Ordnance directed Frankford Arsenal to study the feasibility of producing an 8-in. recoilless cannon (EIK) to replace the medium (8-in.) howitzer as the general support in division artillery and as the reinforcing weapon in Corps artillery. Analyses and experimental test firings with a scale model weapon, as reported in Refs. 15 and 16, showed that it was technically feasible to obtain a weapon system capable of air delivery for direct support of infantry, which meets the following requirements:

- | | |
|-------------------|---|
| 1. Maximum Range: | 30,000 yd desired
20,000 yd acceptable |
| 2. Minimum Range: | 3,000 yd desired
10,000 yd acceptable |
| 3. Traverse: | 360 deg desired
120 deg acceptable |

- 4. Elevation: 0 to plus 65 deg
- 5. Carriage: Unarmored and self-propelled
- 6. Ammunition: HE, chemical, optimum fragmentation (240-lb projectile)

Based on these findings, Frankford Arsenal was directed to continue analytical studies and proceed with experimental investigations. Firings were to be performed in both reduced and full scale test guns to verify the interior ballistic predictions, to evaluate experimentally the effects of blast, and to investigate methods of zoning. These tasks were to be done for range requirements of 10,000 and 20,000 yd.

In addition, for the 20,000-yd range weapon, studies were to be made of the mechanical design of the cannon and design concepts prepared illustrating methods of incorporating the cannon into lightweight towed and self-propelled weapon systems. A designation of Cannon, 8-in. Howitzer, Recoilless, T230E1 was assigned to the 10,000-yd weapon and Cannon, 8-in. Howitzer, Recoilless, T230E2 assigned to the 20,000-yd weapon.

Experimental interior ballistic studies were begun with a 75 mm scale model of the 8-in. weapon, since previous studies had shown that a small caliber test weapon could be designed to have ballistic characteristics similar to a large caliber prototype weapon. The technique of "scale model" studies resulted in considerable savings of both time and money, since less effort was expended on the experimental work performed. Empirical data obtained during the scale model studies were used in the design and construction of the full scale, 8-in., 10,000-yd test Cannon, T230E1.

A total of 25 rounds were fired in the 8-in. T230E1 test weapon for charge establish-

ment, interior ballistic design, and general performance. Based on performance results from the scale model and full size test weapons, the 8-in., 20,000-yd test cannon, ignition studies, ballistic assessment, and long range accuracy firings were performed. These studies indicated that the 8-in. recoilless cannon is lighter than conventional closed breech weapons of equivalent range and fire power, and is more accurate than rockets of the same capability. Its corrected round-to-round range dispersion was about 0.3 percent of range. While it was found that the problems associated with blast were no more serious in the EIK than in comparable rockets, it still was felt that the blast of an EIK would have to be reduced.

While firings were being performed with the EIK test cannons, preliminary weapon system concepts were investigated by the Pitman-Dunn Laboratories Group of Frankford Arsenal. These investigations included breech design and concepts of vehicular components and related ground handling equipment for the EIK weapon system. Ref. 24 describes in detail the following weapon concepts: swing breech, jackknife breech, reciprocating-pivoting breech, and spherical chamber weapon. These weapon designs then were studied for their adaptability to several configurations of mounts and vehicle transports. These studies indicated the following weights for the indicated weapon systems (Ref. 24):

8-in. Recoilless Weapon with	Total System Weight, ton	
	10,000-yd	20,000-yd
Towed mount	2	3
Austere self-propelled carriage	4.5	6.5
Armored self-propelled carriage	8	12

These weight figures along with accuracy and fire power data indicated that in the mid-1950's, the 8-in. recoilless cannon represented a reasonable replacement for existing conventional artillery and rockets.

1-5.4 DEVELOPMENT OF SELF-EJECTING BREECH

In June 1952, the Universal Winding Company began work on the design, development, and fabrication of a scale model 105 mm recoilless rifle with a self-ejecting breech mechanism. Following preliminary studies, development proceeded along two separate paths. The first path followed was the continued development of Frankford Arsenal's "blowback" principle breech design. This design used escaping propellant gases to accomplish automatic cocking of the weapon and ejection of the spent cartridge. The blowback breech weapon as designed by Universal Winding used a round with a combustible case and a shouldered steel base. In the base were a series of blowback orifices (vent holes) through which the propellant gases of the fired round were allowed to escape. As the propellant gases escaped through these orifices, they impinged on the firing mechanism hammer, forcing it back to its cocked position so that it is ready for the next firing. The breech of the rifle is fitted with a split ring that springs open to permit chambering of the round. As the firing mechanism is cocked by the escaping propellant gases, a cam on the hammer engages this split ring, forcing it open. The timing of the hammer is such that when the split ring is opened, the pressure in the chamber has dropped to a level where it safely blows out the case base to the rear (Ref. 19).

The second development path investigated the designs of both electrically and mechanically fired drop-out breech designs. In the drop-out breech, a set of latches or a breech bar acts as a retainer for the cartridge base of a combustible round. During the firing, the chamber pressure forces the cartridge base

against the breech bar or latch detents which held the base in place. When the chamber pressure drops, the cartridge base drops harmlessly through an opening in the breech mechanism. At Universal Winding (Ref. 19), it was felt that the blowback breech system appeared to have more promise in recoilless rifles of larger caliber where it would have a weight and compactness advantage over conventional or drop-out type breeches. In lower caliber weapons, the blowback breech would compare well with other breech types in both weight and functioning, but would be somewhat more complex in breech and firing mechanism design.

1-6 RESEARCH PROGRAMS

1-6.1 INTRODUCTION

Except for a short period of time after World War II, Frankford Arsenal was assigned the responsibility for research and development of recoilless rifles. As a part of its effort to broaden the industrial and engineering base during recoilless rifle development, Frankford Arsenal contracted several facilities to perform research work in the refinement of theoretical design concepts and the general improvement of recoilless rifle technologies. Notable among these facilities were A. D. Little, Inc., Armour Research Foundation, Firestone Tire and Rubber Company, Harvey Aluminum, Midwest Research Institute, United Shoe Machinery Corp., and Universal Winding Company.

A description of all the recoilless rifle research is beyond the scope of this handbook, but the major research activities performed by the previously mentioned organizations are presented in the paragraphs that follow. In these programs, direction and technical specifications were given to the contracted organization by Frankford Arsenal, which then assumed a supervisory role throughout the program.

1-6.2 MIDWEST RESEARCH INSTITUTE

1-6.2.1 Gun Temperature

Among the activities performed at Midwest Research Institute (MRI) were various heat transfer studies for several recoilless rifle programs. In connection with these studies, MRI developed a special surface thermocouple capable of measuring the temperature-time variations at the internal surfaces of a recoilless rifle during firing. First used in 1952, to measure the internal surface temperatures of a 57 mm, T15E13 Recoilless Rifle, the thermocouple was improved by the development and incorporation of special high temperature insulation for the probe assembly. With these improvements, the thermocouple was capable of use in applications involving surface temperatures up to 2000°F and was used extensively in temperature-time studies of the internal surfaces of the Rifle, 106 mm, M40 during the ballistic cycle (Ref. 17).

One of the more extensive studies performed at MRI was conducted to determine the permissible firing procedures for the Rifle, 105 mm, T170 (106 mm, M40). The experimental program consisted of heating the T170 Rifle under various firing conditions in order to define the limitations that should be imposed on the T170 Rifle. In all highly stressed weapons, these limitations arise because the gun steel strength decreases with increasing temperature. When fired under adverse conditions, the rifle temperatures approach the level at which the yield strength decreases very rapidly and it is hazardous to fire the weapon (Ref. 1).

Observed internal gas pressure data were used in conjunction with the rifle stress analysis and tensile properties of the weapon material, to determine the maximum possible rifle temperature. A thermodynamic analysis then was made at selected points of the T170 Rifle to predict the rifle temperatures that would result from certain rates of fire at

chosen ambient conditions. Heat transfer to the rifle wall from the propellant gas was determined experimentally by monitoring twelve thermocouples attached to the rifle. The experimental and theoretical works then were compared to establish that the T170 Rifle was safe to fire at an initial burst of twenty-one rounds at an ambient condition of 125°F without regard to rate. It also was shown that the maximum safe rate of repeat firing was 0.75 round per minute at the same ambient condition. These firing procedures were based upon a limiting rifle temperature of 800°F.

1-6.2.2 Sheet Propellant Studies

During the development of the Frankford Arsenal U-BAT Recoilless Rifle, MRI was contracted to evaluate the feasibility of caseless rounds for the U-BAT weapon. Previously, considerable work had been performed at MRI with the use of sheet propellant charges in both fin- and spin-stabilized projectiles. These studies had indicated the feasibility of using sheet propellants as a means of eliminating the cartridge case. In order that no worthwhile technique to eliminate the cartridge case would be overlooked, sheet, granular, stick, and slotted tubular propellants in various combinations were tested in order to find a satisfactory caseless round.

Since the U-BAT rifle and ammunition designs were still in their formative stages during the MRI investigations, it was decided to perform the tests with a modified 105 mm, M27 Rifle using fin-stabilized test slugs. Embossed sheet propellant was used in disk and scroll forms with different combinations of each placed at various positions along the projectile boom. Experimental firings indicated that a ballistic efficiency of 6.54 was attained with the sheet propellant as compared to 6.26 for a granular propellant. Even though the sheet propellant gave a higher ballistic efficiency, it is not possible to say that the sheet propellant web is the most

efficient. It also was found that the sheet propellant rounds indicated no perceptible unburned propellant ejection from the rifle, whereas, in the granular propellant rounds, approximately 15 percent of the propellant charge was ejected unburned. The various projectile designs and the manner in which the propellant was positioned around the projectile in order to form the caseless round are described fully in Ref. 18.

1-6.2.3 Gun Dynamics

Successive recoilless rifle and mount designs were built to higher performance standards, while at the same time, their weight was undergoing considerable reduction. In order to ensure that the mount strength and weapon accuracy are unaffected by the vibrations caused by the recoil forces, it is necessary to determine the magnitude of these forces. As part of its studies on the Rifle, 105 mm, T170 (M40), MRI conducted pendulum-supported firings to determine the weapon recoil force history.

Recoil forces were obtained from acceleration histories of the pendulum-supported weapon as MRI had done previously for the 37, 57, and 75 mm rifles. The acceleration histories are determined by means of an accelerometer that has its output filtered to determine the various modes of vibration. As described in more detail in Ref. 18, the T170 Rifle gave satisfactory recoil force histories.

1-6.2.4 Ignition Studies

As ballistic requirements became more rigorous for the more sophisticated recoilless rifles, it was apparent that ignition system performance was a vital factor in the ballistic cycle. As part of its BAT activities, MRI was authorized to study the ignition process and establish suitable criteria for evaluating recoilless rifle ignition systems. As concluded in Ref. 18, a good ignition system is one which:

1. Ignites the propellant in any air temper-

ature from -65° to $+125^{\circ}$ F without hang-fires or misfires.

2. Ignites the propellant in such a manner that the burning propellant meets all interior ballistic requirements such as:

- a. Consistent projectile muzzle velocities
- b. Smoothness of pressure-time curves
- c. Uniformity of peak pressures
- d. Acceptable rates of initial pressure rise in all parts of the chamber
- e. Consistent projectile ejection time
- f. Minimum breech and muzzle flash and smoke.

3. Meets the general requirements of:

- a. Minimum costs of ammunition
- b. Suitability to mass production without undue safety hazard
- c. Stability in storage over long periods of time under the conditions as prescribed for the propellant
- d. A minimum of corrosive and toxic combustion products.

1-6.2.5 Flash Characteristics

Midwest Research Institute also investigated the breech flash of recoilless rifles with the goal of accomplishing mechanical flash suppression for the 105 mm recoilless rifle. As described in detail in Ref. 20, the research program consisted of firing tests in both vented chambers and a prototype weapon; aerodynamic tests conducted in a gas dynamics facility; and a theoretical investigation of the flash mechanism. As far as the main question of this program, it was found that a mechanical suppressor with reasonable dimensions could not be designed for the 105

mm rifle. However, during the course of the research, the following conclusions were made about the nature of nozzle flash and nozzle flow (Ref. 20):

1. There are several mechanisms by which a secondary flash may be triggered. Shock ignition may occur, or there may be a continuous reaction from the nozzle exits. A further possibility is that ignition may be caused by energy transfers in the boundary layer. Depending on conditions, some or all of these may be active.

2. The peak pressure in the breech is associated with the triggering mechanism. In general, shock ignition will occur for a lower peak pressure, and a continuous reaction from the nozzle exits will occur at a higher peak pressure.

3. The flash mechanism is more complex and more difficult to suppress for a large nozzle (as in the 105 mm rifle) than for a smaller one.

4. In multiple nozzle systems, there may be a strong interaction of individual jets which may trigger the flash.

5. For the smaller nozzles those suppressor configurations that most effectively destroyed the shock structure of the flow did produce the most effective flash suppression.

6. For conical nozzles, the presence of normal shocks depends mainly on the divergence angle. Larger divergence angle increases the possibility of a normal shock.

7. For the unsteady flow, divergence angles of close to 35 deg can be used without flow separation for expansion ratios of up to about 77:1.

1-6.3 ARMOUR RESEARCH FOUNDATION

1-6.3.1 Interior Ballistic Theory

As part of the development of the Battalion Antitank Weapon, Armour Research Foundation was assigned the task to develop, in cooperation with the Frigidaire Division of the General Motors Corporation, a 105 mm front orifice recoilless rifle. In connection with this task, Armour Research Foundation developed the interior ballistic theory for the rifle.

The ballistic cycle of a front orifice is composed of three stages:

1. A conventional closed breech phase during which the projectile initially seals the nozzle entrance ports

2. A transition stage from closed breech to recoilless phase (partial recoil compensation)

3. A recoilless phase in which the nozzle entrance ports are uncovered completely.

As shown in Ref. 28, accurate solution of the three-stage ballistic system would require the application of numerical methods of calculation. For ease of computation and analysis, personnel at Armour Research Foundation devised a method of putting the ballistic equations in closed form. This was accomplished by reducing the 3-stage system to a 2-stage system consisting of (1) a closed breech phase lasting until the projectile uncovers a portion of the total port area equal to one-half the throat area, and then (2) a recoilless phase thereafter with the discharge of propellant gases controlled by the nozzle throat (equivalent to assuming an instantaneous transition from closed breech to

recoilless operation). The interior ballistic equations developed for a 2-stage system also have application to a recoilless rifle with a nozzle start device, such as a blow-out disk (Ref. 4).

During the analysis of the 2-stage system of interior ballistic equations and their application to the 105 mm T135 Rifle, several observations and discoveries were made (Ref. 4):

1. Since the propellant gases initially are confined in the chamber until the nozzle ports are uncovered, the chamber temperature at the beginning of the second stage is approximately equal to the isochoric flame temperature of the propellant.

2. The gas temperature then decreases to 0.6-0.7 of the isochoric flame temperature at "all burnt" depending upon "all burnt" velocity.

3. Through numerical integration of the energy balance and mass balance equations, it was found that the propellant gas temperature may be represented fairly accurately by assuming the average of the square root of the temperature to be linear with projectile velocity.

By use of these findings to simplify the interior ballistic equations and then comparing the solutions to the solutions obtained by assuming a constant value of propellant gas temperature, it was found both calculations were in good agreement with the solutions obtained from numerical methods. On the basis of these results, the simpler form of the interior ballistic equations, based on constant gas temperature, was used to predict, quite accurately, the performance of front orifice recoilless rifles.

1-6.3.2 Propellants

In connection with the development of the interior ballistic equations for recoilless rifles,

Armour Research Foundation examined the application of the interior ballistic theory to recoilless rifles firing inhibited propellants, composite charges, and liquid propellants. In order to indicate the feasibility of inhibiting propellant grains to provide a progressive type of burning, a series of firing and closed bomb tests were performed with M10 and M1 Propellants. These studies (Ref. 25) showed the effects on burning characteristics caused by different conditions of inhibiting and the use of different types of solvents used to carry the inhibitor into the grain.

Interior ballistic equations were developed for recoilless rifles firing a composite charge; i.e., a charge consisting of a mixture of propellant grains of the same composition, but different web sizes and geometric shapes. The use of an exact form function for the composite charge complicates the solution of the interior ballistic equations, and it was found that in many applications that an equivalent charge of a single web size may be substituted.

Because hydrazine-hydrazine nitrate-water propellants exhibit a lower flame temperature, higher impetus, and greater reduction in flash as compared to solid propellants, significant attention was focused on the use of liquid propellants in recoilless rifles. As part of the nozzle erosion program at Armour Research Foundation, the experimental determination of nozzle erosion due to the firing of hydrazine-type liquid propellants was undertaken. Investigations included the establishment of ballistic parameters and the effects of water and nitrate content on the liquid propellant burning rate for both hydrazine and a hydrazine-hydrazine nitrate-water propellant.

1-6.3.3 Expendable Cartridge Case

As part of the development of the Battalion Antitank Weapons, Armour Research Foundation continued its study of combustible cartridge case materials. The

majority of this investigation centered around cellulose nitrate plastic combustible rubber, acrylic plastic, or a paper-base phenolic material. The conclusion of this investigation (Ref. 25) was that certain of the expendable cased rounds showed considerable promise, particularly those with the cellulose nitrate and paper-phenolic cases. The hard rubber and acrylic materials were considered unworthy of further investigations.

It was established fairly well that perforating the expendable cartridge case has very little effect on the fragment size, but probably has deleterious effects upon the interior ballistic performance. Scoring, or other methods of setting up stress concentrations in the outer surface of the case, proved to be inadequate and of little use. The best results were achieved with heavier wall, paper-phenolic, solid frangible cases.

The cellulose nitrate cases under study were of a convolute structure, formed by rolling a cellulose nitrate sheet to a case diameter, with cement between the convoluted sheets to hold the roll together. As such, the variables for an individual case construction were the sheet thickness and the amount of area to which cement was applied. Ballistic test data indicate that higher muzzle velocities are achieved with cases having a greater cemented area, due to the strengthening of the case, and thus, better ignition, during the initial burning stages. Also, ballistic and piezometric efficiencies were higher when using a thicker sheet of cellulose nitrate.

1-6.3.4 Nozzle Studies

Armour Research Foundation, as part of the 105 mm Battalion Antitank Weapon development, conducted extensive investigations into nozzle performance and nozzle erosion. These investigations included both analytical studies and experimental observations of the phenomena associated with propellant gas flow through a recoilless rifle nozzle and are described fully in Ref. 29.

One of the experimental nozzle studies was the qualitative verification of the nozzle flash theory of re-ignition. This theory supposes that the gases at the nozzle exit are cooled by rapid expansion, thus halting radiation. A subsequent recompression, resulting from oblique interrupting shocks and Mach reinforcement, then reheats the gases and causes further radiation. By high-speed motion pictures of the nozzle flash from 105 mm and 2.75-in. recoilless rifles, it was shown that nozzle flash phenomena do perform according to the re-ignition theory.

Since the nozzle characteristics are an important consideration in the design of a recoilless rifle, the variation of nozzle thrust with the nozzle characteristics was studied in depth by the Armour Research Foundation. The nozzle characteristics examined were expansion angle, expansion ratio, throat area, and approach area. The significant results from these experimental studies (Ref. 25) are:

1. Expansion angles less than 45 deg give essentially the same thrust, while with angles greater than 45 deg, there is a significant decrease in thrust.
2. Thrust unbalance calculated from steady-state isentropic flow theory is in good agreement with experimental thrust data.
3. The percentage change in thrust unbalance is approximately 0.8 of the percentage change in throat area.
4. The 57 mm Rifle, M18 was fired with various internal chamber configurations and nozzle approach areas to study their effect on recoilless rifle operation. It was found that, in general, as the rearward taper of the chamber contours is changed from positive to negative (positive taper indicating a larger diameter at the rear of the chamber), the rifle becomes unbalanced increasingly rearward if the chamber volume and nozzle configurations are kept constant.

Because a bore-size straight-pipe nozzle has the advantage of simplicity and ease of fabrication over a conventional converging-diverging type of nozzle, both the interior- and exterior-mounted straight pipe nozzles were investigated by Armour Research Foundation for possible use in recoilless rifles. On the basis of the experimental data, a bore-size perforated-pipe would give negligible unbalance while exhibiting reasonable ballistic performance. However, the use of a bore-size perforated-pipe nozzle has certain drawbacks. As the result of higher solid propellant loss through the nozzle, the ballistic efficiency of a recoilless rifle is lowered by the use of a bore-size nozzle. In addition, the lateral gas spray through the perforations in the pipe causes a hazard to personnel in the immediate region normal to the rifle axis at the breech end of the weapon.

Other studies conducted at Armour Research Foundation included nozzle erosion studies with M10, T18, and T25 Propellants and hydrazine and hydrazine-hydrazine nitrate-water liquid propellants. Besides determining the erosion rates caused by these propellants at different firing rates, these nozzle studies included the investigation of recoil compensating devices for nozzle erosion. Various recoil compensating devices were tested in 75 mm scale-model and 106 mm Rifle, T170E1 firings. The results of these studies are described in detail in Ref. 25.

1-6.3.5 Stress Analysis

Because of the everpresent emphasis on weight resolution and the incidence of case rupture and bulging in some recoilless rifles, Armour Research Foundation, as a part of its general investigation of cartridge cases, conducted stress analysis of perforated metal cases. As a first step of the stress analysis, it was assumed that a pressure differential exists between the inside of the cartridge case and the chamber. Furthermore, at some time during the firing cycle, the excess internal

pressure becomes large enough to cause a case failure. For purposes of the analysis, the pressure differential was regarded as an equivalent internal pressure resulting from propellant burning or the mechanical compression of the propellant grains caused by bursting of the igniter.

Considering the previous remarks, the perforated cartridge case design problem consisted of first analyzing the static problem of a thin perforated cylindrical shell subjected to uniform pressure with or without end constraints. The overall problem was approached from three directions, namely (Ref. 4):

1. Yield stress calculations for a perforated cylindrical shell subjected only to internal pressure
2. Elastic stress and displacement calculations for the cylindrical shell subjected only to internal pressure
3. Bending stress calculations for the perforated cylindrical shell with internal pressure and built-in ends.

The yield stress calculations are elementary and useful as a guide to design limits, but give no information about the effects of bending. In analyzing problems (2) and (3), an approximate method was adopted from which useful information could be obtained. This method proceeds along the lines of elementary strength of materials, replacing the perforated shell by a nonperforated one having equivalent elastic constants that are different for dilation and bending. This approximate method is outlined fully in par. 11-17.5. In application to the 57 mm perforated cartridge case, it was found that the approximate method gave slightly overdesigned results, however, it was believed that the results obtained by this method were still useful, especially if properly correlated with experimental observations (Ref. 4).

Other stress analysis investigations conducted by Armour Research Foundation were experimental and theoretical analyses of the 106 mm Rifle, T170E1 and 75 mm Rifle, M20. Operational stress levels and margins of safety were determined for these operations as described in Ref. 25.

1-6.4 FIRESTONE TIRE AND RUBBER COMPANY

1-6.4.1 Aerodynamics

As part of its projectile development for the 105 mm BAT weapon system, Firestone performed aerodynamic studies on the T138 slow-spin Projectile (MOBY DICK) prior to undergoing any extensive test firing program (Ref. 21). Through the use of wind tunnel tests at Aberdeen Proving Ground, Firestone was able to define various weaknesses in the T138 Projectile design so that the necessary corrective actions and appropriate types of test firings could be made. In the development of the T119 Projectile, in-flight photography and extensive wind tunnel experiments formed the basis for choosing a fin-sweepback angle of 65 deg. Since the T171 MOBY DICK-type projectile appeared to be very promising, several aerodynamic studies of various tail and nose configurations of the T171 Projectile were performed. These studies indicated that a 6-finned tail with a tee nose provided better aerodynamic stability than either egg-cup tailed or finned egg-cup tailed projectiles with smooth noses.

1-6.4.2 Fuze Studies

During initial design studies of the HEAT round being developed by Firestone for the BAT weapon system, it was concluded that the fuzes used in the HEAT rounds for the Rifle, 105 mm, M27 were not sufficiently quick-acting. A quick-acting fuze is required for the HEAT round because of the sensitivity of shaped charges to standoff. As a result, Firestone investigated the performance of various types of fuzes in the HEAT rounds it

was developing. Among the different types of fuzes investigated were the magneto fuze developed by the Stewart Warner Corporation, the push-button method or electric fuze developed by the National Bureau of Standards, the spit-back fuze extensively studied by the Ballistic Research Laboratories, electronic controlled fuzes, and inertia fuzes. The fuze eventually decided upon for the standardized HEAT round for the BAT weapon system was of the single action.

1-6.5 UNIVERSAL WINDING COMPANY

In June 1952, the Universal Winding Company of Providence, Rhode Island was given a contract to design, develop, and fabricate a scale model of a 105 mm recoilless rifle with a self-ejecting breech mechanism as previously described in par. 1-5.4. Carried on concurrently with this program were a number of investigations of recoilless weapon systems that were adaptable or applicable to the self-ejecting breech design. As described in Ref. 19, these investigations included central nozzle designs of which two systems—the replacing nozzle system and the gas balanced system—were thought to be the most promising. The investigation into the central nozzle concept led to the study of side-firing mechanisms. One type of firing mechanism studied was a circumferential primer that extended around the base of the round.

Under this general program, Universal Winding also designed and manufactured test fixtures for lining 57 mm and 105 mm recoilless rifle cartridge cases. A final task of the program called for an investigation into the design of a semiautomatic recoilless rifle. Development of a side-loading, magazine-fed, blow-back operated, repeating recoilless rifle was carried through 50 percent completion of a test model when work on this particular weapon was discontinued.

As a part of the development of large caliber recoilless rifles, Universal Winding studied the possible alternatives to the

"jackknife" breech system proposed by Frankford Arsenal. Based on one of the suggested breech designs, Universal Winding prepared and submitted a proposal for a complete large caliber rifle system. No further efforts were performed in this area because work on the large caliber recoilless rifles was terminated shortly thereafter.

1-6.6 A. D. LITTLE, INC.

Having compiled an extensive bibliography on recoilless rifle development and shaped charge ammunition, A. D. Little, Inc. was used extensively as a resource for historical and background information as well as in advisory capacities during many of the recoilless rifle development programs. While A. D. Little performed some work in investigating possible solutions to the BAT requirements, a great portion of its recoilless rifle work was performed during its development of the lightweight Rifle, 90 mm, T149 for use as a platoon antitank (PAT) weapon.

During the development of the T149 Rifle, considerable amounts of research were performed in the areas of central nozzle design, rifle chamber contours, cartridge case and liner designs, rocket-assisted and supersonic-launched projectiles, and flash suppression. Some of the specific outcomes of this work were the development of a unique cam-ring breech design, as described in par. 10-22 for the T149 Rifle; the discovery that central nozzles with divergence angles in excess of 40 deg could be used with substantial reduction in nozzle length and consequently, nozzle weight; and the establishment of the need for still a better cartridge liner material than nitrocellulose and polyethylene-coated Kraft paper that had been two of more widely used liner materials.

1-6.7 HARVEY ALUMINUM (HARVEY MACHINE COMPANY)

As early as October 1951, the Harvey Machine Company was performing compre-

hensive studies on the overall problem of an automatic recoilless rifle. Initial studies of the 57 mm rifle indicated that the advantages of semiautomatic operation would be more apparent in a large caliber weapon. Accordingly, the 105 mm recoilless rifle was selected for further development by several organizations in 1952. Ref. 22 serves as an extensive record of the ordnance experience and information obtained by Harvey Machine Company in the development of its own semiautomatic rifle.

Other research performed by the Harvey Machine Company included the investigation of lightweight alloys for application to large caliber recoilless rifles and mounts, and the development of an inexpensive, single-shot, throw-away minor caliber spotting device. Ballistically similar to a cal .50 spotting rifle and ammunition, this spotting device consisted of an integral barrel and chamber combination of very light weight material with provisions for attachment to the major caliber rifle by a clip-on device. The principal achievements made in conjunction with this task were the perfection of tooling and press forming techniques for fabricating the barrel, chamber, and rifling from a single aluminum alloy bar slug; thus eliminating all the customary machining performed on rifled barrels and cartridge cases. These techniques for low cost mass production of precision press-formed riflings in high strength aluminum alloys were considered to be applicable to larger or smaller caliber weapons.

The last major work performed by the then named Harvey Aluminum Company for the recoilless rifle programs was performed in 1958-1962 in connection with the development of the DAVY CROCKETT weapon system. Some of the major achievements resulting from research activities on this program (Ref. 23) were the demonstration that:

1. Titanium was suitable as a recoilless rifle material.

2. Available coatings for titanium nozzles were not satisfactory in erosion resistance.

3. Fiberglas, although a very capable material, did not offer sufficient promise over competitive materials to warrant the extensive development effort that would have been required to prove its suitability in the DAVY CROCKETT application.

1-6.8 CARDE

The Canadian Armament Research and Development Establishment (CARDE) was responsible for several significant contributions to recoilless rifle program. During the BAT program, CARDE was responsible for developing the process for embossing sheet propellant. Sheet propellant is embossed to provide the necessary space for gas flow between adjacent layers of the sheet propellant. Along with its work in the area of sheet propellants, CARDE developed a new type of primer. The CARDE type, high pressure, controlled-venting, hot gas primer employing sheet propellant showed much promise. As a result, similar CARDE type primers were developed by other organizations for use in the BAT weapon system. Other CARDE activities centered around various analyses of existing recoilless weapons and feasibility studies of a medium antitank recoilless rifle.

1-6.9 FRANKLIN INSTITUTE

The Franklin Institute Laboratories for Research and Development made two major contributions to the recoilless weapon program. The first contribution was made in

1948-49 and consisted essentially of collecting all available literature associated with recoilless weapons, reviewing the literature, and compiling selected material in several volumes of which Refs. 1 and 3 are a part. The material was compiled into six volumes. Volumes I, II, and III provide a history of development and the basic principles of recoilless weapons. Volumes IV, V, and VI of the series on recoilless weapons contain descriptive material on recoilless weapons that were developed or were under development at the time of writing in the United States and abroad. This material was in the form of reports and data which described recoilless weapons from a mechanical and a ballistic standpoint.

The second major contribution by Franklin Institute was the preparation of quarterly progress reports on recoilless rifle systems, ammunition, and related items that were being developed at Frankford Arsenal or under the technical supervision of Frankford Arsenal. The purposes of these reports were fourfold:

1. To review local progress and effect coordination as required
2. To serve as a repository for pertinent classified data
3. To permit the transmittal of many classified items in composite form
4. To maintain a backlog of data on these projects so that the accumulation of these progress reports would facilitate the preparation of the final development reports.

REFERENCES

1. *Recoilless Weapons, Volume I, The Recoilless Principle, A Symposium*, Contract No.'s W-36-034-ORD-7652 and -7708, Franklin Institute, May 15, 1948.
2. René R. Studler and W. J. Kroeger, *Battalion Antitank Recoilless Rifles System*, Report No. R1273, Pitman-Dunn Laboratories, Frankford Arsenal, July 1953.
3. *Recoilless Weapons, Volume IV, Description of Weapons*, Contract No.'s W-36-034-ORD-7652 and -7708, Franklin Institute May 15, 1949.
4. *Symposium on Recent Progress of Recoilless Rifles and Ammunition*, Held at Midwest Research Institute, Sponsored by Department of Army, 11-13 January 1954.
5. W. P. Leeper, *Ammunition for 2.75-inch Recoilless Rifle for Aircraft Installation*, Report No. 1376, Frankford Arsenal, June 1957.
6. C. Walton Musser, Edward R. Barber, George Schechter and P. J. Wilds, *Strain Compensated Barrels*, Report No. R-1008, Pitman-Dunn Laboratories, Frankford Arsenal, May 1951.
7. J. E. Copeland and P. J. Wilds, *Development and Manufacture of Cartridge T115E2 for the 57 mm Recoilless Rifle T66E2*, Report No. R-1007, Pitman-Dunn Laboratories, Frankford Arsenal, May 1951.
8. G. S. Bluford, F. W. Dietch and F. J. Shinaly, *Rifle 57 mm T66E2*, Report No. R-1096, Pitman-Dunn Laboratories, Frankford Arsenal, August 1952.
9. G. S. Bluford, *Rifle 57 mm T66 and T66E1*, Report No. R-1011, Pitman-Dunn Laboratories, Frankford Arsenal, May 1951.
10. *Development of the 90 mm Rifle T149*, Interim Technical Report, Contract No. DA-19-020-ORD-40, Arthur D. Little, Inc., June 1, 1955.
11. *Recoilless Rifle Systems, Ammunition and Related Items*, Status Report No. 1, Vol. IV, Report No. R-1316, Frankford Arsenal, 1 January through 31 March 1956.
12. *Recoilless Rifle Systems, Ammunition and Related Items*, Status Report No. 3, Vol. III, Report No. R-1282, Frankford Arsenal, 1 July through 30 September 1955.
13. *Recoilless Rifle Systems, Ammunition and Related Items*, Status Report No. 2, Vol. II, Report No. R-1238, Frankford Arsenal, 1 April through 30 June 1954.
14. *Development of 120 mm Recoilless Heavy Antitank Weapon System (HAW)*, Final Report, Technical Memorandum M64, Frankford Arsenal, 1 April 1959 through 30 June 1962.
15. A. E. Clark, et al., *Feasibility Study of a Large Caliber Recoilless Rifle*, Report No. R-1247A, Pitman-Dunn Laboratories, Frankford Arsenal, March 1955.
16. G. Schechter and L. W. Insetta, *Large Caliber Recoilless Cannon (EIK)*, Report No. R-1345, Pitman-Dunn Laboratories, Frankford Arsenal, March 1956.
17. *Heating of the T170 Rifle Under Various Firing Conditions*, Phase Report No. 1, Contract No. DA-23-072-ORD-637, Midwest Research Institute, December 1953.
18. *Investigation in Connection with Battalion Antitank Recoilless Rifles*, Final Report, Contract No. DA-23-072-ORD-900, Midwest Research Institute, November 1955.

19. *Research and Development of Recoilless Weapons*, Final Report, Contract No. DA-19-020-ORD-1848, Universal Winding Co., 28 February 1957.
20. *Research on Basic Studies of Flash Characteristics of Recoilless Weapons*, Final Report, Contract No. DA-23-072-ORD-762, Midwest Research Institute, 30 September 1955.
21. *105 mm Battalion Antitank Project*, First Progress Report, Contract No. DA-33-019-ORD-33, Firestone Tire & Rubber Company, August 1950.
22. *106 mm Semi-Automatic Recoilless Rifle*, Summary Report No. HMC-1009, Contract No. DA1-04-495-507-ORD-(P)-14, Harvey Machine Company, 18 June 1957.
23. *Study Re Battle Group Systems*, Final Summary Report No. HA-1862, Contract No. DA-04-495-507-ORD-1283, Harvey Engineering Laboratories, Harvey Aluminum, 15 June 1962.
24. R. T. Fillman and D. E. Walters, *Large Caliber Recoilless Cannon (EIK)*, Report No. R-1533, Pitman-Dunn Laboratories, Frankford Arsenal, March 1960.
25. *Battalion Antitank Weapons*, Final Report, Contract No. DA-11-022-ORD-1157, Armour Research Foundation, 15 December 1955.
26. *Recoilless Rifle Technical Information Index (1944-1958)*, Publication Bulletin PB8, Frankford Arsenal, September 1959.
27. *Recoilless Rifle Technical Information Index (1958-1962)*, Publication Bulletin PB8, Supplement 11, Frankford Arsenal, 1962.
28. Samuel Levin and R. G. Wilson, Jr., *Development of 105 mm Battalion Antitank Weapons and Interim Ballistics for the Design of Recoilless Rifles*, Summary Report, Vol. II, Front Orifice, Armour Research Foundation, Project No. L034, 1 July 1954.
29. Ramon L. Olson and A. D. Kafadar, *Nozzle Erosion Studies*, Final Report, Armour Research Foundation, Project 90-812L, December 20, 1951.

CHAPTER 2

SYSTEM DESIGN AND INTEGRATION

2-0 LIST OF SYMBOLS

A	= bore area, in ²	g	= acceleration due to gravity, ft-sec ⁻²
A_t	= nozzle throat area, in ²	I	= impulse, lb-sec
B	= effective burning rate constant, in.-(sec-psi) ⁻¹	K	= nozzle coefficient, sec ⁻¹
C_d	= discharge coefficient of nozzle, dimensionless	K	= $\left[\frac{\gamma g}{F} \left(\frac{2}{\gamma+1} \right)^{\frac{\gamma+1}{\gamma-1}} \right]^{1/2}$, sec ⁻¹
C_i	= initial propellant charge, lb	L_m	= travel of projectile to muzzle, in.
C_s	= total weight of unburned propellant ejected, lb	L_p	= travel of projectile when peak chamber pressure occurs, in.
C_2	= propellant charge burned in rifle, $C_2 = C_i - C_s$, lb	M	= weight of projectile, lb
c_p	= specific heat at constant pressure (ft-lb)-(lb-°R) ⁻¹	m	= mass of projectile, slug
c_v	= specific heat at constant volume, (ft-lb)-(lb-°R) ⁻¹	m'	= effective mass of projectile
E	= energy, ft-lb		= $1.04 \left[m + \frac{(1-\lambda) C_i}{\delta g} \right]$, slug
e	= 2.7182818... base of natural logarithms	N_o	= weight of propellant burnt at projectile start, lb
F	= propellant impetus, (ft-lb)-lb ⁻¹	P_b	= space mean pressure at time charge is all-burnt, psi
f	= safety factory, $f = \sigma_y / \sigma_t > 1$, dimensionless	P_c	= chamber pressure, psi
$f(\lambda, V_m) = \psi'_m k F / (A/A_t)$, dimensionless	P_e	= exit pressure at nozzle, psi
		P_m	= space mean pressure when projectile is at muzzle, psi

P_F	= maximum pressure, psi	α	= $C_{11}/(\rho v_c)$, dimensionless
P_t	= pressure at nozzle throat, psi	γ	= ratio of specific heats, $\gamma = c_p/c_v$, dimensionless
R_2	= gun tube radius, in.		
r'	= $C_2/(\rho A)$	δ	= $(\epsilon - \alpha)/(1 - \alpha)$, dimensionless
V_b	= velocity of projectile at all-burnt, fps	Δ_0	= initial solid propellant loading density, $27.7 C_{11}/v_c$, g-cm^{-3}
V_m	= muzzle velocity of projectile, fps	ϵ	= expansion ratio, $\frac{\text{Total Gun Volume}}{\text{Chamber Volume}}$, dimensionless
V_p	= velocity of projectile at peak chamber pressure, fps	λ	= $kA_1 W_0 / (C_2 B)$, dimensionless
v_c	= chamber volume of rifle, in^3	ρ	= density of propellant, lb-in^{-3}
W_m	= density of metal, lb-ft^{-3}	ρ'	= density of gun material, lb-in^{-3}
W_0	= initial web thickness of propellant grains, in.	σ	= allowable tensile strength of the material, psi
W_r	= weight of bare rifle, lb	σ_y	= stress on rifle tube in y -direction, psi
W_s	= density of steel, lb	σ_t	= tangential stress on rifle tube, psi
w_m	= wall thickness corresponding to pressure at muzzle, in.	ψ'_b	= value of ψ' for $V = V_b$, $(\text{fps})^{-1}$
w_p	= wall thickness corresponding to peak pressure, in.	ψ'_m	= value of ψ' for $V = V_m$, $(\text{fps})^{-1}$
x_m	= effective length of rifle such that Ax_m is the total volume of rifle, (i.e., $Ax_m = v_c + AL_m$), in.	ψ'_o	= value of ψ' for $V = 0$, $(\text{fps})^{-1}$
x_o	= effective length of chamber such that $Ax_o = v_c$, in.	ψ'_p	= $\frac{1}{2} \psi'_o + \left[\left(\frac{\psi'_o}{2} \right)^2 + \left(\frac{\psi'_b - \psi'_o}{V_b} \right) \right]$, $(\text{fps})^{-1}$
x_p	= $x_o + L_p$, in.		

SECTION I

INTRODUCTION

2-1 SCOPE

This chapter describes the logic, technique, and philosophy of integrating a new recoilless weapon system—of “putting it all together” so that the end product serves the customer’s needs and improves the overall defense posture. It treats, more quantitatively and in more explicit detail than does Chapter 1, the definitions of subsystems and components and the design trade-off opportunities available throughout the engineering interval.

Stress is laid on the criticality of the early trade-off analyses when this is possible. The selections among basic alternatives—such as warhead type, projectile stabilization mode, combustible versus frangible versus metal cartridge case, expanded versus bore-size chamber, spigot versus bore-size projectile and the like—become more and more irreversible as the investments of dollars and time grow. Escape from these is often costly in both material terms and professional pain. Sometimes, of course, they are inescapable and either the project is terminated or the defects in the end product haunt you. Insofar as they are instructive, some specific case histories, failures as well as successes, are outlined.

Emphasis is placed on the advantages of the integrated system approach. The continuing tendencies toward specialization in modern technology can lead to compartmentalization and tends to yield a system with incompatible interfaces. For example, a seemingly simple bracket for attaching the telescope sight to the gun tube will not be compatible with the gun tube, if the sight bracket designer did not consider the dynamic elastic behavior of the tube under ballistic stress. Such pitfalls are

illuminated in this chapter and means to avoid them (that have succeeded in the past) are described.

2-2 DEFINITION OF TERMS

To define is (by definition) one of the most arbitrary intellectual activities of man. Nevertheless, the “labels” by which we designate things and the meanings of these labels are indispensable tools for our efficient functioning, especially where engineering endeavors are concerned.

Following is a list of specialized terms used frequently in recoilless weapon system design. These definitions are included here since they are not found in the volume of *Ordnance Technical Terminology* (Ref. 1). All the other terminology not defined herein is fully described in Ref. 1 and is not repeated in this handbook. The asterisked (*) definitions represent an updating of the term as it applies to recoilless weapons rather than the definition given in Ref. 1.

1. Blowout (or rupture) disc: Deliberate obstruction to gas flow to nozzle, designed to be removed by internal pressure of a predetermined level
2. Bore area: Cross-sectional area of gun tube (within lands)
3. Case liner: The membrane covering case perforations to retain granular propellant and exclude moisture
4. Chamber volume: Volume available for propellant gases between projectile in rest position and plane of nozzle throat

5. Gun expansion ratio: Ratio of total gun volume available for propellant gases at instant of projectile exit to the chamber volume

6. Loading density*: Ratio of charge weight to chamber volume

7. Nozzle*: Duct through which a portion of the propellant gases are directed rearward to balance the momentum of the forward moving projectile, thus creating a zero recoil condition in the weapon

8. Nozzle entrance area: Cross-sectional area in upstream portion of nozzle where convergence begins

9. Nozzle erosion: Loss of material from nozzle interface as a result of being exposed to exhausting propellant gases

10. Nozzle exit (or mouth) area: Cross-sectional area at downstream extremity of nozzle.

11. Nozzle expansion angle: Included half-angle of nozzle expansion cone

12. Nozzle expansion ratio: Ratio of exit to throat areas

13. Nozzle throat area: Smallest cross-sectional area of nozzle

14. Perforated case: Metal cartridge case similar in general form to conventional cases but with sidewall multiperforated for propellant gas emission

15. Piezometric efficiency: Ratio of average to peak pressure (Ref. 2, p. 2-29)

16. Projectile travel: Distance from rear of obturator (rotating band), when seated in forcing cone, to end of tube

17. Propellant constants: Chemical composition and physical dimensions of solid granular propellant

18. Propellant force or impetus: Thermochemical energy available per unit weight of propellant

2-3 GENERAL PRINCIPLES OF OPERATION

A recoilless (open-breech) gun, like a closed-breech gun, is essentially a single cylinder heat engine that "loses its piston" (projectile) with each cycle. However, unlike the traditional gun—which transmits the recoil to the earth through a system of slides, hydraulic-mechanical devices, and supporting structures—the recoilless gun counterbalances the recoil force with the thrust of a "rocket motor". This "rocket motor" shares the gases generated in the gun chamber; some of the gases propel the projectile and some are discharged through the recoil balancing nozzle. About 3-4 times more propellant is needed in the recoilless system to do this, as compared to closed breech guns. Also, the "rocket motor" shares the gun structure of the chamber, breech, and nozzle. Schematically, one can visualize the recoilless system as shown in Fig. 2-1.

If this concept as portrayed in Fig. 2-1 were reduced to practice, the following difficulties and inefficiencies could be predicted:

1. Simultaneous ignition of the two propellant charges would be difficult to assure, as would precise congruity of the pressure versus time functions in the two chambers. Large transient unbalanced axial forces would result.

2. Pressure loads on the "fictitious partition" would be considerable both as a function of ballistic time and physical position. This structure and its supporting chamber wall, consequently, would have to be designed to withstand the maximum of such transient loads, adding substantial weight to the gun.

3. Dual ignition systems, dual propellant

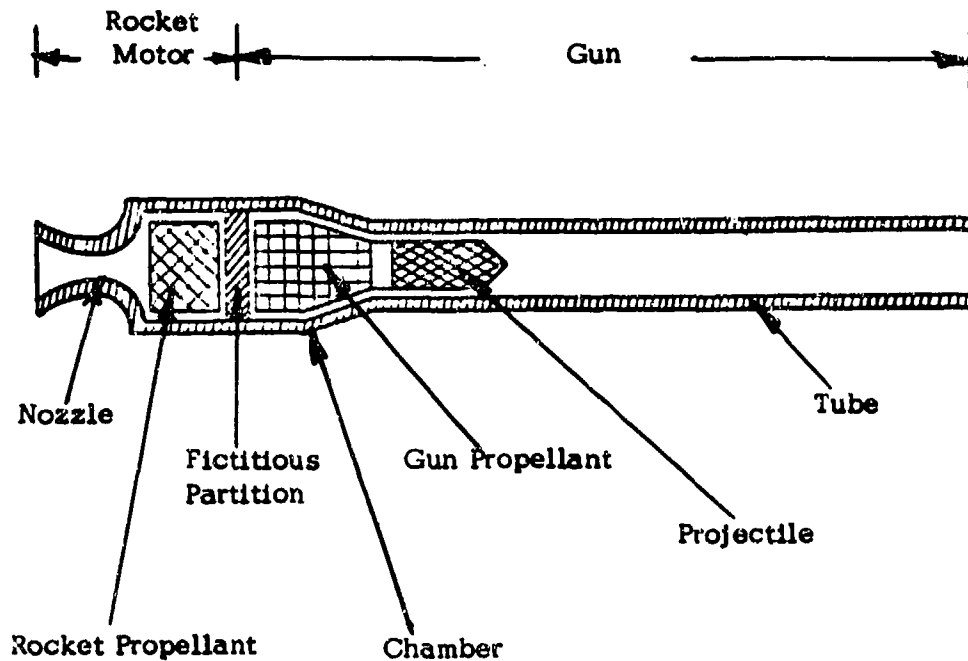


Figure 2-1. Schematic Functional Diagram Showing a Gun Back-to-back With a Rocket Motor To Achieve Recoillessness

charges, and separate loading mechanisms would be required. All of these difficulties and inefficiencies are eliminated by the basic design that has been adopted—the basic design shown schematically in Fig. 2-2 eliminates the partition and shares the propellant gases and structures for both the formation of the recoil balancing jet and for pushing the projectile.

The application of the momentum balancing principle has been made possible and further refined through such developments as the perforated cartridge case, kidney-shaped nozzle, nozzle cant for spin compensation, and others which are described more fully in *Part Three, Design*, of this handbook. It is the application of this principle that yields a lighter weight system which does not penalize accuracy, but has the disadvantages of higher propellant weight, rearward blast with its operating hazards, and intense visual and auditory signatures.

The fundamental principles governing the gas flow through the recoilless gun nozzle and the formation of the jet are similar to those of a rocket and are illustrated in Fig. 2-3. The high pressure P_c of the gases generated in the combustion chamber accelerates the projectile by applying pressure P_b to its base as in conventional guns. Some of the gases move in the opposite direction, converging through the nozzle entrance and accelerating to local sonic velocity at about half chamber pressure P_t in the nozzle throat. In the expansion cone, the gases continue to accelerate into the supersonic region and the pressure continues to drop. At the nozzle exit, the gases transit from the region of constrained expansion to free expansion, provided the expansion angle has prevented flow separation and the expanded gases are still above ambient pressure.

Since the gas is highly turbulent in the

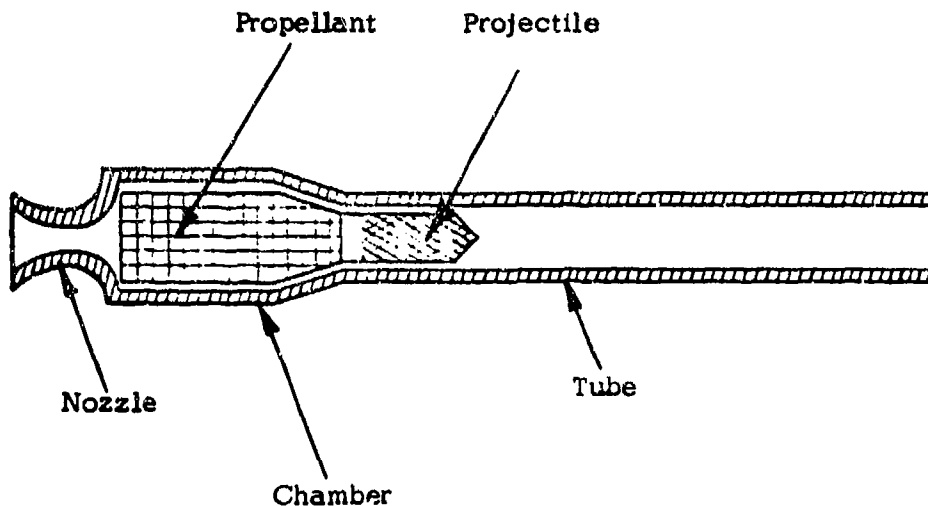


Figure 2-2. Schematic Recoilless Gun

combustion chamber and the chamber pressure is a rapid transient (of the order of 10 msec), it would be erroneous to visualize the flow conditions as laminar and steady-state. Nevertheless, the steady-state laws describe the phenomena adequately for gun design purposes, and the more comprehensible picture of steady-state laminar flow is useful (and more comfortable), provided that one realizes this is an idealization. The general "rules" of basic nozzle design are given briefly in Section III of this chapter and detailed engineering design guidance is given in Chapter 6, "Cancellation of Recoil".

Beyond the nozzle exit is a large region of free expansion and turbulent mixture of the emitted products with ambient air. The gases enter this region at high velocity (about 6000

fps); they contain large volumes of intermediate products of combustion and significant quantities of unburnt solid propellant; and the area is criss-crossed with shock waves, some of them very strong shocks in the locations just downstream of the nozzle exit. Secondary combustion occurs, producing the characteristic large flash, blast, and smoke phenomena. It also is noted that for a given muzzle energy, the muzzle blast from a recoilless gun is no more than that of a closed breech gun. The danger zone created by the gases exiting from the nozzle is conical in shape with its apex at the nozzle. As shown in Fig. 2-4, the danger zone for the 120 mm HAW Weapon is approximately 130 ft deep and 150 ft wide at its base (Ref. 3). For a weapon as large as the 8-in. recoilless cannon, the cone is approximately 400 ft deep and 500 ft wide at its base (Ref. 4).

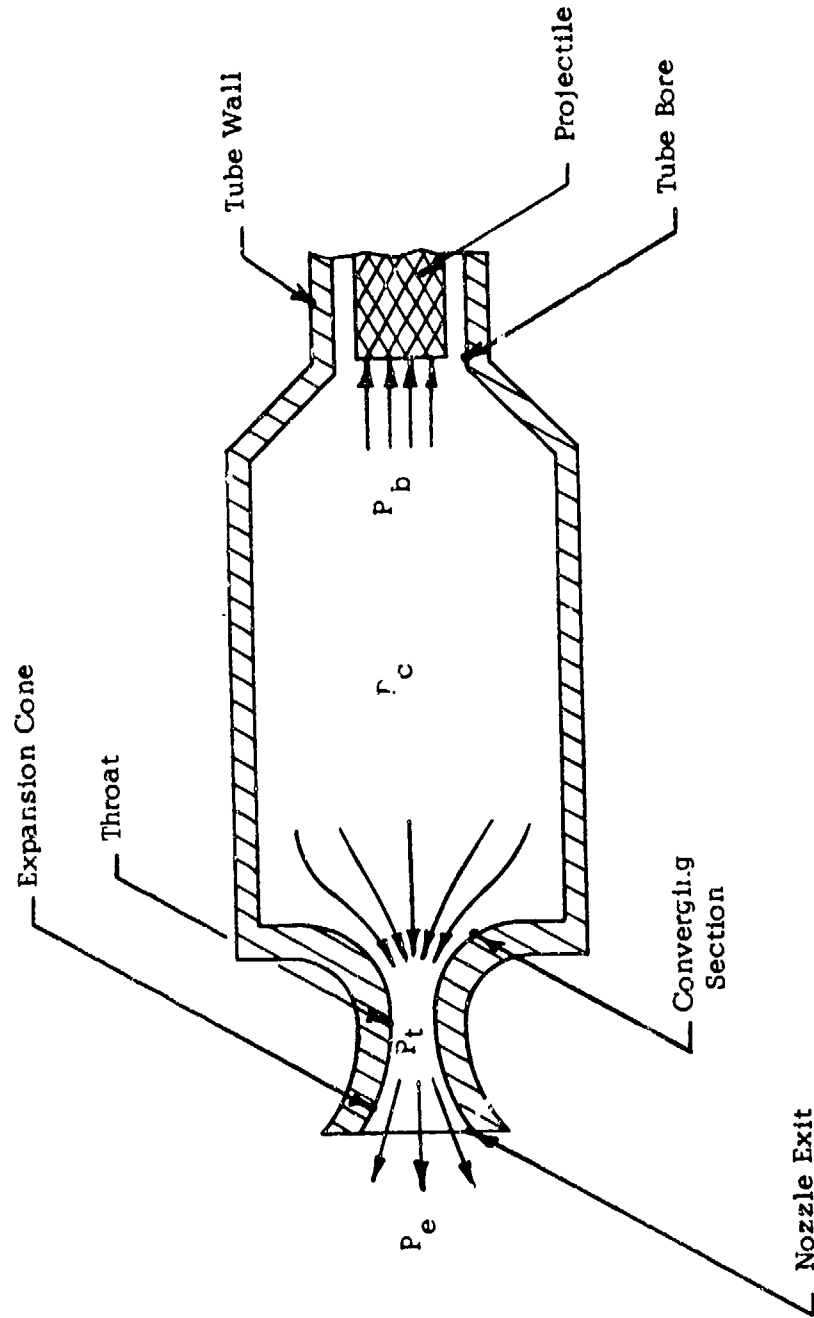
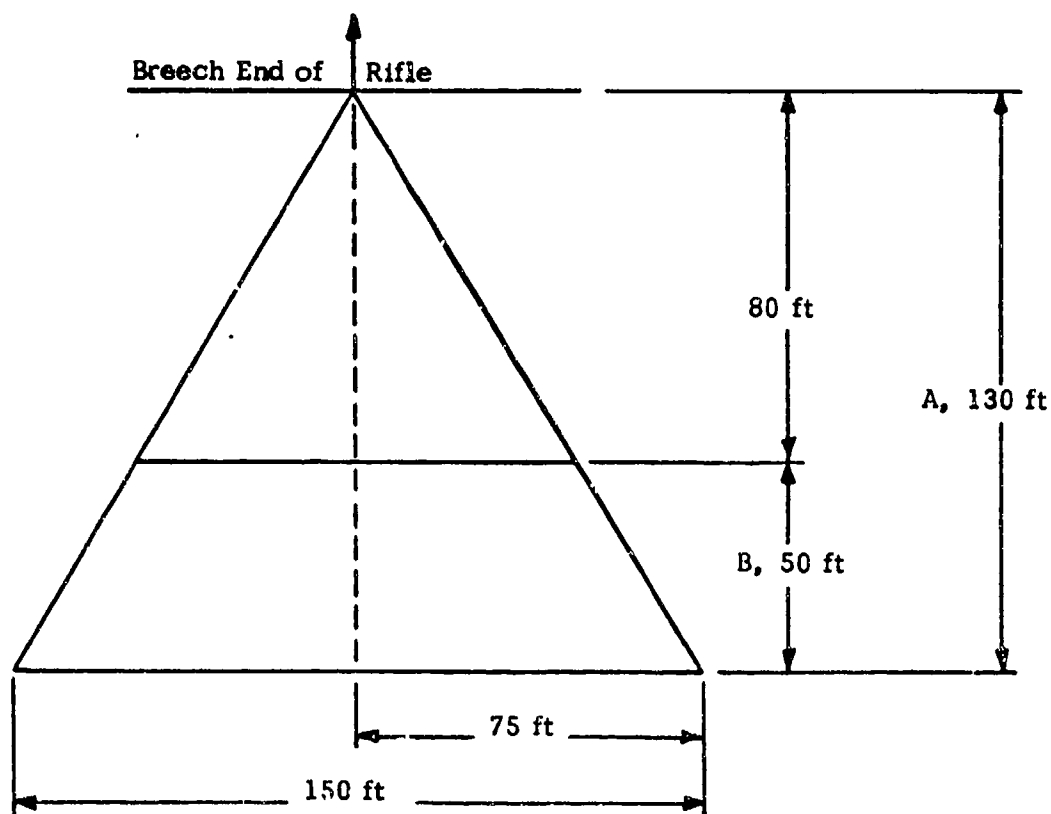


Figure 2-3. Gas Flow in the Chamber and Nozzle



A - Rear Danger Area Due to Blast and Flying Particles

B - Area Considered Safe for Personnel Facing to Rear

Figure 2-4. Rear Blast Danger Area of Rifle, 120 mm, XM105

SECTION II

SYSTEM REQUIREMENTS

2-4 GENERAL

It is possible to outline the various input requirements of the recoilless weapon system in order to see how they relate to the basic design output—weapon system weight. Fig. 2-5 is a block diagram showing these system requirement relations. As seen at the top of this diagram, the basic input requirement to the weapon system is the kill probability for a particular target and specified range.

As shown in Fig. 2-5, the kill probability requirement, in turn, places certain requirements on the hit probability and fire power of the weapon being designed. As these requirements are traced further through the system, it is found that all components of the rifle are affected. The result of this interaction is a system weight for a given terminal ballistic requirement. The remaining paragraphs of Section II more fully describe these requirements and how the problem they create is solved by determining the design parameters that minimize weapon weight.

2-5 REQUIRED MUZZLE ENERGY

2-5.1 KILL PROBABILITY (See Chapter 7)

As stated in Chapter 7, single shot kill probability is defined as the product of hit probability and the conditional probability of a kill given a hit. From the definition of target vulnerable area, conditional kill probability can be expressed as the ratio of the vulnerable area to presented area. From Fig. 2-5, kill probability is shown to be dependent on the type of target and the type of gun-ammunition-fire control combination used in attempting to defeat the target.

2-5.2 HIT PROBABILITY (See Chapter 7)

Hit probability is defined as the probability of a hit or hits on a target occurring out of a given number of rounds fired at the target. For a specified target and weapon system, the hit probability then depends only on the overall weapon dispersions. The principal sources of these dispersions or firing errors are range estimation, aiming, muzzle velocity variation, system jump and cant, crosswind, and the fire control equipment. Weapon system design, production control, and operator training attempt to minimize the random errors contributed by the weapon system and the gun crew. During weapon system design, it is possible to minimize the effects of the nonrandom errors. However, this effort will not be made possible without making some trade-off with the weapon system weight.

One method of increasing the first round hit probability is to increase the muzzle velocity of the projectile. A high muzzle velocity minimizes such errors as range estimation and crosswind, but is achieved by increasing the gun tube length or increasing the chamber pressure—both of which result in an increase in the weapon weight. A sophisticated fire control system could also increase the hit probability, but again, a significant penalty is paid by the additional weight to the weapon. In the last recoilless weapon systems developed (BAT, MAW, HAW, DAVY CROCKETT), it was found that the use of a spotting rifle or spotting pistol presented the most favorable compromise between increased hit probability and increased weight.

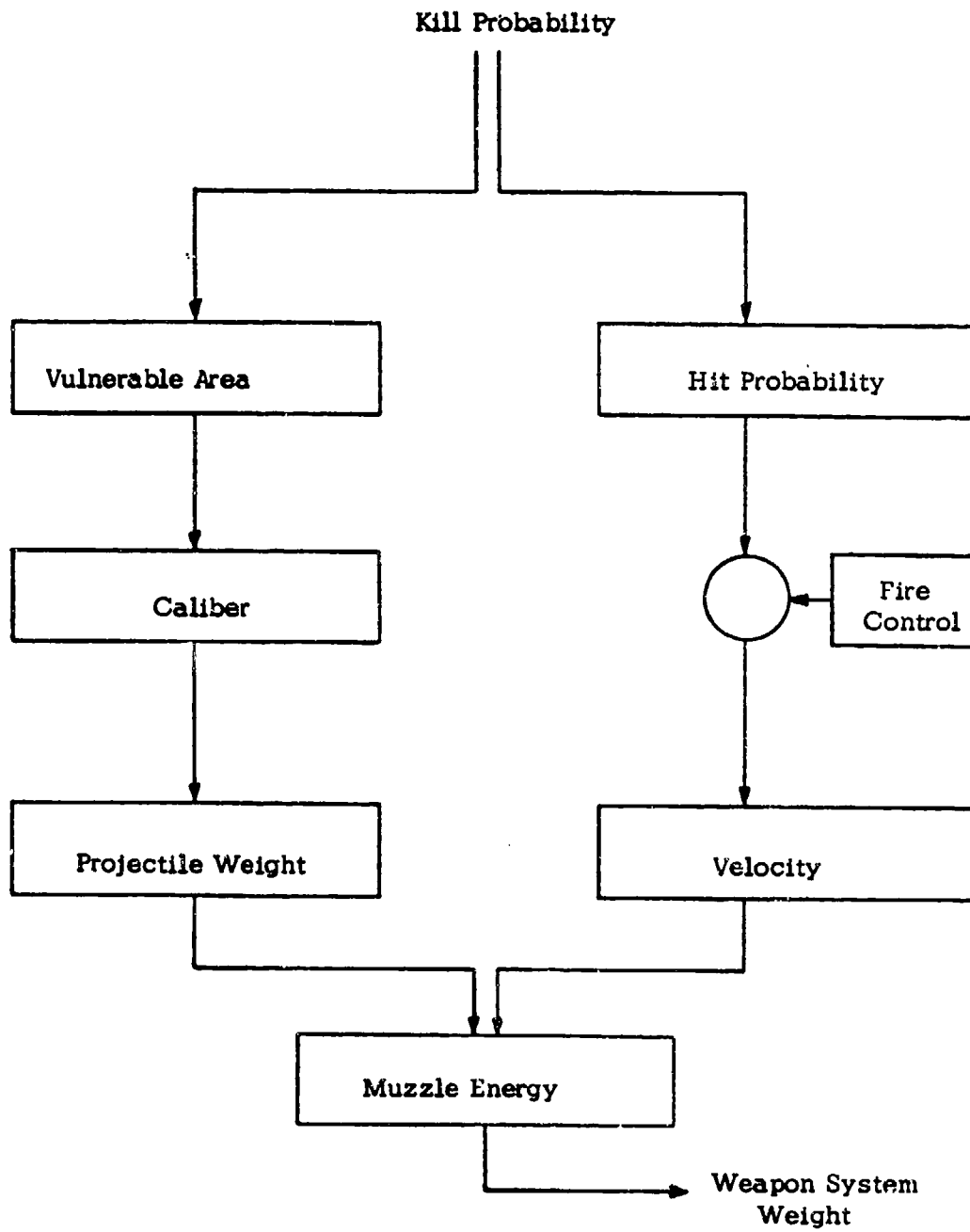


Figure 2-5. System Requirements

SECTION III

DETERMINATION OF BALLISTIC PARAMETERS*

2-7 DETERMINE THROAT AREA

In Chapter 6, it is stated that for the open breech weapon to be recoilless, a certain ratio of bore-to-throat area is required for a given nozzle expansion ratio. From a ballistic and nozzle efficiency viewpoint, it is desirable to use a large expansion ratio nozzle since this permits the use of a small throat area, which acts as a deterrent to the loss of solid unburned propellant. Secondly, the use of a large expansion ratio results in a smaller portion of the propellant charge being used to balance the projectile momentum; i.e., a smaller amount of the propellant gases, expanded to a higher nozzle exit velocity, achieves the same necessary balancing momentum that would be attained by using more of the propellant gas but expanded to a lower velocity. As a result, it would be possible to conserve a significant portion of the propellant charge with a large expansion ratio nozzle.

There is, however, a penalty that arises from using a large expansion ratio nozzle and it is in the form of additional weight to the weapon. Compared to a low expansion ratio nozzle, the large expansion ratio nozzle is larger in actual space required and is proportionately heavier, the greater the expansion.

In the appendix of Ref. 5, it is indicated that nozzle expansion ratios of 1.79 to 3.50 have been used in the various recoilless rifles that have been designed and tested. The specific nozzle expansion ratio to be used will depend upon the type of nozzle employed in the weapon and the compromises that are made between efficiency and weight. For example, in a central nozzle weapon, it is possible to maintain a high expansion ratio,

*See Chapter 5.

with its significant weight decrease, by increasing the divergence angle of the nozzle. A loss in efficiency results, but the weight savings from increasing the divergence angle to as high as 45 deg (Ref. 6) can be significant. Thus, the designer must decide what compromise between weight and efficiency maximizes the weapon system effectiveness. In past recoilless rifle designs, nozzle expansion ratios of 2.0-2.5 have been the most widely used and seem to indicate that they represent the best compromise between efficiency and weight. For the nozzle expansion ratio of approximately 2.0, it is found that the bore area to nozzle throat area ratio should be 1.45, thus determining the nozzle throat area.

2-8 DETERMINE GUN AND PROPELLANT REQUIREMENTS

The previous paragraphs have described how the initial values of the bore and nozzle throat area, projectile weight, and the muzzle velocity are chosen. In Chapter 5, the system of interior ballistic equations is shown not to be readily solved until certain additional variables are determined. These variables are the peak chamber pressure, propellant charge weight, and the propellant wcb. With a specific choice of these quantities, it then is possible to determine the chamber volume and barrel length of the rifle.

The most desirable rifle is, of course, one that is both light and short. Since a light rifle corresponds to a low peak pressure while a short rifle requires a high peak pressure, a compromise between peak pressure and the rifle size will have to be made. In order to make the optimum compromise between peak pressure and gun volume, it is necessary to determine the relation between peak pressure and gun volume. For a given peak pressure,

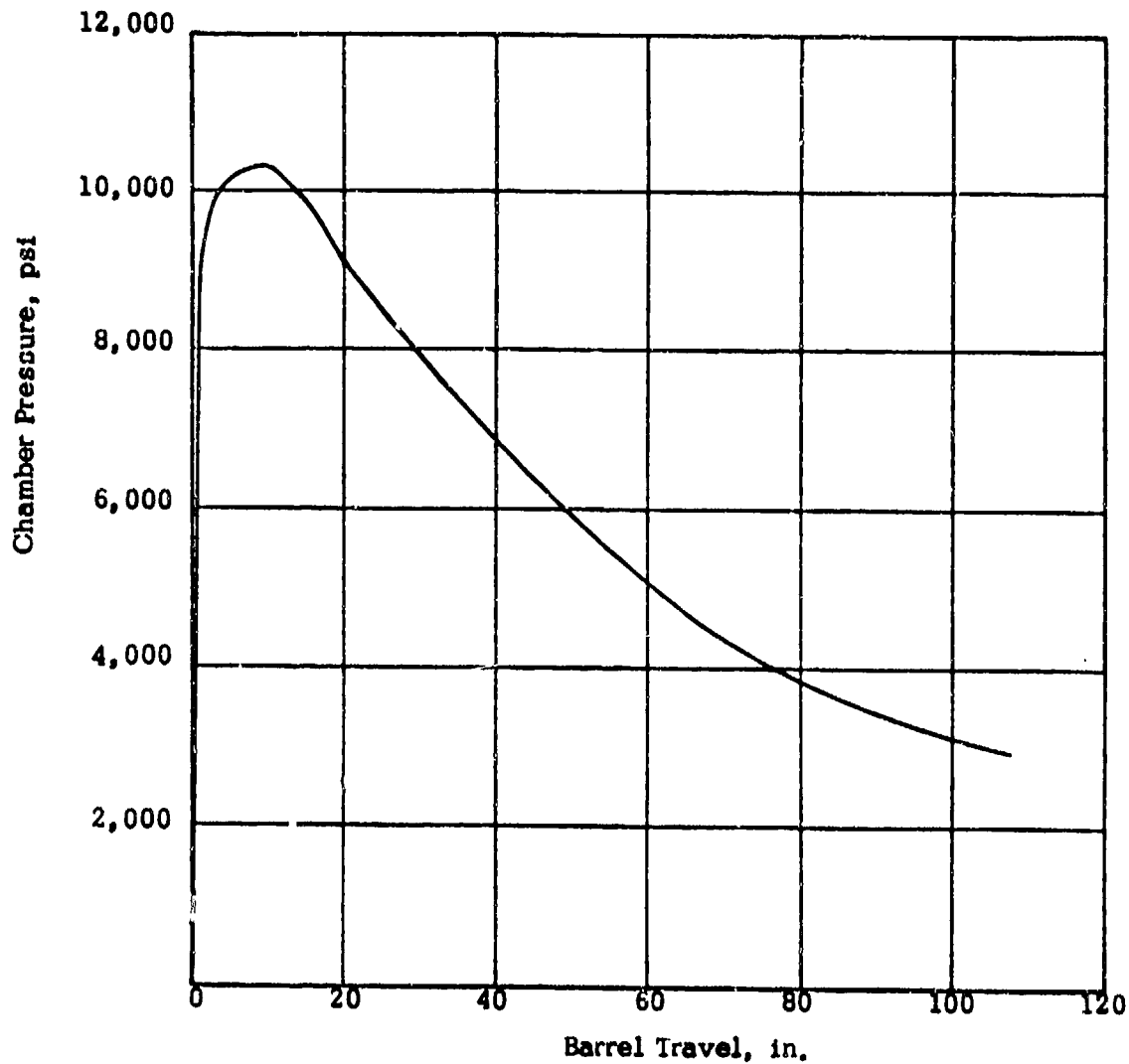


Figure 2-8. Pressure vs Travel 120 mm HAW Recoilless Rifle

however, there is an infinite number of gun volumes corresponding to different choices of charge weight and web size. The designer's problem then is to determine the minimum gun volume for a given peak pressure.

Section V of Chapter 5 shows that it is possible to integrate the system of interior ballistics equations if an average gas temperature is used in place of the instantaneous gas temperature. For a given set of ballistic

parameters, it is possible to use this method of solving the interior ballistic equations and determine the pressure-travel and velocity-travel curves. As an example, Fig. 2-8 shows the pressure-travel curve initially calculated for the 120 mm HAW weapon. Since the bore area is specified, there is a required area under the pressure-travel curve for which the work done by the propellant gases in accelerating the projectile is equal to the desired muzzle energy. By varying the values of the gun and propellant parameters, it would be possible to

generate an infinite number of differently shaped pressure-travel curves for which the desired muzzle energy is attained. Since each of these curves corresponds to a different set of parameters, the task of evaluating one system versus another would be extremely difficult.

Since the weapon weight is primarily a function of the gun volume and peak pressure, it would be desirable to select a peak pressure and then determine the ballistic parameters that result in the minimum weight gun. Section VI of Chapter 5 describes a method that gives this desired result. For a given peak pressure and value of the dimensionless parameter, $\lambda = kA_0 W_0 / (C_2 B)$, it is shown how to use solutions of the simplified interior ballistic equations of Section V of Chapter 5 and be able to calculate the weapon weight. By choosing appropriate values of λ , it is possible to generate a family of curves showing the weapon weight as a function of λ for various peak pressures. However, Section VI of Chapter 5 indicates that there is only one optimum value of λ which satisfies the minimum weight condition and outlines how this value of λ is determined.

For the optimum value of λ , a curve of weapon weight versus peak pressure is obtained. The design that gives the lightest weapon then is chosen—provided that the peak pressure is not so high that it would induce excessive erosion or blast and the corresponding propellant loading density is practical. The optimum value of λ determines the propellant charge and the other propellant parameters. With this information, it is possible to calculate the value of the propellant loading density Δ_0 . For recoilless rifles to be efficient, as described in Section II of Chapter 5, it is necessary that the value of the loading density be about 0.6 g-cm^{-3} . Values above 0.6 tend to give highly peaked pressure-travel curves resulting in low piezometric efficiency and exacting a penalty in

gun weight. Values below 0.6 tend to increase the gun volume and weight.

It should be noted that the minimum weight rifle solution does not specify completely the final parameters of the recoilless weapon system. What it does is specify a small range of peak pressures for the optimum value of λ which leads to the minimum weight gun. Then, it is possible to perform the calculations outlined in Section V of Chapter 5 for the limited range of peak pressures and the optimum value of λ to determine the complete set of weapon system parameters. Through this procedure, the designer has gone from evaluating an infinite number of possible combinations of weapon parameters, to evaluating the solutions obtained from 2 or 3 different peak pressures.

2-9 VERIFY CALCULATIONS WITH TEST WEAPON

Once the specific gun and propellant parameters have been determined, it has been general practice to construct a full scale test weapon in order to verify these theoretically established values. The test weapon is designed with the same ballistic characteristics as the proposed weapon and is equipped with a very simplified configuration of the breech design. In the design of very large caliber recoilless weapon, the 8 in. recoilless cannon being a prime example, a possible intermediate step would be the construction of a scale model test weapon in which preliminary test firings are performed. The use of the scale model test weapon greatly eases the transition from theory to full scale weapon testing while achieving significant savings of both time and money.

Experimental firings of the test weapon are conducted with projectiles cut from cylindrical steel slugs. The propellant charge is contained in a cardboard tube, which serves as the cartridge case, and is positioned in the chamber behind the projectile. Ignition of the round is performed through the use of an

electrical type squib or detonator.

Initial firings are performed to establish the composition and quantity of the propellant charge required to attain the desired peak pressure and muzzle velocity. The exact value of the nozzle throat, and entrance and exit areas are established at this time so that the specified recoil cancellation is attained. Once the charge establishment, interior ballistic design, and general performance requirements have been met, the test weapon is used for ignition studies, ballistic assessment, and accuracy firings.

2-10 COMPLETE DESIGN OF GUN, ROUND, AND ANCILLARY EQUIPMENT

As the design, development, and manufacture of a recoilless rifle weapon system are beyond the expertise of any single organization, it is the responsibility of the developing

agency to coordinate separate developments of the various components of the weapon system. It is necessary to coordinate the design and development of such gun components as the mount and such ancillary equipment as the spotting rifle in order to ensure that these parts have met their respective requirements. Since these components are not integrated into the system until prototype units are made, it is important that the component requirements be compatible.

Part Three of this handbook deals with the design of the components that make up a recoilless rifle weapon system. Chapters 10 through 13 indicate both the considerations to be made in designing the rifle, ammunition, mount, and fire control device, respectively, and how the component design affects or is affected by the design or performance of the other components. Only in light of the design and performance of the other components will the principal components integrate to produce the desired product.

SECTION IV

NUMERICAL EXAMPLE.

The numerical example that follows is based on the procedures outlined in par. 5-20 of Chapter 5 for determining the peak pressure to be used for obtaining the minimum weight gun. The calculations are performed using requirements for the 120 mm HAW Weapon System. Explanation of the various parameters are contained in Chapter 5.

1. Given Constants:

a. P.ellant:

$$1/\rho = 17.09 \text{ in.}^3\text{-lb.}^{-1}$$

$$k = 6.46 \times 10^{-3} \text{ sec}^{-1}$$

$$F = 3.3 \times 10^5 \text{ (ft-lb)-lb}^{-1}$$

b. Weapon System:

$$A = 17.393 \text{ in.}^2$$

$$A_t = 11.911 \text{ in.}^2$$

$$A/A_t = 1.437$$

$$M = 18.1 \text{ lb}$$

$$V_m = 1810 \text{ fps}$$

$$\rho' = 0.3 \text{ lb/in.}^3$$

$$\sigma = 160,000 \text{ psi}$$

$$R_2 = 2.35 \text{ in.}$$

2. Chosen Constant: $P_p = 10,000 \text{ psi}$

3. Assumptions:

$$a. V_b = V_m$$

$$b. N_o = 0$$

4. Solution:

$$\psi'_m = 2/V_m \text{ (fps)}^{-1} \text{ for minimum weight gun (Eq. 5-64)}$$

$$= \frac{2}{1810} = 1.104 \times 10^{-3} \text{ (fps)}^{-1}$$

$$f(V_m, \lambda) = \psi'_m kF/(A/A_t), \text{ dimensionless}$$

$$= \frac{(1.104 \times 10^{-3})(6.46 \times 10^{-3})(3.3 \times 10^5)}{1.46}$$

$$= 1.638$$

From Fig. 5-18 for $f = 1.638$,

$$\lambda = 0.53$$

Estimate Value of C_f

$$C_{est} = 9.60 \text{ lb}$$

$$m = \frac{M}{g} = \frac{18.1}{32.2} = 0.562 \text{ slug}$$

$$m' = 1.04 \left[m + \frac{(1-\lambda)C_f}{3g} \right], \text{ slug}$$

$$= 1.04 \left[0.562 + \frac{(1-0.53)(9.60)}{3(32.2)} \right]$$

$$= 0.63 \text{ slug}$$

From Fig. 5-17 for $P_p = 10,000 \text{ psi}$

$$B = 6.40 \times 10^{-4} \text{ in.-(psi-sec)}^{-1}$$

$$W_o = m'BV_m/A, \text{ in.}$$

$$= \frac{(0.63)(6.40 \times 10^{-4})(1810)}{17.393}$$

$$= 0.042 \text{ in.}$$

$$C_2 = kA_t W_o / (\lambda B), \text{ lb (from definition of } \lambda)$$

$$= \frac{(6.46 \times 10^{-3})(11.911)(0.042)}{(0.53)(6.40 \times 10^{-3})}$$

$$= 9.53 \text{ lb}$$

From Fig. 5-19 for $\psi'_m = 1.104 \times 10^{-3}$
(fps)⁻¹

$$\psi'_p = 1.0 \times 10^{-3} \text{ (fps)}^{-1}$$

For minimum weight gun

$$x_m = \frac{12 m' \exp(\psi'_m V_m)}{P_p A (\psi'_p)^2 e} + r', \text{ in. (Eq. 5-62)}$$

where

$$r' = C_2 / (\rho A) \text{ and } \psi'_m V_m = 2$$

$$x_m = \frac{12 (0.63) (2.718)^2}{(10,000)(17.393)(1.0 \times 10^{-3})^2 (2.178)} + \frac{(9.60) (17.09)}{17.393}$$

$$x_m = 127.6 \text{ in.}$$

For minimum weight gun:

$$x_p = \frac{12 m'}{P_p A (\psi'_p)^2} + r', \text{ in.}$$

$$= \frac{12 (0.63)}{(10,000) (17.393) (1.0 \times 10^{-3})^2} + \frac{(9.6) (17.09)}{17.393}$$

$$= 52.9 \text{ in.}$$

$$x_o = \frac{12 m'}{P_p A (\psi'_p)^2 e} + \frac{C_2}{\rho A}, \text{ in.}$$

$$= \frac{12 (2.718)^2 (0.63)}{(10,000)(17.393)(2.718)(1.0 \times 10^{-3})^2} + \frac{(9.60) (17.09)}{17.393}$$

$$= 25.4 \text{ in.}$$

*Obtained from Eq. 5-61 based on the assumption that $q = 0$ for a minimum weight weapon.

For minimum weight gun:

$$P_m = \frac{P_p (\psi'_p)^2 V_m e}{\psi'_m \rho e^2}$$

(since $\psi'_m V_m = 2$)

$$P_m = \frac{(10,000)(1.0 \times 10^{-3})^2 (1810)(2.718)}{(1.104 \times 10^{-3})(2.718)^2}$$

$$P_m = 6031 \text{ psi}$$

Using a safety factor of 1.15:

$$P'_p = 1.15 P_p$$

$$P'_p = 1.15 \times 10,000 = 11,500 \text{ psi}$$

$$P'_m = 1.15 P_m, \text{ psi}$$

$$P'_m = (1.15) (6031) = 6936 \text{ psi}$$

Calculating the wall thicknesses by Eq. 5-109 corresponding to P'_p and P'_m

$$w_p = P'_p R_2 / \sigma, \text{ in.}$$

$$= \frac{(11,500) (2.35)}{160,000} = 0.169 \text{ in.}$$

$$w_m = P'_m R_2 / \sigma, \text{ in.}$$

$$= \frac{(6936) (2.35)}{160,000} = 0.102 \text{ in.}$$

The weight of the gun then is approximated by Eq. 5-112 and noting that it was assumed $V_b = V_m$, thus $x_o = x_m$. Also Eq. 5-112 shows that the tube weight and the gun weight are estimated by adding the chamber weight to Eq. 5-112.

$$W_{gun} = 2\pi \rho' R_2 \left[(x_o + x_p) w_p + \left(\frac{w_p + w_m}{2} \right) (x_m - x_p) \right] + \pi \rho' \left[w_p^2 (x_o + x_p) \right]$$

$$\begin{aligned}
& + (w_p^2 + w_p w_m + w_m^2) \\
& \times \left(\frac{x_m - x_p}{3} \right) \Big] , \text{lb} \\
& = 2\pi(0.3)(2.35) \left[(25.4 + 52.9) \right. \\
& \quad \times (0.169) + \frac{(0.169 + 0.102)}{2} \\
& \quad \times (127.6 - 52.9) \Big] + \pi(0.3) \\
& \quad \left\{ (0.169)^2 (25.4 + 52.9) \right. \\
& \quad + \left[(0.169)^2 + (0.169)(0.102) \right. \\
& \quad \left. \left. + (0.102)^2 \right] \right. \\
& \quad \left. \times \frac{(127.6 - 52.9)}{3} \right\} \\
& = 104.8 \text{ lb} \\
\Delta_o & = 27.7 \left(\frac{C}{4x_o} \right) , \text{g-cm}^{-3} \\
& = \frac{27.7(9.60)}{17.393(25.4)} = 0.60 \text{ g-cm}^{-3}
\end{aligned}$$

Repeating these calculations for different values of P_p , a curve of bare rifle weight versus peak pressure for $\lambda = 0.53$ is generated as shown in Fig. 2-9. Examining the loading density Δ_o for the various peak pressures, we find the following:

P_p , psi	Δ_o , g-cm ⁻³
8,000	0.518
9,000	0.562
10,000	0.600
11,000	0.636
12,000	0.670
14,000	0.731

From the discussion of par. 2-8, it is shown that the appropriate choice of P_p would be 10,000 psi in order to attain the desired loading density of 0.6 g-cm⁻³. The propellant charge for $\lambda = 0.53$ is 9.6 lb. In the final design of the 120 mm Rifle, XM105, HAW, the following parameters were obtained experimentally for a muzzle velocity of 1800 fps at 70°F:

$$P_p = 10,300 \text{ psi}$$

$$C_i = 9.5 \text{ lb}$$

These values are extremely close to the calculated values obtained for the minimum weight gun. Given the optimum values of P_p and λ for a minimum weight gun, it is possible to determine all the rest of the gun and propellant parameters as well as the pressure-travel relation through the method of solving the interior ballistic equations as described in Section V of Chapter 5. An example of these remaining calculations is given in par. 5-19.

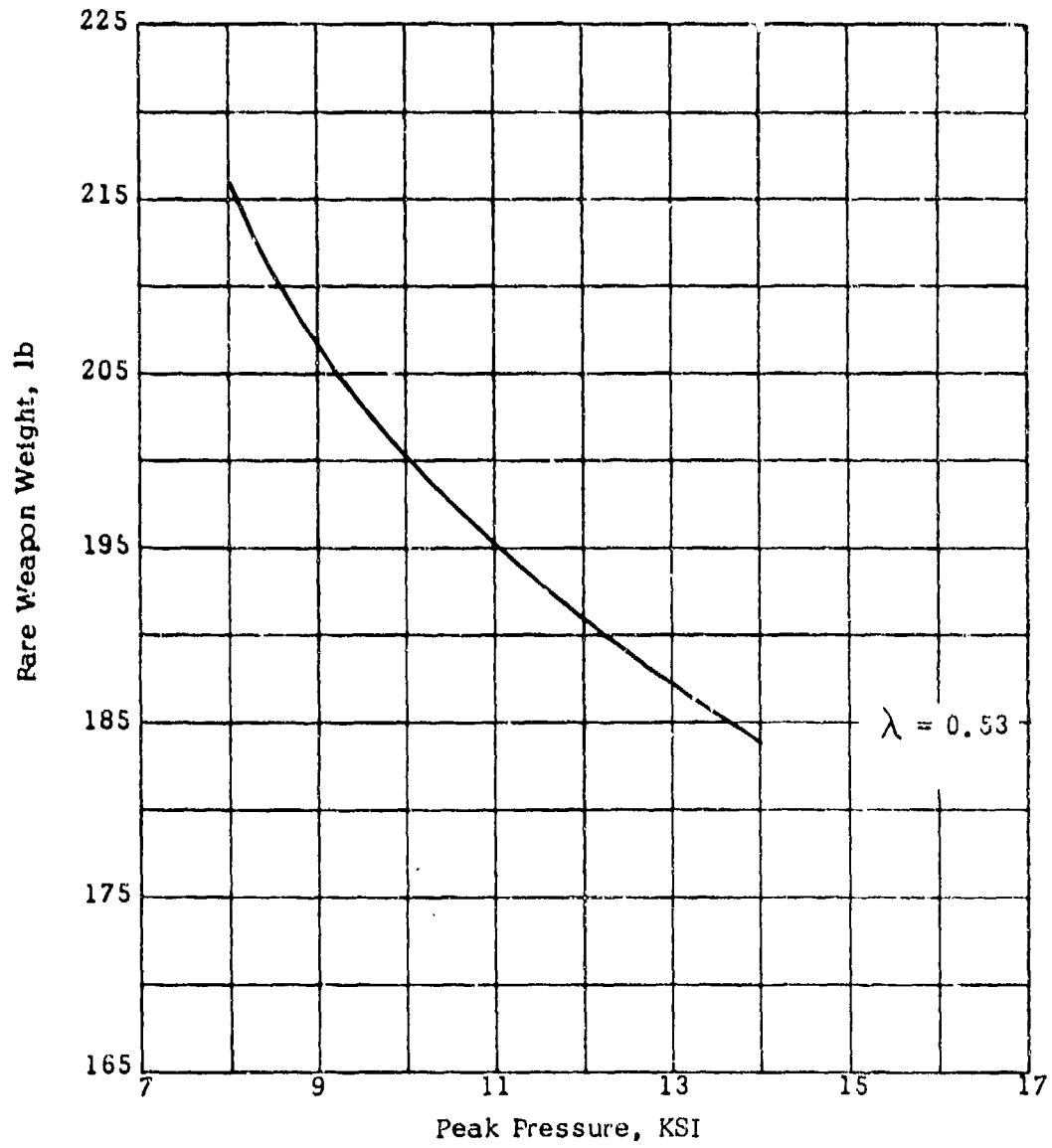


Figure 2-9. Bare Weapon Weight vs Peak Pressure

REFERENCES

1. ST 9-152, *Ordnance Technical Terminology*, US Army Ordnance School, Aberdeen Proving Ground, Maryland, June 1962.
2. AMCP 706-150, *Engineering Design Handbook, Interior Ballistics of Guns*.
3. PDWL S-2, *Notes on Development Type Materiel, 120mm Rifle System XM105E1 Heavy Antitank Weapon (HAW)*, Frankford Arsenal, December 1962.
4. R.T. Fillman and D.E. Walters, *Large Caliber Recoilless Cannon (EIK)*, Report R-1533, Frankford Arsenal, March 1960.
5. *Recoilless Rifle Systems, Ammunition and Related Items*, Status Report No. 1, Vol. II, Report R-1237, Frankford Arsenal, 1 October through 31 March 1954.
6. *Development of the 90mm Rifle T149*, Interim Technical Report, Contract No. DA-19-020-ORD-40, Arthur D. Little, Inc., June 1, 1955.

PART TWO
THEORETICAL ANALYSIS

CHAPTER 3
TERMINAL BALLISTICS

3-0 LIST OF SYMBOLS

A	= constant of Eq. 3-1, dimensionless	$N(m)$	= total number of fragments of weight greater than m
\bar{A}	= average presented area of fragment, ft^2	N_o	= total number of fragments
B	= constant of Eq. 3-5, $\text{g}^{1/2}\text{-in.}^{-7/6}$	R	= outside radius of case, in.
C	= explosive charge weight, g	t	= wall thickness, in.
\bar{C}_D	= average drag coefficient, dimensionless	V	= velocity of fragment, fps
d_i	= projectile inside diameter, in.	V_o	= initial fragment velocity, fps
d_o	= projectile outside diameter, in.	W	= mean width between grooves, in.
e	= base of natural logarithm 2.718281828...	x	= distance from point of burst, ft
$\sqrt{2E}$	= Gurney constant, fps	μ	= quantity in Mott equation related to average fragment mass, g
G	= number of grooves per ring	θ	= angle measured from nose of projectile, deg
K	= constant of Eq. 3-9, lb-ft^{-3}	$\rho(\theta)$	= fragment density, fragments per solid angle (steradian)
M	= total weight of projectile, g	ρ_a	= weight density of air, lb-ft^{-3}
m	= fragment weight, g or lb	ρ_c	= explosive charge weight density, lb-ft^{-3}
		ρ_m	= metal case weight density, lb-ft^{-3}

SECTION I

INTRODUCTION

3-1 SCOPE

Warheads used in recoilless rifle weapon systems are similar to the warheads of conventional artillery ammunition. Since the same or similar types of explosive charge material, fuzes, projectile material, etc., are the same for recoilless and conventional artillery ammunition, this information is not presented herein and the reader is directed to the material on terminal ballistics contained in Refs. 1 and 2. This chapter will direct its discussion to the factors that affect the terminal ballistic performance of recoilless rifle ammunition.

3-2 BACKGROUND

Terminal ballistics is concerned with the principles underlying the effects of weapons on targets. The effects studied include penetration, fragmentation, detonation, shaped charge, blast, combustion, and incendiary effects. Because these effects are dependent upon the firing and flight characteristics of the projectile, the terminal ballistic study includes all actions of the warhead from safing and arming to effect on the target.

In designing weapons and ammunition, maximum desired terminal effect is a primary objective. In order to achieve this objective, a proper balance of many factors is essential. The most important of these factors are shape, weight, and material used in the projectile; type and weight of explosive charge; fuzing system; and terminal velocity. In order to evaluate or determine the scaling of these parameters, various experiments are conducted to determine the principles governing the number, size, velocity, and spatial distribution of fragments resulting from deto-

nations of cased high explosive charges. These experiments also include the study of penetration, impact, blast, and shaped charge effects—depending upon the type of warheads under study. The basic information provided during these terminal ballistic studies and experiments permits the optimization of the parameters and effects on particular types of targets. These studies also provide the information required to evaluate the overall system effectiveness. For example, terminal ballistic studies, i.e., distribution of fragments by size and velocity, provide the data needed to determine kill probability.

3-3 TYPICAL RECOILLESS WARHEADS

Recoilless rifles are large caliber weapons of light weight, great striking power and accuracy, delivering no recoil to its mount or, if shoulder-fired, to the body of the individual firing the weapon. These characteristics make the recoilless rifle ideal for infantry attack against heavily armored vehicles such as tanks.

Most recoilless rifle weapon systems, because of their light weight and relatively low muzzle velocity, cannot function effectively when employing AP (armor-piercing) type warheads that rely totally on the kinetic energy of the projectile to enable it to penetrate the target armor plate. In normal combat conditions, complete incapacitation of armored vehicles is not necessary to put the vehicle out of action. Various components and moving parts such as controls, engine, gun and running gear can become inoperable by being wedged, burred, deformed, or cut off to cause immobilization or uselessness of the vehicle. This can result projectile fragments and blast on the outside of the vehicle or by spall particles on the inside. Furthermore, a

hit on vital components such as ammunition, and sometimes fuel, can cause vehicle destruction by fire.

Because HE (High Explosive), HEAT (High Explosive Antitank), and HEP (High Explosive Plastic) warheads do not rely exclusively on total armor penetration to defeat the

target--i.e., they do not require a high muzzle velocity, but rely on fragmentation, blast, or spalling characteristics to defeat the target--they are used effectively in recoilless rifle weapon systems against armored targets. Figs. 3-1 and 3-2 show the typical configuration of HEAT and HE recoilless warheads, respectively.

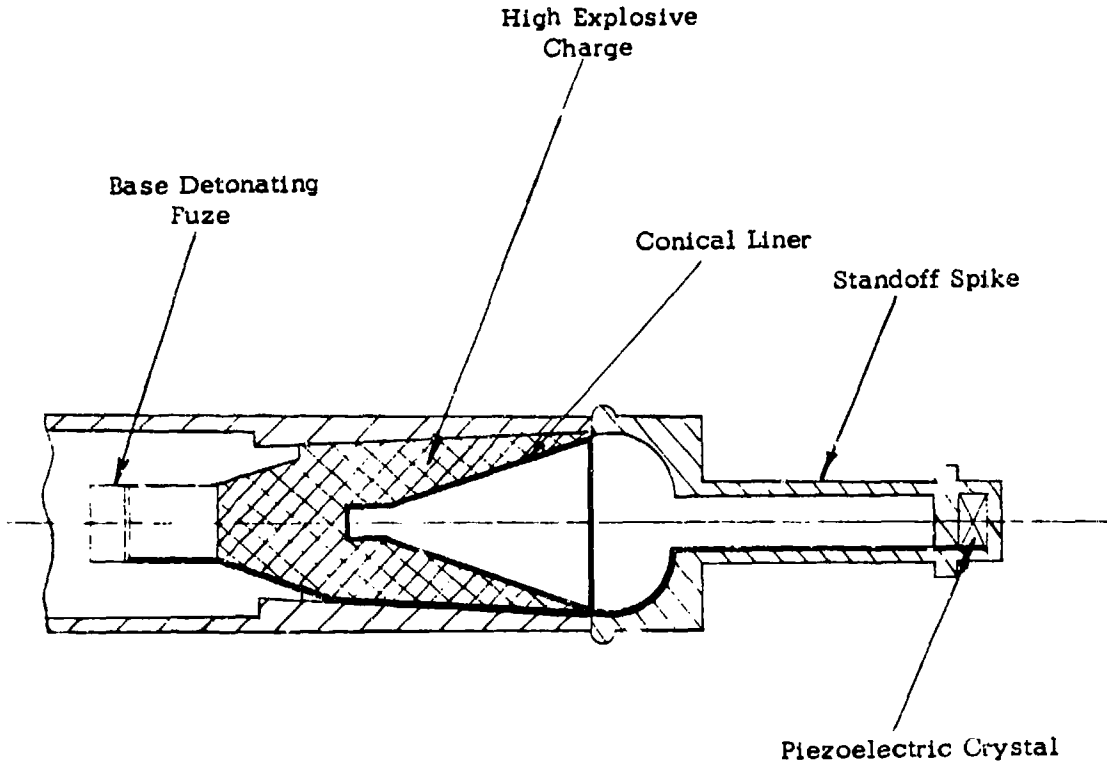


Figure 3-1. Typical HEAT Recoilless Warhead Cross Section

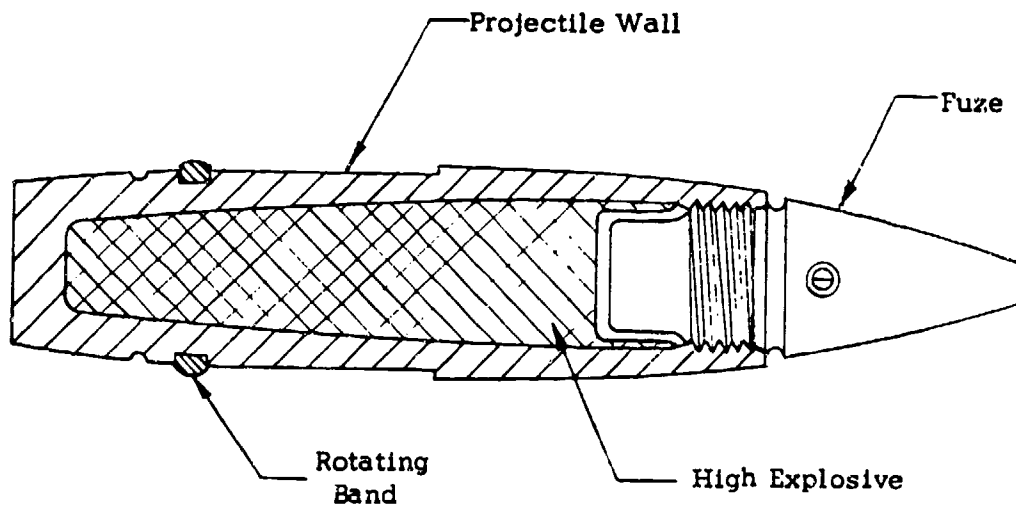


Figure 3-2. Typical HE Recoilless Warhead Cross Section

SECTION II

HEAT WARHEAD

3-4 QUALITATIVE DESCRIPTION

The HEAT warhead is a special type of high explosive warhead that incorporates a shaped charge. The basic components of the shaped charge warhead are container, hollow liner of inert material, fuze, explosive charge, and detonating device. As shown in Fig. 3-1, the shaped charge warhead has an axially symmetric high explosive charge positioned behind an inert liner in the form of a cone with its apex toward the detonator. In operation, the high explosive charge illustrated is initiated by the impact of the warhead which generates a current in the piezoelectric crystal that, in turn, functions the fuze and detonator. The generated shock wave in the explosive collapses some of the liner material into a high velocity stream of metal called a jet. The forward end of the jet attains a velocity approaching the detonation velocity of the explosive (25,000 fps) while the aft end of the jet and the remaining liner material (called the "slug") have a forward velocity of about 1500 fps. If the liner material is sufficiently ductile and there is sufficient space, the liner will be drawn out into a very long thin jet of extraordinary penetrating ability. The distance between the base of the liner and the surface to be attacked is called the "standoff" and depending upon the type of charge, liner material, and other parameters, there will be an optimum standoff for which the greatest penetration is achieved against the specific type of target.

Against armored vehicles, the damage inflicted by a HEAT warhead stems from the ability of the jet to penetrate the armor thickness and from the production of spalls on the opposite side of the armor surface under attack. Properly designed shaped charged warheads detonated at the optimum

standoff can penetrate thicknesses of steel armor equal to three or four times their conical diameter.

For detailed quantitative information on the resistance of armor against HEAT rounds, see Ref. 3.

3-5 FACTORS AFFECTING PERFORMANCE

3-5.1 INTRODUCTION

The performance of shaped charge warheads can be evaluated by several methods that determine the amount or type of penetration in a homogeneous reproducible type of material. In most cases and in the material contained within this chapter, the measure of performance is taken as the total depth of penetration into mild steel, except where otherwise stated. The equivalent penetration in homogeneous armor is obtained by multiplying by a conversion factor. Homogeneous armor generally is not used as a target material because of its much greater cost than mild steel. Fortunately, different grades or types of mild steel all give about the same average penetration for a given shaped charge design. In measuring the depth of penetration, targets often are made up of stacks of mild steel plates 0.5 to 3.0 in. thick.

In various tests as reported in Ref. 1, it is found that the penetration of a given jet into steel at a fixed standoff varies essentially linearly with the Brinell hardness of the steel and that the penetration also is affected by the standoff. Tests also indicate that in comparing the relative performance of the ability of a given shaped charge to penetrate mild steel and homogeneous armor, the armor is more effective than the mild steel in

resisting penetration of a given jet at longer standoffs.

For some purposes, a better measure of performance would be the volume of the hole or its smallest diameter. The best measure of performance, especially when considering the lethality of the warhead, would be the measurement of some factor that indicates the amount of damage done behind a given target plate by the residual jet and spalled material from the back face of the plate.

3.5.2 PROJECTILE SPIN

One of the problems or disadvantages

encountered in the use of shaped charges is that rotation of the warhead in spin-stabilized projectiles reduces the penetration capability of the jet. Increasing standoff increases this effect. Fig. 3-3 shows the relation of penetration to rotational speed, and indicates the undesirable effect of rotation on penetration. The reduction in penetration caused by rotation is attributed to the lateral dispersion of the jet which results in decreasing the effective mean density of the jet.

Attempts have been made to improve the performance of spin-stabilized HEAT projectiles by using nonconical, axially symmetric liners. However, at high spin rates, the results

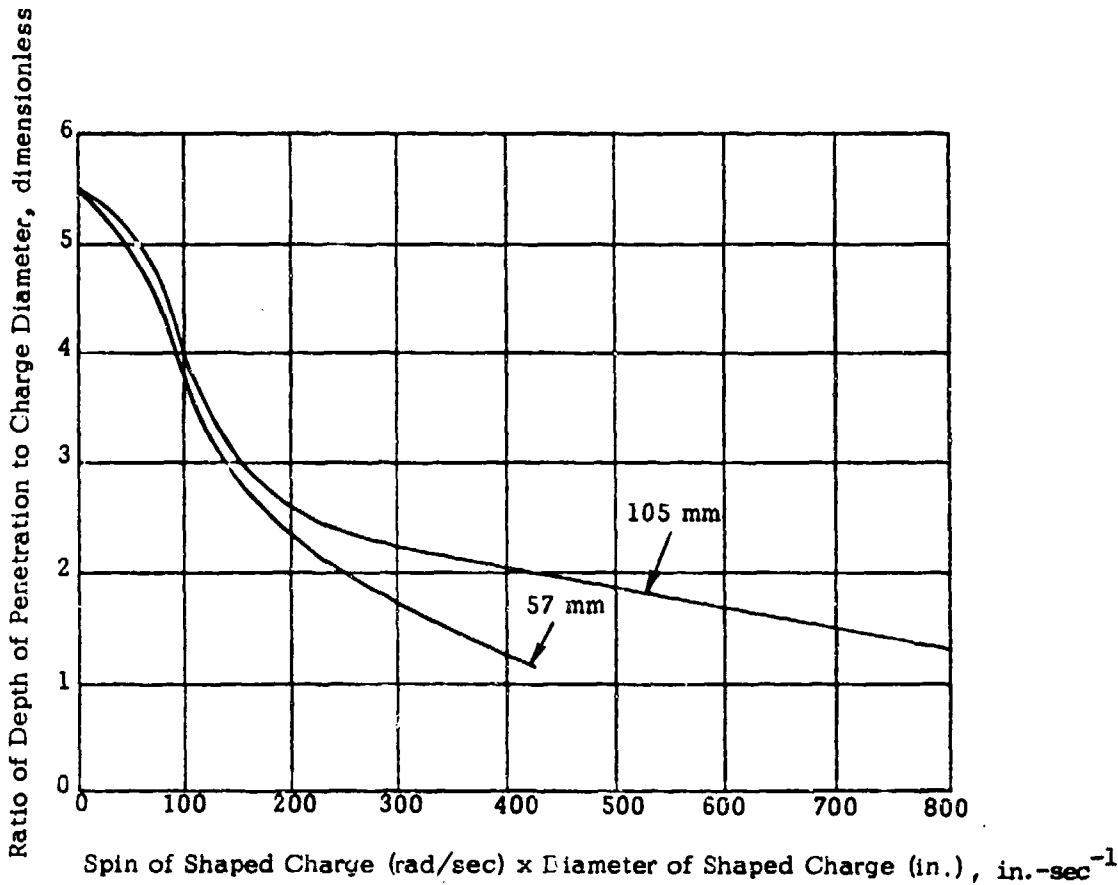


Figure 3-3. Penetration as a Function of Projectile Spin Rate (Ref. 1)

were not promising and the major emphasis shifted to the design of fluted liners not having axial symmetry. The principle underlying the use of fluted liners is that of "spin compensation", i.e., of conserving the angular momentum of the liner so as to inhibit the dispersion of the jet. Generally, spin compensation is achieved by using flutes that are in the plane of the charge axis and that have an increasing thickness as one proceeds from the apex to the base of the cone. However, the mechanism of spin compensation is not yet fully understood, since even the direction of spin compensation can be reversed in some cases by just changing the number of flutings. For the present, it is necessary to rely on available empirical data when considering the use of spin compensation.

3-5.3 PHYSICAL PROPERTIES OF LINER

The formation of a shaped charge jet from the collapsing cone is a critical process and can be affected adversely by deviations in the required geometrical accuracies and metallurgical properties of the liner. In order for the walls of the cone to collapse and meet exactly on the axis of the cone, several geometrical requirements must be satisfied or the sides of the cone will not collapse uniformly on the cone axis and will produce a crooked jet that wanders at the point of contact on the target surface, resulting in poor penetration. Thus, it is important that sections of the cone perpendicular to the cone axis be true circles with centers on the axis and that the walls be of uniform thickness around the section circumference. Uniform density of the metal also is required for even collapse of the walls. The last undesirable characteristic is the existence of waviness along the slant height of the cone.

Deviations in the metallurgical properties of the liner can result in the same reductions in the effectiveness of the warhead as caused by the geometrical inaccuracies of the liner previously discussed. Metallurgical properties of the liner depend strongly on the manufac-

turing method and type of heat treatment. Because of the extremely high pressures, high strain rates, and excessive amount of plastic strain involved in the collapse of the liner, it is difficult to analyze the metallurgical state of the liner in all states of jet formation. Also it must be remembered that the properties of the jet and the cone are not the same, and that the most important properties are those considered under the high pressures and rates of strain previously mentioned. These properties may be very different from those under ordinary conditions, as emphasized by the fact that glass cones give penetrations in concrete targets greater than might be expected from the metallurgical properties of glass. Some very interesting and important correlations exist among properties of the liner, principally crystal structure and melting point, and behavior of the jet. One of the most interesting features is a built-in spin compensation factor in certain cases, apparently resulting from an unusual crystal structure as a consequence of a particular forming process that would give less penetration in static firings.

Theory indicates that the penetration of the jet is proportional to the length of the jet and the square root of the jet density. For a continuous jet the assumption is made that the jet density is the same as that of the cone. As a result of the velocity gradient in the jet, the jet lengthens as it travels and, because of this stretching, eventually breaks up into a series of particles. If the jet did not break up, its length and penetration would increase linearly with time and, consequently, with standoff.

Actual data indicate that penetration increases with standoff up to a maximum value of penetration. The standoff corresponding to this maximum penetration is called the "optimum" standoff. Beyond the optimum standoff, the average penetration decreases with increasing standoff, while the best values of penetration approach an asymptotic value.

The decrease in penetration from the ideal liner value to the asymptotic value is due to the breakup of the jet, whereas the decrease in penetration from the asymptotic value to the average value is due to increasing spread of the jet. Thus, for good penetration, the jet should be capable of attaining a great length before breaking up. The ability of the jet to attain the desired lengths depends upon its metallurgical properties, homogeneity of the explosive filler, and the accuracy of component manufacture and assembly. In tests comparing the penetration capabilities of copper, aluminum, steel, zinc, lead, and glass liners, it is found that copper and aluminum have the best metallurgical properties for shaped charge cones while lead and glass have inferior properties. A desirable liner material would have properties similar to copper and aluminum, and have a high density (Ref. 1).

3.5.4 STANDOFF

Fig. 3-4 shows the relationship between penetration and standoff for copper cones into mild steel targets under test conditions. As indicated in Fig. 3-4, the maximum penetration would occur at a standoff of about 6 cone diameters. In reality, the actual standoff for a well-made conical liner would be limited to one to three cone diameters by such aerodynamic considerations as ogive shape and size, and projectile velocity. However, these shorter standoffs may be sufficient to attain 80 to 90 percent of the penetration expected at optimum standoff indicated in Fig. 3-4.

A properly designed cone will achieve the required level of penetration while exhibiting a fairly flat penetration-standoff curve, i.e., an

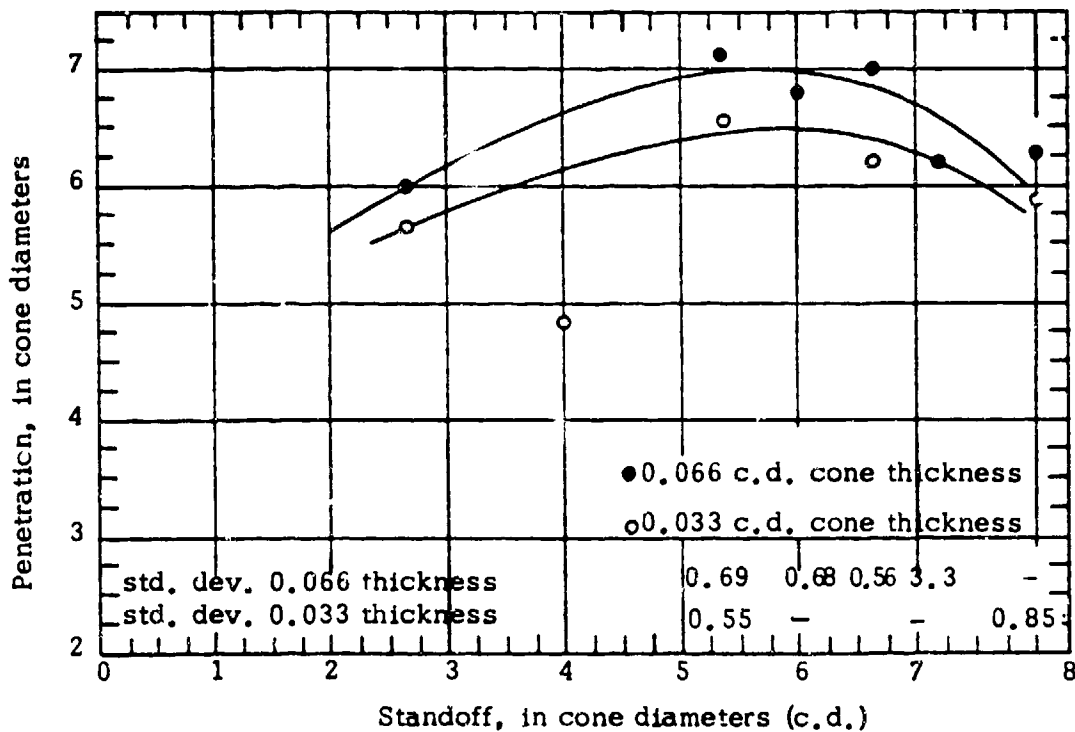


Figure 3-4. Penetration for 30-deg Electroformed Copper Cones into Mild Steel Targets (Ref. 1)

increase or reduction in standoff will not change the penetration greatly. Both aluminum and copper liners exhibit fairly flat penetration-standoff curves, as compared to steel liners which exhibit a sharply decreasing penetration after peaking at a small optimum standoff.

3-5.5 CONE ANGLE

The choice of the cone apex angle is important, both from a performance and a manufacturing standpoint. Data are available that indicate the optimum standoff increases

with increased apex angle up to about 65 deg; optimum standoff or maximum penetration then decreases as the apex angle is increased. However, the optimum standoff is also dependent upon the cone material, wall thickness, and charge length.

With modern, precision-manufacturing methods, the optimum cone angle for projectiles with copper cones is close to 40 to 45 deg. However, certain cases, as indicated in Fig. 3-5, have shown best penetration performance with 20-deg cones, and in others, 60-deg cones. As a first choice, a cone angle

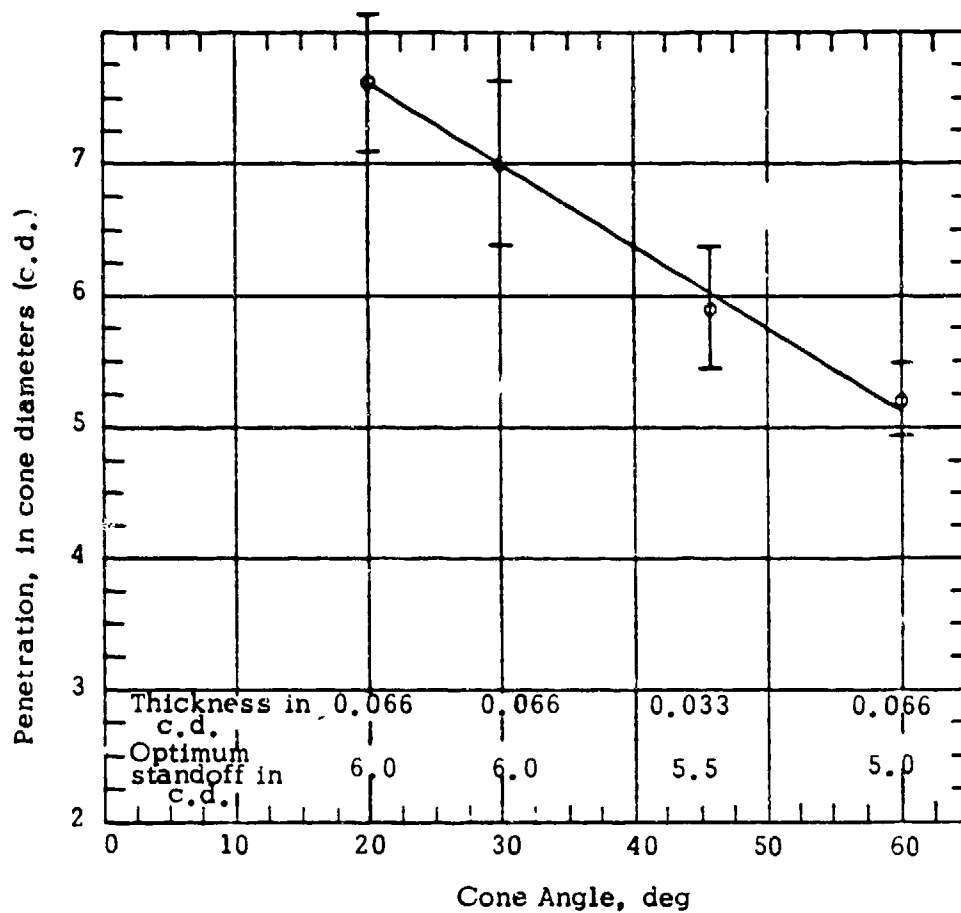


Figure 3-5. Maximum Penetration into Mild Steel Targets at Optimum Standoff vs Cone Angle for Electroformed Copper Cones (Ref. 1)

of either 40 or 45 deg may be selected and will give good performance in projectiles with an ogive length of 2 calibers (Ref. 1).

As with most other cone parameters, the effect of the cone apex angle decreases with increasing projectile spin rate. For example, at 0 rps a 45-deg, 3.4-in. copper cone penetrates 3 in. deeper than a 60-deg cone of the same wall thickness; but at 45 rps, the difference is less than 1 in.

3-5.6 LINER WALL THICKNESS

For each type of cone material, standoff, projectile wall confinement, explosive type, charge shape, and cone apex angle, there is an optimum wall thickness. From a practical consideration of projectile design, the projectile confinement and cone apex angle are the most determining factors.

As a guide for liners of different apex angles, or for shapes other than conical, an approximately correct wall thickness may be obtained by maintaining the thickness constant in the axial direction. As shown in Fig. 3-6, curves of penetration versus wall thickness are frequently unsymmetrical. A thicker wall generally is preferred over a thinner wall since thin-wall performance is typified by excessive variability from charge to charge, whereas the thicker-wall performance is characterized by good reproducibility with only a tolerable decrease in penetration. In practice, a wall thickness about 5 percent greater than the optimum is selected in order to insure that the production wall thickness will not be less than optimum (Ref. 1).

Various studies have indicated that the liner thickness should scale as the diameter, i.e., a cone would logically be thicker at the base than at the apex. The investigations of tapered walls, however, have shown that the real improvement in the penetration performance is slight, if any at all. These studies have indicated, however, that rather wide

tolerances may be placed on the variation in wall thicknesses between apex and base without reducing penetration, provided the wall thickness is held constant at each transverse section of the cone.

3-5.7 LINER SHAPE

Nonconical shapes that have been tried as liners—in addition to the simple cone already described—are hemispheres and spherical caps, trumpets, and combinations of these. The general results are that the penetrations achieved from these configurations are inferior to those obtained with simple cones. Radiographs show that hemispheres do not collapse with the formation of a jet, as do cones; they turn inside out before collapsing, with the whole liner being projected as a stream of particles. Spherical caps (segments) are fragmented and projected as a cluster of particles that may be more or less focused depending upon the curvature. Results obtained from the use of spherical segments show poorer results than those obtained with hemispheres.

Double cone angles in which there is a change from one angle to another have shown good performance in certain cases. When the change in angles is made abruptly, there has been no evidence of any increase in penetration. However, when the change in angles is made smoothly and the liner wall tapered, rounds have given peak performance at normally available standoffs.

3-5.8 ALIGNMENT OF CONE AND CHARGE

For the best and most reproducible performance, the axes of the charge and cone should coincide. In actual practice, however, the axes may not be parallel (tilted), or they may be parallel but displaced (offset). Tilting of the liner results in a reduced average penetration. Although it is possible to obtain good shots with liners tilted as high as 2 deg,

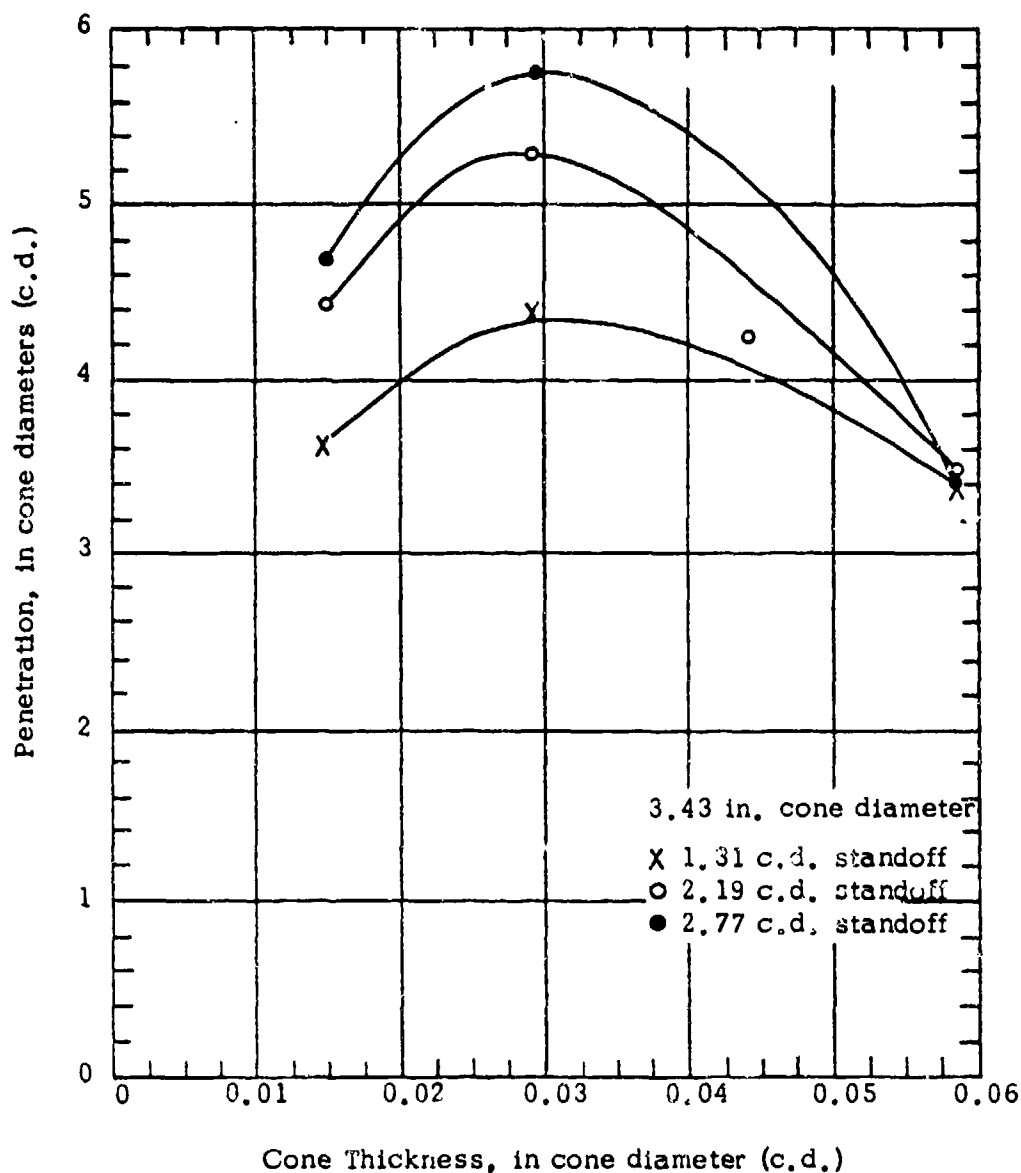


Figure 3-6. Cone Thickness vs Penetration for 45-deg Copper Cones (Ref. 1)

the general findings are that a 1-deg tilt of the cone reduces the average penetration by 50 percent, a 0.5-deg tilt by 20 percent, and a 0.3-deg tilt by 10 percent.

The second type of misalignment results when the cone and charge axes are parallel but slightly offset. Actual tests have shown

that an offset of only 0.015 in. (1 percent of the base diameter) reduced the penetration by approximately 20 percent.

3-5.9 CONFINEMENT

Increasing the confinement of the jet either

by providing an increased wall thickness or a "belt" of explosive greatly increases the hole volume of the penetration. The presence of explosion products at high pressure within the explosive belt retards the expansion of the products in much the same manner as does a steel casing. In the study of the effects of confinement on the performance of flanged and unflanged cones (Ref. 1, par. 2-93) the following conclusions have been drawn:

1. The addition of a small explosive belt obtained by increasing the charge diameter from 1.73 to 2.00 in. produces the same effect on penetration and hole volume for a 1.63 base diameter cone as the addition of 0.25 in. of steel confinement.

2. When heavy base confinement is added to the 2-in. charge, the penetration is decreased about 20 percent.

3. The addition of both lateral and heavy base confinement to the 2-in. charge causes a drastic reduction of about 45 percent in penetration performance.

4. When the larger charge is confined laterally, the presence of a flange causes a relatively small, but significant decrease in penetration, as compared with a similarly confined charge lined with a deflanged cone.

5. The hole volume produced by the 2-in. charge is increased by about 50 percent when lateral confinement of 0.25-in. steel is used (compared with the 100 percent increase which occurs with the 1.63-in. charge); boundary conditions at the base of the charge have little or no effect on hole volume in spite of the large changes in depth of penetration.

SECTION III

HE WARHEAD

3-6 QUALITATIVE DESCRIPTION

The HE warhead consists of a high explosive charge and fuze surrounded by either a wall of preformed metal fragments or a prescored or solid metal casing. Upon detonation of the high explosive, the metal case expands with the fragments being propelled outward at velocities of 6,000 to 10,000 fps. In effect, the fragments are projectiles with the capacity to inflict considerable damage to adjacent objects. Capacity for damage depends upon fragment size, shape, velocity, and distribution.

Fragmentation is not the only result of detonation of the HE warhead. Approximately forty percent of the gas energy normally is expended in the fragmentation process with the balance of the available energy being consumed in the formation of a compressive wave in the air surrounding the projectile.

3-7 DETERMINATION OF FRAGMENTATION CHARACTERISTICS

3-7.1 FRAGMENT SIZE DISTRIBUTION

Mott and Linfoot (see Ref. 1) proposed that the fragmentation of thin-walled projectiles is the result of two-dimensional, rather than three-dimensional, breakup. Based on this assumption, the mass distribution of fragments may be described by the equation

$$N(m) = A \exp(-m/\mu)^{1/2} \quad (3-1)$$

where

$N(m)$ = total number of fragments of weight greater than m

m = fragment weight, g

μ = function of average fragment weight \bar{m} , g

$\mu = \bar{m}/2$

A = constant

If it is assumed that the two-dimensional breakup holds down to the smallest fragment, then

$$N(m) = [M/(2\mu)] \exp(-m/\mu)^{1/2} \quad (3-2)$$

where

M = total weight of projectile, g

2μ = arithmetic average fragment weight, g

Noting that $M/(2\mu)$ represents the total number of fragments N_0 , Eq. 3-2 also may be written

$$N(m) = N_0 \exp(-m/\mu)^{1/2} \quad (3-3)$$

For extremely thick-walled projectiles, the wall thickness will have less effect on the size of the fragment. Also, three-dimensional breakup rather than two-dimensional breakup will be the rule. The weight distribution of fragments for this case is described by

$$N(m) = A \exp(-m/\mu)^{1/3} \quad (3-4)$$

For fragmentation projectiles, Eq. 3-3 is more representative than Eq. 3-4 of the conditions found.

If one assumes the validity of the Mott equation, the quantity μ is a measure of the fragmentation efficiency of the projectile and is dependent both upon the characteristics of the explosive and of the metal case. The

significance of the quantity is made clearer by stating that the number of fragments greater than μ g is equal to the number of fragments having masses between $\mu/11$ and μ g. Thus, if $\mu = 5.5$ g, the number of fragments lying between 0.5 and 5.5 g would be equal to the number of fragments with weight greater than 5.5 g (assuming that the Mott equation is valid down to fragments as small as 0.5 g). Furthermore, if the Mott equation was valid for all fragments, then the number of fragments greater than μ would comprise 37 percent of the total.

As stated in Ref. 1, there has been difficulty in analyzing existing test data because of the nonuniform behavior of the projectiles. Even within a single lot of projectiles, there is considerable variation in the number of fragments produced by the individual warheads. Thus, the rough agreement between existing experimental data and the semitheoretical formula developed by Mott exists. A series of experimental firings with steel projectiles filled with explosives of different characteristics was performed at the US Naval Ordnance Laboratory in order to obtain values of the parameter μ as well as other parameters and characteristics of the fragmentation process. Plots on semilogarithmic paper of the cumulative number of fragments versus the square root of the fragment mass were obtained with several representative plots shown in Fig. 3-7. The Mott equation predicts a straight line of these plots. However, as shown in Fig. 3-7, it can be seen that the experimental points in every case form a curve of increasing negative slope rather than a straight line. Assuming that this experiment was accurate, it would seem to indicate a fundamental defect in the Mott relationship.

The value of μ , in addition to being dependent upon the characteristics of the explosive and projectile material, also is dependent upon the physical dimensions of the projectile. To account for this variability, scaling formulas have been proposed. The

following formula, relating the value of μ to the projectile inside diameter d_i and the wall thickness t has been proposed by Mott:

$$\mu^{1/2} = Bt^{5/6}d_i^{1/3}(1 + t/d_i) \quad (3-5)$$

where

B = constant depending upon the explosive and the physical characteristic of the metal of the casing

d_i = projectile inside diameter, in.

t = wall thickness, in.

3-7.2 INITIAL FRAGMENT SPEED

The initial speed V_o of fragments is predicted quite accurately by the following formulas developed by Gurney:

1. For cylinders:

$$V_o = \sqrt{2E} \left(\frac{C/M}{1 + 0.5(C/M)} \right)^{1/2}, \text{ fps} \quad (3-6)$$

2. For spheres:

$$V_o = \sqrt{2E} \left(\frac{C/M}{1 + 0.6(C/M)} \right)^{1/2}, \text{ fps} \quad (3-7)$$

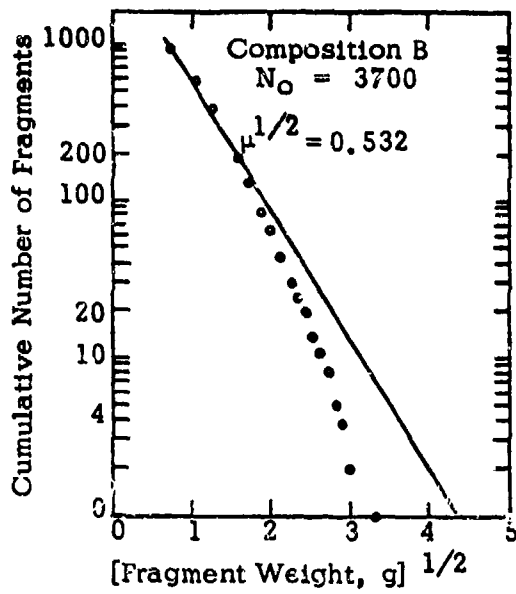
$\sqrt{2E}$ = Gurney constant for each type of explosive, fps

C = weight of explosive charge, g

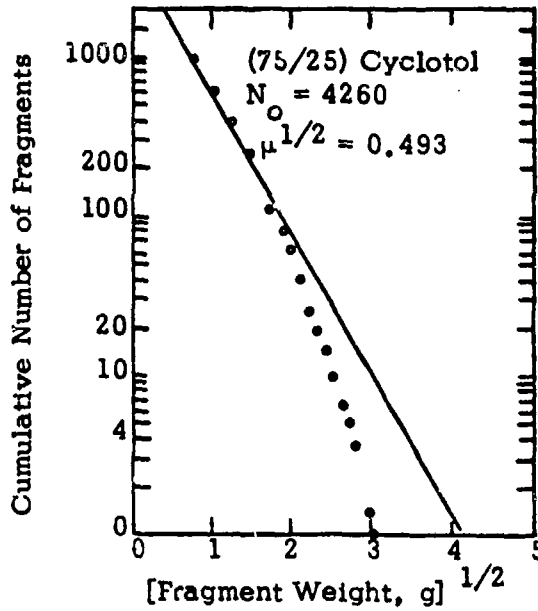
M = weight of fragmenting metal, g

Table 3-1 gives the value of $\sqrt{2E}$, Gurney constant for most of the commonly used high explosives.

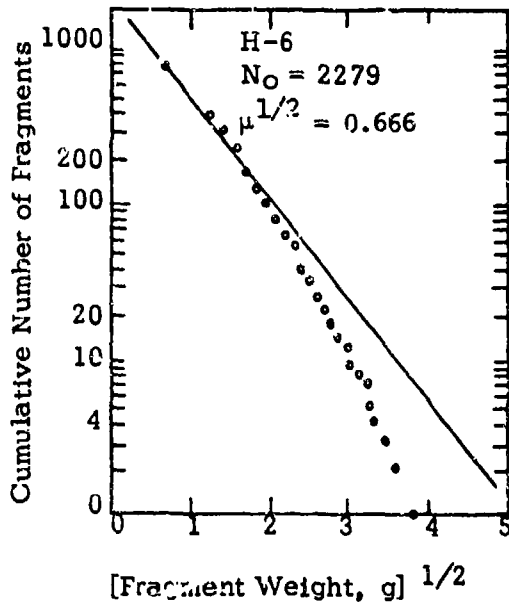
The graphs in Fig. 3-8 simplify the calculations for V_o in terms of the outside diameter d_o and thickness t of the projectile, the ratio



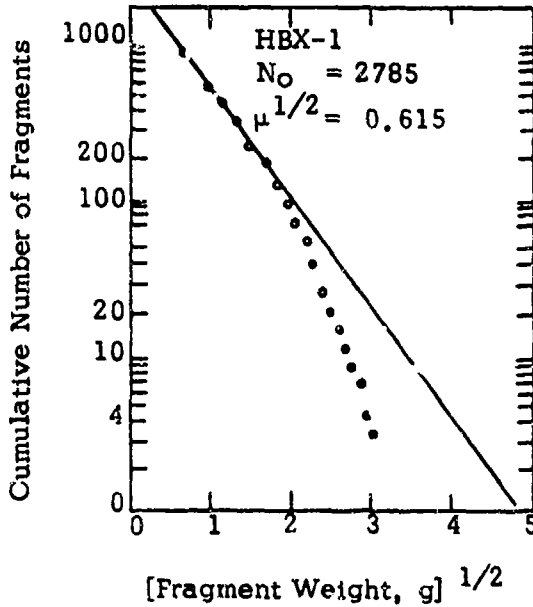
(A) Fragment Mass Distribution For Composition B



(B) Fragment Mass Distribution For 75/25 Cyclotol



(C) Fragment Mass Distribution For H-6



(D) Fragment Mass Distribution For HBX-1

Figure 3-7. Fragment Mass Distribution (Ref. 3)

TABLE 3-1
GURNEY CONSTANT FOR VARIOUS
EXPLOSIVES (Ref. 1)

Explosives	Gurney Constant $\sqrt{2E}$, fps
Composition C-3	8,800
Composition B	8,800
Torpex 2	8,800
Composition H-6	8,400
Pentolite	8,400
Minol 2	8,300
HBX	8,100
TNT	7,600
Tritonal	7,600
Picratol	7,600
Baratol	6,800

ρ_c/ρ_m of the density of the explosive to that of the metal case, and the Gurney constant of the explosive. Knowing the value of t/d_o , one uses Fig. 3-8(A) to solve for $(C/M)/(\rho_c/\rho_m)$. The value of C/M may then be found by multiplying by ρ_c/ρ_m . This value of C/M then may be used to find $V_o/\sqrt{2E}$ from Fig. 3-8(B). Multiplying this expression by the appropriate value of $\sqrt{2E}$ from Table 3-1 gives the value of the initial fragment speed V_o .

3-7.3 FRAGMENT SLOW DOWN

The equation for the velocity V of a fragment at a distance x from the point of burst is given by the following relationship:

$$V = V_o \exp \left[-\frac{\bar{C}_D \bar{A} \rho_a x}{m} \right], \text{ fps} \quad (3-8)$$

where

V = speed of fragment at x feet from point of burst, fps

V_o = initial speed of fragment, fps

\bar{C}_D = average drag coefficient, dimensionless

\bar{A} = average presented area of fragment, ft^2

ρ_a = density of air, lb-ft^{-3}

x = distance from point of burst, ft

m = weight of fragment, lb

For any homologous class of regularly shaped fragments, the weight m and average presented area \bar{A} are related by the following equation:

$$m = K(\bar{A})^{3/2} \quad (3-9)$$

where

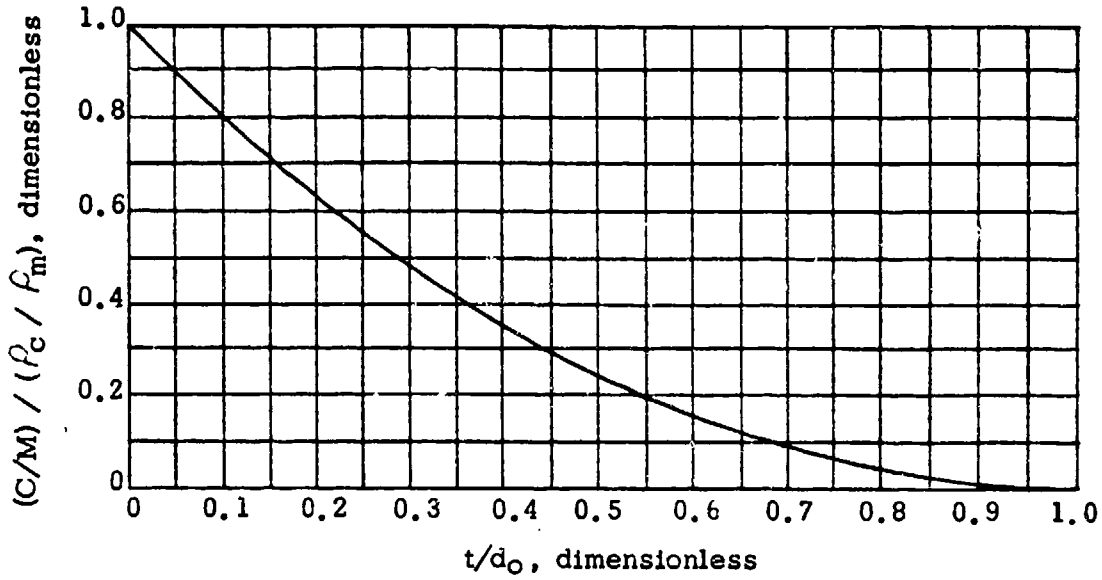
K = constant for the particular class of projectile

The value of K has been shown by experimental results to be roughly constant for the fragments projected from a particular projectile. Values of K are given in BRL Reports 501, 536, and M915 for a variety of projectile and bomb fragments.

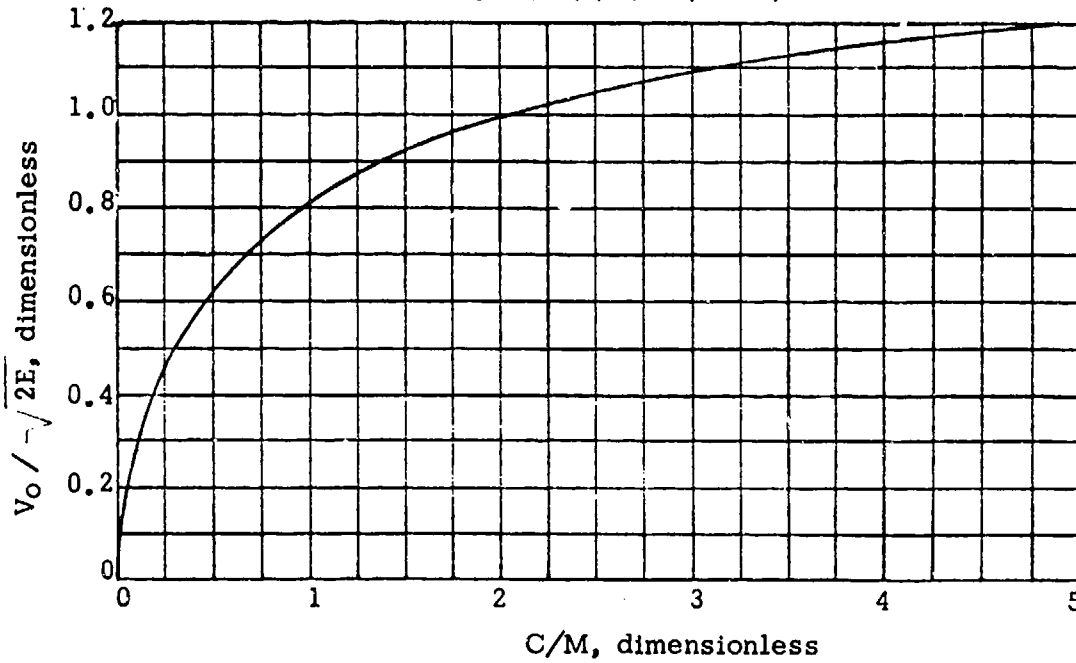
The method used to determine the presented area of the fragment involves measuring the presented area of the fragment for each of 16 positions corresponding to the orientation of 10 of the 20 faces of an icosahedron plus 6 orientations corresponding to the 12 vertices of the icosahedron. The arithmetical average of these values is then used for \bar{A} . The instrument used to obtain the presented area is known as an icosahedron gage.

3-7.4 FRAGMENTATION PATTERNS

When a projectile or warhead bursts, fragments are projected in different directions depending upon the configuration of the projectile. If the projectile were spherical and stationary when detonated, the density of fragments would be substantially constant,



(A) Determining $(C/M) / (\rho_c / \rho_m)$



(B) Determining $V_0 / (2E)$

Figure 3-8. Graphs for Determining the Initial Fragment Velocity V_0
(Ref. 1)

regardless of the direction. If the projectile were entirely cylindrical, the greatest density of fragments would be close to the equatorial plane, with practically all fragments contained in a narrow side-spray of the order of 20-deg width. For an ordinary artillery projectile, the curve of distribution with angle is peaked, and resembles the "normal error curve". An example is shown in Fig. 3-9.

Projectiles and warheads almost always have circular symmetry about their longitudinal axis. Hence, the distribution of fragment mass and velocity may be described as functions of the angle θ measured from the nose of the projectile (see Fig. 3-9). Letting $\rho(\theta)$ be the fragment density in fragments per unit solid angle, the total number of fragments N_o of the given projectile is given by

$$N_o = 2\pi \int_0^\pi \rho(\theta) \sin \theta d\theta \quad (3-10)$$

3-7.5 CONTROLLED FRAGMENTATION

In uncontrolled fragmentation, the range of masses and speeds is very great. In order to secure more effective fragments, it is desired to solve for the optimum mass (depending on the lethality requirements) and design a projectile that would limit all fragments with this mass. Thus, the probability of damage would be greatly increased and the results estimated more correctly.

The methods for controlling fragmentation are described in the paragraphs that follow.

3-7.5.1 Preformed Fragment

The best method of controlling fragment size is to form or precut the fragments to the desired size before incorporation into the projectile wall. The projectile structure usually is formed by a thin metal liner or cover, or

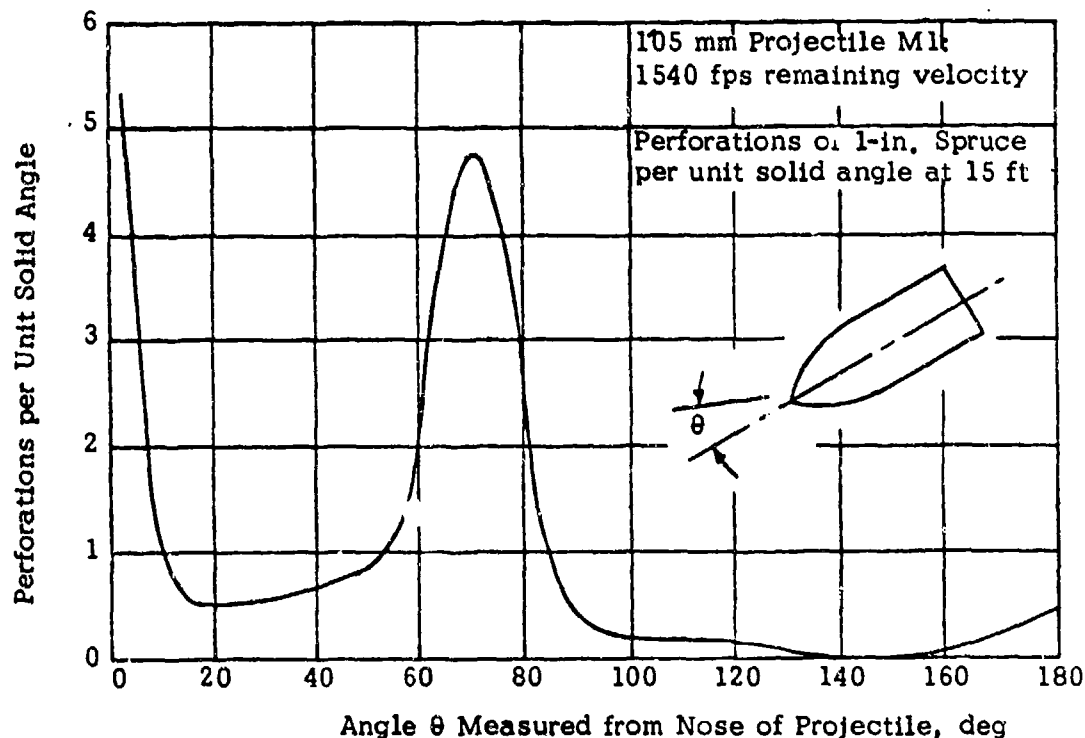


Figure 3-9 Typical Angular Fragmentation Distribution (Ref. 1)

both, to which the fragments are fastened with adhesive. Another method of installing the preformed fragments, especially spherical or fin-stabilized fragments, is to place the fragments in layers between the inner liner and the case and then fill the crevices between them with a plastic matrix.

3-7.5.2 Notched or Grooved Rings

In this method of controlling fragmentation, a series of notched rings are fitted over a plastic or thin metal liner, each ring forming a section of the warhead perpendicular to the axis of symmetry. The forces from detonation operate mostly in the direction of stressing each ring circumferentially and only secondarily to separate adjacent rings. Essentially, the thickness and width of the rings provides control of two dimensions of the fragments while notches along the circumference of the ring provide places of weakness where breakage in the third direction is desired.

The factors that are considered in this type of projectile are:

1. Quality of steel in rings
2. Spacing of the grooves
3. Groove depth
4. Width of rings
5. Timer
6. Length-to-diameter ratio
7. Ring finish.

The material selected for the rings is of relatively minor importance except that it must be homogeneous. Test results to date indicate that mild steel might be preferable to high-carbon steel and that the steel should be sufficiently hot-worked to break up segregated inclusions, and assure their uniform

distribution. The grooving spacing can be determined from the following formula:

$$G = \pi(2R - t)/W \quad (3-11)$$

where

G = number of grooves per ring

R = outside radius of case, in.

t = thickness of case, in.

W = mean width between grooves, in.

The depth of the groove should be from 5 to 10 percent of the ring thickness because excessive groove depth causes the fragments to break up. The grooves should have sharp bottoms and the rings provided with a ground or smooth lathe finish. In general, the width of the ring should be made equal to the thickness, the length to diameter ratio of the case not less than 1.25 to 1, and the length between 2.5 and 5 calibers.

The liner should be made of a material that will produce no important fragments and should be as thin as is consistent with manufacturing and strength considerations. A thickness of 5 percent of its radius has been found satisfactory for laminated phenolic plastic tubing.

3-7.5.3 Notched or Grooved Wire

In general, the notched wire method of controlling fragmentation is similar to the notched rings. This method incorporates a notched wire wound in a helix or spiral into the shape of the warhead casing. The wire must be supported by a liner or fastened together by some means (such as welding) in order to preserve the warhead shape. Notched wires usually are used when a notch ring would be too thin for economical manufacture.

3-7.5.4 Notched Casings

Instead of notching in one direction and having actual discontinuities in the metal in the other direction (such as in the notched ring or wire method), it is possible to cut, punch, or cast a two-dimensional network on a solid casing. Four types of notched casings have been tested for their controlled fragmentation, namely (Ref. 1):

1. Cylinder, 4 in. O.D., 0.25-in. wall with 0.125-in. holes in diamond pattern, punched and plugged; holes, 0.5 in. apart in row, rows 0.5 in. apart.

2. Cylinder, 3.5 in. I.D., with linearly tapered steps cut on outside, steps 0.5 in. long.

3. Cylinder 4 in. O.D., 0.25-in. wall, with left-hand and right-hand helical grooves cut at 45 deg to axis and spaced 0.5 in. apart. Groove profile V-shaped, with included angle of 60 deg.

4. Cylinder, 4 in. O.D., 0.25-in. wall with hexagonal pattern impressed by shearing.

Each cylinder was approximately 12 in. long and each provided with brass endplates to increase the confinement of the explosion. In tests with these cylinders, only the hexa-

gonal sheared pattern provided an excellent degree of fragmentation control.

3-7.5.5 Multiple Walls

The multiple-wall projectile is made by using close-fitted cylinders, each with thickness t/n where t is the thickness of a one-wall projectile and n is the number of walls. Multiple-wall projectiles do not give complete control since only the thickness of the fragments is uniform. The number of fragments is approximately n times the number of fragments of a single-wall projectile. The partial control achieved, however, is an improvement, because the average fragment mass is reduced and the number of fragments emitted is increased. However, the increase in lethality is much less than expected.

3-7.5.6 Metallurgically Modified Material

Another method of fragmentation control is to employ a type of iron, or an alloy, which will fragment in a desirable fashion. For example, pearlite malleable cast iron provides excellent lethality but its use is limited to low setback items. Extrapolating from the cast iron properties, a number of forgeable steel alloys have been developed which yield increased lethality solely as a result of their composition.

SECTION IV

OTHER TYPES OF WARHEADS

3-8 HEP WARHEAD

3-8.1 INTRODUCTION

The HEP warhead is used to defeat armor-protected vehicles. The operational mode of the HEP projectile is based on the fact that, when a "sufficient" quantity of explosive, of sufficient height for a given shape of explosive, is placed in intimate contact with armor plate and detonated, a rupture of a portion of the opposite face of the plate will occur. The ruptured portion of the armor plate is known as a spall and is generally in the form of a rough disk. Dependent upon the quantity of explosive above that needed to cause the rupture, the spall may attain velocities between 100 and 1000 fps. The mass and velocity of the spall depends upon the quality and thickness of the armor, and the mass type and shape of the explosive filler.

In general, HEP warheads are designed to defeat standard tank armor 1.2 calibers in thickness at angles of obliquity of 0 to 60 deg. When considering weights alone, the HEP projectile far surpasses the armor-piercing projectiles in destructive power. Besides depending upon the armor thickness, the effectiveness of solid armor-piercing type projectiles is also highly dependent upon the angle of obliquity (the angle at which it impacts the armor) and therefore must be designed to penetrate a thickness greater than the actual thickness. Since the HEP projectile shock wave is transmitted normal to the armor surface, the spall effect can be accomplished on thicker plates than with a comparable caliber, solid armor-piercing type projectile.

3-8.2 ADVANTAGES AND DISADVANTAGES

While not all the properties and character-

istics of HEP type warheads are known, the following characteristics and trends have been observed:

1. Advantages are:

(a) HEP warheads make low-velocity weapons, such as recoilless rifles, effective antitank destroyers.

(b) While the effectiveness of other anti-tank projectiles decreases as the angle of target obliquity increases, the effectiveness of HEP projectiles decreases at a lower rate.

(c) HEP warheads are cheaper to manufacture than other types of projectiles.

(d) The accuracy of HEP warheads is comparable to or better than HE projectiles fired from the same weapon.

(e) The blast and fragmentation from HEP projectiles provide very desirable secondary effects against primary targets (armored vehicles).

(f) HEP warheads are effective in neutralizing secondary targets (fortifications, weapons, emplacements, personnel and non-armored vehicles).

2. Disadvantages are:

(a) HEP projectiles easily are defeated by means of spaced or spiked armor.

(b) HEP projectiles have a low ballistic coefficient because of their light weight and blunt head shape.

(c) The plastic explosive filler of HEP warheads must be press-loaded rather than cast, taxing limited press-loading facilities.

3-8.3 THEORY OF PERFORMANCE

When a charge of explosive is detonated in contact with a flat steel plate, the explosive energy is transmitted into the plate, normal to the surface. The shock wave produced in the steel is reflected from the rear surface of the plate as another shock wave. The shock waves meet at some line within the steel, and reinforce each other, though not simply additively, as with pure elastic stress waves. If the charge is sufficiently great (the height and shape of the explosive in contact with the plate being important parameters), the steel ruptures and a spall is driven off the rear side of the plate. This action is a result of a complex interaction of the reinforcement of shock waves and the elastic stress waves.

The squashed charge of the HEP warhead is most effective when it is in the form of a flat cone. Since the explosive charge must adhere closely to the surface and not break up, it cannot be crumbly, but must have soft plastic properties like putty which eliminates the use of cast explosives. The spalling effect is best produced with explosives that have a high detonation velocity.

One of the more serious limitations of the HEP warhead is its inability to function satisfactorily outside a range of striking velocities from approximately 1000 to 2000 fps. The maximum velocity limit exists because deflagration of the explosive filler occurs when HEP warheads are fired at velocities much above 2000 fps against armor plate with 0-deg obliquity. The minimum velocity limit exists because the functioning time of existing fuzes and projectile crush-up on the target are not properly coordinated at low velocities. This problem is compounded at low angles of obliquity because the projectile tends to skid-off the target before functioning. The minimum velocity limitation is a serious handicap in the development of HEP projectiles for some recoilless weapon systems.

The fuzing requirements for HEP warheads are that they should have sufficient delay time in fuze functioning to allow for proper projectile deformation. At high angles of obliquity, the delay is shorter than for low angles.

In the design of HEP warheads, it has been found that variations in nose material, nose shape, nose length, nose hardness, and nose thickness can have a marked effect on HEP projectiles performance. Because the explosive shape at time of detonation is very important in causing a spall, it was thought that a softer nose like annealed copper would be more suitable; but in actual tests, an annealed steel nose gave better results. Also, tests have shown that the blunt ogival nose, in addition to giving better explosive effects, also has better ballistic characteristics. In addition to having an ogival shape, it is preferable to have a long nose that will provide a greater contact area upon impact. Existing test data also have indicated that a thin nose gives better results than a thick nose.

3-8.4 GENERAL CONCLUSIONS

The following general conclusions have been drawn from testing HEP warheads:

1. If the charge weight is held constant, the weight of the spall displaced by cylindrical charges will increase as the charge diameter is increased, up to the point where the charge will have less than the minimum thickness required to displace spalls.
2. The area of a displaced spall is usually slightly greater than the area of the charge in contact with the plate.
3. Explosive charges in the shape of a conic frustum are more effective than an equal weight of explosive in cylindrical shape.
4. The most effective shape of a charge is a

frustum of a right circular cone. An oblique circular cone is not as effective.

5. Tough, ductile armor is spalled less readily than higher strength, more brittle armor. As the ductility of armor decreases, the extent of spalling and cracking of the parent metal increases. The difference in performance of armor of two degrees of toughness will be the greatest at lower temperatures. Weight and velocity of spall fragments increase with increasing brittleness of rolled homogeneous armor.

6. The spalling and cracking of rolled homogeneous armor increases as the temperature decreases.

3.9 OTHER TYPES OF WARHEADS

Other types of warheads which find use in recoilless rifle weapon systems are antipersonnel (APERS), incendiary, white phosphorus (WP), smoke, and chemical types.

The APERS or canister type warhead consists of a nonexplosive thin-walled shell loaded with a large number of small preformed missiles. The projectile is designed in such a manner that it breaks up under the action of centrifugal forces as it leaves the weapon muzzle, scattering the missiles in a cone-shaped pattern in front of the rifle in order to obtain a short-range lethal effect on personnel.

The incendiary type warhead contains a

projectile filler that will produce a high enough temperature to ignite any flammable material in the target or incapacitate personnel.

The WP type warhead is designed with a projectile that is very similar to that of the same size HE projectile. The projectile contains a filler of white phosphorus that produces a white cloud when dispersed from the projectile by a high explosive contained in a metal burster tube in the center of the projectile.

The smoke type warhead is again similar in configuration to the HE type projectile. The projectile contains steel canisters filled with a colored smoke composition that is ignited by quick-match in a flash tube which is in turn fired by a black powder initiator from the fuze. When the projectile functions, an ejection charge ejects the steel canisters and the burning dye composition is spread on the ground.

The chemical filled warheads are very similar in design to the WP type except that more rigid fits and tolerances are required to seal against the premature leakage of the contents. The design of the liquid-filled projectile burster casing is similar to the burster casing used in the WP projectile except that it is slightly larger to prevent the burster from whipping around inside the projectile. Sufficient charge is provided to open the projectile and disseminate the liquid, which is either in the form of a persistent or a nonpersistent gas.

REFERENCES

1. AMCP 706-245(C), Engineering Design Handbook, *Ammunition Series, Section 2, Design for Terminal Effects* (U).
2. AMCP 706-107, Engineering Design Handbook, *Elements of Armament Engineering, Part Two, Ballistics*.
3. AMCP 706-170 (S-NOFORN), Engineering Design Handbook, *Armor and Its Applications* (U).
4. AMCP 706-290 (C), Engineering Design Handbook, *Warheads-General* (U).

CHAPTER 4
EXTERIOR BALLISTICS

4-0 LIST OF SYMBOLS

A	= Siacci altitude function for fixed-fin projectiles, dimensionless	C_{M_α}	= static moment coefficient, rad^{-1}
a_o	= speed of sound in air at normal atmosphere conditions = 1120.27 fps	$C_{M_{p\alpha}}$	= magnus moment coefficient, rad^{-1}
C	= ballistic coefficient, lb-in^{-2}	$C_{M_\omega} + C_{M_{\dot{\alpha}}}$	= damping moment coefficient, rad^{-1}
C_D	= drag coefficient, dimensionless	C_N	= aerodynamic force coefficient associated with normal force, dimensionless
C_{D_f}	= wave drag coefficient, dimensionless	C_{N_p}	= aerodynamic force coefficient associated with magnus force, dimensionless
C_{D_o}	= drag coefficient at zero yaw, dimensionless	$C_{N_{p\alpha}}$	= magnus force coefficient, rad^{-1}
C_{D_f}	= drag coefficient of a known projectile design, dimensionless	C_{N_α}	= normal force coefficient, rad^{-1}
C_{D_α}	= $\frac{dC_D}{d(\alpha^2)}$ = rate of change of C_D with α^2 , rad^{-2}	c.p.	= center of pressure
CG	= distance from projectile base to center of gravity, cal	CP	= distance from projectile base to center of pressure, cal
c.g.	= center of gravity	D	= drag force, lb
C_L	= aerodynamic force coefficient associated with lift force, dimensionless	d	= maximum body diameter of projectile, ft
C_{L_α}	= lift coefficient, rad^{-1}	$G(u)$	= drag function $\text{lb}-(\text{in}^2\text{-sec})^{-1}$
		g	= acceleration due to gravity, ft-sec^{-2}

H	$= \frac{\rho S d}{2m} \left[C_{L\alpha} - C_D - \frac{C_{M\omega} + C_{M\dot{\alpha}}}{k_t^2} \right]$	p_e	= equilibrium roll rate, rad-sec ⁻¹
	dimensionless	p_r	= resonance roll rate, rad-sec ⁻¹
h	= altitude Siacci equation in ⁴ -ft-lb ⁻²	q	= dynamic pressure, psf
I	= Siacci inclination function for fixed-fin projectiles, dimensionless	q_1	= inclination, Siacci equation, in ² -lb ⁻¹
I_x	= axial moment of inertia, slug-ft ²	R	= range, yd
I_y	= transverse moment of inertia, slug-ft ²	r_m	= retardation of projectile, sec ⁻¹
i	= (-1) ^{1/2} ; in complex notation indicates rotation by 90 deg	S	= projectile frontal area, ft ²
i_t	= form factor, dimensionless	S_1	= Siacci space function for fixed-fin projectiles, dimensionless
k_a	= axial radius of gyration, cal	s_d	= dynamic stability factor, dimensionless
k_t	= transverse radius of gyration, cal	s_{d_0}	= dynamic stability factor for $\lambda_{max} \leq 0$, dimensionless
L	= lift force, lb	s_g	= gyroscopic stability factor, dimensionless
M	= Mach number, dimensionless	T	$= \frac{\rho S d}{2m} \left[C_{L\alpha} + \frac{C_{M p \alpha}}{k_a^2} \right]$
M_y	= total moment about a horizontal axis through projectile c.g., ft-lb	T_1	= Siacci time function function for fixed-fin projectiles, dimensionless
m	= projectile mass, slug	t	= time, sec
N	= normal force, lb	t_1	= Siacci time equation, in ² -sec-lb ⁻¹
N_p	= magnus force, lb	t_f	= time of flight, sec
p	= roll (spin) rate, rad-sec ⁻¹	U	= upper limit of integration for a specific projectile type, Siacci equation, fps
p_1	= space Siacci equation, in ² -ft-lb ⁻¹		

u	= argument of Siacci functions: component along the line of departure of the velocity relative to air, fps	δ_y	= yaw angle of repose, rad
V	= projectile speed relative to an inertial coordinate system, fps	ϵ	= half angle of nose cone, deg
V_m	= muzzle velocity, fps	λ_1	= nutational damping exponent, dimensionless
V_t	= terminal velocity, fps	λ_2	= precessional damping exponent, dimensionless
V_x	horizontal component of velocity, fps	μ	= static moment factor, (ft-lb)-rad ⁻¹
W	= projectile weight, lb	θ_j	= aerodynamic jump angle, rad
x	= displacement along x-axis, ft	θ	= angle between horizontal (x-axis) and velocity vector, rad
\dot{x}	= velocity along x-axis, fps	ρ	= air density, slug-ft ⁻³
\ddot{x}	= $\frac{d^2x}{dt^2}$, ft-sec ⁻²	ρ'	= air density, lb-ft ⁻³
z	= displacement along z-axis, ft	ϕ	= angle of elevation, mil
\dot{z}	= velocity along z-axis, fps	ω	= angular velocity about horizontal axis when $\alpha = 0$
\ddot{z}	= $\frac{d^2z}{dt^2}$, ft-sec ⁻²		
α	= angle of yaw, vertical component, rad		
$\dot{\alpha}$	= yawing velocity about horizontal axis, rad-sec ⁻¹	B	= body
β	= angle of yaw, horizontal component, rad	i	= dummy index (to be replaced by a sequence of specific indices when the subscripted quantity is to be used in a computation)
λ	= $\rho_0' i_t d^2 / W$, ft ⁻¹	m	= muzzle condition
δ	= total angle of yaw, rad	o	= initial condition or zero yaw value
$\dot{\delta}_o$	= initial yawing velocity, rad-sec ⁻¹	T	= tail or terminal

SUBSCRIPTS

SECTION I

INTRODUCTION

4-1 SCOPE

Exterior ballistics describes the motion of the projectile from muzzle exit to point of impact. The complete theory of exterior ballistics includes only those effects that are of primary interest in the design of recoilless rifle ammunition, i.e., rounds normally of caliber 57 to 120 mm in size that are launched at muzzle velocities up to approximately 2000 fps.

There are two major considerations in the exterior ballistic design of an accurate projectile: (1) the projectile must be stable in flight, i.e., the projectile must be designed to prevent tumbling and limit yaw to small angles, and (2) given the initial conditions, the trajectory of the projectile must be determined.

These two considerations, *stability* and *trajectory calculations*, comprise the major portion of this chapter. These subjects will be supplemented by a discussion of aerodynamic coefficients and other basic material.

4-2 WEAPON SYSTEM INTERACTION

Exterior ballistic factors directly influence the accuracy of the weapon system. To illustrate, the accuracy of a conceptual projectile having a perfectly flat trajectory and zero time of flight is limited only by the accuracy of the sighting device. However, as the time of flight increases, crosswinds and other meteorological effects interact significantly with the projectile; and, further, as the trajectory is elevated, range estimation errors are introduced. In order to minimize these errors, the exterior ballisticians is concerned

with the projectile weight and mass distribution, shape, and muzzle velocity.

4-3 QUALITATIVE DESCRIPTION

The final result of exterior ballistic calculations is a trajectory describing the position of the projectile center of mass as a function of time when fired with a given muzzle velocity and superelevation angle—the angle between the gun axis and the line of sight to the target. Calculation of the trajectory is a routine computer operation, provided projectile drag is known. The FORTRAN particle trajectory program presented in Ref. 1 is an example of such a computer program. However, before making trajectory calculations, the projectile must be stabilized to assure that it will not tumble or yaw excessively during flight. There are two methods of aerodynamic stabilization: (1) gyroscopic stabilization, i.e., spinning the projectile, and (2) fin stabilization. The mass distribution determining the location of the center of gravity and the shape determining the location of the center of pressure are critical in both of these methods.

The theory is well established and stability and trajectory calculations can be made, provided the forces acting on the projectile are known. These forces are expressed in terms of aerodynamic coefficients which are discussed in Section II.

In brief, the projectile is stabilized by adjustment of the mass distribution (location of center of gravity), by adjustment of the external shape (location of center of pressure), and in some cases, by the spin rate of the projectile. The designer then minimizes

drag to obtain the "flattest" and shortest time-of-flight trajectory. Optimization also involves maximizing both the muzzle velocity and sectional density (mass per unit cross-sectional area) of the projectile, subject to constraints on the overall cartridge weight, recoil momentum, peak pressure, cartridge profile, and charge-to-mass ratio.

sectional area) of the projectile, subject to constraints on the overall cartridge weight, recoil momentum, peak pressure, cartridge profile, and charge-to-mass ratio.

SECTION II

AERODYNAMIC FORCES AND MOMENTS

4-4 GENERAL

The aerodynamic forces on a projectile are determined by the pressure distribution existing over the entire projectile exterior. In order to simplify their measurement and mathematical use, the distributed aerodynamic forces are grouped into a specified set of resultant forces. The set of (resultant) forces and moments which have a significant effect on the projectile motion is composed of

1. Normal force
2. Lift
3. Drag
4. Magnus force
5. Static moment
6. Damping moment
7. Magnus moment
8. Roll damping moment.

4-5 AERODYNAMIC FORCES

4-5.1 NORMAL, LIFT, AND DRAG FORCES

The resultant of the pressure forces on a symmetrical nonspinning projectile lies in the plane containing the tangent to the trajectory and the longitudinal axis of the projectile, called the "yaw plane"; the point on the

projectile axis through which this resultant passes is called the center of pressure of the lift or normal force, since the resultant may be resolved either into lift and drag components, or into normal force and axial drag. Lift is parallel to the y, z -plane, drag is parallel to the x -axis; normal force is perpendicular to, and axial drag is in line with, the axis of the projectile. Each possible pair of components lies, of course, in the yaw plane (Ref. 1). Definition of axis is as given in Fig. 4-1.

4-5.2 MAGNUS FORCE

When a projectile is spinning about its longitudinal axis, the pressure distribution over its surface is altered so that the resultant force no longer lies in the plane of yaw. This is resolved by introducing a force component normal to the yaw plane, together with its associated moment. This force, called the "magnus force", is also perpendicular to the longitudinal axis of the projectile, and passes through its own center of pressure. Vector subtraction of the magnus force from the total force on the projectile leaves a force in the yaw plane, which can be resolved into lift and drag (Ref. 1).

4-6 AERODYNAMIC MOMENTS

4-6.1 STATIC MOMENT

The static moment is the product of the normal force and the distance between its c.p. and the c.g. of the projectile, which is considered positive when the c.p. is forward of the c.g. as it practically always is for

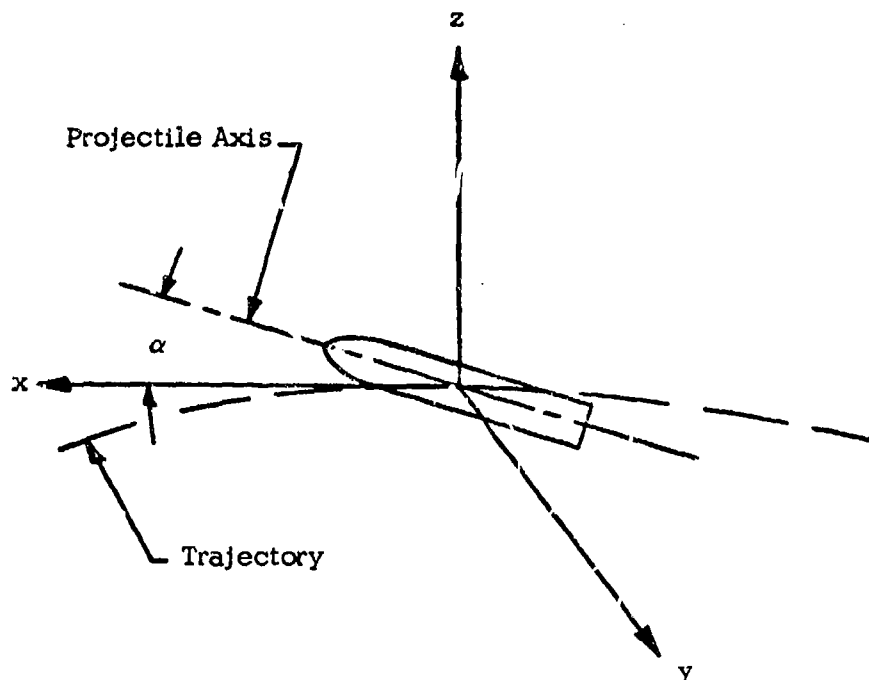


Figure 4-1. Coordinate System

spin-stabilized projectiles. The axis of this moment is a transverse axis through the c.g., normal to the yaw plane. Fin-stabilized projectiles have the c.p. aft of the c.g., so that the static moment opposes an increase in yaw (in normal flight), and can be called a "restoring moment" (Ref. 1).

4-6.2 DAMPING MOMENT

Yaw varies continuously throughout the projectile flight, and, as this angle is changing, the projectile swings about its c.g. This action changes the pressure distribution on the projectile so as to produce a couple about an axis through the c.g. normal to the plane of the yawing velocity (which is not necessarily the plane of yaw). This couple is called the "damping moment" and usually opposes the yawing velocity (Ref. 1).

4-6.3 MAGNUS MOMENT

The magnus force produces a moment

about an axis through the c.g., parallel to the normal force. This magnus moment changes the yawing velocity in a manner depending on the location of the c.p. of the magnus force and its direction. Because the magnus force and moment result from the projectile spin, they are absent on a nonrotating projectile. However, the complete absence of magnus effects on fin-stabilized projectiles generally cannot be stated since fin-stabilized projectiles often are given a slow stabilizing spin.

4-6.4 ROLL DAMPING MOMENT

As defined in Ref. 1, the roll damping moment is a couple about the longitudinal axis of the projectile and, for a spinning body, is related to the friction between projectile and air. Fins produce larger roll damping moments owing to the angle of attack produced by the spin.

4-7 FORCE AND MOMENT COEFFICIENTS

Aerodynamic forces and the static moment have been found to be proportional to the projectile dimensions, to the dynamic pressure of the air, and to the projectile yaw. In addition, the three moments arising from projectile rotation are also proportional to their appropriate angular velocities. The factors of proportionality which relate these quantities are known as "aerodynamic coefficients". These coefficients are not constant for a given projectile, but are functions of Mach number, Reynolds number, spin rate, and yaw as described in pars. 4-7.1 and 4-7.2.

4-7.1 AERODYNAMIC FORCE COEFFICIENTS

The most significant of the aerodynamic force coefficients are defined as follows:

$$C_N = N/(qS) \quad (4-1)$$

$$C_L = L/(qS) \quad (4-2)$$

$$C_D = D/(qS) \quad (4-3)$$

$$C_{N_p} = \frac{N_p}{qS\left(\frac{pd}{V}\right)} \quad (4-4)$$

where

C_N = aerodynamic force coefficient associated with the normal force, dimensionless

C_L = aerodynamic force coefficient associated with the lift force, dimensionless

C_D = drag coefficient, dimensionless

C_{N_p} = aerodynamic force coefficient associated with magnus force, dimensionless

q = dynamic pressure, $\rho V^2/2$, psf
(4-5)

S = $\pi d^2/4$, frontal area of the projectile
(4-6)

N = normal force, lb

L = lift, lb

D = drag, lb

N_p = magnus force, lb

ρ = air density, slug-ft⁻³

V = speed of projectile relative to air, fps

p = roll rate, rad-sec⁻¹

d = maximum body diameter of projectile, ft

The coefficients defined in Eqs. 4-1 through 4-4 are expected to be functions of the yaw angle α , measured in radians. For small yaw angles ($\alpha < 0.17$ rad), all of the aerodynamic force coefficients can be assumed to vary linearly with yaw. This assumption leads to the use of a curve of coefficient vs yaw angle as a more convenient description of the characteristics of the projectile. Eqs. 4-1, 4-2, and 4-4 then can be written in the following form:

$$N = \left(\frac{dC_N}{d\alpha}\right)qS\alpha = C_{N_\alpha}qS\alpha, \text{ lb} \quad (4-7)$$

$$L = \left(\frac{dC_L}{d\alpha}\right)qS\alpha = C_{L_\alpha}qS\alpha, \text{ lb} \quad (4-8)$$

$$N_p = \frac{dC_{N_p}}{d\alpha}qS\left(\frac{pd}{V}\right)\beta = C_{N_{p\alpha}}qS\left(\frac{pd}{V}\right)\beta \quad (4-9)$$

where

$$C_{N_\alpha} = \frac{dC_N}{d\alpha} = \text{normal force coefficient, rad}^{-1}$$

$$C_{L_\alpha} = \frac{dC_L}{d\alpha} = \text{lift coefficient, rad}^{-1}$$

$$C_{N_{p\alpha}} = \frac{dC_{Np}}{d\alpha} = \text{magnus force coefficient, rad}^{-1}$$

$$\alpha = \text{yaw angle, rad}$$

For the sake of simplicity, the symbol α has been used for the yaw angle. As indicated in the notation of Ref. 1, α is the component of the yaw angle in the vertical direction; the component in the horizontal direction given as β , and the total yaw angle δ given by

$$\delta = \beta + i\alpha \quad (4-10)$$

where $i = \sqrt{-1}$, the unit vector in the complex plane. Orientation of the yaw is then $\text{Tan}^{-1}(\alpha/\beta)$. The aerodynamic coefficients can be defined in terms of α because of the rotational symmetry of the projectile, and their values derived from measurements made on a model that is given a yaw in one place, identified as the α -plane.

As indicated earlier in this paragraph, the drag coefficient C_D does not vary linearly with yaw. It has been found that drag D varies with the square of the yaw, so that

$$D = (C_{D_0} + C_{D_{\alpha^2}}\alpha^2) qS \quad (4-11)$$

where

$$C_{D_0} = \text{drag coefficient at zero yaw, dimensionless}$$

$$C_{D_{\alpha^2}} = \text{rate of change of } C_D \text{ with } \alpha^2, \text{ rad}^{-2}$$

4-7.2 MOMENT COEFFICIENTS AND MOMENTS

The moments produced by the aerodynamic forces are referred to the center of gravity of the projectile except as indicated herein. In the terminology of this handbook, the moment coefficients are derivatives with respect to yaw, or with respect to the appropriate angular velocities. The moment coefficients of primary importance are:

1. Static Moment Coefficient C_{M_α}

$$C_{M_\alpha} = \frac{dC_M}{d\alpha}, \text{ rad}^{-1} \quad (4-12)$$

2. Damping Moment Coefficient

$$C_{M_\omega} + C_{M_{\dot{\alpha}}} = \frac{1}{\frac{1}{2}\rho V^2 S d} \left[\frac{\partial M_y}{\partial \left(\frac{\omega d}{V}\right)} + \frac{\partial M_y}{\partial \left(\frac{\dot{\alpha} d}{V}\right)} \right], \text{ rad}^{-1} \quad (4-13)$$

where

$$\dot{\alpha} = \text{yawing velocity about the horizontal axis, rad-sec}^{-1}$$

$$\omega = \text{angular velocity about the horizontal axis when } \dot{\alpha} = 0; \text{ i.e., the total angular velocity about the horizontal axis is } \omega + \dot{\alpha}, \text{ rad-sec}^{-1}$$

$$M_y = \text{total moment about a horizontal axis through the c.g., ft-lb}$$

3. Magnus Moment Coefficient $C_{M_{p\alpha}}$

$$C_{M_{p\alpha}} = \frac{dC_{M_p}}{d\alpha}, \text{ rad}^{-1} \quad (4-14)$$

In coefficient form, the total moment M_y about a horizontal axis through the projectile is given by

$$M_y = \frac{1}{2}\rho V^2 S d \left[C_{M_\alpha} \alpha + C_{M_\omega} \left(\frac{\omega d}{V}\right) + C_{M_{\dot{\alpha}}} \left(\frac{\dot{\alpha} d}{V}\right) + C_{M_{p\alpha}} \left(\frac{p d}{V}\right) \beta \right] \quad (4-15)$$

4-8 DETERMINATION OF AERODYNAMIC COEFFICIENTS

The aerodynamic coefficients can be measured by ballistic range testing or wind tunnel testing. In the typical situation, the recoilless rifle designer is interested in estimating the value of the coefficients for preliminary system design purposes. These

preliminary estimates can be verified and adjusted by actual measurements at a later stage in the system development. The methods of estimating the aerodynamic coefficients are based on interpolation of measurements on existing projectiles and on theoretical calculations. For methods of estimating the various aerodynamic coefficients, the reader is referred to the material found in Ref. 1.

SECTION III

PROJECTILE STABILITY

4-9 INTRODUCTION

Projectile stability relates to the ability of the projectile to quickly reduce the initial yaw to a small value and thus minimize drag and drift. Several stability criteria must be considered. If the projectile is neither *statically* nor *gyroscopically* stable, it will tumble immediately after muzzle exit and be inaccurate.

If it is *dynamically* unstable, the initial yaw will increase with time and the projectile will eventually tumble. In this section, equations are presented for evaluating the various stability criteria of a proposed projectile design.

The material in this section is presented in greater detail in Ref. 1.

4-10 BASIC STABILITY CONSIDERATIONS

As stated in Section II, the aerodynamic forces acting on a projectile can be grouped into a specific set of resultants. These resultants have both magnitude and direction, and also a point of application on the body, i.e., a point through which the resultant acts. This point, called the center of pressure c.p. of the force in question, is assumed to lie in the longitudinal axis of the projectile, while its position along the longitudinal axis depends on the shape of the projectile, the projectile airspeed (Mach number), axial spin rate, and, unfortunately, sometimes on the magnitude of the yaw (Ref. 1).

The c.p. of the lift forces is assumed to be independent of the yaw angle. This assump-

tion is made possible by considering only linear projectile behavior in which yaw seldom exceeds 10 deg. Since the purpose of a good design is to keep the yaw below 5 deg, the assumption of linear projectile behavior is validated further when this design criterion is achieved. However, the c.p. of the Magnus forces will exhibit appreciable movement when the yaw angle changes as much as 10 deg.

The position of the c.p. relative to the projectile c.g. is an important measurement of the projectile stability. A projectile will be statically stable if the c.p. is aft of the c.g., i.e., any yaw of the projectile produces a moment about the c.g. which tends to return the axis of the projectile to the zero-yaw position. If the c.p. is ahead of the c.g., the normal force produces an overturning moment tending to increase the yaw, and the projectile is said to be statically unstable. The statically unstable projectile can be stabilized by either spinning or adding fins to the projectile. By spinning the projectile rapidly about its own axis, the yaw will not grow and the projectile is said to be gyroscopically stable, even though it is still statically unstable. Addition of fins to the rear part of the projectile body moves the c.p. rearward of the c.g. and the fin-stabilized projectile becomes statically stable. Further aspects of the fin- vs spin-stabilization consideration are described in pars. 4-11 and 4-12.

4-11 SPIN STABILIZATION

4-11.1 GYROSCOPIC STABILITY

If the projectile is given sufficient spin, the

yaw angle will be small even though the projectile is statically unstable. This is analogous to the spinning top which remains upright only when the spin rate is sufficiently large. The condition for stability is expressed in terms of the gyroscopic stability factor s_g as follows:

$$s_g = \frac{I_x^2 p^2}{4 I_y \mu}, \text{ dimensionless} \quad (4-16)$$

where

I_x = axial moment of inertia, slug-ft²

I_y = transverse moment of inertia, slug-ft²

p = axial angular velocity, rad-sec⁻¹

μ = static moment factor, lb-ft-rad⁻¹

Assuming that the static moment μ varies linearly with yaw, one obtains:

$$\mu = \frac{\pi}{8} \rho d^3 V^2 C_{M_\alpha}, \text{ (ft-lb)-rad}^{-1} \quad (4-17)$$

where

ρ = air density, slug-ft⁻³

d = maximum body diameter, ft

V = airspeed, fps

C_{M_α} = static moment coefficient, rad⁻¹

If s_g is less than unity, the projectile will tumble within a few hundred feet of the muzzle. If s_g is greater than one, the projectile is gyroscopically stable and dynamic stability must be investigated as described in par. 4-11.3. To allow for variations in air density and other factors, a value of s_g of about 1.3 usually is desired for the preliminary design stages. However, since most projectiles lose airspeed faster than spin rate, the value of s_g increases with flight time. Note that s_g depends on the ratio $(p/V)^2$ and p/V depends

only on the rifling twist, i.e., the spin rate p increases with muzzle velocity and p/V is constant for a given twist. Thus, to a first approximation, gyroscopic stability is independent of muzzle velocity and depends only on rifling twist at the muzzle.

4-11.2 YAW OF REPOSE

During the flight of a spin-stabilized projectile, the angle between the tangent to the trajectory and the direction of the longitudinal axis of the projectile quietes down to a nearly constant yaw, called the yaw of repose. The equilibrium condition is generated when the gravity curvature of the trajectory gives rise to an angle of yaw large enough to create a precession rate that permits the projectile axis to follow the tangent to the trajectory. If the projectile spin is clockwise when viewed from the rear, the equilibrium requirement causes the projectile to point to the right of its flight path (right-hand yaw of repose). This yaw angle generates a lift force that causes the projectile to drift to the right.

An approximate expression for the right hand yaw of repose δ_r is

$$\delta_r = \frac{I_x p g \cos \theta}{\frac{1}{2} \rho S d C_{M_\alpha} V^3} \left[1 + i \left(\frac{C_{M_{p\alpha}}}{C_{M_\alpha}} \right) \frac{p d}{V} \right], \text{ rad} \quad (4-18)$$

where

g = acceleration due to gravity, ft-sec⁻²

θ = angle between the horizontal and velocity vector, rad

An analysis of the first (and most significant) term on the right side of Eq. 4-18 helps to explain the mechanism by which a spinning projectile "trails" as it moves along its trajectory. Multiplying both sides of Eq. 4-18 by $\rho S d C_{M_\alpha} V^2 / 2$ gives

$$\frac{1}{2} \rho V^2 S d C_{M_\alpha} \delta_r = I_x p \left(\frac{g \cos \theta}{V} \right) (1 + \dots) \quad (4-19)$$

The left side of Eq. 4-19 is the static aerodynamic moment. The first term of the right side of Eq. 4-19 is the product of the axial angular momentum $I_x p$ and the rate of change of direction of the tangent to the trajectory $(g \cos \theta)/V$. As explained in Ref. 1, Eq. 4-19 now states that the aerodynamic moment arising from the yaw of repose is just sufficient to change the angular momentum of the projectile at the rate required for the axis of the projectile to remain tangent to the trajectory (in the vertical plane the yaw is in a plane normal to the trajectory plane and the static moment is at right angles to the rotation, or precession, of the projectile axis, which is the well known gyroscopic behavior).

4-11.3 DYNAMIC STABILITY

A spinning projectile has a gyroscopic motion similar to a spinning top. The spin axis of the projectile has a precessional and nutational damping exponent λ_1 and a precessional damping exponent λ_2 . If the associated exponent λ_i ($i = 1, 2$) is positive, the amplitude of motion increases with time and the projectile eventually will tumble even though it is statically stable. If the associated λ_i is negative, the motion is damped and reduces to zero. For dynamic stability both λ_1 and λ_2 must be equal to or less than zero. The analysis of dynamic instability is particularly difficult since, for example, a small dynamic instability might be tolerated for a short time of flight. A complete analysis of dynamic instability requires a sophisticated computer program. However, for preliminary design purposes, a dynamic stability factor s_d can be examined. In Ref. 1 the damping exponents are defined as follows:

$$\lambda_1 = - (1/2) \left[H - \frac{2T - H}{\sqrt{1 - 1/s_g}} \right],$$

dimensionless (4-20)

$$\lambda_2 = - \lambda_1, \text{ dimensionless} \quad (4-21)$$

where

$$H = \frac{\rho S d^2}{2m} [C_{L\alpha} - C_D - k_t^2 (C_{M\omega} + C_{M\alpha})],$$

dimensionless

$$T = \frac{\rho S d}{2m} [C_{L\omega} + k_t^2 C_{M\omega}], \text{ dimensionless}$$

$$k_t = \text{transverse radius of gyration,} \\ = [I_y / (m d^2)]^{1/2}, \text{ dimensionless}$$

$$k_a = \text{axial radius of gyration,} \\ = [I_x / (m d^2)]^{1/2}, \text{ dimensionless}$$

$m = \text{projectile mass, slug}$

Instead of simply requiring that λ_1 and λ_2 be nonpositive for stability, it is possible to set an upper limit on the greater of the two exponents which must not be exceeded if the projectile is to remain stable. This limit, represented by an unsubscripted λ , may be greater than zero because some growth of initial yaw may be tolerable, especially in short flights (Ref. 1).

With the use of λ , the dynamic stability factor s_d can be defined (Ref. 1) by

$$s_d = \frac{2T + 2\lambda}{H + 2\lambda}, \text{ dimensionless} \quad (4-22)$$

In practice λ is often set equal to zero, and the stability factor for $\lambda_{max} \leq 0$, s_{d_0} becomes

$$s_{d_0} = \frac{2T}{H} = \frac{2(C_{L\alpha} + k_a^2 C_{M\omega})}{C_{L\alpha} - C_D - k_t^2 (C_M + C_{M\alpha})} \quad (4-23)$$

In Ref. 1, it is shown that stable values of s_d are related to values of the gyroscopic stability factor s_g as:

$$\frac{1}{s_g} = s_d (2 - s_d) \quad (4-24)$$

This relation is plotted in Fig. 4-2 which shows the span of acceptable values of s_d as a function of $1/s_g$.

4-11.4 AERODYNAMIC JUMP OF SPIN-STABILIZED PROJECTILES

Ideally, the path of the projectile at muzzle exit coincides with the bore-sight of the gun. In practice, the projectile path deviates from

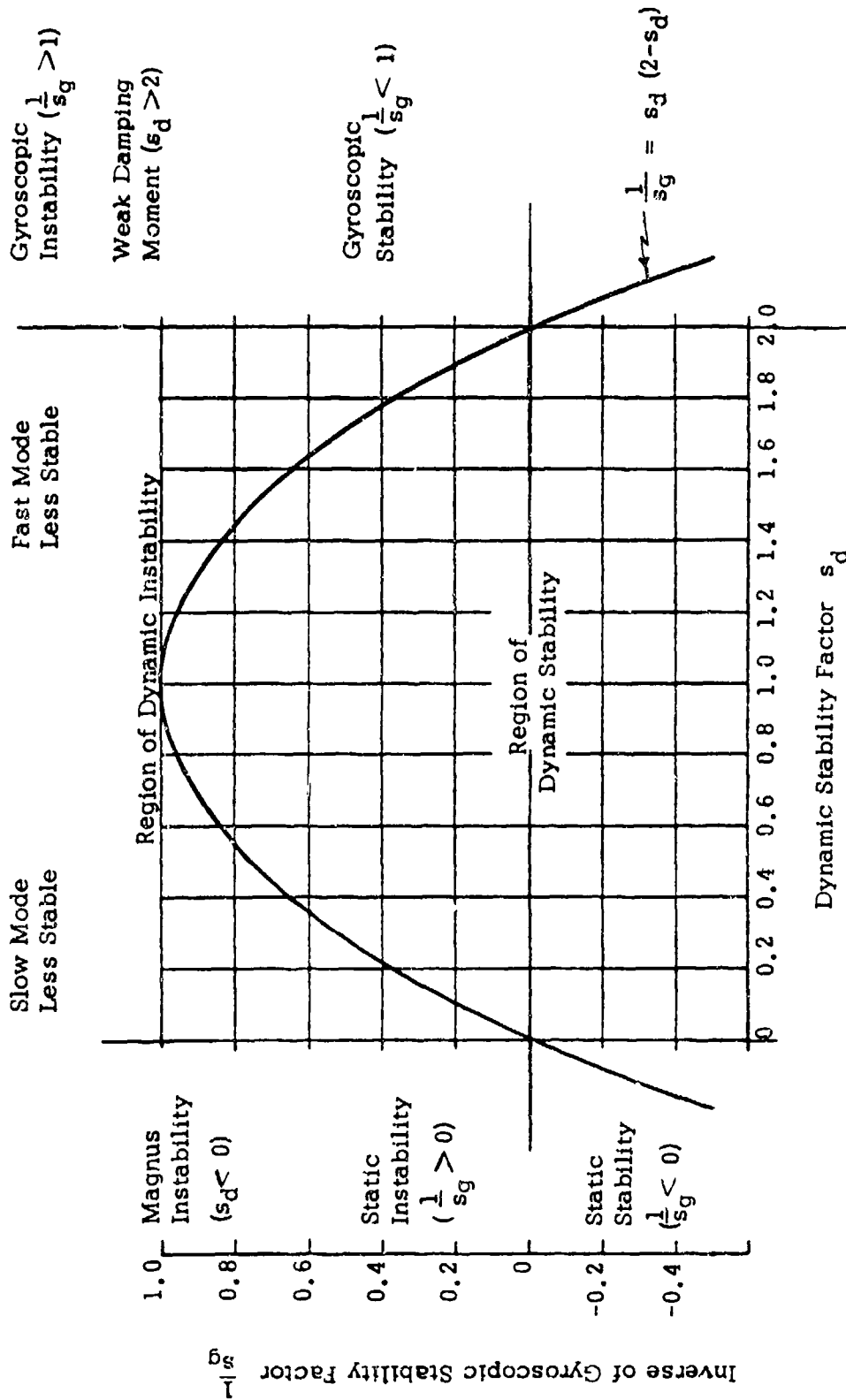


Figure 4.2. Graph of $1/s_g$ vs s_d (Ref. 1)

the gun bore-sight due to gravity, wind, drift, and aerodynamic jump. Aerodynamic jump is defined as the deviation angle that remains after the effects of gravity, wind, and drift have been eliminated. It includes such effects as balloting, poor obturation, motion of the gun tube, projectile asymmetries, and the effects of muzzle blast. The angle of jump θ_j —to a close approximation—is given in complex form by

$$\theta_j = \frac{C_{L\alpha} d}{C_{M\alpha} V_o} (k_1^2 \dot{\delta}_o - i k_2^2 p_o \delta_o), \text{ rad} \quad (4-25)$$

where

V_o = projectile velocity, fps	}	measured at the end of the blast zone
$\dot{\delta}_o$ = yawing velocity, rad sec ⁻¹		
p_o = spin rate, rad-sec ⁻¹		
δ_o = yaw, rad		

Note that Eq. 4-25 describes two components of the jump angle θ_j .

4-12 FIN STABILIZATION

4-12.1 INTRODUCTION

The usual projectile body is not statically stable, i.e., the center of pressure is forward of the center of gravity of the body. By addition of fins rearward of the c.g., the c.p. is moved rearward of the c.g. and the projectile is made statically stable. If, when the fin-stabilized projectile is yawed, the moment produced by the lift forces acting on the fins is greater than the moment produced by the forces acting on the body, the net moment will oppose the yaw and the projectile will be statically stable. In symbolic notation, the stability of a fin-stabilized projectile is defined in terms of aerodynamic moment coefficients as follows:

$$C_{N\alpha} = C_{N\alpha B} + C_{N\alpha T} \quad (4-26)$$

$$C_{M\alpha} = C_{N\alpha B} (CP_B - CG) + C_{N\alpha T} (CP_T - CG) \quad (4-27)$$

$$CP - CG = \frac{C_{M\alpha}}{C_{N\alpha}} \quad (4-28)$$

NOTE: No subscript refers to the overall projectile; subscript *T* refers to the tail; subscript *B* refers to body alone; and the distances from the projectile base to the center of pressure and center of gravity, *CP* and *CG*, respectively, are measured in calibers.

For a statically stable projectile, *CP - CG* is negative, but this quantity usually is treated by its absolute value and referred to as the "CP - CG separation" in units of calibers. Although an optimum magnitude of the *CP - CG* separation is not well-defined, certain limits have been established. The *CP - CG* separation should be far enough above 0.5 cal so that any inaccuracies in estimating $C_{M\alpha}$ and $C_{N\alpha}$ will not cause the *CP - CG* separation to fall below 0.5 cal. On the other hand, *CP - CG* separations above 1.0 cal have been found to increase the dispersion at the target (Ref. 1).

4-12.2 FIN TYPES

The choice of a specific fin type is a trade-off problem involving the utilities of projectile volume, range, accuracy, and cost. The effects of these design criteria on the fin type selection and the overall effect of fin-stabilization on obturation are described briefly in this paragraph.

Fixed fins of one caliber span are easy to make with a high degree of uniformity; this promotes accuracy. However separation is required between the leading edge of the fin and the location of the full body diameter of the projectile in order to permit the air stream to expand and flow over the fin surfaces to develop the expected lift.

Folding fins are bunched behind the projectile when in the gun tube and then fan out to a more than one caliber span after the projectile has left the muzzle blast. Folding fins can produce large $CP - CG$ separations, but are expensive and conducive to large projectile asymmetry. However, they do not reduce the projectile volume-to-length ratio (an important drag consideration) as much as fixed fins.

While fin-stabilization of either type results in a larger and more expensive projectile, the reasons for using fin- instead of spin-stabilization are

1. Shaped charge penetration is degraded by spin.
2. The internal structure of the projectile may be such that it cannot be made gyroscopically stable.
3. Projectile is fired from a smooth bore gun.

4-12.3 DYNAMIC STABILITY

As discussed in par. 4-10, a projectile is said to be dynamically stable if its transient yaw does not increase during flight. Statically stable fin-stabilized projectiles having zero spin are always dynamically stable. However, a condition of zero spin almost never exists since manufacturing tolerances permit some slight twist of the fins that results in a spin producing torque. In fact, zero spin is undesirable, because the lift produced by the projectile asymmetry will steer the projectile away from its predicted trajectory.

The effects of the projectile asymmetry on the trajectory can be minimized by giving the projectile a slow roll called a slow spin. The desired slow roll is much smaller than the spin rates given to spin-stabilized projectiles, and often is produced by "canting" the fins. Computation of this equilibrium roll rate is

described in detail in Ref. 1. It is important to have a good estimate of the equilibrium spin rate. In other words, the spin rate should be kept low enough to avoid magnus effects as described in par. 4-12.5.

4-12.4 AERODYNAMIC JUMP OF FIN-STABILIZED PROJECTILES

The material presented on aerodynamic jump in par. 4-11.4 applies without change to fin-stabilized ammunition except that the drift of a fin-stabilized projectile is kept small by rolling the projectile slowly. However, a very good design is required in order for the fin-stabilized projectile to achieve the same low level of aerodynamic jump as that of a spin-stabilized projectile fired in the same gun.

Since $CP - CG \approx C_{M\alpha} / C_{L\alpha}$ for small angles of yaw, it is seen from Eq. 4-25 that the aerodynamic jump angle θ_j can be reduced by increasing the $CP - CG$ separation. If the increase in the $CP - CG$ separation is achieved by increasing the moment coefficient of the tail (by greater fin area or a longer boom), the initial yawing velocity δ_o is also increased due to the increased effectiveness of the fins in the reversed flow of the blast zone. If the increase in y_o is greater than the increase in $CP - CG$ separation, the aerodynamic jump will be increased and not decreased by the change of $CP - CG$ separation.

By changing the shape of projectile body, it is possible to move the c.p. of the normal force rearward. This change can increase the $CP - CG$ separation of the whole projectile with little or no change in the tail moment. However, if this body change is made by substituting a spike for the ogive, the drag will be increased.

It is noted again that aerodynamic jump has been discussed only for dynamically stable projectiles where δ_o and the $CP - CG$ separation are of primary interest. Fin-stabi-

lized projectiles that are statically stable are also dynamically stable unless they have an unusually high roll rate (Ref. 1).

4-12.5 MAGNUS STABILITY

As stated in Ref. 1, an unbalanced side force can be created on a slowly rolling, fin-stabilized projectile when the projectile is yawed and the body blankets the leeward fins. This force, identified as a magnus force, and its associated moment can be as large as the magnus force and moment acting on a spin-stabilized projectile. If the fins are canted, the fin lift, upon reaching an equilibrium spin, acts in opposite directions on the in-board and outboard fins sections, leading to a nonlinear magnus moment with yaw.

In any case, the magnus moment coefficients of fin-stabilized projectiles are less predictable than those of spin-stabilized projectiles. Thus, it is wise to allow as great a margin of dynamic stability as possible without falling into resonance instability, which is discussed in par. 4-12.6.

4-12.6 RESONANCE INSTABILITY

If either the nutational frequency or precessional frequency is nearly equal to the projectile spin frequency, the magnitude of the yaw due to any projectile asymmetry can become very large. The similarity of this phenomenon to a spring-mass system subjected to an external alternating force has led to the use of the term "resonance instability" as a label for this type of yaw increase. The increase in yaw, unlike the growth of the amplitude of an ordinary spring-mass system, is bounded not so much by the damping in the system as by its nonlinearity. The resonant yaw of a projectile may become

large enough to cause loss of range and accuracy through large drag increases, but not so large as to cause the projectile to tumble. While both spin- and fin-stabilized projectiles theoretically can experience coincidence of spin and yaw frequencies, this phenomenon is much more likely to occur in fin-stabilized projectiles.

In Ref. 1, it is shown that the spin rate which results in this objectionally large yaw angle, identified as the resonance roll rate p_r , can be estimated by

$$p_r = \sqrt{\frac{-\mu}{I_y - I_x}} \text{ rad-sec}^{-1} \quad (4-29)$$

where

$$\mu = qSdC_{M\alpha}, \text{ static moment factor,} \\ (\text{ft-lb})\text{-rad}^{-1}$$

Eq. 4-29 indicates that when I_y is greater than I_x , which is always the case, μ must be negative for resonance, i.e., only statically stable ($C_{M\alpha} < 0$) projectiles can exhibit resonance instability.

The equilibrium roll rate p_e must be designed to avoid the resonance value p_r . If the projectile has zero spin at muzzle exit, the value of p_e should be made sufficiently high so that the spin rate will quickly pass through the value p_r . A ratio of three for p_e/p_r is considered desirable. It also is recommended that the obturator (see Chapter 11, par. 11-12) be designed to produce a spin rate at the muzzle exit greater than p_r and thus avoid passing through the resonance spin rate in flight. This avoids the phenomenon of "roll lock-in" in which the spin rate "locks in" at the resonant frequency rather than increasing to the designed equilibrium spin rate.

SECTION IV

AERODYNAMIC DRAG

4-13 GENERAL

The drag force D was given by Eq. 4-3 as

$$D = qC_D S, \text{ lb} \quad (4-30)$$

where C_D is the drag coefficient which from Eq. 4-11 is a function of yaw angle, i.e.,

$$C_D = C_{D_0} + C_{D_\alpha} \alpha^2 \quad (4-31)$$

The material on aerodynamic drag contained in Section IV is confined to the drag of a projectile flying at zero yaw. The drag coefficient at zero yaw C_{D_0} , in this situation, can be called the axial drag coefficient. For a well behaved projectile, the initial yaw damps rapidly to a small value, so that by far the most important term of C_D in Eq. 4-31 is C_{D_0} . The minimization of C_{D_0} consistent with internal volume requirements, is, therefore, of primary importance in the projectile design. A decrease in C_{D_0} permits the same accuracy with a lower muzzle velocity and a resultant reduction in weapon system weight.

The axial drag at zero yaw can be divided into three components:

1. Wave Drag: the component associated with the formation of shock waves.
2. Friction Drag: the drag due to the flow of air over the projectile body.
3. Base Drag: the component resulting from the reduced air pressure on the base of the projectile.

Each of the drag components depends

strikingly on the Mach number region, which for recoilless weapon projectiles is broken down into the following approximate ranges that will vary slightly according to the specific projectile shape:

1. Subsonic Range: $M < 0.8$
2. Transonic Range: $0.8 < M < 1.1$
3. Supersonic Range: $1 < M < 5$

It is not practical to determine the drag coefficient as a function of Mach number for each projectile design. Instead, the drag coefficient of a projectile shape that differs slightly from a typical projectile design is assumed to be proportional to the drag coefficient of the typical projectile (Ref. 2). If C_{D_t} is the drag coefficient of a known projectile design, the form factor i_t of a projectile whose drag coefficient is C_D is given by

$$i_t = C_D / C_{D_t}, \text{ dimensionless} \quad (4-32)$$

The ballistic coefficient C of the projectile relative to the known drag coefficient is defined as

$$C = W / (144 i_t d^2), \text{ lb-in}^{-2} \quad (4-33)$$

where

W = projectile weight, lb

d = maximum projectile diameter, ft

Values of the form factor i_t and ballistic coefficient C_t are given in Table 4-1 for existing recoilless ammunition.

TABLE 4-1
RECOILLESS AMMUNITION CHARACTERISTICS (Ref. 11)

Rifle	Projectile Diameter, in.	Effective Range, yd	Ammunition	Projectile Weight, lb	Initial Velocity, fps	Ballistic Coefficient <i>C</i>	Form Factor <i>i</i>	Drag* Function <i>G</i>
57 mm M18	2.244	500	M306A1 HE	2.75	1200	0.608	0.90	1
			M307 HEAT	2.74	1200	0.52	1.05	1
75 mm M20	2.953	1000	M309 HE	14.40	990	1.473	1.12	5
			M310 HEAT	13.10	1000	1.781	0.84	6
90 mm M67	3.543	500	M371 HEAT	7.0	800	0.429	1.3	1
105 mm M27	4.134	1000	M323 HE	32.4	1120	2.23	0.85	5
			M324 HEAT	29.3	1250	1.34	1.28	5
106 mm M40	4.173	1200	M344 HEAT	17.5	1650	1	1	M344

*See par. 4-20.3.2

In terms of the known drag, and ballistic coefficients (Eqs. 4-32 and 4-33), the expression for the aerodynamic drag D in Eq. 4-30 becomes

$$D = \left(\frac{\pi}{4}\right) \frac{qWC_{Dt}}{144C}, \text{ lb} \quad (4-34)$$

4-14 SUBSONIC VELOCITIES

For subsonic Mach numbers, the drag coefficient is roughly constant. In this region, the "teardrop" is a good aerodynamic shape, i.e., the projectile should have a rounded nose and a small base diameter. Blunting the nose of projectile (short of a completely flat face) has little effect on overall drag in the subsonic range, but has the important effect of reducing the critical Mach number.

Base drag is the result of a pressure deficiency over the projectile base more

commonly evident in the substatic (less than atmospheric) pressure existing in the wake of a train or automobile. Base drag is reduced by "boattailing" or tapering the rear of the projectile to reduce the base area. However, only a limited amount of tapering can be tolerated since boattailing reduces the lift coefficient and moves the c.p. of the normal force forward, thus reducing the stability of the projectile. Large boattail angles (greater than 16 deg) without a rounded transition from the cylindrical body also can cause air flow separation at the base-body junction, canceling all of the drag reduction achieved by boattailing.

Interruptions in the smooth contour of the projectile may cause an increase in the friction drag. By proper orientation or elimination of such surface irregularities as slots, shallow holes, or protuberances, it is possible to minimize the friction drag.

4-15 TRANSONIC

The transonic range is characterized by the formation of shock waves and a sharp increase in drag due to a rapidly increasing drag coefficient. The greatest part of the drag increase in the transonic range is attributed to the presence of the shock waves and is called the wave drag. Wave drag is affected by abrupt changes in the projectile shape, such as the rotating band and undercuts on the body, because the local Mach number varies from point to point along the projectile surface depending upon the projectile shape. In the transonic range, base drag peaks at $M = 1.0$ and friction drag increases and becomes relatively small as C_{D_o} increases. Since rapid and sometimes unpredicted changes in the aerodynamic coefficients can occur in the transonic range, the designer attempts to minimize the flight time in this region.

4-16 SUPERSONIC

After the shock wave system is fully developed (between Mach 1.1 and 1.2) the drag decreases and is largely determined by the shape of the nose. By the Taylor-Macoll equation:

$$C_{D_f} = [0.0016 + (0.002/M^2)]\epsilon^{1.7},$$

dimensionless (4-35)

where

$$C_{D_f} = \text{wave drag coefficient, dimensionless}$$

$$\epsilon = \text{half angle of nose cone, deg}$$

$$M = \text{Mach number}$$

While this equation is useful for estimating the effect of nose angle, the minimum drag actually is obtained by using an ogive of large radius.

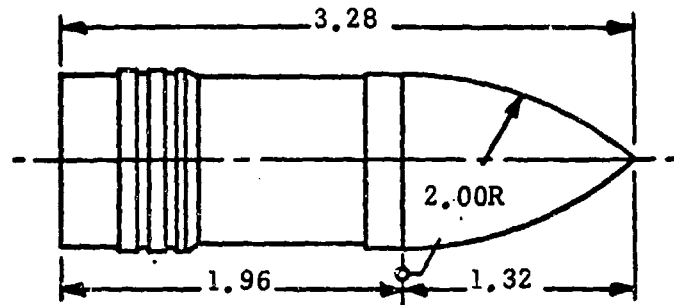
Boattailing reduces the drag at supersonic velocities provided the airflow does not separate from the body. Thus, the boattail angle usually is limited to about 8 deg and one caliber in length. Beyond these critical characteristics, the flow will separate from the projectile forward of the base, resulting in a C_{D_o} that is greater than the minimum attainable.

4-17 TYPICAL VALUES OF DRAG

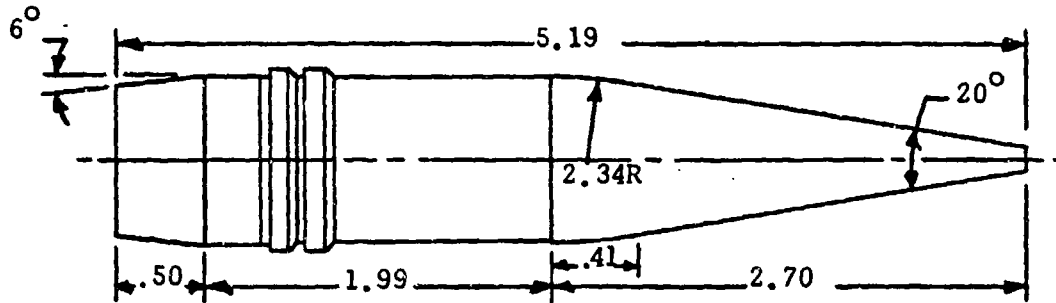
Fig. 4-3 shows four projectile shapes which have been adopted as standards for comparison (Ref. 2). In Fig. 4-4, the value of the drag coefficient C_D is plotted vs Mach number for the four projectile types. As seen in Fig. 4-4, C_D remains fairly constant in the subsonic range, increases rapidly in the transonic range, and then decreases in the supersonic range.

In general, it is assumed that projectiles having the same shape and c.g. location will have the same set of aerodynamic coefficients when fired at the same Mach number. It then is possible to make use of such data as contained in Figs. 4-3 and 4-4 in evaluating a new projectile design. However, there are a few outstanding exceptions to this rule.

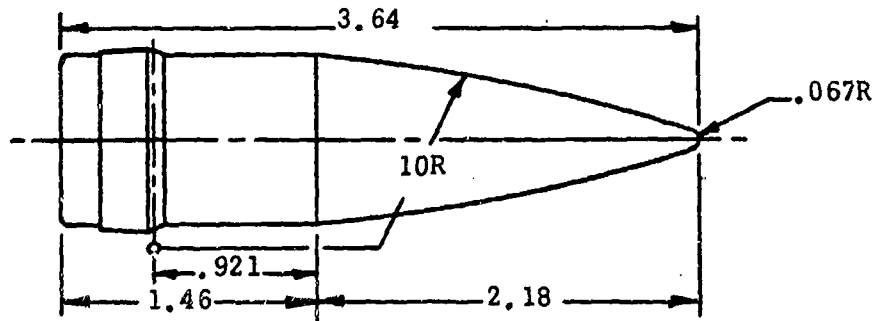
It has been found that stability can be improved by replacing the ogive nose of the projectile with a slender cylinder or "spike" protruding from the flat forward face of the body. During firing tests, it was found that the spiked projectile exhibited essentially two different drag coefficients that were determined according to the position at which the flow separated from the spike. This phenomenon was called dual flow. In order to avoid the condition of dual flow, with its serious effects on accuracy, a tripper ring is added near the tip of the spike to insure the early separation of the flow. Since the spiked-nose projectile does increase drag, it is not commonly used in recoilless rifle projectiles.



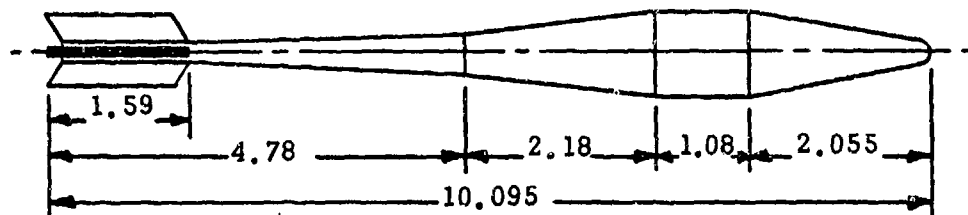
(A) PROJECTILE TYPE 1



(B) PROJECTILE TYPE 2



(C) PROJECTILE TYPE 8



(D) 90 mm HEAT PROJECTILE T108

All Dimensions in Calibers

Figure 4-3. Projectile Shapes (Ref. 2)

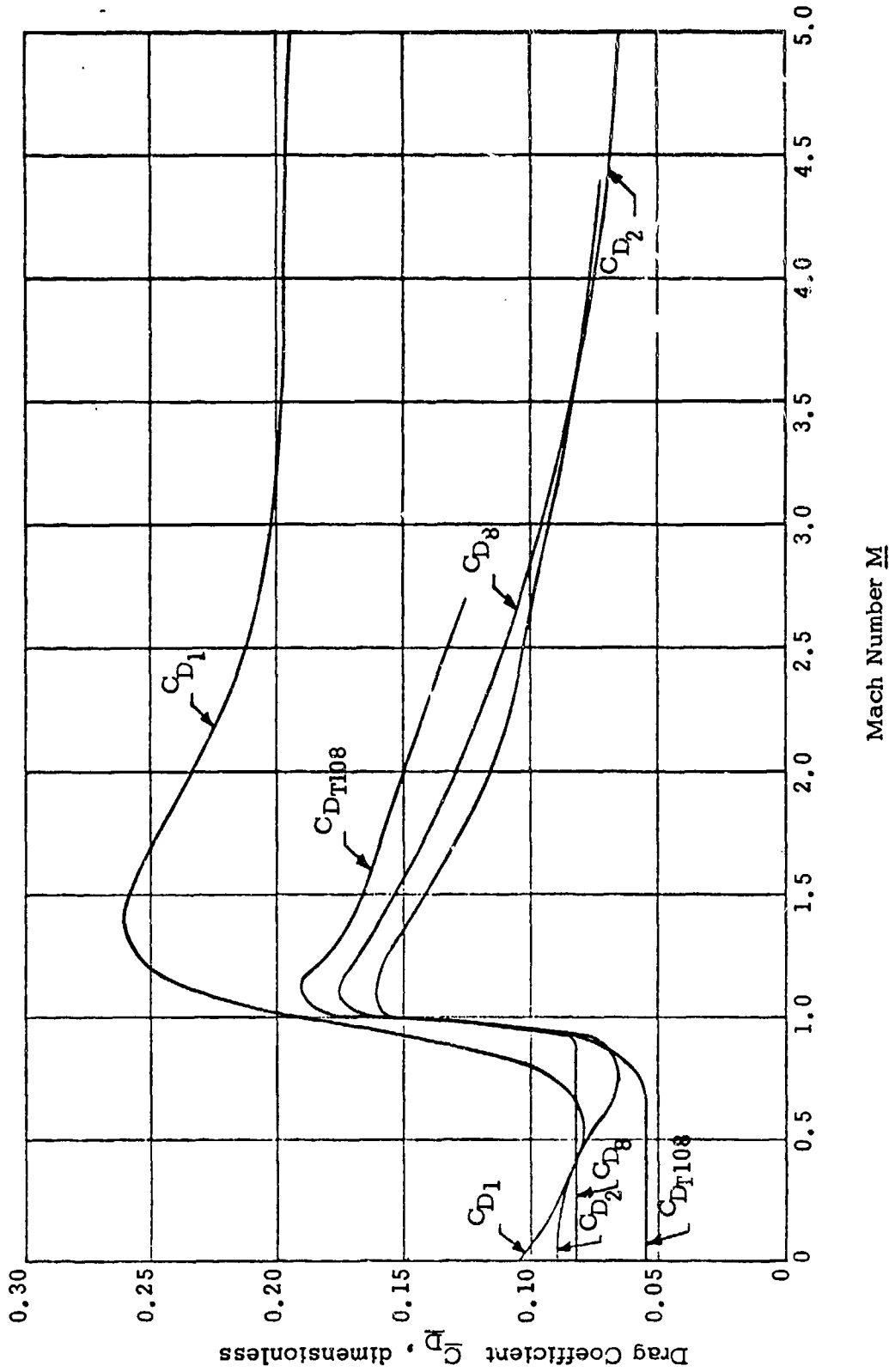


Figure 4-4. Drag Coefficient vs Mach Number (Ref. 2)

SECTION V

PARTICLE TRAJECTORY CALCULATIONS

4-18 TRAJECTORY PROBLEM

A detailed trajectory calculation uses six coordinates to describe the motion of the projectile. Three coordinates determine the position of the projectile center of gravity, two angular coordinates determine the projectile yaw angle, and a third angular coordinate describes the roll or spin. This type of trajectory calculation normally is made on a digital computer (see Ref. 1) and will not be considered in this discussion.

For the purpose of initial design calculations of a proposed recoilless rifle weapon system, a two-degree-of-freedom trajectory calculation provides sufficient information. Thus, the trajectory calculations to be described in this section assume the projectile yaw angle to be zero and the trajectory to lie in the xz -plane. The deviation from the xz -plane is a separate calculation based on the effect of crosswind and drift for the calculated time of flight.

The trajectory problem consists of integrating the equations of motion of the projectile given an initial velocity vector, the vertical force of gravity, and an aerodynamic drag D , acting in a direction opposite to the velocity vector. (The determination of the numerical value of D is performed according to Eq. 4-34.) For the typical short time-of-flight, flat, recoilless weapon trajectory, the effects of variation of air density with altitude, Coriolis force, earth rotation, and similar secondary effects can be neglected with little loss of accuracy.

4-19 TRAJECTORY EQUATIONS

Fig. 4-5 shows the coordinate system and forces acting on the projectile for a two-degree-of-freedom trajectory. Describing the projectile motion in terms of x and z components, the equations of motion are

$$m\ddot{x} = D \cos \theta \quad (4-36)$$

$$m\ddot{z} = D \sin \theta - mg \quad (4-37)$$

subject to the initial condition

$$\tan \theta = \dot{z}_0 / \dot{x}_0 \quad (4-38)$$

where

θ = angle between horizontal (x -axis) and velocity vector, rad

A dot above the coordinate indicates a derivative with respect to time and subscript 0 denotes initial (muzzle) value.

The equations of motion cannot be readily integrated since D is a function of Mach number M and θ varies with time. The usual procedure is to use a numerical integration in which the drag D and flight angle θ are considered constant for short intervals of time.

4-20 SOLUTIONS OF THE EQUATIONS

Until the adoption of high speed digital computers, trajectory calculations were performed exclusively by approximate methods which employed average or effective values of

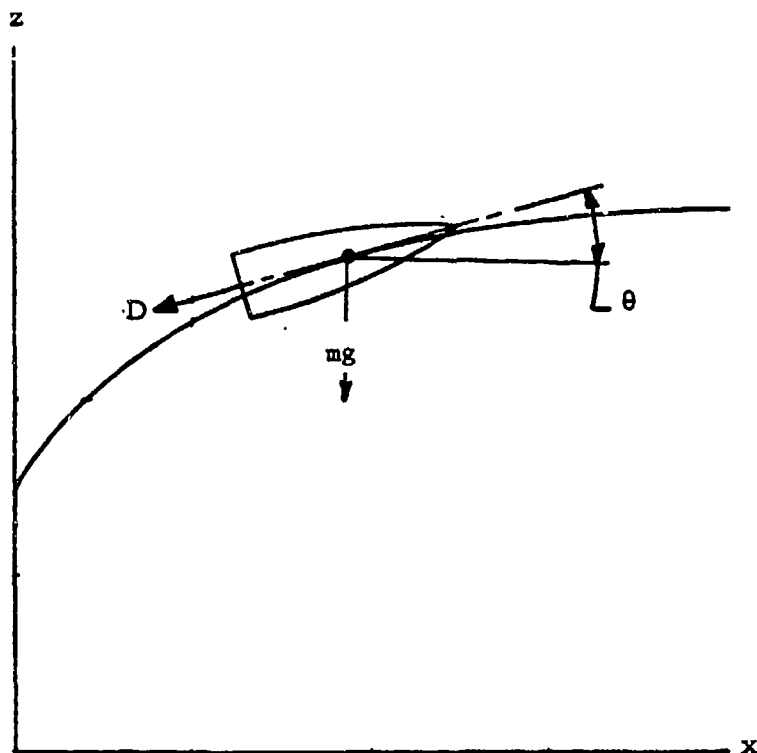


Figure 4-5. Coordinate System for Trajectory Calculations

the drag coefficient. Examples of these approximate methods are the simplified exterior ballistics techniques described in par. 4-20.1 and the Siacci method outlined in par. 4-20.3. While the approximate methods are still used for rapid estimations of the effects of variations in projectile shape, muzzle velocity, and quadrant elevation on range and time of flight, complete trajectory calculations are made on digital computers using numerical integration techniques as described in par. 4-20.2. The use of digital computers has resulted in accuracies of simulation better than one percent, assuming that the drag coefficient curve used averaged within 2 percent of the true C_D at all Mach numbers traversed.

4-20.1 SEMIEMPIRICAL EQUATIONS FOR FLAT TRAJECTORIES

Calculations of the trajectory angle of elevation θ_o , time of flight t_f , terminal velocity V_f , and angle of descent ϕ are necessary for the ballistic evaluation of the weapon system, but are very time consuming because factors such as drag and ballistic coefficients are not readily available. In Ref. 3, a simplified method (based on the assumption of a flat trajectory) for calculating these parameters is presented. From experimental and theoretical work which indicates that the deceleration of a projectile is approximately proportional to the square of

its velocity at any particular time, Ref. 3 shows that

$$t_f = \frac{\exp [(3r_m R)/V_m] - 1}{r_m}, \text{ sec} \quad (4-39)$$

$$\theta_o = \frac{16,100 t_f}{V_m}, \text{ mil} \quad (4-40)$$

$$V_t = \frac{V_m}{1 + r_m t_f}, \text{ fps} \quad (4-41)$$

$$\phi = (1 + r_m t_f) \theta_o, \text{ mil} \quad (4-42)$$

where

$$r_m = \left(\frac{dV_x}{dx} \right)_m = \text{retardation at muzzle,} \\ \text{sec}^{-1}$$

R = range, yd

V_m = muzzle velocity, fps

V_x = horizontal component of velocity, fps

and subscript m indicates muzzle condition. The retardation and muzzle velocity are obtained during charge establishment and uniformity firings with the same system.

Eqs. 4-39 through 4-42 have proven to be accurate within 3 percent for t_f and θ_o and within 5 percent for V_t in the experimental ranges encountered in recoilless rifle systems. In order to facilitate the use of the simplified method, the formulas for t_f , θ_o , V_t , and ϕ have been incorporated into the nomogram shown in Fig. 4-6.

The following sample operation for the use of Fig. 4-6 is presented for the 106 mm, T170 system. Given the following data:

$$R = 1,000 \text{ yd}$$

$$r_m = 0.20 \text{ sec}^{-1}$$

$$V_m = 1,820 \text{ fps}$$

1. Align muzzle velocity V_m (1,820 fps) with range R (1,000 yd) to determine point on reference line 1.

2. Align the point on the reference line 1 with retardation r_m (0.20 fps/ft) to determine a point on reference line 2.

3. Align the point on the reference line 2 with muzzle velocity (already spotted) to determine the desired angle of elevation θ_o (18 mil).

Calculate the other parameters:

$$t_f = \frac{\theta_o V_m}{16,100} = \frac{18(1820)}{16,100} = 2.03 \text{ sec}$$

$$V_t = \frac{V_m}{1 + r_m t_f} \\ = \frac{1820}{1 + (0.2)(2.03)} = 1294 \text{ fps}$$

$$\phi = (1 + r_m t_f) \theta_o \\ = [1 + (0.2)(2.03)]18 = 25.3 \text{ mils}$$

4-20.2 DIGITAL COMPUTER SOLUTIONS

A digital computer program is designed to solve the trajectory equations in the same manner as described in the numerical integration method of par. 4-20.3. An example of this type of program is found in the FORTRAN particle trajectory program of Ref. 1. A table of drag coefficients vs Mach

number is placed in the computer memory so that the program can interpolate the value of a drag coefficient between any two points within the stored data deck. With this drag information, the program can compute the position and velocity of the projectile relative to the coordinate system as well as pertinent angles. With the inclusion of moment coefficient data in the computer memory, it would be possible for the program to verify the gyroscopic and dynamic stability of the projectile.

4-20.3 OTHER METHODS

4-20.3.1 Numerical Integration

Numerical integration of Eqs. 4-36 through 4-38 is performed in the following format for use with an electronic calculator.

Given: V_o , θ_o , and D vs Mach number M

Calculate: $\dot{x}_o = V_o \cos \theta_o$

$\dot{z}_o = V_o \sin \theta_o$

From the table of drag data, determine D for the given V_o . Select an appropriate time interval Δt , say 0.1 sec, depending on desired accuracy. Calculate velocity components at the end of first time increment as follows:

$$\dot{x}_1 = \dot{x}_o - [(D/m) \cos \theta_o] \Delta t, \text{ fps} \quad (4-43)$$

$$\dot{z}_1 = \dot{z}_o - [(D/m) \sin \theta_o + g] \Delta t, \text{ fps} \quad (4-44)$$

Calculate components of position at end of first time increment:

$$x_1 = x_o + \dot{x}_o \Delta t - [(D/m) \cos \theta] \Delta t^2 / 2, \text{ ft} \quad (4-45)$$

$$z_1 = z_o + \dot{z}_o \Delta t - [(D/m) \sin \theta + g] \Delta t^2 / 2, \text{ ft} \quad (4-46)$$

Note: D/m is negative when z is negative

Calculate new angle θ_1 :

$$\theta_1 = \text{Tan}^{-1}(\dot{z}_1/\dot{x}_1), \text{ rad} \quad (4-47)$$

Calculate new velocity:

$$V_1 = (\dot{x}_1^2 + \dot{z}_1^2)^{1/2}, \text{ fps} \quad (4-48)$$

Repeat process for succeeding i th increments as follows:

$$\dot{x}_i = \dot{x}_{i-1} - [(D_{i-1}/m) \cos \theta_{i-1}] \Delta t \quad (4-49)$$

$$\dot{z}_i = \dot{z}_{i-1} - [(D_{i-1}/m) \sin \theta_{i-1} + g] \Delta t \quad (4-50)$$

$$x_i = x_{i-1} + \dot{x}_{i-1} \Delta t - [(D_{i-1}/m) \cos \theta_{i-1}] \Delta t^2 / 2 \quad (4-51)$$

$$z_i = z_{i-1} + \dot{z}_{i-1} \Delta t - [(D_{i-1}/m) \sin \theta_{i-1} + g] \Delta t^2 / 2 \quad (4-52)$$

$$\theta_i = \text{Tan}^{-1}(\dot{z}_i/\dot{x}_i) \quad (4-53)$$

$$V_i = (\dot{x}_i^2 + \dot{z}_i^2)^{1/2} \quad (4-54)$$

4-20.3.2 Siacci Tables

In 1880, the Italian Col. F. Siacci introduced the following Space, Time, Altitude, and Inclination Functions to simplify the calculation of trajectory data for the types 1, 2, and 8 spin-stabilized projectiles described in par. 4-17.

$$\text{Space: } p_1 = \int_u^U \frac{du}{G(u)}, \text{ in.}^2\text{-ft-lb}^{-1} \quad (4-55)$$

$$\text{Time: } t_1 = \int_u^U \frac{du}{uG(u)}, \text{ in.}^2\text{-sec-lb}^{-1} \quad (4-56)$$

$$\text{Inclination: } q_1 = \int_u^U \frac{gdu}{u^2 G(u)}, \text{ in.}^2\text{-lb}^{-1} \quad (4-57)$$

$$\text{Altitude: } h = \int_u^U \frac{q_1 du}{G(u)}, \text{ in.}^4\text{-ft-lb}^{-2} \quad (4-58)$$

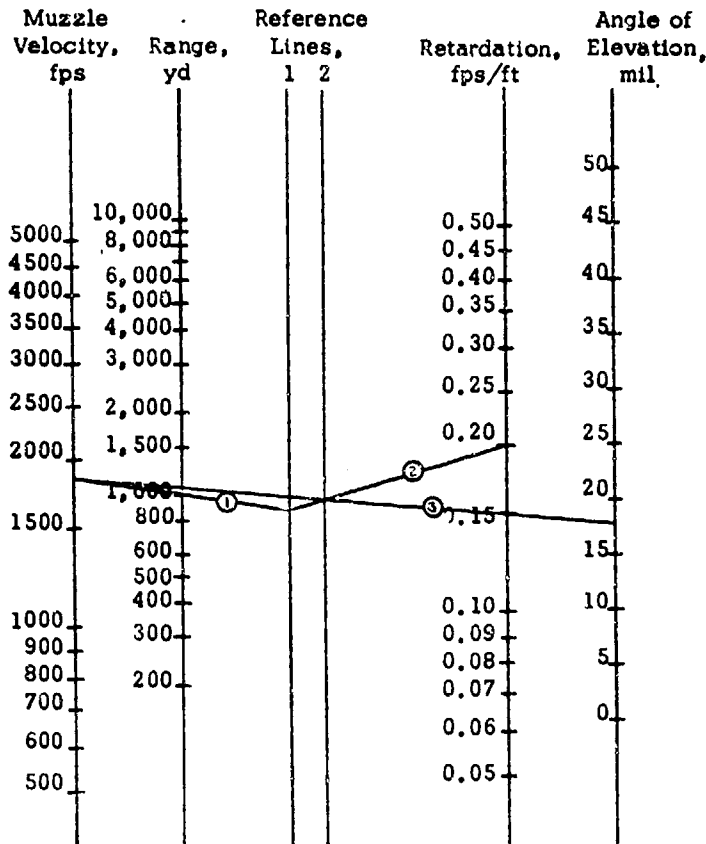


Figure 4-6. Angle of Elevation Nomogram (Ref. 3)

where

u = argument of Siacci functions: component along the line of departure of the velocity relative to air (i.e., u is related to tangential velocity V by $V = u \cos \theta_o / \cos \theta$), fps

$G(u)$ = drag function, $\text{lb}(\text{in}^2\text{-sec})^{-1}$

U = upper limit of integration for a specific projectile type, fps

g = acceleration due to gravity, ft-sec^{-2}

Values of $G(u)$ as a function of u have been determined for the types 1, 2, and 8

projectiles and are contained in Refs. 4, 5, and 6. Based on the applicable drag function $G(u)$, the Siacci functions have been tabulated for the Air Force (Refs. 7, 8 and 9). Since these Siacci Tables were arranged primarily for use in computing aircraft firing tables, they were often called Aircraft Tables. Although the Aircraft Tables are not accurate in computing complete trajectories, they can be used to obtain trajectory data at superelevations below 15 deg according to the following formulas (see Ref. 2) when variations in the air density and Mach number are neglected.

$$x = C(p - p_o) \cos \theta_o, \text{ ft} \quad (4-59)$$

$$t_f = C(t - t_o), \text{ sec} \quad (4-60)$$

$$z = x \tan \theta_o - C^2(h - h_o) + Cq_{1_o} \sec \theta_o, \text{ ft} \quad (4-61)$$

$$\tan \theta = \tan \theta_o - C(q_1 - q_{1_o}) \sec \theta_o \quad (4-62)$$

and for $z = 0$

$$\sin \theta_o = C \left(\frac{h - h_o}{p - p_o} - q_{1_o} \right) \quad (4-63)$$

Note: Subscript o refers to initial value and unsubscripted qualities correspond to the desired value of u for which the trajectory data is being computed.

As an example, suppose it is desired to determine the trajectory data for a type 8 projectile where the velocity is 500 fps, given an initial (muzzle) velocity of 1300 fps. The procedure for evaluating Eqs. 4-59 through 4-63 only involves looking up the values of p , t , h , and q_1 for $u = 500$ fps and 1300 fps from the Siacci Table based on the drag function for a type 8 projectile G_8 and then solving Eqs. 4-59 through 4-63 for these values.

For fin-stabilized projectiles, the Siacci functions are modified based on the drag coefficient for the 900 mm HEAT, T108 Projectile, which has rigid fins. These modified Siacci functions as a function of Mach number M are:

$$\text{Space: } S_1 = \int_M^{2.7} \frac{dM}{MC_D(M)}, \quad \text{dimensionless} \quad (4-64)$$

$$\text{Time: } T_1 = \int_M^{2.7} \frac{dM}{M^2 C_D(M)}, \quad \text{dimensionless} \quad (4-65)$$

$$\text{Inclination: } I = \frac{g}{a_o} \int_M^{2.7} \frac{dM}{M^3 C_D(M)}, \quad \text{dimensionless} \quad (4-66)$$

$$\text{Altitude: } A = \int \frac{I(M)dM}{MC_D(M)}, \quad \text{dimensionless} \quad (4-67)$$

where

$$g/a_o = 32.154/1120.27 = 0.0287 \text{ sec}^{-1}$$

$$a_o = \text{speed of sound in air} \\ = 1120.27 \text{ fps}$$

In terms of the modified Siacci functions, the trajectory equations are as follows (again neglecting variations in air density and Mach number):

$$x = (1/\gamma)(S_1 - S_{1_o}), \text{ ft} \quad (4-68)$$

$$t_f = \left(\frac{\sec \theta_o}{a_o \gamma} \right) (T_1 - T_{1_o}), \text{ sec} \quad (4-69)$$

when the subscript o associated with the Siacci functions indicates initial conditions.

$$z = x \tan \theta_o - \left(\frac{\sec^3 \theta_o}{a_o \gamma^2} \right) (A - A_o) \\ + x \left(\frac{\sec^2 \theta_o}{a_o \gamma} \right) I_o, \text{ ft} \quad (4-70)$$

$$\tan \theta = \tan \theta_o - \left(\frac{\sec^2 \theta_o}{a_o \gamma} \right) (I - I_o) \quad (4-71)$$

and for $z = 0$

$$\sin 2\theta_o = \frac{2}{a_o \gamma} \left[\frac{(A - A_o)}{(S - S_o)} - I_o \right] \quad (4-72)$$

$$V = a_o M \cos \theta_o / \cos \theta \quad (4-73)$$

where

$$\gamma = \rho_o' t_o d^2 / W, \text{ ft}^{-1}$$

As an example, the following problem is presented:

1. Problem: To find the velocity, time of flight, angle of departure, and angle of descent at a range of 1000 yd for 90 mm HEAT, T108E20 Projectile

2. Given Data:

Projectile Caliber d	= 0.29525 ft
Projectile Weight W	= 14.2 lb
Muzzle Velocity V_m	= 2400 fps
Form Factor i_f	= 1.00 based on G_{T108}
Air Density ρ_o	= 0.07513 lb-ft ⁻³
Speed of Sound in Air a_o	= 1120.27 fps

3. Solution:

From the Table of Siacci Functions based on 90 mm HEAT, T108 (Ref. 10)

M	S	T	A	L
1.73650	3.09196	1.427502	0.02537	0.01923
<u>2.14234</u>	<u>1.70836</u>	<u>0.709983</u>	<u>0.00670</u>	<u>0.00851</u>
Difference:	1.38360	0.717519	0.01867	0.01072

Calculating M_o and γ

$$M_o = V_m / a_o = 2400 / 1120.27 = 2.14234 \quad (4-74)$$

$$\gamma = \rho_o i_f d^2 / W = 0.07513 (1.00)(0.29525)^2 / 14.2 = 0.0004612 \text{ ft}^{-1}$$

Substitution of the Siacci function values and the value of M_o and γ into Eqs. 4-68 through 4-73 give the following results at a range of 1000 yd:

$$\text{Angle of departure: } \theta_o = 9.82 \text{ mils} \quad (\text{Eq. 4-72})$$

$$\text{Angle of fall: } \theta = 11.32 \text{ mils} \quad (\text{Eq. 4-71})$$

$$\text{Tangential velocity: } V = 1945.37 \text{ fps} \quad (\text{Eq. 4-73})$$

$$\text{Time of flight: } t_f = 1.389 \text{ sec} \quad (\text{Eq. 4-69})$$

REFERENCES

1. AMCP 706-242, *Engineering Design Handbook, Design for Control of Projectile Flight Characteristics*.
2. AMCP 706-140, *Engineering Design Handbook, Trajectories, Differential Effects, and Data for Projectiles*.
3. R. R. Rhodes, *Simplified Exterior Ballistic Equations*, Memorandum Report MR-672, Frankford Arsenal, Philadelphia, May 1958.
4. G_1 -Table, BRL File N-I-92, Aberdeen Proving Ground, 1945.
5. G_2 - Table, BRL File N-I-20, Aberdeen Proving Ground, 1944. $G_{2.1}$ -Table, BRL File N-I-93, 1945.
6. M. E. Harrington *Table of G_3* , BRL File N-I-68, Aberdeen Proving Ground, 1943, *Table of $G_{3.1}$* , BRL File N-I-96, 1945.
7. *Aircraft Table Based on G_1* , BRL File N-I-122, Aberdeen Proving Ground, 1955.
8. *Aircraft Table Based on $G_{2.2}$* , BRL File N-I-121, Aberdeen Proving Ground, 1955.
9. *Aircraft Table Based on $G_{3.1}$* , BRL File N-I-126, Aberdeen Proving Ground, 1955.
10. C. T. Odom *Drag Coefficient and Slacci Functions for a Rigid Fin Shell Based on the Shell 90 mm HEAT, T108*, BRL MR-882, Aberdeen Proving Ground, 1956 Revision.
11. David E. Walters and Edith F. Reilly, *Hitting Probabilities of the Standard Recoilless Weapons*, Memorandum Report M59-32-1, Frankford Arsenal, Philadelphia, Pa., June 1959.

CHAPTER 5

INTERIOR BALLISTICS

5-0 LIST OF SYMBOLS

A	= bore area, in. ²	C_d	= discharge coefficient of nozzle, dimensionless
A_c	= chamber area, in. ²	C_i	= initial propellant charge, lb
A_e	= nozzle exit area, in. ²	C_o	= hypothetical charge of "ideal" rifle, lb
A_t	= nozzle throat area, in. ²	c_p	= specific heat at constant pressure, (ft-lb)-(lb-°R) ⁻¹
A_w	= surface area of gun being heated, in. ²	C_s	= total weight of unburned propellant ejected, lb
AY	= unoccupied chamber volume, $v_c - C_i/\rho$, in. ³	c_v	= specific heat at constant volume, (ft-lb)-(lb-°R) ⁻¹
a	= $1-\lambda/(2U)$, dimensionless	c_w	= specific heat of weapon, Btu-(lb _{weapon} °F) ⁻¹
a	= constant term in burning law equation, in.-sec ⁻¹	C_2	= propellant charge burned in rifle, $C_2 = C_i - C_s$, lb
a_p	= peak acceleration, ft-sec ⁻²	D	= bore diameter, in.
a_1	= $AC_s/(mV_b)$, in. ² -sec ⁻¹	D_o	= initial grain diameter, in.
a_2	= ψ'_p/ψ'_m , dimensionless	d	= perforation diameter, in.
B	= effective burning rate constant, in.-(sec-psi) ⁻¹	e	= 2.718281828 base of natural logarithms
b	= $\lambda(\gamma-1)/2$, dimensionless	e_b	= ballistic efficiency, dimensionless
C	= effective propellant charge weight and $C = C_i - W_s$, lb	e_c	= thermodynamic efficiency, dimensionless
C'	= burning rate coefficient in linearized burning law equation, in.-(sec-psi) ⁻¹	e_2	= $F \left[\frac{C_2}{A} \left(1 + \frac{W}{L} \right) \left(\frac{B}{W_q} \right) - \Gamma \right]$, fps
C''	= burning rate coefficient in non-linear burning law equation, in.-sec ⁻¹ (psi) ⁻ⁿ	F	= propellant impetus, (ft-lb)-lb ⁻¹

F_g	= gas force, PA, lb	k	= KC_d , sec^{-1}
F_γ	= multiplying factor for converting 7-perforated webs to equivalent single-perforated webs, dimensionless	k_t	= constants in the form function, $N/C = k_o + k_1f + k_2f^2$, dimensionless
f	= fraction of web unburnt, W/W_o , dimensionless	k_t	= thermal conductivity, $\text{Btu}-(\text{in}^2\text{-sec}^{-\circ}\text{F}/\text{in.})^{-1}$
$f(u)$	= $(1+u)^{(1+u)/u}/(1+2u)^{(1+2u)/u}$	L	= travel of projectile at any time, in.
$f(\lambda, V_m)$	= $\left(\frac{T_o}{T}\right)\left(\frac{\lambda}{\theta}\right)$, dimensionless	L_b	= travel of projectile when propellant is all-burnt, in.
g	= acceleration due to gravity, ft-sec^{-2}	L_m	= travel of projectile to muzzle, in.
g_o	= $(1-J_o)\lambda/2$, dimensionless	L_p	= travel of projectile when peak chamber pressure occurs, in.
g_1	= $1-g_o\Gamma_2^2$, dimensionless	l_o	= initial length of propellant grain, in.
H	= Heaviside function	M	= weight of projectile, lb
h	= heat transfer coefficient, $\text{Btu}-(\text{in}^2\text{-sec}^{-\circ}\text{F})^{-1}$	M'	= effective projectile weight, lb ($M' = mg$)
h'	= $h\alpha/(k_t w)$, sec^{-1}	M_1	= θ_o/θ_1 , dimensionless
h''	= $hw/(kt)$, dimensionless	m	= mass of projectile, slug
h_i	= heat transfer coefficient at inner wall, $\text{Btu}-(\text{in}^2\text{-sec}^{-\circ}\text{F})^{-1}$	m'	= effective mass of projectile = $1.04 \left[m + \frac{(1-\lambda)C_i}{\delta g} \right]$, slug
h_n	= $hA_w/(R_f c_w W_w)$, round^{-1}	m_n	= mass of gases flowing through nozzle, slug
h_o	= heat transfer coefficient at outer wall, $\text{Btu}-(\text{in}^2\text{-sec}^{-\circ}\text{F})^{-1}$	N	= weight of propellant burnt, lb
I	= fractional momentum unbalance factor, dimensionless	N_o	= weight of propellant burnt at projectile start, lb
J_o	= 0 for $P_o = 0$	N'	= weight of gas in rifle, lb
K	= nozzle coefficient, sec^{-1}	N'_b	= weight of gas in rifle at all-burnt, lb
K	= $\left[\frac{\gamma g}{F} \left(\frac{2}{\gamma+1} \right)^{(\gamma+1)/(\gamma-1)} \right]^{1/\alpha}$, sec^{-1}		

n	= pressure exponent in burning law equation, dimensionless	R	= universal gas constant, (ft-lb)-(lb-°R) ⁻¹
n	= round number, dimensionless	R_f	= rate of fire, rounds min ⁻¹
n'	= number of grains in gun at any time	R'	= W_o/ρ_o , dimensionless
n'_o	= initial number of grains in gun	R_2	= gun tube radius, in.
P	= space mean pressure at any time, psi	r	= instantaneous burning rate, in.-sec ⁻¹
P'	= pressure at specific point of consideration, psi	r	= radial distance into wall for heat transfer equations, in.
P_b	= space mean pressure at time charge is all-burnt, psi	r'	= $C_2/(\rho A)$, in.
P_c	= chamber pressure, psi	r_1	= effective burning rate, in.-sec ⁻¹
P_e	= exit pressure at nozzle, psi	S	= total area of the propellant charge burning surface, in ²
P_m	= space mean pressure when projectile is at muzzle, psi	S_g	= surface area of single-perforated grain, in ²
P_o	= starting pressure, psi	s	= fraction propellant loss, C_s/C_f , dimensionless
P_p	= maximum pressure, psi	T	= space mean temperature at any time, °R
P_t	= pressure at nozzle throat, psi	\bar{T}	= average gas temperature during ballistic cycle, °F
P_x	= pressure at projectile base, psi	T'	= T/T_o , dimensionless
Q	= $\frac{\left(\frac{A}{C}\right)^2 \left(\frac{C_2}{m}\right)}{F \left(\frac{R}{W_o}\right)^2}$, dimensionless	T_a	= air ambient temperature, °F
Q_o	= heat influx input per round, Btu-(in ² -round) ⁻¹	T_o	= isochoric flame temperature of propellant, °R
Q'_o	= $Q_o w / (k_T \theta_o t_o)$, round ⁻¹	T'_o	= maximum temperature at inner wall, °F
q	= $m k \left(\frac{A_t}{A^2 \lambda}\right) \left(\frac{1}{\rho} - \eta \theta\right)$, in.-sec.ft ⁻¹	T_1	= temperature of gun tube after firing first round, °F
q_o	= heat transferred to weapon per round, Btu-(round) ⁻¹	T_w	= wall temperature of gun, °F

t	= time, sec	w	= wall thickness, in.
t_o	= w^2/α' , sec	w_b	= wall thickness corresponding to pressure at all-burnt, in.
U	= $1 - b$, dimensionless	w_p	= wall thickness corresponding to peak pressure, in.
u	= $\left(\frac{\bar{\gamma}-1}{2}\right) + \left(\frac{W}{L}\right) \left(\frac{C_i}{A^2}\right) \left(\frac{B}{W_o}\right)^2 Fm'$, dimensionless	x	= effective distance of projectile to breech such that Ax is the volume behind the projectile, $L + x_o$, in.
V	= velocity of projectile at any time, fps	x_b	= $x_o + L_b$, in.
V_b	= velocity of projectile at all-burnt, fps	x_o	= effective length of chamber such that $Ax_o = v_c$, in.
V_m	= muzzle velocity of projectile, fps	x_m	= effective length of rifle such that Ax_m is the total volume of rifle, (i.e., $Ax_m = v_c + AL_m$), in.
V_n	= velocity of gases flowing through nozzle, fps	x_p	= $x_o + L_p$, in.
V_p	= velocity of projectile at time of peak chamber pressure, fps	Y	= unoccupied chamber length = $x_o - C_i/(\rho A)$, in.
v_c	= chamber volume of rifle, in. ³	Y'	= x/x_b , dimensionless
v_p	= volume of all single-perforated propellant grains, in. ³	α	= $C_i/(\rho v_c)$, dimensionless
v_x	= $A(L + x_o) - (C_i - N)/\rho$ = free volume in gun, in. ³	α'	= diffusion constant, in. ² -sec ⁻¹
W	= web thickness of a burning grain, in.	β	= ratio of heat loss to kinetic energy of the projectile, dimensionless
W_g	= weight of gun tube, lb	γ	= ratio of specific heats, $\gamma = c_p/c_v$, dimensionless
W_o	= initial web thickness of propellant grains, in.	$\bar{\gamma}$	= pseudo ratio of specific heats, $\bar{\gamma} = (1 + \beta)(\gamma - 1) + 1$
W_s	= weight of unburned propellant ejected, lb	Γ	= $\gamma C_d K \left(\frac{A_i}{A}\right) \left(\frac{T}{T_o}\right)^{1/2}$, sec ⁻¹
W_w	= weapon weight, lb	Γ_2	= $[(\gamma - 1)\lambda + 1]^{1/2}$, dimensionless
W_γ	= web thickness of 7-perforated grain, in.	Δ_o	= initial solid propellant loading density, $27.7 C_i/v_c$, g-cm ⁻³
W/L	= effective propellant charge regressiveness, dimensionless		

δ	$= (\epsilon - \alpha)/(1 - \alpha)$, dimensionless	ξ	$= r/w$, dimensionless
ϵ	$=$ expansion ratio, $\frac{\text{Total Gun Volume}}{\text{Chamber Volume}}$, dimensionless	ξ'	$= Ax/(v_c - C_i \rho)$, dimensionless
ζ	$= \frac{(1 + \beta)(\gamma - 1)}{2kF} \left(\frac{A}{A_t}\right) \lambda$, sec-ft $^{-1}$	ν	$= P(v_c - C_i/\rho)/(12 C_i F)$, dimensionless
ζ_2	$= \frac{12 m V_b^2 (x_o/x_b)}{v_c P_b \phi_2^2 (2 - \gamma)}$, dimensionless	ρ	$=$ density of propellant, lb-in. $^{-3}$
η	$=$ covolume of propellant gases, in. 3 -lb $^{-1}$	ρ'	$=$ density of gun material, lb-in. $^{-3}$
θ	$= 1 - \lambda(T_o/\bar{T})^{1/2}$, dimensionless	σ	$=$ allowable tensile strength of the material, psi
$\theta(n)$	$=$ wall temperature above ambient, $\theta = T - T_a$ or $\theta(n) = \theta_e [1 - \exp(-nh_n)]$, °F	τ	$= t/t_o$, dimensionless
$\bar{\theta}$	$= 1 - \lambda(T_o/\bar{T})^{1/2}$ up to burnt; N'_b/C_2 after all-burnt, dimensionless	$\bar{\tau}$	$= \frac{12 Ft}{v_c - \frac{C_i}{\rho}} \left(\frac{C_i B}{W_o}\right)$, dimensionless
θ'	$= N'/N$, dimensionless	τ_R	$=$ dimensionless time between rounds $= 1/(t_o R_f)$
θ_d	$=$ temperature decay at wall after initial temperature rise, °F $\theta_d = \theta_1 \exp[-hA_w t/(c_w W_w)]$	ϕ	$= \theta/\theta_o$, dimensionless
θ_e	$=$ equilibrium temperature, °F	ϕ	$= 1 - \lambda\gamma U/2 - \zeta V$, dimensionless
θ_g	$=$ gas temperature above ambient, deg F	ϕ'	$= N/C_2$, dimensionless
θ_o	$=$ maximum temperature rise at inner wall, °F	ϕ_2	$= 2(g_i - N'_b/C_2)/(N'_b/C_2)$, dimensionless
θ_1	$= \theta(1) - \theta(0) = \theta_e [1 - \exp(-h_n)]$, °F	ψ	$= 1/\phi_2 + 1$, dimensionless
λ	$= kA_t W_o/(C_2 B)$, dimensionless	ψ'	$= \left(\frac{T_o}{T}\right) \left(\frac{A}{A_t}\right) \frac{\lambda}{\theta F k}$, (fps) $^{-1}$
μ	$=$ piezometric efficiency, $= \frac{12(1/2)m V_m^2}{(P_p A L_m)}$, dimensionless	ψ'_b	$=$ value of ψ' for $V = V_b$, (fps) $^{-1}$
		ψ'_m	$=$ value of ψ' for $V = V_m$, (fps) $^{-1}$
		ψ'_o	$=$ value of ψ' for $V = 0$, (fps) $^{-1}$
		ψ'_p	$= \psi'/2 + [(\psi'_o/2)^2 + (\psi'_b - \psi'_o)/V_b]$
		ω	$=$ fraction of propellant web burnt, $\omega = 1 - f$, dimensionless
		Ω	$= (N - N')/N$, dimensionless

SECTION I

INTRODUCTION

5-1 SCOPE

The theory of interior ballistics provides the bases for the calculation of pressure within the gun and projectile velocity as functions of projectile displacement. Those factors which affect projectile motion in the gun are within the scope of the subject of interior ballistics. Many contributory factors such as the theory of propellant burning are the same for recoilless weapons and conventional guns, and hence are covered in other references given at the end of this chapter.

The material in this chapter provides an understanding of the interior ballistic processes and the relationships among interior ballistic parameters and weapon system characteristics. Approximate solutions and graphical methods are presented which allow the designer to estimate quickly the effects of these relationships, however, a digital computer program as outlined in Section VII is recommended for more accurate calculations.

5-2 QUALITATIVE DESCRIPTION OF THE INTERIOR BALLISTIC PROBLEM

The interior ballistics of a recoilless rifle is a complex subject, and it is helpful to obtain a qualitative understanding of all factors that influence the motion of the projectile before undertaking the detailed mathematical analysis. All appropriate thermodynamic constants are space averaged.

The projectile is accelerated by the propellant gas pressure acting on its base. The instantaneous pressure in the gun is determined by the amount of propellant that has burned, the amount of propellant gas that has been discharged through the nozzle, the available volume behind the projectile into which

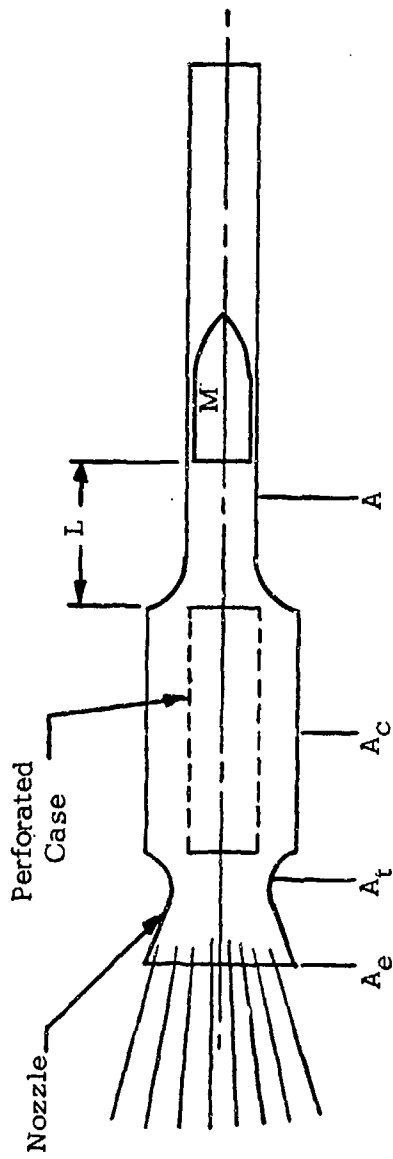
propellant gas expands, and the temperature of the propellant gas. The pressure is then determined by use of an appropriate equation of state.

The rate at which propellant burns is a function of the gas pressure, the amount of burning propellant surface, and the density of the solid propellant. The surface area is determined by the geometry of the propellant grain and the number of grains or total weight of propellant that is burning. The propellant grain is typically cylindrical in shape and its burning surface is controlled by the number, distribution, and diameter of holes through the length of the grain. The integrated propellant burning rate determines the amount of propellant burnt at any time.

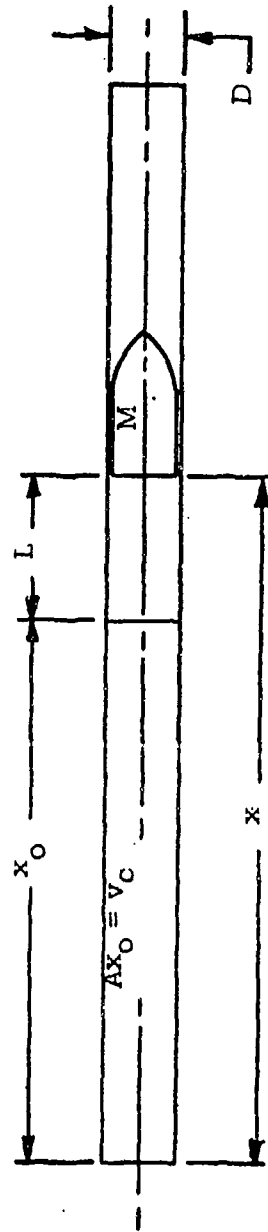
The rate at which gas is discharged through the nozzle is determined primarily by the pressure in the rifle, the weapon, the geometry of the nozzle, and to a lesser extent the temperature of the propellant gas. The configuration of the nozzle, of course, determines the recoil thrust and must be designed to eliminate the net system recoil.

The gas temperature in the gun is a function of the particular propellant used, the effects of gas expansion, and heat conduction to the gun wall.

In a later section, these processes will be described quantitatively by means of a set of simultaneous differential equations yielding the gas pressure and projectile velocity as functions of projectile displacement. The gas pressure influences the design wall thickness of the gun tube; the desired muzzle velocity determines, in part, the length of gun tube. The wall thickness and tube length largely determine the system weight of a given caliber rifle.



(A) Idealized Cross Section



(B) Equivalent Cross Section

Figure 5-1. Schematic of Gun Showing Interior Ballistic Parameters

The typical interior ballistic problem is the determination of the complete set of ballistic parameters which will lead to the optimum gun design (usually the lightest gun) that will provide the projectile with the specified energy.

This qualitative discussion is illustrated in Fig. 5-1 that presents schematically an idealized recoilless rifle and an equivalent recoilless rifle showing the interior ballistic parameters, each consisting of a tube of cross-sectional area A with an orifice at one end of throat area A_t . In the equivalent rifle, the initial position of the projectile is at a distance x_0 from the throat giving a chamber volume $v_c = Ax_0$. The instantaneous gun volume behind the projectile is Ax .

5-3 USE OF EXISTING REFERENCES ON INTERIOR BALLISTIC THEORY

There is no convenient, closed-form solution to the set of the differential equations of interior ballistics. Approximate solutions have

been obtained by making appropriate simplifying assumptions. There are a number of different methods for solving the ballistic equations, such as Corner's or Hirschfelder's, which are indicated in the references. These procedures are available, effective, and interesting. However, graphical and analytical methods of solution will be presented in sufficient detail to provide choices based on required accuracy. These choices range from simple graphs of dimensionless parameters for quick approximate solutions to more precise digital computer solutions of the basic differential equations.

5-4 DESIGN DATA FOR SEVERAL RECOILLESS RIFLES AND AMMUNITION

A simple and useful method for predicting the performance of a conceptual recoilless rifle is the comparison with the performance of a similar existing rifle of known characteristics. The conceptual design parameters are estimated through the application of

TABLE 5-1

BALLISTIC PARAMETERS FOR SEVERAL GUNS AND ROUNDS

<u>Gun</u>	<u>57 mm M18</u>	<u>75 mm M20</u>	<u>90 mm M67</u>	<u>105 mm M27</u>	<u>106 mm M40</u>
<u>Round</u>	<u>M306A1</u>	<u>M309A1</u>	<u>M371</u>	<u>M323</u>	<u>M344</u>
L_m , in.	47.5	65.1	27.5	106	109.8
P_p , psi	7,500	10,000	3,700	9,260	10,280
m , slug	0.0854	0.4361	0.42	1.006	0.544
V_m , fps	1200	990	450	1120	1650
C_f , lb	1.00	3.309	1.31	7.87	7.46
Type Propellant*	M10	M10	M5	M10	M10
A , in ²	3.96	7.00	10.1	13.72	13.72
A_t , in ²	2.95	4.67	6.82	9.30	10.00
x_0 , in.	32.8	40.9	14.8	60.9	32.4
Web, in.	0.0179	—	—	0.0336	0.035
Grain	Single Perf	—	—	Multi-Perf	Multi-Perf
v_c , in ³	120	286	150	840	444
A_0/A_t	2.39	2.07	3.5	1.88	1.79
A/A_t	1.34	1.49	1.48	1.47	1.38

*See Table 11-3, Chapter 11, "Ammunition", for Propellant Parameters

similitude relationships. These methods are discussed in the next section.

Table 5-1 presents design parameters and performance details for a series of existing recoilless rifles to aid the designer of new

systems in scaling the ballistic parameters. These data are useful also for checking the accuracy of an analytical solution or of a digital computer program of the ballistic equations.

SECTION II

EMPIRICAL AND GRAPHICAL METHODS
FOR QUICK APPROXIMATIONS5-5 SOLUTIONS BASED ON EFFICIENCY
CONSIDERATIONS

5-5.1 INTRODUCTION

The methods of this section are based on the observation that if an existing gun yields a certain projectile muzzle energy per unit charge, then other guns of the same efficiency can be designed to meet different requirements of performance and size. These methods do not provide detailed gun design data but are useful for rapid estimates of the gross dimensions (weight, length, volume) and propellant requirements.

5-5.2 THERMODYNAMIC EFFICIENCY

For conventional guns, thermodynamic efficiency e_c is defined as the ratio of the projectile kinetic energy to the available energy of the propellant. In the recoilless rifle system, however, some of the useful available propellant energy goes into balancing the rifle—i.e., preventing recoil—so that in comparing fairly identical recoilless rifles by using the conventional efficiency definition one rifle will appear more efficient and require a smaller charge when it recoils rearward, and less efficient when it recoils forward. Therefore, in order to compare effectively the ballistic performance or potentiality of recoilless systems, the efficiency of a recoilless rifle is now defined as the ratio of useful work obtained from the system to the available propellant energy (Ref. 1). The useful work from the system is the kinetic energy of both the projectile and nozzle gases. Considering the case of an "ideal" rifle, i.e., a rifle in which there are no energy losses, the ballistic efficiency e_b of the recoilless rifle can be written as

$$e_b = C_o/C_i, \text{ dimensionless} \quad (5-1)$$

where

C_o = hypothetical charge that contributes to the energy of the projectile and the gases balancing the recoil forces, lb

C_i = initial propellant charge, lb

Considering the "ideal" rifle system, the conservation of energy and momentum can be written, respectively, as

$$m_n V_n^2/2 + m V_m^2/2 = C_o F/(\gamma - 1) \quad (5-2)$$

and

$$m_n V_n + I m V_m = m V_m \quad (5-3)$$

where

γ = specific heat ratio, c_p/c_v , dimensionless

F = propellant impetus, (ft-lb)-lb⁻¹

I = fractional momentum unbalance factor, dimensionless

m = projectile mass, slug

m_n = mass of gases flowing through nozzle, slug

V_n = velocity of gases flowing through nozzle, fps

V_m = muzzle velocity of projectile, fps

The term $C_o F/(\gamma-1)$ is the total available

propellant energy of the ideal propellant charges and ImV_m is the momentum of the rifle and accessories; I is defined as the fractional momentum unbalance factor which is positive for rearward recoil and negative for forward recoil.

Solving Eq. 5-3 for V_n and substituting into Eq. 5-2, and then solving the resulting quadratic equation for C_o , the ballistic efficiency e_b of a recoilless rifle becomes as shown in Ref. 1.

$$e_b = \left[\frac{mV_m^2(\gamma - 1)}{2C_i F} \right] \left[1 + \left(\frac{1 - I}{V_m} \right) \sqrt{\frac{2gF}{\gamma - 1}} \right] \quad (5-4)$$

It should now be noted that for a closed breech weapon $I = 1$ and e_b reduces to the conventional thermodynamic efficiency definition e_c ,

$$e_c = \frac{mV_m^2(\gamma - 1)}{2C_i F} \quad (5-4a)$$

5-5.3 PIEZOMETRIC EFFICIENCY

Piezometric efficiency is the ratio of the equivalent constant pressure (average pressure) of the ballistic cycle to the actual peak pressure of the system. Hence, piezometric efficiency μ is

$$\mu = \frac{1}{P_p L_m} \int_0^{L_m} P(L) dL \quad (5-5)$$

From the equation of motion, force equals mass times acceleration

$$P(L)A = m \left(\frac{dV}{dt} \right)$$

and from

$$12V = \left(\frac{dL}{dt} \right)$$

it follows that

$$P(L)A = 12mV \left(\frac{dV}{dL} \right) \quad (5-5a)$$

Evaluating the integral of Eq. 5-5

$$\int_0^{L_m} P(L) dL = 12 \frac{m}{A} \int_0^{V_m} V dV = 12 \left(\frac{m}{A} \right) \left(\frac{V_m^2}{2} \right) \quad (5-5b)$$

Substituting Eq. 5-5b into Eq. 5-5, we obtain

$$\mu = 12 \left[\frac{\left(\frac{1}{2} \right) m V_m^2}{A P_p L_m} \right] \quad (5-6)$$

where

P = space mean pressure at any time, psi

P_p = maximum pressure, psi

L_m = gun barrel length, in.

A = bore area, in²

Peak pressure is a significant design parameter affecting gun weight, blast, and flash. Thus, a characteristic piezometric efficiency provides a quick estimate of tube length given a required projectile weight and velocity, and a specified allowable maximum pressure. The larger the piezometric efficiency, the shorter the travel required for a given muzzle energy. Hence, an important consideration in the determination of the propellant charge and gun design is the maximizing of the area defined by the pressure-travel relationship, while attempting to minimize both tube length and peak pressure.

5-5.4 EFFICIENCY TABLES AND GRAPHS

Table 5-2 lists values of thermodynamic and piezometric efficiencies for some existing recoilless rifles. These efficiencies correspond to the systems identified in Table 5-1. This

TABLE 5-2
PIEZOMETRIC, BALLISTIC, AND THERMODYNAMIC EFFICIENCIES
OF SOME EXISTING RECOILLESS RIFLES

Weapon	Round	Piezometric Efficiency μ	Conventional Thermodynamic Efficiency e_c	Ballistic Efficiency e_b
57 mm M18	M308A1	0.52	0.052	0.44
75 mm M20	M309A1	—	—	0.50
105 mm M27	M323	0.55	0.058	0.54
106 mm M40	M344	0.56	0.071	0.47

table indicates that a typical, well designed recoilless system should have a ballistic efficiency e_b and piezometric efficiency μ of about 0.50, and a conventional thermodynamic efficiency e_c of 0.06.

5-5.5 NUMERICAL EXAMPLE

Assume that a 105 mm, 8-lb projectile is to be launched at $V_m = 2000$ fps with $F = 3.3 \times 10^5$ ft-lb/lb and that peak pressure P_p is not to exceed 10,000 psi. Applying a conventional thermodynamic efficiency e_c of 0.06 and $\gamma = 1.24$, one calculates from Eq. 5-4a

$$C_i = \frac{(\gamma - 1) \left(\frac{1}{2}\right) m V_m^2}{(0.06) F}$$

$$= \frac{(0.24) \left(\frac{1}{2}\right) \left(\frac{8}{32.2}\right) (2000)^2}{(0.06)(3.3 \times 10^5)}$$

$$\approx 6 \text{ lb of propellant}$$

A piezometric efficiency μ of 0.5 yields, using Eq. 5-6,

$$AL_m = 12 \left[\frac{\frac{1}{2} m V_m^2}{P_p (0.5)} \right]$$

$$= 12 \left[\frac{\left(\frac{1}{2}\right) \left(\frac{8}{32.2}\right) (2000)^2}{10^4 (0.5)} \right] = 12 \times 10^2 \text{ in}^3$$

$$A = \frac{\pi}{4} \left(\frac{10.5}{2.54} \right)^2$$

$$= 13.4 \text{ in}^2 \text{ (for 105 mm projectile)}$$

hence

$$L_m = \frac{12 \times 10^2}{13.4} = 90 \text{ in.}$$

It is often convenient to use dimensionless coefficients instead of the ballistic parameters themselves. For example, by review of empirical data, the dimensionless propellant weight coefficient (propellant weight per unit projectile weight) is found to be closely approximated by a single valued function of projectile velocity. This relation appears in Fig. 5-2 with the two curves representing two values of ballistic efficiency e_b (0.4 and 0.5).

Fig. 5-3 shows the relation between chamber volume and both projectile travel and propellant weight through the use of the dimensionless coefficients—expansion ratio ϵ and loading density Δ_p .

Fig. 5-4 is the projectile travel L_m required to obtain a specified muzzle velocity for given values of peak acceleration based on Eq. 5-7.

$$L_m = \frac{12 V_m^2}{2 \mu a_p}, \text{ in.} \quad (5-7)$$

where

V_m = muzzle velocity, fps

a_p = peak acceleration of projectile, ft-sec⁻²

μ = piezometric efficiency, dimensionless

Piezometric efficiency μ is assumed to be 0.60.

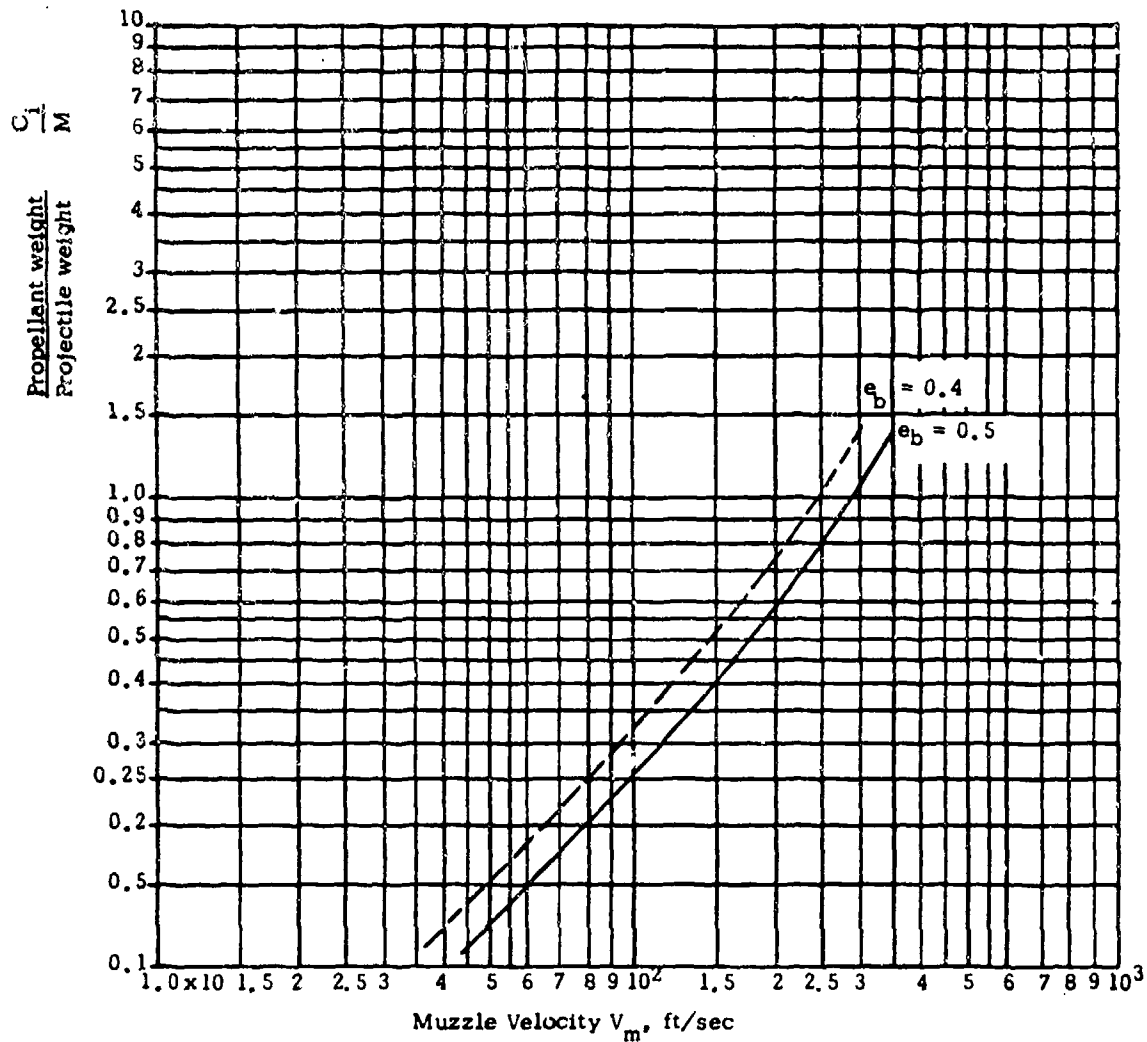


Figure 5-2. Weight of Propellant C_1 per Unit Projectile Weight M as a Function of Muzzle Velocity V_m for Ballistic Efficiencies ($e_b = 0.4$ and 0.5)

5-6 TABULATED DESIGN DATA

5-6.1 METHOD

In Ref. 2, a series of interior ballistic calculations have been made and the results tabulated. These data are shown in Table 5-3(A). If the projectile weight and bore area are specified, this table can be used to estimate various combinations of chamber

volume, barrel length, and peak pressure to produce a specified muzzle velocity. Note that there are three sets of calculations corresponding to propellant loss of 0, 10, and 20 percent. The choice of most appropriate data will be at the discretion of the designer based on the nozzle design and the point where propellant burning ends. The method for using the table follows:

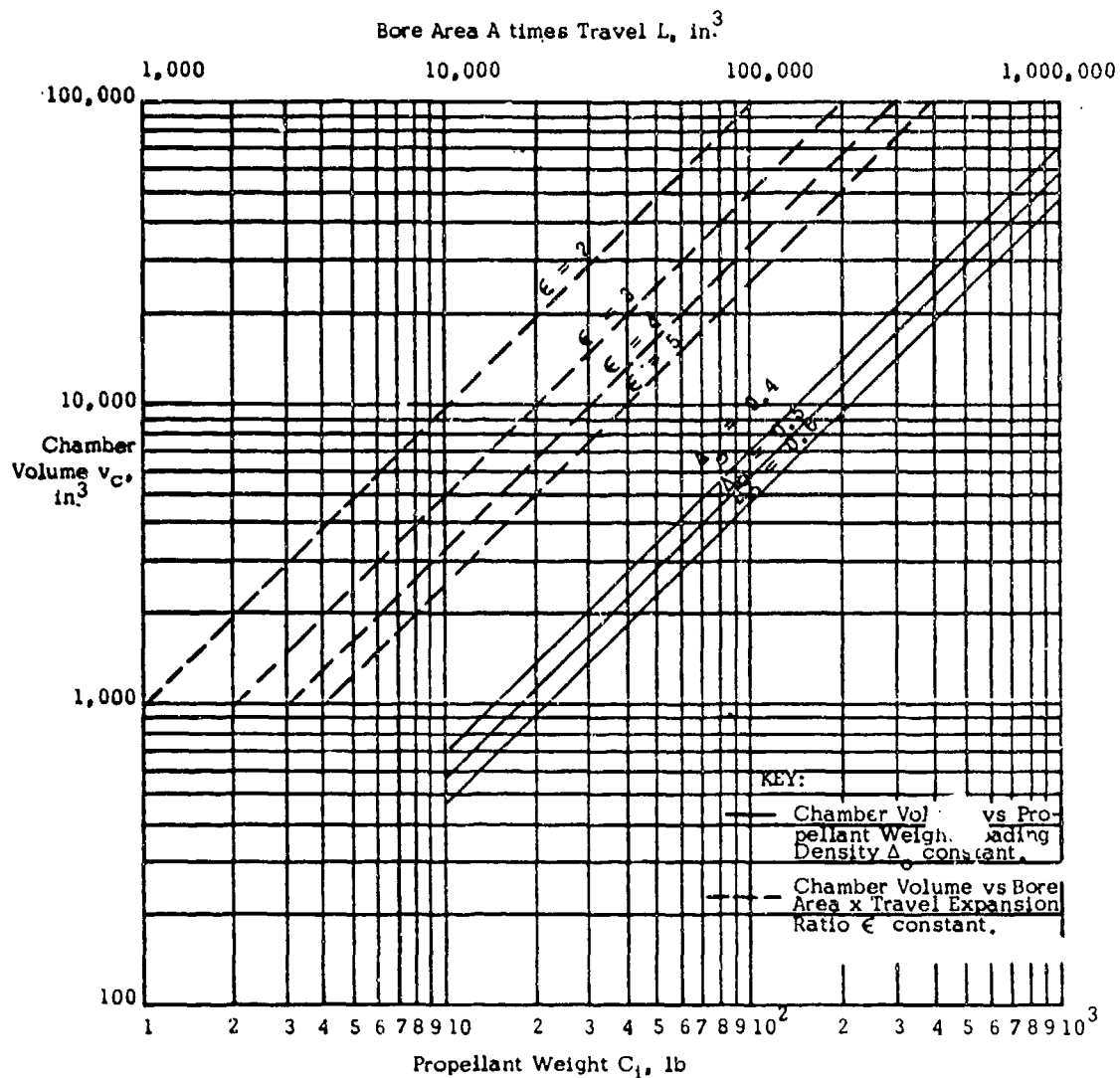


Figure 5-3. (A) Lower abscissa: Chamber Volume as a Function of Propellant Weight for Loading Densities 0.4, 0.5, 0.6 g-cm⁻³
 (B) Upper abscissa: Chamber Volume as a Function of Barrel Volume (Bore Area Times Travel) for Expansion Ratios 2, 3, 4, and 5.

Given V_m , m' , A , and P_p :

(1) Compute ratio m'/A where the m' is the effective projectile mass (see par. 5-10).

(2) Choose a set of values for the flow factor λ (see par. 5-7.2) in the range $0.45 \leq \lambda < 0.65$.

(3) From Table 5-3(A), for each λ in the set of Step (2), read $L_m(m'/A)^{-1}$ and v_c/m' corresponding to the given maximum pressure and muzzle velocity. This should be done for each propellant loss; 0 percent, 10 percent, and 20 percent.

(4) Compute the total travel L_m for each λ

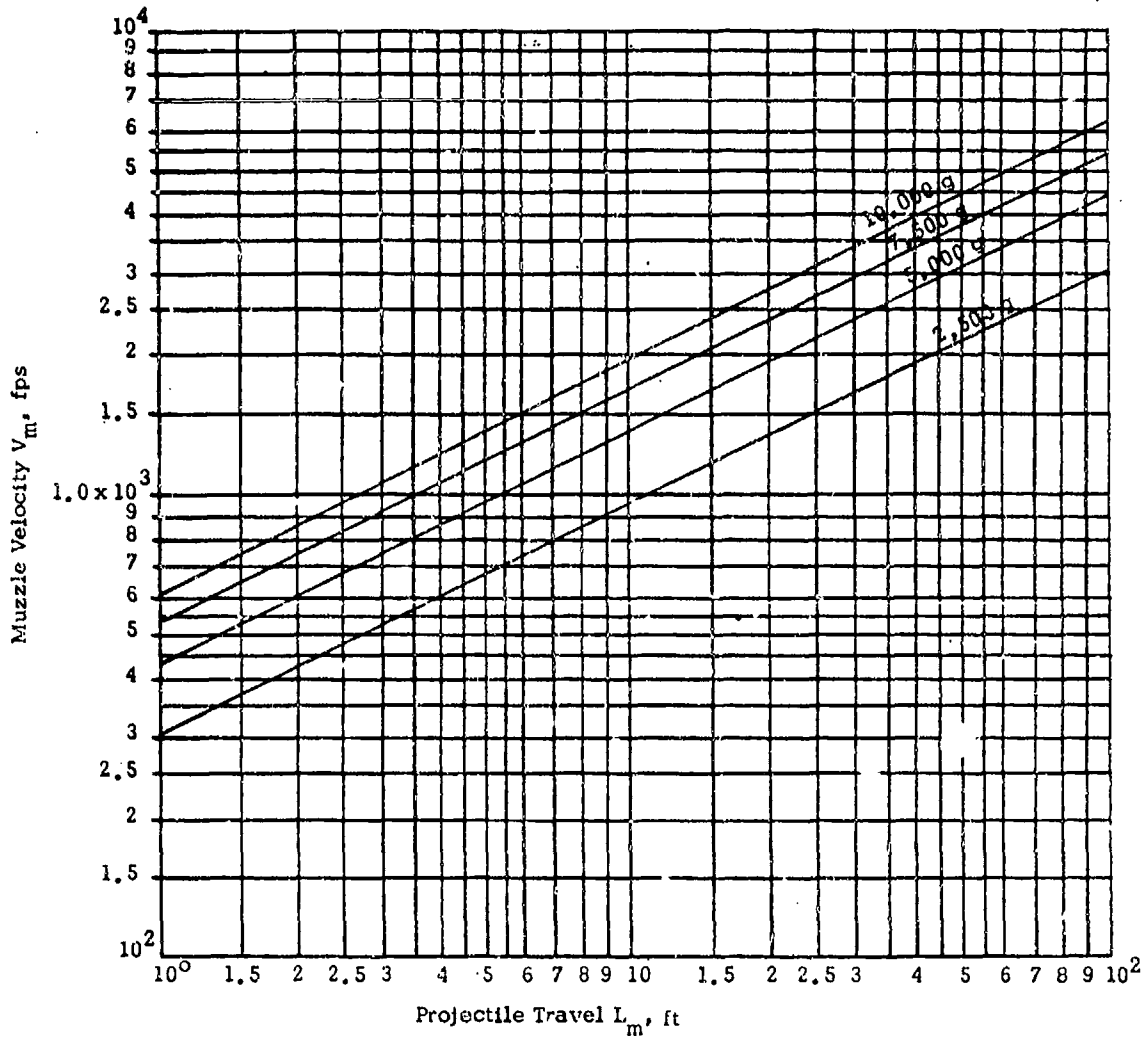


Figure 5-4. Muzzle Velocity as a Function of Projectile Travel in the Barrel for Peak Projectile Acceleration 2,500, 5,000, 7,500, and 10,000 g's.

and propellant loss by

$$L_m = \left(\frac{L_m}{m'} \right) \frac{m'}{A}$$

(5) Compute the chamber volume v_c by:

$$v_c = \left(\frac{v_c}{m'} \right) m'$$

(6) Tabulate results L_m and v_c versus λ

(7) Determine the value of C_1 for the various values of λ from:

$$C_1 = \frac{100C_2}{100 - \% \text{ propellant loss}}$$

where

$$C_2 = \left(\frac{C_2}{M'} \right) m'g$$

TABLE 5-3(A)
GENERAL BALLISTIC DESIGN DATA BASED ON SIMPLIFIED THEORY

λ	V_m fps	P_p psi	v_c/m' in. ³ /slug	$L_m \left(\frac{m}{A}\right)^{-1}$ in. ³ /slug	λ	V_m fps	P_p psi	v_c/m' in. ³ /slug	$L_m \left(\frac{m}{A}\right)^{-1}$ in. ³ /slug	
										Powder Loss = 0 percent
0.45	1500	6000	1575	3180	0.45	1500	6000	1758	3392	
		10000	1003	1997			10000	1114	1956	
		15000	717	1238			15000	799	1291	
		20000	574	926			20000	638	932	
		30000	431	600			30000	478	622	
	2000	6000	1708	5267	2000	6000	2022	5758		
		10000	1113	3132		10000	1309	3581		
		15000	815	2065		15000	950	2270		
		20000	668	1537		20000	713	1722		
		30000	521	1010		30000	595	1136		
	3000	15000	1035	6605	3000	15000	1261	6699		
		20000	874	4966		20000	1053	4867		
0.50	1500	6000	1139	2991	0.50	1500	6000	1311	3298	
		10000	729	1682			10000	848	1962	
		15000	528	1177			15000	617	1298	
		20000	431	871			20000	501	905	
		30000	334	571			30000	375	595	
	2000	6000	1209	5201	2000	6000	1548	5682		
		10000	812	3148		10000	1020	3270		
		15000	613	2087		15000	757	2183		
		20000	513	1572		20000	626	1626		
		30000	382	1032		30000	487	1136		
	0.55	1500	6000	805	2895	0.55	1500	6000	990	3170
			10000	538	1722			10000	653	1917
15000			404	1146	15000			495	1325	
20000			337	841	20000			400	950	
30000			261	614	30000			317	727	
2000		6000	910	6140	2000	6000	1172	6428		
		10000	630	3670		10000	795	3845		
		15000	490	2430		15000	605	2555		
		20000	400	1800		20000	511	1929		
		30000	317	1325		30000	400	950		
0.60		1500	6000	581	3429	0.60	1500	6000	767	3573
			10000	403	2067			10000	518	2102
	15000		314	1391	15000			394	1406	
	20000		251	1032	20000			317	1095	
	30000		191	727	30000			243	727	
	2000	6000	701	8922	2000	6000	919	8500		
		10000	503	5442		10000	639	5145		
		15000	400	3845		15000	504	3525		
		20000	317	2555		20000	400	2102		
		30000	243	1406		30000	317	1095		
	0.65	1500	6000	421	4938	0.65	1500	6000	577	4425
			10000	307	3018			10000	404	2685
15000			243	2102	15000			317	1406	
20000			191	1406	20000			243	1095	
30000			140	1095	30000			191	850	
2000		6000	534	6428	2000	6000	701	6428		
		10000	404	3845		10000	534	3845		
		15000	317	2555		15000	404	2555		
		20000	243	1406		20000	317	1406		
		30000	191	1095		30000	243	1095		

TABLE 5-3(A)

GENERAL BALLISTIC DESIGN DATA BASED ON SIMPLIFIED THEORY (CONCLUDED)

λ	V_m	P_p	v_c/m'	$L_m \left(\frac{m'}{A}\right)^{-1}$	λ	V_m	P_p	v_c/m'	$L_m \left(\frac{m'}{A}\right)^{-1}$	
	fps	psi	in. ³ /slug	in. ³ /slug		fps	psi	in. ³ /slug	in. ³ /slug	
Powder Loss = 20 Percent										
0.45	1500	6000	1927	4013	0.55	1500	6000	1220	3860	
		10000	1231	2401			10000	800	2280	
		15000	882	1558			15000	590	1530	
		20000	708	1132			20000	485	1141	
		30000	533	760			30000	380	759	
	2000	6000	2348	6812	2000	6000	1492	7278		
		10000	1516	4014		10000	997	4363		
		15000	1101	2669		15000	750	2818		
		20000	893	1971		20000	626	2199		
		30000	686	1289						
	3000	15000	1516	8134	3000	20000	917	7082		
		20000	1257	6063						
		30000	996	4054						
	0.50	1500	6000	1473	4017	0.60	1500	6000	993	3937
			10000	954	2386			10000	658	2392
15000			695	1575	15000			492	1592	
20000			566	1164	20000			410	1193	
30000			436	756						
2000		6000	1805	6775	2000	6000	1224	7762		
		10000	1188	4102		10000	832	4852		
		15000	880	2710		15000	637	3262		
		20000	725	2025		20000	539	2462		
		30000	571	1339						
3000		15000	1234	7537	0.65	1500	6000	788	4497	
		20000	1041	5687			10000	538	2772	
							15000	413	1868	
							2000	10000	707	6440
							15000	553	4400	

The ratio C_2/M' of charge burned C_2 to effective projectile weight M' is obtained from Table 5-3(B).

5-6.2 EXAMPLE

Consider a 75 mm gun with a round which has the following parameters:

$$P_p = 10,000 \text{ psi}$$

$$A = 6.85 \text{ in}^2$$

$$V_m = 2000 \text{ fps}$$

$$m' = 0.34 \text{ slug}$$

$$m'/A = 0.05 \text{ slug/in}^2$$

From Table 5-3(A) for $\lambda = 0.5$ and zero propellant loss

$$v_c/m' = 812 \text{ in}^3/\text{slug}$$

and

$$L_m(m'/A)^{-1} = 3148 \text{ in}^3/\text{slug}$$

TABLE 5-3(B)

TABLE OF PARAMETERS BASED ON
SIMPLIFIED THEORY

λ	V_m	C_2/M'
	<u>$V_m = 1500$ fps</u>	
0.45		0.316
0.50		0.314
0.55		0.310
0.60		0.305
0.65		0.301
	<u>$V_m = 2000$ fps</u>	
0.45		0.460
0.50		0.456
0.55		0.450
0.60		0.440
0.65		0.436
	<u>$V_m = 3000$ fps</u>	
0.45		0.788
0.50		0.777
0.55		0.757
0.60		0.745
0.65		0.723

therefore

$$v_c = (812)(0.34) = 276 \text{ in.}^3$$

and

$$L_m = (3148)(0.05) = 157 \text{ in.}$$

The propellant charge corresponding to these values is determined in the manner that follows.

$$\text{From Table 5-3(B), } C_2/M' = 0.456$$

Therefore, since $M' = m'g$

$$\begin{aligned} C_2 &= \left(\frac{C_2}{M'} \right) m'g = (0.456)(0.34)(32.2) \\ &= 4.99 \text{ lb} \end{aligned}$$

and, since zero propellant loss was assumed,

$$C_t = \frac{100C_2}{100 - 0} = \frac{100}{100}(4.99) = 4.99 \text{ lb}$$

A complete table of combinations of chamber volume and barrel length is then obtained by repeating these calculations for the other values of λ , and for 10 and 20 percent propellant loss.

5-7 GRAPHICAL SOLUTIONS

5-7.1 INTRODUCTION

In this paragraph a step-by-step procedure is described for determining recoilless rifle design parameters graphically. The bases for these graphs are described in Ref. 3.

This graphical method does not permit a calculation of pressure and velocity as a function of projectile travel but it does provide recoilless rifle and propellant parameters that will yield a specified muzzle energy and peak pressure. In general, these graphs are based on the simplified Hirschfelder Theory as found in Ref. 4. It is assumed that V_m , m , A , and the type of propellant are specified. Then A_t , A_e , and A_c are chosen and determined as dimensionless quantities such that the rifle will be recoilless (A/A_t usually taken as 1.45, and A_c/A_t close to unity). For these conditions A_e is nearly double A_t .

Figs. 5-5 through 5-13 contain several parameters (represented by the following symbols: λ , ψ_p' , ψ_b' , and ψ_o') that are discussed in Section V of this chapter. Most of these parameters are of no special interest to the weapon designer, however, the factor λ is of special interest. It is defined as $\lambda = kA_t W_o / (C_2 B)$ which shows that a specific value of λ determines the propellant charge C_2 . The use of Figs. 5-5 through 5-13 enables the weapon designer to estimate a value of λ based on previous experience and then, per-

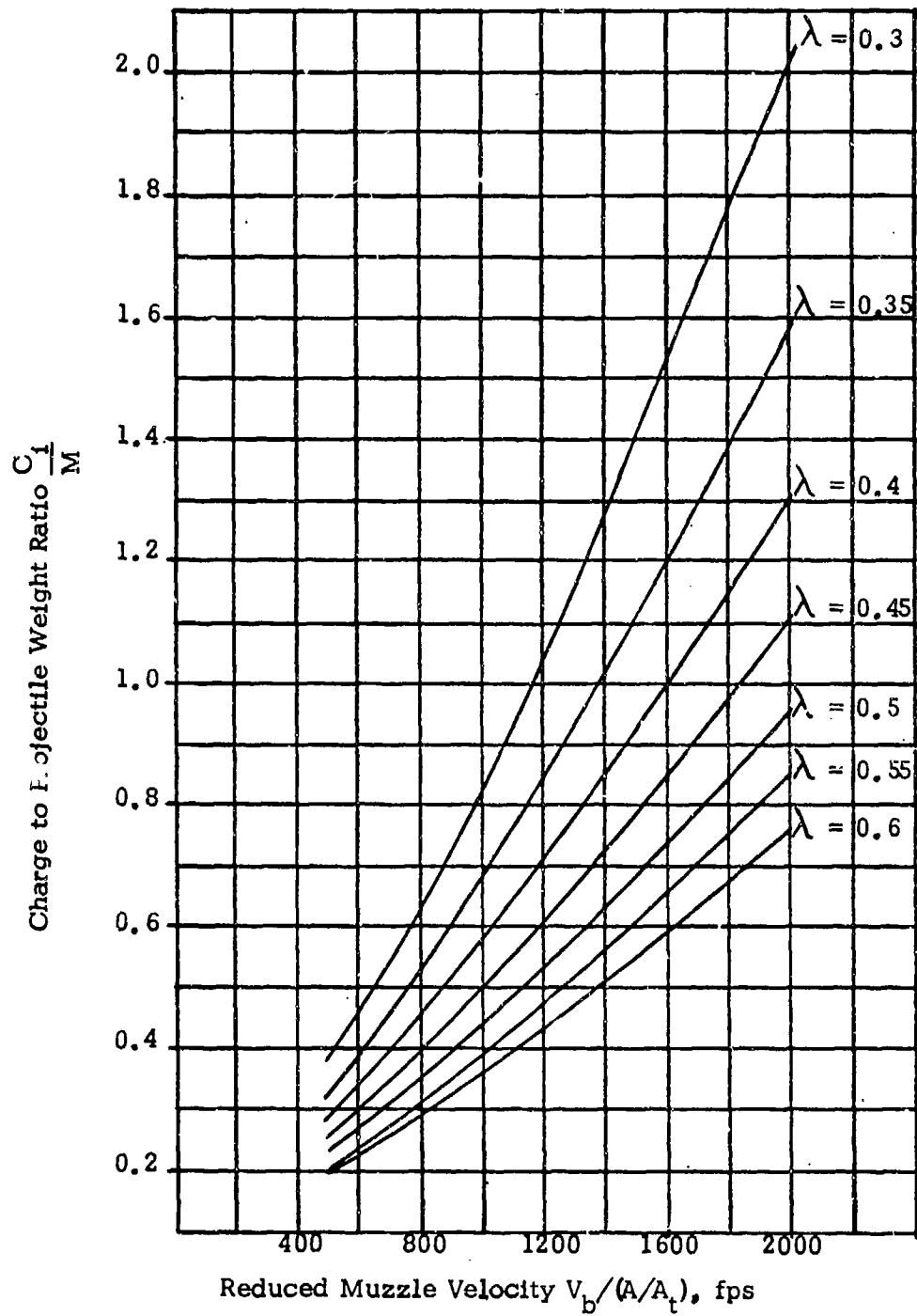


Figure 5-5. Charge to Projectile Weight Ratio as a Function of Reduced Muzzle Velocity $V_b/(A/A_t)$ for Values of λ from 0.3 to 0.6

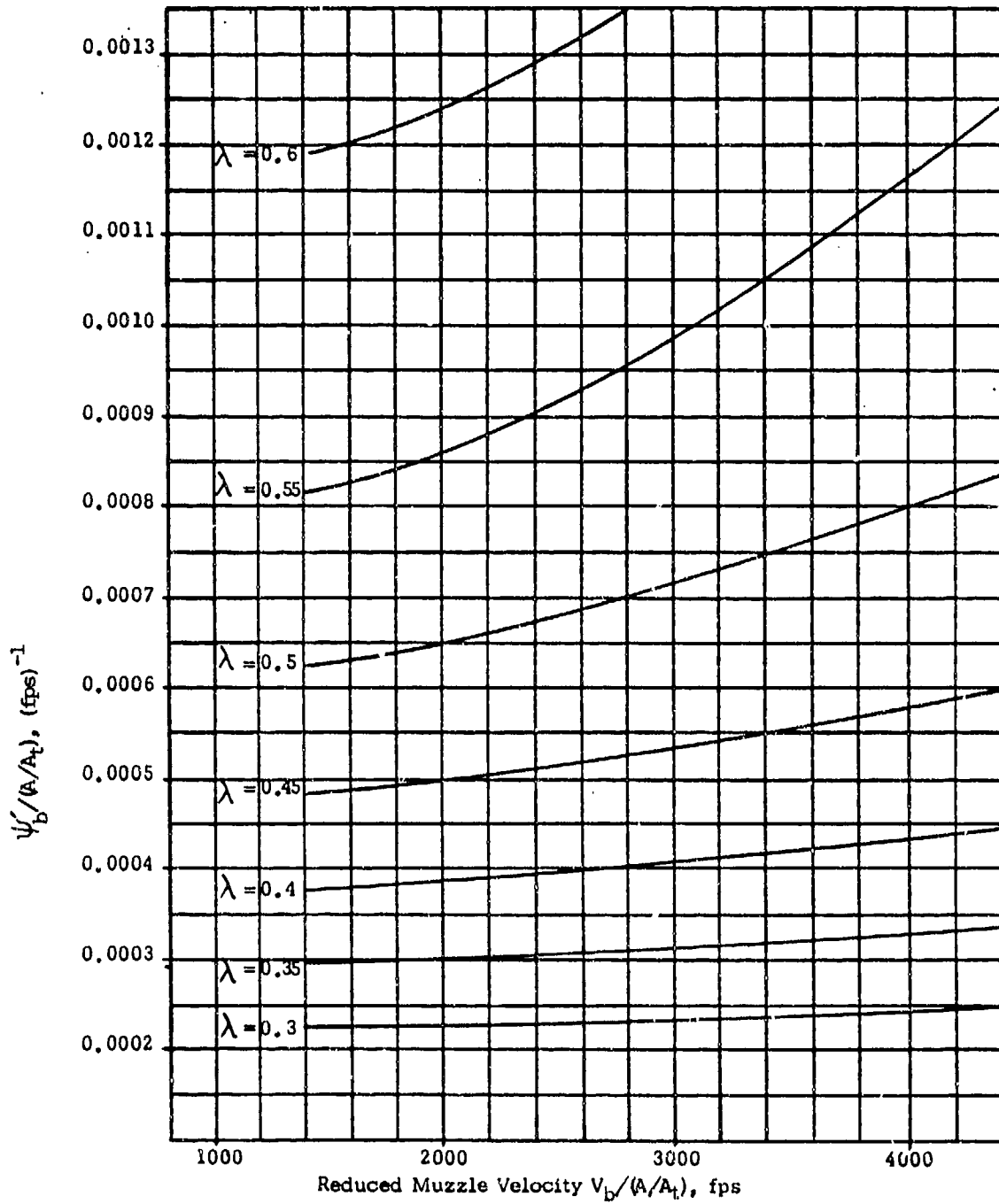


Figure 5-6 $\psi_b/(A/A_t)$ as a Function of $V_b/(A/A_t)$ and λ

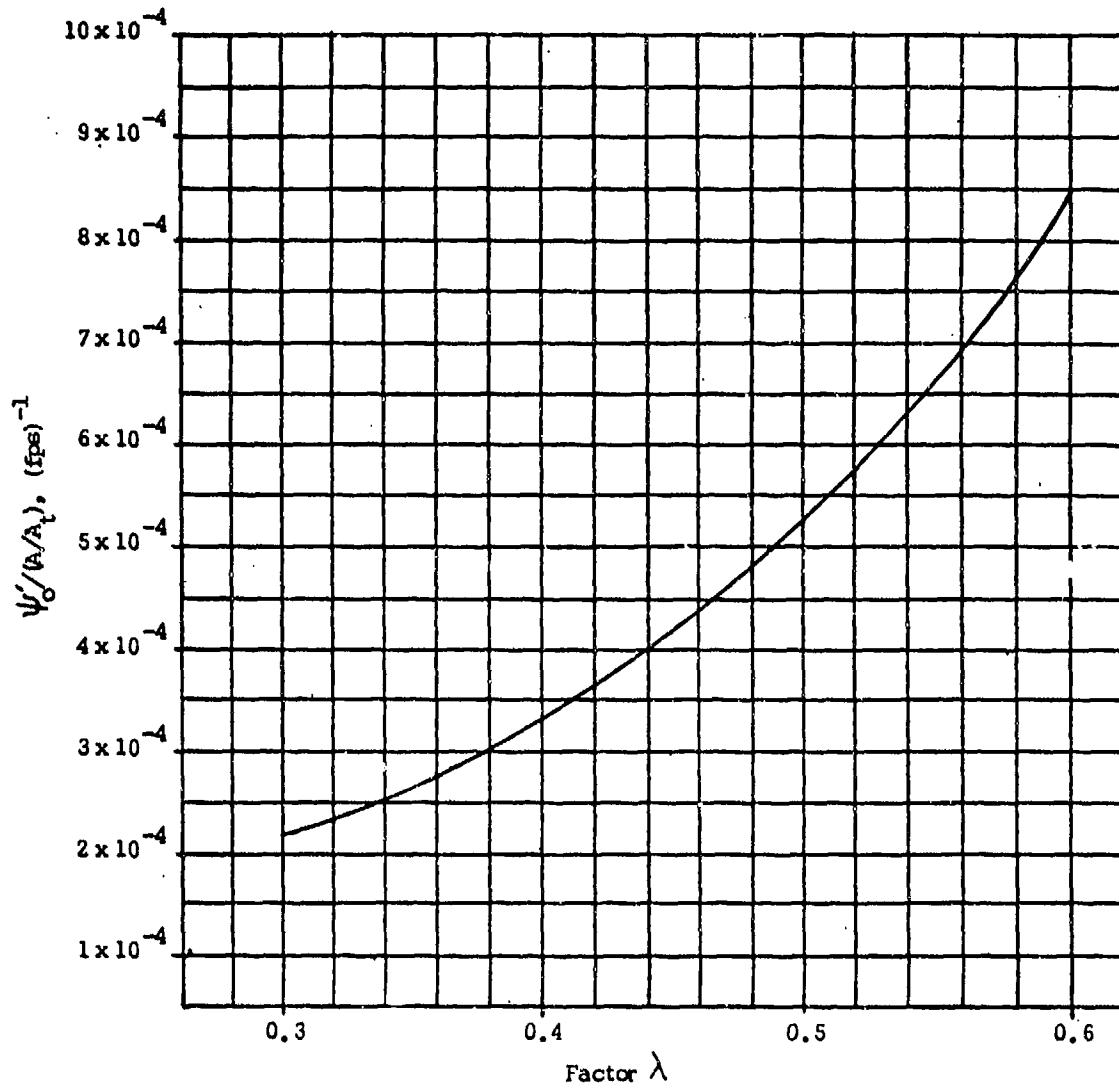


Figure 5-7. $\psi_0/(A/A_1)$ as a Function of Factor λ

forming a minimum number of limiting calculations, obtain the optimum value of λ which will lead to a practical loading density. The curves in the figures that follow indicate the exact value of charge and peak chamber pressure which correspond to the desired loading density. With this information, the chamber volume and propellant web can be

determined, respectively, from the definition of loading density Δ_0 and λ where

$$\Delta_0 = 27.7C_i/v_c, \text{ g-cm}^{-3} \quad (5-8)$$

where

C_i = initial propellant charge, lb

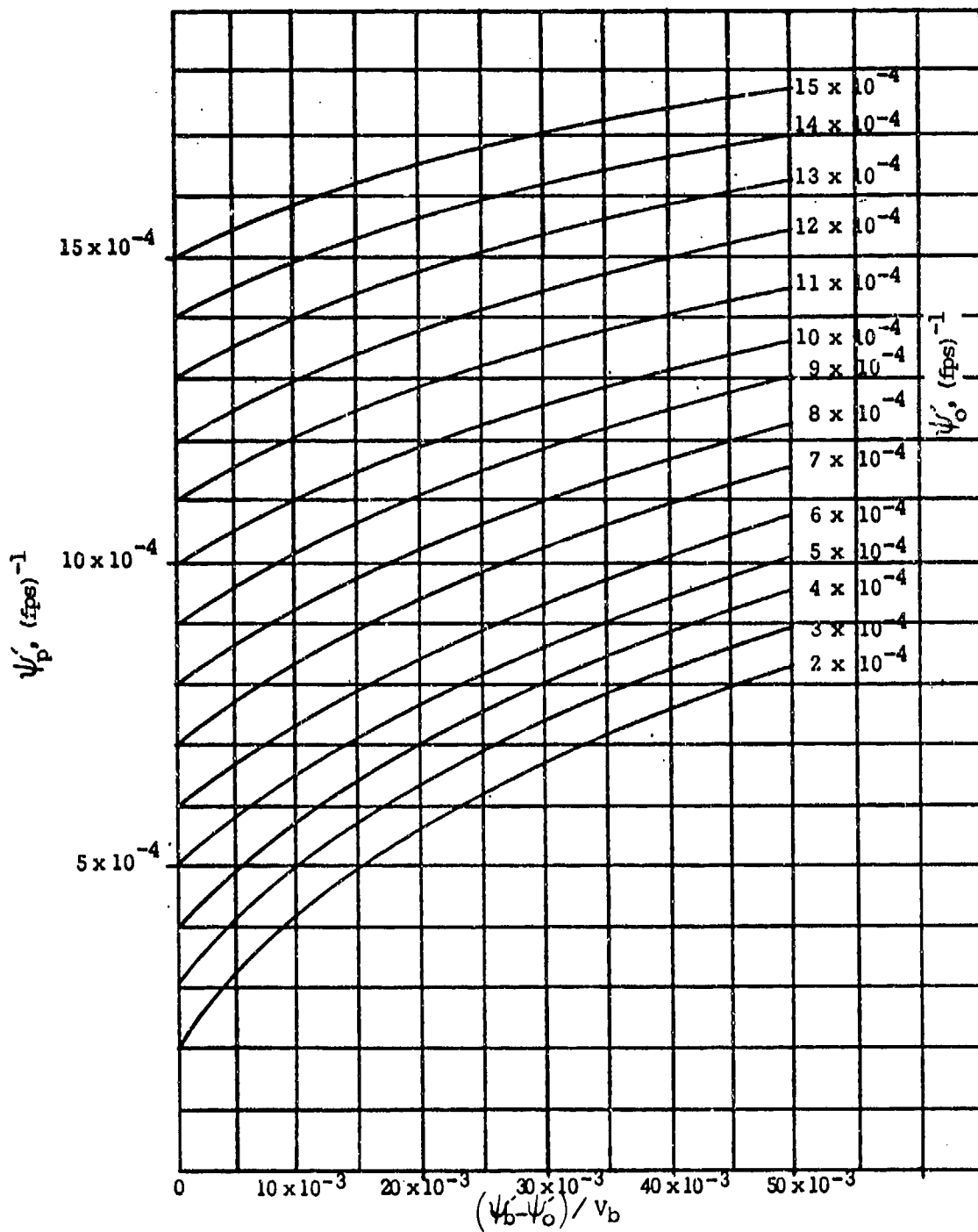


Figure 5-8. ψ_p' as a Function of ψ_o' and $(\psi_b' - \psi_o') / V_b$

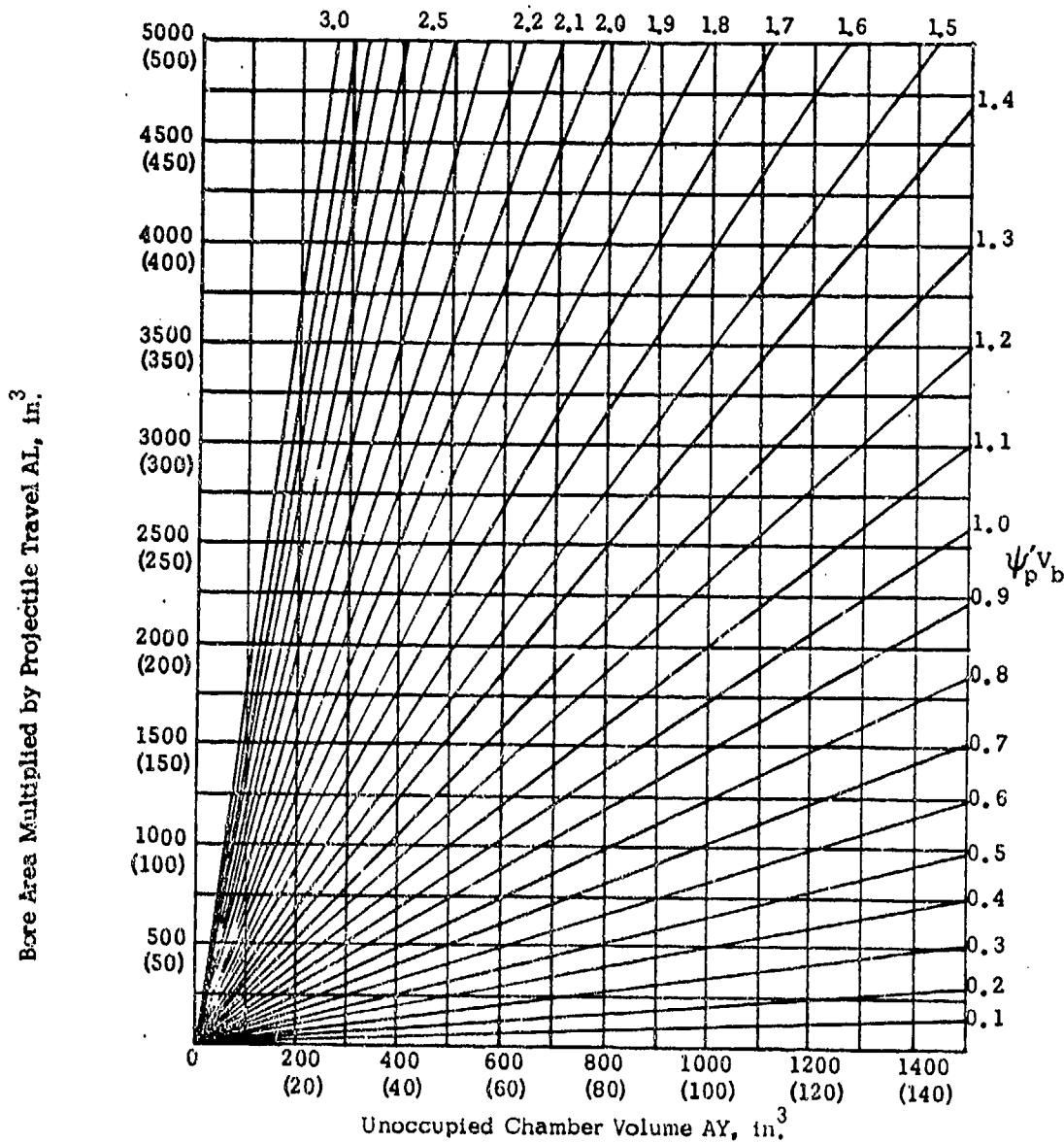
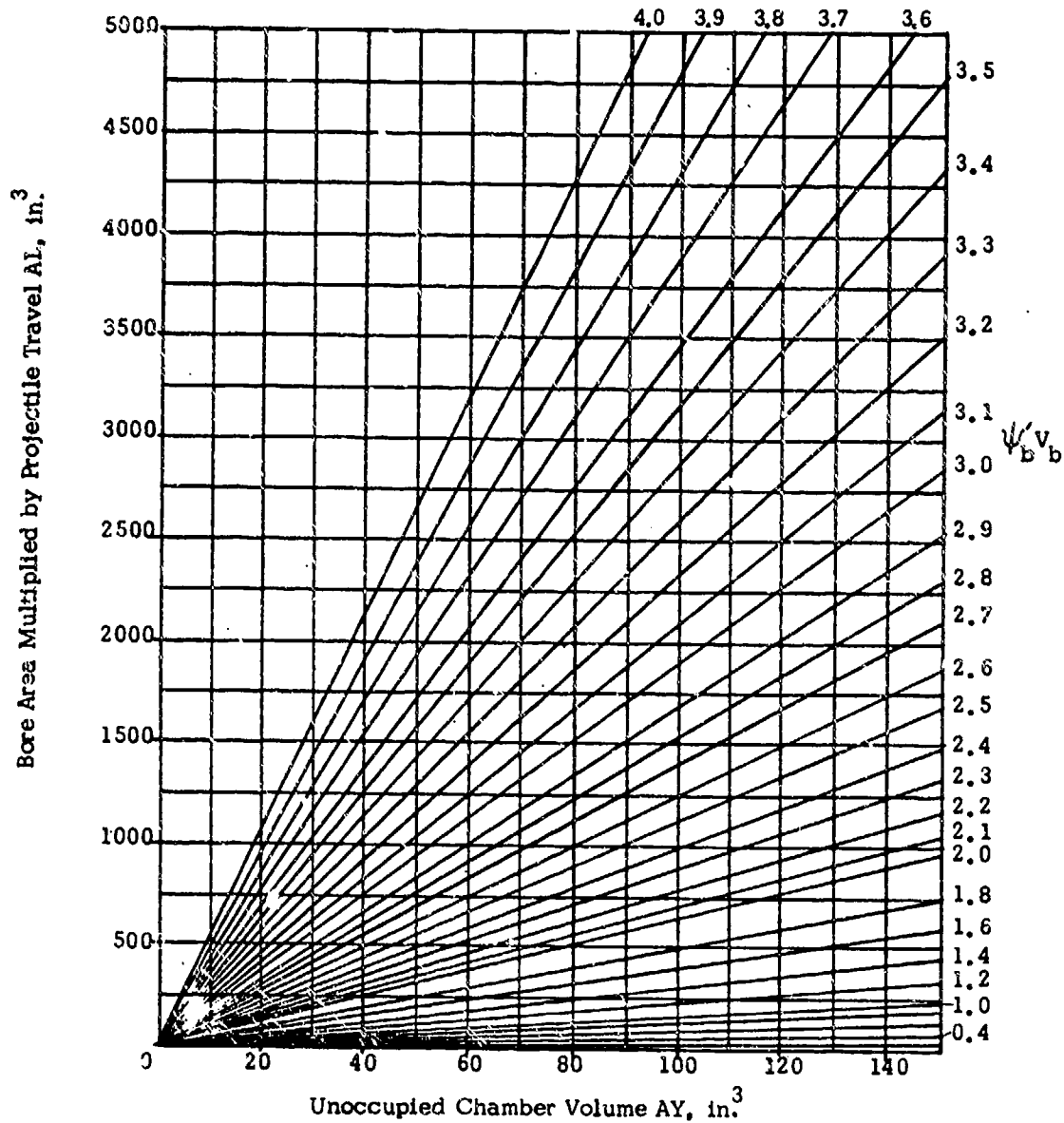


Figure 5-9. Bore Area Times Projectile Travel AL as a Function of AY and $\psi'v_b$

Although the burning rate determined from the definition of λ is not very accurate and must be determined by experimental firing of the particular weapon, the ratio W/B can be determined from the definition of λ with reasonable accuracy, where W is the web thickness of the propellant grain in inches and

B is the effective burning rate constant in in.-(sec-psi)⁻¹.

Figs. 5-5 through 5-13 are plots of the equations of Ref. 4 and are based on the assumption that the projectile velocity V_b , at the instant the propellant is all burned, is



Figures 5-10. Bore Area Times Projectile Travel AL as a Function of AY and $\psi'_b V_b$

approximately 95 percent of the muzzle velocity V_m . However, in order to simplify the curves, it is assumed that $V_b = V_m$ with only a small error being introduced.

5-7.2 PROCEDURE FOR USING GRAPHS

Given V_m , m , and A/A_i :

- (1) Determine C_i from Fig. 5-5.
- (2) Determine ψ'_b , ψ'_o , and ψ'_p from Figs. 5-6, 5-7 and 5-8, respectively.
- (3) Determine AY from Fig. 5-9 or 5-10. The scales of both coordinates on these figures may be simultaneously multiplied by the same constant factor.

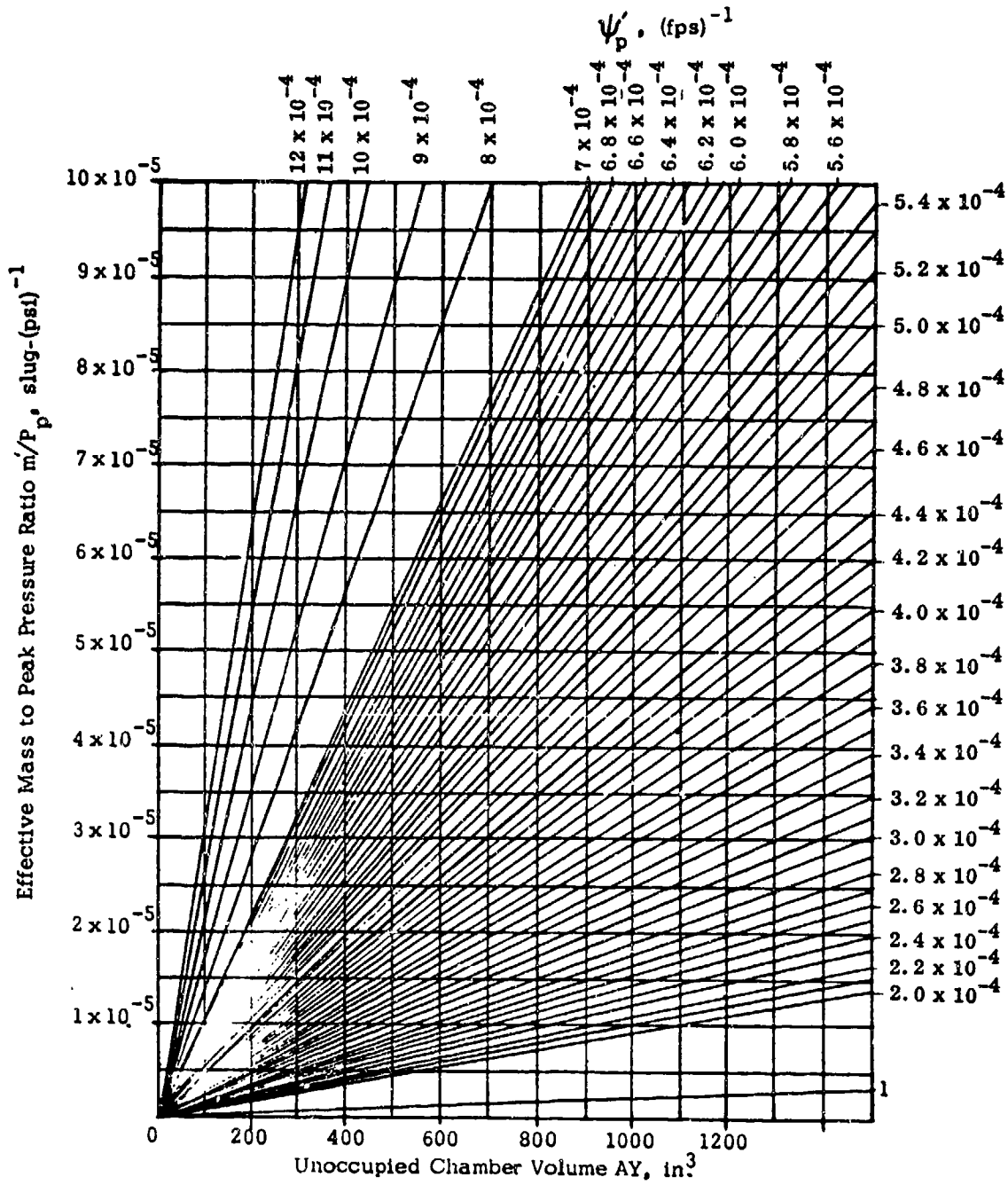


Figure 5-11. Effective Mass to Peak Pressure Ratio m'/P_p as a Function of AY for $\psi'_p \times 10^{-4}$ from 1 to 12

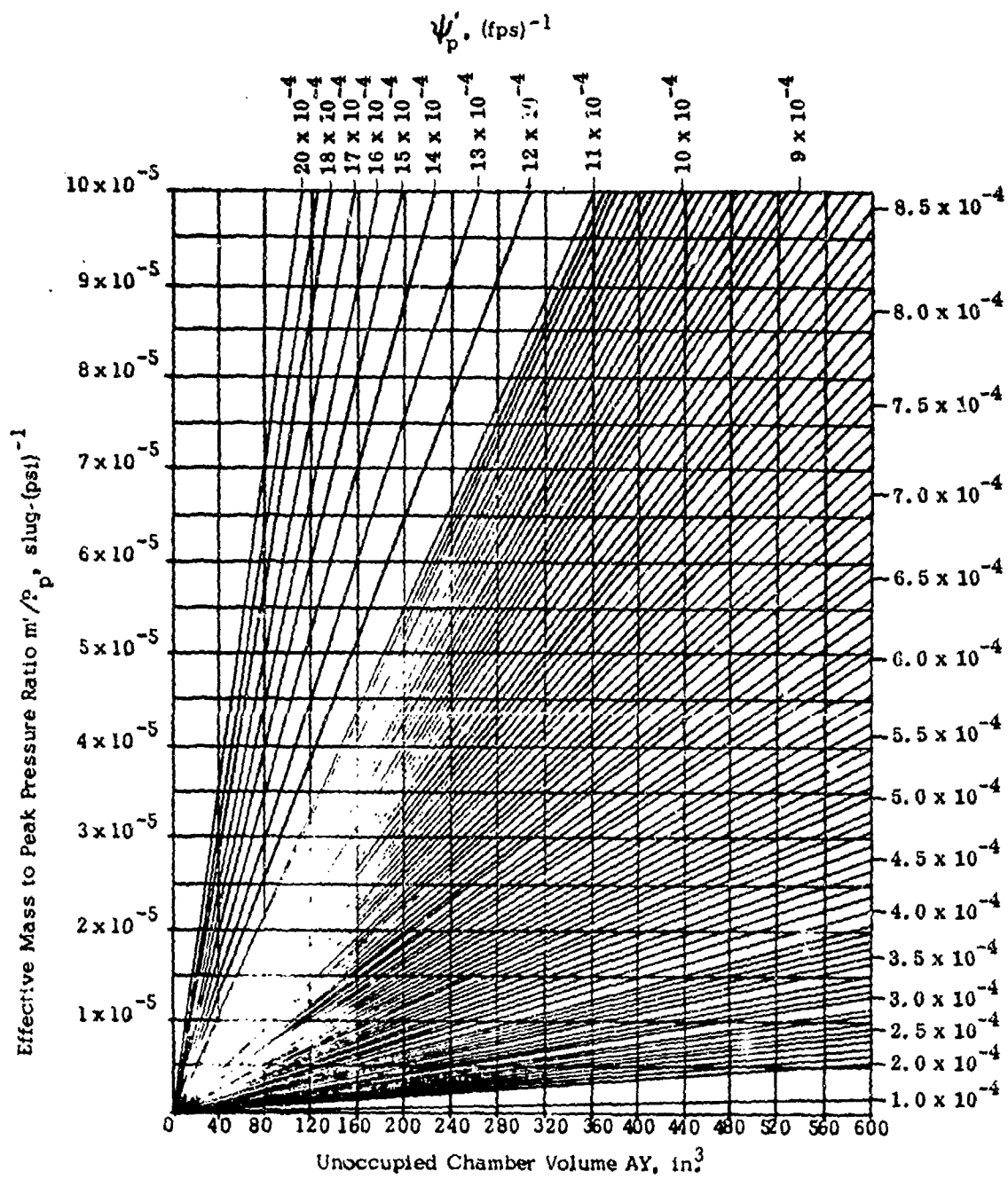


Figure 5-12. Effective Mass to Peak Pressure Ratio m'/P_p as a Function of AY for $\psi_p' \times 10^{-4}$ from 1 to 20

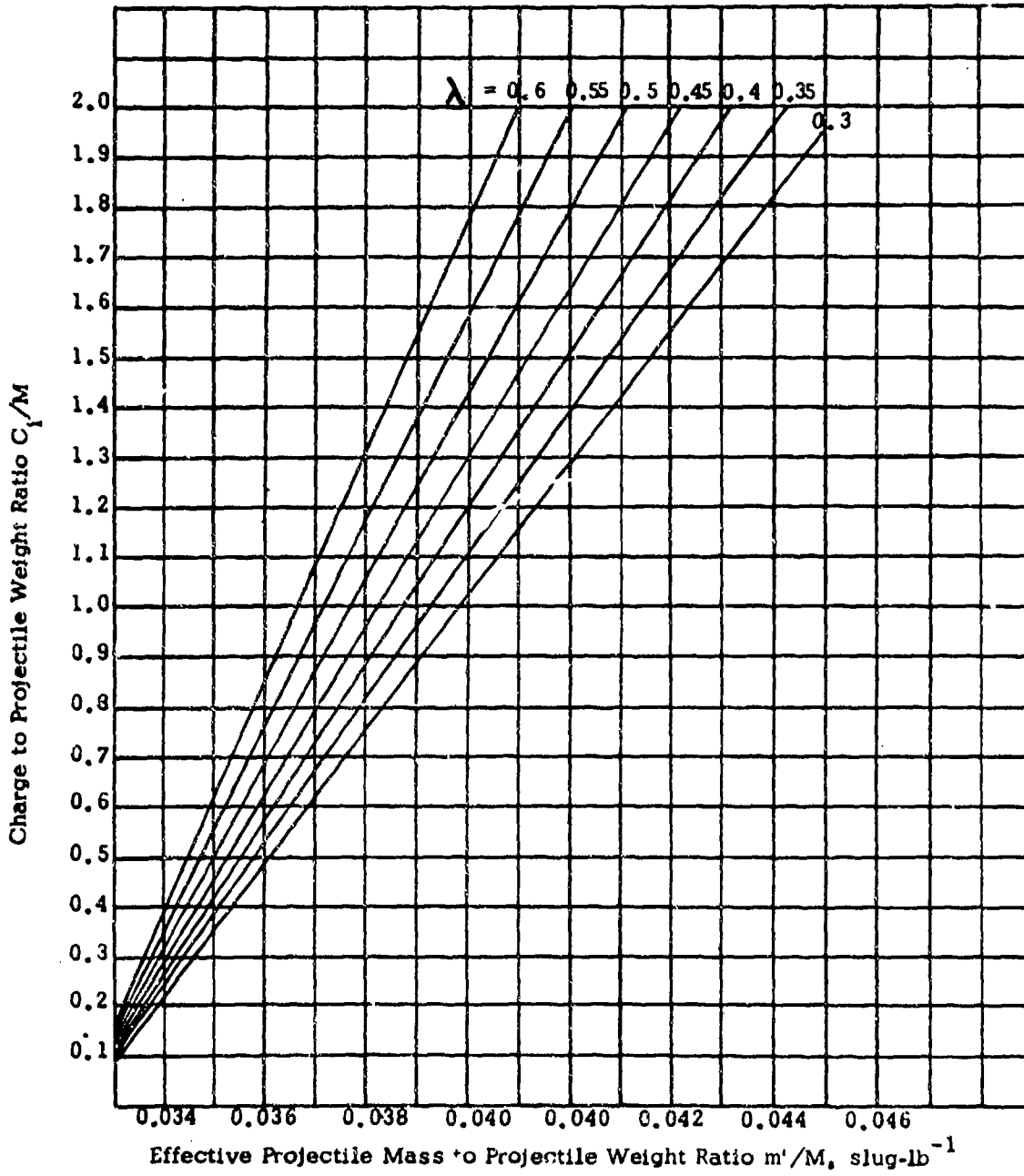


Figure 5-13. Charge to Projectile Weight Ratio C_1/M as a Function of Effective Projectile Mass to Projectile Weight Ratio m'/M for Values of λ from 0.3 to 0.6

(4) Determine m'/P_p from Fig. 5-11 or Fig. 5-12. The scales in these figures may also be simultaneously multiplied by a constant factor as in Step (3).

(5) Determine m' from Fig. 5-13.

(6) Compute $P_p = m'/(m'/P_p)$.

(7) Compute chamber volume v_c

$$v_c = AY + C_i/\rho \text{ (where } \rho \text{ is the density of solid propellant in lb-in.}^{-3}\text{)}$$

(8) Calculate the loading density Δ_o

$$\Delta_o = 27.7 C_i/v_c$$

(9) A set of recoilless rifle and propellant parameters has been determined corresponding to a particular value of λ . The process is repeated with a change of λ to yield another set of parameters consistent with the required muzzle velocity and tube length. By tabulating and plotting the results of these calculations a suitable choice of λ will result in an optimization of peak pressure, chamber volume, and propellant charge under the constraints of the weapon system.

5-7.3 NUMERICAL EXAMPLE

Given the following parameters for a 105 mm M27 Recoilless Rifle using an M323 Projectile and M10 Propellant:

$$A = 13.72 \text{ in}^2$$

$$A_i = 9.31 \text{ in}^2$$

$$A/A_i = 1.473$$

$$M = 32.4 \text{ lb}$$

$$V_m = 1120 \text{ fps}$$

$$L_m = 106 \text{ in.}$$

$$F = 3.31 \times 10^5 \text{ (ft-lb)-lb}^{-1}$$

$$\gamma = 1.24$$

$$\eta = 17.09 \text{ in}^3\text{-lb}^{-1}$$

$$K = 6.46 \times 10^{-3} \text{ sec}^{-1}$$

The results of the calculations performed based on these parameters are plotted in Figure 5-14 which shows that for a loading density (0.6 g-cm^{-3}), the factor λ would be 0.585; the charge C_i , 9 lb; and the peak pressure P_p , 7500 psi.

5-8 SIMILITUDE RELATIONS

5-8.1 INTRODUCTION

The basic interior ballistic equations as derived in Section III can be written in dimensionless form by use of the following dimensionless variables:

$$\phi' = N/C_i$$

$$\Omega = (N - N')/N$$

$$\theta' = N'/N$$

$$T' = T/T_o$$

$$\nu = P(v_c - C_i/\rho)/(12C_iF)$$

$$\xi' = Ax/(v_c - C_i/\rho)$$

$$\bar{\tau} = \left(\frac{12 \text{ Ft}}{v_c - C_i/\rho} \right) \left(\frac{C_i B}{W_o} \right)$$

Substitution of these variables into the basic equations of par. 5-16 and assuming that $\theta\eta\rho = 1$ in the equation of state, yields the following dimensionless governing equations:

(1) Equation of Motion:

$$\frac{d^2 \xi'}{d\bar{\tau}^2} = Q\nu \quad (5-9)$$

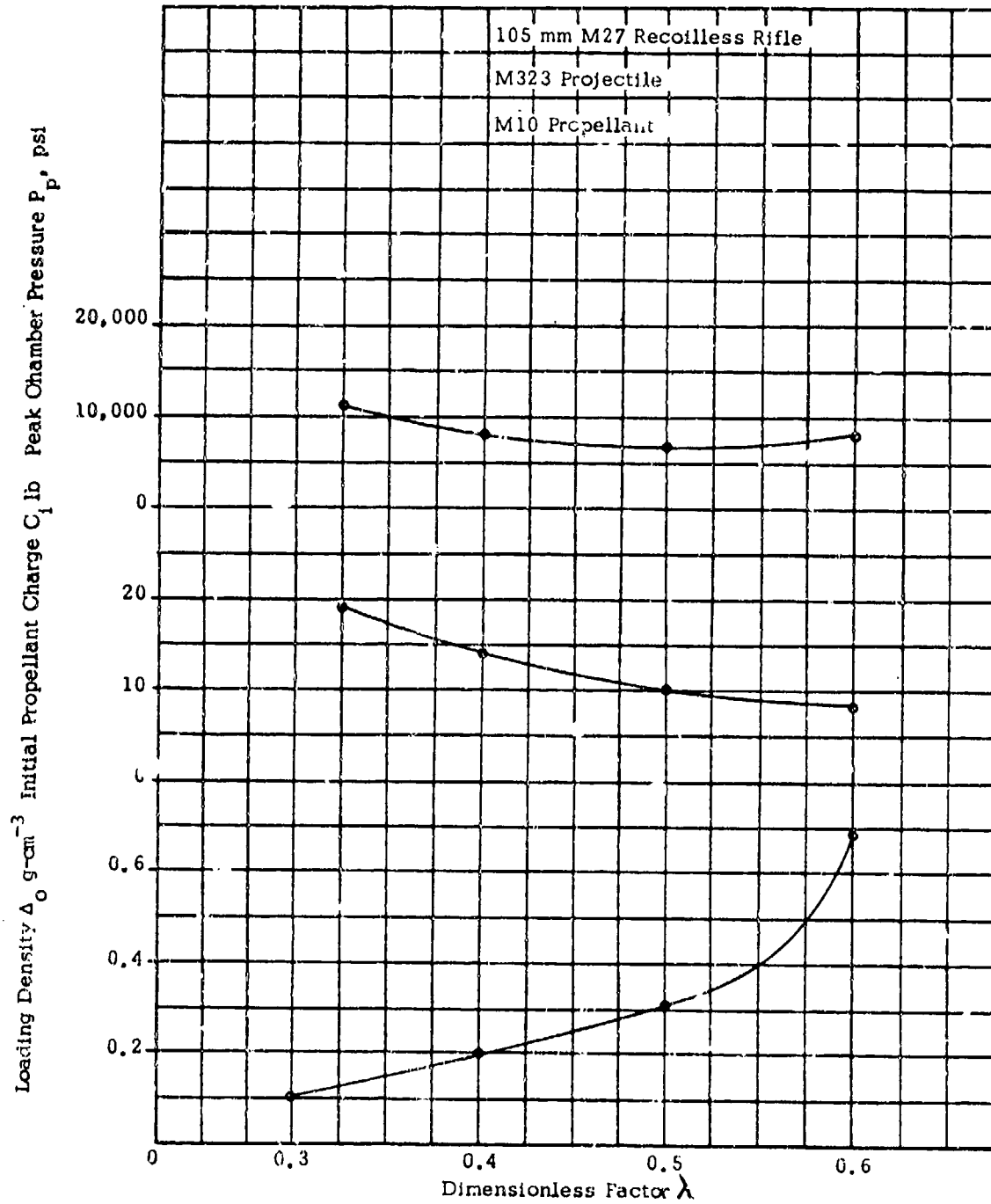


Figure 5-14. Ballistic Parameters as a Function of Factor λ

where

$$Q = \frac{\left(\frac{A}{C_1}\right)^2 \left(\frac{C_1}{m'}\right)}{F \left(\frac{B}{W_0}\right)^2}$$

(2) Gas Production Equation:

$$\frac{d\xi'}{d\bar{r}} = \nu \quad (5-10)$$

(3) Gas Discharge Equation:

$$\Omega = \lambda (T')^{-1/2} \quad (5-11)$$

where

$$\Omega = k A_1 W_0 / (C_1 B)$$

(4) Continuity Equation:

$$(1 - \Omega) = \theta' \quad (5-12)$$

(5) Equation of State:

$$\theta' \phi' T' = \nu (1 + \xi') \quad (5-13)$$

(6) Energy Equation:

$$\theta' \phi' T' = \phi' - \frac{\gamma \Omega T'}{Q} \left(\frac{d\xi'}{d\bar{r}}\right) - \frac{(\gamma - 1)(1 + \beta)}{2Q} \left(\frac{d\xi'}{d\bar{r}}\right)^2 \quad (5-14)$$

It is seen from these dimensionless governing equations that if the numerical value of the coefficients Q , λ , γ , and β remain constant the solution to the governing equations is the same; i.e., systems for which these coefficients are the same will have identical theoretical ballistic performance.

5-8.2 CHARACTERISTIC SIMILITUDE RELATIONS

If the performance of a particular gun is

known, the performance of a similar gun can be predicted through the use of the similarity relations developed by maintaining the same value for Q and λ . In practice, Q is held constant by preserving the charge to bore area ratio C_1/A , the relative quickness B/W_0 , impetus F , and projectile sectional density M/A . If Q is constant and the ratio of bore area to throat area is also unchanged, then the gas discharge equation is also unchanged. The specific heat ratio γ is not a widely varying coefficient and can be assumed constant within the accuracy of this interior ballistics model. The ratio β of heat loss to projectile kinetic energy also must be constant for similitude conditions, which is expected, since similar guns are expected to have similar fractions of heat loss to projectile kinetic energy.

Identifying the known system parameters with a subscript 1, the parameters for the model system should be as follows in order to obtain the same pressure-travel and velocity-travel solutions:

$$m/A = m_1/A_1$$

$$C_1/A = C_{1_1}/A_1$$

$$A/A_t = A_1/A_{t_1}$$

$$x_0 = x_{0_1}$$

$$B/W = B_1/W_1$$

$$T' = T'_1$$

$$F = F_1$$

5-9 EFFECT OF BALLISTIC VARIATIONS

5-9-1. INTRODUCTION

In many cases, it is desirable to determine the effect of the variation of such ballistic parameters as flow factor, impetus, and burning rate on the ballistic performance of a recoilless rifle—especially as affecting peak

pressures and muzzle velocity. For example, an increase in throat area due to nozzle erosion will cause a significant increase in forward recoil and may affect the muzzle velocity to such an extent that the rifle becomes useless for operation after a certain amount of usage. Therefore, it is necessary to be able to estimate the life of the gun nozzle based on the variation of muzzle velocity with throat area. The approximations for peak pressure and muzzle velocity that follow as given in Ref. 5 are differentiated with respect to the designated ballistic parameters and the effects evaluated in subsequent paragraphs.

$$P_p = \frac{12m'e_2^2 f(u)}{v_c(1-\alpha)}, \text{ psi} \quad (5-15)$$

$$V_m = \frac{e_2}{u}(1 - \delta^{-u}), \text{ fps} \quad (5-16)$$

where

$$f(u) = (1+u)^{(1+u)/u} / (1+2u)^{(1+2u)/u},$$

dimensionless

$$\delta = (\epsilon - \alpha) / (1 - \alpha), \text{ dimensionless}$$

$$\alpha = C_d / (\rho v_c), \text{ dimensionless}$$

$$\epsilon = \text{expansion ratio, total volume / chamber volume, dimensionless}$$

The parameters e_2 and u are given by

$$e_2 = F \left[\frac{C_2}{A} \left(1 + \frac{W}{L} \right) \left(\frac{B}{W_o} \right) - \Gamma \right], \text{ fps}$$

$$u = \frac{(\bar{\gamma} - 1)}{2} + \left(\frac{W}{L} \right) \left(\frac{C_2}{A^2} \right) \left(\frac{B}{W_o} \right)^2 F m',$$

dimensionless

where

$$\Gamma, \text{ flow factor} = \gamma C_d K \left(\frac{A_t}{A} \right) \left(\frac{\bar{T}}{T_o} \right)^{1/2}, \text{ sec}^{-1}$$

$$\bar{\gamma} = (1 + \beta)(\gamma - 1) + 1, \text{ dimensionless}$$

$$\beta = \text{ratio of heat loss to burning energy of projectile, dimensionless}$$

$$C_d = \text{discharge coefficient of nozzle, dimensionless}$$

5-9.2 EFFECT OF QUICKNESS FACTOR B/W_o

The quickness factor is defined as B/W_o . The effect of quickness factor on peak pressure is obtained by differentiating the log pressure given in Eq. 5-15 with respect to the quickness B/W_o .

$$\frac{dP_p}{P_p} = 2 \left[\left(1 + \frac{\Gamma F}{e_2} \right) - \left(u - \frac{\bar{\gamma} - 1}{2} \right) \frac{(u + 1.5)}{(u + 1)^2} \right] \times \frac{d(B/W_o)}{(B/W_o)} \quad (5-17)$$

For the usual range of parameters a 1 percent change of quickness factor produces a change of peak pressure of 1.5 to 4 percent.

The effect of quickness factor on muzzle velocity is found by taking the derivative of the log V_m , as given in Eq. 5-16, with respect to B/W_o as shown in Ref. 5, Chapter II.

$$\frac{dV_m}{V_m} = \left[\frac{\Gamma F}{e_2} - 1 + \frac{\bar{\gamma} - 1}{2} + \frac{2 \left(u - \frac{\bar{\gamma} - 1}{2} \right) \ln \delta}{\delta^u - 1} \right] \times \frac{d(B/W_o)}{(B/W_o)} \quad (5-18)$$

As a typical example of the effect of quickness, the 57 mm M18 Recoilless Rifle has a change in muzzle velocity of 0.8 times the change in quickness.

5-9.3 EFFECT OF IMPETUS F

The change in peak pressure due to a

change in impetus is, taking the derivative of P_p with respect to F ,

$$\frac{dP_p}{P_p} = \left[2 - \left(u - \frac{\bar{\gamma} - 1}{2} \right) \frac{(u + 1.5)}{(u + 1)^2} \right] \frac{dF}{F} \quad (5-19)$$

Substitution of typical numerical values indicates that a 1 percent change in impetus results in a 1.5 percent change in peak pressure.

The variation in muzzle velocity is

$$\frac{dV_m}{V_m} = \left[\frac{\bar{\gamma} - 1}{2u} + \left(u - \frac{\bar{\gamma} - 1}{2} \right) \frac{\ln \delta}{\delta^u - 1} \right] \frac{dF}{F} \quad (5-20)$$

For the 57 mm M18 Rifle, it is found that the change in muzzle velocity is about one-half the change in impetus.

5-9.4 EFFECT OF PROPELLANT REGRESSIVENESS W/L

Propellant regressiveness is defined as a fictitious web to length ratio W/L and, in the case of single perforated grains, is given by:

$$\frac{W}{L} = \left(1 - \frac{C_s}{C_i} \right)^{-1} \left[\frac{W_o}{l_o} + \frac{C_s}{C_i} \frac{\left(1 - \frac{W_o}{l_o} \right)}{\left(1 - \frac{W_o}{3l_o} \right)} \right] \quad (5-21)$$

where

W_o = initial web thickness, in.

l_o = initial propellant grain length, in.

C_s = total weight of solid propellant ejected from rifle, lb

C_i = initial propellant charge, lb

A change in net regressiveness W/L causes the following change in peak pressure as found by

taking the derivative of P_p with respect to W/L ,

$$\frac{dP_p}{P_p} = 2 \left\{ 1 - \frac{1}{e_2} \left[\frac{C_2 F}{A} \left(\frac{B}{W_o} \right) - \Gamma F \right] - \left(u - \frac{\bar{\gamma} - 1}{2} \right) \frac{(u + 1.5)}{(u + 1)^2} \right\} \frac{d(W/L)}{W/L} \quad (5-22)$$

For small values of W/L , the term

$$\frac{1}{e_2} \left[\frac{C_2 F}{A} \left(\frac{B}{W_o} \right) - \Gamma F \right]$$

is close to unity and u is close to $(\bar{\gamma} - 1)/2$, therefore, the effect on peak pressure may be negligible. A typical value of this coefficient as given for the 57 mm M18 Rifle is

$$\frac{dP_p}{P_p} = (0.8) \frac{d(W/L)}{W/L}$$

The equation relating change of regressiveness to a change in muzzle velocity is:

$$\frac{dV_m}{V_m} = \left[\frac{F}{e_2} \left(\frac{C_2}{A} \right) \left(\frac{B}{W_o} \right) \frac{W}{L} - \left(1 - \frac{\bar{\gamma} - 1}{2u} \right) \times \left(1 + \frac{u \ln \delta}{\delta^u - 1} \right) \right] \frac{d(W/L)}{W/L} \quad (5-23)$$

For the M18 Rifle this term is negative and approximately one-half. For longer rifles, i.e., larger values of δ , the effect of regressiveness becomes negligible.

5-9.5 EFFECT OF FLOW FACTOR Γ

The flow factor Γ is a significant factor defined by a combination of ballistic parameters as follows:

$$\Gamma = \gamma C_d K \left(\frac{A_t}{A} \right) \left(\frac{\bar{T}}{T_o} \right)^{1/2}, \text{ sec}^{-1} \quad (5-24)$$

The effect of flow factor on peak pressure is

determined by taking the derivative of P_p with respect to Γ and given by,

$$\frac{dP_p}{P_p} = -2 \left(\frac{F\Gamma}{e_2} \right) \frac{d\Gamma}{\Gamma} \quad (5-25)$$

For a typical case of the M18 Rifle, $F\Gamma/e_2 = 0.75$, so that a corresponding change in peak pressure varies inversely about 1.5 times the change in flow factor.

The effect on muzzle velocity is deter-

mined by taking the derivative of V_m with respect to Γ and is given by,

$$\frac{dV_m}{V_m} = - \left(\frac{\Gamma F}{e_2} \right) \frac{d\Gamma}{\Gamma} \quad (5-26)$$

Since $F\Gamma/e_2$ is, for example, = 0.75 for the M18 Rifle, the change in muzzle velocity will be about 0.75 times the inverse change in flow factor.

SECTION III

BASIC INTERIOR BALLISTIC EQUATIONS

5-10 EQUATIONS FOR PROJECTILE ACCELERATION

In the absence of friction, the equation of motion of the projectile

$$\frac{dV}{dt} = \frac{AP_x}{m} \quad (5-27)$$

where

V = instantaneous projectile velocity, fps

P_x = pressure acting on the projectile base, psi

A = bore area, in²

m = mass of the projectile, slug

t = time, sec

It is obvious that there must be a greater pressure in the weapon chamber since the propellant gas itself must be accelerated by the difference in pressure between the chamber and the base of the projectile. There is an additional, usually smaller, pressure drop required to overcome the effects of gun-wall friction against the motion of the gas. This real drop in pressure is effected by artificially increasing the mass of the projectile in order to produce the correct acceleration. The relation between the space-mean pressure and the pressure at the base of the projectile is estimated as

$$P = (1.04)P_x \left[1 + \frac{(1 - \lambda)C_i}{\delta M} \right] \quad (5-28)$$

where

P = space-mean pressure, psi

P_x = pressure at projectile base, psi

C_i = propellant charge, lb

δ = $(\epsilon - \alpha)/(1 - \alpha) \approx 3$

λ = $kA_i W/(C_i B)$, dimensionless

k = KC_d , sec⁻¹

The factor δ is plotted as a function of M/C_i in Fig. 5-15.

Eq. 5-27 can now be written as

$$\frac{dV}{dt} = \left(\frac{A}{m} \right) \left\{ \frac{P}{1.04 \left[1 + \frac{(1 - \lambda)C_i}{\delta g} \right]} \right\} \quad (5-29)$$

By defining an effective mass m' as

$$m' = 1.04 \left[m + \frac{(1 - \lambda)C_i}{\delta g} \right] \quad (5-30)$$

where the factor 1.04 accounts for friction.

Eq. 5-29 can now be written

$$\frac{dV}{dt} = \frac{AP}{m'} \quad (5-31)$$

It is seen from Fig. 5-15 that for values of M/C_i larger than one the value of δ is approximately 3, and this is the value normally used for calculations of m' .

5-11 EQUATION OF STATE FOR PROPELLANT GAS

The equation of state for the propellant gas can be taken with sufficient accuracy as

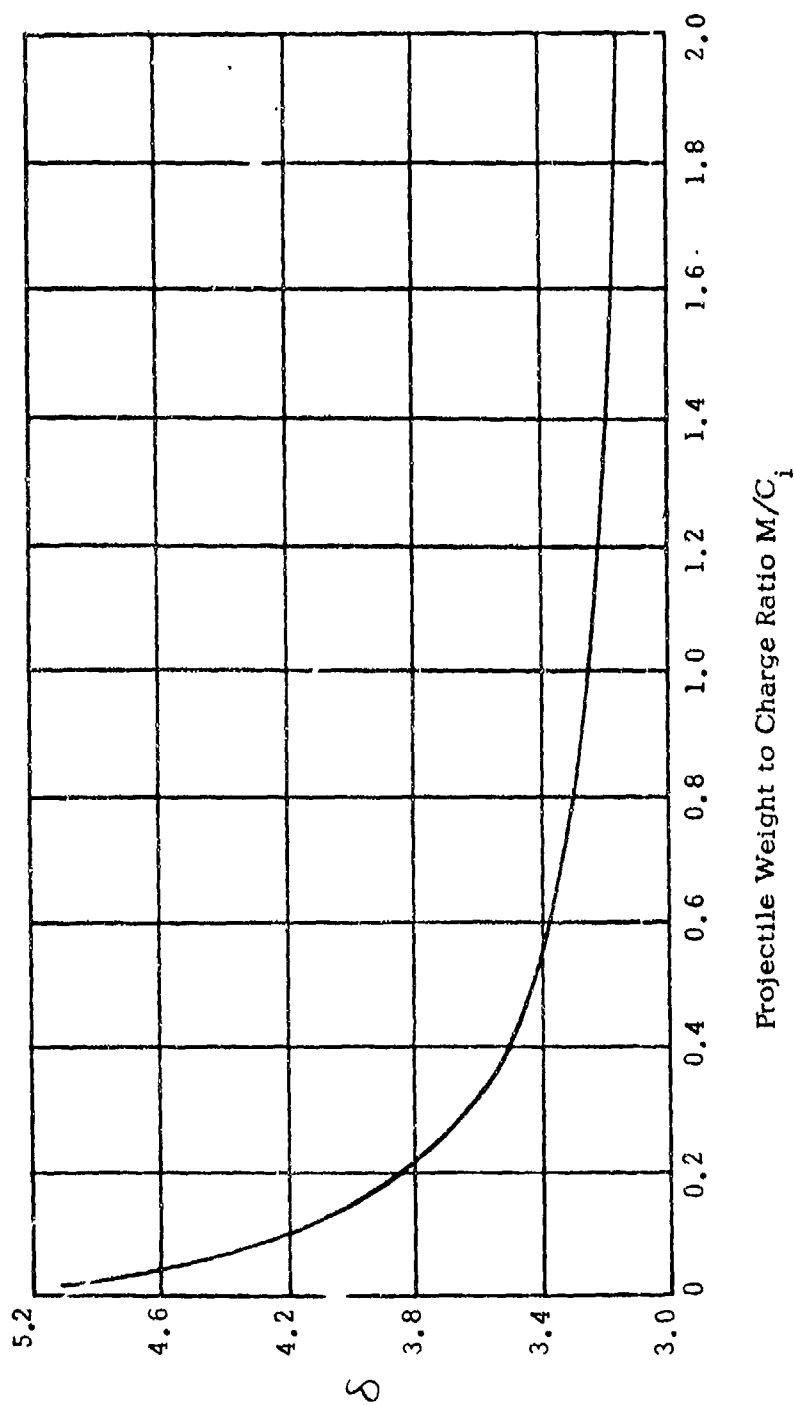


Figure 5-15. The Parameter δ as a Function of the Projectile Weight to Charge Weight Ratio M/C_1

$$P(v_x - \eta N') = 12N'RT \quad (5-32)$$

where

$$\eta = \text{gas covolume, in}^3\text{-lb}^{-1}$$

$$N' = \text{quantity of gas in the weapon, lb}$$

$$T = \text{gas temperature, } ^\circ\text{R}$$

$$R = \text{gas constant, (ft-lb)-(lb-}^\circ\text{R)}^{-1}$$

$$v_x = \text{free volume in gun, in}^3$$

The gas covolume η is the space occupied by the gas when it is compressed to its limit. The free volume v_x in the recoilless rifle is defined as the total volume behind the projectile less the volume occupied by the unburnt propellant and can be expressed as

$$v_x = A(L + x_0) - (C_2 - N)/\rho \quad (5-53)$$

where

$$x_0 = \text{equivalent chamber length, in.}$$

$$= V_c/A$$

$$L = \text{projectile displacement, in.}$$

$$N = \text{quantity of gas produced, lb}$$

$$\rho = \text{density of the solid propellant, lb-in.}^{-3}$$

Introducing the propellant impetus F

$$F = RT_0, \text{ (ft-lb)-lb}^{-1} \quad (5-34)$$

where

$$T_0 = \text{isochoric (constant volume) flame temperature, } ^\circ\text{R, and is the temperature which the gases would attain if all the propellant energy was converted into the formation and heating of gases}$$

$$R = \text{universal gas constant (ft-lb)-(lb-}^\circ\text{R)}^{-1}$$

With these substitutions the equation of state, Eq. 5-32 becomes

$$P[A(L + x_0) - (C_2 - N)/\rho - \eta N'] = 12N'FT/T_0 \quad (5-35)$$

It should be noted that the difference $(N - N')$ is the amount of gas discharged through the nozzle.

5-12 EQUATION FOR RATE OF PROPELLANT BURNING

The rate at which propellant gas is produced is given as

$$\frac{dN}{dt} = \rho S r \quad (5-36)$$

where

$$\rho = \text{density of solid propellant charge, lb-in.}^{-3}$$

$$S = \text{instantaneous burning surface area, in}^2$$

$$r = \text{instantaneous burning rate, in.-sec}^{-1}$$

The instantaneous rate r is expressed in general form for propellant burning as

$$r = a + C' P^n \quad (5-37)$$

where a , C' , and n are constants depending upon the specific propellant composition. For the pressures encountered in most recoilless rifles, the value of $C' P^n \gg \gg a$ and as a result the burning rate equation is used with $a = 0$. Also, it is found that in recoilless rifles, the value of n is close to unity and therefore as a useful approximation the burning rate may be considered linear and is expressed as

$$r = G' P, \text{ in.-sec}^{-1} \quad (5-38)$$

with the value of the burning rate C' (in.-(sec-psi)⁻¹), chosen to give the best agreement with Eq. 5-37 for the range of pressure considered for the specific propellant. The linearized burning rate Eq. 5-38 is shown plotted in Fig. 5-16 for two different pressure ranges for M10 Propellant that has the following nonlinear burning rate per Eq. 5-37

$$r = 4.53 \times 10^{-3} p^{0.7}$$

where

$$C'' = 4.53 \times 10^{-3} \text{ in. sec}^{-1}\text{-psi}^{-0.7}$$

$$n = 0.7$$

In the case of the single perforated grain where burning occurs normal to all the surfaces, outer surface, perforation surface, and both ends, the surface area S for a charge comprising a single-grain is

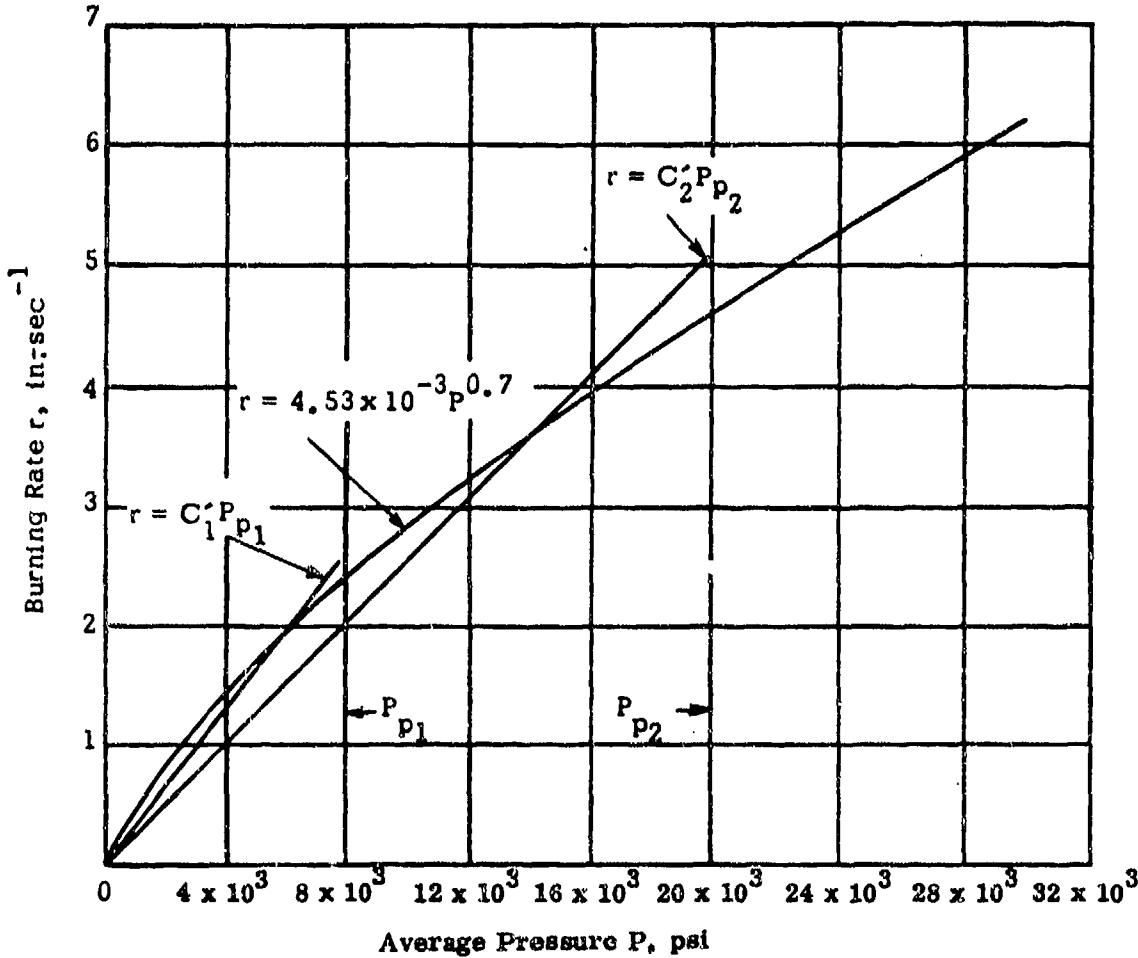


Figure 5-16. Burning Rate as a Function of Average Pressure for M10 Composition Propellant, Lot FDAP 81

$$\left. \begin{aligned}
 S &= 2\frac{\pi}{4} \left[(D_o - \omega W_o)^2 - (d + \omega W_o)^2 \right] \\
 &+ \pi \left[(D_o - \omega W_o) + (d + \omega W_o) \right] \\
 &\times (l_o - \omega W_o) \\
 \text{or} \\
 S &= \pi(D_o + d)l_o \left[\left(1 + \frac{W_o}{l_o} \right) \right. \\
 &\quad \left. - 2 \left(\frac{W_o}{l_o} \right) \omega \right] \text{ in.}^2
 \end{aligned} \right\} (5-38a)$$

where

D_o = outer grain diameter, in.

d = perforation diameter, in.

W_o = $(D_o - d)/2$ = web, the minimum distance the flame front can burn through and consume the grain, in.

ω = fraction of web consumed, dimensionless

l_o = initial length of grain, in.

It should be noted that as long as $l_o > W_o$, the grain will be consumed when half of the web W_o is burnt because the grain is burning from the perforation outward and simultaneously from the outer surface inward. Obviously, for the same burning rate, the flame fronts will meet when half of the web is consumed.

The corresponding density for the single perforated grain is

$$\left. \begin{aligned}
 \rho &= \frac{C_2}{\frac{\pi}{4}(D_o^2 - d^2)l_o} \\
 \text{or} \\
 \rho &= \frac{2}{\pi} \left[\frac{C_2}{(D_o + d)W_o l_o} \right] \text{ lb-in.}^3
 \end{aligned} \right\} (5-38b)$$

where

ρ = density of the solid propellant, lb-in.⁻³

C_2 = propellant charge burned, lb

Substituting Eqs. 5-38b, 5-38a, and 5-38 in Eq. 5-36, one obtains

$$\frac{dN}{dt} = \frac{2C' C_2 P}{W_o} \left[\left(1 + \frac{W_o}{l_o} \right) - 2 \left(\frac{W_o}{l_o} \right) \omega \right] \text{ lb-sec}^{-1} \quad (5-38c)$$

The surface area can be obtained from Eqs. 5-38b and 5-38a as

$$S = \frac{2C_2}{\rho W_o} \left[\left(1 + \frac{W_o}{l_o} \right) - 2 \left(\frac{W_o}{l_o} \right) \omega \right], \text{ in.} \quad (5-38d)$$

For the condition of constant burning surface propellant, $W_o/l_o = 0$, which is a good approximation for a single perforated grain, Eq. 5-38d can be written as

$$S = 2C_2/(\rho W_o), \text{ in.}^2 \quad (5-39)$$

and Eq. 5-38c as

$$\frac{dN}{dt} = \frac{BC_2 P}{W_o}, \text{ lb-sec}^{-1} \quad (5-40)$$

where

$$B = 2C', \text{ in.} \cdot (\text{sec-psi})^{-1}$$

The quantity B/W_o is known as the propellant quickness with dimensions $(\text{sec-psi})^{-1}$. Values of B as a function of peak pressure for M10 Propellant are plotted in Fig. 5-17.

For multiperforated grains the web thickness is the actual measured minimum thickness of propellant between perforations. A factor F_7 is shown in Fig. 5-33 which relates the seven perforated web thickness to an equivalent single perforated web thickness. Thus, the equation for gas generation of a seven perforated grain is estimated as

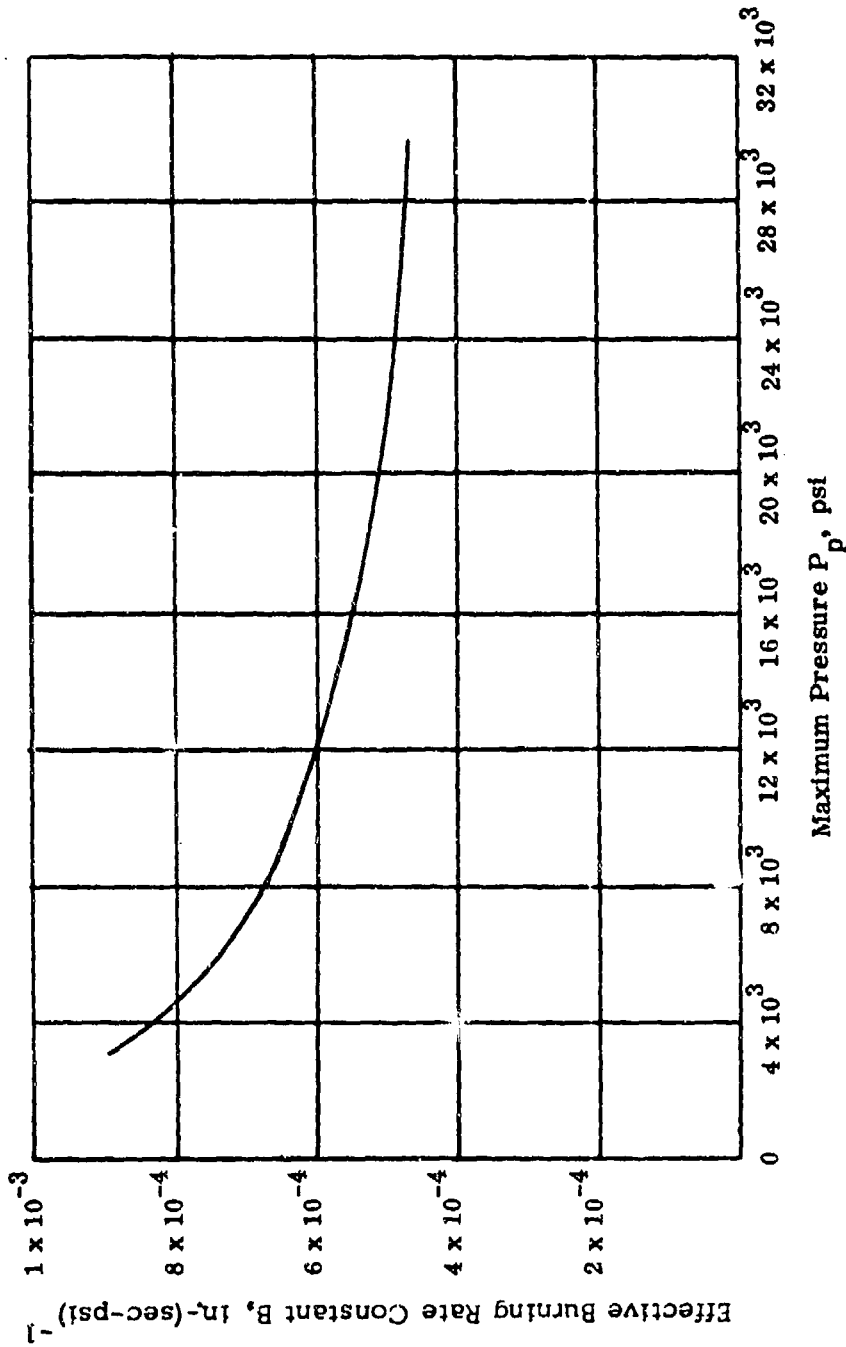


Figure 5-17. "Effective" Burning Rate Constant B_p as a Function of Maximum Pressure P_p

$$\frac{dN}{dt} = \frac{C_2 B P}{F_1 W_1}, \text{ lb-sec}^{-1} \quad (5-40a)$$

For further information on specific propellants and propellant geometries, reference is made to the propellant section of Chapter 11, "Ammunition".

5-13 EQUATION FOR DISCHARGE OF PROPELLANT GAS THROUGH NOZZLE

The amount of gas discharged through the nozzle is equal to the amount of propellant burnt minus the gas in the recoilless rifle. The rate of nozzle discharge in pounds per second is

$$\frac{d(N - N')}{dt} = k A_t \left(\frac{T_0}{T} \right)^{1/2} P \quad (5-41)$$

where

N' = propellant gas accumulation in recoilless rifle, lb

A_t = nozzle throat area, in²

k = $C_d K$, sec⁻¹

K = nozzle coefficient
 $= \left[\frac{\gamma g}{F} \left(\frac{2}{\gamma + 1} \right)^{(\gamma+1)/(\gamma-1)} \right]^{1/2}$, sec⁻¹

C_d = nozzle discharge coefficient, dimensionless

P = space-mean pressure, psi

γ = ratio of specific heats, dimensionless

For an isentropic nozzle, the discharge coefficient is taken as unity by definition. However, due to losses in an actual nozzle, the discharge coefficient is less than one. In short nozzles the friction and heat losses are usually small but, when the additional effect

of throat blockage by ejection of solid propellant is taken into account, a discharge coefficient of approximately 0.9 is used in order to satisfy the mass balance equation.

5-14 EQUATION FOR ACCUMULATION OF GAS IN GUN

The rate of propellant gas being generated minus the rate of propellant gas discharged through the nozzle is the rate of gas accumulation in the gun. From Eqs. 5-40 and 5-41 the rate of gas accumulation in the gun becomes

$$\frac{dN'}{dt} = \left[\frac{C_2 B}{W_0} - k A_t \left(\frac{T_0}{T} \right)^{1/2} \right] P, \text{ lb-sec}^{-1} \quad (5-42)$$

Define the following dimensionless parameters

$$\lambda = k A_t / (C_2 B), \text{ dimensionless,}$$

and

$$\theta = 1 - \lambda \left(\frac{T_0}{T} \right)^{1/2}, \text{ dimensionless}$$

then the rate of gas accumulation in the gun becomes

$$\frac{dN'}{dt} = \theta \left(\frac{C_2 B}{W_0} \right) P \quad (5-43)$$

and from Eq. 5-40, Eq. 5-43 can be written

$$\frac{dN'}{dt} = \theta \left(\frac{dN}{dt} \right) \quad (5-44)$$

5-15 ENERGY EQUATION

The total energy available by burning N pounds of propellant is $N c_v T_0$ where c_v is the specific heat at constant volume, (ft-lb)(lb⁻¹R)⁻¹.

The total available energy is divided among the following four applications:

(1) Kinetic energy of the projectile:

$$\frac{1}{2} m' V_m^2$$

(2) Heat loss to the gun:

$$\frac{\beta}{2} m' V_m^2$$

where β is estimated as shown in Ref. 4 as

$$\beta = \frac{5.8 L_m}{\left(\frac{2M}{C_t} + 0.3\right) V_m^2} \left(\frac{T_o - 300}{D}\right)^{4/3}$$

dimensionless (5-45)

where

T_o = isochoric flame temperature, °R

D = bore diameter, in.

A rough approximation of β is sufficient. Values of β range from about 0.4 for 57 mm rifles to about 0.2 for 105 mm rifles. A more detailed discussion of heat transfer is given in Section IX.

(3) Nozzle discharge energy:

It is shown in Ref. 4 that the energy dissipated in the nozzle discharge is

$$\gamma c_v k (T_o \bar{T})^{1/2} \left(\frac{A_t}{A}\right) m' V \quad (5-46)$$

where

$(T_o \bar{T})^{1/2}$ represents the average value of $(T_o \bar{T})^{1/2}$ over the discharge time.

(4) Internal energy of gas remaining in weapon:

$$N' c_v T$$

The total energy balance equation is then:

$$N c_v T_o = N' c_v T + \gamma c_v k (T_o \bar{T})^{1/2} \left(\frac{A_t}{A}\right) m' V + \frac{(1 + \beta)}{2} m' V^2 \quad (5-47)$$

5-16 SUMMARY OF EQUATIONS

Use the relation

$$\frac{dV}{dt} = V \left(\frac{dV}{dL}\right) \quad (5-48)$$

and the average value of θ

$$\bar{\theta} = 1 - \lambda \left(\frac{T_o}{\bar{T}}\right)^{1/2} \quad (5-49)$$

The basic interior ballistic equations then can be summarized as

(1) Equation of Projectile Motion

From Eq. 5-31

$$PA = m' \left(\frac{dV}{dt}\right)$$

and the definition of velocity

$$12V = \frac{dx}{dt} = \frac{dL}{dt} \quad (5-50)$$

$$P = 12 \left(\frac{m'}{A}\right) V \left(\frac{dV}{dL}\right)$$

(2) Equation of Burning

From Eq. 5-44 and considering the start condition

where

$$N = N_0$$

$$N' = N_0$$

$$N' = \bar{\theta}N + (1 - \bar{\theta})N_0$$

(5-51)

where

N_0 = weight of propellant burnt at projectile start, lb

(3) Energy Equation:

The energy remaining in the recoilless

rifle is obtained from Eq. 5-47 as

$$N'c_vT = Nc_vT_0 - \gamma c_v k(T_0\bar{T})^{1/2} \left(\frac{A_t}{A}\right) m'V + (1 + \beta)m'V^2/2 \quad (5-52)$$

(4) Equation of State

Eq. 5-35 yields

$$12F\left(\frac{T}{T_0}\right) = \frac{P}{N'} \left[A(x_0 + L) - \left(\frac{C_2 - N}{\rho}\right) \eta N' \right] \quad (5-53)$$

SECTION IV

DISCUSSION OF SOLUTION TO EQUATIONS

In Section III, four equations were obtained based on the assumptions indicated and relate the chamber pressure, projectile motion, gas temperature, and propellant gas accumulation in the recoilless rifle. This handbook will not present the detailed analytical solutions to these equations as obtained by Hirschfelder or Corner and others who have simplified the equations by choosing values of certain propellant, projectile, and weapon parameters such as λ , v_c , and W , in order to obtain analytical solutions of the ballistic equations. Since these methods involve lengthy calculations, it is not recommended that they be used.

By making the simple approximation that the instantaneous gas temperature T can be replaced with an average value, the ballistic equations can be solved by a simple integration that is discussed in detail in Section V. The solutions obtained by this method give results within reasonable accuracy so that, for first approximations, this simplified solution or the graphical solutions presented in par. 5-7 should be used. For more accurate solutions to the ballistic equations, a digital computer program for the numerical integration of the basic equations should be employed.

SECTION V

SIMPLE SOLUTION BASED ON CONSTANT AVERAGE TEMPERATURE

5-17 INTRODUCTION

In order to make the system of ballistic equations derived in Section III readily integrable, a gas temperature averaged over the integration limits is used in place of the instantaneous gas temperature. With this assumption, a solution of the ballistic equations is obtained as shown in the discussion that follows. The method of solution presented herein serves as a general procedure for solving these equations since similar solutions also can be obtained after making certain assumptions about other ballistic parameters and using the outlined procedure.

The resulting solutions are simple and displayed in such a manner that the qualitative effects and relationships of the ballistic parameters are seen clearly. The resulting simplified equations are readily optimized for determining minimum volume and minimum weight rifles, and are used with little loss of accuracy when compared to the more complicated solutions.

5-18 METHOD

The equation of state, Eq. 5-35, can be written as

$$\frac{dx}{dV} = \psi'(x + qV - r'), \text{ in.} \cdot (\text{fps})^{-1} \quad (5-54)$$

where

P , N , and N' have been eliminated by the use of the following substitutions

$$\psi' = \left(\frac{T_o}{\bar{T}}\right) \left(\frac{A}{A_t}\right) \frac{\lambda}{\theta F k}, \text{ sec-ft}^{-1} \quad (5-54a)$$

$$\left(\frac{T_o}{\bar{T}}\right) = \text{the average value of } T_o/\bar{T} \text{ over the ballistic cycle} \quad (5-54b)$$

$$\lambda = k A_t W_o / (C_2 B), \text{ dimensionless} \quad (5-54c)$$

$$q = m' k \left(\frac{A_t}{A^2 \lambda}\right) \left(\frac{1}{\rho} - \eta \theta\right), \text{ in.} \cdot \text{sec-ft}^{-1} \quad (5-54d)$$

$$r' = \frac{C_2}{\rho A}, \text{ in.} \quad (5-54e)$$

The general solution of the differential Eq. 5-54 is

$$x = K_1 \exp(\psi' V) - qV - \frac{q}{\psi'} + r' \quad (5-55)$$

With the initial condition that at $x = x_o$, $V = 0$

$$x_o = K_1 - \frac{q}{\psi'} + r'$$

Solving for K_1 and substituting into Eq. 5-55, the specific solution becomes

$$x = \left(x_o + \frac{q}{\psi'} - r'\right) \exp(\psi' V) - qV - \frac{q}{\psi'} + r', \text{ in.} \quad (5-56)$$

Eq. 5-55 is an exact analytical solution of Eq. 5-52 provided that the correct value T_o/\bar{T} can be determined. In Ref. 6 it is shown that with some simplification of the basic energy equation a good approximation of $(T_o/\bar{T})^{1/2}$ is

$$\left(\frac{T_0}{T}\right)^{1/2} = \frac{1}{2} \left[\frac{1}{U} + \left(\frac{T_0}{T}\right)^{1/2} \right] \quad (5-57)$$

where

$$\left(\frac{T}{T}\right)^{1/2} = \left(\frac{\phi}{a}\right)^{1/2} - \frac{b}{2a}, \text{ dimensionless} \quad (5-57a)$$

$$U = 1 - b, \text{ dimensionless} \quad (5-57b)$$

$$\phi = 1 - \lambda\gamma U/2 - \zeta V, \text{ dimensionless} \quad (5-57c)$$

$$a = 1 - \lambda/(2U), \text{ dimensionless} \quad (5-57d)$$

$$b = \lambda(\gamma - 1)/2, \text{ dimensionless} \quad (5-57e)$$

$$\zeta = \frac{(1 + \beta)(\gamma - 1)}{2kF} \left(\frac{A}{A_t}\right) \lambda, \text{ sec-ft}^{-1} \quad (5-57f)$$

The expressions for x and dV/dx are substituted into the equation of motion, Eq. 5-50, to give the resulting equation

$$P = \frac{12m'V}{A\psi'} \left[\left(x_0 + \frac{q}{\psi'} - r' \right) \times \exp(\psi'V) - \frac{q}{\psi'} \right]^{-1}, \text{ psi} \quad (5-58)$$

Pressure as a function of projectile travel can now be determined parametrically.

The maximum pressure P_p that occurs is of particular importance since it strongly affects rifle chamber and tube design, nozzle blast damage, and muzzle flash effects. Maximum pressure is derived on the basis that $\partial P/\partial V = 0$ at V_p (provided that V_p is less than V_b) where V_p is the projectile velocity at the time when maximum pressure occurs in the recoilless rifle. Differentiating Eq. 5-58 with respect to V and solving for V_p it is

found that for the usual range of parameters

$$V_p = 1/\psi'_p \quad (5-58a)$$

where

$$\psi'_p = \frac{1}{2}\psi'_0 + \left[\left(\frac{\psi'_0}{2}\right)^2 + \left(\frac{\psi'_b - \psi'_0}{V_b}\right)^2 \right]^{1/2}, \text{ (fps)}^{-1} \quad (5-59)$$

and ψ'_0 and ψ'_b refer to the values of ψ' for V equal to 0 and V_b , respectively.

5-19 EXAMPLE

The following is a demonstration of the method of par. 5-18. Given:

$$\beta = 0.2$$

$$\gamma = 1.24$$

$$\eta = 28.6 \text{ in}^3\text{-lb}^{-1}$$

$$1/\rho = 17.99 \text{ in}^3\text{-lb}^{-1}$$

$$k = 6.46 \times 10^{-3} \text{ sec}^{-1}$$

$$F = 3.3 \times 10^5 \text{ (ft-lb)-lb}^{-1}$$

$$B = 6.46 \times 10^{-4} \text{ in.-(psi-sec)}^{-1}$$

The following gun and projectile values have been chosen:

$$A = 13.72 \text{ in}^2$$

$$A_t = 9.31 \text{ in}^2$$

$$m = 1.0 \text{ slug}$$

$$C_2 = 10 \text{ lb}$$

$$x_0 = 50 \text{ in.}$$

Required:

$$V_m = 1120 \text{ fps}$$

Find:

$$L_m$$

The calculations that follow are made according to the steps outlined in par. 5-18.

The value of W usually is chosen such that the propellant will be "all burnt" about the time the muzzle velocity is attained or slightly before. A longer burning time results in loss of unburnt propellant, and a shorter time causes excessive peak pressures given in the same parameter set. The relation between the web and muzzle velocity is then estimated as

$$W_o = m' BV_m/A \quad (5-60)$$

After a reasonable value of C_2 has been chosen and a value of 0.5 assumed for λ the web W can be calculated from Eq. 5-60.

If

$$\begin{aligned} m' &= 1.04 \left[1 + \frac{(1 - 0.5)10}{(3)(32.2)} \right] \\ &= 1.095 \text{ slugs} \quad [\text{Eq. 5-30}] \end{aligned}$$

then by Eq. 5-60,

$$W_o = \frac{1.095(6.5 \times 10^{-4})(1120)}{13.72} = 0.058 \text{ in.}$$

The value of λ is then calculated from its definition

$$\begin{aligned} \lambda &= \frac{kA_t W_o}{C_2 B} = \frac{(6.46 \times 10^{-3})(9.31)(0.058)}{(10)(6.5 \times 10^{-4})} \\ &= 0.537 \end{aligned}$$

$$b = \frac{1}{2}(1.24 - 1)(0.537) = 0.0644 \quad [\text{Eq. 5-57e}]$$

$$U = 1 - 0.064 = 0.936 \quad [\text{Eq. 5-57b}]$$

$$a = 1 - \frac{0.537}{(2)(0.936)} = 0.713 \quad [\text{Eq. 5-57d}]$$

$$\begin{aligned} \zeta &= \frac{(1 + 0.2)(1.24 - 1)(1.474)(0.53)}{2(6.46 \times 10^{-5})(3.31 \times 10^5)} \\ &= 0.535 \times 10^{-4} \text{ sec-ft}^{-1} \quad [\text{Eq. 5-57f}] \end{aligned}$$

$$\begin{aligned} \phi &= 1 - \frac{(0.537)(1.24)(0.936)}{2} \\ &\quad - (0.535 \times 10^{-4})(1120) = 0.629 \quad [\text{Eq. 5-57c}] \end{aligned}$$

$$\left(\frac{T}{T_o}\right)^{1/2} = \left(\frac{0.629}{0.713}\right)^{1/2} - \frac{0.0644}{2(0.713)} = 0.894 \quad [\text{Eq. 5-57a}]$$

$$\left(\frac{T_o}{\bar{T}}\right)^{1/2} = \frac{1}{2} \left(\frac{1}{0.936} + \frac{1}{0.894} \right) = 1.093 \quad [\text{Eq. 5-57}]$$

$$\left(\frac{T_o}{\bar{T}}\right) = (1.093)^2 = 1.19$$

$$\theta = 1 - (0.537)(1.093) = 0.413 \quad [\text{Eq. 5-49}]$$

Ref. 6 shows that for $V=0$ the gas temperature T equals the average temperature \bar{T} and correspondingly

$$\left(\frac{\bar{T}}{T_o}\right)^{1/2} = \left(\frac{T}{T_o}\right)^{1/2} = U$$

$$\bar{\theta}_o = 1 - \frac{0.537}{0.936} = 0.426$$

Since propellant is assumed to be all burnt at time of muzzle exit

$$V_b = V_m$$

and

$$\begin{aligned} \psi'_m = \psi'_b &= \frac{(1.19)(1.474)(0.537)}{(0.413)(3.31 \times 10^5)(6.46 \times 10^{-3})} \\ &= 1.067 \times 10^{-3} \text{ (fps)}^{-1} \quad [\text{Eq. 5-54a}] \end{aligned}$$

$$\psi'_0 = \frac{(1.274)(0.537)}{(0.936)^2(0.427)(3.31 \times 10^5)(6.46 \times 10^{-3})}$$

$$= 0.992 \times 10^{-3} \text{ (fps)}^{-1} \quad [\text{Eq. 5-54a}]$$

$$\psi'_p = \frac{1}{2}(0.992 \times 10^{-3}) + \left[\left(\frac{0.992 \times 10^{-3}}{2} \right)^2 + \left(\frac{1.067 - 0.992}{1120} \right) \times 10^{-3} \right]^{1/2}$$

$$= 1.055 \times 10^{-3} \text{ (fps)}^{-1} \quad [\text{Eq. 5-59}]$$

$$q = (1.095)(6.46 \times 10^{-3}) \left[\frac{9.31}{(1372)^2(0.537)} \right]$$

$$\times [17.1 - 28.6(0.413)]$$

$$= 3.445 \times 10^{-3} \text{ in. -sec-ft}^{-1} \quad [\text{Eq. 5-54d}]$$

$$r' = \frac{(10)(17.1)}{13.72} = 12.46 \text{ in.}$$

$$x_m = \left[50 + \frac{3.445 \times 10^{-3}}{1.067 \times 10^{-3}} - 12.46 \right]$$

$$\times e^{1.067 \times 10^{-3}(1120)} - 3.445 \times 10^{-3}(1120)$$

$$- \frac{3.454 \times 10^{-3}}{1.067 \times 10^{-3}} + 12.46$$

$$= 140 \text{ in.} \quad [\text{Eq. 5-56}]$$

$$L_m = x_m - x_0 = 140 - 50 = 90 \text{ in.}$$

$$v_c = Ax_0 = (13.72)(50) = 685 \text{ in}^2$$

$$V_p = \frac{1}{\psi'_p} = \frac{1}{1.055 \times 10^{-3}} = 947.9 \text{ fps}$$

$$[\text{Eq. 5-58a}]$$

$$P_p = \frac{(12)(1.095)(947.9)}{(13.72)1.055 \times 10^{-3}}$$

$$\times \left[\left(50 + \frac{3.445 \times 10^{-3}}{1.055 \times 10^{-3}} - 12.46 \right) \right]$$

$$\times e^{1.055 \times 10^{-3}(947.9)} - \frac{3.445 \times 10^{-3}}{1.055 \times 10^{-3}} \Big]^{-1}$$

$$= 7993 \text{ psi} \quad [\text{Eq. 5-58}]$$

$$P_m = \frac{(12)(1.095)(1120)}{(13.72)(1.067) \times 10^{-3}}$$

$$\times \left[\left(50 + \frac{3.445 \times 10^{-3}}{1.067 \times 10^{-3}} - 12.46 \right) \right]$$

$$\times e^{1.067 \times 10^{-3}(1120)} - \frac{3.445 \times 10^{-3}}{1.067 \times 10^{-3}} \Big]^{-1}$$

$$= 7647 \text{ psi} \quad [\text{Eq. 5-58}]$$

SECTION VI

ANALYTIC EQUATIONS FOR OPTIMIZING CERTAIN GUN PARAMETERS

5-20 THE LIGHTEST GUN FOR A SPECIFIED MUZZLE ENERGY

In Section V, methods were presented for calculating pressure-travel and velocity-travel functions from a given set of ballistic parameters. By variation of these ballistic parameters, it is possible to calculate families of gun design alternatives from which an optimum configuration may be chosen. It is desired to design the lightest gun of specified caliber, projectile weight, and muzzle velocity. Neglecting certain auxiliary equipment of approximately fixed weight for all calibers, the weapon weight is primarily a function of the recoilless rifle volume and peak pressure. It is desirable to select a peak pressure and determine the ballistic parameters that result in the minimum volume weapon of specified A , m , and V_m .

In Section V, Eq. 5-56 showed that

$$x_m = \left(x_0 + \frac{q}{\psi'_m} - r' \right) \exp(\psi'_m V_m) - q V_m - \frac{q}{\psi'_m} + r', \text{ in.}$$

and from Eq. 5-58 and Eq. 5-58a

$$P_p = \frac{12m'}{A(\psi'_p)^2} \left[\left(x_0 + \frac{q}{\psi'_p} - r' \right) e - \frac{q}{\psi'_p} \right]^{-1}, \text{ psi} \quad (5-61)$$

where

ψ'_p is defined in Eq. 5-59.

For a specified bore area, the minimum weight rifle corresponds to the minimum value of x_m . In determining the minimum

value of x_m , it is satisfactory to neglect small quantities that vary slowly. Therefore, the following simplifications are introduced.

- (1) $q = 0$
- (2) $\psi'_p = a_2 \psi'_m$ where a_2 is an undetermined constant
- (3) $\left(\frac{T_0}{T} \right) = \text{function of } V \text{ alone.}$

With these assumptions Eqs. 5-56 and 5-61 can be combined as shown in Eq. 5-62

$$x_m = \frac{12m' \exp(\psi'_m V_m)}{P_p A e a_2^2 (\psi'_m)^2} + r' \quad (5-62)$$

For a given bore area the weapon volume is determined by Eq. 5-62 and for a given muzzle velocity and peak pressure is a function of ψ' and C_2 alone.

As shown in Ref. 7, the value of ψ' which minimizes the recoilless rifle volume can be determined from

$$\frac{dx_m}{d\psi'_m} = 0 \quad (5-63)$$

The condition for minimum volume as determined from Eq. 5-62 is

$$\psi'_m = 2/V_m \quad (5-64)$$

In order to determine the charge associated with the optimum value of ψ'_m , it is necessary to determine a value of λ for a given ψ'_m . The value of λ is determined from the following equation:

$$\frac{\psi'_m k F}{\left(\frac{A}{A_t} \right)} = \left(\frac{T_0}{T} \right) \frac{\lambda}{\theta} = f(\lambda, V_m), \text{ dimensionless} \quad (5-65)$$

The function of f can be evaluated as shown in Ref. 6 and, by plotting f as a function of λ , a family of curves is obtained with V_m as a parameter. For a given V_m there is only one value of f and λ which satisfies Eq. 5-65. The family of curves then reduces to a single curve of f as a function of λ which satisfies the optimum condition. This curve is plotted in Fig. 5-18 where f_1 applies to minimum volume guns. The value of C_2 can then be determined, knowing the value of λ , as follows

$$C_2 = kA_t W_o / \lambda B, \text{ lb} \quad (5-66)$$

The chamber volume Ax_o then can be determined from Eqs. 5-62, 5-64, and 5-65.

The complete method of solution for the minimum volume recoilless rifle, which for a specific bore area and chosen value of P_p corresponds to the minimum weight rifle for a specified muzzle velocity, is as follows:

Given: A, m, V_m, A_t , propellant constants

Chosen: P_p

Assumptions: (1) $V_b = V_m$

(2) $N_o = 0$

Solution

$$(1) \psi'_m = 2/V_m$$

$$(2) f(V_m, \lambda) = \psi'_m k F / (A/A_t)$$

(3) λ determined from curve f_1 of Fig. 5-18.

$$(4) m' = 1.04 \left[m + \frac{(1 - \lambda)C_1}{3g} \right]$$

At this point C_1 is estimated.

(5) B is determined from Fig. 5-17.

$$(6) W_o = m' B V_m / A$$

$$(7) C_2 = kA_t W_o / (\lambda B)$$

If the estimate of C_1 in Step (4) was poor, Steps 4 through 7 should be repeated. (Note: $C_2 = C_1 - C_3$)

(8) $\psi'_p = g_2(\psi'_m)$ determined from Fig. 5-19.

$$(9) x_m = x_o + L_m = \frac{12m'}{P_p A (\psi'_p)^2 e} \times \exp(\psi'_m V_m) + \frac{C_2}{A\rho}$$

$$(10) L_m = \frac{12m' [\exp(\psi'_m V_m) - 1]}{P_p A (\psi'_p)^2 e}$$

$$(11) v_c = Ax_o$$

$$(12) x_o + L_p = \frac{12m'}{P_p A (\psi'_p)^2} + \frac{C_2}{\rho A}$$

$$(13) P_m = \frac{P_p (\psi'_p)^2 V_m e}{\psi'_m \exp(\psi'_m V_m)}$$

$$(14) \Delta_o = 27.7 C_1 / v_c$$

It can be shown that for high muzzle velocities the desirable minimum volume rifles occur at high loading density. If the required loading density is impractical, there are two possible remedies. The loading density may be reduced by using smaller values of λ or smaller values of V_b . In the usual case, it would be better to use smaller values of λ than to use smaller values of V_b . In general, however, some calculations for smaller V_b should be made to determine which procedure for reducing the loading density yields the smallest final weapon volume. For calculations involving $V < V_b$, the equations of Ref. 6 can be used up to $V = V_b$. For $V > V_b$ an "after burnt" solution such as given by Hirschfelder (Ref. 8) must be used.

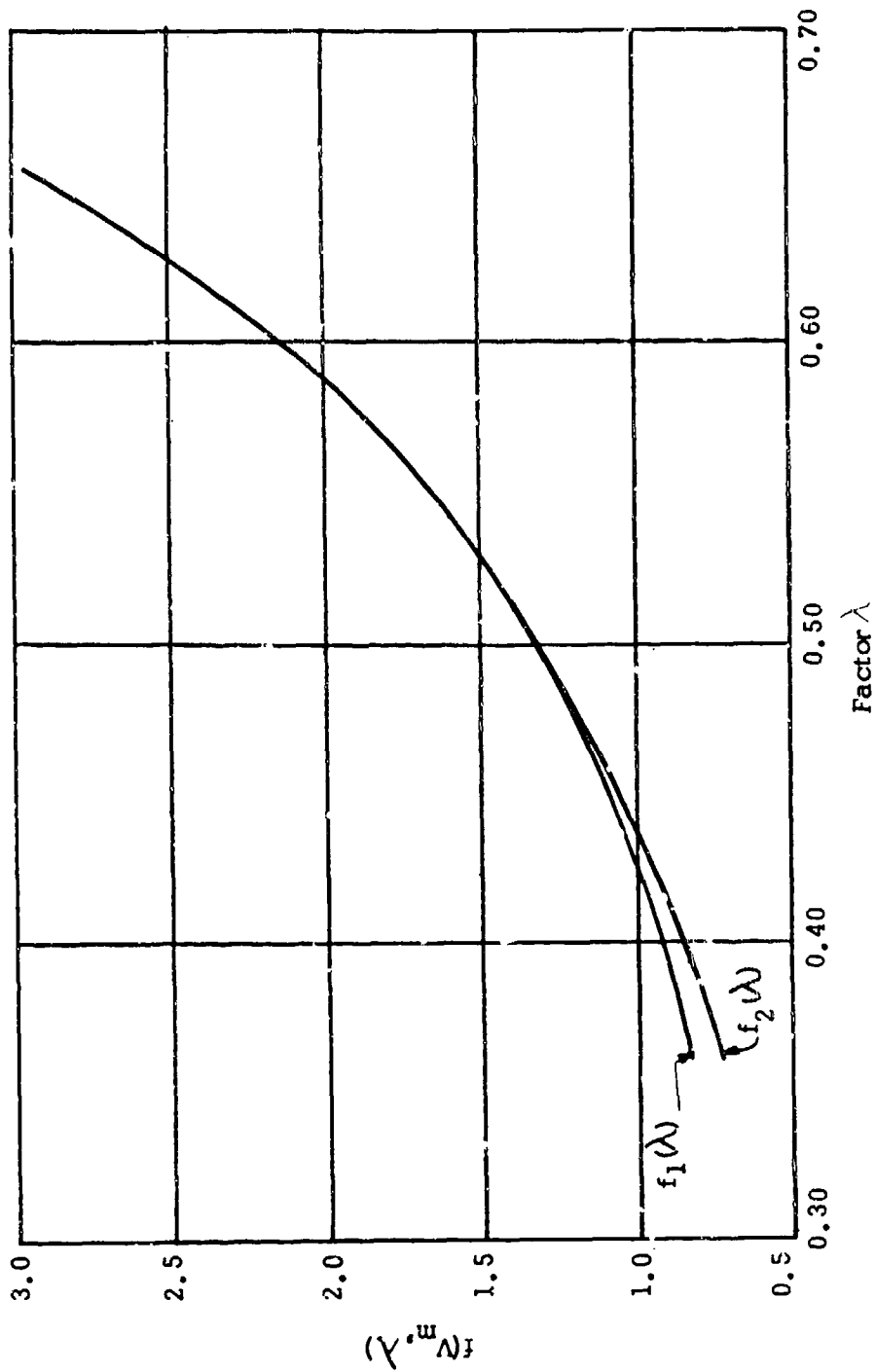


Figure 5-12. $f(V_m, \lambda)$ as a Function of λ

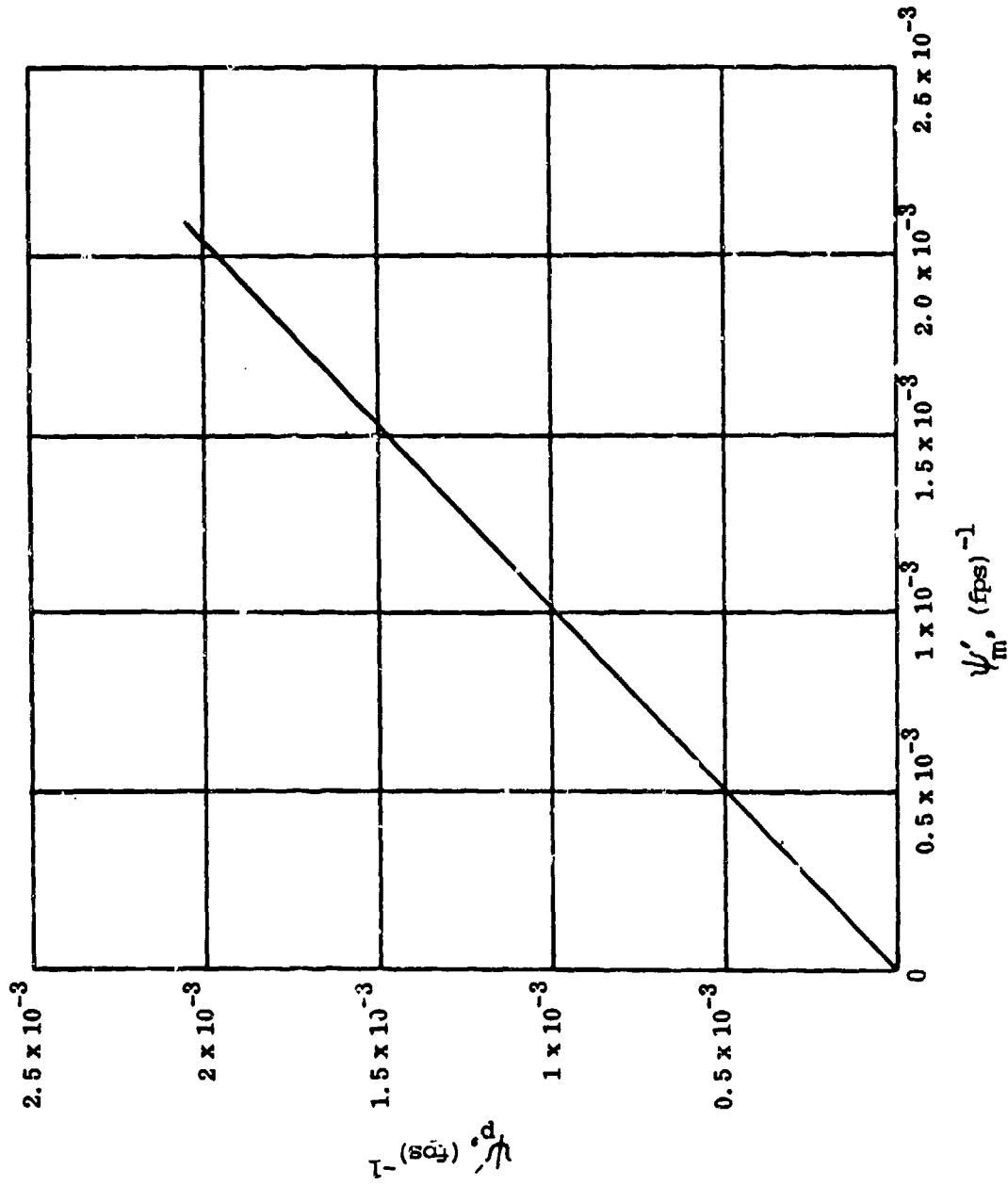


Figure 5-19. ψ'_m as a Function of ψ'_m

5-21 THE SHORTEST GUN FOR A SPECIFIED MUZZLE VELOCITY

The barrel length can be obtained from

$$L_m = x_m - x_0$$

Substituting x_m from Eq. 5-62, x_0 from Eq. 5-61 for the condition $q = 0$ into the above obtain

$$L_m = \frac{12m'}{P_p A_e a_2^2 (\psi'_m)^2} [\exp(\psi'_m V_m) - 1] \quad (5-67)$$

The minimum barrel length is determined when

$$\frac{\partial L_m}{\partial \psi'_m} = 0$$

Hence

$$-\frac{2[\exp(\psi'_m V_m) - 1]}{\psi'_m} + V_m \exp(\psi'_m V_m) = 0 \quad (5-68)$$

The solution to Eq. 5-68 yields

$$\psi'_m = 1.594/V_m$$

The complete solution for the minimum barrel length rifle is then the same as outlined in the preceding section with the exception that for a calculated f , the corresponding value of λ is determined from the f_2 curve as shown in Fig. 5-18.

5-22 NUMERICAL EXAMPLE

The following is a demonstration of the method of par. 5-20 applying the indicated steps.

Given the following propellant values:

$$\eta = 28.6 \text{ in}^3 \text{-lb}^{-1}$$

$$1/\rho = 17.1 \text{ in}^3 \text{-lb}^{-1}$$

$$k = 6.5 \times 10^{-5} \text{ sec}^{-1}$$

$$F = 3.3 \times 10^5 \text{ (ft-lb)-lb}^{-1}$$

The following gun and projectile values have been chosen.

$$A = 12 \text{ in}^2$$

$$m = 0.5 \text{ slug}$$

$$A_t = 8 \text{ in}^2$$

$$V_m = 1500 \text{ fps}$$

It is required to determine the barrel length L_m for minimum volume rifle. For the first calculation, a peak pressure of 10,000 psi is chosen

$$\psi'_m = \frac{2}{1500} = 1.33 \times 10^{-3} \text{ (fps)}^{-1}$$

$$f(V_m, \lambda) = (1.33 \times 10^{-3})(6.5 \times 10^{-3}) \times (3.3 \times 10^5)/(12/8) = 1.92$$

$$\lambda = 0.58 \text{ (from Fig. 5-18)}$$

$$C_t = 6 \text{ lb (estimated)}$$

$$m' = 1.04 \left[0.5 + \frac{(1 - 0.58)6}{3(32.2)} \right] = 0.546 \text{ slug}$$

$$B = 6.5 \times 10^{-4} \text{ in.-(psi-sec)}^{-1} \text{ (from Fig. 5-17)}$$

$$W_0 = \frac{(0.546)(6.5 \times 10^{-4})(1500)}{12} = 0.044 \text{ in.}$$

$$C_2 = \frac{(6.5 \times 10^{-3})(8)(0.044)}{(0.58)(6.5 \times 10^{-4})} = 6.06 \text{ lb}$$

$$\psi'_p = 1.28 \times 10^{-3} \text{ (from Fig. 5-19)}$$

$$x_m = \frac{12(0.546)(2.71828)^2}{10^4(12)(1.28 \times 10^{-3})^2(2.71828)}$$

$$+ \frac{6.06(37.1)}{12} \text{ (Note } V_m \psi'_m = 2)$$

$$= 90.6 + 8.6 = 99.2 \text{ in.}$$

$$L_m = \frac{12 (0.546) [(2.71828)^2 - 1]}{10^4 (12) (1.28 \times 10^{-3})^2 (2.71828)}$$

$$= 78.3 \text{ in.}$$

$$v_c = 12[99.2 - 78.3] = 250.8 \text{ in.}^3$$

$$L_p = \frac{12(0.546)}{10^4(12)(1.28 \times 10^{-3})^2}$$

$$+ \frac{(6.06)(17.1)}{12} - \frac{250.8}{12}$$

$$= 33.3 + 8.6 - 20.9 = 21.0 \text{ in.}$$

$$P_m = \frac{10^4(1.28 \times 10^{-3})^2(1500)(2.71828)}{1.33 \times 10^{-3}(1500)(2.71828)^2}$$

$$= 6830 \text{ psi}$$

The rifle weight can then be calculated by the method of par. 5-35.

The process is repeated for several choices of peak pressure and a plot of weapon weight vs peak pressure results.

SECTION VII

INTERIOR BALLISTIC SOLUTION USING DIGITAL COMPUTER

The digital computer is an excellent tool for solving the interior ballistic equations without the need for additional simplifying assumptions.

An actual computer program will not be presented in this handbook since it is simple to write a program given a thorough understanding of the physical principles. It is important, however, that the user of the program determine that the program indeed represents his physical problem, or requires modification.

A basic rationale employed in writing the program follows:

(1) An initial shot-start pressure as discussed in Chapter 11 is chosen.

(2) Over a short interval of time, e.g., 0.0001 sec, the pressure in the gun is assumed to be constant. If P_1 is the actual pressure at the beginning of the time increment and P_2 the pressure at the end of the time increment then it is assumed that an average pressure $\bar{P} = (P_1 + P_2)/2$ is constant over the time increment. The error of this assumption is negligible over a sufficiently short time increment. The velocity V , travel L , propellant burnt N , and propellant gas accumulation N' , based on the assumed average pressure are then

$$V_2 = V_1 + \frac{A}{m} \bar{P}(\Delta t), \text{ fps} \quad (5-69)$$

$$x_2 = x_1 + \frac{12}{2} (V_1 + V_2) \Delta t, \text{ in.} \quad (5-70)$$

$$N_2 = N_1 + \frac{C_2 B}{W_0} \bar{P} \Delta t, \text{ lb} \quad (5-71)$$

$$N'_2 = N'_1 + \left[\frac{C_2 B}{W_0} - k \left(\frac{T_0}{T} \right)^{1/2} A_t \right] \bar{P} \Delta t, \text{ lb} \quad (5-72)$$

where a value of T is obtained from solving the energy equation, Eq. 5-47.

(3) The pressure P'_2 at the end of the time increment can then be calculated from the equation of state, Eq. 5-35, as follows:

$$P'_2 = 12FN'_2 \frac{T}{T_0} \left[A(x_0 + L) - \left(\frac{C_1 - N_2}{\rho} \right) - \eta N'_2 \right]^{-1}, \text{ psi} \quad (5-73)$$

The calculated average pressure $\bar{P}' = (P_1 + P'_2)/2$ is then compared with the assumed average pressure.

(4) If $|\bar{P}' - \bar{P}| > 100$ psi, for example, repeat the calculation using the value of \bar{P}' as the assumed average pressure. After a few iterations the assumed and calculated values of average pressure will converge toward a true value and

$$|\bar{P}' - \bar{P}| < 100 \text{ psi}$$

At this point the calculation is sufficiently accurate and the next time increment can be calculated.

(5) For the first time increment, P_1 is taken as the value of shot-start pressure with $x_1 = 0$ and $V_1 = 0$. As a first approximation in each increment, the assumed average pressure can be taken as equal to the initial pressure of the increment.

(6) A running tabulation of all variables is kept and, when the amount of propellant burnt equals the propellant charge, the program switches to the governing equations applicable to the "all burnt" condition.

Since the computer program only calcu-

lates $P(t)$, $v(t)$, and $x(t)$ for a given set of weapon parameters, it is recommended that approximate values of optimum gun parameters first be calculated by the method of Section VI. The parameters then can be used as inputs to the digital computer for a more accurate solution.

SECTION VIII

SOLUTION FOR AFTER "ALL-BURNT" CONDITION

5-23 INTRODUCTION

In the previous discussions of the interior ballistic equations, it had been assumed that the propellant continued to burn to muzzle exit so that a solution after "all-burnt" was not required. This is often the case in the design of a recoilless rifle since it results in a high piezometric efficiency and therefore a light gun.

However, it may be desirable to end propellant burning sooner than muzzle exit. When the propellant charge is consumed before muzzle exit, the interior ballistic equations must be modified to reflect simple gas expansion. The projectile velocity coinciding with end of burning is designated V_b . Normally the minimum weight weapon corresponds to $V_b = V_m$, however, in practice, it is usually desirable to end propellant burning before muzzle exit to avoid excessive discharge of unburnt propellant.

5-24 MODIFICATION OF EQUATIONS FOR "ALL-BURNT" CONDITION

The basic equation for the rate of accumulation of gas in the rifle must be modified after all-burnt. The weight of gas N'_b in the weapon at the end of burning is

$$N'_b = \bar{\theta}_b C_2, \text{ lb} \quad (5-74)$$

where

$$\bar{\theta}_b = 1 - \lambda \left(\frac{T_o}{\bar{T}_b} \right)^{1/2}, \text{ dimensionless}$$

C_2 = propellant charge weight burned,
lb

Thereafter, the amount of gas in the recoilless

rifle decreases as gas is discharged through the nozzle. At this point, the equation for the weight N' of the residual gas in the weapon is

$$N' = N'_b - k \left(\frac{T_o}{T} \right)^{1/2} \left(m' \frac{A_t}{A_b} V \right), \text{ lb} \quad (5-75)$$

The introduction of this equation for N' permits a solution for the pressure and velocity.

5-25 SOLUTION OF EQUATIONS FOR "ALL-BURNT" CONDITION

The step-by-step procedure presented in Section V can be continued for the case where $V > V_b$ as follows:

The equations are

- (1) $N'_b/C_2 = \bar{\theta}$, dimensionless
- (2) $\Gamma_2 = [(\gamma - 1)\lambda + 1]^{1/2}$, dimensionless
- (3) $g_o = (1 - J_o)\lambda/2$, dimensionless
where $J_o = 0$ for $P_o = 0$
- (4) $g_1 = 1 - g_o \Gamma_2$, dimensionless
- (5) $N'_b/C_2 = g_1 - g_o / (T_b/\bar{T}_b)^{1/2}$,
dimensionless

where

$$\left(\frac{\bar{T}_b}{T_o} \right)^{1/2} = 1 / (T_o/\bar{T})^{1/2} \text{ for up to "all-burnt"}$$

$$(6) \quad \phi_2 = 2 \left(g_1 - \frac{N'_b}{C_2} \right) / (N'_b/C_2),$$

dimensionless

$$(7) \quad \psi = 1/\phi_2 + 1, \text{ dimensionless}$$

(8) $\bar{\gamma} = 1 + (1 + \beta)(\gamma - 1)$, dimensionless

(9) $\xi_2 = \frac{12m'V_b^2 \left(\frac{x_o}{x_b}\right)}{v_c P_b \phi_2^2 (2 - \gamma)}$, dimensionless

(10) $Y' = \left\{ 1 + [1 + (2 - \bar{\gamma})\phi_2] \phi_2^{(\bar{\gamma}-2)} \xi_2 \right.$
 $\left. - \xi_2 \left[\psi - (\bar{\gamma} - 1) \frac{V}{V_b} \right] \right\} /$
 $\psi - \left(\frac{V}{V_b} \right)^{(\bar{\gamma}-1)} \left\}^{-1/(\bar{\gamma}-1)}$

(11) $x = Y' x_b$

(12) $P = P_b \left[\frac{\phi_2}{Y'} \left(\psi - \frac{V}{V_b} \right) \right]^{\bar{\gamma}}$

5-26 EXAMPLE

In par. 5-19, a numerical example was given in which burning ended with a muzzle velocity V_m of 1120 fps. Assume that nothing is changed in the previous example except that the required muzzle velocity is 1200 fps. Thus, at the end of burning

$V_b = 1120$ fps

$x_b = 140$ in.

$P_b = 7641$ psi

The problem is to calculate new values of x_m and P_m as follows, using the steps outlined in par. 5-25:

$\Gamma_2 = [(1.24 - 1)(0.537) + 1]^{1/2} = 1.062$

$g_o = 0.537/2 = 0.268$

$g_1 = 1 - (0.268)(1.062) = 0.715$

$\frac{N'_b}{C_2} = 0.715 - \frac{0.268}{1.093} = 0.470$

$\phi_2 = 2 \left(\frac{0.715 - 0.470}{0.470} \right) = 1.043$

$\psi = \frac{1}{1.043} + 1 = 1.959$

$\bar{\gamma} = 1 + (1 + 0.2)(1.24 - 1) = 1.288$

$\xi_2 = \frac{12(1.095)(1120)^2 \left(\frac{50}{140}\right)}{685(7641)(1.043)^{1.288}(2 - 1.24)}$
 $= 1.402$

$Y' = \left\{ 1 + [1 + (2 - 1.288)(1.043)](1.043)^{(1.288-2)}(1.402) \right.$
 $\left. - \frac{(1.402) \left[1.959 - (1.288 - 1) \left(\frac{1200}{1120}\right) \right]}{1.959 - \left(\frac{1200}{1120}\right)^{(1.288-1)}} \right\}^{-1/(1.288-1)}$
 $= 1.406$

$x_m = 1.406(140) = 197$ in.

$L_m = x_m - x_o = 197 - 50 = 147$ in.

$P_m = 7641 \left[\frac{1.043}{1.406} \left(1.959 - \frac{1200}{1120} \right) \right]^{1.288}$
 $= 4460$ psi

SECTION IX

HEAT TRANSFER

5-27 INTRODUCTION

The transport of thermal energy from propellant gases to the bore and nozzle surfaces of the recoilless rifle deserves serious consideration. Heat transfer degrades interior ballistic performance, increases the erosion of nozzle and bore surfaces, may cause premature ignition or chemical deterioration of a round of ammunition, introduces difficulty in the handling of a shoulder-fired recoilless rifle, limits the maximum rate of fire and finally, but not the least important, diminishes the physical strength of the gun material as the temperature of the barrel rises. For example, in the latter consideration, the strength of some gun steel alloys drops approximately 18 percent for a rise in temperature from 70° to 500°F. This loss in strength assumes even greater importance when one considers that the recoilless rifle has a very low overall heat capacity compared to the conventional closed breech system; this fact is reflected in a significantly higher and more rapid temperature rise.

The problem of estimating the temperature distribution through the wall of the chamber and barrel as a function of time is challenging. The paragraphs that follow provide some of the theoretical bases upon which a satisfactory method of temperature estimation is obtained when combined with a minimum of experimental support.

5-28 BASIC EQUATIONS

Based on the assumptions that (1) heat is transferred conductively only in the radial direction of the gun barrel, since the effects of longitudinal and circumferential heat flow are slight, (2) the gun barrel is of infinite

length, and (3) convective heat transfer occurs at the interior and exterior gun walls, the basic equations for thin walls and little curvature describing the heat transfer in the recoilless rifle are:

$$\alpha' \left[\frac{\partial^2 \theta(r, t)}{\partial r^2} \right] = \frac{\partial \theta(r, t)}{\partial t} \quad (5-76)$$

with the boundary conditions

$$(1) -k_T \left[\frac{\partial \theta(0, t)}{\partial r} \right] = h_i [\theta(0, t) - \theta_a]$$

$$(2) -k_T \left[\frac{\partial \theta(w, t)}{\partial r} \right] = h_o \theta(w, t)$$

and the initial condition that

$$\theta(w, 0) = 0$$

where

$$\theta(r, t) = T_w(r, t) - T_a = \text{wall temperature above ambient, } ^\circ\text{F}$$

$$T_w(r, t) = \text{wall temperature at position } r \text{ and time } t, ^\circ\text{F}$$

$$T_a = \text{ambient temperature, } ^\circ\text{F}$$

$$r = \text{outward radial distance into wall, in.}$$

$$t = \text{time, sec}$$

$$\alpha' = \text{diffusion constant, in}^2\text{-sec}^{-1}$$

$$k_T = \text{thermal conductivity of rifle, Btu-(in}^2\text{-sec-}^\circ\text{F/in.)}^{-1}$$

$$h_i = \text{heat transfer coefficient at interior wall, Btu-(in}^2\text{-sec } ^\circ\text{F)}^{-1}$$

- h_o = heat transfer coefficient at exterior wall, $\text{Btu}-(\text{in}^2\text{-sec}.\text{°F})^{-1}$
- w = wall thickness, in.
- θ_g = propellant gas temperature above ambient, deg F.

5-29 SOLUTION OF THE EQUATIONS

The temperature of the recoilless rifle now will be determined by two different methods of solving the basic equations presented in par. 5-28. The first method defines an equilibrium temperature on a single shot basis, and then determines the round necessary to achieve any particular percentage of this equilibrium temperature at a specific rate of fire. The second method deals with the determination of the weapon temperature as a continuous function of the number of rounds for a given rate of fire.

Before discussing either method of solution, it is possible to write the basic equations in dimensionless form by introducing the following dimensionless quantities which are referred to as reduced distance ξ , reduced time τ , and reduced temperature φ :

$$\xi = r/w$$

$$\tau = t/t_o$$

$$\varphi = \theta/\theta_o$$

where θ_o = maximum temperature above ambient at inner wall, °F, and t_o is defined as

$$t_o = w^2/\alpha', \text{ sec}$$

Substitution of these quantities into Eq. 5-76 yields

$$\frac{\partial^2 \varphi(\xi, \tau)}{\partial \xi^2} = \frac{\partial \varphi(\xi, \tau)}{\partial \tau} \quad (5-77)$$

where

$$\varphi(\xi, \tau) = \frac{\theta(r, t)}{\theta_o} = \frac{\theta(w\xi, t_o\tau)}{\theta_o}, \text{ dimensionless}$$

Since the ballistic cycle of a recoilless rifle is approximately 12 msec, and the rate of fire usually does not exceed 20 rounds per minute (3 sec between rounds), the heat input to the rifle can be defined as a delta "function", i.e., a certain quantity of heat is instantaneously transferred each time a round is fired. The entire formal problem can then be described as follows:

$$\frac{\partial^2 \varphi(\xi, \tau)}{\partial \xi^2} = \frac{\partial \varphi(\xi, \tau)}{\partial \tau} \quad 0 < \xi < 1, \quad \tau > 0 \quad (5-78)$$

$$\frac{\partial \varphi(0, \tau)}{\partial \xi} = -Q'_o \sum_{n=1}^N \delta[\tau - (n-1)\tau_R] \quad (5-79)$$

$$\frac{\partial \varphi(1, \tau)}{\partial \xi} = -h'' \varphi(1, \tau) \quad (5-80)$$

$$\varphi(1, 0) = 0 \quad (5-81)$$

where

$$Q'_o = \frac{Q_o w}{k_T \theta_o t_o}, \text{ round}^{-1}$$

$$Q_o = \text{heat flux input per round, Btu}-(\text{in.}^2\text{-round})^{-1}$$

$$h'' = hw/k_T, \text{ dimensionless}$$

$$h = \text{heat transfer coefficient, Btu}-(\text{in.}^2\text{-°F-sec})^{-1}$$

$\delta[\tau - (n-1)\tau_R]$ is the delta function defined in such a manner that

$$\int_{-\infty}^{\infty} \delta(x) dx = 1, \text{ and } \delta(x) = 0 \text{ for } x \neq 0;$$

where in this case, $x = \tau - (n-1)\tau_R$.

$$\tau_R = \text{dimensionless time between rounds} \\ = (t_o R_f)^{-1}$$

To determine the temperature of the exterior wall on the basis of pulsed heat input at the inner boundary and convective heat loss at the outer boundary, the dimensionless Eqs. 5-77 through 5-81 are solved through the use of Laplace and inverse Laplace transforms as outlined in Ref. 9. The final solution of the reduced temperature at the exterior is written as

$$\varphi(1, \tau) \\ = \sum_{n=1}^N \frac{H[\tau - (n-1)\tau_R] \exp\{-h''[\tau - (n-1)\tau_R]\}}{M_1} \quad (5-82)$$

where

$\varphi(1, \tau)$ = reduced temperature at exterior wall for reduced time τ , dimensionless

H = Heaviside function which has the following property

$$H(t = S) = \begin{cases} 0, & t < S \\ 1, & t \geq S \end{cases}$$

$1/M_1$ interpreted as initial, reduced temperature rise

$$M_1 \approx (h'' + 1)/(2Q_o'), \text{ dimensionless} \quad (5-82a)$$

In the determination of an equilibrium temperature by the single shot analysis the assumption of convective cooling at the exterior surface still holds with the additional assumption that the heat transfer coefficient h is constant with change in temperature. From an energy balance, the following holds:

$$R_f c_w W_w \frac{d\theta}{dn} = q_o R_f - 60hA_w \theta, \text{ Btu-min}^{-1} \quad (5-83)$$

where

q_o = heat transferred to the weapon per round, Btu-round⁻¹

R_f = rate of fire, rounds min⁻¹

$q_o R_f$ = heat transferred to weapon per unit time, Btu-min⁻¹

$60hA_w \theta$ = heat loss by cooling per unit time, Btu-min⁻¹

$R_f c_w W_w \frac{d\theta}{dn}$ = net gain of heat in weapon per unit time, Btu-min⁻¹

W_w = weapon weight, lb

c_w = specific heat of weapon, Btu-(lb weapon⁻¹ °F)⁻¹

A_w = surface area of weapon being heated, in²

$\frac{d\theta}{dn}$ = change in weapon temperature per round, °F-round⁻¹

The solution to Eq. 5-83 may be written as

$$\theta(n) = \theta_e [1 - \exp(-nh_n)], \text{ °F} \quad (5-84)$$

where

$\theta_e = \frac{q_o R_f}{60hA_w}$ = equilibrium temperature, °F

$$h_n = \frac{60hA_w}{R_f c_w W_w}, \text{ round}^{-1}$$

The initial temperature rise θ_1 , i.e., $n = 1$, is then expressed as

$$\theta_1 = \theta(1) - \theta(0) = \theta_e [1 - \exp(-h_n)] \quad (5-85)$$

Solving Eq. 5-85 for θ_e

$$\theta_e = \frac{\theta_1}{1 - \exp(-h_n)}$$

The temperature decay θ_d after the initial temperature rise is given by

$$\theta_d = \theta_1 \exp [hA_w t / (c_w W_w)]$$

Therefore, the temperature rise θ_{12} just before firing the second round is

$$\theta_{12} = \theta_1 \exp \left(- \frac{60hA_w}{R_f c_w W_w} \right) = \theta_1 \exp (-h_n)$$

or

$$\frac{\theta_{12}}{\theta_1} = \exp (-h_n)$$

Substituting into Eq. 5-85 and then Eq. 5-84, the equilibrium temperature θ_e becomes

$$\theta_e = \frac{\theta_1}{1 - \frac{\theta_{12}}{\theta_1}} = \frac{\theta_1^2}{\theta_1 - \theta_{12}} \quad (5-86)$$

and the temperature of the weapon at round "n" given by

$$\theta = \left[\frac{\theta_1^2}{\theta_1 - \theta_{12}} \right] \left[1 - \left(\frac{\theta_{12}}{\theta_1} \right)^n \right] \quad (5-87)$$

5-30 TEMPERATURE DISTRIBUTION DATA

5-30.1 THEORETICAL CALCULATION

The solutions for both the single-shot analysis, Eqs. 5-86 and 5-87, and the multiple number of rounds for a given rate of fire, Eq. 5-82, methods have been determined and described in graphical form, Ref. 9, and are presented in pars. 5-30.1.1 and 5-30.1.2. Given the round number n , rate of fire R_f , cooling factor h' , the maximum temperature at inner wall T'_0 , and the temperature of inner wall after first firing T_1 , the exterior wall temperature easily is calculated by either of the procedures outlined in pars. 5-30.1.1 and 5-30.1.2.

5-30.1.1 Single-shot Analysis

The solution to the single-shot analysis has been plotted in the form of nomograms as shown in Figs. 5-20 and 5-21. Fig. 5-20 is a nomogram of equilibrium temperature as a function of initial temperature rise θ_1 , and subsequent temperature decay θ_d until the second round is fired. The quantities θ/θ_e , R_f , n , and h' are paired, respectively, with an indexing axis drawn between θ/θ_e and R_f (Fig. 5-21). In order to determine θ/θ_e —given $h' = 0.033$, $n = 40$, and $R_f = 2$ —the following procedure is used.

(1) Construct the straight line determined by the points h' and n , and extend the line to intersect the index (Fig. 5-21).

(2) Construct the straight line determined by the point of intersection on the index and the point on the R_f -axis determined by the rate of fire. This line intersects the θ/θ_e -axis at the correct value (0.5).

The results obtained by using these results from the single-shot analysis have proven successful, being within the experimental errors shown in Table 5-4(A).

5-30.1.2 Determination of Temperature as a Function of Round Number and Rate of Fire

The solution for the exterior wall temperature as found in Eq. 5-82 may be interpreted as discussed in the paragraphs that follow.

After the initial temperature rise, the temperature begins its decay in such a manner that when the second round is fired, its contribution to the exterior surface temperature is added to the residual effects of the first round. In a similar manner, immediately after firing the third round, the temperature is calculated by adding the contribution of the third round to the residual effects of the first and second rounds. This process continues until no further rise in the peak temperature

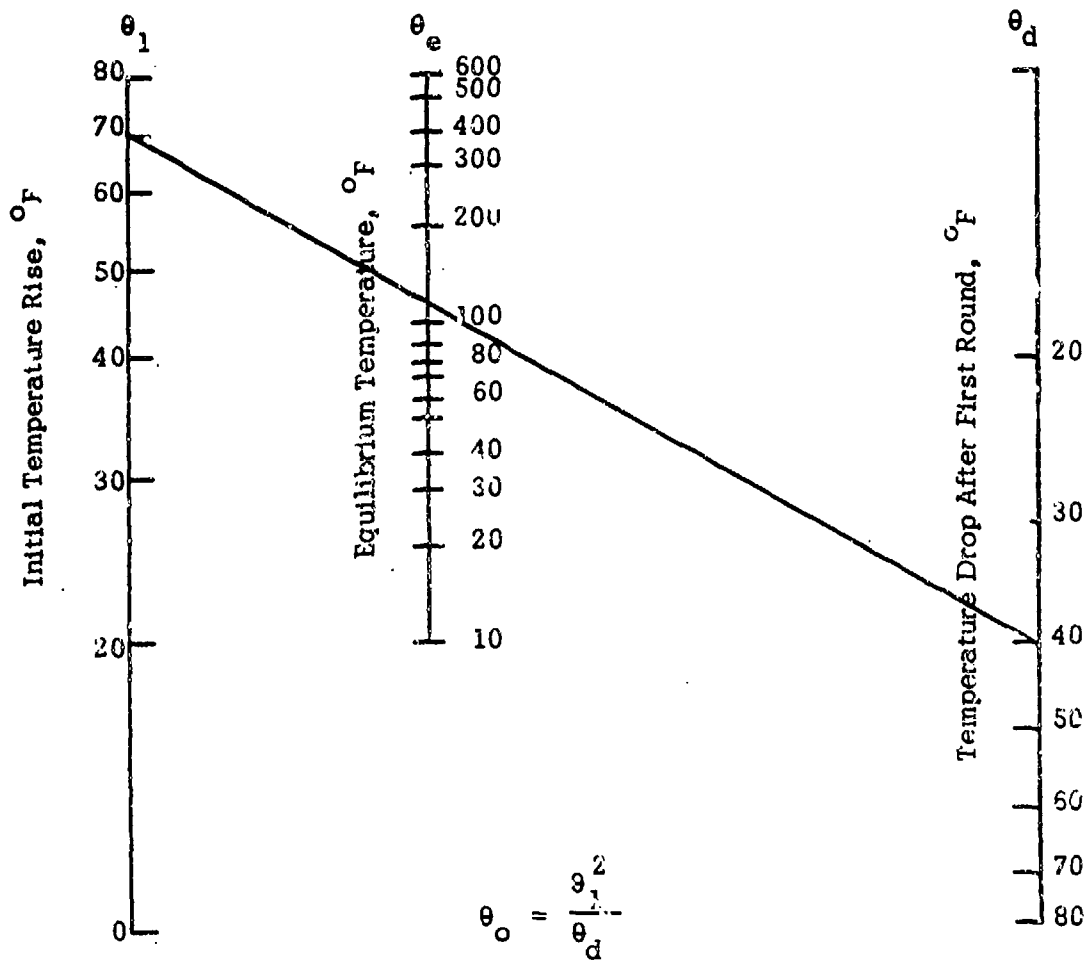


Figure 5-20. Equilibrium Temperature as a Function of initial Temperature Rise and Decay

occurs, i.e., the equilibrium temperature has been attained. In other words, the contribution of the last round is exactly negated by the decay of the preceding rounds.

The quantity $1/M_1$ may also be interpreted as the initial, reduced temperature rise

$$M_1^{-1} = \frac{1}{M_1} = \frac{\theta_1}{\theta_o} \quad (5-88)$$

where θ_o is the maximum temperature rise at the inner wall. This quantity is independent of the rate of fire and is a function of caliber

insofar as Q_o and H are functions of caliber. Therefore, the dimensionless quantity M_1 is a generalized quantity not only with respect to temperature, but also with respect to caliber. Figs. 5-22 through 5-31 are graphs of $M_1 \varphi$ vs n for surface conditions $h = 0.02$ to 0.20 min^{-1}

A typical calculation would be

Given:

$$T_a = 50^\circ \text{F}$$

$$T'_o = 500^\circ \text{F}$$

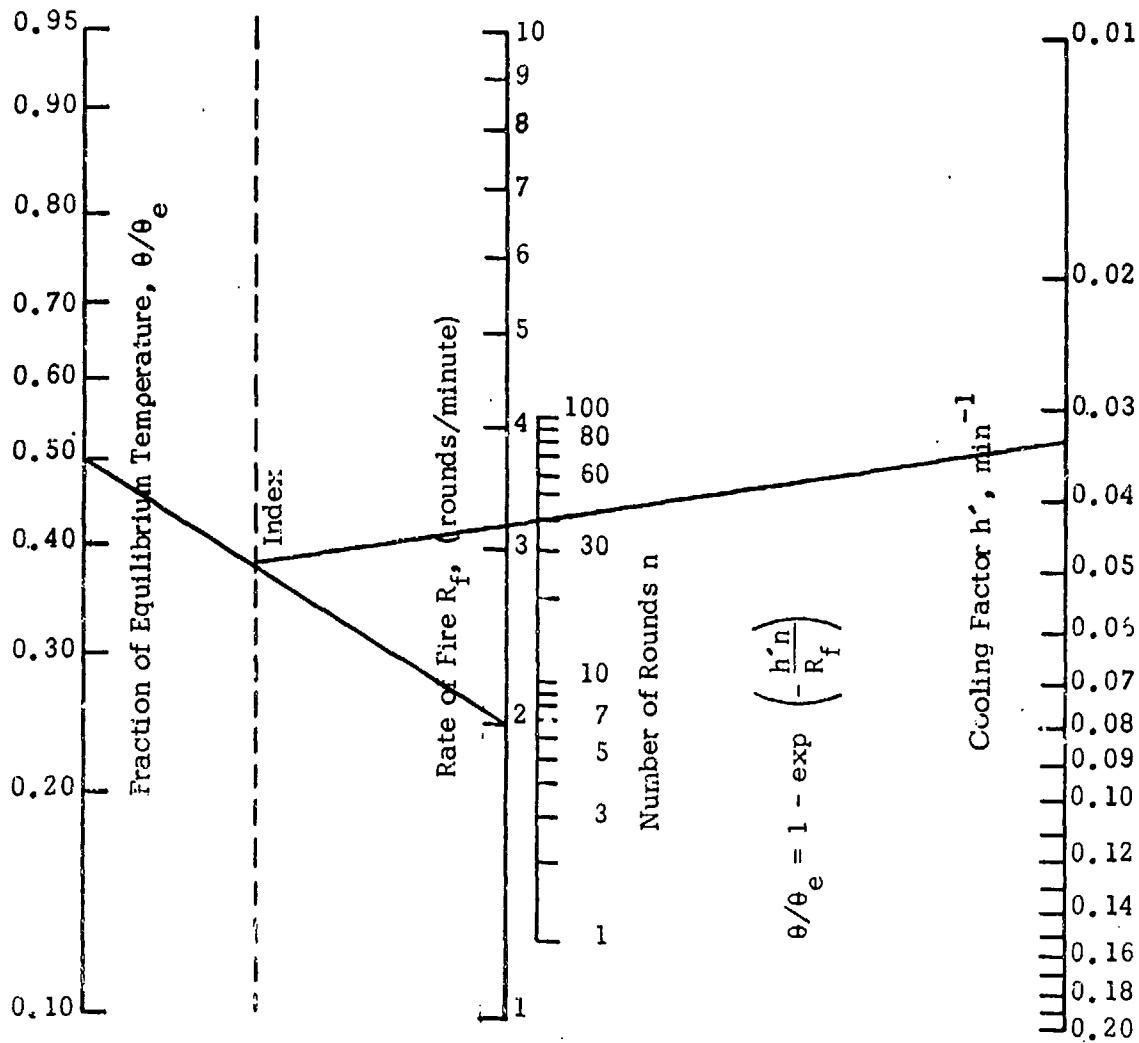


Figure 5-21. Number of Rounds To Achieve Given Fraction of Equilibrium Temperature

$T_1 = 85^\circ\text{F}$

$n = 15$

$R_f = 2 \text{ rd/min}$

$\theta_o = 500^\circ\text{F} - 50^\circ\text{F} = 450 \text{ deg F}$

$h' = 0.18 \text{ min}^{-1}$

$\theta_1 = 85^\circ\text{F} - 50^\circ\text{F} = 35 \text{ deg F}$

TABLE 5-4

COMPARISON OF THEORETICAL AND OBSERVED TEMPERATURE DATA

(A) Based on Single-shot Analysis

Caliber, mm	Rate of Fire R_f , rd/min	Equilibrium Temperature θ_e , °F				
		θ_i	θ_d	Calculated	Observed	Error, %
57	0.5	45	9	225	213	6.0
57	2.0	46	5	423	443	4.5
105	0.5	29	7	120	127	5.5
105	0.5	28	6	130	133	2.2

(B) Comparison of Observed and Calculated Results for the 57 mm, TGGE2 Recoilless Rifle based on Determination of Temperature as a Function of Round Number and Rate of Fire

Round No., n	Calculated*	Temperature, °F		Theoretical***
		Observed**		
1	85	85		80
2	121	120		114
3	149	150		140
4	171	170		161
5	188	190		177
6	202	200		190
7	213	215		200
8	221	220		208
9	228	230		215
10	233	235		219
11	237	240		223
12	241	240		227
13	243	245		227
14	245	245		231
15	247	250		231
16	248	250		233
17	249	250		234
18	250	250		235
19	250	250		235
20	251	250		236

- * The initial temperature rise alone is taken from empirical data.
- ** Observed temperatures are recorded to within 5 deg F.
- *** The initial temperature rise is calculated on the basis of Eq. 5-82a.

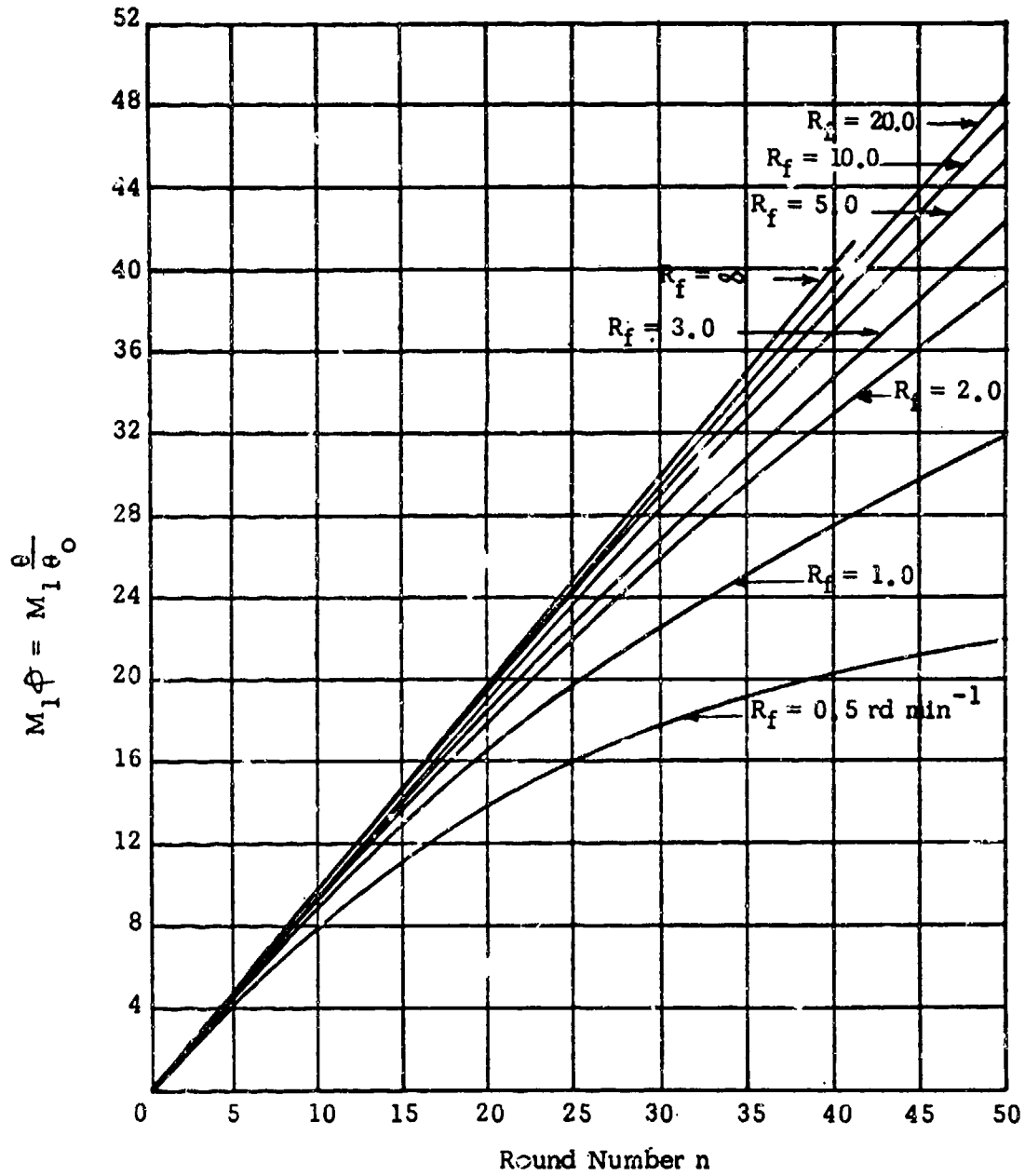


Figure 5-22. Reduced Temperature vs Round Number for Given Rate of Fire ($h' = 0.02 \text{ min}^{-1}$)

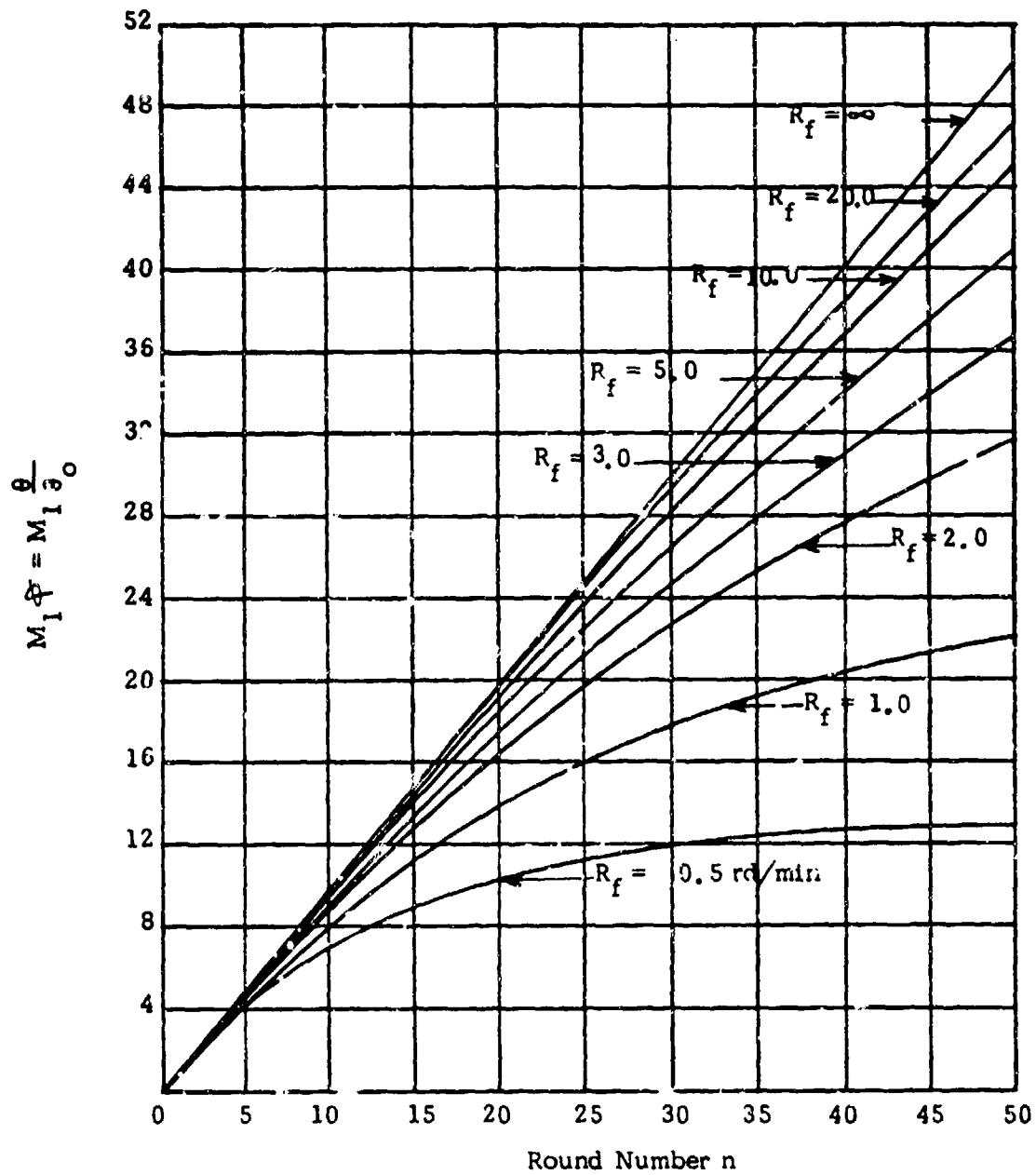


Figure 5-23. Reduced Temperature vs Round Number for Given Rate of Fire ($h' = 0.04 \text{ min}^{-1}$)

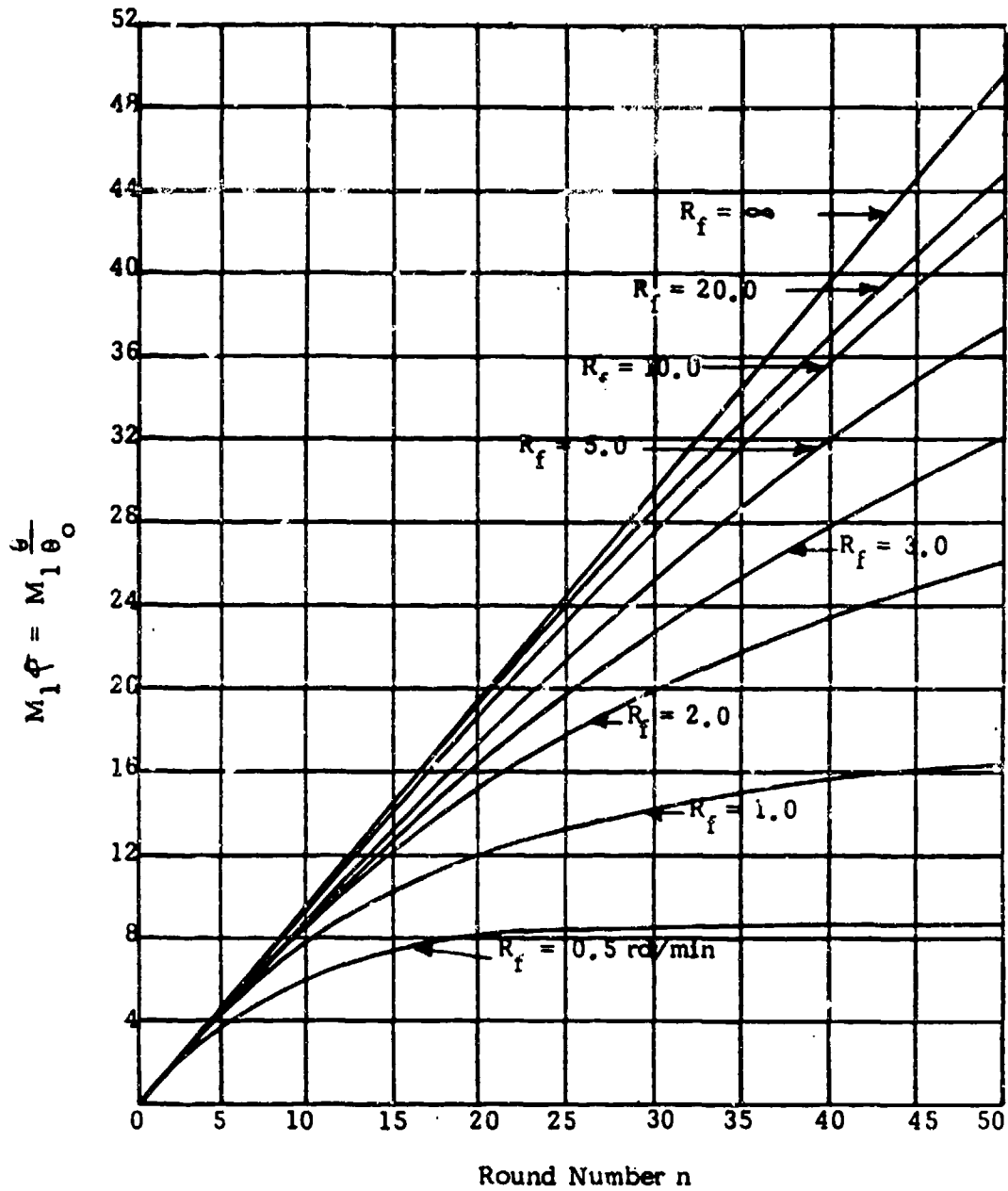


Figure 5-24. Reduced Temperature vs Round Number for Given Rate of Fire ($h' = 0.06 \text{ min}^{-1}$)

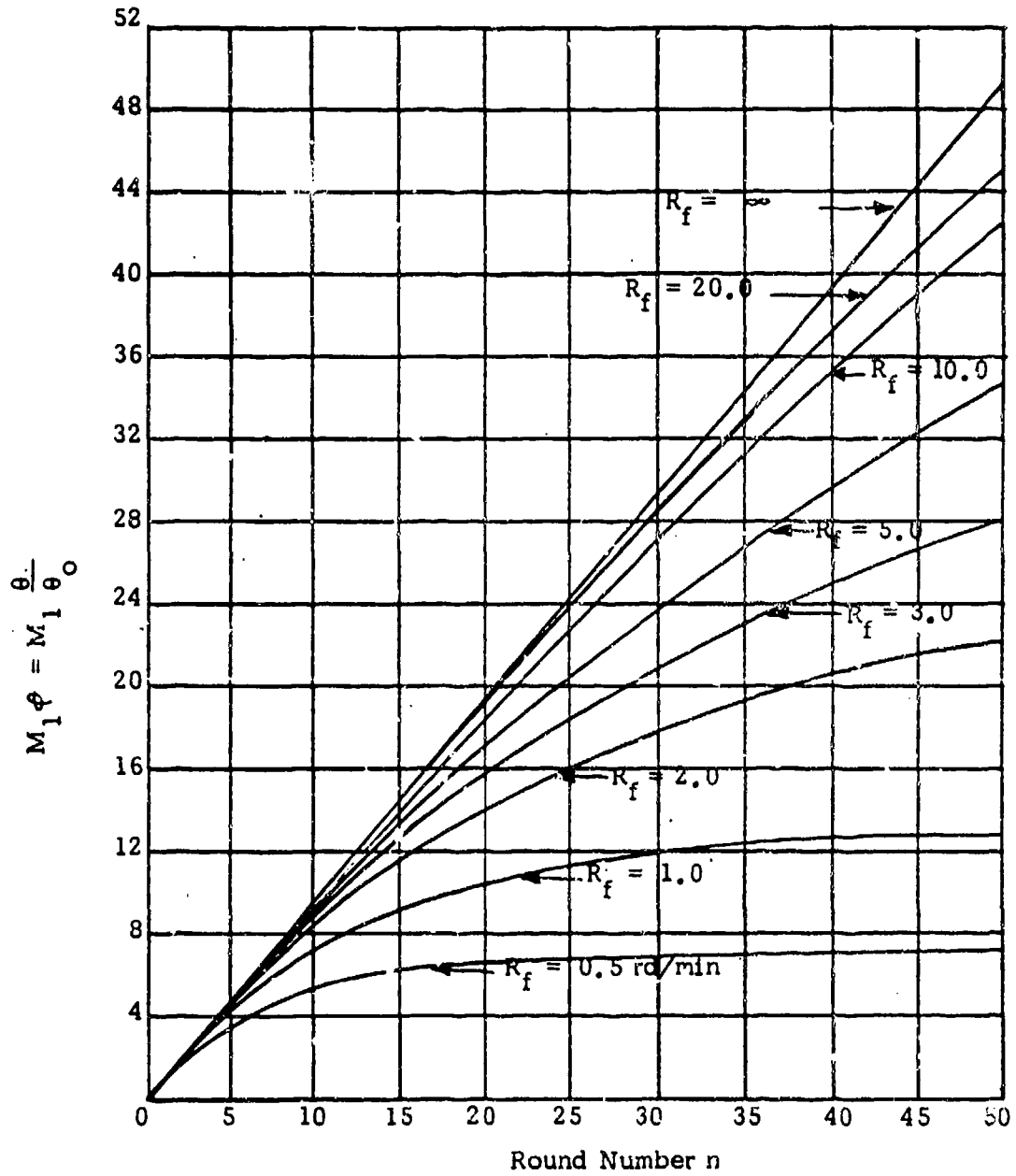


Figure 5-25. Reduced Temperature vs Round Number for Given Rate of Fire ($h' = 0.08 \text{ min}^{-1}$)

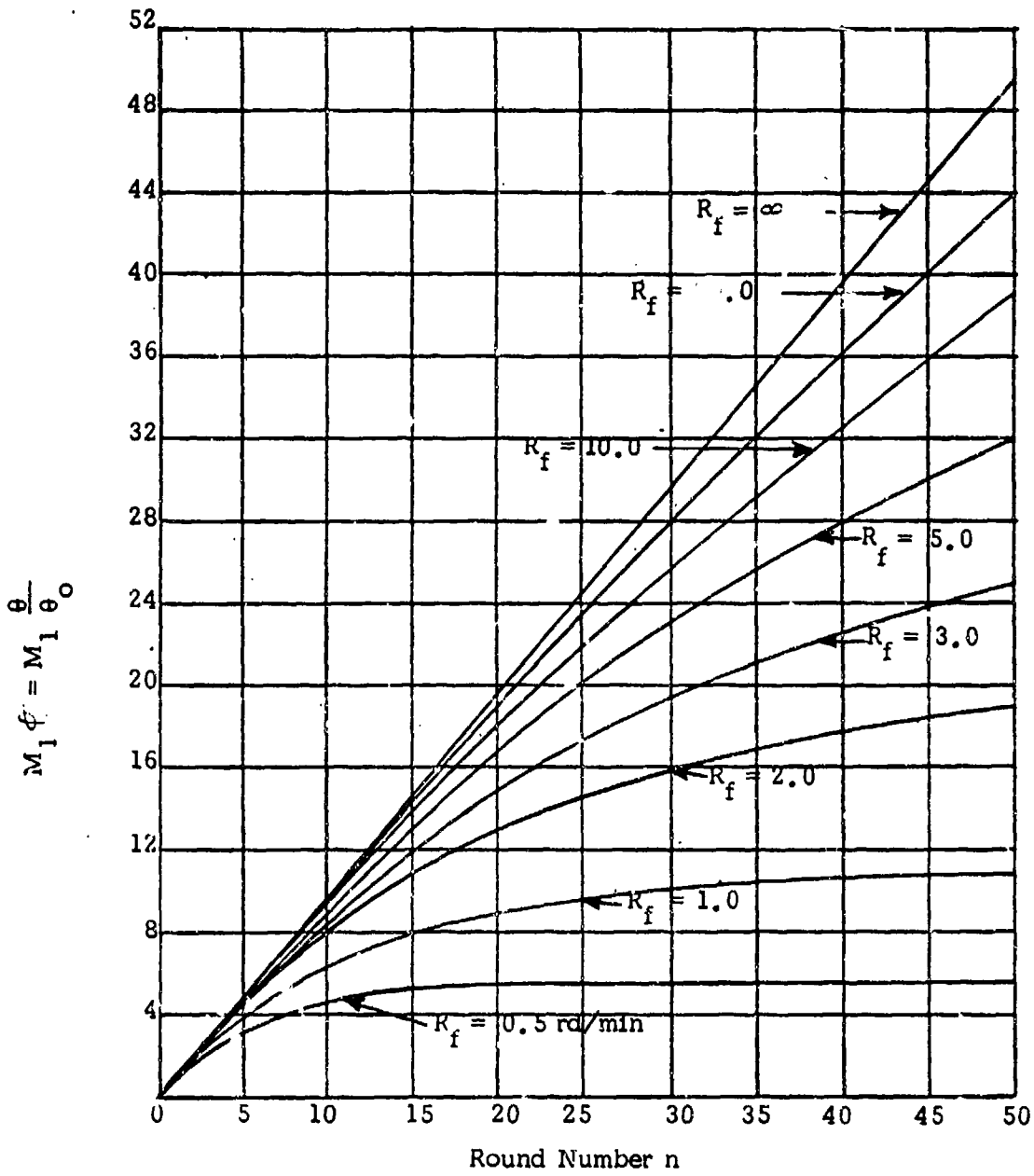


Figure 5-26. Reduced Temperature vs Round Number for Given Rate of Fire ($h' = 0.10 \text{ min}^{-1}$)

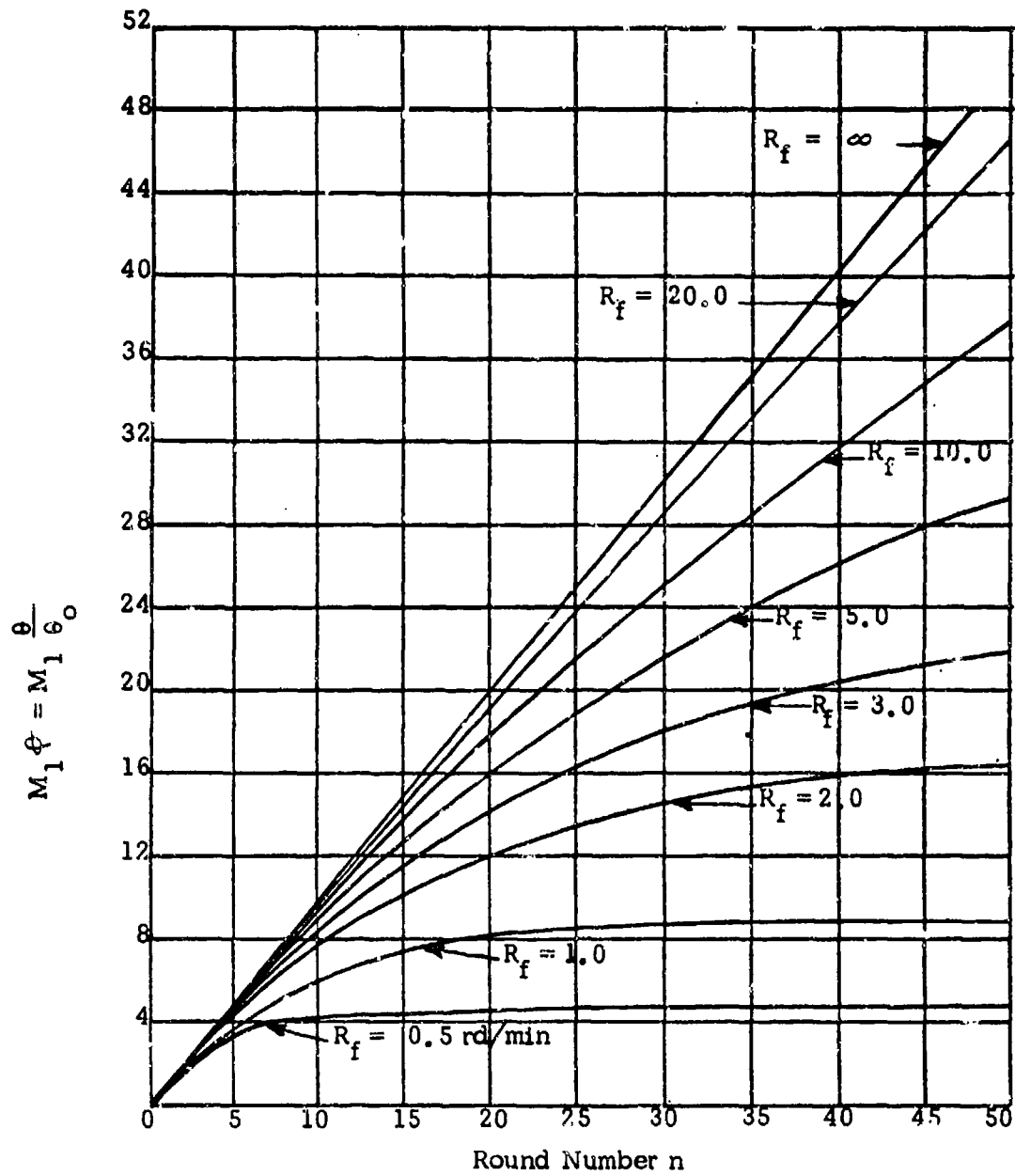


Figure 5-27. Reduced Temperature vs Round Number for Given Rate of Fire ($h' = 0.12 \text{ min}^{-1}$)

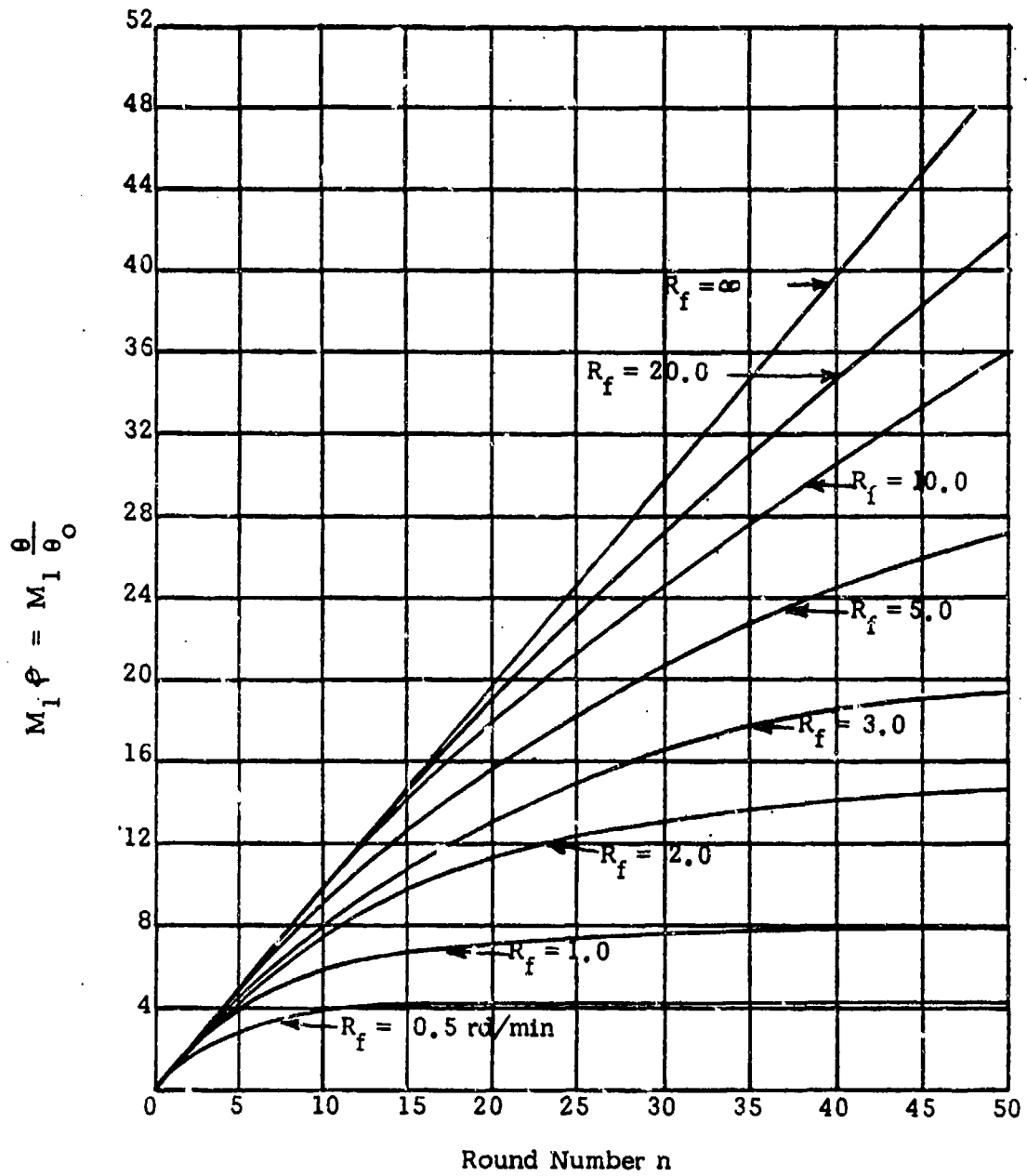


Figure 5-28. Reduced Temperature vs Round Number for Given Rate of Fire ($h' = 0.14 \text{ min}^{-1}$)

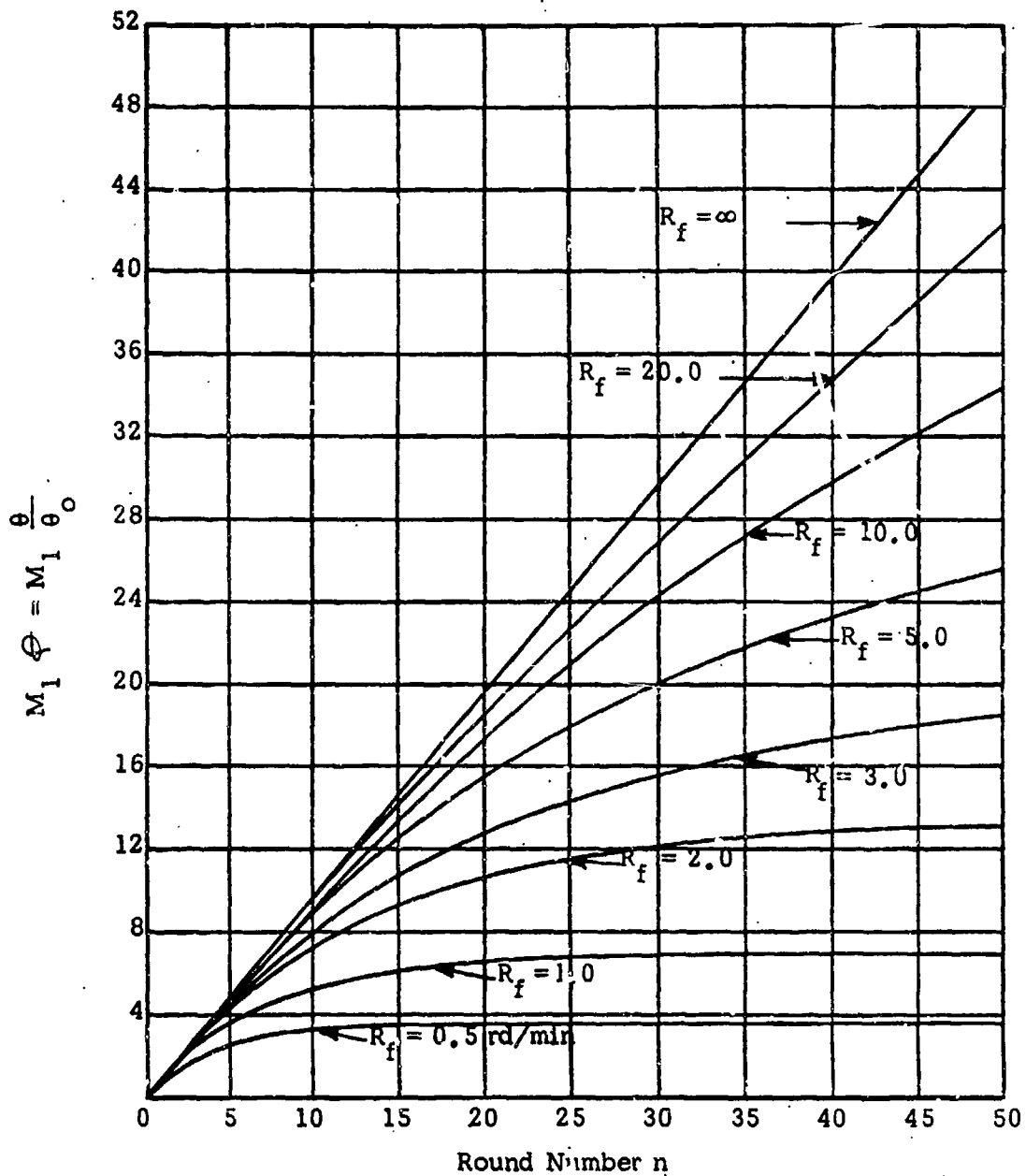


Figure 5-29. Reduced Temperature vs Round Number for Given Rate of Fire ($h' = 0.16 \text{ min}^{-1}$)

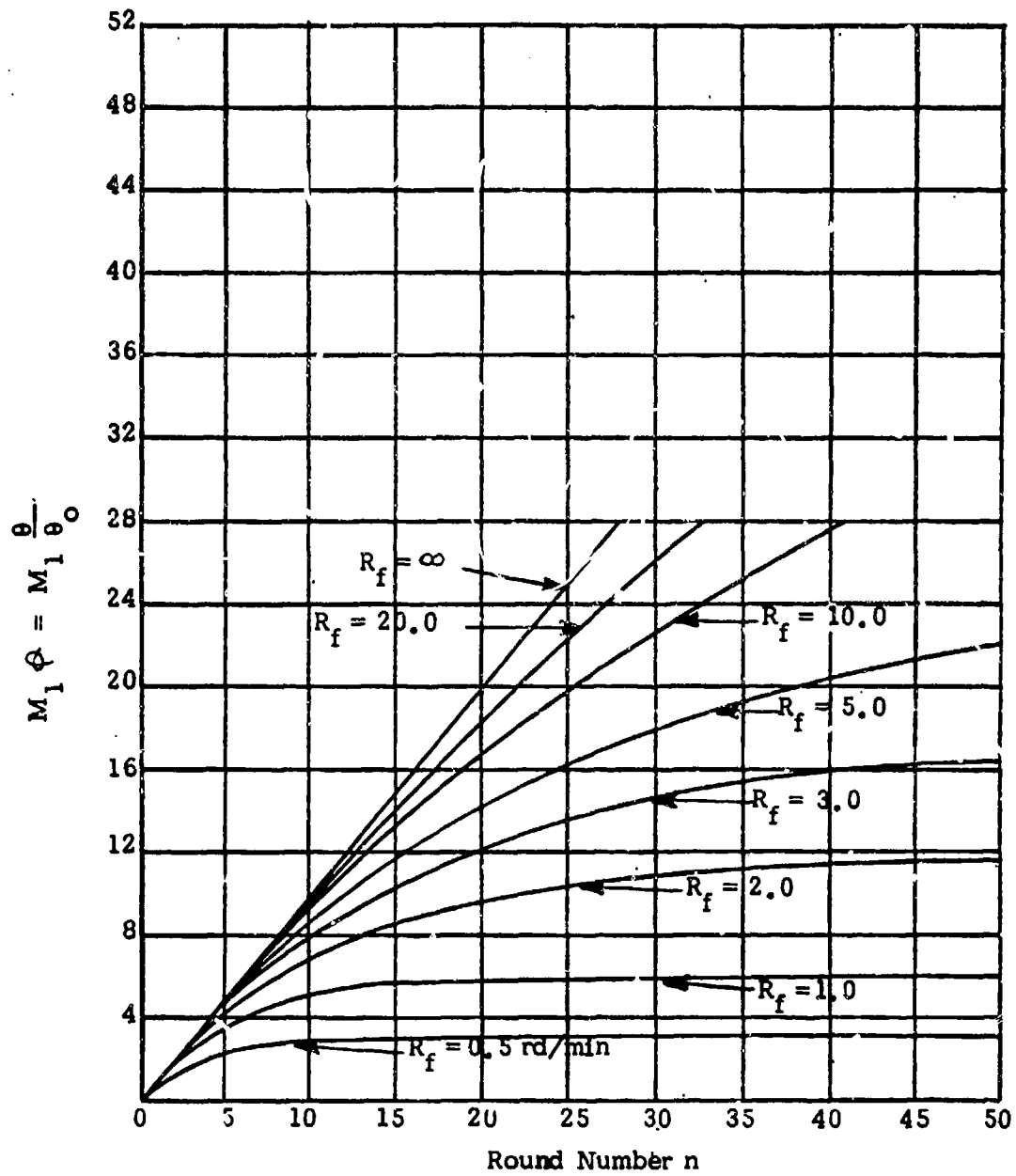


Figure 5-30. Reduced Temperature vs Round Number for Given Rate of Fire ($h' = 0.18 \text{ min}^{-1}$)

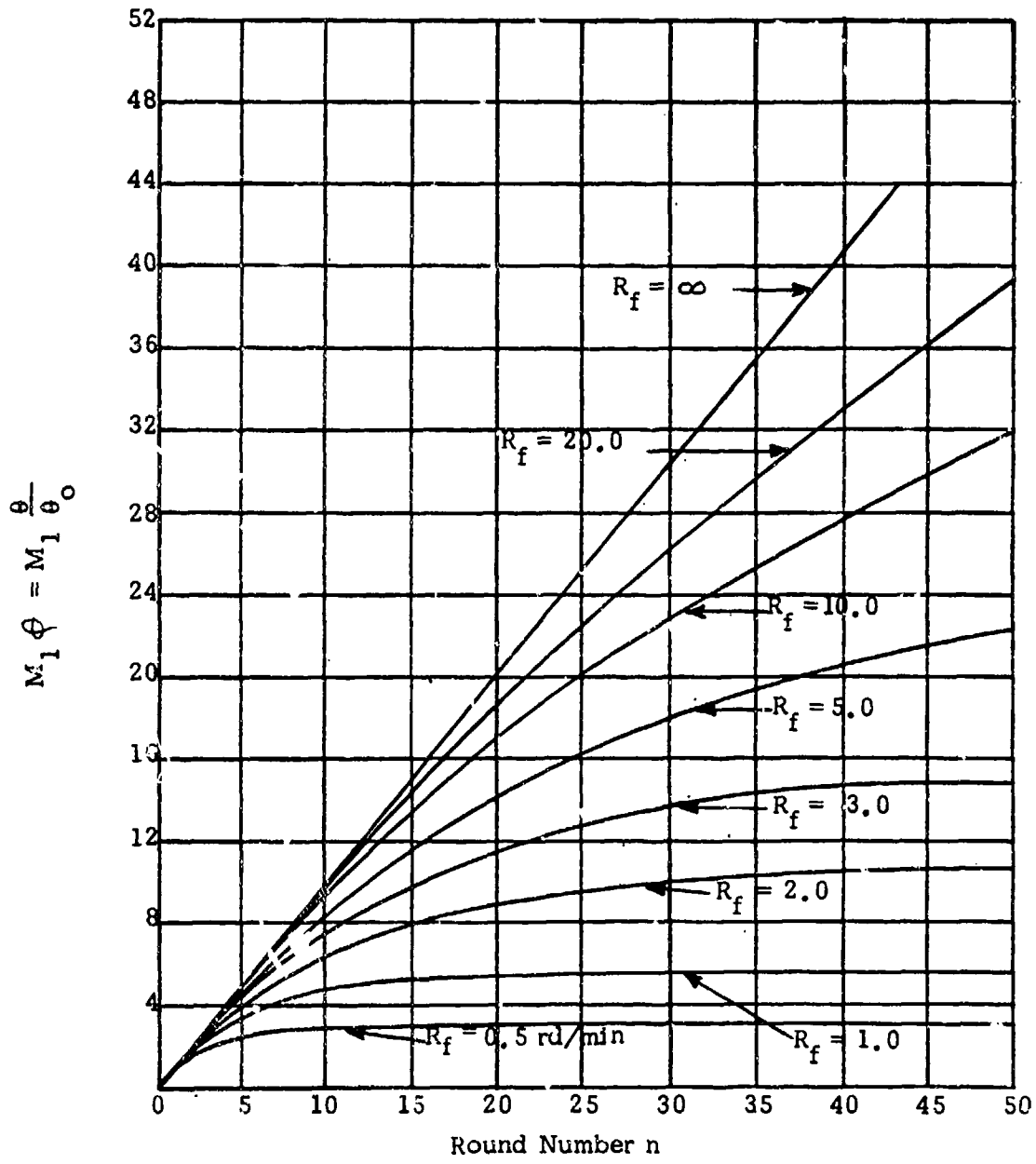


Figure 5-31. Reduced Temperature vs Round Number for Given Rate of Fire ($h' = 0.20 \text{ min}^{-1}$)

where

T_a = air ambient temperature, °F

T_o = maximum temperature at inner wall, °F

T_1 = temperature of inner wall after firing first round, °F

$$M_1^{-1} = \frac{\theta_1}{\theta_o} = \frac{35}{450} = 0.078$$

From Fig. 5-30 for $h' = 0.18 \text{ min}^{-1}$ with $R_f = 2$ and $n = 15$

$$M_1 \phi'_{15} = 8.60$$

$$\phi'_{15} = \frac{8.60}{M_1}$$

$$\phi'_{15} = 8.60 \times 0.078 = 0.67$$

$$\theta_{15} = \phi'_{15} \theta_o \text{ (remembering } \phi = \theta/\theta_o \text{)}$$

$$\theta_{15} = 0.67 \times 450$$

$$\theta_{15} = 302 \text{ deg F}$$

$$T_{15} = \theta_{15} + T_a = 302 + 50$$

$$T_{15} = 352 \text{ deg F}$$

Table 5-4(B) also contains a comparison of observed and calculated results for the 57 mm T66E2 Recoilless Rifle for the following conditions:

$$R_f = 0.5 \text{ rd/min}$$

$$h' = 0.12 \text{ min}^{-1}$$

$$T_1 = 85 \text{ °F}$$

$$T_a = 41 \text{ °F}$$

$$T_o = 500 \text{ °F (assumed)}$$

$$M_1^{-1} = 0.096$$

5-30.2 EXPERIMENTAL PHASE

Fig. 5-32 shows the experimental exterior surface temperature distribution obtained during firing tests of a 57 mm T66E2 Recoilless Rifle. The rifle was outfitted with firing stand and ten Chromel-Alumel thermocouples of 40 gage wire spot welded into minute slots along the barrel as indicated in Fig. 5-32. These thermocouples measured the rifle temperature as a function of time for various rates of fire. In this case, as described in Ref. 10, the output from each thermocouple was recorded on a multichannel galvanometer type recorder. The recorder is calibrated by substituting an equivalent resistance for the thermocouple circuit, impressing on it a known millivoltage, and recording the deflection obtained. Since the deflection of each galvanometer is not exactly linear, the calibration is accomplished in steps at approximately 1-in. intervals up to 4-in. total deflection to establish a calibration curve.

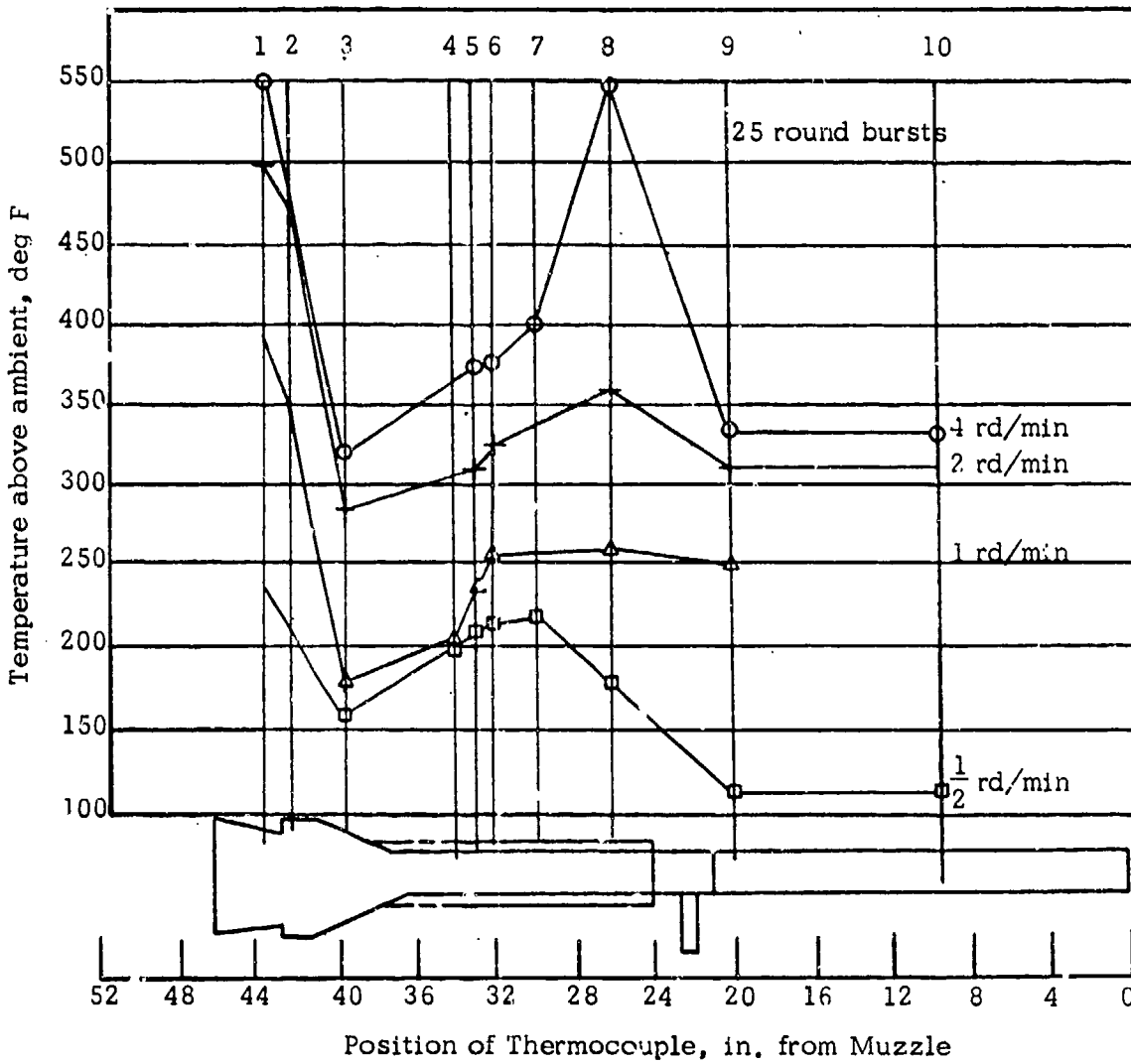


Figure 5-32. Experimental Temperature Distribution in Rifle

SECTION X
SPECIAL TOPICS

5-31 LOSS OF UNBURNT PROPELLANT

If unburned propellant ejection through the nozzle is W_s at any time and the initial charge is C_i , the following relation exists:

$$C - N = C_i - W_s - N, \text{ lb} \quad (5-89)$$

where

C = effective propellant charge weight, lb

N = weight of propellant burnt, lb

From experimental investigations of the powder loss from a 57 mm M18 Recoilless Rifle as reported in Ref. 3, it was found that

$$\frac{dW_s}{dt} = a_1 P$$

Substituting $P = \frac{m'}{A} \left(\frac{dV}{dt} \right)$ from the equation

of projectile motion and integrating up to time of all burnt, the value of a_1 is found to be

$$a_1 = \frac{AC_s}{m'V_b}, \text{ in.}^2 \text{-sec}^{-1}$$

where C_s is the total unburned propellant charge ejected through the nozzle. The value of W_s at any time t is then

$$W_s = a_1 \int_0^t P dt = a_1 m' V/A, \text{ lb}$$

By substituting this result into Eq. 5-89, the weight of unburned propellant remaining in

the rifle at any time is

$$C - N = C_i - a_1 m' V/A - N \quad (5-90)$$

From the definition of the propellant web thickness W

$$W = W_o - 2 \int_0^t r dt \quad (5-91)$$

and from the approximation of a linear burning rate r

$$r = C' P$$

the following expression is obtained for the unburnt propellant web

$$W = W_o - 2C' \int_0^t P dt$$

or in dimensionless form

$$f = 1 - \frac{2C'}{W_o} \int_0^t P dt \quad (5-92)$$

where

$$f = W/W_o = \text{fraction of web unburnt}$$

Since the amount of unburned propellant ejected is proportional to the pressure

$$\frac{dW_s}{dt} = a_1 P$$

then from Eq. 5-92 the amount of unburnt

propellant ejected at any time t is

$$W_s = a_1 \left[\frac{(1-f)W_o}{2C'} \right] \quad (5-93)$$

Therefore, the amount of unburned propellant in the gun at any time is obtained by using Eq. 5-89.

$$C - N = C_t - N - a_1 W_o (1-f)/(2C') \quad (5-94)$$

If we let n' be the number of grains in the gun at any time and n'_o the initial number of grains, Eq. 5-94 can be written as

$$n' = n'_o - a_2 W_o (1-f)/(2C') \quad (5-95)$$

By knowing the fraction of propellant loss, $s = C_s/C_t$, the constant a_2 in Eq. 5-95 can be determined from the following relation

$$s = - \int_1^0 \left(\frac{a_2 W_o}{2C'} \right) \left[\left(1 - \frac{W_o}{l_o} \right) + \left(\frac{W_o}{l_o} \right) f \right] \frac{f}{n'_o} df \quad (5-96)$$

where

$$\left[\left(1 - \frac{W_o}{l_o} \right) + \left(\frac{W_o}{l_o} \right) f \right] \frac{f}{n'_o}$$

represents the ratio of ejected charge volume to the total initial charge volume, and l_o is the initial length of the propellant grains. The result of integration yields

$$\frac{a_2 W_o}{2C'} = \frac{2s n'_o}{1 - \frac{1}{3} \left(\frac{W_o}{l_o} \right)}$$

which upon substituting into Eq. 5-96 and defining $R' = W_o/l_o$

$$\begin{aligned} n' &= \frac{n'_o}{1 - \frac{R'}{3}} \left(1 - \frac{R'}{3} - 2s + 2sf \right) \\ &= \frac{n'_o}{1 - \frac{R'}{3}} \left[\left(1 - \frac{R'}{3} \right) - 2s(1-f) \right] \end{aligned} \quad (5-97)$$

Since the surface area S_g of single-perforated grain at any time is given by

$$\begin{aligned} S_g &= \frac{2C_2}{W_o \rho} (1 - R' + 2R'f) \\ &= \frac{2C_2}{W_o \rho} [(1 + R') - 2R'(1-f)] \end{aligned}$$

where

$$C_2 = C_t - C_s$$

the total surface area S of the number of grains in the rifle at any time t can be written as the product of the number of grains in the rifle and the surface area per grain. The result is

$$\begin{aligned} S &= \frac{2C_2}{W_o \rho} \left(1 - \frac{R'}{3} \right)^{-1} \left[\left(1 - \frac{R'}{3} \right) - 2s(1-f) \right] \\ &\times [(1 + R') - 2R'(1-f)] \end{aligned} \quad (5-98)$$

The burning rate equation may be written in the following form

$$r = - \frac{W_o}{2} \left(\frac{df}{dt} \right)$$

and substituting this value of r into

$$\frac{dN}{dt} = \rho S r$$

obtain

$$\frac{N}{C_2} = - \frac{\rho W_o}{2C_2} \int_1^f S df \quad (5-99)$$

Substituting Eq. 5-98 into Eq. 5-99 results in the following integral

$$\frac{N}{C_2} = -\frac{1}{1-s} \int_1^f \left[1 - \left(\frac{2s}{1 - \frac{R'}{3}} \right) (1-f) \right] \times [1 + R' - 2R'(1-f)] df$$

The integration of this equation yields a cubic in f which is reduced to a quadratic expression by the following substitution

$$f^3 \approx \frac{3}{2}f^2 - \frac{1}{2}f$$

From these operations, it follows that

$$\frac{N}{C_2} = 1 - \left(1 - \frac{W}{L} \right) f - \left(\frac{W}{L} \right) f^2$$

where W/L is the charge regressiveness considering propellant loss and is found to be

$$\frac{W}{L} = \frac{1}{1-s} \left[R' + s \left(\frac{1-R'}{1 - \frac{R'}{3}} \right) \right]$$

or

$$\frac{W}{L} = \frac{1}{1 - \frac{C_s}{C_t}} \left[\frac{W_o}{l_o} + \frac{C_s}{C_t} \left(\frac{1 - \frac{W_o}{l_o}}{1 - \frac{W_o}{3l_o}} \right) \right] \quad (5-100)$$

5-32 PRESSURE GRADIENT IN GUN

The complete derivation for the effective projectile mass is found in par. 5-10. The purpose of the effective projectile mass is to compensate for the difference in the chamber pressure and the pressure acting on the base of the projectile and the additional pressure drop caused by friction at projectile-barrel interface. With the introduction of effective projectile mass m' it is possible to write the

equation of projectile motion in terms of the chamber pressure as follows

$$\frac{dV}{dt} = \frac{AP}{m'}$$

5-33 FORM FACTOR FOR PROPELLANT BURNING

In par. 5-12 the rate of propellant burning was given as

$$\frac{dN}{dt} = \frac{3C_2}{W_o}$$

and upon integrating

$$\frac{N}{C_2} = \frac{Bm'V}{AW_o}$$

assuming that the burning surface of the propellant is constant (single-perforated grains) or as discussed in par. 5-12 for seven-perforated grains

$$\frac{N}{C_2} = \frac{Bm'V}{AW_7F_7}$$

where the factor F_7 is shown in Fig. 5-33.

This approximation can be improved by use of a form function that expresses the fraction of propellant charge burned N/C_2 as a quadratic function of the fraction of the unburned web f . The following function fits accurately the common propellants in use

$$\frac{N}{C_2} = k_o - k_1f + k_2f^2 \quad (5-101)$$

where k_o , k_1 , and k_2 are constants that depend upon the propellant granulation.

The values of k_o , k_1 , and k_2 are given in the subsequent paragraph for the following granulations with no unburned propellant loss through nozzle injection.

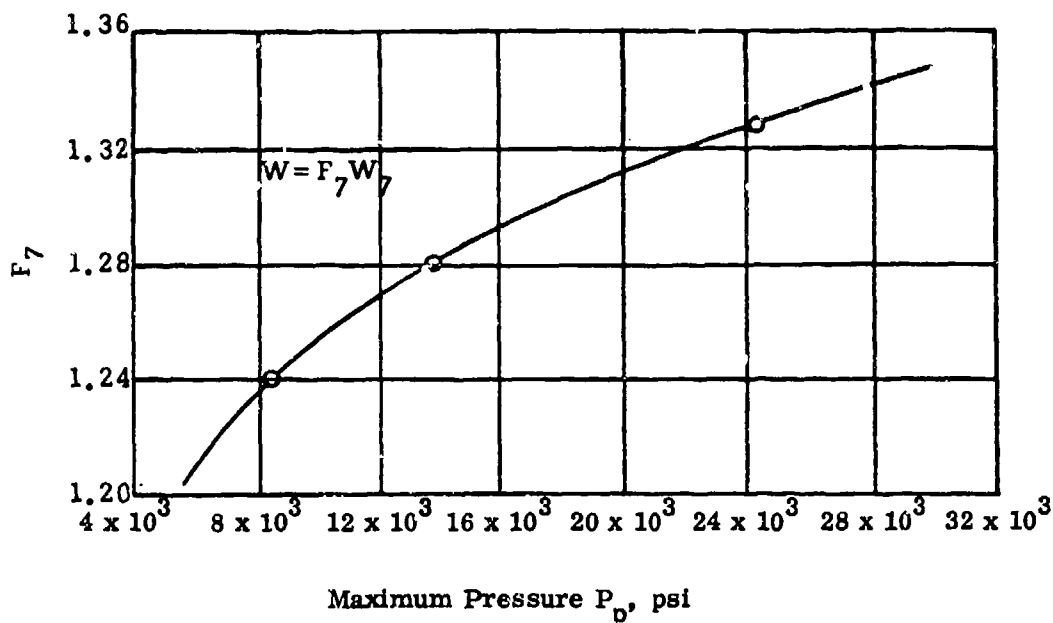


Figure 5-33. Multiplying Factor F_7 for Converting 7-perforated Webs (W_7) of M10 Propellant to Equivalent Single-perforated Webs (W)

(1) Single-perforated Grain:

$$\frac{N}{C_2} = 1 - \left(1 - \frac{W_e}{l_o}\right) f - \left(\frac{W_e}{l_o}\right) f^2 \quad (5-102)$$

$$k_3 = \frac{1}{4} \left[1 - \frac{3}{\left(\frac{D_e}{d}\right)}\right] \left\{ \frac{1}{\left(\frac{l_o}{D_o}\right)} + 2 \frac{\left[1 + \frac{7}{\left(\frac{D_e}{d}\right)}\right]}{\left[1 - \frac{7}{\left(\frac{D_e}{d}\right)^2}\right]} \right\} \quad (5-104)$$

(2) Seven-perforated Grain:

The form function of the seven-perforated grain to splintering can be written in slightly different form in terms of the fraction of propellant web burnt.

$$k_4 = \frac{1}{8} \left[1 - \frac{3}{\left(\frac{D_e}{d}\right)}\right]^2 \left\{ \frac{3}{1 - \frac{7}{\left(\frac{D_e}{d}\right)^2}} - \frac{1}{\left(\frac{l_o}{D_o}\right)} \frac{\left[1 + \frac{7}{\left(\frac{D_e}{d}\right)}\right]}{\left[1 - \frac{7}{\left(\frac{D_e}{d}\right)^2}\right]} \right\} \quad (5-105)$$

$$\frac{N}{C_2} = k_3 \omega + k_4 \omega^2 + k_5 \omega^3 \quad (5-103)$$

$$k_5 = \frac{3}{32} \left[1 - \frac{3}{\left(\frac{D_e}{d}\right)}\right]^3 \left\{ \frac{1}{\left(\frac{l_o}{D_o}\right)} \frac{1}{\left[1 - \frac{7}{\left(\frac{D_e}{d}\right)^2}\right]} \right\} \quad (5-106)$$

where

$\omega = 1-f$ = fraction of propellant web burnt

where

D_o = initial diameter of grain

d = perforation diameter

l_o = initial length of grain

The constants k_3 , k_4 , and k_5 are as follows:

(3) *Cord and Sheet Propellants:*

(a) Cord or Cylindrical Solid:

$$\frac{N}{C_2} = 1 + \left(\frac{W_0}{2L_0}\right)f - \left(1 + \frac{W_0}{2L_0}\right)f^2 \quad (5-107)$$

(b) Sheet Propellant:

$$\frac{N}{C_2} = 1 + f \quad (5-108)$$

5-34 MUZZLE FLASH**5-34.1 BASIC THEORY**

When a recoilless rifle is fired, the hot gases discharged from the muzzle and nozzle are luminous, resulting in a visible flash. Since flash reveals the location of the weapon, it is an undesirable effect that should be minimized or eliminated. The flash resulting from gases issuing from the nozzle of a recoilless rifle is similar to muzzle flash, but is of much greater intensity because of the larger amount of gases discharged. A study of flash phenomenon reveals three regions of luminosity (Refs. 11, 12, and 13):

(1) A small region of low luminosity at muzzle or nozzle called primary flash.

(2) A region of high intensity just beyond the muzzle or nozzle and separated from primary flash known as intermediate flash.

(3) An ill-defined region of high intensity, beyond but not well separated from the intermediate flash, called the secondary flash.

Although the flash mechanisms are not understood fully, it generally is agreed that the propellant gas emerging from the gun is sufficiently energetic to be self-luminous. The gas immediately expands and cools below the luminous temperature, resulting in a dark zone. Following this, the gas is overexpanded

and is recompressed adiabatically through a shock. This recompression raises the gas temperature and the gas becomes luminous again. The propellant gases have entrained air during this process, thus forming a combustible mixture. If the recompression has raised the mixture temperature to the ignition point, it will form a secondary flash.

Most of the luminosity in flash is due to metallic impurities in the propellant gases. The spectrum of the emitted gases reveals strong radiation from sodium, potassium, and calcium, and the oxides of calcium and copper which are expected since these materials are used in propellant manufacture with copper originating predominately from the rotating bands.

5-34.2 FLASH SUPPRESSION

In principle, flash can be partially suppressed by the elimination of metallic impurities. However, this approach is not economically feasible. It has been determined experimentally that flash can be partially suppressed by the addition of propellant additives or suppressed mechanically by the insertion of flow spoilers.

Chemical suppressors inhibit combustion in the secondary flash zone only. Many of the additives that have been effective include the following compounds of potassium: iodide, bromide, oxalate, acid oxalate, and sulphate.

Mechanical methods have been more successful in suppressing flash. The general effect of mechanical suppressors is the inhibition of combustion since the gas dynamics are suitably perturbed. For example, when steel bars are introduced into the gas stream, the flash is reduced significantly.

Experimental studies also have been performed to determine the effect of gun design on flash. This work indicates that flash intensity is suppressed with reduction of peak

chamber pressure and increase in nozzle expansion ratio. Flash intensity reductions of 50% were achieved by this means but only by using a nozzle expansion ratio of seven which is not usually optimum.

5-35 CALCULATION OF "BARE" GUN WEIGHT

An important impact of interior ballistic design is the effect upon the minimum weighted gun. The calculation of "bare" weapon weight suffices since ancillary equipment, gun sights, and spotting rifle, are approximately the same weight for most gun designs.

One proceeds to estimate weight considering the recoilless rifle a cylindrical tube of length x , cross-sectional area A with wall thickness w , required to sustain the internal gas pressure.

The required wall thickness is

$$w = P'R_2/\sigma, \text{ in.} \tag{5-109}$$

where

P' = pressure at point in consideration, psi

R_2 = radius of tube, in.

σ = allowable tensile strength of material, psi

P' then is expressed in terms of P , the space average pressure in the weapon. At the instant $P=P_p$, any point of the tube up to $x=x_p$ must withstand a maximum pressure P'_{max} of

$$P'_{max} = 1.15 \left(\frac{M + \frac{C_2 \bar{\theta}}{2}}{M + \frac{C_2 \bar{\theta}}{3}} \right) P_p \tag{5-110}$$

where the factor 1.15 represents a 15 percent safety factor. The pressure in the gun is estimated to be P'_{max} for $0 \leq x \leq x_p$, and then to decrease linearly from P' to P'_b for $x_p \leq x \leq x_b$ and then with a linear decrease from P'_b to P'_m for $x_b \leq x \leq x_m$ where

$$P'_b = 1.15P_b$$

$$P'_m = \frac{1.15mgP_m}{\left(mg + \frac{C_2 \bar{\theta}}{3} \right)}$$

The wall thicknesses w corresponding to these pressures are determined as

$$w = w(x) = \begin{cases} w_p, & 0 \leq x \leq x_p \\ w_p - \left(\frac{w_p - w_b}{x_b - x_p} \right) (x - x_p), & x_p \leq x \leq x_b \\ w_b + \left(\frac{w_b - w_m}{x_m - x_b} \right) (x - x_b), & x_b \leq x \leq x_m \end{cases} \tag{5-111}$$

The tube weight W_g is then given by

$$W_g = 2\pi\rho' \int_0^{x_m} \left[R_2 + \frac{w(x)}{2} \right] w(x) dx$$

$$W_g = 2\pi\rho'R_2 \left[w_p x_p + \left(\frac{w_p + w_b}{2} \right) (x_b - x_p) + \left(\frac{w_b + w_m}{2} \right) (x_m - x_b) \right] + \pi\rho' \left[w_p^2 x_p + (w_p^2 + w_p w_b + w_b^2) \frac{(x_b - x_p)}{3} + (w_b^2 + w_b w_m + w_m^2) \frac{(x_m - x_b)}{3} \right] \tag{5-112}$$

where ρ' = density of gun material.

In the case that V_b is less than V_p , $P_p = P_b$ and $x_b = x_p$, which eliminates the second and fifth terms of Eq. 5-112. In the case that $x_h = x_m$, the third and sixth terms of Eq. 5-112 are eliminated.

5-36 LIST OF NUMERICAL CONSTANTS USED IN INTERIOR BALLISTIC CALCULATIONS

Table 5-5 is a list of the numerical values of the constants for M10 Propellant and other parameters used in the interior ballistic calculations.

TABLE 5-5
NUMERICAL CONSTANTS USED IN
INTERIOR BALLISTIC CALCULATIONS

For M10 Propellant:

η	=	28.55 in. ³ -lb ⁻¹
$1/\rho$	=	17.09 in. ³ -lb ⁻¹
T_o	=	2859° K
F	=	3.31×10^5 (ft-lb)-lb ⁻¹
r_1	=	$4.53 \times 10^{-3} p^{0.7}$ in.-sec ⁻¹
μ	=	1.24

Other Parameters:

K	=	6.46×10^{-3} sec ⁻¹
A/A_t	=	1.5
A_e/A_t	=	2.3

REFERENCES

- AD 95182, D. J. Katsanis, *A New Concept of the Ballistic Efficiency of Recoilless Rifles*, Frankford Arsenal Report R-1312, March 1956, 9 pp.
- Interior Ballistics of Recoilless Rifles*, Final Report ORD Project No. TS4-4004, Armour Research Foundation of Illinois Institute of Technology, Frankford Arsenal, Philadelphia, Pa., April 1952, 3 Volumes.
- D. J. Katsanis, *A Graphical Method of Solution of Interior Ballistic Problems in Conventional Recoilless Rifle Design*, Report No. MR-604, Pitman-Dunn Laboratories, Frankford Arsenal, Philadelphia, Pa., May 1955, 18 pp.
- S. G. Hughes, *Summary of Interior Ballistics Theory for Conventional Recoilless Rifles*, Report No. R-1140, Pitman-Dunn Laboratories, Frankford Arsenal, Philadelphia, Pa., September 1953, 39 pp.
- AD 36531, *Development of 105mm Battalion Antitank Weapons and Interior Ballistics for the Design of Recoilless Rifles*, Summary Report, Volume I, ORD Project TS4-4020, Armour Research Foundation of Illinois Institute of Technology, July 1, 1954.
- S. G. Hughes, *Simplified Interior Ballistic Equations for Recoilless Rifles with Zero Starting Pressure*, Report No. R-1061, Pitman-Dunn Laboratories, Frankford Arsenal, Philadelphia, Pa., April 1952, 12 pp.
- S. G. Hughes, *Conditions for Theoretically Optimum Recoilless Rifles*, Report No. R-1102, Pitman-Dunn Laboratories, Frankford Arsenal, Philadelphia, Pa., October 1952, 13 pp.
- J. O. Hirschfelder, R. B. Kershner, C. F. Curtis, and R. E. Johnson, *Interior Ballistics of Recoilless Guns*, OSRD Report No. 1801, NDRC Report No. A-215, September 1943.

9. AD 115524, H. Kahn, *Temperature Distribution in Recoilless Rifles*, Report No. R-1321, Frankford Arsenal, Philadelphia, Pa., May 1956, 29 pp.
10. AD 34245, *Symposium of Recent Progress of Recoilless Rifles and Ammunition*, Department of the Army, January 1954.
11. Rudolf Ladenburg, *Report on Muzzle Flash*, BRL Report No. 426, 1943.
12. AD 224762, Rudolf Ladenburg, *Studies of Muzzle Flash and Its Suppression*, BRL Report No. 618, 10 February 1947, 23 pp.
13. AMCP 706-255, *Engineering Design Handbook, Spectral Characteristics of Muzzle Flash*.

BIBLIOGRAPHY

- AMCP 706-150, *Engineering Design Handbook, Interior Ballistics of Guns*.
- AD 73766, *Research on Basic Studies of Flash Characteristics of Recoilless Weapons*, Dept. of the Army, September 1955.
- G. Seitz, *The Influence of the Geometric Forms of Powder Grains on Their Burning Rates*, (report translated by K. P. Gerhard from *Sprengtechnik* No. 12, 1952 and *Explosivstoffe* No. 1/2), Picatinny Arsenal, 1953, 30 pp., Picatinny Arsenal Translation No. 1.
- Jerome M. Frankle and James R. Hudson, *Propellant Surface Area Calculations for Interior Ballistics Systems*, AD 213-441, BRL Memo Report 1187, January 1959, 33 pp.
- J. Corner, *Theory of the Interior Ballistics of Guns*, J. Wiley & Sons, New York, 1950.
- T. J. Hayes, Major General, *Elements of Ordnance*, J. Wiley & Sons, New York, 1938.
- AD 105-887, L. E. Stout and W. A. Dittrich, *Analog Computer Study of Interior Ballistic Equations*, Report No. R-1313, Frankford Arsenal, March 1956, 24 pp.
- AD 296-282, A. Magar, *Burning Rate Characteristics of M5 Propellant*, Frankford Arsenal, FA Report R-1642, June 1962, 27 pp.
- AD 265-123, J. Harris Shulman, and C. Lenchitz, *Burning Characteristics of Standard Gun Propellants at Low Temperatures (21°C to -52°C)*, Picatinny Arsenal, November 1961, 101 pp.
- A. Magar, *Burning Rate Characteristics of T18 and M6 Propellants*, Frankford Arsenal, October 1958.
- CPIA/M2 Solid Propellant Manual*, Revised Edition, October 1965.
- Sorrow, *Recherches Theoriques Sur le Chargement des Bouches a Feu* (Paris, 1882).
- AD 229-048, D. J. Katsanis, *A Theoretical Interior Ballistic Study of Recoilless High-Low Pressure Guns*, Report R-1513, Frankford Arsenal, June 1959, 47 pp.
- W. A. Dittrich, *Ninth Tripartite AXP Conference*, Paper A.2(a)1, 1958.
- J. Mar, (S), *A Feasibility Study of the Internal Ballistics of a New Medium Anti-Tank Recoilless Gun* (U), CARDE Tech Memo 292164, March 1960.
- Hypervelocity Guns and the Control of Gun Erosion*, Summary Technical Report of Division 1, NDRO, Volume 1, 1946.
- C. L. Anni, et al., *Measurement of Heat Input to the Bore Surface of Caliber .50 Gun*

Barrels, OSRD 6470, Report A-399, Leeds & Northrup Co., July 23, 1945.

J. O. Hirschfelder et al., *Heat Conduction, Gas Flow, and Heat Transfer in Guns*, OSRD 863, Progress Report A-87, Geophysical Lab., Carnegie Institute of Washington, July 1943.

G. S. Fulcher, Ed., *The Temperature of the Bore Surface of Guns*, OSRD 1966, Report No. A-201, Geophysical Lab., Carnegie Institute of Washington, July 1943.

J. O. Hirschfelder et al., *Interior Ballistics, Part I*, OSRD 1236, Report No. A-142, Geophysical Lab., Carnegie Institute of Washington, February 1943.

E. P. Hicks, C. K. Thornhill, *The Heating of Gun Barrel by the Propellant Gases*, Report No. 507-1, Watertown Arsenal, December 1942.

Heat Transfer in a 57 mm Recoilless Rifle Based Upon Measured Internal Surface Temperature, Phase Report No. 3, Midwest Research Institute, Contract DA-23-072-ORD-637, October 1954.

AD 404-467, Bannister et al., *Heat Transfer, Barrel Temperature and Thermal Strains in Guns*, Report No. 1192, Ballistic Research Labs., February 1963, 59 pp.

AMCP 706-107, Engineering Design Handbook, *Elements of Armament Engineering, Part Two, Ballistics*.

AD 73766, *Research on Basic Studies of Flash Characteristics of Recoilless Weapons*, Department of the Army, September 1955.

AD 801-763, Douglas C. Vest, *An Experimental Traveling Charge Gun*, BRL Report No. 773, October 1951, 72 pp.

Fast Burning Propellant, Final Report, Contract DA-23-072-ORD-369, Phases I, II and

IV, Olin Mathieson Chemical Corp., East Alton, Illinois, 1955.

AD 36566, D. C. Vest et al., *A Qualitative Discussion of the Burning Mechanism of Porous Propellants*, BRL Report No. 902, April 1954, 30 pp.

AD 250-053, Paul G. Baer and Kenneth R. Bryson, *Design Data for the Constant Pressure Traveling Charge Gun*, BRL Tech Note No. 1360, November 1960, 23 pp.

(C) *Hypervelocity Weapons Feasibility Study* (U), Final Report, Contract AF08(635)-3543, Illinois Institute of Technology, No. 1965.

CARDE 316/59(C), *Launcher Rocket, ATK, 100 mm Xc-1* (U), May 1960.

O. E. Teichman, *Investigation of Temperature Distribution and Powder Gas Flow in Recoilless Rifles*, Summary Report, Contract W-11-022-ORD-11171, Armour Research Foundation, Jan. 1949.

Development 2.76 in. Recoilless Rifles T-190 and T-191 for Mounting on Aircraft, Final Report, Vol. I, Contract DA-11-022-ORD-865, Armour Research Foundation.

J. N. Kapur, *The Internal Ballistics of a Recoilless High-Low Gun*, Appl. Science Research, Section A, Vol. 6, No. 5-6.

S. P. Carfagno, (C) *Handbook on Gun Flash* (U), Prepared for Ammunition Branch, Office of Chief of Ordnance, U S Army, The Franklin Institute, Philadelphia, Pa., 1961.

AMCP 706-255, Engineering Design Handbook, *Spectral Characteristics of Muzzle Flash*.

AD 467617, A. G. Edwards, *Interior Ballistic Analysis of Various Guns and Launcher Systems*, Picatinny Arsenal, TR-3193, June 1965, 88 pp.

AMCP 706-238

AD 201104, *Calculation of Interior Ballistics of Recoilless Guns by Analog Computer*, Picatinny Arsenal, TR-2541, November 1958, 31 pp.

Recoilless Rifle Handbook (Unpublished), Prepared at Frankford Arsenal, Philadelphia, Pa.

CHAPTER 6
 CANCELLATION OF RECOIL

6-0 LIST OF SYMBOLS

A	= cross-sectional area of nozzle at arbitrary location, ft ²	c_p	= specific heat of propellant gas at constant pressure, (ft-lb)-(lb ^o F) ⁻¹
A_b	= cross-sectional area of bore of rifle, ft ²	c_v	= specific heat of propellant gas at constant volume, (ft-lb)-(lb ^o F) ⁻¹
A_c	= cross-sectional area of chamber of rifle, ft ²	D_B	= bore diameter of rifle, in. or mm
A_e	= cross-sectional area of nozzle at exit, ft ²	D_1, D_2, D_t	= throat diameter of nozzle, in.
A_i	= cross-sectional area of nozzle at inlet (also called nozzle approach area, or nozzle entrance area), ft ²	F	= thrust force of nozzle, lb
A_o	= cross-sectional area of nozzle at reference location, ft ²	F_R	= recoil force (rearward) of rifle, lb
A_t	= cross-sectional area of nozzle at throat, ft ²	G	= mass velocity, slug-(ft ² sec) ⁻¹
a	= acoustic velocity at arbitrary section of nozzle, ft-sec ⁻¹	G'	= mass flux (mass flow, or mass flow rate), slug-sec ⁻¹
a_t	= acoustic velocity at throat section of nozzle, ft-sec ⁻¹	G'_a	= actual mass flow rate, slug-sec ⁻¹
b	= subscript which refers to bore of rifle	ΔH	= theoretical specific enthalpy change, (ft-lb)-slug ⁻¹
C_F	= thrust coefficient, dimensionless	h, h_1, h_2	= heat transfer coefficient from propellant gas to nozzle surface, cal-(cm ² -sec ^o C) ⁻¹
c	= specific heat of nozzle material, cal-(g ^o C) ⁻¹	k	= thermal conductivity of nozzle material, cal-(cm ² -sec ^o C/cm) ⁻¹
c	= subscript which refers to chamber of rifle	M'	= molecular weight of propellant gas, dimensionless
		$M = v/a$	= Mach number at arbitrary location of nozzle, dimensionless
		M_e	= jet Mach number, dimensionless

%MP	= percent of melting point	ΔT_t	= temperature rise of propellant gas at nozzle throat (with reference to nozzle initial temperature), °R
p	= pressure at arbitrary location of nozzle, lb-ft ⁻²	t	= time, sec
p_a	= ambient pressure external to rifle, lb-ft ⁻²	t	= subscript which refers to throat of nozzle
p_c	= chamber pressure of rifle, lb-ft ⁻²	t_m	= time for projectile to leave muzzle of rifle, sec
p_e	= pressure at exit section of nozzle, lb-ft ⁻²	v	= gas velocity at arbitrary location of nozzle, fps
p_i	= pressure at inlet section of nozzle, lb-ft ⁻²	v_e	= gas velocity at exit section of nozzle, fps
p_o	= ideal reservoir pressure (pressure at reference location), lb-ft ⁻²	v_i	= gas velocity at inlet section of nozzle, fps
p_t	= pressure at throat section of nozzle, lb-ft ⁻²	v_t	= gas velocity at throat section of nozzle, fps
p_e/p_a	= jet pressure ratio, dimensionless	v_e/v_i	= velocity ratio, dimensionless
p_o/p_e	= pressure ratio, dimensionless	x	= abscissa of a point on jet boundary
R	= gas constant (= 49,709/ M'), ft ² -(sec ² -°R) ⁻¹	y	= ordinate of a point on jet boundary
r	= radius of exit section of nozzle (jet radius), in.	α	= divergence angle of nozzle (angle of inclination of diverging nozzle wall to nozzle axis), deg
$r' = A_c/A_t$	= ratio of chamber area to rifle bore area, dimensionless	2α	= cone angle of nozzle (nozzle expansion angle), deg
ΔT_m	= difference between melting temperature of nozzle material and initial temperature of nozzle, °R	β	= angle of inclination of converging plug wall to nozzle axis, deg
T_o	= ideal reservoir temperature of propellant gas (temperature at reference location), °R	$\gamma = c_p/c_v$	= ratio of specific heats of propellant gas, dimensionless
ΔT_s	= temperature rise of inner surface of nozzle throat (with reference to nozzle initial temperature), °R	ϵ	= expansion ratio of nozzle, dimensionless

ϵ_1, ϵ_2	= fractional increase in nozzle throat area, dimensionless	λ	= divergence correction factor, dimensionless
η	= overall efficiency of nozzle, dimensionless	ρ'	= density of nozzle material, g-cm^{-3}
η_d	= discharge correction factor of nozzle, dimensionless	ρ_o	= density of propellant gas in reservoir, slug-ft^{-3}
η_{KE}	= kinetic energy efficiency of nozzle, dimensionless	ρ_t	= density of propellant gas at nozzle throat, slug-ft^{-3}
η_v	= velocity coefficient of nozzle, dimensionless	ω	= dimensionless recoil (momentum ratio parameter), dimensionless

SECTION I

INTRODUCTION

6-1 CONSERVATION OF MOMENTUM

The so-called "Recoilless Principle" is derived from the general "Momentum Theorem" for a system of particles. This theorem states that the time rate of change of the momentum of the system is equal to the sum of all the *external* forces acting on the system. Accordingly, in the absence of *external* forces, the momentum of the system undergoes no change. This result is known popularly as the principle of "Conservation of Momentum". When applied to a gun discharging a projectile forward, this principle shows that the gun will itself be driven in motion in a direction opposite to that of the projectile, a phenomenon well known as recoil. In the event that the gun is to experience no recoil, it is evident that an equivalent amount of rearward momentum must be generated by use of a scheme in which the recoiling mass is something other than the gun and, consequently, the recoilless guns do not, in general, have the breech closed as in the case of conventional guns.

Among the various schemes proposed, one of the first was a gun that used a single straight tube to simultaneously fire projectiles of equal mass from both ends. A similarly awkward scheme was employed in the Davis gun that ejected simultaneously a projectile with high velocity from the muzzle and a heavy lump of lead with low velocity from the breech of the weapon.

A simpler, though somewhat less obvious, way of obtaining the recoilless effect is to permit the transfer of a large portion of the

propellant gas to the rear, so that the rearward momentum of the gas escaping from the breech is employed to balance the forward momentum of the projectile. A constriction of the gun tube at a point behind the propellant charge was employed in the Cooke recoilless gun. The constriction of the rear passage increases the velocity of the escaping gas, raises the internal pressure, and also increases the muzzle velocity of the projectile. Recoillessness then becomes a function of the ratio of the bore area to exit-port area, ratio of the projectile mass to charge mass, loading density, powder granulation and compositions, burning temperature, and other factors.

6-2 THE SUPERSONIC NOZZLE

In actual practice, the constriction in the rear passage is realized by having the propellant chamber open into a rearward orifice of a cross section somewhat smaller than the bore and then into a divergent nozzle. The convergent-divergent (de Laval) nozzle thus formed allows the passage of a large portion of the propellant gas and its associated momentum to the rear. Upon ignition of the charge, the propellant gases are generated at a greater rate than can be maintained in the efflux from the nozzle. The rising pressure in the chamber then exerts a force on the projectile to set it into motion, and finally establishes a state of approximate pressure equilibrium in the chamber during the remainder of propellant combustion. In this process the rearward momentum acquired by the gas escaping through the nozzle is controlled by the size of the nozzle throat area and the expansion ratio (defined by Eq.

6-1) of the nozzle. By proper selection of these quantities, the forward thrust exerted by the reaction of the escaping gas on the chamber and nozzle walls can be used to neutralize the rearward thrust (recoil) which otherwise would be communicated to the gun by the reaction of the gas pressure driving the projectile forward. Ideally, the nozzle will maintain the weapon motionless during the firing cycle. However, perfection is not sought since slight variations in performance from round to round are unavoidable. In the long run, the progressive wear in the tube and nozzle will aggravate these variations, and a slight amount of recoil is tolerated. In fact, some initial recoil is deliberately planned in the rearward direction at as high a level as can be tolerated, since this is desirable for longer nozzle life. As the nozzle throat wears, rearward recoil diminishes to zero and ultimately becomes regenerated in the forward direction. Newly designed nozzles should, therefore, have the throat restricted more than necessary in the test gun to assure a substantial rearward recoil.

Thus, recoilless weapons of given nozzle design and geometry, to a certain extent, can be adjusted to the desired recoil balance by increasing the throat area to decrease rearward recoil, or by decreasing the nozzle length to increase rearward recoil. Increasing the throat area is simpler than decreasing the nozzle length and is most commonly used.

To recapitulate, the forward momentum of the projectile, together with that of the small amount of the propellant gases accompanying it, is to remain practically equal to the rearward momentum of the greater fraction of the gases that issue from the nozzle in order for the rifle to be recoilless. Strictly speaking, however, impulses due to such small factors as projectile friction and engraving, gas drag, and the resistance of any diaphragm initially restraining the exit of the propellant gases from the nozzle must be compensated, along with the elimination of the rotary recoil (torque neutralization) of the rifle which

results from the helical motion of the spin-stabilized projectile inside the gun tube.

For a given amount of recoil to be eliminated, less mass of propellant gas is required by use of high-velocity gas. The convergent-divergent nozzle can produce supersonic gas velocity. When the flow completely fills the nozzle, exit pressures below the *critical* level (defined by Eq. 6-6) cannot exist in a convergent nozzle, and the exit velocity can never exceed the sonic value. In a convergent-divergent nozzle, however, the pressure along the nozzle can be less than the critical value at any point past the throat, and supersonic flow results in the divergent portion of the nozzle—provided that the ratio of the chamber pressure to the exit pressure is sufficiently high to induce supersonic flow—since the exhaust velocity of the nozzle is a function (see Eq. 6-14) of this pressure ratio. Very high gas exhaust velocities can be obtained in this type of nozzle, the increase in the kinetic energy of the gas being derived from a corresponding decrease in the temperature.

Additional information on nozzle theory is contained in par. 6-7 dealing with nozzle design.

6-3 EFFECT ON INTERIOR BALLISTICS

The efficiency of a nozzle is based upon the thrust it can produce. The thrust F is proportional to the thrust coefficient C_F (see Eq. 6-20) which is a function of the expansion ratio e as shown in Figs. 6-4 and 6-5. A large expansion ratio nozzle is highly efficient and permits the use of a smaller throat area for a given recoil balance and, consequently, requires a smaller amount of propellant charge. On the other hand, a large expansion ratio nozzle is larger and heavier than a low expansion ratio nozzle to the extent that expansion ratios greater than 3 have not been worth the increased weight they incur. Past practice has been to use nozzle expansion ratios between about 2.0

and 3.0. In general, a value of about 2.5 represents a good compromise between efficiency and weight. For this value of the expansion ratio, the ratio of the area of the bore to that of the throat required for recoillessness is about 1.45 (refer to par.

6-11). For recoilless rifles, the ratio of the area of the bore to the area of the throat varies, in general, between approximately $4/3$ and $3/2$. This corresponds to a nozzle approach-area to rifle bore-area ratio of approximately 1.5 or greater.

SECTION II
THEORY OF THE DE LAVAL
(CONVERGENT-DIVERGENT) NOZZLE

6-4 ASSUMPTIONS

The de Laval nozzle is of the "convergent-divergent" type and has axial symmetry. In the simplified, one-dimensional (hydraulic) theory of nozzles, the following assumptions are made:

1. The propellant gas is homogeneous throughout the chamber and nozzle.
2. The propellant gas is ideal, i.e., it obeys the perfect gas law.
3. The gas has no viscosity.
4. There is no heat transfer across the walls.
5. The gas flow is steady and irrotational, with no shock, discontinuity, or separation.
6. The flow is axially symmetric, the velocity being axially directed.
7. The velocity and pressure of the gas are uniform across any circular cross section of the nozzle.
8. Chemical equilibrium prevails.

Based on these simplifying assumptions, the calculated ideal values of performance are usually within 1 to 10 percent of the measured values, so that the theory still gives good prediction of results.

6-5 DEFINITIONS

Fig. 6-1 is a schematic of the de Laval nozzle showing various design parameters.

The propellant gas enters the nozzle at the inlet section *i*.

The minimum nozzle area is called the throat area. The section at which the gas leaves the nozzle to enter the surrounding atmosphere is known as the exit *e*, and the associated area of cross section is called the exit area. The nozzle area expansion ratio ϵ or, simply, the expansion ratio is defined as

$$\epsilon = A_e/A_t, \text{ dimensionless} \quad (6-1)$$

where

$$A_e = \text{nozzle exit area, ft}^2$$

$$A_t = \text{nozzle throat area, ft}^2$$

and the reciprocal of ϵ may be calculated by Eq. 6-12. The pressure at the throat for which the gas flow per unit area of the throat is a maximum is called the critical pressure. The ratio of the critical pressure to the pressure at the inlet (or, more precisely, the constant pressure p_o of a large reservoir from which the flow in the nozzle could have arisen by purely isentropic flow) is called the critical pressure ratio. This ratio is a function of γ

where

$$\gamma = c_p/c_v = \text{ratio of specific heats, dimensionless} \quad (6-2)$$

$$c_p = \text{specific heat of propellant gas at constant pressure, (ft-lb)-(lb-}^\circ\text{F)}^{-1}$$

$$c_v = \text{specific heat of propellant gas at constant volume, (ft-lb)-(lb-}^\circ\text{F)}^{-1}$$

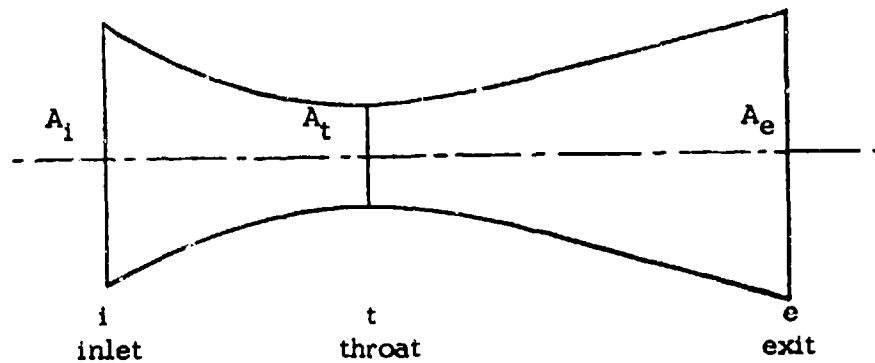


Figure 6-1. Schematic of Nozzle Showing Design Parameters

6-6 BASIC EQUATIONS

6-6.1 RATE OF FLOW

From the assumptions of par. 6-4, it follows that isentropic expansion relations can be used in the de Laval nozzle flow. By use of the energy equation, the equation of continuity, and the assumption of the isentropic flow of a perfect gas, it can be shown (Ref. 1, p. 120) that the velocity v and the pressure p at any section are related by

$$v = \frac{1}{\sqrt{1 - \left(\frac{A}{A_t}\right)^2 \left(\frac{p}{p_o}\right)^{2/\gamma}}} \times \sqrt{\left(\frac{2\gamma}{\gamma-1}\right) RT_o \left[1 - \left(\frac{p}{p_o}\right)^{(\gamma-1)/\gamma}\right]}, \text{ fps} \quad (6-3)$$

where

A = cross-sectional area of nozzle at location under consideration, ft^2

p = gas pressure at A , lb-ft^{-2}

v = gas velocity at A , fps

R = gas constant ($= 49,709/M'$),
 $\text{ft}^2 \text{-(sec}^{-2} \text{-}^\circ\text{R)}^{-1}$

M' = molecular weight of gas, dimensionless

γ = ratio of specific heats, dimensionless

A_o = cross-sectional area of nozzle at a reference location, ft^2

p_o = gas pressure at A_o , lb-ft^{-2}

T_o = gas temperature at A_o , $^\circ\text{R}$

Selecting the conditions of the reference location to be those of an infinite reservoir maintaining the isentropic flow in the nozzle, one obtains from Eq. 6-3 the simpler expression

$$v = \sqrt{\left(\frac{2\gamma}{\gamma-1}\right) RT_o \left[1 - \left(\frac{p}{p_o}\right)^{(\gamma-1)/\gamma}\right]}, \text{ fps} \quad (6-4)$$

where p_o and T_o now refer, respectively, to the pressure and the temperature of the gas in the inlet reservoir. In Eq. 6-4, p is the only variable and it, in turn, governs the magnitude of the velocity.

The mass flow rate per unit area A of the nozzle (or, mass velocity G) is obtained from Eq. 6-4, the equation of continuity, and the perfect gas law, as

$$G = \frac{G'}{A} = \rho_o \sqrt{\left(\frac{2\gamma}{\gamma-1}\right) RT_o \left(\frac{p_t}{p_o}\right)^{(2/\gamma)} \left[1 - \left(\frac{p_t}{p_o}\right)^{(\gamma-1)/\gamma}\right]}, \quad \text{slug-(ft}^2\text{-sec)}^{-1} \quad (6-5)$$

where

G = mass velocity, slug-(ft²-sec)⁻¹

G' = constant rate of flow of mass of gas (mass flux), slug-sec⁻¹

ρ_o = density of propellant gas in reservoir, slug-ft⁻³

The value of the pressure ratio p_t/p_o for which the mass velocity G is a maximum, occurs at the throat and is obtained from Eq. 6-5 as

$$\frac{p_t}{p_o} = \left(\frac{2}{\gamma+1}\right)^{\gamma/(\gamma-1)}, \quad \text{dimensionless} \quad (6-6)$$

This is known as the so-called critical pressure ratio and depends on the specific heat ratio γ . The density ρ_t and the temperature T_t at the throat are given by

$$\frac{\rho_t}{\rho_o} = \left(\frac{2}{\gamma+1}\right)^{1/(\gamma-1)} \quad (6-7)$$

and

$$\frac{T_t}{T_o} = 2/(\gamma+1) \quad (6-8)$$

The gas velocity at the throat v_t is obtained from Eq. 6-4, with $p = p_t$, and Eq. 6-6 as

$$v_t = \sqrt{\left(\frac{2\gamma}{\gamma+1}\right) RT_o} = \sqrt{\gamma RT_t} \quad (6-9)$$

Since $\sqrt{\gamma RT_t} = a_t$, represents the acoustic velocity at the throat, Eq. 6-9 indicates that the critical velocity (throat velocity) v_t is always equal to the local acoustic velocity in the ideal nozzle in which critical conditions prevail. The Mach number v_t/a_t at the throat of the ideal nozzle is, therefore, unity provided that the critical pressure exists at the throat. It will be seen shortly (see Eq. 6-14) that if the exit pressure p_e is such that

$$\frac{p_e}{p_o} \leq \left(\frac{2}{\gamma+1}\right)^{\gamma/(\gamma-1)}$$

then, the divergent portion of the nozzle permits a further decrease in pressure below that at the throat and a corresponding increase in velocity above the sonic throat velocity; supersonic flow results in the divergent portion of the nozzle.

Theoretically, the maximum possible value of the nozzle exhaust (exit) velocity $(v_e)_{max}$ is reached by letting $p_e/p_o \rightarrow 0$ in Eq. 6-4, i.e.,

$$(v_e)_{max} = \sqrt{\left(\frac{2\gamma}{\gamma-1}\right) RT_o} \quad (6-10)$$

This corresponds, for example, to the case of the nozzle exhausting into a vacuum. The maximum value is never achieved in actual practice because the temperature falls below the point of liquefaction during the expansion of the gas.

It is seen from Eq. 6-4 that the exhaust velocity v_e of the nozzle is a function of the pressure ratio p_o/p_e and the specific heat ratio γ of the propellant gas. Furthermore, v_e is proportional to the square root of the gas constant R and the square root of the absolute temperature of the ideal reservoir. The gas constant R is inversely proportional to the molecular weight of the gas. The exit velocity v_e increases with the pressure ratio p_o/p_e and decreases slightly with the specific heat ratio γ . The influence of either of these two factors on v_e (or v , in general) is,

however, less pronounced than that of the absolute combustion temperature divided by the molecular weight of the gas.

The area ratio for the divergent section of a supersonic nozzle can be expressed, by use of Eqs. 6-5 and 6-6, as a function of the pressure ratio and the specific heat ratio, as

$$\frac{A_t}{A} = \left(\frac{\gamma + 1}{2}\right)^{1/(\gamma-1)} \times \sqrt{\frac{\gamma + 1}{\gamma - 1} \left[\left(\frac{p}{p_0}\right)^{2/\gamma} - \left(\frac{p}{p_0}\right)^{(\gamma+1)/\gamma} \right]} \quad (6-11)$$

where A is the downstream area where the pressure is p . At the exit, $A = A_e$ and $p = p_e$, so that the expansion ratio ϵ defined by Eq. 6-1 is given by

$$\frac{1}{\epsilon} = \frac{A_t}{A_e} = \left(\frac{\gamma + 1}{2}\right)^{1/(\gamma-1)} \left(\frac{p_e}{p_0}\right)^{1/\gamma} \times \sqrt{\frac{\gamma + 1}{\gamma - 1} \left[1 - \left(\frac{p_e}{p_0}\right)^{(\gamma-1)/\gamma} \right]} \quad (6-12)$$

The ratio of the velocity v at any point downstream of the throat with pressure p to the velocity v_t at the throat follows from Eqs. 6-4 and 6-9 as

$$\frac{v}{v_t} = \sqrt{\frac{\gamma + 1}{\gamma - 1} \left[1 - \left(\frac{p}{p_0}\right)^{(\gamma-1)/\gamma} \right]} \quad (6-13)$$

and the velocity ratio v_e/v_t is

$$\frac{v_e}{v_t} = \sqrt{\frac{\gamma + 1}{\gamma - 1} \left[1 - \left(\frac{p_e}{p_0}\right)^{(\gamma-1)/\gamma} \right]} \quad (6-14)$$

In a supersonic nozzle, $v_e > v_t = \sqrt{\gamma RT_t}$. From this and Eq. 6-14, it follows that

$$\frac{p_e}{p_0} \leq \left(\frac{2}{\gamma + 1}\right)^{\gamma/(\gamma-1)} \quad (6-15)$$

6-12

a result already cited previously, following Eq. 6-9.

The expansion ratio ϵ given by Eq. 6-12 together with the velocity ratio of Eq. 6-14 are tabulated in Table 6-1 versus the pressure ratio p_0/p_e for $\gamma = 1.23$. Note that the velocity ratio has the finite value of $\sqrt{(\gamma + 1)/(\gamma - 1)}$ in the event of the exhausting into a vacuum, while both the expansion ratio ϵ and the pressure ratio p_0/p_e are infinitely large.

6-6.2 MASS FLOW

The rate of flow of mass of gas G' is obtained, by considering the flow through the throat area, as

$$G' = A_t v_t \rho_t, \text{ slug-sec}^{-1} \quad (6-16)$$

From Eqs. 6-16, 6-7, 6-9, and the equation of state of the perfect gas, it follows that the mass flow through the critical section of a supersonic nozzle is

$$G' = \frac{A_t p_0}{\sqrt{\gamma RT_0}} \gamma \sqrt{\left(\frac{2}{\gamma + 1}\right)^{(\gamma+1)/(\gamma-1)}} \text{ slug-sec}^{-1} \quad (6-17)$$

Eq. 6-17 shows that the mass flow through the de Laval nozzle is proportional to the throat area A_t , the reservoir pressure p_0 ; inversely proportional to the square root of the absolute temperature of the reservoir, and is a function of the properties of the gas. Note that Eq. 6-17 is independent of the exit pressure p_e , provided the latter remains below its critical value of $p_0 (2/\gamma + 1)^{\gamma/(\gamma-1)}$. In other words—provided that the flow in the divergent portion of the nozzle is supersonic—lowering the exit pressure will not increase the throat velocity or the mass flow, and Eq. 6-17 represents the maximum value of the mass flow. In fact, this maximum value is obtained more directly by use of Eq. 6-5 in which $A = A_t$ and $p = p_t$, and Eq. 6-6, together with the equation of state of the perfect gas.

TABLE 6-1
VELOCITY RATIO AND EXPANSION RATIO AS
FUNCTIONS OF PRESSURE RATIO ($\gamma = 1.23$)

Pressure Ratio, p_o/p_e	$\gamma = 1.23$	
	Velocity Ratio, v_e/v_t	Expansion Ratio, $\epsilon = A_e/A_t$
2	1.085656	1.008103
4	1.487956	1.292250
6	1.661412	1.609248
8	1.767347	1.911414
10	1.841766	2.199208
20	2.036213	3.409333
30	2.136047	4.631886
40	2.198073	5.687256
50	2.242835	6.682456
60	2.277429	7.632444
80	2.328697	9.431303
100	2.365893	11.129566
∞	3.113784	∞

6-6.3 THRUST GENERATED BY NOZZLE

When a fluid in a duct experiences a change in momentum, thrust is said to be developed. For the axisymmetric and unidirectional flow through the nozzle of Fig. 6-2, the thrust is axial and its magnitude is equal to the surface

integral of the pressure forces acting on the nozzle in the x -direction. In the event of steady flow, the magnitude of the thrust force can be shown to be (Ref. 2, p. 54)

$$F = G'v_e + A_e(p_e - p_a), \text{ lb} \quad (6-18)$$

where p_a is the ambient external pressure. The thrust F , which is the external force acting on the nozzle, is seen to be the sum of two terms. The first, which is the product of the mass flow rate G' and the exit velocity v_e relative to the nozzle, is called the momentum thrust. The second, which is the product of the cross-sectional area of the exit of the nozzle and the difference between the jet exit pressure and the ambient pressure, is called the pressure thrust. Since $G' = A_t v_t \rho_t$, Eq. 6-18 may be rewritten in the general form of

$$F = A_t \rho_t v_t v_e + A_e(p_e - p_a), \text{ lb}$$

For constant value of γ during nozzle expansion, Eq. 6-18 is rewritten by use of Eqs. 6-17, 6-14, and 6-9 as

$$F = A_t p_o \sqrt{\left(\frac{2\gamma^2}{\gamma-1}\right) \left(\frac{2}{\gamma+1}\right)^{(\gamma+1)/(\gamma-1)}} \left[1 - \left(\frac{p_e}{p_o}\right)^{(\gamma-1)/\gamma}\right] + A_e(p_e - p_a), \text{ lb} \quad (6-19)$$

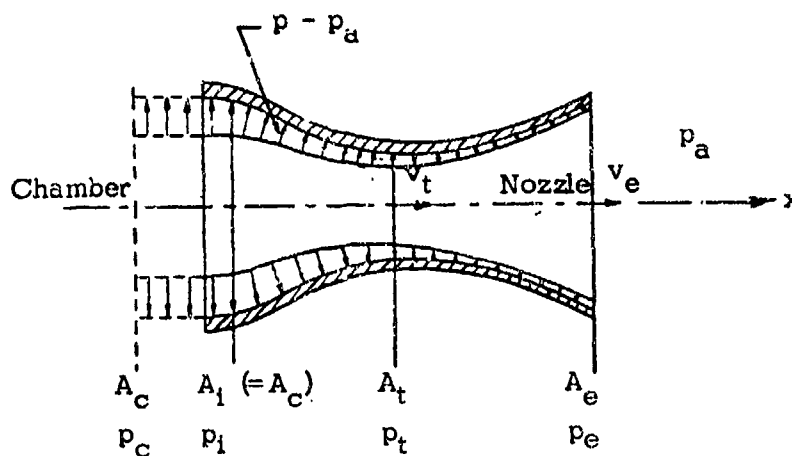


Figure 6-2. Distribution of Forces Acting on Nozzle

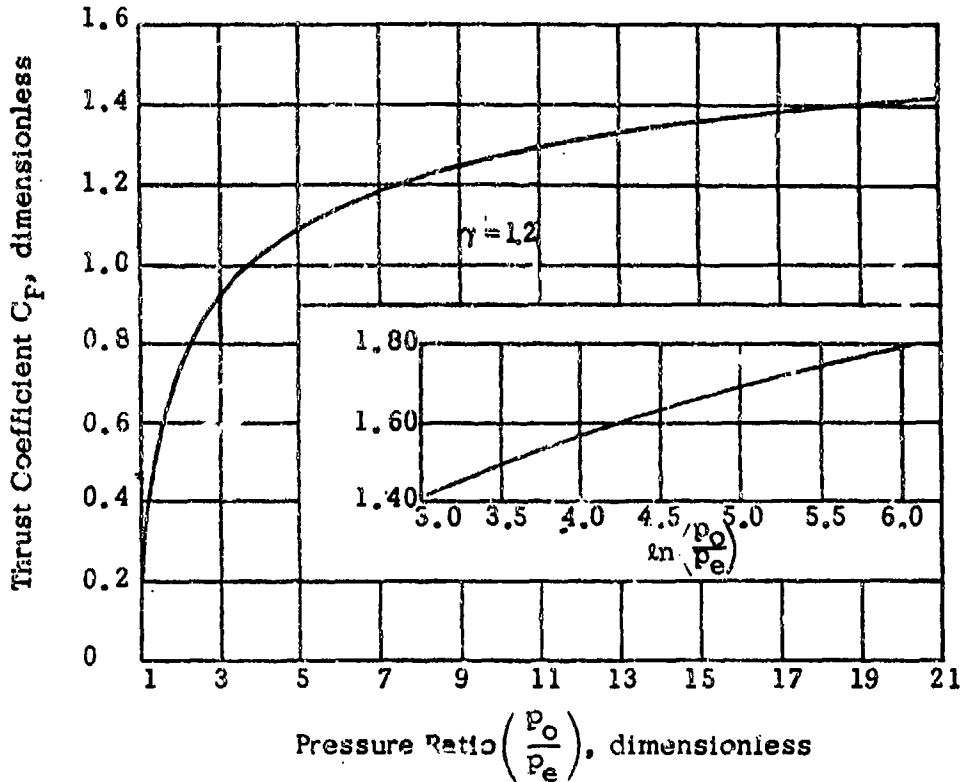


Figure 6-3. Thrust Coefficient C_F as a Function of Pressure Ratio p_0/p_e .

It is seen from Eq. 6-19 that the thrust generated by the nozzle is proportional to the throat area A_t , reservoir pressure p_0 , pressure thrust; and is a function of the pressure ratio p_0/p_e and the specific heat ratio γ .

With the definition of the thrust coefficient C_F by

$$C_F = F/(A_t p_0), \text{ dimensionless} \quad (6-20)$$

Eq. 6-19 leads to the expression

$$C_F = \sqrt{\left(\frac{2\gamma^2}{\gamma-1}\right)\left(\frac{2}{\gamma+1}\right)^{(\gamma+1)/(\gamma-1)} \left[1 - \left(\frac{p_e}{p_0}\right)^{(\gamma-1)/\gamma}\right]} + \left(\frac{A_e}{A_t}\right)\left(\frac{p_e - p_a}{p_0}\right) \quad (6-21)$$

where A_e/A_t is the nozzle expansion ratio. By use of experimentally measured values of the

reservoir pressure p_0 , throat diameter, and thrust F , the thrust coefficient is determined from Eq. 6-20. This coefficient represents the amplification of the thrust generated by the expansion of the gas in the nozzle as compared with the thrust that would be generated were the reservoir pressure to act over the throat area only.

If p_e is less than p_a , the pressure thrust is negative. Nozzles are usually so designed as to have the exit pressure p_e equal to or slightly higher than the ambient pressure p_a . In the case of $p_e = p_a$, C_F is known as the optimum thrust coefficient and the nozzle is called a perfect nozzle. It should be recalled, however, that this ideal case can be valid only in the event of irrotational, steady, isentropic flow with no viscosity and no heat conduction.

Fig. 6-3 shows the variation of the optimum thrust coefficient with the pressure

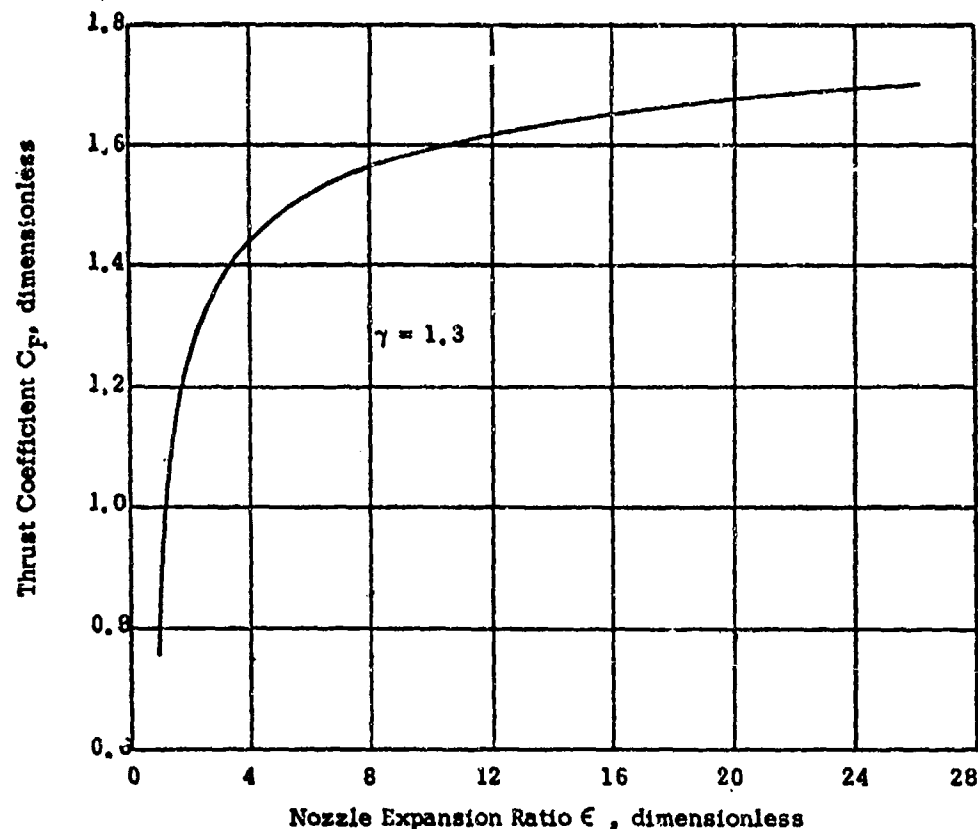


Figure 6-4. Calculated Optimum Thrust Coefficient C_F as a Function of Nozzle Expansion Ratio ϵ ($\gamma = 1.3$)

ratio p_o/p_e for $\gamma = 1.2$ and 1.3 , while Figs. 6-4 and 6-5 show C_F as a function of $A_e/A_t = \epsilon$ for $\gamma = 1.3$ and $\gamma = 1.2$, respectively. In all of these curves, C_F refers to theoretical values not incorporating any losses.

Because of the finite size of the chamber area of cross section A_c , a loss occurs in the amount of the thrust generated by the nozzle. In the event of an infinitely large reservoir, the situation corresponds to a theoretical case of ideal thrust generation since the thrust is proportional to the product of the exit velocity and mass flow of the gases. The losses in thrust are progressively larger for successively smaller ratios of chamber to throat cross sections and for successively lower

pressure ratios p_o/p_e . For example, a straight tubular chamber has approximately 22 percent less thrust than the equivalent ideal chamber with infinite cross section. For a chamber with an area ratio of 2, the loss in thrust is only 6 percent. These figures are for a chamber pressure to nozzle exit pressure ratio of 10, and the influence of variation of the specific heat ratio on the loss in thrust is considered negligible.

6-7 DESIGN CONSIDERATIONS

In designing nozzles, various losses and the associated correction factors are to be taken into account for adapting the "one-dimensional" or hydraulic theory (O. Reynolds —

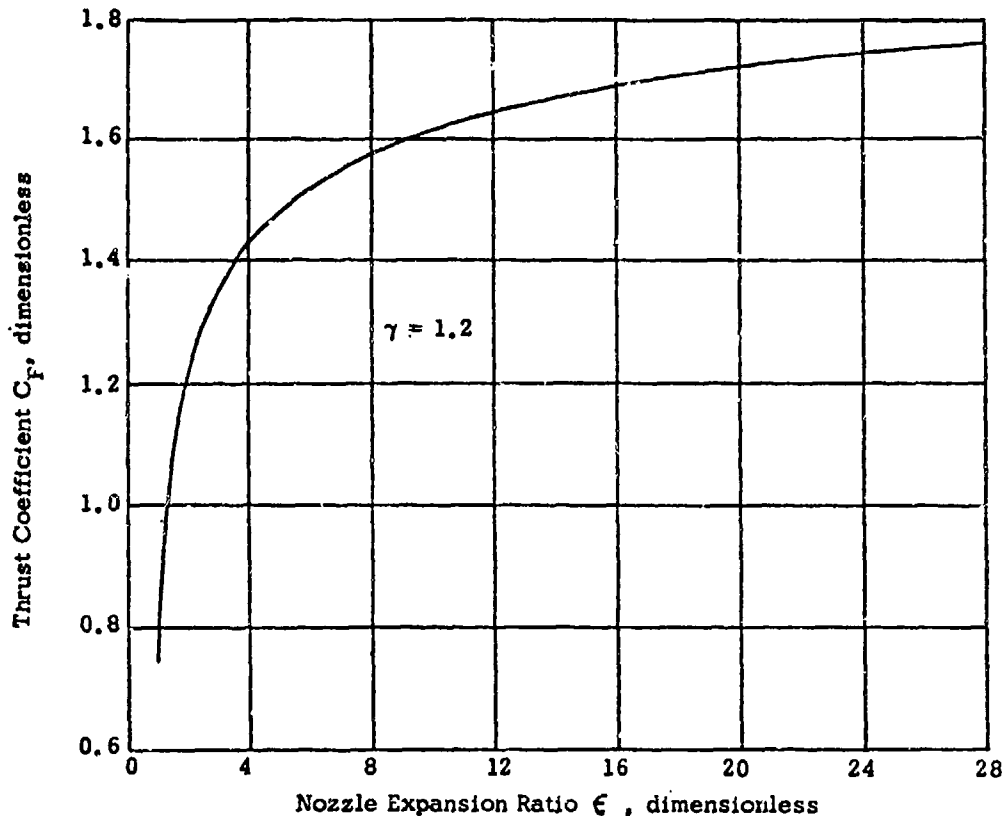


Figure 6-5. Calculated Optimum Thrust Coefficient C_F as a Function of Nozzle Expansion Ratio ϵ ($\gamma = 1.2$)

1885) of compressible flow to real nozzles. These losses are due to the effects of such factors as nonaxial and nonuniform flow, imperfect gases, heat transfer, and friction.

In the convergent section of the nozzle, the kinetic energy of the gases is relatively small so that losses are very low, almost independent of the convergent nozzle shape provided that the wall contour is symmetrical and well-rounded particularly at the entrance and throat sections. This is because discontinuities give rise to shock waves in the nozzle.

In the divergent section of the nozzle, however, nozzle losses depend markedly on the configuration, shape, and angle of

divergence for a given expansion ratio ϵ . Since the rounding of the edge of the exit section of the nozzle would lead to over expansion and flow separation, this section customarily is made to have a sharp edge. With increased divergence at the exit, the radial component of the velocity also is increased to result in a reduction of the thrust generated by the nozzle. Furthermore, in the event of a large divergence at any single cross section of the nozzle, losses due to separation, turbulence, and divergence may become excessively high. On the other hand, short nozzles with large divergence give rise to low friction losses.

Contoured nozzles designed to give parallel, uniform exit flow usually are excessively long

and heavy and, in most instances, conical shapes of divergence have been found satisfactory because they are simple and relatively easy to manufacture. The potential flow in such a nozzle may be represented closely by the flow due to a point source of suitable strength and located at the vertex of the cone. If 2α is the angle of the cone, α is called the divergence angle of the nozzle. Since thrust is based on the axial component of momentum acting against the exit area normal to the nozzle axis, the thrust of a conical nozzle will be less than that of a contoured nozzle. Simple geometric considerations give the ratio of the momentum flux in the conical nozzle to that in the contoured nozzle as

$$\lambda = (1 + \cos \alpha)/2, \text{ dimensionless} \quad (6-22)$$

The factor λ is called the correction factor for divergence angle α or, simply, the divergence factor. The validity of Eq. 6-22 has been confirmed by experiment for values of α up to about 25 deg (Ref. 3). For a conical nozzle, then, the thrust coefficient of Eq. 6-21 becomes modified as

$$(C_F)_{\text{conical}} = \lambda \sqrt{\left(\frac{2\gamma^2}{\gamma-1}\right) \left(\frac{2}{\gamma+1}\right)^{(\gamma+1)/(\gamma-1)} \left[1 - \left(\frac{p_e}{p_o}\right)^{(\gamma-1)/\gamma}\right]} + \left(\frac{A_e}{A_t}\right) \left(\frac{p_e - p_a}{p_o}\right), \text{ dimensionless} \quad (6-23)$$

Another method of producing axially aligned flow is by means of a plug nozzle. Dependent on the particular plug configuration the expansion may be completely or partially internal expansion (converging central plug); the performance is similar to that of the conventional convergent-divergent nozzle. In this configuration the nozzle length is decreased by use of the plug, without increasing the flow inclination; however, because of the extra area, the skin friction is increased. For complete internal expansion by

means of a conical plug (of cone angle 2β) and conical nozzle section, the flow may be assumed to be emanating from a source situated at the hypothetical intersection of the plug and nozzle surfaces. With this approximation and the additional assumption that the vertex of the central conical plug lies in the nozzle exit plane, the exit momentum of such a flow can be evaluated by integrating across the exit plane to give the divergence correction factor as

$$\lambda_{\text{plug}} = \frac{(\sin \alpha + \sin \beta)^2}{2[(\alpha + \beta) \sin \beta + \cos \beta - \cos \alpha]} \quad (6-24)$$

dimensionless

where

α = angle of inclination of diverging nozzle wall to axial direction (nozzle divergence angle), deg

β = angle of inclination of converging plug wall to axial direction, deg

It is seen that when $\beta = 0$, Eq. 6-24 reduces to Eq. 6-22. When the outer wall is parallel to the nozzle axis, $\alpha = 0$ and Eq. 6-24 reduces to

$$\lambda_{\text{plug}} = \frac{\sin^2 \beta}{2(\beta \sin \beta + \cos \beta - 1)} \quad (6-25)$$

It may be seen from these expressions that conical plugs of large vertex angles can be used without undue loss from flow divergence. In addition, the volume (and weight) of the nozzle required to generate comparable thrust can be less for a plug nozzle than for a conventional nozzle, and cooling problems may also be simplified. Plug nozzles of types designed to create completely or partially internal expansion have the added advantage that the throat area can easily be varied to compensate for changes in operating conditions (Ref. 4). Further information on the performance of plug nozzles may be found, for example, in Ref. 5.

Although many nozzles use a divergence

angle of about 15 deg, experience has shown that the divergence angle α can be as great as 40 deg without incurring flow separation. Consequently, the conical nozzle may be reasonably short, quickly designed, and easily produced. However, when α is 40 deg, Eqs. 6-22 and 6-24 show that a loss in thrust of about 12 percent is incurred and, in many cases, the advantage of short length is more than offset by the thrust loss. A nozzle accurately designed to give parallel flow at the exit is theoretically more efficient than a conical nozzle of the same expansion ratio operating at the same exit pressure. The design of such a nozzle (contoured nozzle) involves an expansion section, in which the flow deviates from the axial direction, as well as a straightening section in which the flow is redirected along the axis. In order to provide shock-free flow axially aligned at the exit, the nozzle contour must be designed accurately by means of the method of characteristics. Details of this method for axially-symmetric flow are given in Refs. 6 through 9. Ref. 10 gives an approximate method for determining the contour of the optimum-thrust nozzle by purely geometric means. Nozzle contour design and performance are also covered in Refs. 11 and 12.

One of the disadvantages of the contoured nozzle is that thrust loss is experienced when the nozzle operates at pressure ratios and gas compositions other than those for which it is designed. In the event of an underexpanding nozzle, exit pressure is greater than the ambient pressure. In the case of an overexpanding nozzle, the exit pressure is smaller than the ambient pressure. The effect of either overexpansion or underexpansion is a reduction in the exhaust velocity and a corresponding loss of energy and thrust. In highly overexpanded nozzles flow separation occurs with the result that a large and, usually, heavy portion of the nozzle is not used; thus the nozzle is longer and bulkier than required. In the absence of separation, Eq. 6-21 is in good agreement with measured results for underexpanded and for slightly

overexpanded nozzles. With a plug nozzle where the plug is used so that all or most of the expansion is external, the ambient air behaves as the outer wall and thus gives this type of nozzle the advantage of an automatic adjustment of the exhaust expansion to ambient pressure and prevents loss due to over- or underexpansion.

As for the convergent section of the nozzle, losses are usually very low. In the event of relatively steep convergent sections and comparatively small radius-of-curvature throats, however, losses are no longer negligible, and the influence of the entrance contour on the performance of such nozzles is discussed in Ref. 13.

The overall efficiency of a nozzle is based upon the thrust it can produce and usually is defined as the ratio of actual thrust to ideal thrust, and is denoted by η . The ideal thrust is based on the assumption of the one-dimensional flow of an ideal gas. A measure of how closely an actual flow approaches the condition of an adiabatic expansion of a perfect gas is given by the kinetic energy efficiency η_{KE} defined as

$$\eta_{KE} = \frac{v_e^2}{2(\Delta H)}, \text{ dimensionless} \quad (6-26)$$

where

v_e = nozzle exit velocity (average value over the cross section), fps

ΔH = theoretical specific enthalpy change of gas from chamber to nozzle exit, (ft-lb)-slug⁻¹

The values of efficiency have the range $0.90 < \eta_{KE} < 0.99$. The efficiency of a nozzle may be affected by the nonuniform distribution of both the magnitude and direction of the velocity across the exit, and an associated velocity coefficient η_v is defined as

$$\eta_v = \frac{(v_e)_{\text{effective}}}{(v_e)_{\text{theoretical}}}, \text{ dimensionless} \quad (6-27)$$

where the effective velocity $(v_e)_{\text{effective}}$ could properly replace $(v_e)_{\text{theoretical}}$ in the one-dimensional equations. The discharge correction factor η_d is defined as the ratio of the actual mass flow rate G'_a in a real nozzle to the ideal critical flow rate G' at the throat of the nozzle working with the same inlet conditions and the same exit pressure, i.e.,

$$\eta_d = G'_a / G', \text{ dimensionless} \quad (6-28)$$

From Eqs. 6-28 and 6-17 it follows that

$$\eta_d = \frac{G'_a \sqrt{\gamma R T_0}}{A_t p_0 \gamma \sqrt{\left(\frac{2}{\gamma+1}\right)^{(\gamma+1)/(\gamma-1)}}},$$

dimensionless (6-29)

The value of η_d varies from 0.98 to 1.15. The

reason that η_d is usually greater than one is based on the following facts:

1. The molecular weight of the gases increases slightly when flowing through a nozzle, thereby changing the density.
2. The heat transferred to the walls lowers the gas temperature and raises the density.
3. The change in γ down the nozzle is such as to increase η_d .

In summary, for a nozzle operating with $p_e = p_a$, since the thrust is given directly by the momentum of the exhaust gases, the overall nozzle efficiency η may be expressed by

$$\eta = (\eta_{KE})^{1/2} (\eta_v) (\eta_d) \quad (6-30)$$

In general, the value of η can vary from 0.85 to 1.10, depending on design parameters.

SECTION III

THEORY OF RECOIL CANCELLATION

6-8 DEFINITION OF MOMENTUM RATIO
PARAMETER

The analysis of flow of propellant gas with entrained solid propellant grains is very complex and beyond the scope of the present handbook. In all of the standardized recoilless rifles in the US, the perforated cartridge case helps to confine the propellant grains so that most of the charge is consumed in the chamber (or rifle). In the 57 mm M18 Recoilless Rifle, the solid propellant ejection through the nozzle was experimentally determined to be approximately 0.3 lb (or about 30% of the total charge). The amount of unburnt propellant does not vary appreciably from round to round at a given temperature so the performance of the rifle is not affected. It should be pointed out that from the logistic standpoint, elimination of solid propellant ejection would lead to a smaller and lighter round. However, even in the recoilless rifle with nozzles in front of the chamber and initially closed by the projectile (Front Orifice Recoilless Rifles such as 105 mm T135), approximately 10 percent of the propellant charge is expelled unburnt. In the Battalion Antitank Weapon (BAT), the M40 Recoilless Rifle unburnt propellant ejection is about 20 percent.

From a design standpoint, the nozzle of a recoilless rifle can be designed in accordance with this chapter. The unburnt propellant ejection does not affect appreciably the dimensions of the nozzle designed on the basis of gas flow only.

Denoting by F_R the instantaneous total force on the rifle, which produces the recoil, and assigning to it the positive sign for rearward recoil, Ref. 14 derives the following expression for F_R :

$$F_R = A_b p_c \left\{ 1 - \left(\frac{A_e}{A_b} \right) \left(\frac{p_e}{p_o} \right) \left(\frac{p_o}{p_c} \right) - \sqrt{\frac{2\gamma^2}{\gamma-1} \left(\frac{2}{\gamma+1} \right)^{(\gamma+1)/(\gamma-1)} \left[\left(\frac{p_e}{p_o} \right)^{(\gamma-1)/\gamma} \right]} \right. \\ \left. \times \left(\frac{p_o}{p_c} \right) \left(\frac{A_t}{A_b} \right) \right\} + (A_e - A_b) p_a, \text{ lb} \quad (6-31)$$

where

A_b = bore area of rifle, ft²

A_e = exit area of nozzle, ft²

A_t = throat area of nozzle, ft²

F_R = force of recoil, lb

p_a = ambient pressure external to rifle, lb-ft⁻²

p_c = chamber pressure, lb-ft⁻²

p_e = pressure at exit section of nozzle, lb-ft⁻²

p_o = pressure in a large reservoir from which the flow in nozzle could have arisen by purely isentropic flow, lb-ft⁻²

γ = c_p/c_v , ratio of specific heats, dimensionless

The last term $(A_e - A_b) p_a$, in Eq. 6-31, which is the force contribution due to ambient pressure, is generally small and usually can be neglected. This expression is to be considered approximate in the sense that

its derivation is based on certain simplifying assumptions. For practical purposes, however, it is of sufficient accuracy consistent with those of the foregoing. It is noted that Eq. 6-31 can be recovered more directly as

$$F_R = A_b(p_c - p_a) - F \quad (6-32)$$

where F is the instantaneous thrust generated by the nozzle and given by Eq. 6-19. It is apparent from Eq. 6-32, that one of the simplifying assumptions employed in the derivation of Eq. 6-31 is that of the projectile base pressure being equal to the chamber pressure.

In order to estimate the total impulse delivered to the rifle, Eq. 6-31 is integrated from $t = 0$, when it is assumed that the projectile is free and the nozzle open, to time t_m when the projectile leaves the muzzle. The dimensionless recoil (momentum ratio parameter) ω is then introduced by the definition

$$\omega = \frac{\int_0^{t_m} F_R dt}{\int_0^{t_m} (p_c A_b) dt} \quad (6-33)$$

By referring to this definition, it is seen that the numerator is the impulse delivered to the rifle while the projectile is in the barrel (i.e., rifle momentum of recoil). For a large class of recoilless rifles, i.e., those in which the pressure on the projectile base is nearly equal to the pressure of the chamber, the denominator of Eq. 6-33 is nearly equal to projectile momentum at the muzzle. Thus ω , the dimensionless recoil, is for a large group of rifles equal to the ratio of rifle momentum (positive to the rear) to projectile momentum at the instant of projectile ejection; hence, the term "momentum ratio parameter".

6-9 EQUATION FOR MOMENTUM RATIO AS A FUNCTION OF GUN AND NOZZLE PARAMETERS

Neglecting the term $(A_e - A_b)p_a$ in Eq. 6-31 and combining it with Eq. 6-33, and using Eq. 6-12, one obtains

$$\frac{A_b}{A_t} \cdot \frac{p_c}{p_o} = \left(\frac{1}{1-\omega} \right) \left\{ \left(\frac{2}{\gamma+1} \right)^{(\gamma+1)/[2(\gamma-1)]} \right. \\ \left. \times \sqrt{\frac{2\gamma^2}{\gamma-1}} \left[\frac{1 - \left(\frac{\gamma+1}{2\gamma} \right) \left(\frac{p_e}{p_o} \right)^{(\gamma-1)/\gamma}}{\sqrt{1 - \left(\frac{p_e}{p_o} \right)^{(\gamma-1)/\gamma}}} \right] \right\} \quad (6-34)$$

where the ratio p_e/p_o must satisfy Eq. 6-15. For each value of p_e/p_o , a value of the nozzle expansion ratio A_e/A_t is obtained from Eq. 6-12, and a value of the ratio $(A_b/A_t) \cdot (p_c/p_o)$ is obtained from Eq. 6-34 for a given value of ω . Thus, the dependent variable of Eq. 6-34 is a function of the expansion ratio ϵ of the nozzle, the quantities ω and γ being parameters. The curve represented by this function is called a *line of constant dimensionless recoil*. For $\gamma = 1.25$ and for values of ω from -0.10 to 0.10 at increments of 0.01 , Fig. 6-7(A) gives the lines of constant dimensionless recoil.

6-10 EQUATIONS FOR RATIO OF CHAMBER PRESSURE TO IDEAL RESERVOIR PRESSURE

The momentum equation in steady flow

between a postulated plane of zero gas velocity in the cylindrical chamber (see Fig. 6-9) and the plane of intersection of the nozzle with the chamber-inlet section of the nozzle—is

$$G'v_i = A_c(p_c - p_i) \quad (6-35)$$

where the subscript i refers to quantities at the inlet of the nozzle, and the mass flow rate G' is given by Eq. 6-17. Substituting into Eq. 6-35 the value of v_i from Eq. 6-4 in which $p = p_i$, one has

$$\frac{p_c - p_i}{p_o - p_o} = \frac{A_t}{A_c} \sqrt{\frac{2\gamma^2}{(\gamma-1)} \left(\frac{2}{\gamma+1}\right)^{(\gamma+1)/(\gamma-1)} \left[1 - \left(\frac{p_i}{p_o}\right)^{(\gamma-1)/\gamma}\right]} \quad (6-36)$$

As in the case of Eq. 6-11, use of Eq. 6-5 leads to

$$\frac{A_t}{A_c} = \sqrt{\frac{\left(\frac{2}{\gamma-1}\right)^{(\gamma+1)/(\gamma-1)} \left[\left(\frac{p_i}{p_o}\right)^{2/\gamma} - \left(\frac{p_i}{p_o}\right)^{(\gamma+1)/\gamma}\right]}{\left(\frac{2}{\gamma+1}\right)^{(\gamma+1)/(\gamma-1)}}} \quad (6-37)$$

and the substitution of this into Eq. 6-36 results in

$$\frac{p_c}{p_o} = p_o \left(\frac{2\gamma}{\gamma-1}\right) \left[\left(\frac{p_i}{p_o}\right)^{1/\gamma} - \left(\frac{p_i}{p_o}\right)\right] \quad (6-38)$$

where

$$\frac{p_i}{p_o} > \left(\frac{2}{\gamma+1}\right)^{\gamma/(\gamma-1)}$$

If p_i/p_o is eliminated between Eqs. 6-37 and 6-38, p_c/p_o is expressed as a function of

A_c/A_t . The curve representing this function is shown in Fig. 6-6 for $\gamma = 1.25$.

6-11 GRAPHICAL SOLUTION OF THE EQUATIONS

In the problem of design where the throat area A_t is sought, the relation between bore cross-sectional area A_b and chamber cross-sectional area A_c usually is known. Let $A_c = r'A_b$, where the dimensionless constant $r_i = A_c/A_b$ is known (typical values of r_i may vary between 2.0 and 3.0). Fig. 6-6 then gives the relation between p_c/p_o and r' (A_b/A_t), and one can obtain the corresponding values of p_c/p_o and $A_b/A_t = r' A_c/A_t$. By use of this relationship, the factor p_c/p_o appearing in the ordinate of Fig. 6-7(A) can be eliminated to obtain the corresponding A_b/A_t versus A_e/A_t curves of constant dimensionless recoil ω , all for a particular value of r' . This set of curves is presented in Fig. 6-7(B) for the special case of $r' = 1$ (bore cross section being equal to chamber cross section). It is interesting to note that for zero recoil ($\omega = 0$) and with $A_e = A_t$, Fig. 6-7(B) gives the required ratio of $A_b/A_t = 1$. This is the straight tube, open at both ends, which often is cited as an example of a recoilless rifle.

If at any point on a curve of Fig. 6-7(B) the abscissa is divided by the ordinate, one obtains the ratio A_e/A_b . The relation $A_e/A_b = \text{constant}$ appears as a straight line in Fig. 6-7(B) where these are shown in dashed lines for $A_e/A_b = 1.5, 2.0, 2.5,$ and 3.0 . Along such a line, the throat cross-sectional area varies while A_b and A_e each can be considered constant. Nozzle erosion results in an increase in A_t with little, if any, change in A_b and A_e . Obviously, then, the change in recoil which accompanies nozzle erosion may be predicted by moving down the line of constant A_e/A_b starting at the initial (uneroded) values of A_t and ω for the rifle. The $A_e/A_b = \text{constant}$ type of a straight line is also useful in estimating the change in throat area necessary to eliminate excessive recoil.

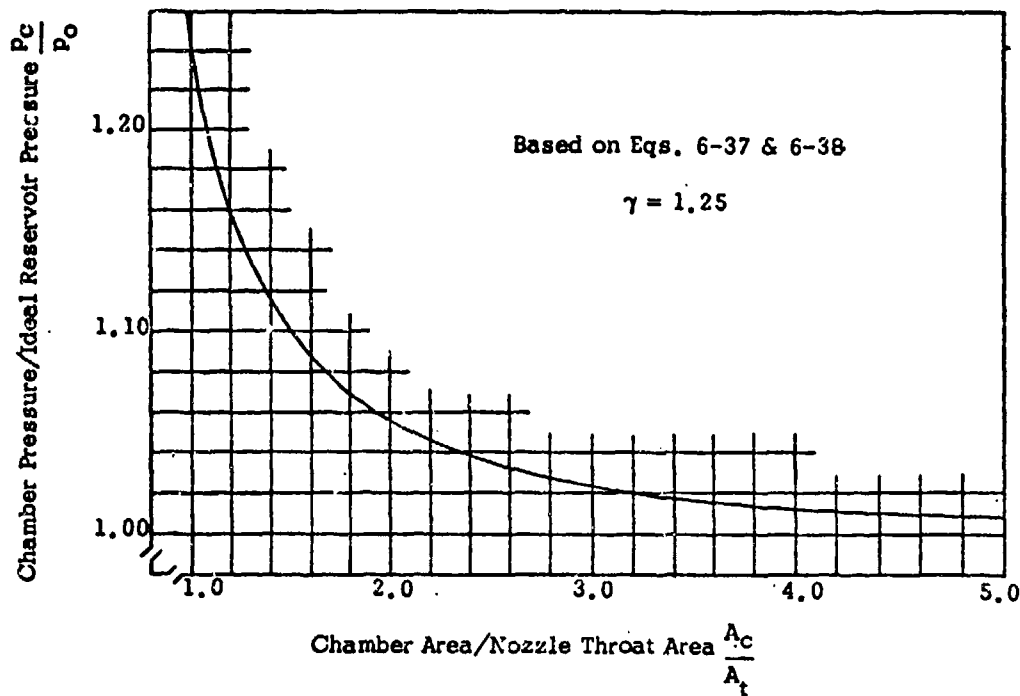


Figure 6-6. Chamber Pressure/Ideal Reservoir Pressure as a Function of Chamber Area/Nozzle Throat Area ($\gamma = 1.25$)

To sum up, by use of Fig. 6-6 and Fig. 6-7(A), a corresponding set of curves (as in Fig. 6-7(B)) is constructed for a given value of $r' = A_c/A_b$ and for a selected range of values of ω . The resulting figure, together with the appropriate lines of $A_c/A_b = \text{constant}$, is valuable in actual problems of recoil considerations of guns.

6-12 NOZZLE PERFORMANCE FACTORS

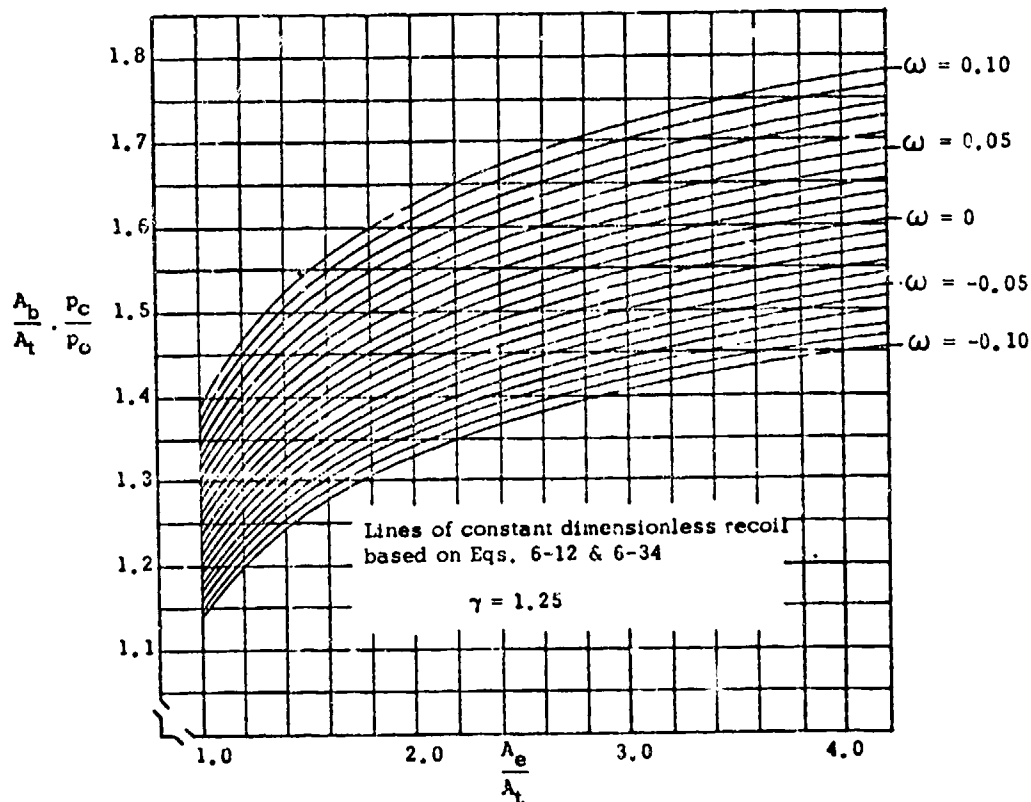
6-12.1 VARIATION OF NOZZLE THRUST WITH NOZZLE EXPANSION ANGLE

An important consideration in the design of a recoilless rifle is the nozzle expansion angle 2α which is twice the divergence angle treated in par. 6-7. In rear orifice recoilless rifles, a larger expansion angle means a shorter

nozzle for a given expansion ratio and, hence, a corresponding saving in nozzle weight. In some front orifice recoilless rifles (see Ref. 26), a long nozzle is required to carry the gases beyond the rifle breech. Hence, a small expansion angle is desirable to obtain a small frontal area and minimum weight.

The effect of the angle α on nozzle thrust F , which is given by Eq. 6-19, is represented by the divergence correction factor λ of Eq. 6-22. As expressed by Eq. 6-23, nozzle thrust varies linearly with λ . For a perfect nozzle ($p_e = p_a$), F becomes proportional to λ for a given expansion ratio. The percentage loss in thrust then becomes $100(1 - \lambda)$. For a conical nozzle, Table 6-2 shows the variation of this loss with the angle 2α .

It should be noted that, since Table 6-2 is



(A) (Bore Area/Nozzle Throat Area) x (Chamber Pressure/Ideal Reservoir Pressure) as a Function of Nozzle Expansion Ratio ($\gamma = 1.25$)

Figure 6-7. Lines of Constant Dimensionless Recoil ω

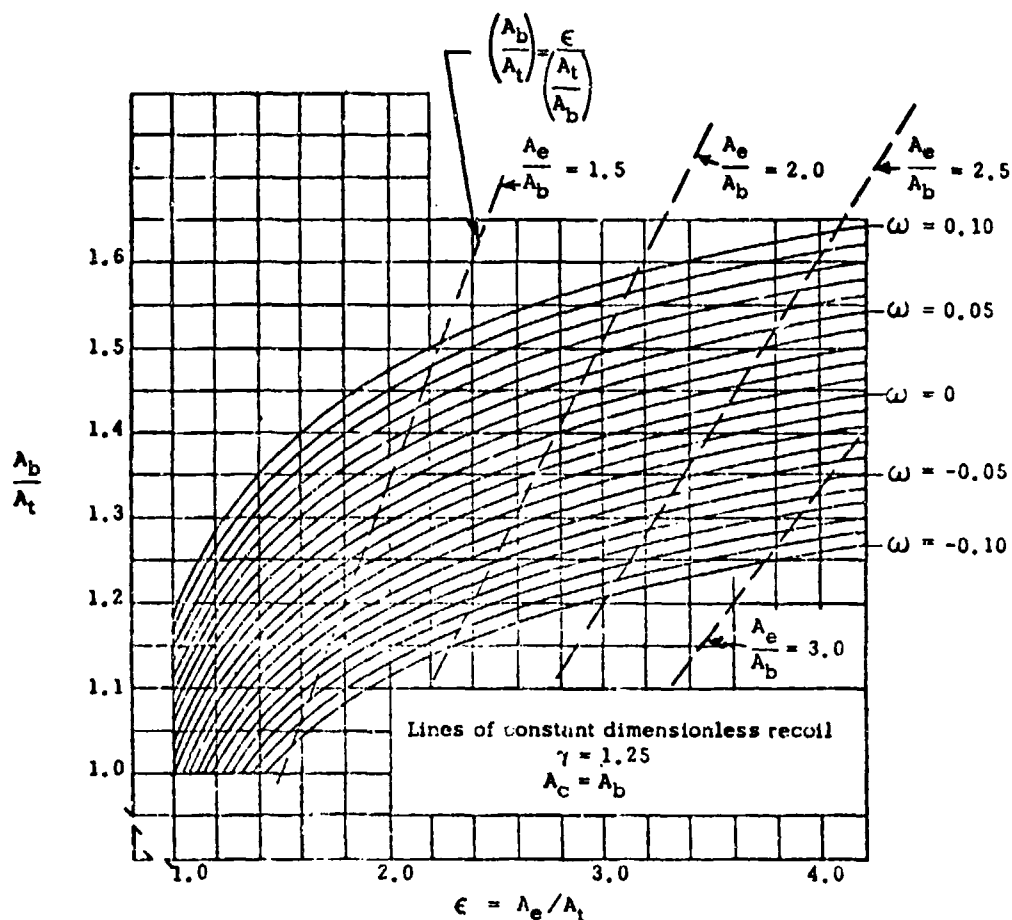
based on Eq. 6-22, the validity of which has been confirmed by experiment (Ref. 3) for values of α up to about 25 deg, this table is valid for $0 \leq 2\alpha \leq 50$ deg. It thus is concluded that the decrease in nozzle thrust due to expansion angles not exceeding 50 deg is less than 5 percent.

As to the influence of the expansion angle on unbalanced *forward* recoil force $-F_R$, given by Eq. 6-32, results of tests (Ref. 15, p. 63) conducted in the differential thrust bomb on nozzles with expansion angles of 5, 15, 30, 45, and 60 deg, and expansion ratios of $\epsilon = 4.5$ indicate that angles less than 45 deg give

essentially the same $[-F_R/(A_b p_c)]$ (100) value but, in the event of $2\alpha \geq 45$ deg, there is a significant decrease.

6-12.2 VARIATION OF NOZZLE THRUST WITH EXPANSION RATIO

The results of a study (Ref. 15, p. 65) of the effect of nozzle expansion ratio on the recoil force of nozzles are summarized in Table 6-3 where both experimental and theoretical values are given for the variation of percent rearward recoil force imbalance $[F_R/(A_b p_c)]$ (100), with nozzle expansion ratio. Various nozzles having circular throat



(B) (Bore Area/Nozzle Throat Area) as a Function of Nozzle Expansion Ratio ($\gamma = 1.25$)

Figure 6-7. Lines of Constant Dimensionless Recoil ω

sections and radial expansion cones with expansion ratios of 1.0, 3.15, 6.77, and 9.68, and identical throat areas were tested in the differential thrust bomb. Except for the case of $\epsilon = 9.68$, the experimental and theoretical data (based on a discharge coefficient of 0.94) of Table 6-3 are in good agreement. The discrepancy in the event of $\epsilon = 9.68$ is, in part, due to flow separation, and increased friction and heat losses.

In a recoilless rifle, as previously noted, the

increase of the forward recoil force imbalance, which results from the erosion of the nozzle throat, shortens the useful life-span of its nozzle. The nozzle life is determined by the acceptable level of augmentation in recoil force imbalance, and can be predicted provided that the erosive properties of the nozzle material and the change in recoil force imbalance with change in throat area are known. Fig. 6-8 shows the close correlation between the experimental and theoretical results (based on a nozzle discharge coeffi-

TABLE 6-2

VARIATION OF NOZZLE THRUST WITH
NOZZLE EXPANSION ANGLE 2α

Nozzle Expansion Angle 2α , deg	Loss in Nozzle Thrust, %
0	0.00
10	0.20
20	0.76
30	1.70
40	3.02
50	4.68
<hr style="border-top: 1px dashed black;"/>	
60	8.70
70	9.04
80	11.70
90	14.64

cient of 0.94) on the variation of recoil force imbalance with nozzle throat area (Ref. 15, p. 68).

6-12.3 EFFECT OF NOZZLE APPROACH AREA AND CHAMBER CONFIGURATION ON RIFLE PERFORMANCE

In order to study the effect of chamber configuration on recoilless rifle operation, a series of firing tests was conducted on the 57 mm Recoilless Rifle, M18 (see Ref. 15), employing various internal chamber configurations and nozzle entrance areas of cross section. The M18 chamber was modified by use of a variety of five liner inserts described in Ref. 15. For these tests the chamber volume was kept constant at 80 in³, and a charge of M2 Propellant, Lot RAD 459, was contained in a standard 57 mm perforated cartridge case. The nozzle used had a throat area A_t of approximately 3.0 in² with an expansion ratio of $\epsilon = 2$. The ballistic data obtained for the rifle fired with the liners are given in Table 6-4. This table indicates that, as the nozzle approach area A_i is decreased, the rearward recoil imbalance increases. A plot of

TABLE 6-3

VARIATION OF RECOIL FORCE IMBALANCE
WITH NOZZLE EXPANSION RATIO

Expansion Ratio ϵ	Percent Rearward Imbalance of Recoil Force	
	Experimental (average of four rounds)	Theoretical
1.00	+ 4.0	+ 4.0
3.15	-18.6	-18.6
6.77	-26.5	-27.0
9.68	-29.2	-30.6

this variation versus the ratio of nozzle approach area to nozzle throat area is shown in Fig. 6-9. It is seen from this plot that, for a given nozzle throat area, percent recoil imbalance is an inverse, nonlinear, function of the nozzle approach area, the imbalance increasing at a progressive rate with decreasing approach area.

The experimental plot in Fig. 6-9 is correlated by a theoretical plot also shown in the figure and obtained from Fig. 6-6. It is noted that the two plots have a close similarity through the range of $A_i/A_t = A_c/A_t$, the divergence of the curves occurring at area ratios lower than 2. This divergence is explained by the difference of the "effective" nozzle approach area, attributed to chamber configuration and heat losses.

It is seen from Table 6-4, that chamber configurations such as employed with chamber liners Nos. 2 and 3 do not give satisfactory recoil compensation, and it is concluded from Fig. 6-9 that the ratio of nozzle approach area to throat area should be equal to, or greater than, 2.0. For recoilless rifles, the bore area to throat area ratio is, in general, approximately equal to 4/3. This would give an approach-area to bore-area ratio of approximately 1.5, or greater, as used, for

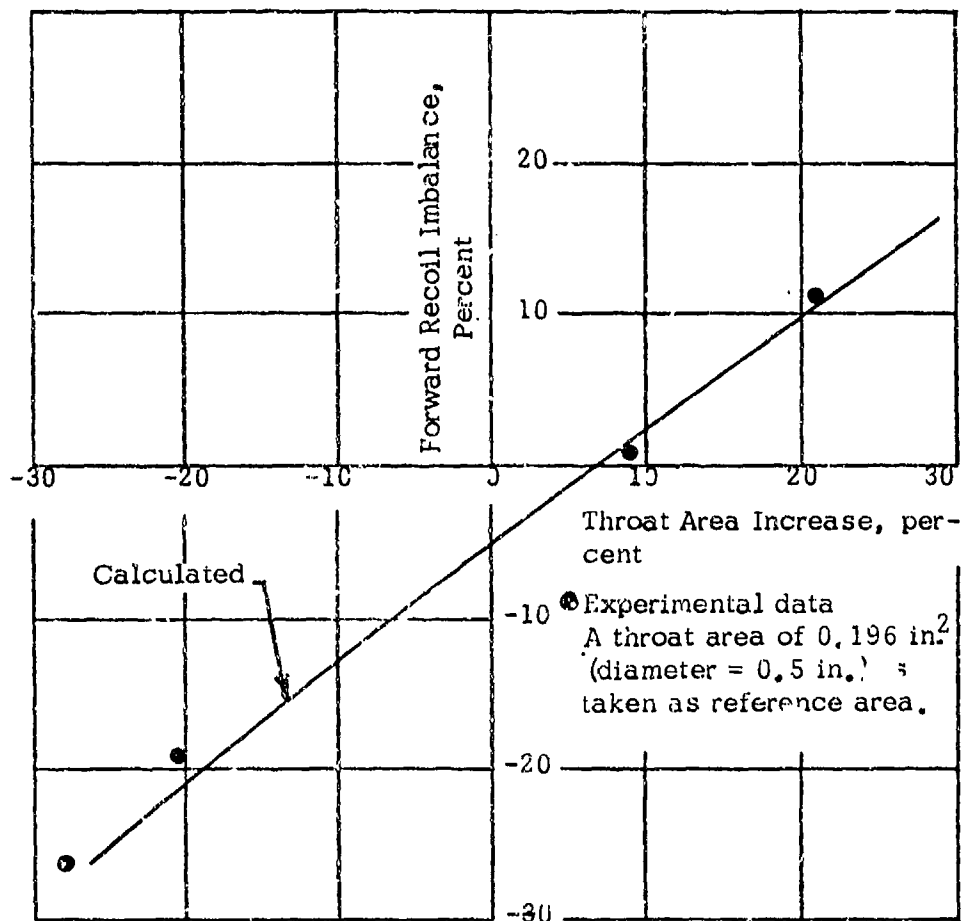


Figure 6-8. Percent Recoil Force Imbalance as a Function of Nozzle Throat Area

example, in the design of the 75 mm Recoilless Rifle, T41.

Due to the close radial confinement of the burning charge in the front portion of the chamber, the chamber design given by liner No. 5 results in chamber pressures higher than for an equal volume chamber with a uniform annular space as exemplified by chamber liner No. 3. Liner No. 5 also gives the highest ballistic efficiency (i.e., ratio of projectile kinetic energy to total propellant energy) when compared with liner Nos. 1 and 4. Furthermore, it is to be noted that the maximum pressure and recoil imbalance are

considerably higher with liner No. 5 than with liner No. 1, which has a fully tapered configuration, even though they both have the same geometric approach areas. The maximum pressure is approximately 30% greater and the recoil imbalance is 2.5% greater for the configuration of liner No. 5.

Results of similar studies repeated with the 57 mm Recoilless Rifle, M18, fitted with a centrally-located circular nozzle (in lieu of the annularly-located kidney nozzle) indicate that (see Ref. 15):

1. The expansion of gases in the central

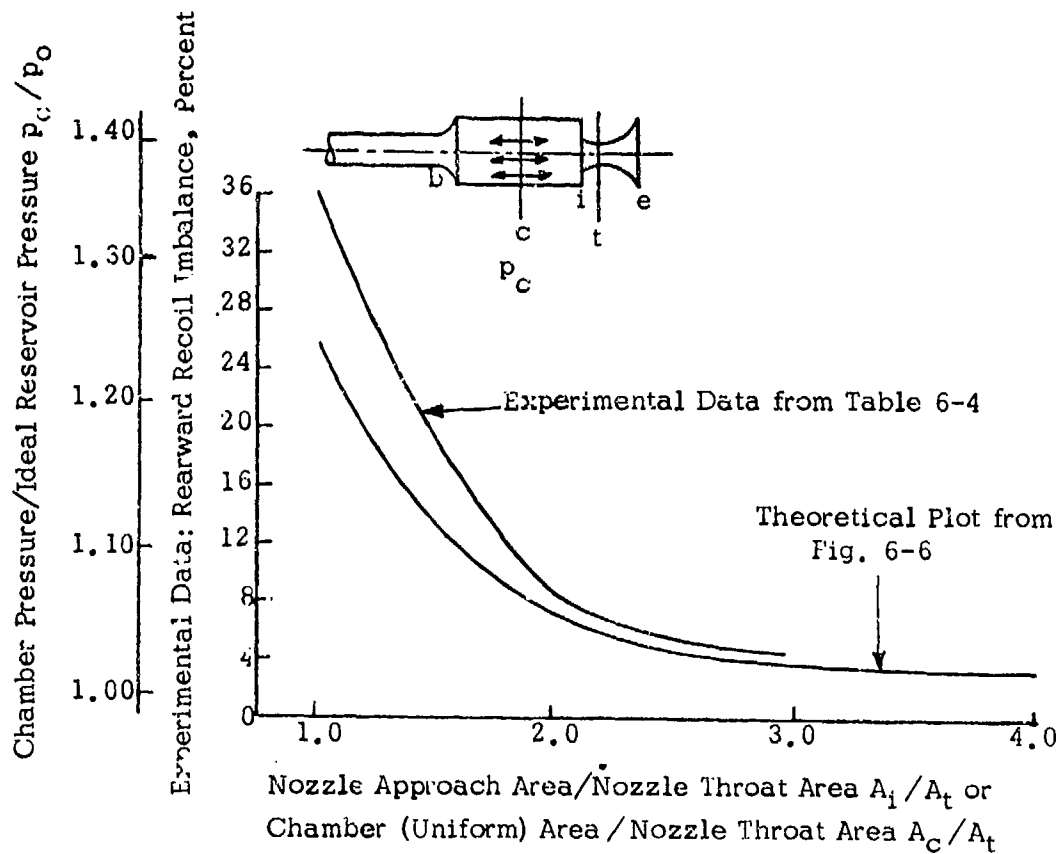


Figure 6-9. Effect of Approach Area A_1 on Recoil Imbalance of the 57 mm Recoilless Rifle, M18

nozzle is slightly more efficient than in the kidney-shaped nozzle.

2. The recoil compensation is less sensitive to change in geometric approach area for the central nozzle as compared to the kidney-

shaped nozzle in the critical region between ratios of approach area to throat area of one to two.

3. The ballistic efficiency of the rifle is slightly greater for the central nozzle than for the kidney-shaped nozzle.

TABLE 6-4

**BALLISTIC DATA FOR THE 57 mm RECOILLESS RIFLE, M18, FIRED WITH
VARIOUS CHAMBER CONFIGURATIONS (Ref. 15)**

Liner Charge, No. *	g	Instrument Velocity, fps	Maximum Pressure, psi	Rearward	Nozzle	Propellant Loss, %	Ballistic Efficiency %	A_r/A_t
				Recoil Imbalance, %	Approach Area, A_r , in. ²			
1	426	1232	7200	4.5	9.0	25.2	3.46	3.00
2	360	1282	7450	36.0	3.05	20.0	4.43	1.02
3	405	1282	7900	17.7	4.37	23.0	3.94	1.46
3	426	1366	9100	17.4	4.37	21.8	4.22	1.46
4	426	1272	8050	8.6	6.0	23.6	3.66	2.00
5	426	1294	9400	7.0	9.0	24.2	3.82	3.00

A_t = Nozzle throat area = 3.0 in.²
Chamber volume = 80 in.³

Propellant: M2, Lot RAD 459
Cartridge Case: 57 mm, M30

*Liner No. 1: similar to conventional tapered chamber rifles with a nozzle approach area 3.0 times throat area

Liner No. 2: reversed taper and a nozzle approach area of 1.02 times throat area

Liner No. 3: constant cross section, with a nozzle approach area 1.46 times throat area

Liner No. 4: tapered, with an approach area 2.0 times throat area

Liner No. 5: constant cross section, but only one-half the chamber length. The nozzle approach area equals that of the 57 mm, M18 chamber, or 3.0 times the throat area

SECTION IV

NOZZLE EROSION

6-13 GENERAL DISCUSSION

Of all phenomena unfavorable to long nozzle life, nozzle erosion is the worst offender. Erosion is the progressive wearing away of the inner surface of the nozzle as the gun is used. It is greatest at the throat section and, as the bore of the throat tends to become enlarged, the effect is to diminish the rearward recoil to zero and even ultimately generate forward recoil.

The erosion process is very complex and its details are not fully understood. The process involves mechanical, chemical, and thermal effects which are interrelated. Erosion is primarily a physical activity although chemical action can increase its rate. The abrasive effects of propellant gases and particles impinging at high velocities on the nozzle surface are highly damaging because they sweep away some of the nozzle surface material. This phenomenon is known as gas wash. Erosion is particularly sensitive to the heating of metal surfaces. By melting a very thin layer of the nozzle surface, and thereby making it easier for the gases to carry off the nozzle surface material, intense heat contributes indirectly to the process of erosion. At high temperatures, some constituents of the propellant gases may undergo chemical combination with the nozzle surface material to form brittle compounds that may crack and peel off under the action of propellant gases.

Erosion is particularly severe if hot-burning propellants are used. Under these circumstances, the erosion induced by the gases is most significant. As the flame temperature is increased, the erosion rate increases much more rapidly than the rate of increase of the flame temperature to such an extent that the thermal effects become dominant. Another

form of damage to the nozzle as a result of firing is that of the large thermal and mechanical stresses developed. The result is that the nozzle surface develops a characteristic pattern of cracks which lead to a developing roughness that increases the heat transfer to the nozzle. These cracks erode locally, and the surface ultimately becomes quite rough. In contrast, low-energy weapons using cool propellants erode very slowly.

6-14 THEORY

Erosion is an ever-present problem in recoilless guns. The phenomenon of erosion has been studied quite extensively, but only a portion of the literature is useful (Ref. 16). Many articles written on the subject of erosion in guns elaborate the theories that have been advanced, although there is little reliable experimental data available.

One method of study of the erosion process has been to allow the hot propellant gases to flow through a hole or vent in a block of known weight and determine the weight loss. This method is applicable to weapons using nozzles, and the results show that erosion in vents is of two types: (1) a melting type found above a minimum density of loading, and (2) a chemical type found below this minimum. In the chemical type of erosion, chemical composition of the ingredients, particularly of the primer, is found to be of importance. A comprehensive study concludes that erosion is due to the melting of the surface and shows that this melting starts at a definite pressure independent of the size of the chamber in which the propellant is burned. Above this pressure, the rate of increase of erosion per unit of added charge is independent of chamber size. However, correlation between weight of eroded material and charge weight appears to be better.

The vent plug test—either as a cylindrical plug with a hole, or as two flat plates of different material with the gas passage between, or as several rings of metal forming the tube—appears most analogous to erosion in nozzles. Increasing the pressure in the vented bomb at first causes but slight erosion up to a critical pressure, while further increase causes a rapid increase of erosion in a linear manner. Increasing the area of the hole causes a decrease in erosion, approximately proportional to the area. This is an indication of the effect of the length of time of contact. Increasing the flame temperature of the propellant increases the erosion in a linear manner, roughly a 10 percent increase in erosion per 100 deg C increase in flame temperature.

The erosion of metal by the hot gases produces a characteristic appearance of the metal surface. In ferrous metals, the surface takes on a checked appearance, while in nonferrous metals the surface has a streaked washed-out appearance. Metallographic examination of ferrous alloys shows several layers, beginning with one or more white layers at the surface, of martensitic structure, with lower layers of troostitic and sorbitic structure.

Nonferrous alloys show some changes in grain structure and, of course, more of the martensitic appearance. While the checked structure usually accompanies erosion, it is not certain whether or not it is a cause of erosion. One theory is that the checked structure results from the rapid cooling of the metal surface following the heating by the hot gases.

The two main theories of erosion, then, are the surface fusion theory, and the chemical reaction theory. Supporting the surface fusion theory is the relation among the melting point of the metal and the amount of erosion, and the agreement with heat transfer theories. Chemical reaction theory may apply in vent plugs only below some critical pressure at which melting starts.

6-15 EROSION RESISTANCE OF VARIOUS METALS

In the design of the nozzle of a new recoilless rifle, the designer must be supplied with reliable design data with respect to material, configuration, and dimensions of the nozzle for a projected performance of the gun. In line with this objective, the results of a comprehensive program of study on nozzle erosion are summarized in Ref. 17. Included in this study is a theoretical analysis of the transfer of heat to nozzles, which leads to a useful classification of engineering metals and metallic alloys on the basis of the surface melting under conditions of gun firing, followed by an extensive experimental program to evaluate the erosion of nozzles manufactured from all of the known promising materials in order to correlate the experimental data with the thermal properties of the materials.

The nozzle erosion tests described in Ref. 17 were carried out in a vented bomb, constructed from a 37-mm breech with a chamber volume of 19.5 in.³, with a standard shape nozzle. The rate of increase of nozzle throat, rather than the weight loss per round, was adopted as a criterion of erosion. By use of the M1, M10, and M2 Propellants—the isochoric flame temperatures of which are 2580°K, 3040°K, and 3510°K, respectively—the experimental results pertinent to erosion resistance of various materials are summarized as follows:

1. Molybdenum:

Pure molybdenum possesses the highest erosion resistance of all the materials tested. This is in agreement with predictions by the theoretical classification of metals based on their thermal properties.

Porosity in molybdenum increases the relative erosion rate appreciably. Erosion of pure molybdenum is characterized by deep radial cracks and some spalling. Localized melting along the cracks is apparent.

2. Sintercast:

Nozzles of composition of 60% Mo and 40% Cu and with a throat lining of either molybdenum or chromium behave in much the same way as pure copper does, indicating that—after the throat line is blown off—erosion is probably caused by the melting of the copper and subsequent spalling of the molybdenum particles. The nozzles have a roughened appearance characteristic of this type of erosion.

Nozzles of composition of 80% Mo and 20% Cu and with a throat liner of either molybdenum or chromium exhibit approximately the same relative erosion rates under continued firing conditions. Before the chromium liner completely erodes away after 15 rounds at 35,000 psi, the chromium-lined throat walls are somewhat superior to those with molybdenum liners.

3. Tantalum:

The erosion of tantalum is found to be higher than expected on the basis of the heat transfer theory alone. The surface of the tantalum liner becomes darkened under firing, pointing to a change of chemical nature.

Unlike molybdenum, however, no signs of spalling or cracking exist. Under conditions of rapid fire at 35,000 psi, the rate of erosion of tantalum is found to be more than twice that of molybdenum.

4. Tungsten Carbide. Tungsten carbide nozzles employing approximately 5% Co as a binder exhibit appreciable erosion at the entrance section and along the external edges of the nozzle because of the melting of the cobalt binder, while undergoing less than one percent increase in the throat area at pressure levels of up to 30,000 psi. At 35,000 psi, however, complete shattering of one and serious damaging of another nozzle has been recorded.

5. Copper and Copper Alloys:

Pure electrolytic copper compares very well with gun steel and possesses excellent erosion characteristics at pressures below 20,000 psi. After 40 rounds at this pressure and with the M2 Propellant, no appreciable erosion is observed, as compared with gun steel that erodes 10% after 15 rounds at 20,000 psi.

Because of its relatively low mechanical strength, copper is not recommended for use at pressures in excess of 20,000 psi. While the change in throat area is not excessive at 30,000 psi with the M10 Propellant, the extrusion of the copper-lined nozzle and the deformation of the solid copper nozzle are appreciable. Below 20,000 psi, however, the deformation of copper is less than that of gun steel.

Alloys of copper erode somewhat more rapidly than pure copper but, unlike copper, do not erode appreciably at 30,000 psi. This is to be expected because slight amounts of alloying elements cause a reduction in the thermal conductivity while increasing the strength.

6. Gun Steel. Under tests with the M2 Propellant, gun steel (SAE-4150) exhibits negligible erosion at 10,000 psi. At 20,000 psi and 30,000 psi, the increase in throat area is 3.4% and 8.4%, respectively, for five rounds of firing. These figures are higher, approximately by one order of magnitude, than the corresponding ones for copper.

7. Cast Steel. A cast steel having a composition comparable to SAE-4340 exhibits the same order of magnitude of erosion as that of gun steel, when subjected to the standard erosion test with the M2 Propellant. The actual figures are somewhat lower in the case of cast steel. Furthermore, this steel is exceptional in that the amount of erosion with the M1 Propellant (flame temperature 2580°K) is almost identical to that with the

M10 Propellant (flame temperature 3010°K). This is confirmed by a theoretical analysis (Ref. 17) based on heat transfer and surface melting considerations, showing that a combination of conditions can exist under which the erosion rates will be the same despite the different flame temperatures.

8. Stellite. This is a cobalt-base alloy used for facing valves and high-speed cutting tools. Stellite maintains a high tensile strength even at red heat. All four alloys of stellite tried as nozzle material suffered extreme erosion. The thermal conductivity of these alloys is so low that the surface temperature of the nozzle probably reaches the melting point.

9. RAF Styria Stainless Steel. Results of tests with the best of these stainless steels indicate that this material does not have good erosion characteristics. Nozzles made from a sample of the best RAF styria stainless steel can undergo an erosion of 26% when subjected to the standard test procedure at a pressure of 30,000 psi.

10. Titanium Carbide. Titanium carbide nozzles also appear to have considerably less erosion resistance than gun steel. A sample of a cobalt-bonded titanium carbide with smaller amounts of other ingredients to promote oxidation resistance is reported to have undergone an erosion of 11.5% after 5 rounds at 10,000 psi and 5 rounds at 20,000 psi with the M2 Propellant.

11. Timken Alloy. The principal alloying elements in Timken alloy are approximately 16% Cr, 25% Ni, and 6% Mo. On the basis of weight loss, the erosion of Timken alloy nozzles fired with the M2 Propellant at a nominal pressure of 20,000 psi is reported to be 0.42 g/round. The corresponding figures for gun steel, cast steel, and cast molybdenum are 0.165, 0.08, and 0.002 g/round, respectively.

12. Graphite. It is reported in Ref. 17 that a nozzle made from pure carbon-bonded

graphite shattered after one round of testing at 10,000 psi. Graphite does not possess sufficient mechanical strength for this application.

13. Titanium. When a pure titanium-lined nozzle is tested at 15,000 psi with M10 Propellant, it erodes very severely. The type and degree of erosion indicate the occurrence of a chemical reaction between the titanium and some of the constituents of the propellant gases.

14. Ceramics. The mechanism of erosion in ceramic nozzles is quite complicated. Two theories of the erosion of ceramics have been advanced: spalling, and thermal shock. Spalling is caused, at least in part, by the penetration of gases into small cavities and their subsequent expansion after the pressure is released. Consequently, porosity is an important factor in these nozzles. In the thermal shock theory of erosion, localized failure of the material occurs because of the sudden rise of the surface temperature of the nozzle throat. The surface temperature of ceramic nozzles will reach practically the gas temperature in 2 to 5 msec. For adiabatic flow with M2 Propellant, the gas temperature is approximately 2300°C at the throat and may even exceed 3000°C should combustion occur there. Even in the best ceramics, erosion is characterized by spalling and apparent melting at the surface, and the best of the ceramic nozzles are found to be inferior to gun steel.

15. Coated Materials:

In the coating of nozzles, a thin liner or inner surface coating, usually of some material with a high melting point or particularly desirable chemical resistance properties, is backed by a material having good thermal properties. Experimental studies of the possibility of using composite nozzles to reduce nozzle erosion have been very limited. The results of tests on sintered molybdenum nozzles with oxide-resistant

coating indicate that it is doubtful that the coating has any more than a temporary effect in reducing erosion, since the increase in the average radius at the throat is considerably greater than the thickness of the coating. Aluminum alloy and magnesium alloy nozzles equipped with special coatings are reported also to have undergone complete and severe erosions, respectively (Ref. 17).

In order to estimate theoretically the amount of erosion of the nozzle due to surface melting, the following approximate expression, derived in Ref. 17, for the temperature of the surface is useful:

$$\frac{\Delta T_s}{\Delta T_t} = \frac{2(ht^{1/2})}{(\pi k \rho' c)^{1/2} + \frac{4}{3}(ht^{1/2})},$$

dimensionless (6-39)

where

ΔT_s = temperature rise of inner surface of nozzle throat (with reference to nozzle initial temperature), °R

ΔT_t = temperature rise of propellant gas at nozzle throat (with reference to nozzle initial temperature), °R

h = heat transfer coefficient from propellant gas to nozzle surface, cal-(cm²-sec-°C)⁻¹

k = thermal conductivity of the nozzle material, cal-(cm²-sec-°C/cm)⁻¹

ρ' = density of nozzle material, g-cm⁻³

c = specific heat of nozzle material, cal-(g-°C)⁻¹

t = time, sec

Eq. 6-39 has the advantage of showing the surface temperature rise as being practically proportional to the heat transfer coefficient for small values of time. For $t = 5$ to 10 msec,

which is the case in gun vents and barrels, the deviation of Eq. 6-39 from the exact solution is reported to be less than 2 percent (Ref. 17).

If ΔT_m = difference between melting temperature of nozzle material and initial temperature °R of nozzle, and %MP = percent of melting point, then

$$\begin{aligned} \%MP &= 100 \left(\frac{\Delta T_s}{\Delta T_m} \right) \\ &= 100 \left(\frac{\Delta T_t}{\Delta T_m} \right) \frac{2(ht^{1/2})}{(\pi k \rho' c)^{1/2} + \frac{4}{3}(ht^{1/2})} \end{aligned}$$

(6-40)

On the basis of Eq. 6-40, a theoretical classification of metals is made for their use as erosion-resistant materials. For heat transfer coefficient values of $h = 2, 4,$ and 6 cal - (cm² - sec - °C)⁻¹, and for an exposure time to the hot gases of 5 msec, Eq. 6-40 generates the curves of Fig. 6-10. This figure indicates that the pure metals tungsten, molybdenum, tantalum, iridium, chromium, and copper are the most promising metals since they exhibit lower %MP values for the magnitudes of h and t considered. This conclusion is in agreement with experimental results of erosion studies.

Since the surface temperature rise of these nozzles is approximately inversely proportional to $(k\rho'c)^{1/2}$, ceramics to be used in making the nozzles should have a large $k\rho'c$ product. Although the product $\rho'c$ for ceramics may be of the same order of magnitude as for metals, for most ceramic materials k is 10 to 100 times smaller than for metals. For an advantageous application, then, the constituents of the ceramic nozzles must have high melting points preferably of the order of 3000°K. This would minimize the major cause of the severe erosion of ceramic nozzles believed to be due to the melting of the throat surface where the temperature rise reaches the level of the gas temperature in a very short period of time.

In summary, nozzle materials fall into two

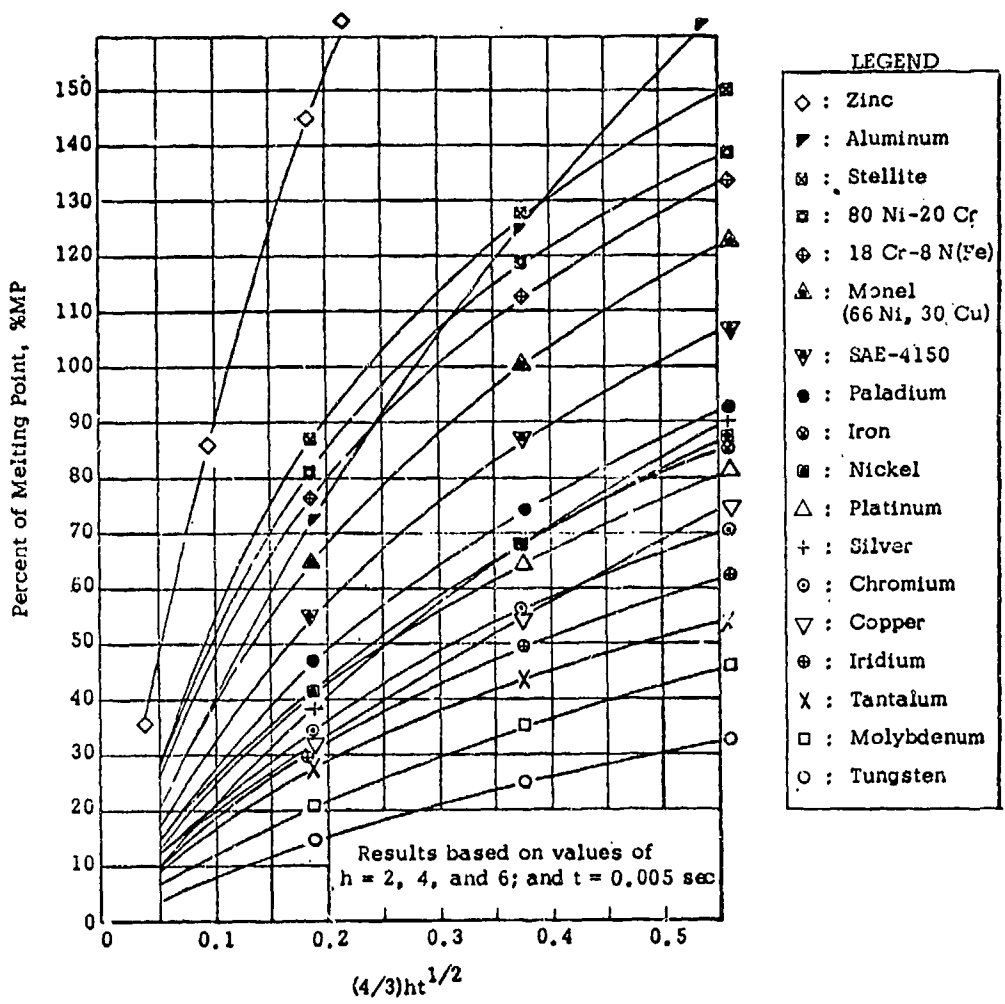


Figure 6-10. Theoretical Classification of Metals on the Basis of Heat Transfer Properties

general classifications: the heat-absorbing type and the heat-resisting type. To the heat-absorbing class belong the simple metals and alloys which, because of their higher thermal conductivity, are able to remove the heat from the surface of the nozzle. To the heat-resisting class belong materials like ceramics, having low thermal conductivity and high melting points. Ceramics as a class have been found to lack sufficient mechanical strength to withstand the erosive forces of the gases.

6-16 SIMILITUDE RELATIONSHIPS

For the purpose of extending the experimental erosion results obtained on nozzles with a 0.5-in. throat diameter to the larger size nozzles used in recoilless rifles, a similitude relation in nozzle erosion is required. For two nozzles of throat diameters D_1 and D_2 , and working with the same pressure-time curve it follows, from the Boelter-Dittus equation for forced convection heat transfer in a pipe, that

$$\frac{h_1}{h_2} = \left(\frac{D_2}{D_1}\right)^{1/5} \quad (6-41)$$

where h_1 and h_2 are the respective heat transfer coefficients. Denoting the fractional increase in the throat area by $\epsilon_1 = 2(\Delta D_1)/D_1$ and $\epsilon_2 = 2(\Delta D_2)/D_2$, and assuming the respective increases in throat diameters to be proportional to the surface conductance, one finally gets

$$\frac{\epsilon_1}{\epsilon_2} = \left(\frac{D_2}{D_1}\right)^{6/5} \quad (6-42)$$

On the basis of this relationship the erosion of nozzles of recoilless rifles with bore diameters from 15 mm to 381 mm (15 in.) have been estimated for various materials, and the results are shown in Table 6-5 for the case of the ratio of the bore area to nozzle throat area being equal to 1.5 (Ref. 17). Furthermore, erosion data given in Table 6-5 correspond to a duration of gas flow of about 10 msec, the average chamber pressure during the cycle being approximately 20,000 psi. For longer duration of gas flow at the same chamber pressure and gas temperature, the erosion figure in Table 6-5 must be multiplied by a correction factor. Based on heat conduction theory, it is suggested that for nozzles of less than 5 in. in throat diameter this factor be the time ratio, and for nozzles having a throat diameter greater than 5 in. the multiplying factor be the square of the time ratio in order to estimate erosion for flow duration longer than 10 msec.

6-17 OTHER FACTORS THAT AFFECT EROSION RATE

The effects of other factors on nozzle erosion are discussed in Ref. 17. These include such factors as the isochoric flame temperature of the propellant, the shape of the nozzle, the initial temperature of the nozzle, and the test history. A summary of these effects follows:

1. Effect of Isochoric Flame Temperature. The three types of propellant—M1, M10, and M2—used to study the effect of propellant flame temperature on the rate of erosion of metals have the isochoric flame temperatures of 2580°K, 3010°K, and 3540°K, respectively. Results of the tests with seven metals indicate (Ref. 17) that, in general, erosion is reduced appreciably through the use of a propellant with a lower flame temperature. One exception to this is found in the tests with cast steel (approximately SAE-4340) for which the erosion with the M1 Propellant was almost identical to that with the M10 Propellant. This has been confirmed theoretically by an analysis based on considerations of heat transfer and surface melting. The results show that a combination of conditions can exist under which the rate of erosion will be the same despite the different flame temperatures.

2. Effect of Nozzle Shape. Four nozzle shape characteristics were investigated (Ref. 17) to determine their relative effects on erosion rate. The results are

a. The erosion rate of nozzles with cylindrical sections at the throat 0.25 in., 0.50 in., and 0.91 in. long showed that cylindrical throat sections of the lengths considered had no appreciable effect in terms of throat area increase when compared with standard test nozzles of the same material (SAE-4150).

b. Tests with a nozzle having a square cross section indicate that no discernible erosion takes place at the corners. As anticipated from gas flow and heat transfer patterns, sharp corners have practically no effect on erosion.

c. In order to quantitatively compare oblong nozzles with circular nozzles of the same cross-sectional area, oblong nozzles with cross sections having length-to-width ratios equal to 1.875 and 4.33 exhibited a spread of less than one percent in the measured

TABLE 6-5

ESTIMATED EROSION OF GUN NOZZLES AS A FUNCTION OF BORE
DIAMETER ($A_b/A_t = 1.5$) AT 30,000 psi MAX PRESSURE

D_B^* , mm	D_B^* , in.	D_t^* , in.	$\left(\frac{D_t}{D_B}\right)^{6.5}$	Erosion per 100 Rounds (percent throat area increase)		
				Gun Steel	Elkaloy A	Cupeloy and Tantalum
15	0.59	0.482	1.0460	62.8	12.10	23.40
30	1.18	0.963	0.4560	27.3	5.30	10.20
45	1.77	1.448	0.2790	16.7	3.20	6.30
60	2.36	1.930	0.1980	11.9	2.30	4.40
75	2.95	2.410	0.1510	9.1	1.75	3.40
105	4.13	3.375	0.1010	6.1	1.20	2.20
150	5.91	4.820	0.0660	4.0	0.77	1.50
200	7.87	6.390	0.0463	2.8	0.54	1.00
250	9.85	8.050	0.0357	2.1	0.42	0.80
300	11.80	9.620	0.0290	1.7	0.34	0.65
381	15.00	12.250	0.0215	1.3	0.25	0.50

* D_B = bore diameter of rifle; D_t = throat diameter of nozzle

At 30,000 psi (M10 Propellant) erosion of cast molybdenum, sintered molybdenum (sp gr 10.0), or molybdenum copper (sintered) should be negligible for all sizes in Table 6-5.

increases in throat area after 50 rounds at 15,000 psi with the M10 Propellant. The cross section shape does not appear to have a critical effect on the erosion rate.

d. Tests with nozzles having divergence angles of 7.5 deg, 15 deg, and 30 deg indicate that the divergence angle has no appreciable effect on the conditions of gas flow affecting the rate of erosion at chamber pressures of up to 15,000 psi.

3. Effect of Initial Temperature. In a recoilless rifle with a high cyclic rate of firing, the effect of an elevated initial temperature on the erosion of nozzles is expected to be appreciable. Tests have shown that when the initial temperature is 225°C, the erosion of gun steel at 30,000 psi (M2 Propellant) is twice as high as the erosion at an initial temperature of 25°C, as predicted on the basis of heat transfer and surface melting considerations.

4. Effect of Test History. To study the effect of test history on subsequent rate of erosion, three cast steel nozzles using the M10 Propellant were tested. Firing on one was started at the 10,000 psi level while the firing on another was begun at the 20,000 psi level. The subsequent rates of erosion of these nozzles at 35,000 psi were compared with the erosion rate of the third nozzle on which testing was initiated at 35,000 psi. All were found to erode at very nearly the same rate. This indicates that the lower pressure portion of the firing schedule is not a severe test for the cast steel, and it is to be expected that the subsequent rates of erosion of other metals superior to gun steel at the higher pressure levels would not be significantly affected either. This was shown also to be true for cast molybdenum tested with the M2 Propellant. No general conclusion applicable to other metals may be drawn on the basis of these results alone.

SECTION V

BORE-SIZE NOZZLE

During the course of study (Ref. 15) of the feasibility of a recoilless rifle that permits rear loading without a breech mechanism, the 57 mm Recoilless Rifle, M18, was modified to have a concentrically mounted nozzle that simply consisted of a straight pipe of uniform cross section with an inside area of about 1.02 times the bore area of the rifle. The study was initiated in recognition of the obvious practical advantages of the straight-pipe nozzle over the conventional de Laval nozzle. These advantages are simplicity; ease of fabrication, which is of greater importance when the nozzle must be replaced after erosion has changed rifle performance beyond a desired level; and the elimination of a costly breech mechanism.

On the basis of the experimental data obtained, it is concluded that a perforated pipe of length less than 5 in. will meet the requirements of negligible recoil imbalance with reasonable ballistic performance. In the event that a higher ballistic efficiency is desired, the bore-size system of internal rings and external perforated pipe can be used and, with the application of a combustible cartridge case and the improvement of ignition conditions to diminish the propellant loss, the total charge required can be reduced considerably.

Use of several types of the bore-size nozzle, including perforated and nonperforated pipes as well as combinations of externally located pipes with internally located rings, was made in the series of tests conducted.

The first series of tests consisted of firing the M18 Rifle with a 4 in. long straight pipe located externally at the rear of the chamber. The recoil imbalance recorded was approximately 16 percent in the forward direction.

This correlates well with the theory when a nozzle discharge coefficient of 0.72 is incorporated to account for the further decrease of the stagnation pressure and mass flow rate at the sharp-edged entrance of the straight-pipe nozzle (Ref. 15). In order to obtain a balanced rifle with a bore-size nozzle, the forward recoil imbalance was reduced by diverting a portion of the rearward momentum of the gases away from the rifle axis, thereby reducing the momentum transfer to the rifle. This was accomplished in two ways. One, by adding a device similar to a "muzzle brake" to the end of the straight pipe; and two, by perforating the wall of the straight pipe. In both of these systems, the amount of momentum change is a function of the amount of gas diverted and the angle of diversion. Experimental data indicate that the effect of the brake is greater if the slot width is increased to gain bleed-off area, compared to simply increasing the number of slots, when the wider slots are used. Also, the influence of the "nozzle brake" on the interior ballistics of the rifle is negligible, so that the net effect is to reduce the forward thrust on the rifle without measurable effect on the mass flow entering the straight-pipe nozzle.

As to the use of the perforated, straight-pipe nozzle with perforations at 90 deg to the axis, an obvious disadvantage is the spraying of hot gases in the immediate region normal to the rifle axis. A conical shield or deflector employed as a device to deflect the bleed-off gas flow toward the rear of the rifle did not prove to be satisfactory because it gave unacceptable recoil imbalance. Consequently, a bore-size nozzle was designed with perforations at angles of 45 deg and 65 deg to the bore axis. Flash pictures indicated qualitatively that there is less eddying of gases into

the gunner's area with the holes at 65 deg to the bore axis than with the holes at 90 deg.

A straight-pipe, sharp-edged entrance nozzle with an expansion cone was tested in the differential thrust bomb for comparison with a straight-pipe, sharp-edged entrance nozzle without an expansion cone. The net difference of thrust imbalance between the two nozzles was about 20 percent, which is 7 percent less (in the forward direction) than the value predicted by the theory. The difference is attributed to decreased thrust efficiency of the nozzle due to a discontinuity of surface slope, which could cause formation of oblique shock waves and vortex flow, with resulting loss of forward thrust.

In the series of tests employing straight-pipe nozzles located internally, several other types of bore-size nozzles were employed for location inside the chamber of the M18 Rifle. This was an effort to achieve mass flow control by effecting the dynamic flow contraction of a main gas stream by the introduction of a second high-velocity gas stream at right angles to the main stream. Thus, the net effect is, in general, entropy increase, or total pressure decrease of the combustion gases in the nozzle. When compared with the results of the externally located, perforated, bore-size nozzles, the ballistic results are, in general, favorable.

However, in order to maintain a balanced rifle, it was found necessary to use the externally located straight-pipe nozzle with 65-deg perforations in combination with these internal devices. As a result of the higher propellant loss with these systems, it was obvious that the ballistic efficiency of the M18 Rifle was lowered by the use of a bore-size nozzle, as compared with its operation with a standard convergent-divergent type of nozzle. In the event that higher ballistic efficiency is desired, the bore-size system of internal rings and external perforated pipe could be used and, with the application of a combustible cartridge case and the improvement of the ignition conditions to reduce the propellant loss, the required amount of charge could be reduced considerably.

Lastly, in connection with the erosion rate of the straight-pipe, bore-size nozzle with sharp-edged entrance, investigations performed in the vented bomb indicated the eroding of the entrance to a radial contour shape and the uniform erosion of the inside pipe surface over the full length. The total erosion rate was about one-sixth that of a convergent-divergent nozzle throat and there was little change in the thrust of the nozzle when tested in the differential thrust bomb—in good agreement with the theoretical prediction when the very low expansion ratio of the nozzle is taken into account.

SECTION VI

RECOIL COMPENSATORS

The effectiveness of recoilless rifles can be increased considerably if the effects of nozzle erosion on rifle performance could be compensated for continuously during the life of the rifle. This is achieved by use of recoil compensators for nozzle erosion.

It is reported (Ref. 15) that during the investigation of the effects of chamber configuration and nozzle approach area on rifle performance, tests were performed whereby the average muzzle velocity was maintained approximately constant by variation of the charge weight. It is noted that, had the charge weight remained constant during these tests, muzzle velocity and chamber pressure could have been maintained constant by enlarging the nozzle throat, which would also have brought the rifle closer to a balanced condition. Thus, these tests indicated that compensation by means of flow throttling was entirely practicable; however, a mechanical set-up using a set of chamber liners is impracticable. Rather, such throttling devices as tested in the study of the internally located bore-sized nozzles in the 57 mm Rifle, M18, are more practical if the chamber design permits variable throttling by variation of the axial position of the compensator from the nozzle. The opportunity for this type of correction would not exist if the gases were not so much underexpanded in the production rifles.

Devices that have been designed and tested in the 75 mm Rifle, M20, to compensate for nozzle erosion are described in Ref. 15. These devices were rings, of various cross-sectional

shapes and sizes, located at various positions in front of the nozzle. The effects of size, shape, and position on rifle imbalance and projectile muzzle velocity were determined. The results indicate that the change of percent imbalance in recoil is, in general, greater than the percent change of the projectile muzzle velocity. This effect is greater with a ring of square cross section, a ring of circular cross section having the least effect. Test results also indicate that, with rings of square cross section, the ring with a larger cross section provides greater compensation throughout the entire range of axial adjustment, and also, for an adjustment less than 0.5 in. from the nozzle, its effect increases at a faster rate. This generally superior effect of the square ring with a larger cross section is due to the greater restriction of flow provided.

Studies of the devices to compensate for nozzle erosion were also conducted with the 106 mm Recoilless Rifle, T170. Results of tests reported (Ref. 15) indicate that a conical recoil compensator in the 106 mm Rifle appears to be more efficient, since the change of percent rifle imbalance is nearly equal to the percent change of projectile muzzle velocity. This is attributed to its throttling of gas against a forward chamber wall instead of the nozzle entrance, as in the ring compensators.

Complete and detailed information on rotational recoil compensators for nozzle erosion is given in Ref. 15.

SECTION VII

BLAST EFFECTS

6-18 INTRODUCTION

The nozzle blast from recoilless rifles contains several components that are potentially damaging or dangerous. These include: the nozzle or back jet of high-velocity air and gases; the unburned propellant grains ejected from the breech at high-velocity; the flame illuminating the surrounding area; and the air blast, i.e., the airborne shock wave or blast pressure pulse.

When a recoilless rifle is fired, a very large volume of propellant gas streams from the nozzle at supersonic speed and compresses the surrounding atmosphere, thus initiating a shock wave. The shock wave is bounded by an extremely sharp front, called the shock front, which represents a discontinuity in density, pressure, and temperature of the atmosphere. As the shock front continues to move outward, the peak pressure, the velocity of propagation, and the impulse of the shock wave decrease while the transient duration of the shock increases. When its velocity decreases to the sonic level, the shock wave becomes simply an impulse sound wave.

The phase where the pressure first rises very sharply from atmospheric to a peak value and then declines to the atmospheric level is known as the positive or pressure phase of the shock wave. Immediately after the pressure phase, the pressure continues to decline to subatmospheric levels and then returns to normal. This second phase is known as the negative or suction phase and lasts considerably longer than the positive phase, the peak negative pressure being only a fraction of the peak pressure of the positive phase.

The effectiveness of a blast wave may be measured by the peak overpressure and the

impulse of the positive phase at various distances from the origin of the blast. The peak pressure is the pressure jump at the shock front, which is the highest pressure in the shock wave. As a measure of both the intensity of the pressure and its duration, the impulse of the positive phase is of basic importance. This positive impulse is equal to the area under the pressure-time wave of the positive phase, and is approximately equal to one-half the peak pressure multiplied by the duration of the positive phase. For highly elastic structures, the positive impulse of the wave will be effective; for brittle structures, the damage is generally determined by the peak overpressure.

6-19 VARIOUS DAMAGE MECHANISMS

In the design of a recoilless rifle, an important factor to be considered is the damaging effect of the backblast on personnel and structures behind the nozzle of the gun and, since the early 1950s, the characteristic blast zone behind the recoilless rifle has been the object of extensive analytical and experimental investigations, with a view toward determining blast danger zones and establishing techniques of blast reduction or diverting. Strictly analytical solutions to the blast problem have been found inadequate in determining the characteristics of the shock structure, and a combined empirical-analytical approach usually is employed (Ref. 18).

Blast studies usually consist of the experimental mapping of the blast pressure field (Refs. 19, 20, 21) and the determination of the response of structures to the blast loadings. The objective of the first part of the study of blast is to determine the degree to which recoilless rifle and ammunition design can influence the blast envelope in terms of

both intensity and location of the overpressure. The second part of the study treats the effects of the blast overpressure on nearby objects, both structurally and from a control aspect, in order to explore the possibility of optimizing the rifle for both zero recoil and minimum blast effects. However, a minimum blast field requirement may not be realized by designing breech nozzles for a single steady-state flow condition obtained for the single set of values of chamber pressure, nozzle expansion ratio, and nozzle length that will balance the total impulse. In order to optimize nozzle design for both recoil balance and minimum blast field effects, a detailed evaluation of the time-dependent flow field may be required. To date, such a study has not been available in the literature.

In addition to structural damage due to the blast from the nozzle of a recoilless rifle, the danger of physiological damage also exists. The extent and nature of the damage caused by the concussion produced by the blast wave depend on the intensity of the blast, its impulse, the position of the subject with respect to the blast, angle of incidence of the blast, and the presence of reflected blast wave. At close range, the nozzle jet (back jet) is very destructive especially along the axis of the gun. Generally, a significant amount of unburned propellant is also ejected during backblast, ranging in size from whole grains down to small slivers. This is a most serious component of backblast danger, since its missile effect extends over wider angles and to greater distances behind the rifle than any of the other injuring factors. The amount of the solid propellant ejected is a function of the chamber, nozzle and cartridge case designs, the ignition of the propellant, and the pressure level at which the rifle operates; the higher the operating pressure, the smaller the percentage quantity of unburned propellant ejected. Inasmuch as the back jet and propellant missile effects are severe in regions where the flame causes only the minor damage of singeing the hair, the flame component of backblast appears to be negligible. The blast-type injury caused by

high pressures associated with the back jet usually occurs only in regions where the effects of the back jet and ejected propellant are very large so that the blast wave pressure factor is overridden in severity by the other two. Consequently, the pressure wave is not a primary source of danger to life, but is a possible complication added to the other already severe injury mechanisms. Injuries to the lungs and the auditory mechanisms (Ref. 29), and damage to the nervous system are the most common and easily produced effects of the blast pressure. Detailed information on the effects of nozzle blasts is contained in the experimental investigation of Ref. 22. Other, less frequently occurring, blast induced injuries have been reported by the National Research Council in Ref. 23.

Apart from causing physiological effects, blast from recoilless rifles also creates psychological factors which may be significant. Ref. 23 reports that blast intensities that are too small to induce serious physiological disruption often cause psychological effects of extreme lethargy and feelings of fatigue. It is not possible to derive concrete conclusions that define the limits of blast pressure which can be tolerated by humans and animals; there is much disagreement on these limits since there have been only very few experimental studies conducted under controlled conditions.

6-20 BLAST AND FLASH PATTERNS

Since the early stages of the development of the recoilless rifle, backblast has been considered the principal objectionable by-product of the recoil-balancing nozzle. The tremendous blast that results from the escape of propellant gas to the rear of the rifle is an inherent characteristic of the design of the weapon, and constitutes the main drawback to the use of recoilless rifles. The magnitude of the blast is determined by the projectile energy, and studies have indicated that it is incapable of considerable reduction. Personnel and materiel therefore must be adequately protected for many yards to the rear. In the

event of the 57 mm rifle, for example, the danger zone is a cone extending 50 ft to the rear and 40 ft wide at its widest point. Because of the danger of flying particles thrown up by the blast action, personnel within 100 ft of the rear of the breech must not face the weapon. Another, but much less serious, effect of the blast is that it may be the means of enemy observation of battery locations. Obviously, it would be desirable to have this disadvantage reduced or eliminated.

Studies have indicated that the backblast levels developed by a recoilless rifle can be reduced by firing at lowered maximum operating pressures. A propellant grain that provides a high piezometric efficiency (neutral pressure-time characteristic) will permit attaining a high muzzle velocity with the lowest maximum operating chamber pressure.

The structure of the high-velocity nozzle jet and the major factors influencing it are discussed extensively in the experimental and theoretical studies reported in Ref. 24. These studies pertain to axisymmetric free jets exhausting from sonic and supersonic nozzles into still air and into supersonic streams. For jets exhausting into still air, the primary variables considered are jet Mach number, nozzle divergence angle α , jet pressure ratio p_e/p_a , and the ratio of specific heats of the jet. The effects of most of these variables upon jet structure, primary wavelength, and the shape and curvature of the jet boundary are studied in Ref. 24. The gaseous jet exhausting supersonically into still air has been known to exhibit a periodic or chain-like structure at least as early as the observations of Lord Rayleigh in 1879. Since then, several theories have been advanced for the prediction of the primary wavelength (length of the first periodic segment of the jet) and the secondary wavelength (length of the succeeding periodic segments) which is known to differ from the primary, particularly at the higher jet pressure ratios. At a constant value of p_e/p_a and α , the experimental results show that the primary wavelength increases with increasing Mach number. Divergence angle α is

indicated to be of secondary importance within the range from 0 deg to 20 deg. When a jet exhausts from a nozzle into still air, it will undergo a two-dimensional expansion if $p_e/p_a > 1$. The amount of this expansion can be measured by the resulting initial inclination of the jet boundary. In the event of extreme jet pressure ratios, results indicate that large initial inclinations will occur. Preliminary calculations based on the method of characteristics to determine the shape of the jet boundary and to observe the formation of the jet structure indicate that the effect of increasing α is to promote the formation of shocks within the jet. The effect of increasing γ from 1.2 to 1.4 is also to favor the formation of shocks within the jet. Approximately 3,000 calculated boundaries are presented which cover p_e/p_a ratios from 1 to about 42,000; values of γ of the jet from 1.115 to 1.667; values of α from 0 deg to 20 deg; and the jet Mach numbers from 1.0 to 3.0. Most of these boundaries (2,960) comprise a systematic study in the jet pressure ratio range from 1 to 10 for conically divergent nozzles.

Typical curves of the calculated jet boundaries for a jet Mach number M_e of 2.0 and $\gamma = 1.2$ for the jet are presented in Fig. 6-11 for $\alpha = 5$ deg, and in Fig. 6-12 for $\alpha = 10$ deg. In these curves, x is the abscissa and y is the ordinate of a point on the boundary of the jet, and r is the radius of the exit section of the nozzle; the origin of the coordinate axes being at the center of the nozzle exit section. The effect of increasing the jet pressure ratio is obvious from these figures. Effects of the other variables at a jet pressure ratio of 5 (arbitrarily chosen) are shown in Fig. 6-13. The effect of increasing M_e is to decrease the initial inclination of the boundary, to increase the maximum diameter of the free jet, and to move the maximum diameter farther away from the plane of the jet exit. The effect of increasing γ is to decrease the initial inclination of the boundary, to decrease the maximum diameter of the free jet, and to move the maximum diameter closer to the plane of the jet exit.

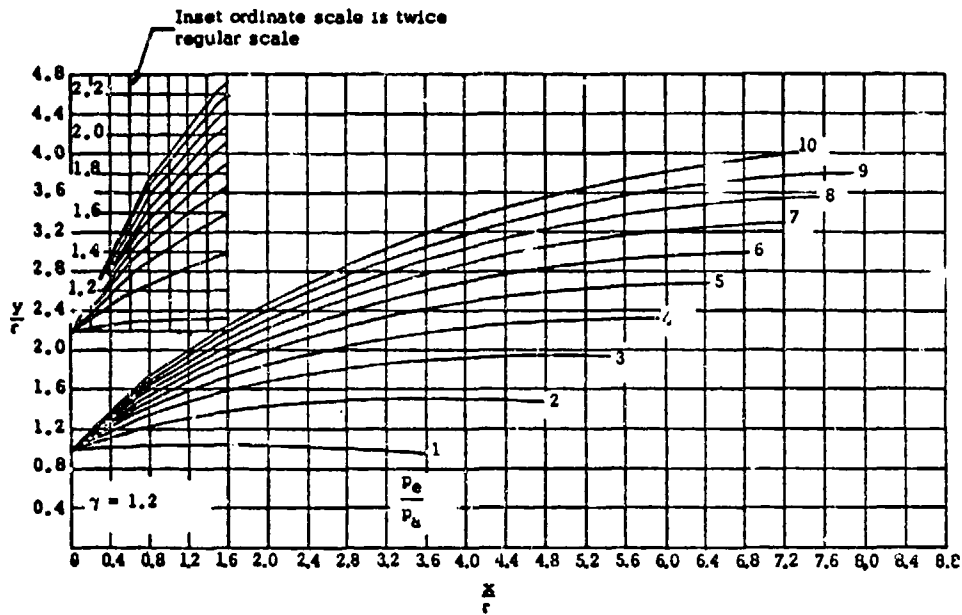


Figure 6-11. Jet Boundaries for Jet Pressure Ratios from 1 to 10
 ($\alpha = 5 \text{ deg}$, $\gamma = 1.2$, $M_e = 2.0$)

The effect of increasing the nozzle divergence angle α is to increase the initial inclination of the boundary, to increase the maximum diameter of the free jet, and to move the maximum diameter closer to the plane of the jet exit. These effects appear to be typical of

all other jet pressure ratios. It is also apparent that, for a particular value of γ of the jet, there are a number of combinations of M_e , α , and p_e/p_a which produce essentially the same boundary. At large values of p_e/p_a , the calculated jet boundaries also are presented in

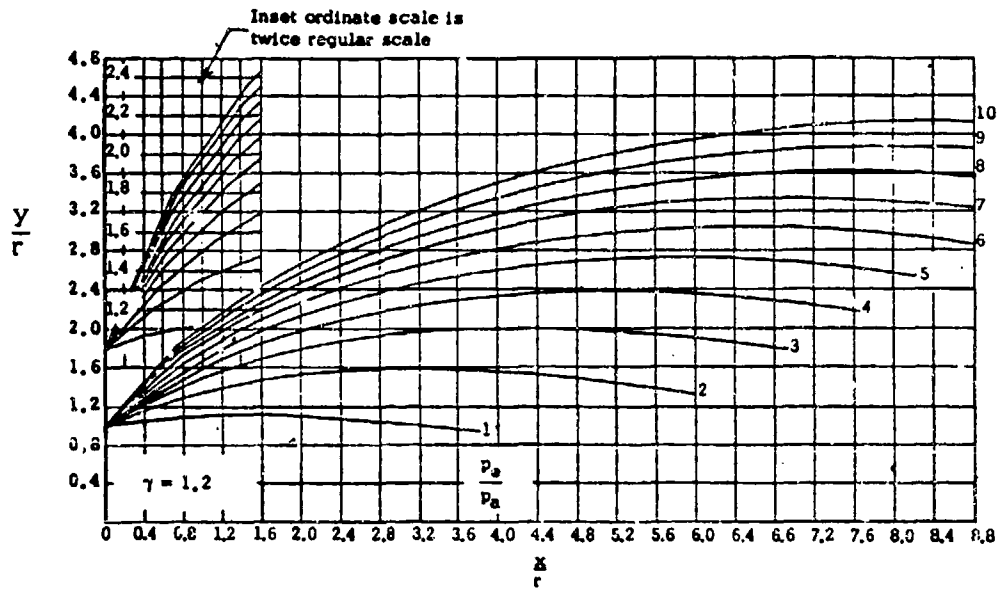


Figure 6-12. Jet Boundaries for Jet Pressure Ratios from 1 to 10
 ($\alpha = 10 \text{ deg}$, $\gamma = 1.2$, $M_e = 2.0$)

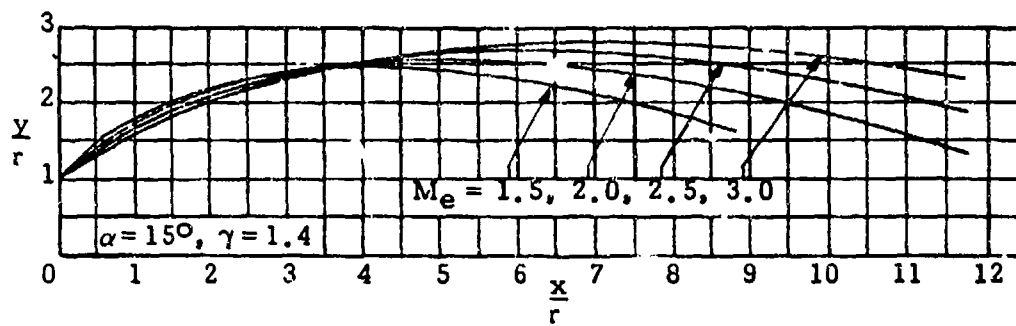
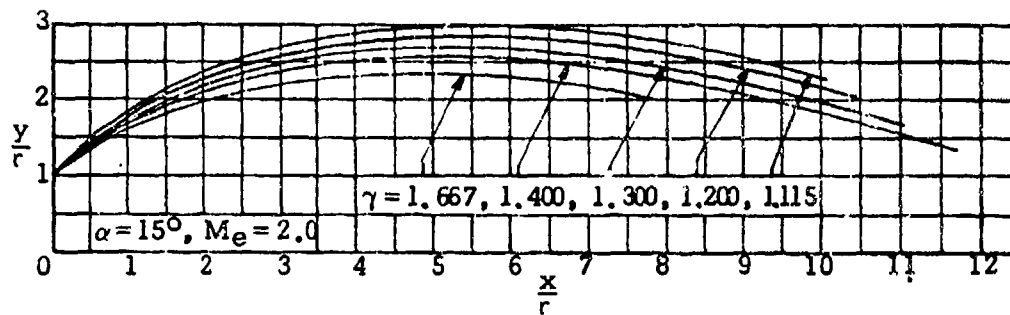
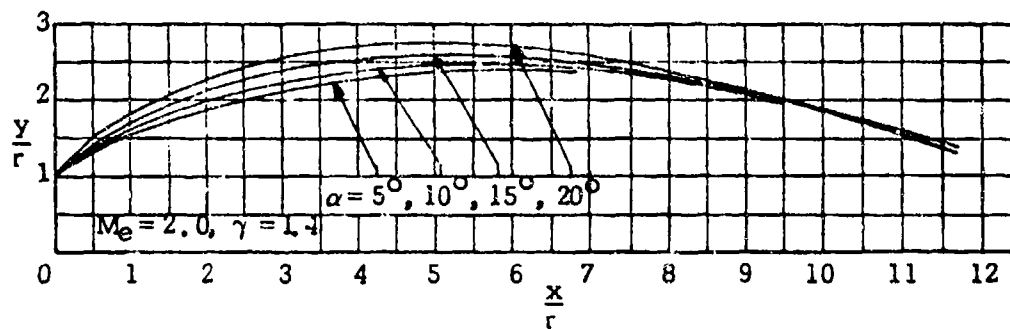
(A) Effect of M_e (B) Effect of γ (C) Effect of α

Figure 6-13. Jet Boundary Patterns for Various Parameters (Example of the effects of jet Mach number, ratio of specific heats of the jet, and nozzle divergence angle upon the shape of the jet boundary, $p_e/p_a = 5$)

Ref. 24 for values of α and γ larger than those shown in Figs. 6-11 and 6-12. The enormous size that the free jet may attain at large ratios of jet pressure is apparent, particularly for $\gamma = 1.20$, when the initial inclination of the boundary approaches and exceeds 90 deg.

Indicated also is the elimination of the jet shock with increasing p_e/p_a at large values of the latter.

The analytical method of Ref. 18 for predicting the backblast overpressure field to

the rear of the recoilless rifle is based on the assumption that the solution of the spherically symmetric blast problem due to a point source can be made applicable to the nozzle blast problem by incorporating an empirical factor to account for the directional effect of the nozzle gases. This factor, called the directional coefficient, is a function of the angle included by the rifle axis and the line joining the center point of the nozzle exit plane to the point under consideration, and is given in Ref. 18. While this procedure does, in general, correlate reasonably well with the experimental results of nozzle blast studies, it is not applicable at positions close to the nozzle (less than 5 ft away from nozzle) where the shock is only partially formed and the flow apparently is undefined.

Recent observations of a series of high-speed movies indicate that the behavior of the overall nozzle blast phenomenon associated with the firing of standard recoilless rifles is as follows. The initial shock front, driven by the hot gas to cold air contact surface, emanates from the breech nozzle exit and appears to diffract about the nozzle exterior, forming a bubble which expands and translates aft. The bubble is rendered partially visible due to the intense radiation field directed to the aft. The radiation is scattered by multicomponent and multiphase efflux, becoming more isotropic and less intense with increasing efflux density and distance from the exit plane of the nozzle. It is concluded that:

1. The initial shock front from a recoilless rifle emanates from a finite "line-source" that directs the blast so that it does not possess spherical symmetry. The classical, "point-source" blast wave theory does not allow for directivity of the blast field nor for the continuous addition of energy to the blast field produced by such a source.

2. The arrival of shock phenomena as measured by pressure transducers located on a plane containing the axis of the rifle yields a Mach number distribution that builds up to

Mach 2 intensity before decreasing aft to transonic intensities.

3. The existing data indicate that overall backblast damage may be due to a composite of two recoilless rifle overpressures consisting of the initial shock front with its reflected overpressures and the quasi steady-state jet plume impingement overpressures.

Another important and objectionable by-product of the recoil-balancing nozzle of a recoilless rifle is the nozzle flash that results from the luminosity of the hot gases issuing from the nozzle. Muzzle flash in recoilless rifles is negligible in comparison with nozzle flash which is of much greater intensity and longer duration. For example, the flash from the nozzle of the 75 mm M20 Recoilless Rifle has an integrated intensity of the order of 10^4 candle-seconds. Its shape is approximately that of an ellipsoid of revolution with a diameter of about 10 ft and a major axis of about 30 ft. Obviously, nozzle flash is detrimental from the standpoint of detection by the enemy and, to a lesser extent, due to the danger of impairment of vision of the user of the rifle. If adequate flash suppression measures are not taken, the flash problem can become very serious.

While the mechanism of flash is not understood in complete detail, the long duration of nozzle flash has enabled the examination of its structure and time-development in greater detail than has been possible in the case of conventional gun flash. The details have been recorded by means of high-speed motion pictures. Studies of the flash structure over a range of variables—including nozzle shape, chamber pressure, and propellant composition—have led to a clearer understanding of the mechanism of the flash and the methods of reducing it. Qualitative results indicate that, for a given chamber pressure, the flash decreases as expansion ratio increases and, for a given expansion ratio, flash decreases with chamber pressure increase (see Ref. 14).

In the study of flash, three regions of luminosity have been observed. As the propellant gases exit from the nozzle of a recoilless rifle, they are sufficiently hot to be self-luminous and constitute a small region of low luminosity at the nozzle. This is called the *primary flash*. Upon exit from the nozzle, the gases rapidly expand and cool and the luminosity disappears, forming the dark zone. Here the gases are overexpanded and subsequently are recompressed *adiabatically* through a shock. This process raises the temperature to a level almost equal to that of the nozzle exit temperature, so that the gases are again luminous and form the *intermediate flash*. In the meantime, the gases have entrained air, and a combustible mixture has been formed of the unburned hydrogen and carbon monoxide in the nozzle gases. When the recompression process raises the temperature of this mixture above its ignition level, the combustible mixture will ignite and burn as a diffusion flame constituting the *secondary flash*.

Such metallic impurities as sodium, potassium, and calcium—which are always present in propellants—are responsible for most of the luminosity in flash. However, it does not seem possible to eliminate flash by eliminating these impurities. It has been found that flash can be greatly reduced by either the addition of such salts of potassium as iodide, bromide, oxalate, and sulfate to the propellant, or by use of a mechanical device on the nozzle. Chemical suppressors act by inhibiting combustion in the secondary flash and hence suppress only the secondary flash. Mechanical suppressors reduce the intensity of the shocks and therefore suppress both the intermediate and the secondary flash. Extensive treatment of gun flash and its suppression can be found in Refs. 25, 28, and 29.

6-21 EXPERIMENTAL DATA

6-21.1 PRESSURE CONTOURS

The blast field behind several types of

recoilless rifles has been experimentally determined (Refs. 18, 19, 20).

In the experimental study reported in Ref. 18, the 57 mm Rifle M18, the M18 with central nozzle adapter, the 75 mm Rifle T21, and the 105 mm Rifle M27, were fired and the peak pressures to the rear of these rifles were measured at angles ranging from zero to 70 deg from the nozzle axis and at distances up to approximately 22 ft from the nozzle exit. The results of these field tests indicate, generally, that the pressures build up to a peak at about 4 or 5 ft from the nozzle exit followed by quasi-steady-state pressures thereafter. Until the maximum peak pressure is reached, i.e., at positions close to the nozzle (less than 5 ft away from nozzle), the flow phenomenon appears to be undefined for all the rifles fired. The major experimental problem in these pressure measurements is in the design of pressure gages which can withstand the blast without damage.

The experimental results indicate (Ref. 18) that, while the standard 57 mm Rifle M18 yields a maximum peak overpressure of 41 psi at 4 ft from the nozzle exit along the axis of the nozzle, the corresponding maximum peak overpressure in the event of the central-nozzle adaptation of the M18 Rifle is 14 psi at the same distance. The standard 57 mm rifle burns approximately 0.76 lb of charge producing a peak chamber pressure of about 6500 psi, while the central-nozzle 57 mm rifle burns about 0.67 lb at a peak chamber pressure of approximately 4800 psi.

Extensive firing of the 75 mm Rifle T21 indicated (Ref. 18) that the maximum peak overpressure to the rear is approximately 50 psi at 4 to 5 ft away from the nozzle, and that the pressure wave along the nozzle axis fluctuates considerably. The charge weight for the rifle was 2.90 lb.

The experimental results (Ref. 18) obtained from the 105 mm Rifle M27 show that the corresponding peak overpressures are

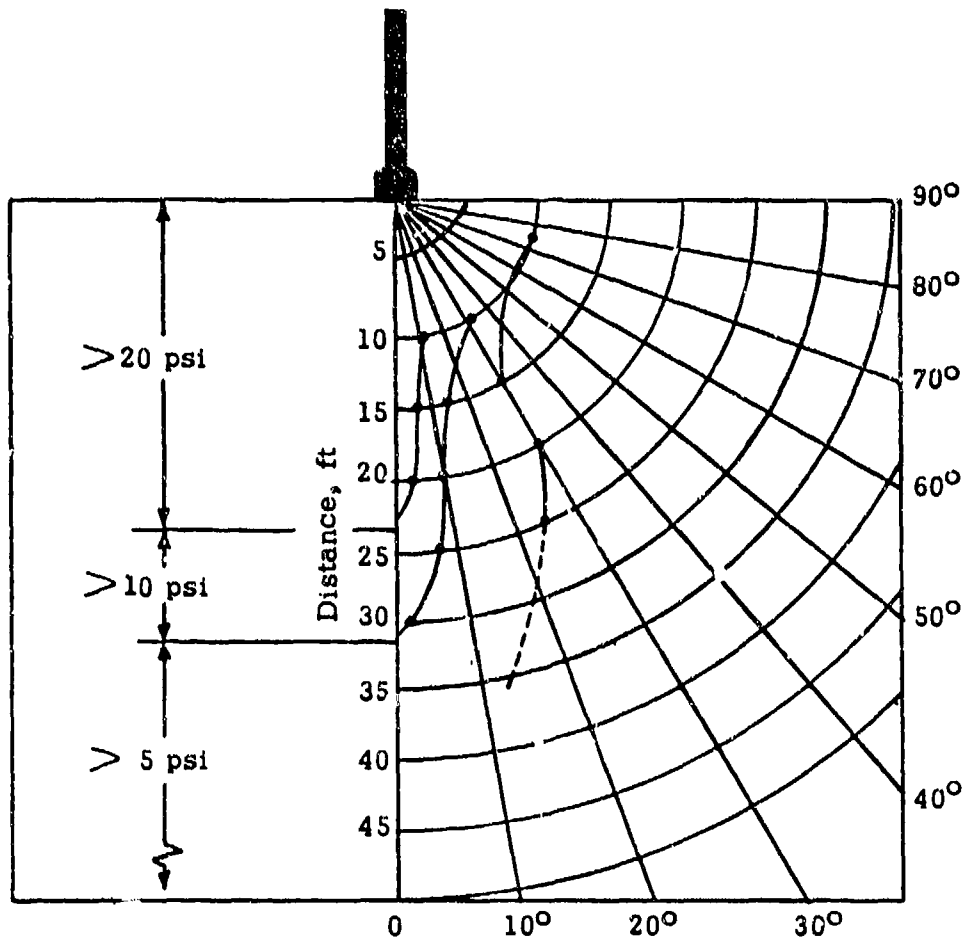


Figure 6-14. Peak Pressure Contours for Backblast of the 105 mm Recoilless Rifle, M27

lower than those obtained from the 75 mm Rifle T21. In particular, the maximum peak overpressure measured from the 105 mm rifle is about 25 psi at 7 to 8 ft from the nozzle, while that from the 75 mm rifle is approximately 32 psi at about the same distance. The charge weight for the M27 was 7.9 lb and for the T21 was 2.9 lb. The number of the nozzles for each rifle was 4. Fig. 6-14, given in Ref. 20, is a contour map of the peak pressures for the backblast of the 105 mm M27 Recoilless Rifle. It is seen from this figure that the pressures behind the M27 are very high at distances of less than 15 ft from the breech, near the line of fire. Twelve feet to either side of the line of fire and to

distances greater than 35 ft back, the pressures rise to more than 5 psi above ambient. For pressures greater than 10 psi, these distances are 5 ft to either side of the line of fire and 30 ft along the rifle axis.

Correlation of the wide range of experimental results of such blast studies with a theoretical model, which is based on shock sphere energy (and, ultimately, on chamber pressure and nozzle size) and which also includes a factor to account for the effect of directivity, appears to be reasonably good except in regions close to the nozzle (see Ref. 18).

6-21.2 DANGER AREAS

Both personnel and materiel in the immediate vicinity of a recoilless rifle must be protected from the dangerous effects of the blast from its nozzle. Results of an experimental investigation of the physiological effects of such blasts on goats have been reported in Ref. 22. The following are the conclusions of this investigation.

1. The danger areas behind recoilless rifles have roughly a tear-drop shape; the danger decreases as one goes farther behind the gun and farther off the gun axis.

2. The maximum backward extent of the danger zone occurs on the gun axis and extends to about 30 ft for the 57 mm and to about 80 ft for the 75 mm and the 105 mm rifles.

3. At its widest extent, the danger area reaches about 8 ft on either side of the axis for the 57 mm rifle and about 15 ft on either side of the axis for the 75 mm and the 105 mm rifles.

4. The most important single injuring factor is the missile effect of unburned propellant expelled at high velocity from the breech of the rifle, and it is this factor that determines the maximum extent of the danger areas.

5. The back jet of high velocity air and gases is very dangerous within about 10 deg either side of the gun axis up to distances of about 30 ft for the 75 mm and the 105 mm rifles, and up to about 10 ft for the 57 mm rifle.

6. During backblast, conditions are probably incompatible with life on the axis of the rifle within about 5 ft of the 57 mm rifle and within about 20 ft of the 75 mm and the 105 mm rifles. Here, back jet and propellant missile effects combine to cause extremely serious injury or death.

7. Improvement in efficiency of propellant burning should result in reduction of the extent of the danger areas.

8. Flame (flash) present in backblast presents an extremely minor hazard for the animal body, whether clothed or unclothed.

9. Blast pressure waves may cause injury to the unprotected ear even in those locations near the rifle that are outside the danger areas found in Ref. 22.

10. The danger region extends from the ground to a height of at least 6 ft.

11. The danger areas for the 75 mm and the 105 mm recoilless rifles are closely similar in extent. The danger zones for the 57 mm rifle extend over a region the dimension of which is about half as large in any direction as the corresponding ones for the two larger caliber rifles.

It is recommended that attempts be continued to improve the efficiency of burning of the propellant since unburned propellant is the most important single factor in determining the maximum extent of danger regions.

6-21.3 DUCTING

Apart from physiological damage due to the blast from the nozzle of a recoilless rifle, there is the danger of structural damage. In certain recoilless rifle applications—e.g., in such enclosed installations as aircraft and helicopter fuselages, and tank turrets—it is necessary to devise methods of conducting and diverting the backblast of the nozzle gases out of the inclosure. These methods usually consist of the channelling of the nozzle gases through metal ducts and are known as ducting. The purpose of ducting is to divert the flow and also tend to dissipate the shock wave of the blast in such a way as to protect personnel and structures in the immediate area of the rifle. Ducting of the recoil

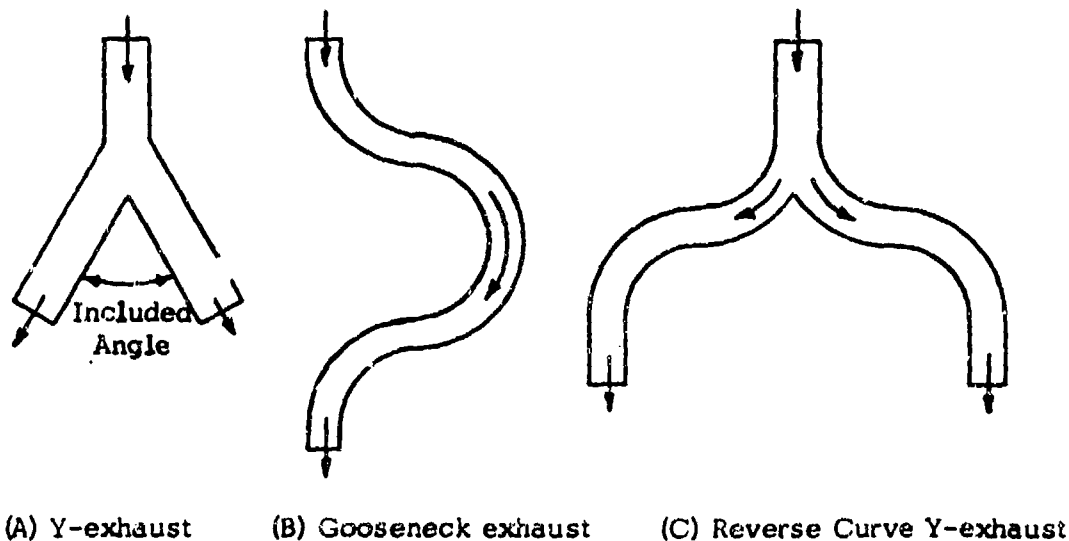


Figure 6-15. Typical Ducting Configurations

compensating gases is employed also in front-orifice type of recoilless rifles (Ref. 26) that differ from the conventional type of rear-orifice rifles in that the propellant gases used to achieve recoil balance are bled from the forward end of the chamber, thus providing for simple breech mechanisms as in the case of the closed breech guns.

Typical ducting configurations include the Y-exhaust, the gooseneck exhaust, and the reverse curve Y-exhaust which are illustrated in Fig. 6-15.

The principal effects of ducting are on the recoil and performance of the rifle, and on the structural integrity of the ducts. In the event the gas flow from the nozzle into the ducts is subsonic, the disturbances of the ducts are propagated upstream and, through a time lag, are felt at the chamber. The result is a direct influence of ducting on the pressure-time history of the rifle chamber. This, in turn, affects the motion of the projectile in the barrel and, ultimately, the muzzle velocity.

In the event the gas flow through the ducts

is supersonic, flow disturbances cannot be propagated upstream and the ducts can only influence the pressure-time history of the chamber if shock waves develop and travel toward the chamber and render the flow subsonic. The prediction of the formation of shock waves in ducted flow and that of the influence of the subsonic duct flow, requiring unsteady flow analyses, on rifle performance are far from being developed in sufficiently simplified form for handbook use. In order to determine these factors and the effect of ducting on recoil, use must be made of rigorous gas dynamic analyses together with experimental data. However, as a reasonable guide, some simplified results for the Y-duct configuration given in Ref. 26 can be used to determine the effect of ducting on recoil. Obviously, a minimum quantity of gases need to be bled from the rifle if the forks of the Y-ducting are parallel to the rifle axis. In the event of an included angle between the forks, an additional amount of gases is required to be bled off in order to insure recoillessness of the rifle. These additional gases come from an increase in the amount of the propellant used. Table 6-6 (see Ref. 26) shows the percent increase in the weights of ammunition and

TABLE 6-6
 INCREASE IN CHARGE AND AMMUNITION
 WEIGHTS—Y-DUCT COMPARED WITH
 CASE OF ZERO INCLUDED ANGLE

Included Angle, deg	Increase in Charge Weight, %	Increase in Ammuni- tion Weight, %
0	0	0
10	1.1	0.3
20	3.7	1.4
30	9.1	3.4

charge associated with the Y-duct as compared with the case in which the included angle is zero.

The structural integrity of the duct is determined by the geometry of the duct and the characteristics of the ammunition interior ballistics. In addition to the possibility of bursting due to high pressures, a curved duct can be subjected to moderate tensile and shear loads, and large bending moments as a result of the centrifugal action of the mass flow through the duct and has the tendency to straighten itself out. This holds true whether the curved duct is composed of continuously smooth or piecewise smooth curves. In general, evaluation of the dynamic loading in curved ducts is a difficult problem because the flow is of a complicated nature. In addition to the axial flow along the duct, there arises a secondary flow in each plane of

the cross section of the duct, called circulatory motion. This vorticity, the existence of shock waves, and effects of viscosity and of heat transfer contribute to the complexity of the flow pattern. However, a rough theory of the effects of the changes in the direction of gas flow—which impose centrifugal thrusts on the duct systems, thus producing shearing, tensile, and bending stresses—is outlined in Ref. 27 to deal with the problems of loading and induced stresses in the system. In this simplified procedure, each of the components of the more complex shapes—which may consist of such elements as a nozzle, straight-pipe section, curved sections, abrupt changes of direction, increases in pipe sections, diverging pipes—is considered separately with respect to the gas thrusts introduced by each of the elements, and these separate pieces are then combined to obtain the load on the entire system. The stresses induced as a result of the loading due to gas thrusts are determined at various sections of interest by methods of the elementary theory of strength of materials. Some safety factor for the effects of impact loading, shock compression, and nonstationary flow should be included.

Ref. 27 also gives illustrations of this procedure in dealing with the stresses induced in a gooseneck exhaust and a reverse curve Y-exhaust, together with a discussion of a Y-exhaust design. It is concluded that the level of these stresses can be very high, and adequate structural strength must be incorporated in the design of ducting.

REFERENCES

1. A. B. Cambel and B. H. Jennings, *Gas Dynamics*, McGraw-Hill Book Company, New York, 1958.
2. C. P. Sutton, *Rocket Propulsion Elements*, John Wiley & Sons, Inc., New York, 3rd Ed., 1963.
3. C. R. Foster and F. B. Cowles, *Experimental Study of the Divergence Angle Effect in Rocket-Motor Exhaust Nozzles*, Jet Propulsion Laboratory, California Institute of Technology, Progress Report No. 20-134, January 1952.

4. H. G. Krull, W. T. Beale and R. F. Schmiedlin, *Effect of Several Design Variables on Internal Performance of Convergent-Plug Exhaust Nozzles*, NACA RM E56G20, October 1956.
5. K. Berman and F. W. Crimp, Jr., "Performance of Plug-Type Rocket Exhaust Nozzles", *ARS Journal*, Vol. 31, January 1961, pp. 18-23.
6. A. Fern, *Application of the Method of Characteristics to Supersonic Rotational Flow*, NACA Report 841, September 1946.
7. R. Sauer, *Method of Characteristics of Three-Dimensional Axially Symmetric Supersonic Flows*, NACA TM1133, January 1947.
8. L. L. Cronvich, "A Numerical-Graphical Method of Characteristics for Axially Symmetric Isentropic Flow", *Journal of the Aeronautical Sciences*, Vol. 15, No. 3, March 1948, pp. 155-162.
9. I. L. Warren, R. B. Abbadessa and G. J. Pietrangeli, *Application of the Method of Characteristics to the Supersonic Rotational Flow Through a Circular Conical Inlet*, CM-668, Applied Physics Laboratory, The Johns Hopkins University, September 1951.
10. G. V. R. Rao, "Approximation of Optimum Thrust Nozzle Contour", *ARS Journal*, Vol. 30, June 1960, p. 561.
11. J. M. Farley and C. E. Campbell, *Performance of Several Method-of-Characteristics Exhaust Nozzles*, NASA TND-293, October 1960.
12. G. V. R. Rao, "Recent Developments in Rocket Nozzle Configurations", *ARS Journal*, Vol. 31, No. 1 November 1961, pp. 1488-1494.
13. L. H. Back, R. F. Cuffel, and P. F. Massier, "Influence of Contraction Section Shape and Inlet Flow Direction on Supersonic Nozzle Flow and Performance", *Journal of Spacecraft and Rockets*, Vol. 9, No. 6, June 1972, pp. 420-427.
14. *Symposium on Nozzle Design for Recoilless Rifles*, Supplement Report, Pitman-Dunn Laboratories, Frankford Arsenal, Philadelphia, Pa., 10-11 December 1951, 40 pp.
15. *Development of 105 mm Battalion Anti-tank Weapons and Interior Ballistics for the Design of Recoilless Rifles*, Final Report, Contract No. DA-11-022-ORD-1157, Armour Research Foundation of Illinois Institute of Technology, Chicago, Ill., December 15, 1955, 160 pp.
16. *Recoilless Weapons, Vol. II, Nozzles, A Symposium*, Contract No. W-36-034-ORD-7652, W-36-034-ORD-7708, The Franklin Institute Laboratories for Research and Development, Philadelphia, Pa., for Ordnance Department, U S Army, March 15, 1948.
17. *Nozzle Erosion Studies*, Final Report, Contract No. DA-11-022-ORD-10, Armour Research Foundation of Illinois Institute of Technology, Chicago, Ill., for Frankford Arsenal, Philadelphia, Pa., December 20, 1951.
18. *Investigation of the Effect of Blast from Recoilless Rifles*, Final Report, Contract No. DA-11-022-ORD-1227, Armour Research Foundation of Illinois Institute of Technology, Chicago, Ill., June 30, 1954, 55 pp.
19. C. N. Kelber and R. D. Koenitzer, *Blast Field Behind a 75 mm M20 Recoilless Rifle*, Frankford Arsenal Report No.

- R-1145, August 1953, 18 pp., Pitman-Dunn Laboratories, Frankford Arsenal, Philadelphia, Pa.
20. C. N. Kelber, *Blast Field Behind a 105 mm M27 Recoilless Rifle* Frankford Arsenal Report No. R-1162, August 1953, 8 pp., Pitman-Dunn Laboratories, Frankford Arsenal, Philadelphia, Pa.
21. C. N. Kelber, et al., *Recoilless Rifle Systems Ammunition and Related Items, Status Report Vol. I, No. 2*, Frankford Arsenal Report No. R-1145, December 1952, 149 pp., Frankford Arsenal, Philadelphia, Pa.
22. A. J. Dziemian, et al., *Recoilless Rifle Backblast Danger Areas*, Medical Laboratories Research Report No. 72, Army Chemical Center, Chemical Corps, Medical Laboratories, Maryland, July 1951, 69 pp.
23. *Report on Blast Injuries*, National Research Council, Division of Medical Sciences, Office of Medical Information, 11 June 1943.
24. E. S. Love, C. E. Grigsby, L. P. Lee, and M. J. Woodling, *Experimental and Theoretical Studies of Axisymmetric Free Jets*, Technical Report R-6, NASA, 1959.
25. S. P. Carfagno, *Handbook on Gun Flash*, Prepared for Ammunition Branch, Office of Chief of Ordnance, U S Army, The Franklin Institute, Philadelphia, Pa., 1961.
26. *Front Orifice Recoilless Rifles*, OEA Document No. 6184, Ordnance Engineering Associates, Inc., Chicago, Illinois, August 1961.
27. W. J. Kroeger, *The Piping of Recoilless Gun Gases Through Straight Channels and Bends*, Report No. R-860, July 1948, 26 pp., Pitman-Dunn Laboratories, Frankford Arsenal, Philadelphia, Pa.
28. AMCP 706-255. Engineering Design Handbook, *Spectral Characteristics of Muzzle Flash*
29. AMCP 706-251. Engineering Design Handbook, *Muzzle Devices*.

BIBLIOGRAPHY

Symposium on Nozzle Design for Recoilless Rifles, Pitman-Dunn Laboratories, Frankford Arsenal, Philadelphia, Pa., 10-11 December 1951, 205 pp.

AMCP 706-150, Engineering Design Handbook, Ballistics Series, *Interior Ballistics of Guns*.

AMCP 706-107, Engineering Design Handbook, *Elements of Armament Engineering, Part Two, Ballistics*.

L. W. Nordheim, H. Soodak, and G. Nordheim, *Thermal Effects of Propellant Gases in Erosion Vents and in Guns*, Report No. A-262, National Defense Research Committee, Duke University, May 1944.

J. Matsushino and C. F. Price, *Investigation of the Effect of Blast From Recoilless Rifles*, Reports 1 through 12, Armour Research Foundation of Illinois Institute of Technology, Chicago, Ill., May 1953 to April 1954.

R. L. Olson and A. D. Kafadar, *Special Report on Recoilless Rifles for Navy BUORD*, Mechanics Research Department, American Machine and Foundry Company, Chicago, Ill., 4 April 1957, 19 pp.

J. R. Zimmerman and R. A. Vecchio, *Back Blast Determination of a 105 mm Recoilless Rifle for An Aerial Artillery Weapon System*, Technical Report 3420, Picatinny Arsenal, Dover, New Jersey, August 1966, 124 pp.

R. D. Meade and R. T. Eckenrode, *Psychological and Physiological Effects of Gun Blast with Special Reference to Recoilless Rifles, A Preliminary Literature Survey*, Human Engineering Report No. 7, Frankford Arsenal Report No. R-1283, Pitman-Dunn Laboratories, Frankford Arsenal, Philadelphia, Pa., September 1955, 34 pp.

J. J. Donnelly and G. Schechter, *Firing Tests of*

Duct for Discharging Nozzle Gases from Recoilless Guns in Enclosed Installations, Report No. R-861, Frankford Arsenal, Philadelphia, Pa., July 1948, 49 pp.

Recoilless Rifle Handbook (Unpublished), Prepared at Frankford Arsenal, Philadelphia, Pa.

CHAPTER 7

SYSTEM EFFECTIVENESS

7-0 LIST OF SYMBOLS

A	= presented area of target, in. ²	V	= muzzle velocity, fps
A_v	= vulnerable area of target, in. ²	w	= angle of fall, deg
$E(K)$	= expected number of personnel incapacitations within an area target, dimensionless	x	= horizontal target coordinate, ft
L_A	= lethal area, in. ²	y	= vertical target coordinate, ft
p_H	= total hit probability, $p_H = p_v p_h$, dimensionless	\bar{x}, \bar{y}	= mean values of target coordinate, ft
p_h	= horizontal hit probability, dimensionless	δ_h	= mismatch between main and spotting rifle in horizontal direction, ft
P_K	= kill probability, dimensionless	δ_v	= mismatch between main and spotting rifle in vertical direction, ft
$p_{K H}$	= conditional probability of a kill given a hit on target, dimensionless	σ_x^2	= total variance in horizontal direction, ft ²
p_v	= vertical hit probability, dimensionless	$\sigma_{x_i}^2$	= i th variance of the n independent sources of error in horizontal direction, ft ²
$p(x)$	= Gaussian hit probability density function in horizontal direction, ft ⁻¹	σ_y^2	= total variance in vertical direction, ft ²
$p(y)$	= Gaussian hit probability density function in vertical direction, ft ⁻¹	$\sigma_{y_i}^2$	= i th variance of the n independent sources of error in vertical direction, ft ²
$p_K(x, y)$	= probability of kill function for a hit at point (x, y) , dimensionless	σ_x	= standard deviation in horizontal direction, ft
R	= range, ft	σ_y	= standard deviation in vertical direction, ft
		$\sigma(x, y)$	= density of personnel targets within area A , in. ⁻²

SECTION I

INTRODUCTION

A comparison of similar weapon systems is made by examining the effectiveness by which each weapon system defeats a specific type of target. There are several ways to measure effectiveness, but in most cases it is defined as the ratio of target damage to unit cost. This chapter will discuss the manner in which target damage (kill probability) is determined. Unit cost usually is measured in dollars for munitions expended per killed target.

Single shot kill probability is defined as the product of hit probability and conditional probability of kill given a hit, and can be expressed as the probability that a particular weapon system with a prescribed method of employment will inflict a specified level of damage on a particular target. The determination of hitting and killing with a single round will depend on making certain assumptions and the type of target and gun-ammunition combination employed.

SECTION II

HIT PROBABILITY

7-1 GENERAL

Hit probability is defined as the probability of a hit or hits on a target occurring out of a given number of rounds fired at the target and thus, for a given weapon system, depends only on the target size and the overall weapon dispersions (scattering of shots due to unavoidable variations). In determining the probability of hitting a particular target, it is assumed that the distribution of impact points about the aiming point is a Gaussian (normal) distribution. It also is assumed that the vertical and horizontal dispersions are statistically independent so that the probability density functions of a Gaussian distribution in the horizontal and vertical directions are (Ref. 1):

$$p(x) = \frac{1}{\sigma_x \sqrt{2\pi}} \exp\left[-\frac{(x - \bar{x})^2}{2\sigma_x^2}\right]$$

(horizontal), ft⁻¹ (7-1)

$$p(y) = \frac{1}{\sigma_y \sqrt{2\pi}} \exp\left[-\frac{(y - \bar{y})^2}{2\sigma_y^2}\right]$$

(vertical), ft⁻¹ (7-2)

where

\bar{x}, \bar{y} = mean values, ft

σ_x^2, σ_y^2 = variances, ft²

The variance σ_x^2 is the mean-square value of x about the mean \bar{x} and is given by the following equation:

$$\sigma_x^2 = \int_{-\infty}^{+\infty} (x - \bar{x})^2 p(x) dx, \text{ ft}^2 \quad (7-3)$$

The square root of the variance is the standard deviation σ .

The standard deviation for the weapon system is usually a combination of various sources of error. If $\sigma_{x_i}^2$ is the variance of one of n independent sources of error in the horizontal direction, then the combined standard deviation σ_x is

$$\sigma_x = \left[\sum_{i=1}^n \sigma_{x_i}^2 \right]^{1/2} \quad (7-4)$$

and, similarly, in the vertical coordinate σ_y ,

$$\sigma_y = \left[\sum_{i=1}^n \sigma_{y_i}^2 \right]^{1/2} \quad (7-5)$$

7-2 SOURCES OF ERROR

Sources of errors that must be considered in determining hit probability are described briefly in the following paragraphs:

1. Vertical jump. Vertical deflections (jump) are caused by an upward flip of the gun tube as it reacts to the motion of the projectile while in the vicinity of leaving the muzzle.

2. Lateral jump. Lateral jumps are the horizontal deflections caused by the same reactions of the gun tube to the projectile as it leaves the gun muzzle.

3. Nonstandard conditions. Nonstandard

conditions are the variations in ambient weather conditions—such as temperature, air pressure, humidity, and wind.

4. Cant. Cant error is the horizontal deflection of the projectile due to a leaning or tilting to one side of the gun (i.e., the gun does not elevate in the true vertical plane).

5. Determination of target range. In the case of unaided, visual observations (no rangefinder), estimation of the target ranges causes deviations from the actual range.

6. Variation in muzzle velocity. Variation in muzzle velocity caused by gun tube wear and lot-to-lot variations in propellant performance result in vertical deviations in the trajectory.

7. Zeroing error. Zeroing errors, caused by both changing conditions during zeroing and firing for effect and observation error in zeroing, result in horizontal and vertical variations. Variations in cant, jump, and crosswind and range error are examples of changing conditions from round to round; while observation errors include the errors in estimating the center of impact of a group of shots and the error resulting from the fact that a finite number of rounds are used to establish the center of impact.

8. Gun laying error. Inability of the gunner to place the crosshairs of his sight precisely on the center of target results in gun laying errors.

9. Wind deflection. Wind deflection that results from day-to-day variation in wind.

10. Round-to-round dispersion. Round-to-round dispersion is the irreducible residual error that remains.

7-3 CALCULATION OF HIT PROBABILITY

7-3.1 GENERAL

Based on independence of the lateral and vertical dispersions and a rectangular target, the equation for calculating the total hit probability p_H is

$$p_H = p_v p_l \quad (7-6)$$

where

p_v = vertical hit probability

p_l = lateral hit probability

The overall error in each of the lateral and vertical directions in the target plane is then the square root of the sum of the individual component errors in their respective directions.

In order to calculate hit probability, certain assumptions have to be made as to what sources of error are present and how they are distributed for the specific weapon system. Sources of error as discussed in par. 7-2 can be categorized into either fixed biases, variable biases, or random errors:

1. Fixed biases. Defined as those errors inherent in a specific gun-ammunition design and implies that the nature and characteristic of the fixed bias are known. While a fixed bias may vary with target range, it is constant for a given target range and does not vary from occasion to occasion or round to round. An example of a fixed bias would be projectile drift.

2. Variable biases. Defined as those errors whose magnitudes are constant from round to round during a given firing but vary from occasion to occasion, such as crosswind and cant.

3. Random errors. Defined as those errors that vary from round to round during a given firing, gunner aiming being a prime example.

7-3.2 ERRORS ASSOCIATED WITH TYPE OF FIRE CONTROL SYSTEM

As to the types of fire control that are employed in the weapon system, recoilless rifles can be divided into two groups—either with or without a spotting rifle. Depending upon the type of fire control used, certain assumptions are made in order to perform the necessary error analysis.

1. Without Spotting Rifle. The total standard deviations for lateral and vertical directions of the mounted recoilless rifle without a spotting rifle become

$$\sigma_x(\text{total}) = (\sigma_{x_C}^2 + \sigma_{x_{JM}}^2 + \sigma_{x_W}^2 + \sigma_{x_Z}^2 + \sigma_{x_{RRM}}^2 + \sigma_{x_{AP}}^2)^{1/2} \quad (7-7)$$

where

$$\sigma_{x_Z} = (\sigma_{x_{FC}}^2 + \sigma_{x_{ZRRM}}^2 + \sigma_{x_C}^2 + \sigma_{x_{ZJM}}^2 + \sigma_{x_W}^2)^{1/2}$$

$$\sigma_y(\text{total}) = (\sigma_{y_{JM}}^2 + \sigma_{y_{MVM}}^2 + \sigma_{y_{RE}}^2 + \sigma_{y_Z}^2 + \sigma_{y_{AP}}^2)^{1/2} \quad (7-8)$$

where

$$\sigma_{y_Z} = (\sigma_{y_{FC}}^2 + \sigma_{y_{ZRRM}}^2 + \sigma_{y_{ZJM}}^2 + \sigma_{y_{RE}}^2 + \sigma_{y_{MVM}}^2)^{1/2}$$

Table 7-1 gives numerical values and definitions for the individual component errors for recoilless rifles without spotting rifles. The numerical values listed in Table 7-1 are believed to be descriptive of actual firing conditions. This group of error sources is fairly complete for describing first round accuracy, and the probability of hitting which is premised on the combination of these errors should be realistic (Ref. 2). Each error

source of Table 7-1 is assumed to occur at random and follows a normal distribution.

2. With Spotting Rifle. Inherent in the employment of a spotting rifle on a recoilless weapon is the elimination of errors due to ranging, and the addition of jump variation, muzzle velocity variation, and round-to-round dispersion of the subcaliber spotting ammunition. With the assumption of an "ideal" spotter system (no trajectory mismatch) the errors due to cant, range estimation, and crosswind are eliminated. This assumption is reflected primarily in zeroing error since the errors due to cant and crosswind are differential in nature if trajectory mismatch does exist.

The total standard deviations for lateral and vertical directions for a mounted recoilless rifle with a spotting rifle become

$$\sigma_x(\text{total}) = (\sigma_{x_{JM}}^2 + \sigma_{x_{JS}}^2 + \sigma_{x_{RRM}}^2 + \sigma_{x_{RRS}}^2 + \sigma_{x_{AP}}^2)^{1/2} \quad (7-9)$$

and

$$\sigma_y(\text{total}) = (\sigma_{y_{JM}}^2 + \sigma_{y_{JS}}^2 + \sigma_{y_{MVM}}^2 + \sigma_{y_{MVS}}^2 + \sigma_{y_{RRM}}^2 + \sigma_{y_{RRS}}^2 + \sigma_{y_{AP}}^2)^{1/2} \quad (7-10)$$

Table 7-1 also contains the magnitudes of errors associated with recoilless rifles which use spotting rifles.

3. Linearization of Error. As stated previously, in order to breakdown the errors into their components along the lateral and vertical directions, it is necessary first to convert all errors into linear errors. For example, some of the linear standard deviations of the errors in the vertical direction on the target plane are computed as follows (Ref. 2):

TABLE 7-1
MAGNITUDE OF ERRORS FOR CALCULATING HIT PROBABILITY (Ref. 2)

Source	Symbol	Standard Deviation	
		Vertical <i>y</i>	Horizontal <i>x</i>
Range estimation	σ_{RE}	21% $R^{a,c}$	-
Round-to-round, main weapon	σ_{RRM}	0.35 mil ^a 0.5 mil ^b	0.35 mil ^a 0.5 mil ^b
Round-to-round, spotting weapon	σ_{RRS}	0.5 mil ^b	0.5 mil ^b
Muzzle velocity, main weapon	σ_{MVM}	10 fps ^{a,b}	-
Muzzle velocity, spotting weapon	σ_{MVS}	10 fps ^b	-
Cant	σ_C	-	3 deg ^a
Wind	σ_W	-	11 fps ^a 1 fps ^b
Aim point	σ_{AP}	1.25 ft ^{a,b}	1.25 ft ^{a,b}
Fire control	σ_{FC}	0.1 mil ^{a,b}	0.1 mil ^{a,b}
Jump, main weapon	σ_{JM}	0.1 mil ^{a,b}	0.1 mil ^{a,b}
Jump, spotting weapon	σ_{JS}	0.1 mil ^b	0.1 mil ^b
Zeroing			
round-to-round, main weapon	σ_{ZPRM}	$\sigma_{RRM}/\sqrt{5}$ ^{a,b}	$\sigma_{RRM}/\sqrt{5}$ ^{a,b}
round-to-round, spotting weapon	σ_{ZRRS}	$\sigma_{RRS}/\sqrt{5}$ ^b	$\sigma_{RRS}/\sqrt{5}$ ^b
jump, main weapon	σ_{ZJM}	0.1 mil ^{a,b}	0.1 mil ^{a,b}
jump, spotting weapon	σ_{ZJS}	0.1 mil ^b	0.1 mil ^b

^aM18, M20 and M27 Rifles, i.e., rifles having no ranging device
^bM40 and M67 Rifles, i.e., rifles having a ranging device
^cR = range

$$\sigma_{yRE} = \sigma_{RE} \tan w$$

$$\sigma_{yRRM} = \sigma_{RRM} \times R$$

$$\sigma_{yRRS} = \sigma_{RRS} \times R$$

$$\sigma_{yMVM} = \left(\frac{\partial y}{\partial V}\right) \sigma_{MVM}$$

$$\sigma_{yMVS} = \left(\frac{\partial y}{\partial V}\right) \sigma_{MVS}$$

(7-11)

where

w = angle of fall, deg

R = range, ft

V = muzzle velocity, fps

7-3.3 LATERAL AND VERTICAL SINGLE SHOT HIT PROBABILITIES

It has been stated earlier that the delivery error can be characterized as being distributed normally in two dimensions, lateral and vertical. The single shot hit probabilities for the two fire control systems are presented.

1. Without Spotting Rifle. With the assumption of no fixed bias errors, in the case of the weapon without a spotting rifle, this establishes that the mean of the errors in the lateral and vertical directions will be at the center of the target ($x = 0, y = 0$). For the recoilless weapon without spotting system, the lateral p_h and vertical p_v single shot hit probabilities, assuming normal distribution of errors, for a target that extends from $-a$ to $+a$ along both x - and y -axes are

$$p_h = \frac{1}{\sqrt{2\pi}\sigma_x} \int_{-a}^{+a} \exp\left(-\frac{x^2}{2\sigma_x^2}\right) dx, \quad \text{dimensionless} \quad (7-12)$$

and

$$p_v = \frac{1}{\sqrt{2\pi}\sigma_y} \int_{-a}^{+a} \exp\left(-\frac{y^2}{2\sigma_y^2}\right) dy, \quad \text{dimensionless} \quad (7-13)$$

2. With Spotting Rifle. In the case of the recoilless rifle with spotter system, the lateral p_h and vertical p_v single shot hit probabilities, again assuming a normal distribution of errors, can be expressed as

$$p_h = \frac{1}{\sqrt{2\pi}\sigma_x} \int_{-a-\delta_h}^{a-\delta_h} \exp\left(-\frac{x^2}{2\sigma_x^2}\right) dx \quad (7-14)$$

$$p_v = \frac{1}{\sqrt{2\pi}\sigma_y} \int_{-a-\delta_v}^{a-\delta_v} \exp\left(-\frac{y^2}{2\sigma_y^2}\right) dy \quad (7-15)$$

where

δ_h = mismatch between main and spotting rifles in lateral (horizontal) direction, ft

δ_v = mismatch between main and spotting rifles in vertical direction, ft

The total single shot hit probability p_H is then the product of the separate single shot hit probabilities in the lateral and vertical directions, i.e., Eq. 7-6.

7-4 USE OF SPOTTING ROUND

7-4.1 GENERAL

As in all weapon systems, it is desirable to obtain a high first round hit probability when using recoilless weapon systems. In some of the antitank recoilless rifles, the trajectories are considerably arched and tend to reduce the first round hit probability unless the target range is known accurately. In order to supply range information, many recoilless rifles make use of a spotting system that consists of a small caliber semiautomatic spotting rifle rigidly attached to the major weapon.

The purpose of the spotting rifle is to fire a projectile containing a tracer in its base and an incendiary or spotting mix in its nose so that both the flight path and impact point are visible to the gunner. In operation, the gunner fires the spotting rifle until a hit on the target is obtained, whereupon the major weapon is fired. If the major projectile follows the same path as the spotting rifle, the target will be hit provided there is small dispersion with respect to target size. Ideally, the major weapon and spotting systems should be designed to obtain the same trajectory. The process of achieving this correspondence is known as matching. The difference between trajectory heights or horizontal positions is defined as mismatch.

One of the basic matching problems is caused by the difference in the exterior ballistics of the major and spotting rifle ammunition. Since the small spotting projectile decelerates more rapidly, it will fall below the major projectile trajectory if both projectiles are given the same muzzle velocity. In order to compensate for the difference in caliber, the spotting projectile often is fired with a higher muzzle velocity and at an elevation slightly less than the major weapon. The difference in elevation is built into the spotting rifle mount and is called bias. While

somewhat effective for short ranges, this type of fix becomes marginal for larger ranges and inadequate in the presence of moderate crosswinds.

One method that helps the smaller spotting projectile better maintain its original velocity, so as to make its flight velocities and times more equal to the major projectile, is to increase the ballistic coefficient of the spotting projectile. The ballistic coefficient of the spotting projectile can be increased in four ways: (1) better streamlining, (2) the use of higher density materials, (3) longer projectiles, and (4) larger caliber spotting projectiles.

The remaining matching problems are associated with recoilless rifles that employ

fin-stabilized projectiles. Fin-stabilized major projectiles with a slow right hand spin have a slightly nose-up attitude to the left of the projectile path, whereas most spin-stabilized spotting projectiles have a nose-up attitude to the right of the projectile path. In order to compensate for the aerodynamic forces that cause the spotting projectile to curve to the right, it is necessary to introduce a small bias angle in azimuth between the major and spotting rifles.

7-4.2 MAGNITUDE OF MISMATCH

Tables 7-2, 7-3, and 7-4 contain the calculated matching velocities, vertical and lateral bias angles, and the residual vertical and lateral mismatches for three major recoilless weapons with spotting rifle systems.

**TABLE 7-2
MAGNITUDE OF MISMATCH SYSTEM 1 (Ref. 3)**

Ammunition	Velocity, fps	Bias Angle, mil	
		Vertical	Horizontal
105 mm, HEAT, T119E11	1650		
Cal .50 ST, T189E1	1723	- 0.48	10.33
105 mm, HEP, T139E44	1635		
105 mm, HE, T268	1606		

Range, yd	Mismatch in Inches					
	T119E11 Minus T189E1		T189E1 Minus T139E44		T189E1 Minus T268	
	V	H	V	H	V	H
400	0.4	3.3	1.0	- 7.9	4.5	- 8.0
500	-0.4	3.6				
600	-0.8	3.5	3.5	-14.8	10.6	-14.9
700	-0.9	3.3				
800	-0.4	2.5	4.4	-24.1	12.7	-24.2
900	0.7	1.4				
1000	1.9	0.1	1.4	-36.9	6.5	-36.3
1100	1.2	-2.0				
1200	-2.1	-4.5	-4.7	-52.6	-13.0	-51.4

TABLE 7-3

MAGNITUDE OF MISMATCH SYSTEM 2 (Ref. 3)

Ammunition	Velocity, fps	Bias Angle, mil	
		Vertical	Horizontal
105 mm, HEAT, T119E11	1650		
Cal .50 ST, T189E1	1816	-1.27	10.30
105 mm, HEP, T139E1	1601		
105 mm, HE, T268	1660		

Mismatch in inches

Range, yd	T119E11 Minus T189E1		T189E1 Minus T139E44		T189E1 Minus T268	
	V	H	V	H	V	H
	400	-4.0	3.0	-6.0	-7.3	-3.7
500	-2.2	3.1				
600	-0.4	3.2	-5.3	-13.7	2.0	-13.9
700	1.4	2.9				
800	2.5	2.3	-2.1	-22.5	6.3	-22.7
900	2.4	1.1				
1000	1.1	0.0	1.0	-34.2	5.4	-34.1
1100	0.6	-1.6				
1200	-2.0	-4.1	2.8	-49.4	-5.2	-48.3

7-5 PROBABILITY OF HIT WITH RECOIL-LESS RIFLES**7-5.1 COMPARISON OF SIMPLE SIGHT AND SPOTTING ROUNDS**

Fig. 7-1 shows the hit probability vs range of a typical recoilless rifle with and without a spotting system. This figure definitely indicates the advantage of using a spotting rifle beyond the range of 400 yd.

7-5.2 PROBABILITY OF HIT FOR STANDARD WEAPONS

Figs. 7-2 through 7-9 show the results of first round hit probability computations for the set of error sources described in par. 7-3.2 as a function of range for eight standard recoilless rifles which can be divided into two groups according to their fire control. The

first group consists of first generation recoilless weapons that do not have a spotting device. This group of recoilless rifles firing spin-stabilized ammunition follows:

Rifle	Ammunition	Fig. No.
57 mm M18	M306A1 HE Projectile	7-2
57 mm M18	M307 HEAT Projectile	7-3
75 mm M20	M309 HE Projectile	7-4
75 mm M20	M310 HEAT Projectile	7-5
105 mm M27	M323 HE Projectile	7-6
105 mm M27	M324 HEAT Projectile	7-7

The second group of rifles consists of

TABLE 7-4
MAGNITUDE OF MISMATCH SYSTEM 3 (Ref. 3)

Ammunition	Velocity, fps	Bias Angle, mil	
		Vertical	Horizontal
105 mm, HEAT, T119E11	1650		
Cal .50 ST, T189E1	1626	2.44	10.72
105 mm, HEP, T139E44	1598		
105 mm, HE, T268	1522		

Range, yd	Mismatch in Inches					
	T119E11 Minus T189E1		T189E1 Minus T139E44		T189E1 Minus T268	
	V	H	V	H	V	H
400	-26.4	8.6	33.4	-13.5	45.0	-13.7
500	-29.0	11.1				
600	-28.9	11.4	44.7	-23.2	67.4	-23.6
700	-25.5	12.2				
800	-18.8	12.8	47.3	-35.3	85.2	-36.2
900	-9.0	12.9				
1000	3.4	12.5	38.8	-50.6	93.6	-51.6
1100	16.8	11.6				
1200	28.8	10.5	23.7	-70.3	88.8	-70.3
1300	33.9	8.6				
1400	27.8	6.4	6.2	-93.4	64.6	-92.4
1500	19.3	3.6				
1600	9.0	0.0	-8.9	-122.1	32.0	-118.1
1700	2.0	-4.1				
1800	-9.1	-8.6	-14.6	-156.4	-22.3	-147.5
1900	-21.4	-13.9				
2000	-30.7	-19.6	-11.5	-197.4	-100.7	-180.8

newer recoilless rifles that fire spin-stabilized ammunition and are equipped with a spotting rifle, i.e.,

Rifle	Ammunition	Fig. No.
90 mm M67	M371 HEAT Projectile	7-8
106 mm M40	M344 HEAT Projectile	7-9

As shown in Figs. 7-2 through 7-9 the weapon systems which employ spotting rifles have much higher first round hit probabilities than those rifles which rely on visual range estimation. Figs. 7-8 and 7-9 also show that the hit probabilities of those weapons with spotting rifles remain high even up to their maximum range.

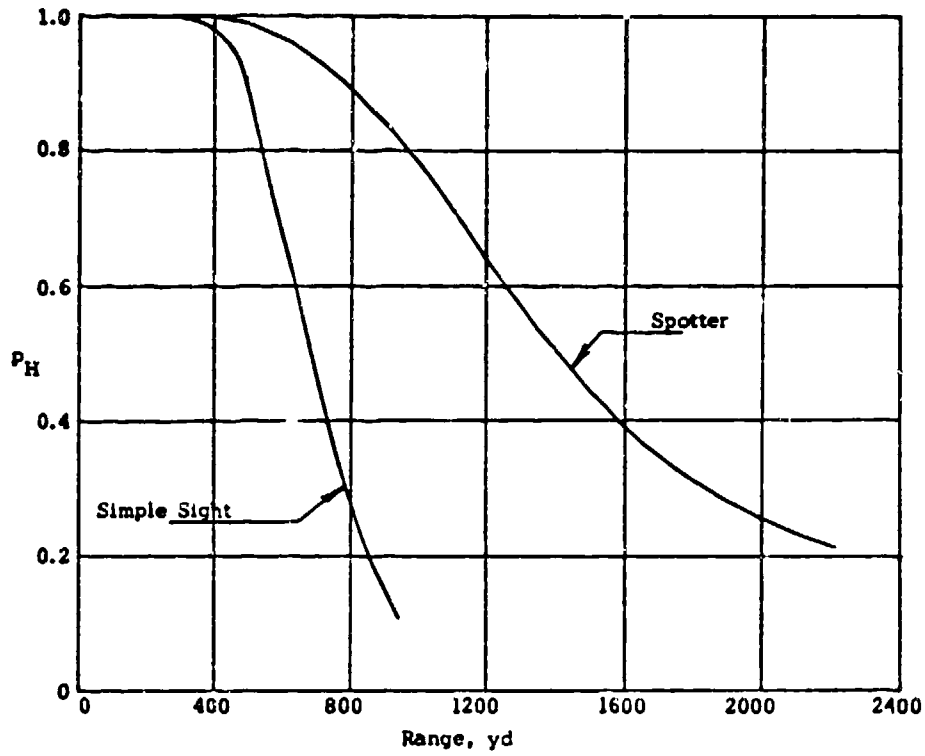


Figure 7-1. Comparison of Total Hit Probability p_H for Different Fire Control Systems as a Function of Range (Ref. 4)

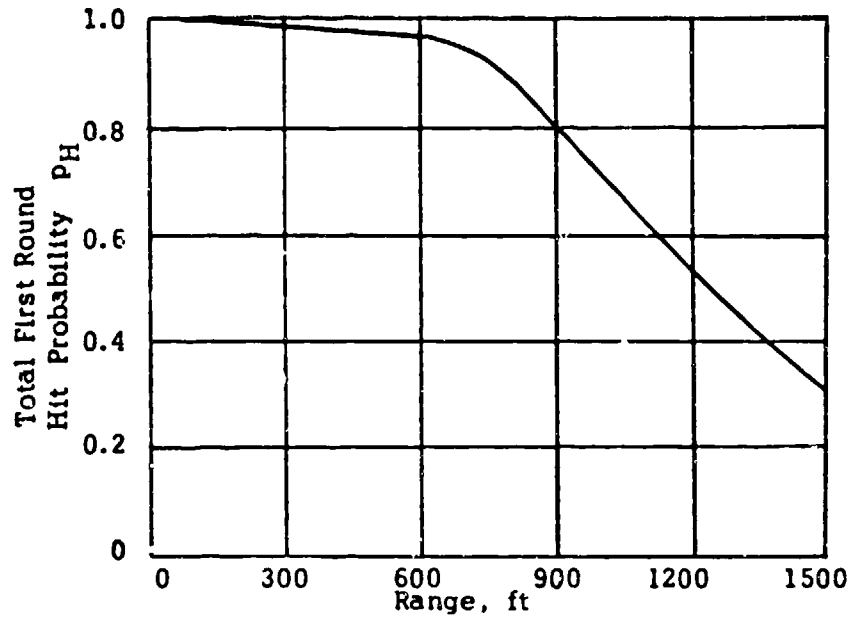


Figure 7-2. Probability of Hit - 57 mm M18 Rifle; M306A1 HE Projectile (Ref. 2)

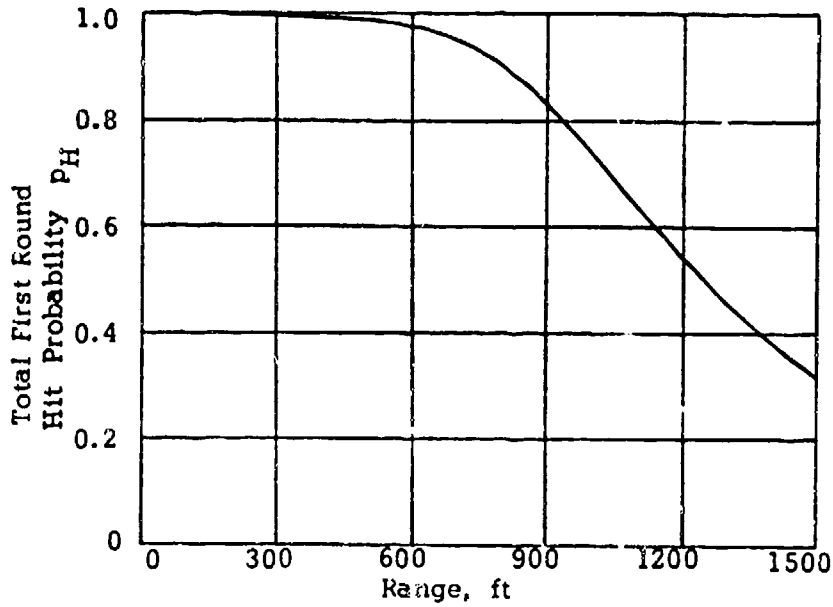


Figure 7-3. Probability of Hit – 57 mm M18 Rifle;
M307 HEAT Projectile (Ref. 2)

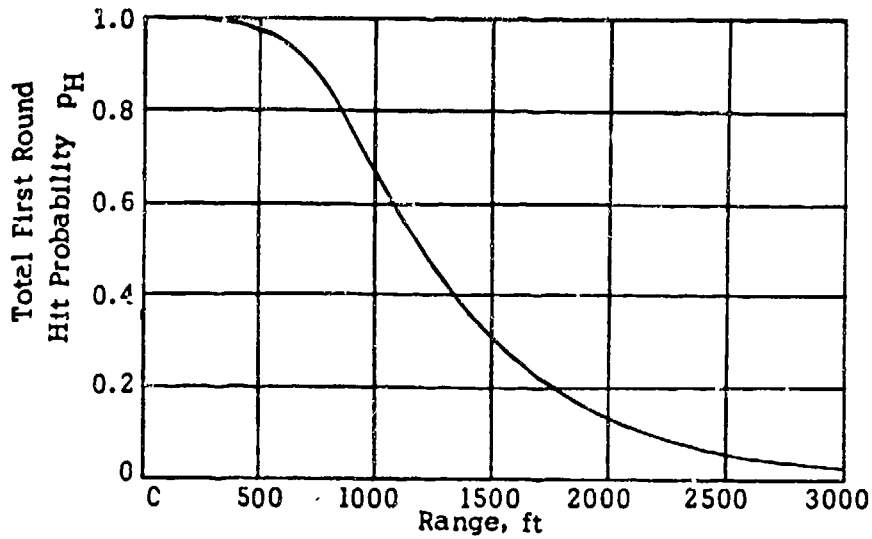


Figure 7-4. Probability of Hit – 75 mm M20 Rifle;
M309 HE Projectile (Ref. 2)

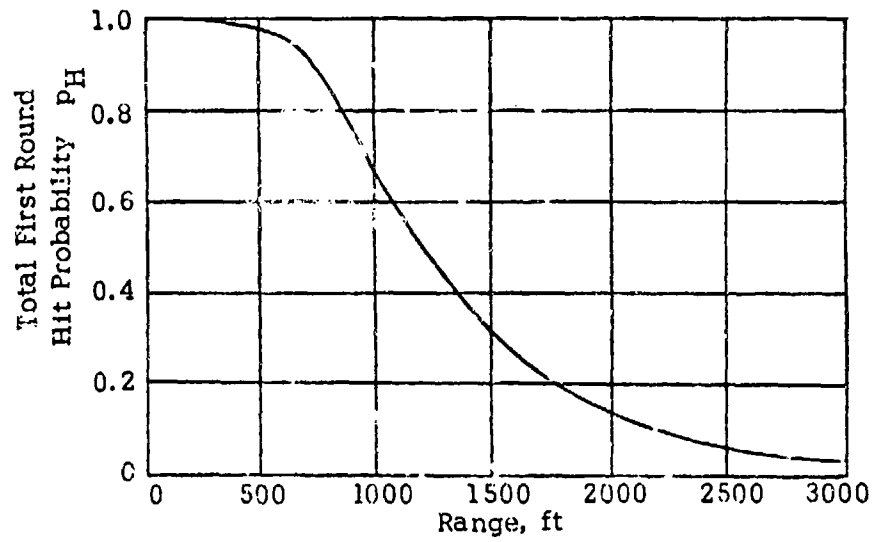


Figure 7-5. Probability of Hit – 75 mm M20 Rifle;
M310 HEAT Projectils (Ref. 2)

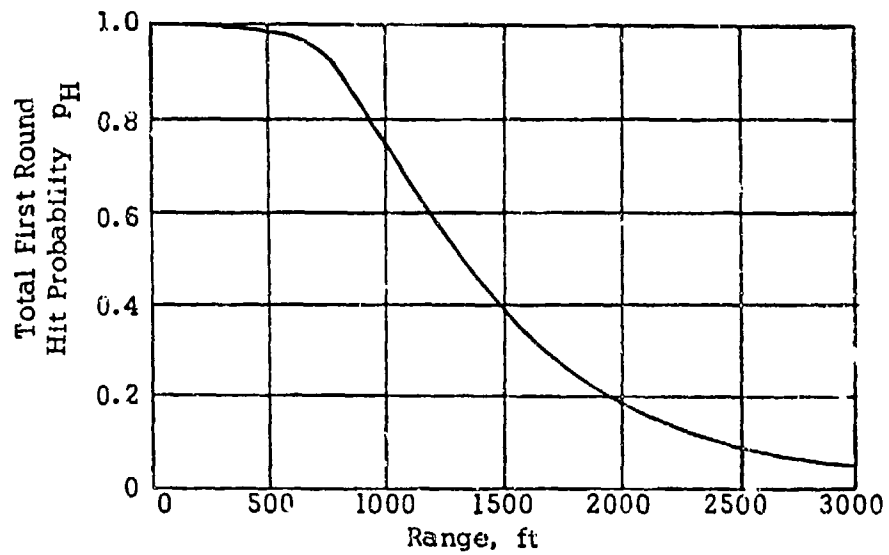


Figure 7-6. Probability of Hit – 105 mm M27 Rifle;
M323 HE Projectile (Ref. 2)

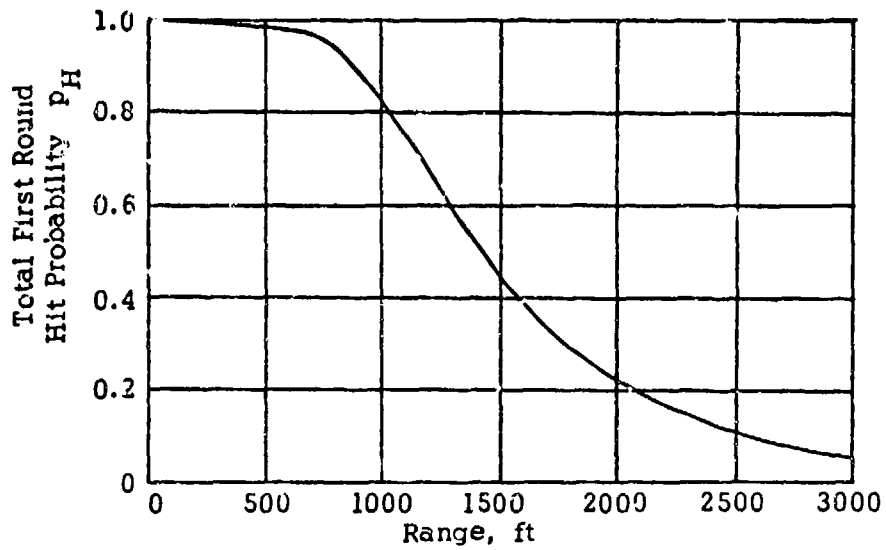


Figure 7-7. Probability of Hit - 105 mm M27 Rifle;
M324 HEAT Projectile (Ref. 2)

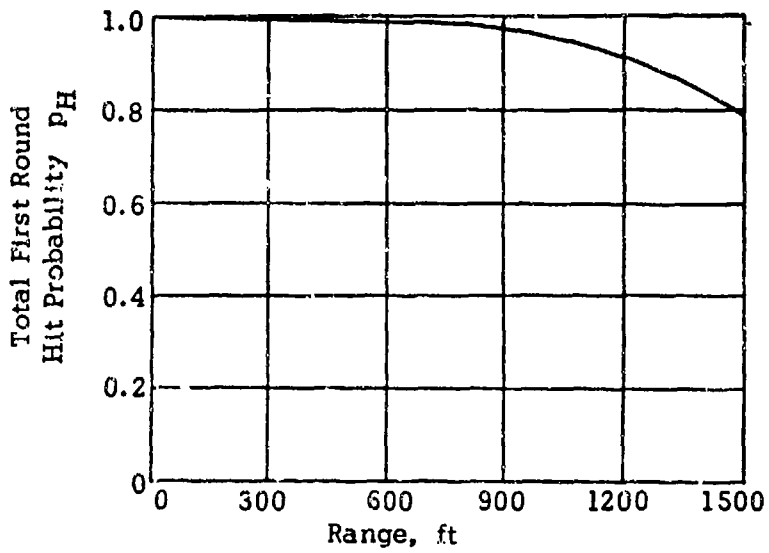


Figure 7-8. Probability of Hit - 90 mm M67 Rifle;
M371 HEAT Projectile (Ref. 2)

TABLE 7-5

SINGLE-SHOT HIT PROBABILITY—VISUAL RANGE ESTIMATION (Refs. 5 AND 6)

<u>Weapon</u>	<u>Velocity, fps</u>	<u>Range, yd</u>	<u>Single Shot Hit Probability p_H</u>
57 mm	1200	200	0.99
		400	0.37
		600	0.08
		800	0.02
75 mm	1000	200	0.89
		400	0.37
		600	0.11
		800	0.03
90 mm	700	100	0.99
		200	0.79
		300	0.30
		400	0.11
106 mm	1600	200	0.99
		400	0.62
		600	0.24
		800	0.12
		1000	0.07
		1200	0.04
	1400	0.02	

TABLE 7-6

SINGLE-SHOT HIT PROBABILITY—CRUDE RANGE FINDER (Refs. 5 AND 6)

<u>Weapon</u>	<u>Velocity, fps</u>	<u>Range, yd</u>	<u>Single Shot Hit Probability p_H</u>
57 mm	1200	200	0.99
		400	0.55
		600	0.26
		800	0.10
75 mm	1000	200	0.99
		400	0.57
		600	0.28
		800	0.11
90 mm	700	100	0.99
		200	0.81
		300	0.45
		400	0.26
106 mm	1600	200	0.99
		400	0.65
		600	0.39
		800	0.23
		1000	0.14
		1200	0.09
	1400	0.06	

TABLE 7-7

SINGLE-SHOT HIT PROBABILITY—SPOTTING RIFLE (Refs. 5 & 6)

Weapon	Velocity, f/s	Range, yd	Single Shot Hit Probability p_H
57 mm	1200	200	0.99
		400	0.95
		600	0.74
		800	0.49
		1000	0.26
		1200	0.15
75 mm	1000	200	0.99
		400	0.95
		600	0.77
		800	0.53
		1000	0.28
		1200	0.16
90 mm	700	200	0.99
		400	0.92
		600	0.56
		800	0.25
		1000	0.10
		1200	0.09
106 mm	1600	200	0.99
		400	0.97
		600	0.88
		800	0.72
		1000	0.50
		1200	0.37
		1400	0.26
		1600	0.18
		1800	0.12
		2000	0.09

7-5.3 PROBABILITY OF HIT AS A FUNCTION OF VARIOUS CONDITIONS

Tables 7-5 through 7-7 list typical single shot hit probabilities for several hypothetical recoilless rifle systems with either visual range estimation, crude range finder, or spotting rifle fire control systems.

7-5.4 PROBABILITY OF HIT AS A FUNCTION OF MUZZLE VELOCITY

Figs. 7-10 through 7-12 show the total

single shot hit probability, the total probability of at least one hit in two shots, and the total probability of at least one hit in three shots, respectively, as a function of muzzle velocity. These figures are based on calculations for a medium sized recoilless rifle with spotting rifle fired at a 7.5 ft by 7.5 ft vertical target. The independent and normally distributed quasi-combat errors assumed to cause impact deviations at the target are shown in Table 7-8. The quasi-combat errors listed in Table 7-8 are the errors expected in a typical combat situation.

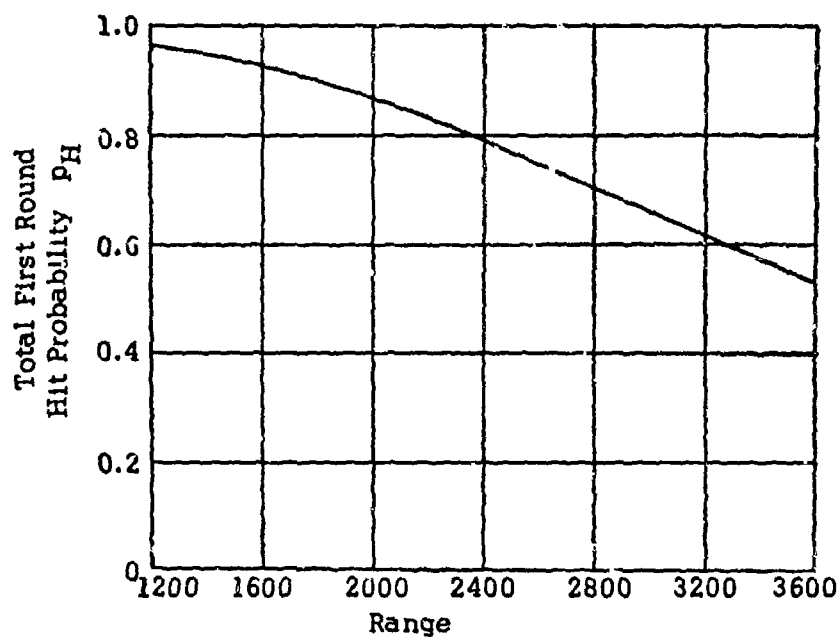


Figure 7-9. Probability of Hit -- 106 mm M40 Rifle;
M344 HEAT Projectile (Ref. 2)

TABLE 7-8

INDEPENDENT AND NORMALLY DISTRIBUTED QUASI-COMBAT ERRORS
ASSUMED TO CAUSE IMPACT ERRORS (Ref. 7)

Cause	Standard Deviation	
	Vertical	Horizontal
Round-to-Round, Main Weapon	0.5 mil	0.5 mil
Round-to-Round, Spotting Weapon	0.5 mil	0.5 mil
Jump, Main Weapon	0.25 mil	0.25 mil
Jump, Spotting Weapon	0.25 mil	0.25 mil
Muzzle Velocity, Main Weapon-to-Weapon	7.5 fps	-
Muzzle Velocity, Spotting Weapon-to-Weapon	7.5 fps	-
Aim Point	1.25 ft	1.25 ft
Crosswind	-	11 fps
Cant	-	40 mils

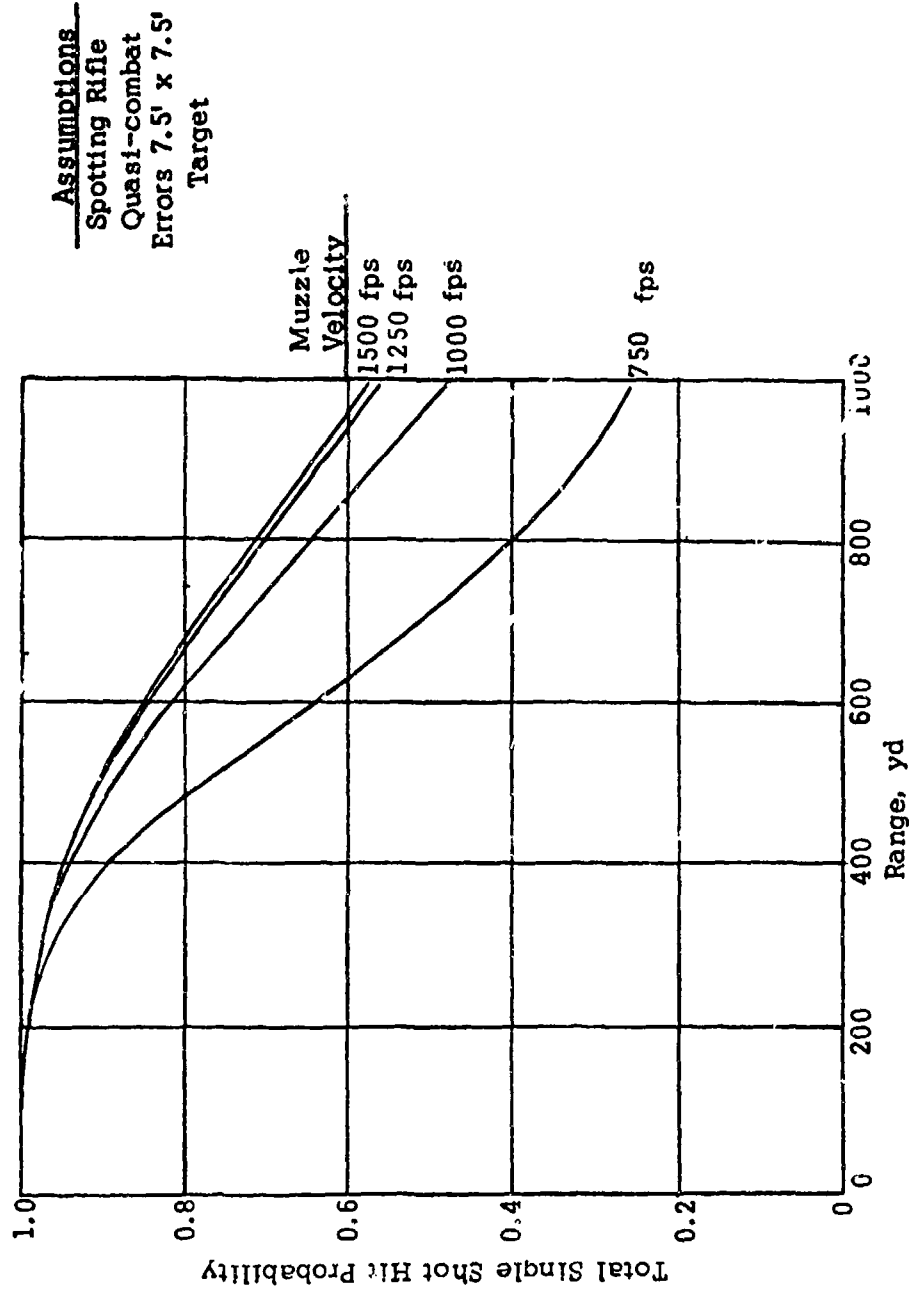


Figure 7-10. Effect of Muzzle Velocity on Single Shot Hit Probability (Ref. 7)

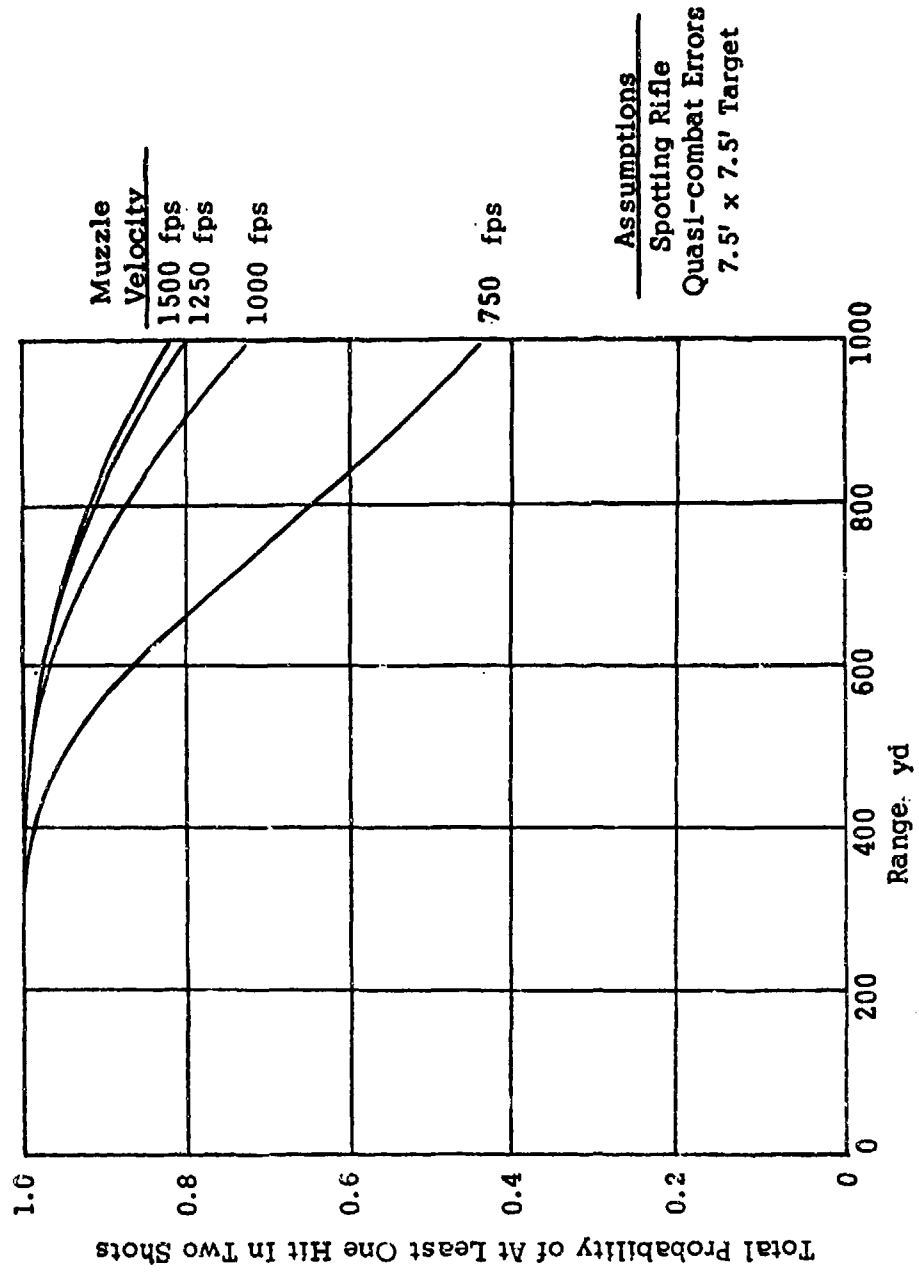


Figure 7-11. Effect of Muzzle Velocity on Probability of One Hit Out of Two Shots (Ref. 7)

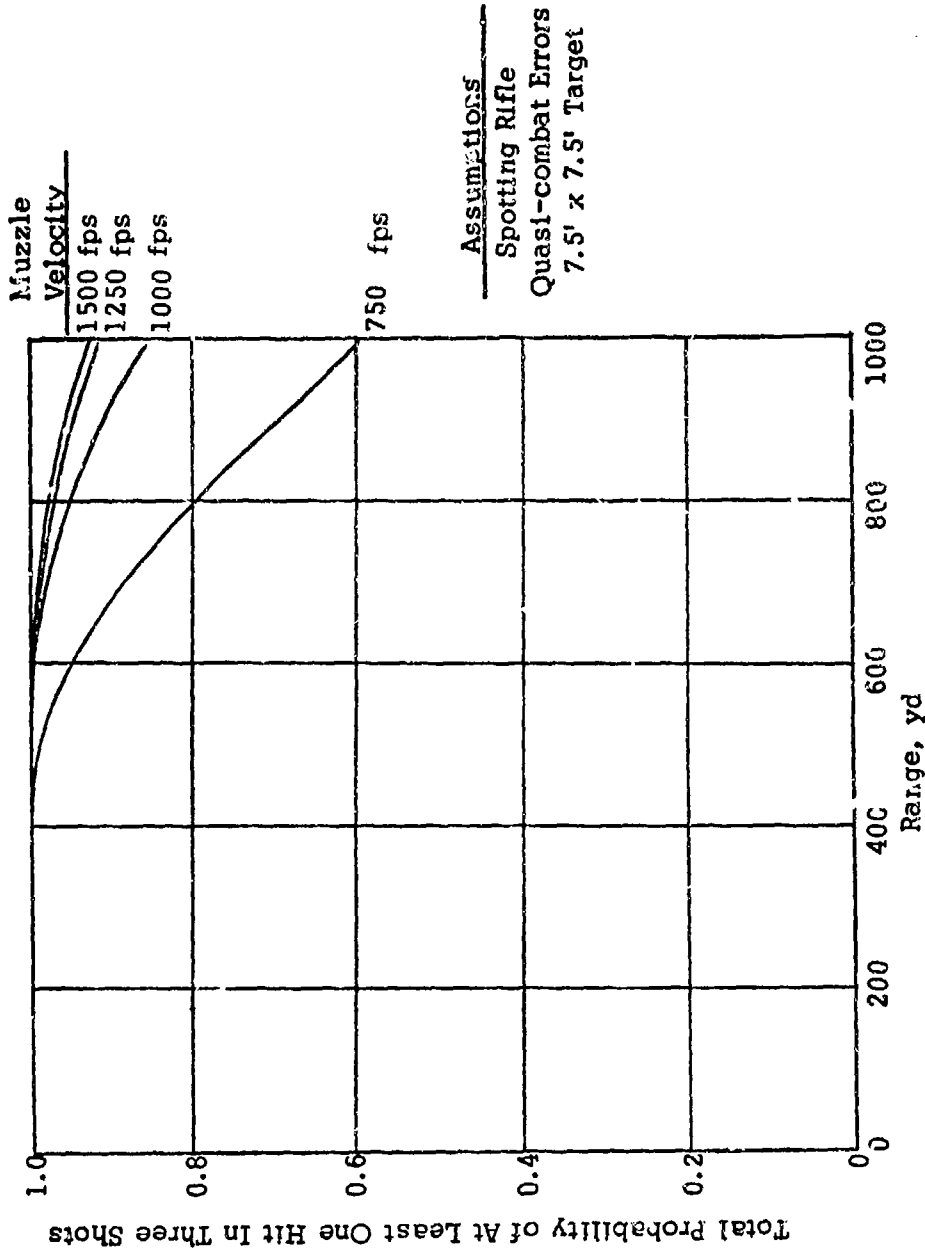


Figure 7-12. Effect of Muzzle Velocity on Probability of One Hit Out of Three Shots (Ref. 7)

SECTION III

KILL PROBABILITY

7-6 INTRODUCTION

Kill probability p_K is defined as the product of total hit probability p_H and conditional probability of a kill given a hit $p_{K|H}$, where kill means to destroy the target to the degree defined in par. 7-7.2. From this general definition it is seen that, given a hit on a target, the calculation of kill probability depends only on the type of warhead used against a specific type of target. In this general sense, kill probability is a measure of the effectiveness of the weapon system in that it involves the delivery accuracy of the weapon system and the lethality of the warhead on a particular target.

7-7 HARD TARGET

7-7.1 INTRODUCTION

Kill probability is dependent upon the particular type of target. The first type of target to be considered is the hard target that is typified by the type of target a tank presents. The hard target is small in dimensions in contrast to an area target over which personnel are scattered and, in general, requires a hit on the target in order for a kill to occur. Most hard targets are protected by some type of armor and generally will require penetration of the armor by a HEAT or HEP type warhead in order to defeat the target.

7-7.2 TYPES OF KILL

The three categories or types of kill of an armored target are defined (Ref. 8):

1. K Kill. The type of kill in which the

armored target is destroyed and is dependent to a great extent on the ignition of fuel or ammunition.

2. F Kill. The type of kill which causes complete or partial loss of the ability of the tank to fire its main armament and machine guns.

3. M Kill. The type of kill which causes immobilization of the tank.

As detailed in Refs. 8 and 9, a list of standard damage assessments can be established to be able to quantitatively define which type of kill has taken place.

7-7.3 VULNERABLE AREA

The vulnerable area of a target is defined as the product of the presented area of the target and the probability that a hit on the presented area will be a kill. Since the presented area of a particular target is known, the evaluation of the vulnerable area depends upon determining a value for the probability that a hit on the presented area will be a kill. Considering two types of warheads, HEAT and HEP, which could be used in attempting to defeat a hard target such as a tank, one can see that this probability function will depend on where a specific type of warhead strikes the target or if the warhead penetrates the armor. It will be necessary to know the probability of the warhead penetrating the armor at the specific point of the target and, if penetration occurs, the probability that the warhead will cause the defeat of essential components of the target. In certain areas of the tank, it will only be necessary for the

projectile to penetrate the armor in order to cause a kill, whereas hits on or near areas—such as the suspension and turret ring—may be enough to cause an M-type kill of the target.

Vulnerable areas are calculated separately for each of the three types of kill described in par. 7-7.2. The general method of calculating the vulnerable area of hard targets for HEAT and HEP type warheads is given in the next subparagraph.

7-7.4 CALCULATIONS OF KILL PROBABILITY

Kill probability with a single shot as earlier defined can be written in the following manner:

$$p_K = p_H p_{K|H} \quad (7-16)$$

where

p_K = kill probability

p_H = total hit probability

$p_{K|H}$ = conditional probability of a kill given a hit

The hit probability of any point on the target is determined by the methods described in Section II so that upon determining the value of $p_{K|H}$, the kill probability essentially is determined. The definition of vulnerable area A_v is

$$A_v = p_{K|H} A \quad (7-17)$$

where

A_v = vulnerable area, in²

A = presented area, in²

With Eq. 7-17, the kill probability can be

expressed as the product of the hit probability and the ratio of vulnerable area to presented area or

$$p_K = p_H \left(\frac{A_v}{A} \right) \quad (7-18)$$

More precisely, the vulnerable area for a two dimension target is given by the following relationship (Ref. 1):

$$A_v = \iint_A p_K(x, y) dx dy \quad (7-19)$$

where

x, y = coordinates centered at the center of gravity of the target and in a plane perpendicular to the projectile trajectory

$p_K(x, y)$ = probability of kill function for a hit at the point (x, y)

The probability-of-kill function $p_K(x, y)$ assigns a probability value that the target will be killed if there is a hit at the point (x, y) .

A complex target such as a tank can be considered to be made up of individual vulnerable components. If the components do not overlap or mask one another and are not redundant, the total vulnerable area is merely the sum of the vulnerable areas of these components.

In practice, vulnerability drawings of the target are prepared, showing the arrangement of the interior components to the line of fire. By use of an overlay grid, a conditional kill probability is entered into each square of the grid for a given point of aim. This probability value depends upon the damage that would result on the component behind the particular grid square as a result of a specific type of warhead striking the designated point (x, y) of the target and is determined from target

vulnerability studies and existing vulnerability data on similar components. The vulnerable area of the whole target for one of the three types of kill then would be computed by summation of the component vulnerable areas, taking into account masking and redundancy.

7-7.5 TYPICAL VALUES OF KILL PROBABILITY

Fig. 7-13 obtained from Ref. 7 shows the expected variation of kill probability with range, caliber, and muzzle velocity for several hypothetical recoilless weapon systems when fired against a JS III tank. The kill potential of these weapons was made on the basis of the quasi-combat error conditions as defined in par. 7-5.4. As shown in Fig. 7-13, the combined effect of caliber and muzzle velocity on the expected number of kills is clearly evident. As expected, the longer the range, the lower the kill probability and, for any selected value of range and muzzle velocity, the larger the caliber of the weapon, the higher its kill probability.

7-8 AREA TARGET

7-8.1 INTRODUCTION

The recoilless rifle weapon system also is employed in the defeat of personnel distributed over an area. This type of target is called an area target and is a definite contrast to the hard target described earlier. The area target is usually large in dimensions and, except for foxholes and cover by the natural terrain, there is no armored protection for the personnel within the area. The defeat of personnel in the area target is accomplished by the fragmentation of the HE type or antipersonnel type warheads.

7-8.2 LETHAL AREA

Evaluating the lethal area of a fragmenting projectile permits the prediction of how many

casualties a projectile will produce upon detonation under specified conditions. The basic concept used in arriving at a suitable lethality index is that of the expected number of incapacitations $E(K)$ of personnel targets which is given by

$$E(K) = \iint_A \sigma(x, y) p_K(x, y) dx dy \quad (7-20)$$

where $\sigma(x, y)$ is the density of the personnel targets and p_K is the probability of a target within area A being incapacitated from a hit at a point (x, y) . For a constant target density Eq. 7-20 becomes

$$E(K) = \sigma(x, y) \iint_A p_K dx dy \quad (7-21)$$

Lethal area L_A is

$$L_A = \iint_A p_K dx dy \quad (7-22)$$

The probability p_K is really the joint probability of the target being exposed, the target being hit if exposed, and the target being incapacitated if hit. The valuation of the function p_K depends upon the following parameters:

1. Projectile angle of fall
2. Projectile terminal velocity
3. Burst height
4. Projectile external geometry
5. Projectile internal geometry
6. Projectile casing composition
7. Projectile filler composition
8. Target presented area, which depends on:
 - a. target attitude
 - b. cover (natural or artificial)

Assumptions

D	P	K/H
mm		
90	0.5	
105	0.6	
120	0.7	

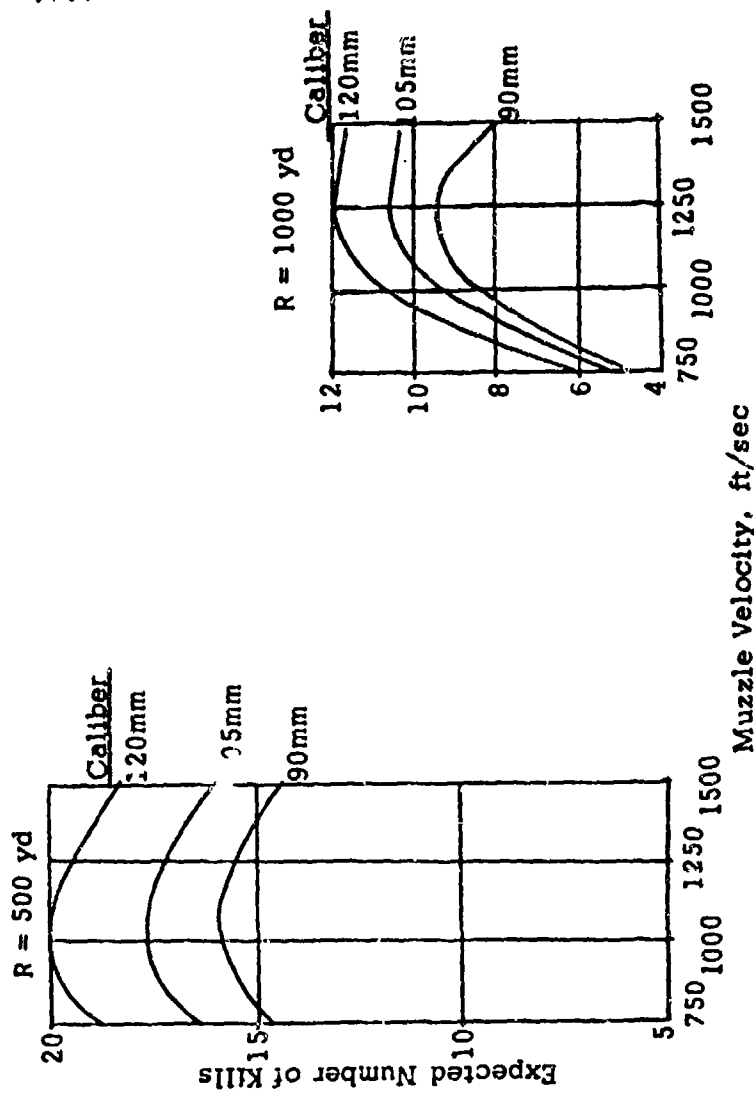


Figure 7.13. Variation of Expected Number of Kills With Range, Caliber, and Muzzle Velocity (Ref. 7)

c. fragment aspect angle

9. Target incapacitation criteria.

As seen from this list, the function p_K , and as a result L_A , is only a function of the warhead and target area characteristics and is independent of weapon accuracy.

REFERENCES

1. AMCP 706-327, Engineering Design Handbook, *Fire Control Series, Section 1, Fire Control Systems - General*.
2. David E. Walters and Edith F. Reilly, *Hitting Probabilities of the Standard Recoilless Weapons*, Memorandum Report M59-32-1, Frankford Arsenal, Research and Development Group, Philadelphia, Pa., June 1959.
3. AD 34245, *Symposium on Recent Progress of Recoilless Rifles and Ammunition*, Department of Army, January 1954.
4. *Recoilless Rifle Handbook* (Unpublished), prepared at Frankford Arsenal, Philadelphia, Pa.
5. AD 392 365, Frank A. Lepold, Jr. and Ned I. Yates, Jr., *An Effectiveness Study of Infantry Antitank Weapons*, Technical Memorandum No. 13, Aberdeen Proving Ground, Maryland, August 1968.
6. AD 351 905, Capt. L. R. Creelman, *A Parametric Study of the Probability of Hit of Unguided Ballistic Weapons*, Canadian Armament Research and Development Establishment, Valcartier, Quebec, March 1965.
7. *MAW Long Range Report 1303-20* (Unpublished), Frankford Arsenal, Philadelphia, Pa.
8. AMCP 706-245(C) Engineering Design Handbook, *Artillery Ammunition Series, Section 2, Design for Terminal Effects* (U).
9. AMCP 706-170(S), Engineering Design Handbook, *Armor and Its Applications* (U).

BIBLIOGRAPHY

- AD 119-560, *Estimates of a Spotting System for the T41 Light Tank*, Pitman-Dunn Laboratories Group, Frankford Arsenal, Memorandum Report MR-637, December 1956.
- An Analytical Comparison of Fin and Spin-Stabilized Spotting Projectiles for the Ultimate Battalion Antitank Weapon System, Phase Report No. 1*, Midwest Research Institute, Contract No. DA-23-072-ORD-901, for Frankford Arsenal, Philadelphia, Pa., 15 August 1955.
- AD 312-558, *Accuracy of the Recoilless Light Assault Weapon*.
- AD 3826, Helen J. Coon and Frank E. Grubbs, BRL Memorandum Report No. 636, *On Estimating Probabilities of Hitting for the Battalion Antitank Weapon*, January 1953.
- AMCP 706-107, Engineering Design Handbook, *Elements of Armament Engineering, Part Two, Ballistics*.
- David Walters, *A Spotting Rifle for the 90 mm Gun Mounted on the T42 Tank*, Report R-1123, Pitman-Dunn Laboratories, Frankford Arsenal, Philadelphia, Pa., April 1953.
- J. L. Wright, *Dynamic Tests for the Light Measurement on Caliber .50 Spotter-Tracer Ammunition*, Pyrotechnics Lab. Report

Picatinny Arsenal, Dover, N.J., September 1961.

R. T. Eckenrode, *The Spotting Technique*. Memorandum for Record, Project TS4-4020 Frankford Arsenal, Philadelphia, Pa., November 1954.

E. Arnold, *Sensitivity Test for Primer Compositions*, PIC Bulletin No. 10, Frankford Arsenal, Philadelphia, Pa., June 1942.

AD 153-036, Harold Brodtkin, *Fire Control Studies—Tank Gunnery Accuracy Evaluation*,

Report R-1380A, Frankford Arsenal, Philadelphia, Pa., February 1958.

D. E. Walters, *Hit Probability of T114 BAT Vehicle System*, Memorandum Report M63-8-1, Frankford Arsenal, Philadelphia, Pa., August 1962.

D. E. Walters and E. F. Reilly, *Hitting Frequency of the 57 mm T66 Recoilless Rifle*, Technical Memorandum No. M61-5-1, Frankford Arsenal, Philadelphia, Pa., September 1960.

CHAPTER 8
MEASUREMENT TECHNIQUES

8-0 LIST OF SYMBOLS

A	= bore area, in ²	N	= number of cycles of the Doppler signal measured from time equal zero, dimensionless
A_1	= piston area, in ²	P	= internal chamber pressure, psi
a_o	= sonic speed, fps	P_a	= partial pressure of air at temperature T , psi
C	= unit of electrical charge, C	P_b	= peak blast pressure, psi
C_L	= line capacitance, μF	P_K	= pressure constant, psi-V ⁻¹
C_T	= total input capacitance, μF	P_o	= atmospheric pressure, psi
c	= speed of light, fps	P_w	= partial pressure of water vapor temperature T , psi
D	= horizontal displacement of pendulum, in.	R	= resistance, ohm
$D_{1 \text{ thru } 4}$	= spacing between fixed points for velocity measurement, ft	R_g	= gage resistance, ohm
F	= unit of capacitance, F	R_r	= retardation of projectile velocity, fps-ft ⁻¹
f_d	= Doppler frequency, Hz	S_v	= output voltage charge, μvolt
f_R	= radar operating frequency, Hz	T	= air temperature, °F
g	= acceleration due to gravity, ft-sec ⁻²	t	= time, sec or μsec
GF	= gage factor, dimensionless	t_1, t_2	= time to traverse fixed distances for velocity measurement, sec
I	= current, A	V	= power supply voltage, V
I_m	= recoil impulse, lb-sec	V_m	= muzzle velocity, fps
K	= gage constant, lb-(μC) ⁻¹		

V_p	= projectile velocity, fps	\ddot{x}	= acceleration, g's
V_R	= radial velocity, fps	γ	= ratio of specific heats of air = 1.4, dimensionless
V_s	= velocity of shock wave, fps	ϵ	= strain, $\mu\text{in.}-(\text{in.})^{-1}$
V_T	= triggering voltage, V	θ	= angle of radar beam with respect to projectile trajectory, deg
V_1, V_2	= average projectile velocity ob- tained from time to traverse fixed distances, fps	λ	= radar wavelength, ft
W	= projectile weight, lb	μ	= 10^{-6} , dimensionless
W_t	= weight of pendulum and recoil- less rifle, lb	τ	= period of pendulum, sec
x	= displacement, ft		

SECTION I

INTRODUCTION

The experimental studies performed in the design of recoilless systems require the use of a variety of special purpose instrumentation to record important test data. Determination of flight characteristics may require measurement of velocity at a number of points along the trajectory as well as at the muzzle, determination of yaw, spin rate, and projectile integrity in flight. Interior ballistic performance studies will require, at the least, information on pressure-time history in the chamber, muzzle velocity, and may, in addition, require information on interior transient temperatures, projectile displacement-time, and projectile base pressure measurement. Nozzle throat design will require information on recoil impulse and possibly recoil force and velocity-time history. Investigation of firing safety hazards may require a plot of the blast pressure field around the system and additional information such as muzzle flash and recoil torque also may be necessary. Design of the gun tube often will require experimental verification of stress levels at various points in the weapon and temperature measurements during rate-of-fire tests.

The short duration of the transients associated with a system of this nature—coupled with the high pressures and tempera-

tures, and the difficulty of ready attachment of measuring devices to a lightweight system—may make the use of especially designed instrumentation, recording equipment, and test weapons necessary. Recording equipment used for tests of rocket devices and other slow varying phenomena usually is not suitable.

While most equipment components necessary for the recording of recoilless rifle experimental results are now available commercially, proper selection and application will be described in this chapter and construction of certain special purpose devices explained. It will be assumed that the reader has a familiarity with basic principles of measurements and general equipment available. The systems mentioned have been tried and are practical; however, the rapid advance in the technology of measurements may in some cases have already obsoleted them in favor of more reliable or accurate equipment. Use of such equipment is recommended where one can ascertain that equivalent or better performance is possible, however, thoughtful consideration should be given to the dynamic environment encountered in the system and assurance made that the specification on the equipment chosen will apply in such an environment.

SECTION II

MEASUREMENT OF VELOCITY

8-1 GENERAL

Probably the most important measurement in the design of the overall system is that of velocity of the projectile. It is desirable to know the velocity of the projectile at all times from ignition of the propellant to target impact, however, the most often used measurement is that of velocity at the muzzle of the gun.

Muzzle velocity usually is determined from the time taken for the projectile to travel between two detectors a known distance apart. This time is measured with an electronic time interval meter or chronograph. Since this method gives the average velocity over the distance of measurement, it is necessary to record two or more velocities ahead of the muzzle and extrapolate back to muzzle velocity. A diagram of a typical setup is shown in Fig. 8-1. From the arrangement of Fig. 8-1, the following may be determined:

$$\left. \begin{aligned} \text{Average velocity: } V_1 &= D_2/t_1, \text{ fps} \\ \text{Average velocity: } V_2 &= D_4/t_2, \text{ fps} \\ \text{Retardation } R_r: &= \frac{V_1 - V_2}{\frac{D_2}{2} + D_3 + \frac{D_4}{2}} \\ &\text{fps-(ft)}^{-1} \end{aligned} \right\} \quad (8-1)$$

Considering the retardation to be linear, which is approximately true for short distances (e.g., 100 ft), the muzzle velocity V_m is given by the equation

$$V_m = V_1 + R_r(D_1 + D_2/2) \quad (8-2)$$

When range space is limited, it may be desirable to stagger detectors as shown in Fig.

8-2 to achieve greater velocity accuracy by permitting longer baselines with a reduction, however, in distance between velocities and hence an increased retardation error. From the arrangement of Fig. 8-2, the following may be determined:

$$\left. \begin{aligned} V_1 &= (D_2 + D_3)/t_1 \\ V_2 &= (D_3 + D_4)/t_2 \\ R_r &= 2(V_1 - V_2)/(D_2 + D_4) \\ V_m &= V_1 + R_r[D_1 + (D_2 + D_3)/2] \end{aligned} \right\} \quad (8-3)$$

Errors inherent in both these methods are:

1. Error in distance measurement (usually in the range of ± 0.01 ft)
2. Detector error—error caused by time delays in the detector uncertainty in projectile location at which the electrical pulse output is generated
3. Error in time measurement— ± 1 μ sec with a 1 MHz time interval meter, providing that electrical time delays do not occur in transmission lines between detectors and meter.

The use of a long baseline (distance between detectors) can decrease both timing and distance measurement errors; however, its length often will be limited by firing range facilities, especially if a rather high firing angle is used. It is necessary to make two velocity measurements for accurate determination of muzzle velocity; if a linear extrapolation is used, the two velocity measuring systems should be close together.

The determination of muzzle velocity, as

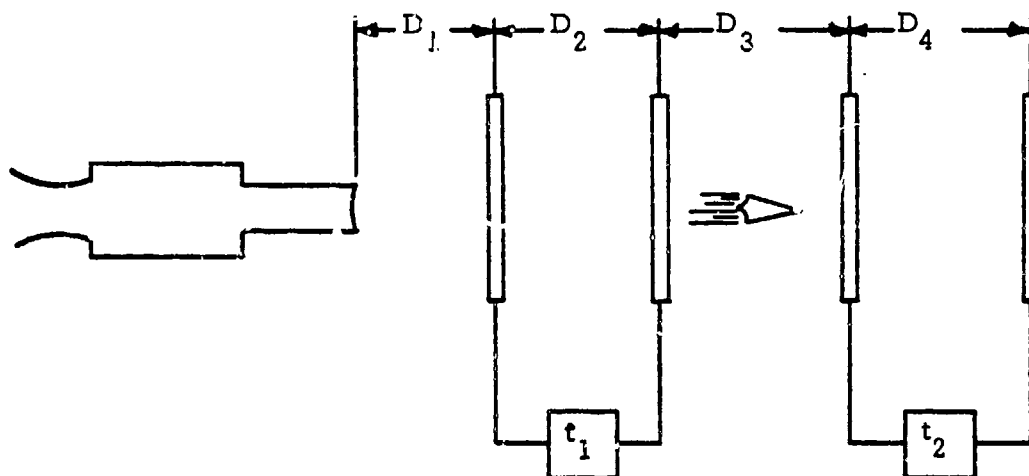


Figure 8-1. Velocity Measurement Schematic

described, actually gives the velocity at some point slightly forward of the muzzle since escaping gases accelerate the projectile after it leaves the muzzle. In normal recoilless systems this increase is not significant due to the reasonably low pressures and velocities encountered. It is desirable to locate the first velocity detector some distance from the muzzle to prevent muzzle blast or flash from affecting the detector performance. This distance may vary from 15 ft for a 57 mm gun to as much as 50 ft for high velocity

larger caliber guns. The recommended baseline for a velocity system is in the nature of 25 to 50 ft to assure an error of ± 0.1 percent (± 1 fps at 1000 fps) or less in velocity caused by distance measurement and detection error.

8-2 DETECTING DEVICES

The purpose of the detecting device is to produce an electrical signal indicating the passage of the projectile at a known point in space. There are several types of detectors

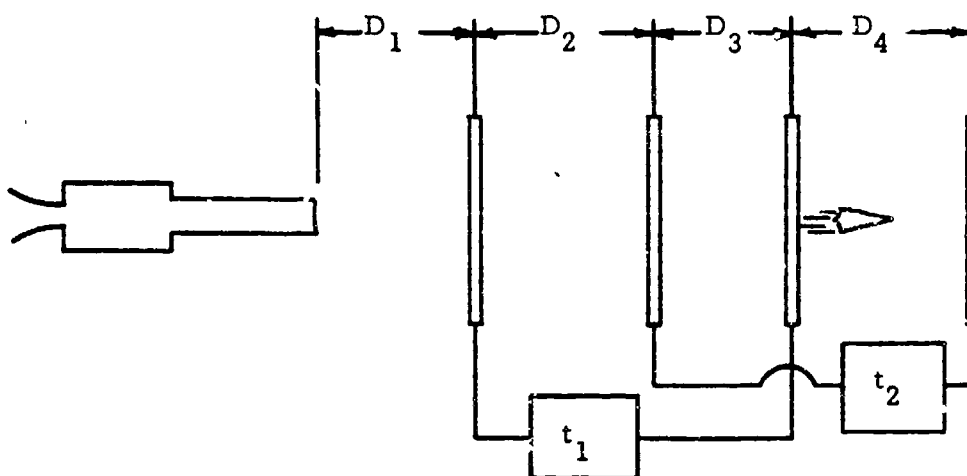


Figure 8-2. Velocity Measurement With Staggered Array of Detectors

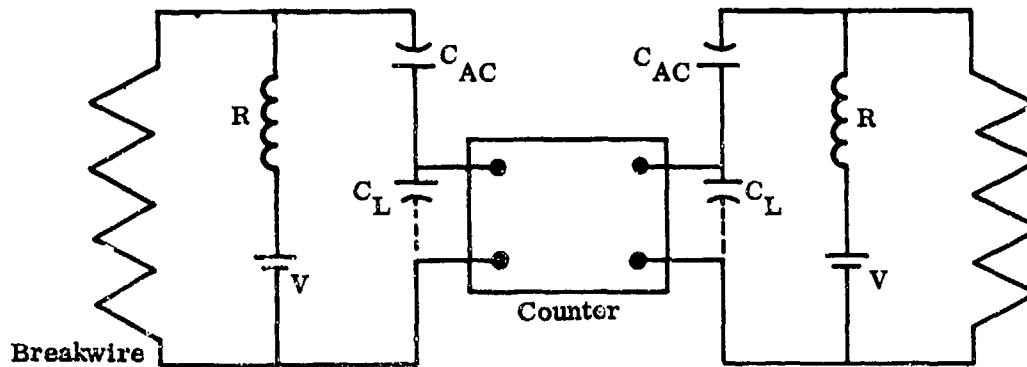


Figure 8-3. Circuit for Breakwire System

suitable for velocity determinations of recoilless systems, each of which have certain advantages and disadvantages.

8-2.1 BREAKWIRE SYSTEM

This system consists of a grid of wire, or paper with a conductive grid strung across a frame made of an insulating material such as wood. The wire is broken by the passage of a projectile through it. Normally, a current is passed through the wire, and a chronograph is used to sense the reduction in current when the wire is broken. While this is probably the most simple detecting device, it requires replacement of the wire after each firing. In addition, the wire has a tendency to stretch before breaking, especially when pointed projectiles are used, causing an error in baseline measurement. This error may be minimized by using hard drawn wire, keeping it stretched taut, and using narrowly spaced grid wires. The circuit used with this system is shown in Fig. 8-3.

The breakage of the wire will cause the voltage across the terminals of the chronograph or time interval meter to rise to V , considering that the input resistance of the counter is high with respect to R . Since the

line between the breakwire and the chronograph normally will have a capacitance C_L , the rise to V will not be instantaneous. The approximate value for any value of C_L the line capacitance, and V_T the triggering voltage of the chronograph may be determined from the equation

$$I = V/R = C_L V_T / t, \text{ A} \quad (8-4)$$

(for $V_T \ll V, C_L \ll C_{AC}$)

where

I = current in closed circuit, A

V = power supply voltage, volt, $\geq 50 V_T$

R = series resistance, ohm

C_L = capacitance of line, chronograph input and break circuit, μF

t = signal delay time, μsec , for error permitted

V_T = triggering voltage of chronograph example, V

An example of the application of Eq. 8-4 follows:

Given:

$$t = 1 \mu\text{sec}$$

$$C_L = 0.005 \mu\text{F}$$

$$V_T = 1 \text{ volt}$$

$$V = 50 \text{ volts}$$

Determine: R by Eq. 8-4

$$I = \frac{0.005 \times 1}{1} = 0.005 \text{ A}$$

Since

$$V \approx 50V_T$$

$$R = \frac{V}{I} = \frac{50}{0.005} = 10,000 \text{ ohms}$$

The use of C_{AC} is to provide AC coupling into the chronograph if required. This example considered the value of the breakwire resistance to be low in comparison to R . Since the length of wire for the two breakwire circuits usually will be similar, the signal delays will be similar and the timing error will be less than that caused by either one alone.

Where long cables or higher triggering voltages are required, it is desirable to use pulse-shaping and line-matching techniques which are well known in electronics, see Fig. 8-4. For example, one might have an integrated-circuit connected as a Schmitt trigger feeding into a 50-ohm cable. If the input and output impedances are appropriately matched, the pulse will suffer little degradation in shape (or amplitude) even over fairly long distances. Electronic technicians or equipment vendors ought to be consulted for the proper equipment to use. Circuit delays can be made the same by making the 2 cable lengths the same, or the equipment can be set to account for the different delays automatically.

8-8

8-2.2 MAKE SYSTEM

The make-circuit consists in principle of two conductors, separated by an insulator, which are connected by the passage of the projectile. In practice, the system consists of a sandwich of sheets of aluminum foil glued on Styrofoam about one inch thick. Screen wire electrodes with hardboard or thin plywood as a separator also have been used successfully. The make circuit is especially useful in the measurement of terminal velocity where large size screens are necessary and replacement of breakwires difficult. Make screens as large as 20 feet square have been fabricated and used for many firings before being destroyed to the point where some contact is not made between the projectile and the two electrodes. Other materials have been tried including a sandwich of foil and cardboard; however, it was found that the insulator tended to extrude over the rear foil and prevent contact. When using a separator other than Styrofoam, it is advisable to leave an air space between the rear electrode and the insulator to provide good contacts. The circuit, Fig. 8-5, used is similar to that used with the break circuit. The circuit has a time delay proportional to both the series resistance of the line and battery, and the capacitance of the line. For V large with respect to the triggering voltage and the line resistance R , small with respect to chronograph input resistance, the approximate time required t to reach the triggering voltage V_T will be

$$t = C_L V_T R / V, \mu\text{sec} \quad (8-5)$$

where

$$t = \text{time, } \mu\text{sec}$$

$$C_L = \text{capacitance of line plus make circuit, } \mu\text{F}$$

$$V_T = \text{trigger voltage, V}$$

$$V = \text{supply voltage, volt}$$

$$R = \text{series resistance of battery and line, ohm}$$

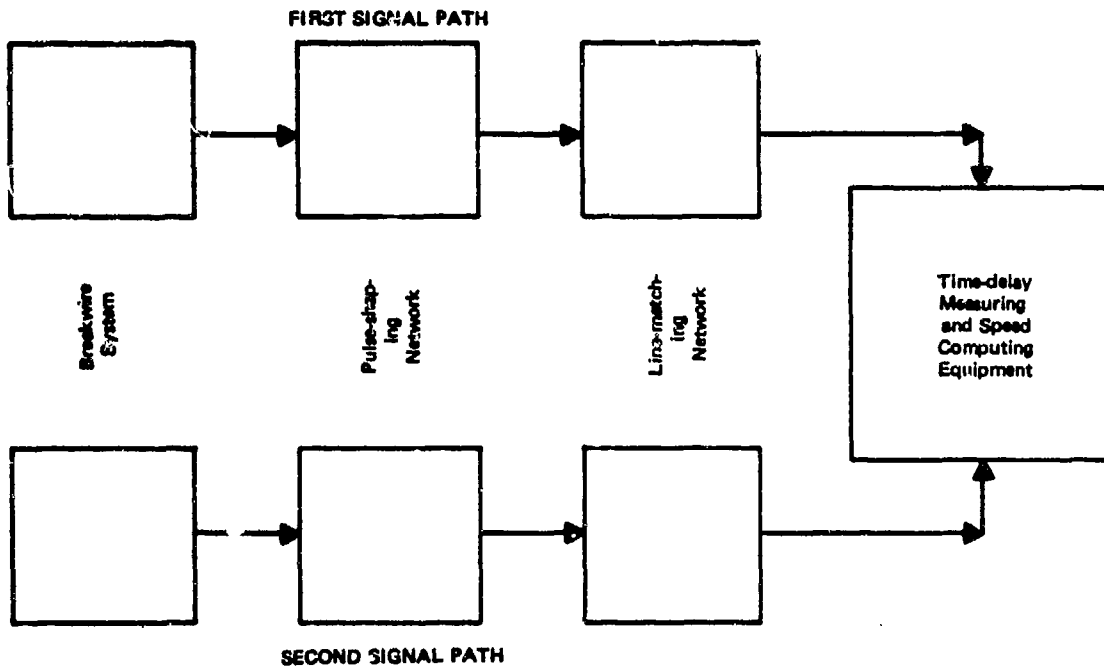


Figure 8-4. Measuring Projectile Speed

An example of the application of Eq. 8-5 follows:

Given:

- $C_L = 0.01 \mu\text{F}$
- $V_T = 1 \text{ volt}$
- $V = 45 \text{ volts}$
- $R = 100 \text{ ohm}$

Determine: t

$$t = \frac{0.01 \times 1 \times 100}{45} = \frac{1}{45} \mu\text{sec}$$

(Negligible compared to other circuit delays). For long lines or where a high trigger voltage is required, refer to the paragraph just above par. 8-2.2.

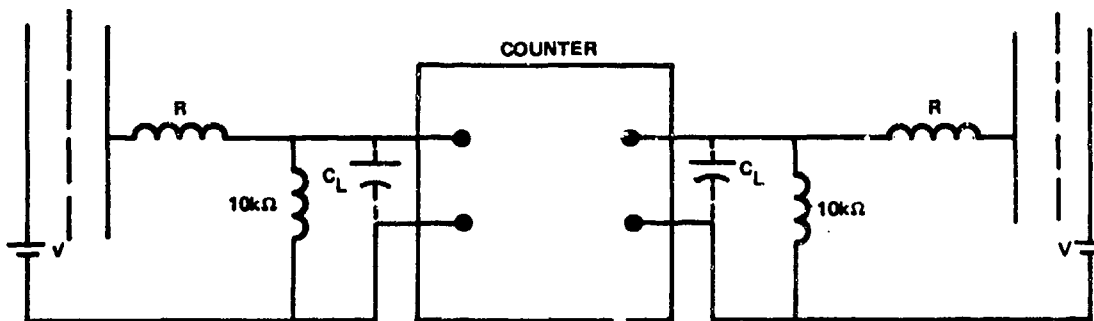


Figure 8-5. Make System Circuit

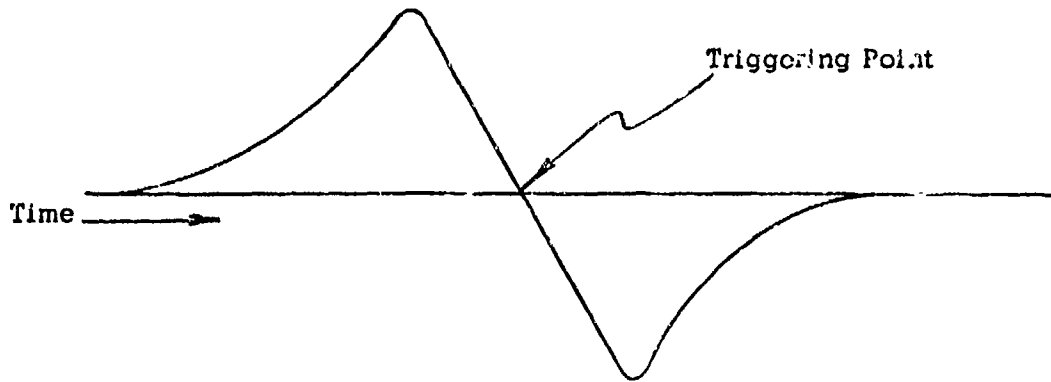


Figure 8-6. Solenoid Output Waveform

8-2.3 SOLENOID COIL DETECTORS

Probably the most used method for the velocity detection of recoilless rifle projectiles is the solenoid coil system where a magnetized projectile passes through a coil of wire to produce a current, indicating its passage. The coil normally is wound about 200 turns of No. 20 to No. 24 magnet wire in a loop 20 to 30 in. in diameter, dependent on the diameter of the projectile. While originally wound loosely on a wooden frame, it was found that the excessive blast from a recoilless system caused enough vibration of the wire in the magnetic field of the earth to produce extraneous signals. Latter coils were tightly bound and rigidly mounted to a wooden donut-shaped disc.

It is necessary to magnetize the projectile in the proper direction prior to firing, or, if the projectile is nonmagnetic, to insert a magnet where it will not be excessively shielded by the material of the projectile. It is common practice to mount a cylindrical magnet in the nose so that at least 0.5 in. protrudes beyond the projectile nose.

The design of the solenoid coil and the pulse shaping circuit is important to assure triggering of the chronograph at a known point in space. As shown in Fig. 8-6, the wave

shape of the signal from the coil is much like a sine wave. As the projectile approaches the coil, the increasing magnetic flux induces an EMF which reaches a maximum and then rapidly drops to zero as the projectile field is centered in the coil. The EMF then rapidly drops to some negative value and slowly returns to zero as the projectile passes out of the coil. It is advisable to use a shaping circuit to pick off the point of rapid negative rate of change, where the signal passes through zero, as the trigger point for the chronograph. A shaping adapter is available to perform this function, or it may be performed on most universal time interval meters having high gain amplifiers by setting slope control to negative and amplitude control slightly negative. To ascertain the accuracy of trigger point, it is useful during initial system test to record concurrently on an oscilloscope the output signal from the coil and the gate pulse from the chronograph. Normally, coils are wired in series and connected to a common ("period" or "coils") input on the chronograph. A sketch is shown in Fig. 8-7.

Proper polarity of coils and projectile magnetization may be checked by the use of a compass and a DC polarizing current of about 100 mA applied across the coils at the chronograph input. A rule of thumb prescribes that magnetization of the projectile

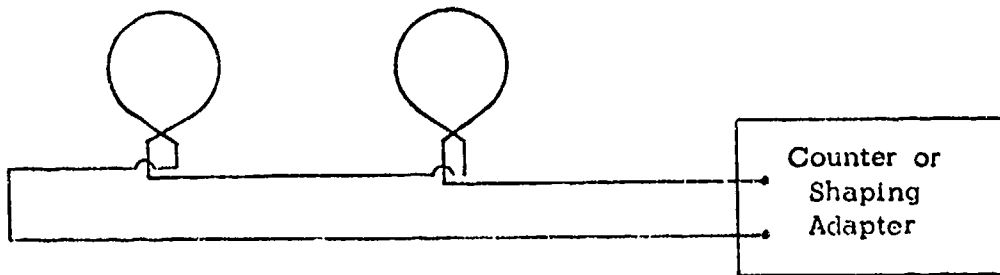


Figure 8-7. Series Wiring of Coils

should be strong enough to deflect a compass 45 deg from the magnetic field of the earth when 4 in. from the nose of the projectile. This test also may be used after magnetization to assure relative consistency of magnetic field strength between projectiles. Projectiles normally are magnetized by placement in a coil equal to the length of the major portion of the projectile through which a steady or impulsive high current is applied.

8-2.4 SKY SCREEN

Another method of detecting passage of a projectile in space is the sky screen. It has the advantages over other systems of not interfering in the visual path of the projectile, and permitting a number of velocities to be taken down range. The device consists basically of an optical system, collimating slit, and photomultiplier tube which produces a pulse when a rapid change in ambient light level occurs in its field of view. It has a fan-shaped field of view which will produce an error of about 0.2 to 0.5 percent, depending on the setup method, due to its spread. For muzzle velocity, it is normally positioned directly below the trajectory; while for time of flight measurement, it is placed off to one side to increase the field of view. It cannot be used on dark or hazy days and cannot be pointed into the sun. Extreme care must be taken in positioning the unit since a small change in angle of the lens can cause a considerable error in baselines. One method to determine the sighting point of the device on flat trajectory firings is to

suspend objects at points directly above the screens (when the screens are pointed vertically) on the trajectory. A meter measuring photomultiplier cathode current will dip when the screen is pointed directly at the object. Measuring the distance between objects will give the baseline.

8-2.5 RADAR VELOCITY MEASUREMENTS

Microwave interference (Doppler radar) techniques may be used to measure the velocity and displacement of the projectile in the barrel and its velocity over its entire trajectory. The basic system consists of a microwave transmitter that transmits a signal of known frequency in a beam along the axis of the projectile and a receiver that receives a signal reflected from the projectile. Transmitted and received frequencies are compared, and the difference or Doppler frequency obtained is proportional to the projectile velocity along the axis of the microwave beam by the relationship of Eq. 8-6.

$$V_R = \left(\frac{\lambda}{2}\right) f_d, \text{ fps} \quad (8-6)$$

where

V_R = radial velocity, fps

λ = radar wavelength, ft

f_d = Doppler frequency, Hz

$$\lambda = c/f_R, \text{ ft}$$

where

$$c = \text{speed of light, fps}$$

$$f_R = \text{radar operating frequency, Hz}$$

Since it is difficult to have the angle between the radar beam axis and the projectile trajectory equal to zero at all times, the radial velocity measured by the radar, i.e., the component of velocity of the projectile in the direction of the radar beam, will be somewhat less than actual projectile velocity along the axis of its trajectory. A typical setup is shown in Fig. 8-8. The velocity V_R measured by the radar will at any point in space equal the actual projectile velocity V_p , multiplied by the cosine of the angle θ , i.e., $V_R = V_p \cos \theta$. In recoilless firing experiments, it obviously is not possible to locate the radar directly behind the gun. It, therefore, is necessary to locate the radar as close to the side of the gun as possible, considering blast effects on the equipment, to obtain good down range measurements. For accurate muzzle velocities or velocity of the projectile while in the barrel, the radar may be located just off the trajectory down range and pointed toward the gun.

The radar systems produce a sinusoidally varying signal proportional to the radial velocity of the projectile which may be recorded by a number of methods. For recording the velocity over the complete trajectory, the Doppler signal may be converted by a frequency meter to a voltage proportional to frequency and, hence, velocity that may be recorded on an optical oscillograph as a trace of velocity versus time of flight. The signal also may be recorded digitally as a series of points containing the number of cycles of the Doppler signal occurring in given time increments, i.e., a number of velocities measured during the flight of the projectile.

The microwave system may be pointed toward the gun to measure velocity and displacement within the bore as shown in Fig. 8-9. To reduce the effect of radar off the axis of the projectile, the setup shown in Fig. 8-10 has been applied to advantage. Here a reflector made of foil backed with Styrofoam is placed about 25 ft forward of the muzzle at an angle to reflect the signal into the gun. The system is best aligned by placing a microwave detector connected to a meter in the gun tube and positioning for best signal strength as indicated on the meter. Since, by Eq. 8-6

$$V_R = \left(\frac{\lambda}{2}\right) f_d$$

it also holds that

$$x = \left(\frac{\lambda}{2}\right) N \quad (8-7)$$

where

x = displacement of the projectile from rest, ft

N = number of cycles of the Doppler signal measured from time $t = 0$

By recording the raw Doppler signal on an oscillograph, drum camera, or similar device, it is possible to obtain projectile displacement-time information.

In recording Doppler information in a gun tube, an error is caused by an apparent change in the wavelength of the microwave signal when traveling in a waveguide, which the gun tube may be considered. The error is significant when the diameter of the gun barrel approaches the wavelength of the radar system which is the case when the X-band microwave equipment is used with normal size recoilless systems. To avoid this effect, the system may be calibrated statically by positioning a piston in the gun at measured amounts equal to null in the microwave

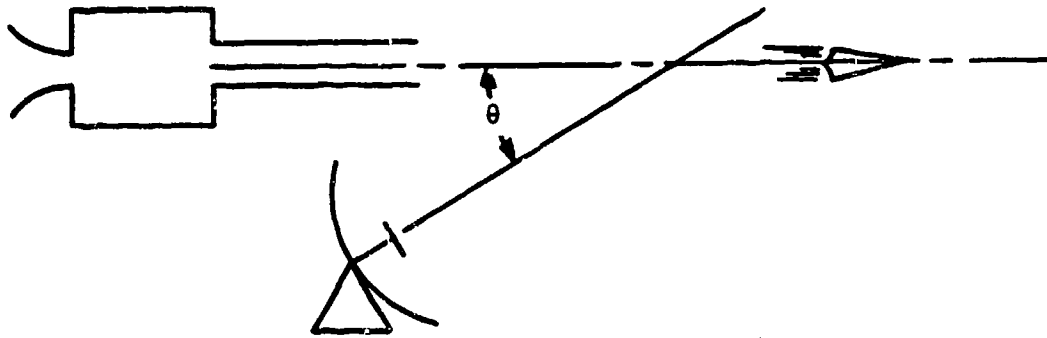


Figure 8-8. Radar Velocity Measurement Schematic

signal. In-bore microwave systems are described more fully in Refs. 2, 3, and 4.

The simplest radar system applied in recoilless tests is shown schematically in Fig. 8-11. It consists of a highly stable X-band low power klystron coupled through a "magic tee" to a 10-in. parabolic antenna and diode detector. This system produces a usable Doppler signal for short ranges (50 ft or less) with large caliber (57-280 mm) systems. For longer ranges (165 to 320 ft) the M36 Chronograph has been used with filter by-passed. To obtain results over ranges of up to 10,000 ft, a modified HAWK CW illuminator radar is applicable.

8-2.6 PHOTOGRAPHIC METHODS

Velocity also may be measured by means

of high speed (Fastex) motion cameras. A typical setup is shown in Fig. 8-12. A board several feet long with distance marks painted on its side is placed parallel to the trajectory as a distance reference. Parallax caused by the board being behind the projectile axis will cause an error in measurement. The correction may be determined by knowledge of the camera to object and camera to reference distances, and simple trigonometry. Timing marks normally are placed on the film for a time reference. While less accurate and more time consuming than previously described measurement techniques, photography can observe projectile integrity and launch characteristics as well as verifying velocity determined by other systems.

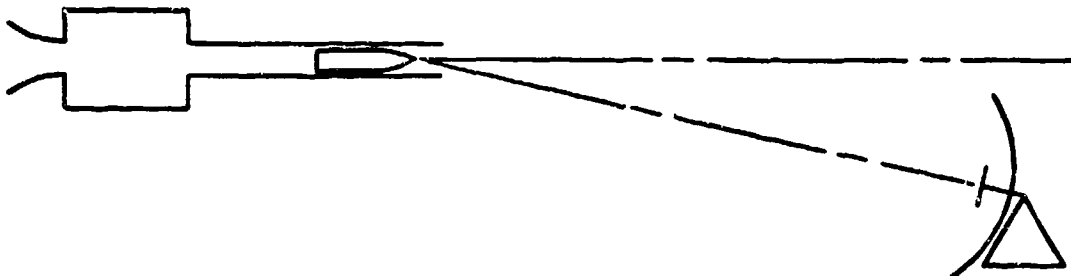


Figure 8-9. Radar Velocity and Displacement Schematic

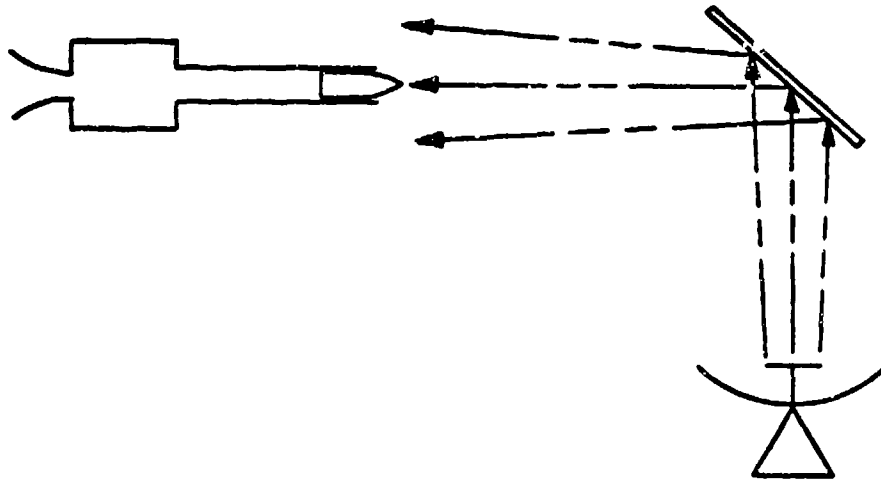


Figure 8-10. Radar Velocity and Displacement Schematic Using a Reflector

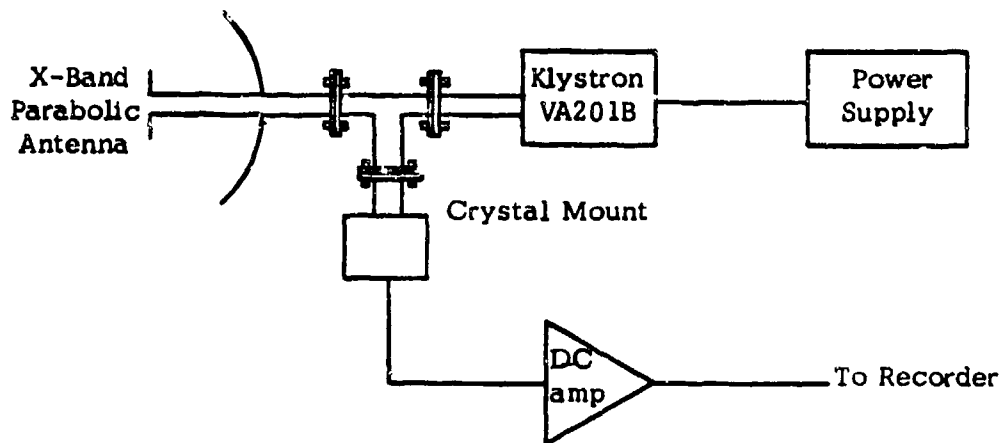


Figure 8-11. Simple X-band Interferometer

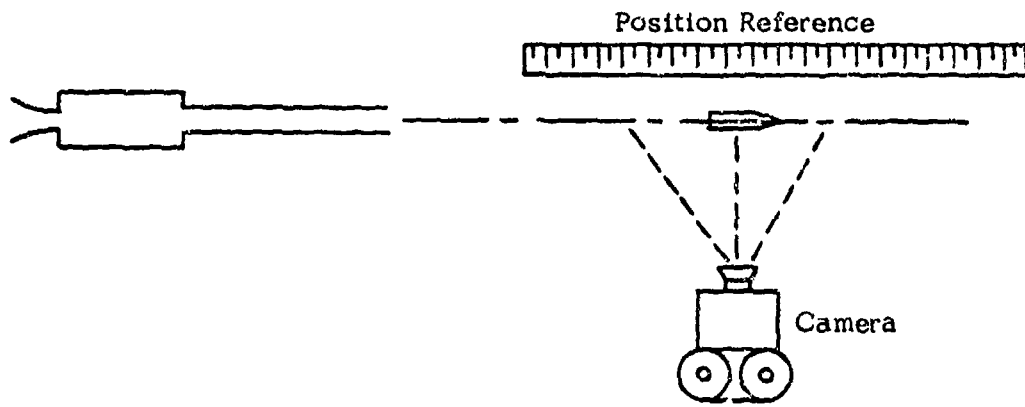


Figure 8-12. Photographic Method for Velocity Measurement

SECTION III

PRESSURE MEASUREMENTS

8-3 GENERAL

Next in importance to the measurement of velocity is the measurement of internal combustion pressures. Measurement of approximate values of peak pressure may be made with a copper crusher gage, however, measurement of overall pressure-time information is really necessary for interior ballistic and gun tube design. In addition to peak pressure, the pressure-time curve will indicate ignition delays, poor propellant burning characteristics, excessively high muzzle exit pressures, etc.

8-4 COPPER CRUSHER GAGE

The copper crusher gage as shown in Fig. 8-13 provides a measure of peak pressure based on the measurement of compression of a copper sphere or cylinder. It is used mainly in proof firings, in development firings with prototype weapons that do not permit modification for instruments, and as a simple check on transient pressure measurements. The pressures measured by these devices will be from 5-25 percent below the actual pressures read by the electronic gages when the crusher cylinders are calibrated statically.

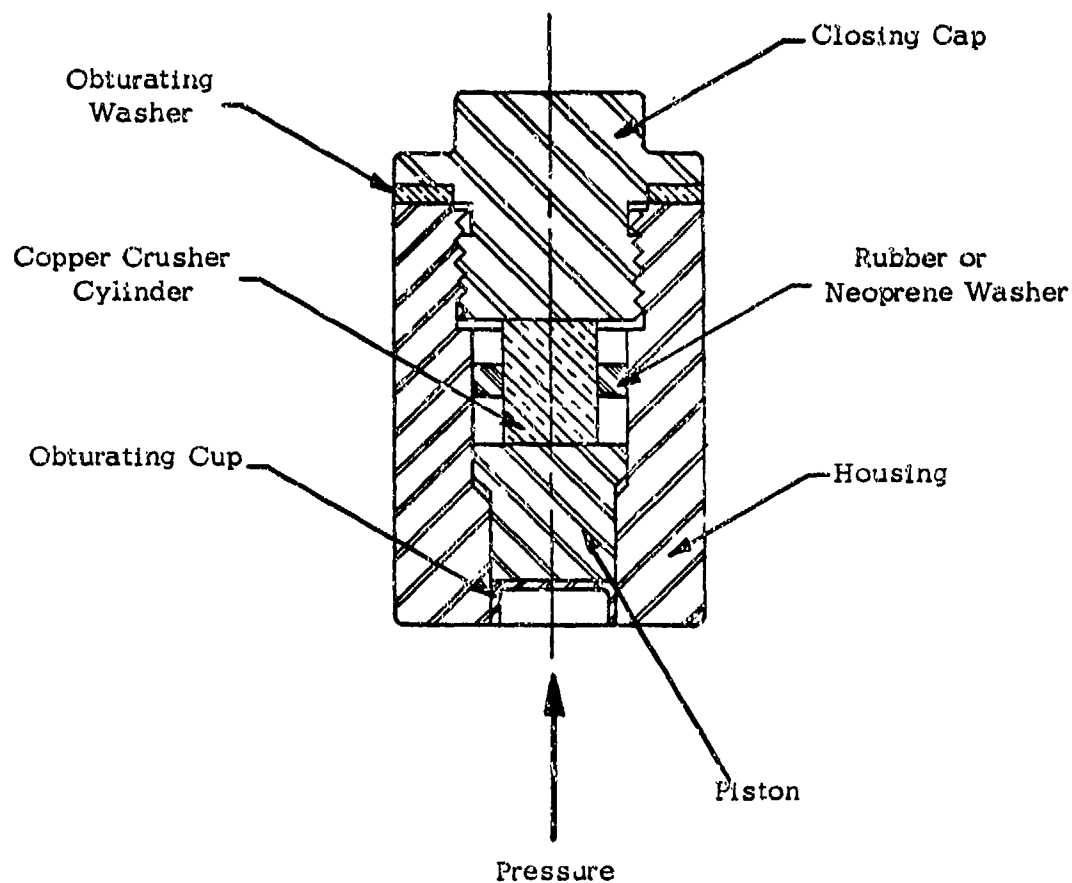


Figure 8-13. Copper Crusher Gage

Crushers are available as internal gages for direct insertion into the propellant bed, which are ejected from the gun on firing, and as externally mounted gages on test guns. While their absolute accuracy is poor, it is possible to generate empirically a correction factor for a given ballistic system for use in routine firings and as a check and an indicator of trouble in an electronic system. The correction, however, may change from gun to gun or ammunition lot to ammunition lot.

8-5 PIEZOELECTRIC GAGE

A number of dynamic systems are in use for the measurement of chamber pressures in recoilless systems. Transient pressures normally are measured by either a piezoelectric or strain gage type pressure transducer inserted in the chamber of the weapon and recorded on an oscilloscope-camera or a magnetic tape recording system. For normal recoilless systems having ballistic cycle times of approximately 5 to 25 msec, the equipment should have flat frequency response over the range of 0.5 to 10,000 Hz with response to DC (zero Hz) an advantage. In addition, phase shift must be low in this range to avoid distortion of the transient.

The piezoelectric transducer offers certain advantages for measurement of pressure in recoilless systems. A piston of accurately known area converts the incident pressure to a compressive force on a piezoelectric crystal or stack of crystals. Piston area of $1/6$ in² is used for pressures of 3000 to 20,000 psi while $1/30$ in² pistons cover the range of 12,000 to 90,000 psi. While barium titanate and tourmaline crystals have been used, quartz offers low temperature coefficient, high stability, excellent high frequency response, and reasonably high output. The gage is self-generating, producing a charge proportional to incident pressure. The calibration changes little with aging or excessive overloading, and the transducer readily can withstand the vibrations encountered in recoilless

firings. The major disadvantages are the high impedance output that requires a matching amplifier, the transient distortion, and the poor low frequency response that may occur if dampness or poor insulation effectively lowers the output impedance. The lowered output impedance effectively discharges the gage circuit capacitance while the transient is still being generated. A negative final (muzzle) pressure on the trace is indicative of excessively low impedance or leakage resistance in the gage circuit.

The formula used for computing the pressure constant P_K is

$$P_K = KC_T/A_1, \text{ psi-V}^{-1} \quad (8-8)$$

where

$$K = \text{gage constant, lb-(}\mu\text{C)}^{-1}$$

$$C_T = \text{total input capacitance—including capacitance of gage, line, and amplifier—}\mu\text{F}$$

$$A_1 = \text{piston area, in}^2$$

where the input circuit of Fig. 8-14 is used. The time constant RC_T , where R is the leakage resistance of the circuit including amplifier input impedance, should be greater than 100 times the ballistic cycle time to assure good low frequency response and low distortion. Values in the nature of 100 M Ω for R and 0.05 μF for C_T are common for recoilless systems. Use of a capacitive feedback or charge amplifier with this type of gage is also feasible where lines between the gage and the amplifier are short (100 ft or less). This amplifier permits the calibration to be independent of cable length.

8-6 STRAIN GAGES

Strain type pressure gages have the advantage of being capable of measuring static pressure and, hence, may be calibrated by static hydraulic systems. A typical strain type

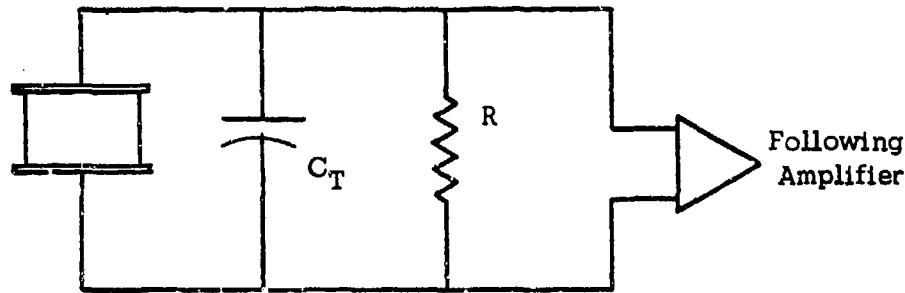


Figure 8-14. Input Circuit

pressure gage is shown in Fig. 8-15. It consists of a ferrule or cylinder to which are bonded foil or wire type strain gages. The cavity normally is filled with silicone grease that transmits the gun pressure to the ferrule, expanding it and causing a change in gage resistance. The strain gage makes up one or more arms of a low impedance wheatstone bridge circuit that generates a voltage proportional to its excitation voltage and the pressure measured. This voltage is usually in the millivolt range and considerable amplification is required to permit recording. This is a disadvantage in field application where good signal to noise ratios are sometimes difficult to obtain. The strain type pressure gage also is subject to changes in calibration factor when overloaded by short duration transients. It is advisable to verify its calibration frequently

or to replace the gage whenever excessively high pressures or bridge imbalance is noticed.

All pressure gages have natural resonance frequencies that can cause errors in measurement if the resonances are low in comparison with frequency components in the phenomena under study. Step function response of a gage should be investigated to ascertain that ringing or overshoot does not occur in the recorded output when subjected to a high rate of change of pressure. A rapid pressure rise for test of an individual gage may be produced by a high pressure shock tube, by a small closed bomb in which a primer or detonator is fired, or by inserting pressure gages in the barrel of a recoilless test gun where they will be subjected to rapid pressure rise as the projectile passes the transducer.

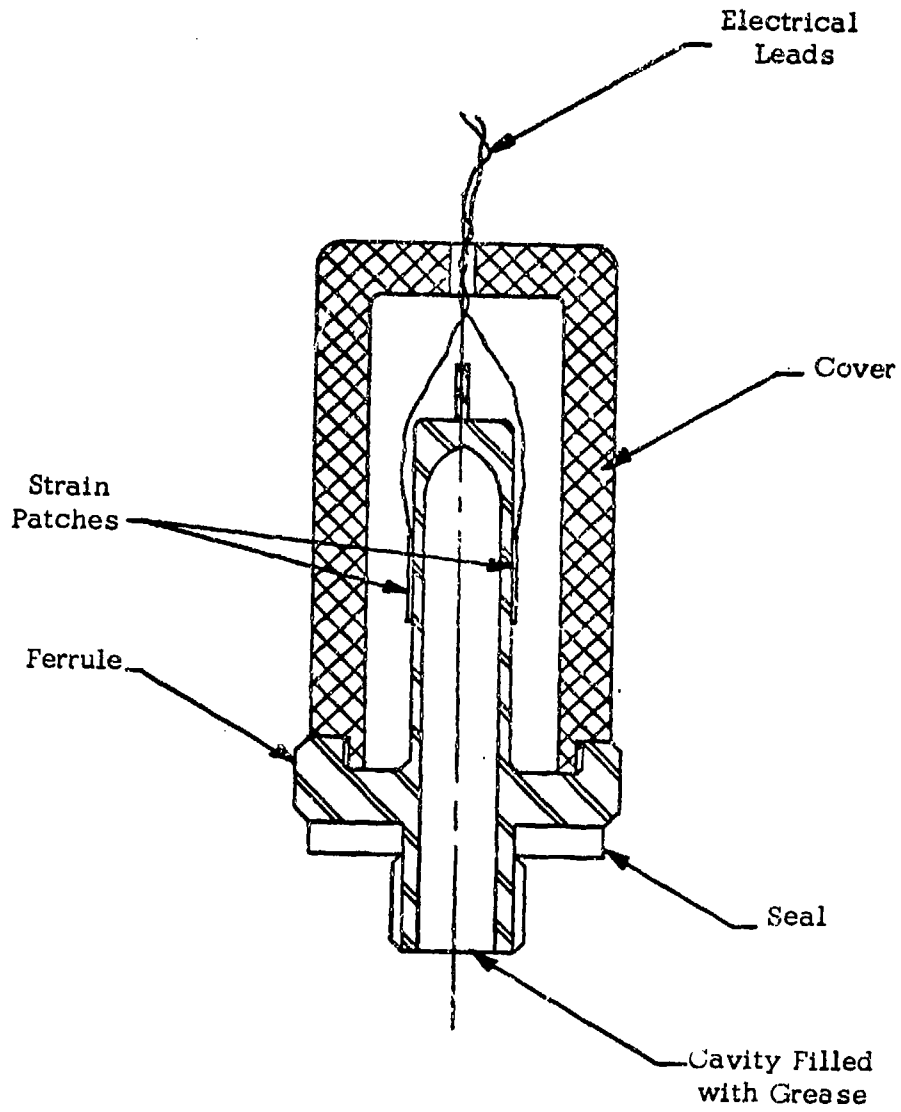


Figure 8-15. Strain Gage

SECTION IV

OTHER MEASUREMENT TECHNIQUES

8-7 STRAIN MEASUREMENTS

8-7.1 GENERAL

Recoilless rifle design normally stresses the minimization of weight with an associated reduction in the thickness of chambers and other components to that essential to safely contain pressures anticipated. This requires the accurate determination of dynamic stresses on the system to assure that safety margins are not surpassed. The use of strain gages, brittle lacquer, "stresscoat" and similar experimental techniques are therefore of importance in the design of the prototype system.

8-7.2 THE GAGE

The strain gage produces a change in resistance proportional to the change in strain in the surface to which it is applied. When a known current is passed through the gage, the output voltage change across the gage will be proportional to strain occurring in the metal as expressed by Eq. 8-9.

$$S_v/\epsilon = R_g(GF)I, \mu \text{ V per } \mu \text{ in.-(in.)}^{-1} \text{ strain} \quad (8-9)$$

where

S_v = output voltage change, as expressed in μV

R_g = gage resistance, Ω

GF = gage factor, dimensionless

I = current passed through the gage, A

ϵ = strain, $\mu\text{in.-(in.)}^{-1}$

Since the strains encountered are dynamic, it is not necessary to use a static bridge circuit

with the gage. A simple divider circuit such as that shown in Fig. 8-16 may be used. The capacitor C should be large enough to prevent low frequency attenuation, considering the impedance of the amplifier used. To produce a constant current in the gage, it is necessary that R be in the order of 20 times the gage resistance R_g . 120- Ω or 350- Ω gages of the "advance" wire (copper nickel) type are usually used, having a foil resistance element and epoxy backing. Since the gun may be allowed to cool between rounds in a strain test, it normally is not necessary to use high temperature bonding techniques or temperature compensation circuits. Outputs in the order of millivolts are attainable for strains encountered, using an excitation current in the range of 10 mA. Strain gage application techniques are covered in more detail in Refs. 5 and 6.

8-7.3 OTHER USES OF STRAIN GAGES

In addition to use in strain measurement, strain gages also may be used on a chamber to indicate pressure-time functions in a thin-wall gun where attachment of pressure gages is otherwise impossible. In some weapons, it is possible theoretically to determine the relationship between internal chamber pressure and external strain at a point by knowing chamber geometry. It is possible to determine this experimentally by hydrostatic pressurization of the system or by the expedient of firing a group of uniform charges first in pressure instrumented test guns of the same internal geometry. The same charge fired in the strain instrumented prototype should produce a strain curve of the same shape which can be related by an amplitude factor if the average muzzle velocities coincide.

Strain gages also may be used to detect passage of the engraving band on the

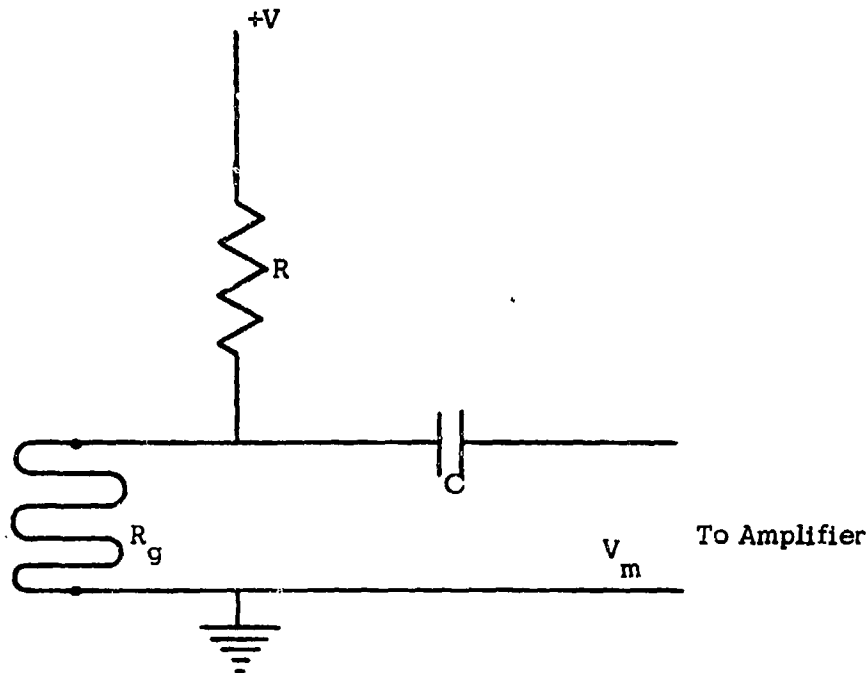


Figure 8-16. Divider Circuit for Strain Gage

projectile at certain points on the barrel for displacement-time on muzzle exit information.

8-8 ACCELERATION MEASUREMENT

8-8.1 GENERAL

The design of fuzing or sighting mechanisms sometimes requires the measurement of acceleration on the projectile or weapon mounts. These measurements have been accomplished using piezoelectric accelerometers designed specifically for shock applications. Acceleration also may be determined with reasonable accuracy by relating to internal chamber pressure by Eq. 8-10.

$$PA = W\ddot{x} \quad (8-10)$$

where

P = internal chamber pressure, psi

A = bore area, in²

W = projectile weight, lb

\ddot{x} = acceleration, g's

In most recoilless systems where bore friction and pressure gradients are low, errors of less than 5 percent are attainable by this method.

8-8.2 ACCELEROMETERS

It has been found possible to make acceleration measurements by mounting piezoelectric accelerometers in the nose of a blunt test projectile. A usable signal is transmitted out the bore over a low noise coaxial cable and picked up by a cup on the projectile nose during its travel down the tube.

Also, accelerometers mounted in simulated sights have been used to measure sight

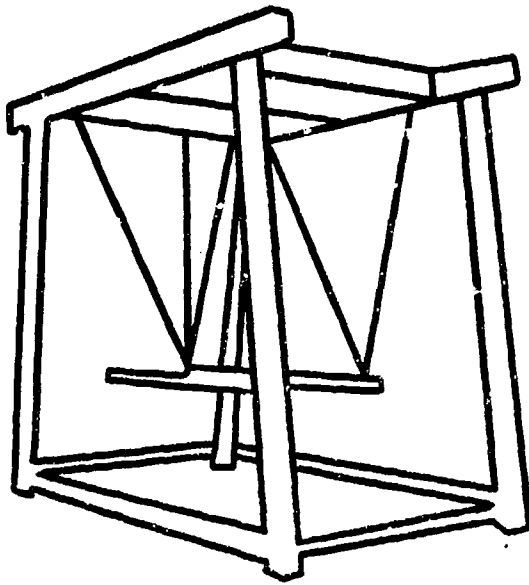


Figure 3-17. Portable Pendulum

vibrations and, mounted to barrels, to measure recoil forces as well.

Doppler radar (interferometer) also may be used to produce projectile position-time which may be double differentiated to obtain acceleration. Some accuracy will be lost, however, in the smoothing process.

8-9 RECOIL MEASUREMENTS

8-9.1 GENERAL

The measurement of recoil is of primary importance in the evaluation of performance of recoilless systems. The most used measurement is that of recoil impulse; however, it is sometimes necessary to have information on instantaneous recoil forces. Recoil impulse is measured by recording the displacement of a simple ballistic pendulum upon which the gun is mounted. The triangular suspension system of the ballistic pendulum reduces the effect of torque on the pendulum displacement. The

weapon is mounted so that its center of gravity is located as close as possible to the center of gravity (which should also be the geometrical center) of the pendulum frame.

8-9.2 MEASUREMENT OF RECOIL IMPULSE

Displacement of the pendulum is shown in Fig. 8-17, and direction of initial movement may be determined visually using an indicator mounted to the pendulum and a fixed scale, or it may be photographed using a movie camera. Recoil impulse I_m may be determined from Eq. 8-11.

$$I_m = \frac{\pi W_t D}{6g\tau}, \text{ lb-sec} \quad (8-11)$$

where

W_t = weight of pendulum with recoilless rifle attached, lb

D = horizontal displacement, in.

g = acceleration due to gravity, ft-sec^{-2}

τ = period of pendulum, sec

Where visual methods are not suitable for safety or other reasons, a displacement transducer may be used to convert the information to an electrical signal suitable for recording. The transducer, however, must not impede the movement of the pendulum.

The schematic diagram, Fig. 8-18, shows another method used with good results for measuring recoil displacement. A scale engraved with reflecting marks spaced 0.1 to 0.25 in. apart reflects the light from a light source to a photocell that produces a change in current as each mark passes the cell. Positive and negative directions of recoil are sensed by a difference in thickness of the marks producing a different output signal.

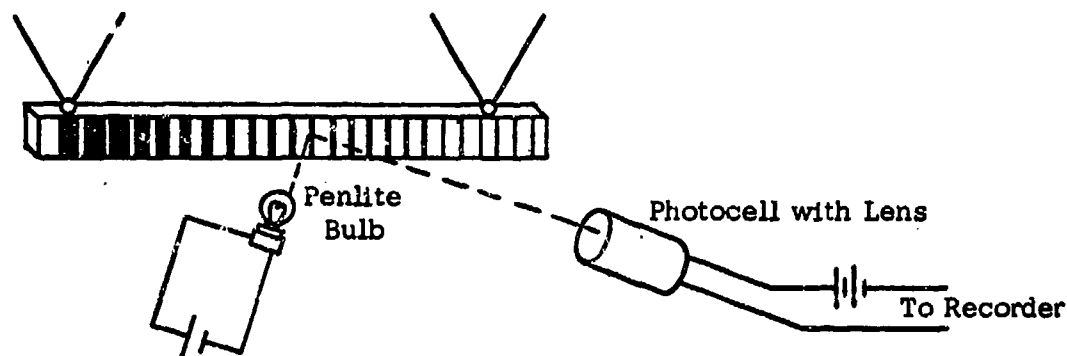


Figure 8-18. Photoelectric Recoil Measuring Device

8-9.3 MEASUREMENT OF RECOIL FORCES

Recoil force may be measured through the use of an accelerometer mounted along the axis of the gun. Best results are obtained by using strain gage type accelerometers having low cross axis sensitivity, natural frequencies in the order of 2000 Hz, and "g" ranges in the order of several hundred "g's". The force at any time may be calculated approximately from Newton's law, knowing the mass of the pendulum and associated components. The accelerometer output may be integrated electrically by operational amplifiers to obtain recoil velocity and position versus time.

8-10 MEASUREMENT OF TEMPERATURE

8-10.1 GENERAL

In the design of recoilless rifles, several aspects require the need for temperature measurement at various points on the weapon. Temperature rise measurements during high rate of firing studies are used for weight reduction studies and stress analyses for barrel, chamber, and head sections of the rifle. Interior ballistic studies require temperature measurements on the interior of the chamber wall and at the nozzle throat in order to relate or determine quantities or parameters such as mass rate of flow and heat transfer.

8-10.2 TECHNIQUES

As previously stated, temperature measurements are required at various points on the weapon in several areas of design study. This commonly is performed through the use of thermocouples welded to the exterior of the weapon. Differential (ungrounded) inputs are required on the recording equipment to prevent interaction between thermocouples and noise pickup. Normally iron-constantan junctions will suffice.

Measurement of temperature on the interior of the chamber wall and at the nozzle throat is accomplished by the bore-surface thermocouple shown in Fig. 8-19. The thermocouple is made of an iron bolt through which a nickel wire coated with nickel oxide as an insulator is threaded. A layer of nickel approximately 1 micron thick is plated across the finely polished surface connecting the bolt to the nickel wire and forming the junction. It is necessary to replat the thermocouple after each firing to insure reliable performance.

8-11 PROJECTILE MOTION

8-11.1 YAW

Exterior ballistic studies require the measurement of projectile yaw. Precise measure-

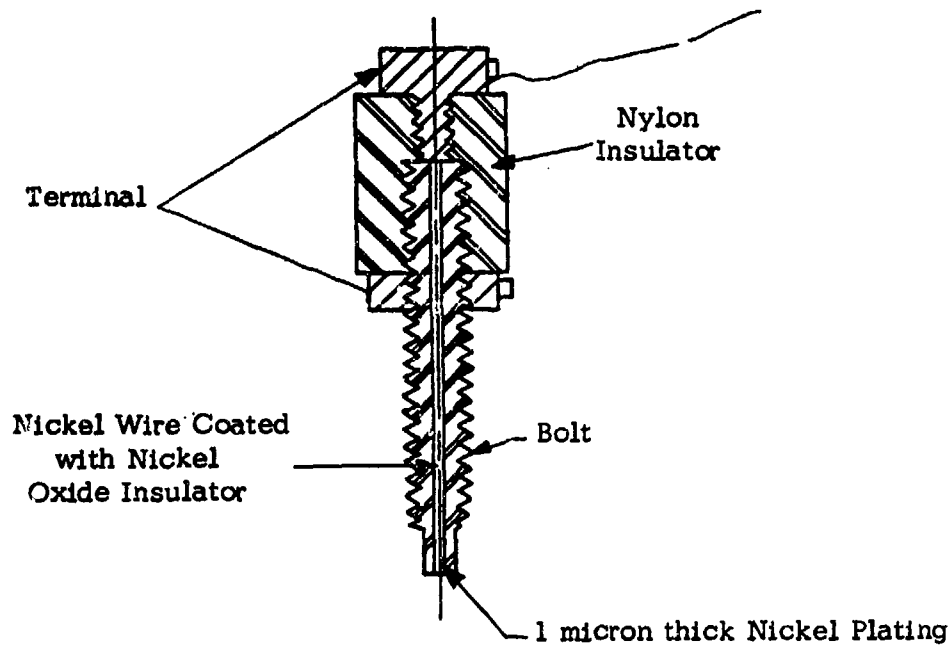


Figure 8-19. Bore-surface Thermocouple

ment of yaw requires the use of a series of spark or motion picture cameras located in two places at intervals down range. Reduction of data will produce information on yaw frequency and magnitude. Yaw may also be measured with a lesser degree of accuracy by the use of yaw cards, cardboard targets about the thickness of shirt cardboard placed at intervals down range through which the projectile is fired. Measurement of hole elongation in the case of spin-stabilized rounds and fin impression in the case of fin-stabilized rounds along with measurements of length of projectile (base to beginning of taper or rotating band to fin) will give an indication of magnitude of yaw while frequency may be determined by observing the distance between cards showing maximum amplitudes and knowing the projectile velocity at the cards.

3-11.2 SPIN

Spin may be measured in much the same way as yaw. A spring loaded pin is inserted in

the side of the projectile which pops out when the projectile leaves the barrel. The angle of rotation occurring between two successive targets is measured by observing the impressions made by the pin in the targets. It is necessary that two of the targets be close enough together to assure that the projectile has completed less than one revolution between the targets. The spin rate may be computed knowing the projectile velocity at that position in the trajectory. Increased accuracy may be obtained using another set of targets spaced far enough apart to permit several revolutions of the projectile between targets.

Similar results have been obtained by stretching thin wires (break circuits) across the path of the projectile and noting marks on a flat nosed projectile caused when it struck the wires.

A method of obtaining spin versus time makes use of a spin sonde in which a transistor oscillator with a loop antenna is mounted in the projectile nose. The RF signal

is picked up by an antenna that parallels the projectile flight. Signal strength is a function of polarization of loop with respect to antenna and produces a signal varying at two cycles per revolution.

The current method for measuring spin is by the induced emf technique. Projectiles are magnetized and fired parallel to a passive coil. This method has proved very successful in applications where the projectile is ferromagnetic. The method is very low in cost and extremely accurate.

Spin also has been obtained on fin type projectiles using the Doppler radar mentioned before. In addition to the Doppler frequency produced by velocity, a lower frequency in the order of 200 Hz will be produced by a slow spinning, finned projectile since the Doppler return will be at a maximum when any set of fins is parallel to the polarization of the antenna. The Doppler frequency will equal the spin rate times the number of fins on the projectile.

8-12 BLAST

8-12.1 GENERAL

The expansion of exhaust gases of a recoilless rifle produces a pressure wave in the surrounding air which is appreciably higher than the pressure wave or blast from a closed breech weapon of equivalent size. Pressure wave measurement is necessary to determine the boundaries of the zone from which personnel must be excluded for safety.

The blast pressure curve ideally will be of the shape shown in Fig. 8-20. The initial compression wave of a few milliseconds in duration will be followed by a negative rarefaction wave of lower amplitude but longer duration. Reflections from objects surrounding the pressure measurement equipment may cause additional peaks; however, the information of greatest importance is the initial positive pressure peak.

8-12.2 BLAST GAGES

Pressure may be measured directly by the use of blast pressure gages, which are basically microphones of special design, or by determination of shock velocity at a point and computing the peak pressure. Gages are located at a number of points around the weapon under test at various heights, and a plot is made of blast pressure versus position. Blast pressure as low as 0.03 psi (140 dB) can be detrimental to human hearing and, hence, accurate measurements are of importance. Pressures in the range of 30 psi (200 dB) may be measured a few feet from the nozzle of a recoilless weapon.

It is necessary that the gage used to measure air blast pressures produce as little restriction to the flow of the pressure wave as possible while having a frequency response high enough (in the order of 20 kHz) to respond to the rapid rise of the blast transient. Capacitor microphones having a small diaphragm (0.25 in.) or pencil-shaped piezoelectric blast gages have been used for these measurements.

The pencil gage has produced the most uniform results at blast pressures over 0.05 psi. It consists of a ring shaped barium titanate sensing element mounted flush with the outer surface of the pencil shaped body to provide a minimum effect in the air flow across it. The gage is pointed directly into the origin of the wave. It must be mounted on a fixture that does not resonate when disturbed by the blast wave, and it should have a streamlined appearance in the area of the gage to prevent reflections from affecting the wave front incident on the gage. In order to reduce the effects of noise in the cable leading from the gage to the recording equipment, the cable should be buried, be of a nonmicrophonic type, and it may be necessary to attach a low microphonic emitter follower close to the gage to transform the signal to a low impedance for long transmission lines. The output of the gage is a charge

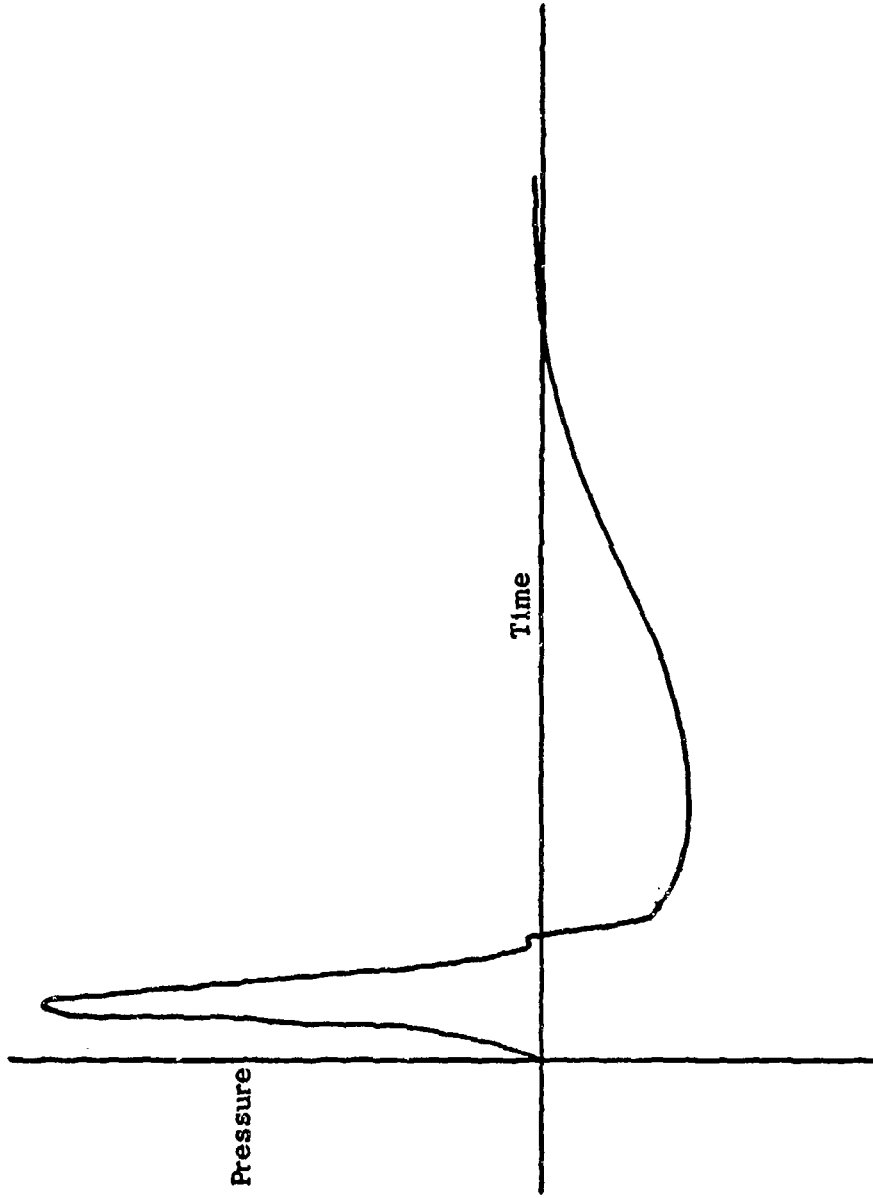


Figure 8-20. Typical Blast Waveform

proportional to pressure in the order of 500 pC-(lb-in.²)⁻¹ or about 0.25 V (psi)⁻¹, if connected directly to an amplifier by a short cable. Parallel capacitors may be used, if necessary, across the gage output to reduce the signal level.

Blast pressure gages are calibrated in a shock tube by comparison with a standard or by measuring the velocity of the shock front at the point of impingement on the gage and computing pressure. A field check on calibration is also possible by setting two gages a known distance apart (in the order of one to three feet) along the direction of propagation of the wave and measuring the time for the wave to travel between the gages. The peak pressure P_b of the wave may be computed from Eq. 8-12 (see Ref. 7):

$$P_b = P_o \left(\frac{2\gamma}{\gamma + 1} \right) \left[\left(\frac{V_s}{a_o} \right)^2 - \left(\frac{\gamma - 1}{2\gamma} \right) \right], \text{ psi} \quad (8-12)$$

where

P_o = atmospheric pressure, psi

V_s = velocity of shock wave, fps

γ = 1.40 (specific heat ratio for air)

a_o = speed of sound, fps

$$= \left(1052 \sqrt{1 + \frac{T}{459}} \right) \left(1 + 0.149 \frac{P_w}{P_a} \right)$$

T = air temperature, °F

P_w = partial pressure of water vapor at temperature T , psi

P_a = partial pressure of air at temperature T , psi

The site chosen for the blast measurement should be flat and free of obstacles that might cause reflections. The recording equipment

used may be oscilloscope, magnetic tape, or equipment similar to that used for recording of pressure and acceleration.

8-13 RECORDING EQUIPMENT

8-13.1 OSCILLOSCOPE

Most of the measurement devices previously mentioned produce as an output either time-varying analog voltages or pulses that initiate or stop time interval counters. Where only one or two channels of analog voltage information are required, the oscilloscope-polaroid camera method is most economical.

For calibration, a series of voltage steps are applied to the vertical amplifier prior to firing while the horizontal axis is modulated with a time reference from a crystal marker oscillator. Such a system is capable of providing recording accuracies in the order of ± 2 percent. The oscilloscope is triggered by an electrical signal used to fire the gun or may be triggered internally if the initial pressure rise is not important for the test conducted. The trace may be blanked at muzzle exit by a pulse on the horizontal axis produced by a muzzle breakwire or a pressure gage located at the muzzle. A typical record obtained is shown in Fig. 8-21.

8-13.2 MAGNETIC TAPE

Where a large number of channels of analog information is to be recorded simultaneously, the FM magnetic tape system is more advantageous. This permits the reduction of multichannel analog information on pressure, strain, and other parameters at usable chart speeds. Accuracies within ± 2 percent or better are attainable if voltage steps and time markers are recorded prior to firing and carried through on playback.

Another item associated with the recording equipment is a group of analog computer operational amplifiers which may be pro-

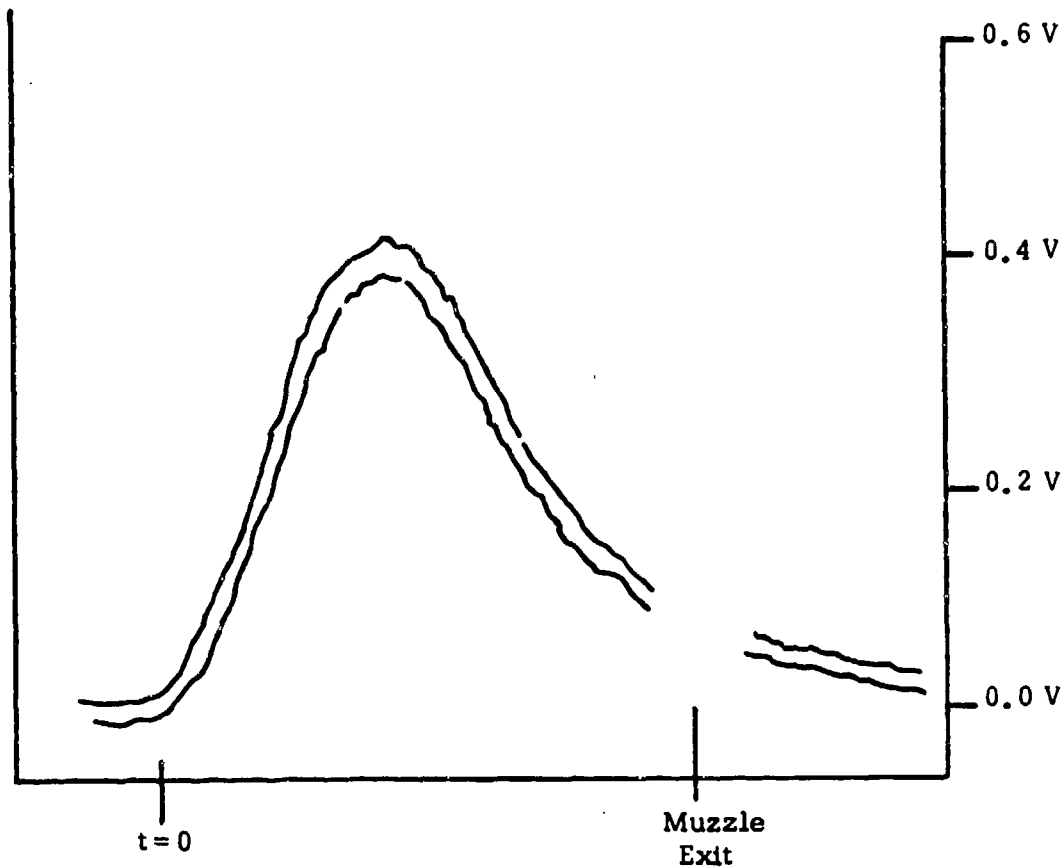


Figure 8-21. Typical Pressure-Time Curve

grammed to integrate pressure and accelerometer output to permit a real time recording of velocity and displacement time information.

The blast effect of recoilless systems on recording equipment as well as safety considerations normally require that the recording equipment be placed some distance away from the test site. This may require cables of 500 ft or more which are sources of noise and attenuation of the signal. High impedance piezoelectric transducers will require coaxial lines of very high leakage resistance unless line driving amplifiers are used at the test site. It has been found in

practice that mounting of outside termination points in heated boxes will reduce leakage resistance caused by moisture better than attempting to seal such terminals from the environment.

While strain gage lines are of low impedance, care must still be taken to avoid pickup from stray fields that will often surpass the millivolt signal being transmitted. Proper grounding of shields can best be determined by experiment. Where calibration resistors are used to calibrate strain gages, additional leads usually are required to bring the resistance effectively to the gage.

SECTION V

GENERAL CONSIDERATIONS

In measurement of recoilless rifle parameters as well as those of any other system, it is essential to make use of redundant measurements whenever possible to indicate existence of instrument malfunctions. The use of two different methods of obtaining the same piece of information is better than merely duplicating equipment to obtain duplicate measurements. While velocity, for example, may be measured by two successive velocity systems (the one further down range should indicate a lower velocity), an integration of a pressure gage record will provide a cross-check as well. By use of formulas and empirical relationships, pressure may be checked against strain, terminal velocity against muzzle velocity, acceleration against pressure, etc.

Equipment should be calibrated periodically and, in addition, a standard round of ammunition should be fired immediately prior to a test to check out equipment under

dynamic conditions to avoid loss of data in an important test series.

Records should be kept during each firing program of instruments and transducers used, calibration factors, setup methods, and unusual results noticed in addition to actual test data. When at all possible, photography should be used to show test setups as well as being applied as a measuring technique. While quantitative data are sometimes difficult to obtain by photographic means, high speed photos of the weapon and projectile during firing are an invaluable tool in determining causes of malfunctions.

Certain aspects of measurements, safety considerations, test procedures, and the like are covered in more detail in Refs. 1 and 6, and in texts of test equipment manufacturers' brochures on measurement equipment. The reader is encouraged to refer to these for further information.

REFERENCES

1. AMCP 706-181, Engineering Design Handbook, *Explosions in Air, Part One*.
2. AMCP 706-150, Engineering Design Handbook, *Ballistics Series, Interior Ballistics of Guns*.
3. BRL Report 968, *Ballistic Studies with a Microwave Interferometer, Part I*, 1955.
4. BRL Report 1006, *Ballistic Studies with a Microwave Interferometer, Part II*, 1957.
5. *Measurement Engineering*, Stein Engineering Services, Inc., Phoenix, Arizona, 1964.
6. NPG Report 1241, *Development of a Pressure Time Recording System for the 20 mm Anti Aircraft Gun*, U S Naval Proving Ground, Dahlgren, Virginia, 1954.
7. H. W. Liepmann and A. Roshko, *Elements of Gasdynamics*, John Wiley and Sons, N. Y., 1957, p. 64.

PART THREE DESIGN

CHAPTER 9

BASIC DESIGN CONSIDERATIONS

SECTION I

INTRODUCTION TO DESIGN CONSIDERATIONS

9-1 ADVANTAGES OF RECOILLESS RIFLES

The major advantage of a recoilless rifle over closed breech weapons and the reason for its development are found in the light weight of this weapon system; the ratio of projectile kinetic energy to system weight is very favorable for a recoilless rifle compared to a closed breech weapon. In small caliber recoilless rifles, less than 100 mm, this advantage is more pronounced because the recoilless principle produces a portable gun, capable of being shoulder fired with a probability of hit at battle ranges quite comparable to that obtained by the conventional closed breech gun. The light weight of the recoilless rifle is made possible mainly by the cancellation of recoil, and, to a certain extent, by the high piezometric efficiency inherent to recoilless rifles.

Recoil is cancelled in the recoilless rifle by providing sufficient propellant to produce gases to accelerate the projectile forward and to discharge rearward through a nozzle such that the impulse of gases discharged equals the projectile momentum. The result is that substantially no recoil impulse is imparted to the rifle, and the weapon does not require any of the heavy recoil mechanisms that a conventional gun would require, i.e., no heavy carriages and no pneumatic or spring recoil systems ordinarily present in the weapon system are needed. Likewise, the mount for

the rifle is made relatively light in comparison with the mounts required to support the heavier conventional guns.

The weight saving realized by use of a recoilless rifle is shown in Table 9-1.

The data in this table clearly show the weight advantage of a recoilless rifle over a comparable closed breech gun. Comparison of the 75 mm system shows the closed breech to be 8.6 times as heavy as the comparable recoilless rifle.

9-2 IMPORTANCE OF SYSTEM DESIGN APPROACH

The usefulness of the recoilless rifles, because of their light-weight, lies in the ability to give infantry the capability of defeating small fortifications, armored targets, and area targets. When necessary, it is possible to hand-carry the 57 mm, 75 mm, and 106 mm and even the 120 mm and 155 mm, recoilless rifles for short distances, over average terrain, in order to support combat rifle units in any situation. Accordingly, it is necessary that human engineering, maintainability, and reliability be considered in the design approach - i.e., these factors together with the goal of providing a specific terminal effect form the criteria which are studied and weighed in designing the recoilless rifle as a totally integrated system. The roles that human engineering, reliability, and maintenance factors play in the design of recoilless rifles are

TABLE 9-1

COMPARISON OF 75 mm RECOILLESS AND CLOSED BREECH WEAPON SYSTEMS

Weapon	Projectile Weight, lb	Muzzle Velocity, ft-sec ⁻¹	Weapon System Weight, lb	Ratio Projectile Kinetic Energy to Weapon Weight, ft
75 mm, M20 Recoilless	13.1	1000	168	1210
75 mm, M1A1 Howitzer	13.4	1000	1440	144

discussed in the last three sections of this chapter. The remaining part of this paragraph will describe briefly the various components of the recoilless rifle and their interrelationship with other components of the system.

The two largest components of the recoilless rifle, which together account for approximately two-thirds of the rifle weight, are the gun tube (or barrel) and chamber. The gun tube for the recoilless rifle is similar to the barrel of a standard artillery gun. The gun tube has a rifled bore and fires a conventional projectile that incorporates a standard fuze. The ammunition used in the recoilless rifle is of a special type in which the cartridge case is perforated to permit the easy escape of the propellant gases (see Fig. 9-6 and 11-9). As in the case of the standard artillery projectile, the perforated cartridge case remains in the chamber during firing, the projectile being the only component that is ejected from the weapon. The chamber of the recoilless rifle is considerably larger than the chamber of the similar caliber conventional gun and is closed only partially at the rear by the breechblock. The breechblock often contains the nozzle which allows for the rearward release of the propellant gas, and contains part of the firing mechanism for detonating the cartridge primer. The remaining components of the recoilless rifle are the triggering mechanism, the mount, and the sighting mechanism. The design and types of recoilless rifles are described in more detail in Chapters 10 through 13 of this handbook.

9-3 DESCRIPTION OF VARIOUS WEAPON CONFIGURATIONS

9-3.1 BASIC PRINCIPLE

The basic principle underlying the operation of the recoilless weapon is the principle of "Conservation of Momentum". Chapter 6 of this handbook contains a detailed presentation relating to cancellation of recoil including the basic principle on conservation of momentum. In application to recoilless rifles balance is achieved by producing an impulse of the gases discharged through the nozzle equal to the effective momentum of the projectile and the gases accelerating the projectile. After shot ejection, the impulse of the gases discharging through the nozzle may exceed that of the gases discharging through the muzzle and a slight forward balance may result. However, it is the practice to select the nozzle throat area such that the weapon recoils slightly rearward. Thus, as the nozzle erodes as a result of successive firing, the rearward unbalance becomes less and with sufficient erosion will become forward. The contribution of the recoil unbalance after shot ejection is quite small and is compensated in the initial selection of throat area.

9-3.2 THE DAVIS GUN

The application of the principle of the recoilless gun dates back to World War I, when it was incorporated in the basic patent of the Davis gun. As shown in Fig. 9-1, the

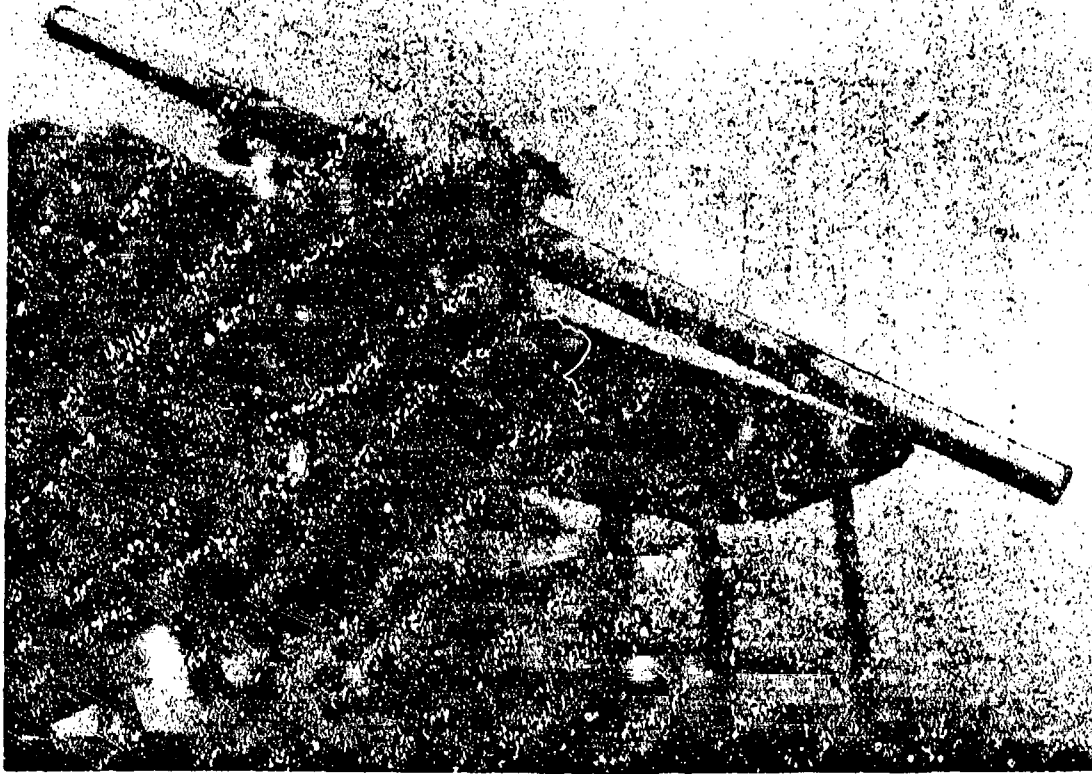


Figure 9-1. Davis Gun Mounted on WW I Martin Bomber

Davis gun consisted mainly of a straight tube that simultaneously ejected a projectile from the muzzle and a heavy lead shot with low velocity from the breech of the weapon (Ref. 1). Considered for use as a possible weapon for airplanes, the Davis gun had the disadvantages of being both awkward and shooting the lead shot rearward. As a result, the gun was abandoned by the Army and the Navy.

9-3.3 RUSSIAN AND GERMAN DESIGNS

The early Russian and German recoilless guns were different from the US and British designs in that they did not use perforated cartridge cases. Instead, they preferred using a conventional type of cartridge case with a

plastic burst or blow-out disc in its base. As shown in Fig. 9-2, the chamber is much smaller than that of a comparable US recoilless rifle (Ref. 1), see Fig. 9-6. The resulting difference in operation was that the early German and Russian rifles operated at higher chamber pressures with short barrels, whereas US and British guns employed lower chamber pressures with longer barrels.

An obvious disadvantage of the German and Russian guns was the discharge of solid particles through the nozzle. Another, more important, disadvantage of these guns was the reduced efficiency of their projectile. Since these guns operated at higher chamber pressures, the projectiles had to be designed to withstand the higher acceleration forces.

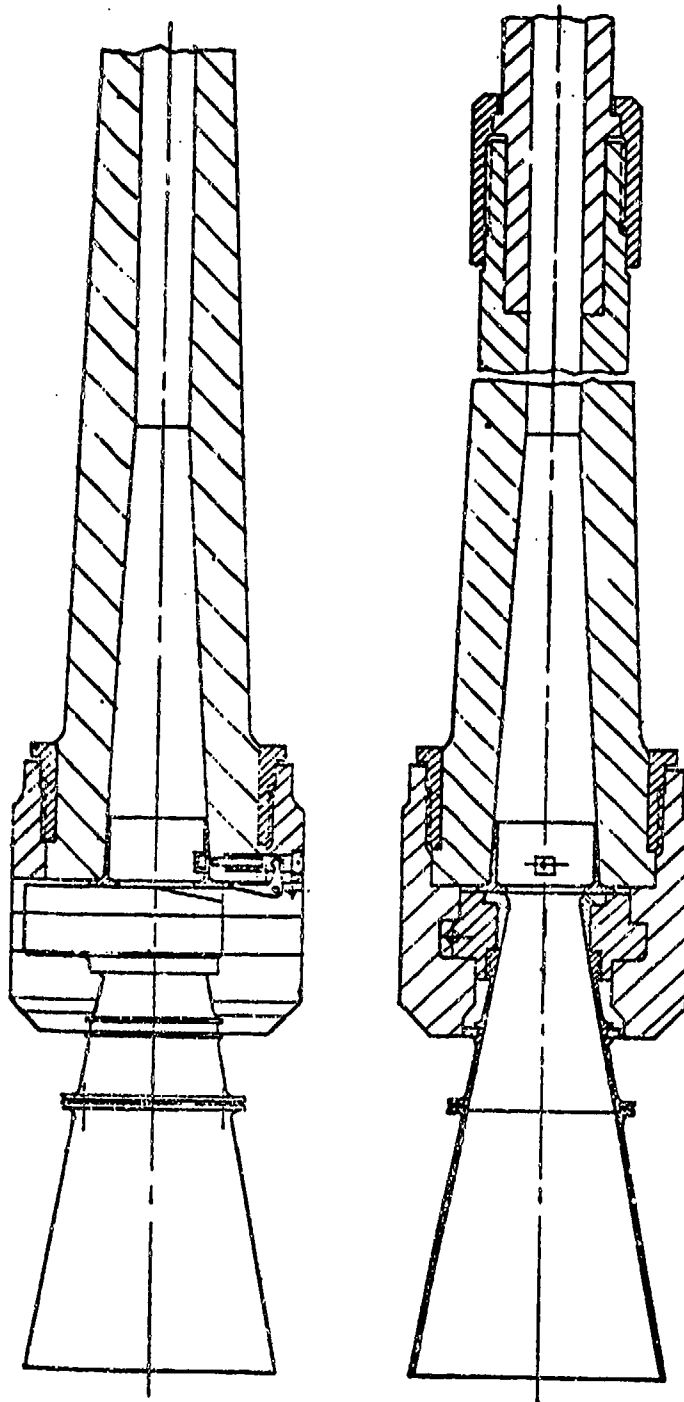


Figure 9-2. 28 cm German Recoilless Gun

When the projectile walls and base are made thicker to meet the higher strength requirements, the amount of high explosive that will fit in the projectile cavity is reduced. If the projectile base thickness is increased to withstand the higher acceleration stresses, it is also necessary to reduce the amount of metal at the nose of the projectile, so that the acceleration stresses due to the weight of the nose are not being transmitted to the base. The resulting projectile design, with its uneven distribution of metal and reduced explosive content, results in a projectile that is less efficient with regard to both explosive charge to projectile weight ratio and fragmentation.

9-3.4 THE BURNEY GUN

During World War II, British designer Sir Dennis Burney applied the recoilless principle to a series of weapons which were developed for the British Government. The first of the Burney guns was the 95 mm R.C.L. Twin Jet Gun which is shown in Fig. 9-3 (Ref. 1, Vol. VI). Sir Burney incorporated the use of multiple nozzles with large expansion ratios. The divergent nozzles were mounted on the sides of the breech ring. This allowed the use of a standard sliding block type breech mechanism, similar to that used on a 95 mm howitzer, which would accommodate a conventional cartridge case flange. In this manner, loading, firing, breech opening, and cartridge extraction functions remained the same as for the standard 95 mm howitzer. Recoil adjustments were made through the use of interchangeable throat rings of varying diameters. Although the Burney guns were recoilless, the total weight saving that could have been made was not achieved. For example, the 95 mm Twin Jet Gun shown in Fig. 9-3 weighs 700 lb without any carriage as compared with the US 106 mm, M40 Recoilless Rifle which weighs only 274 lb.

In 1944, a series of recoilless mortars 60 mm, 81 mm, and 4.2 in. applied the current technology to these high angle fire weapon

systems. Many experimental models were designed and built. Figs. 9-4 through 9-6 illustrate a representative technology in these three tube calibers.

9-3.5 THE HYBRID WEAPON

It was not until the late 1940's that the principles of the front orifice recoilless rifles were studied in detail. The front orifice rifle, which is shown in Fig. 9-7 (Ref. 2), has the distinct feature that the projectile covers the nozzle ports at the beginning of the ballistic cycle. The propellant charge is confined to the closed chamber which provides for good ignition. The advantages of this design as compared with rear orifice weapons are:

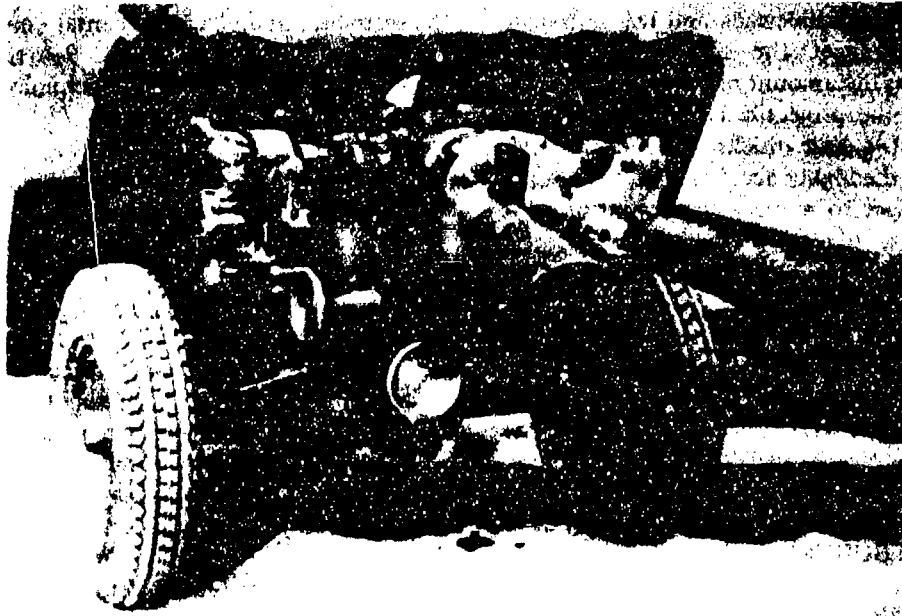
1. Unperforated cartridge cases can be used.
2. Good ignition characteristics are attained.
3. Propellant loss through nozzle is negligible.
4. Nozzles of large expansion ratio can be used without increasing weapon length.

The disadvantages of the front orifice rifle are:

1. An initial rearward momentum is generated until nozzle ports are uncovered.
2. Added weight due to heavier chamber design, longer nozzles, and added gas ducting system.

9-3.6 SIDE-LOADING CONFIGURATION

Fig. 9-8 (Ref. 3), comprises sectional views of a proposed side-loading, magazine-fed, blow-back operated, repeating, recoilless system. The basic components of the system are the guide tube, the barrel and the box-type, and spring-loaded magazine mounted below the weapon. A magazine latch



BURNEY 95MM R.C.L. TWIN JET GUN AND CARRIAGE
(REAR VIEW)



BURNEY 95MM R.C.L. TWIN JET GUN AND CARRIAGE
(REAR VIEW)

Figure 9-3. Burney 95 mm R.C.L. Twin Jet Gun and Carriage

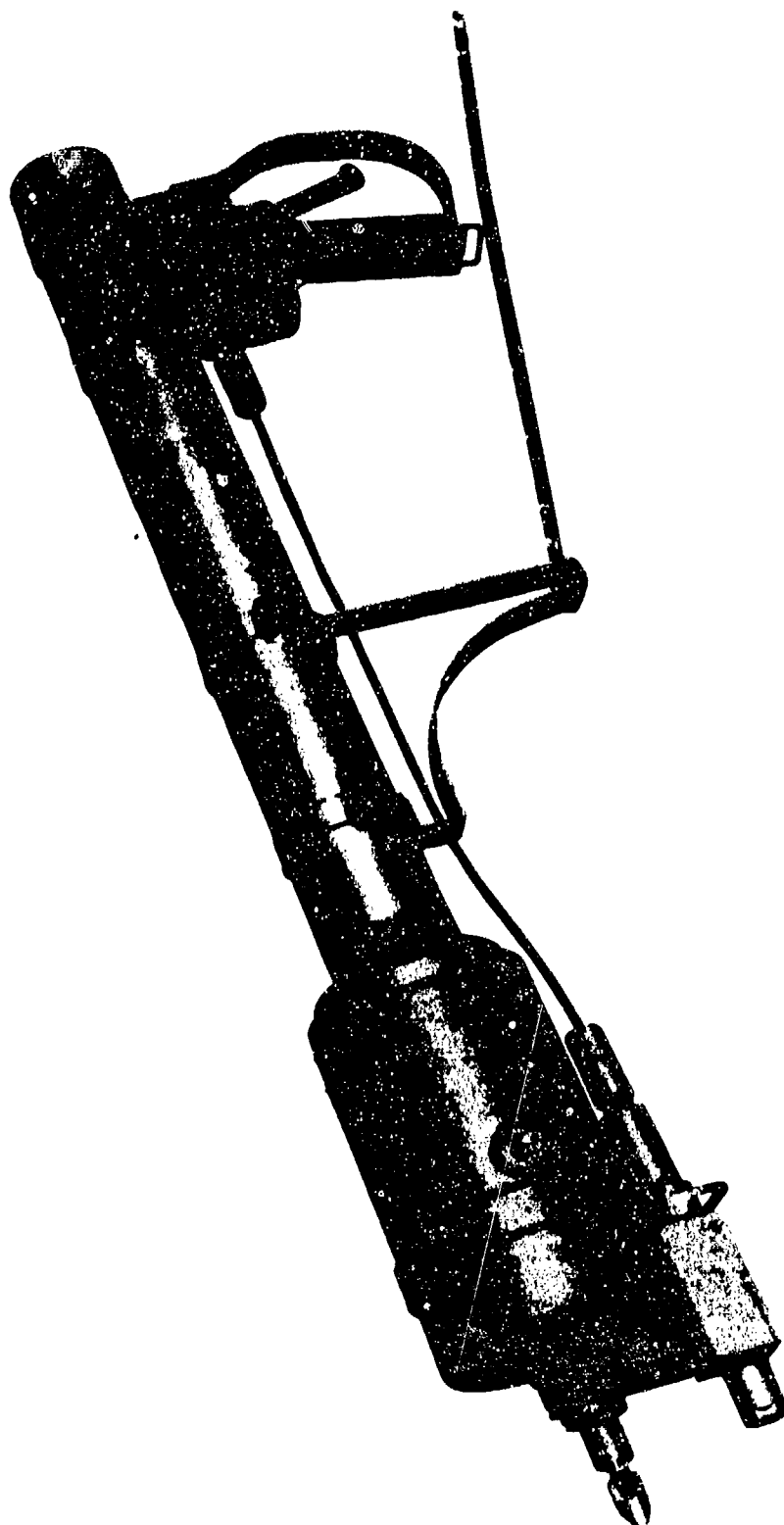


Figure 9-4. 60 mm Recoilless Mortar



Figure 9-5. 81 mm Recoilless Mortar

is provided for opening and locking the magazine in the closed position. A detent handle actuates the mechanism for holding the round in place during loading. A cocking handle is provided for initial cocking of the weapon.

Operation of the system includes initial cocking of the weapon, which involves pulling the gun barrel forward after the magazine has

been loaded, closing the magazine, releasing the magazine detent, and allowing the barrel to return. This action places the first round in the chamber, and the weapon is ready to fire. As each round is fired, the barrel automatically cocks, the weapon is loaded, and the barrel returns to the "ready-for-firing" position. After the last round is fired, the barrel is locked forward and the magazine may be opened for reloading. Closing the magazine automatically releases the barrel.

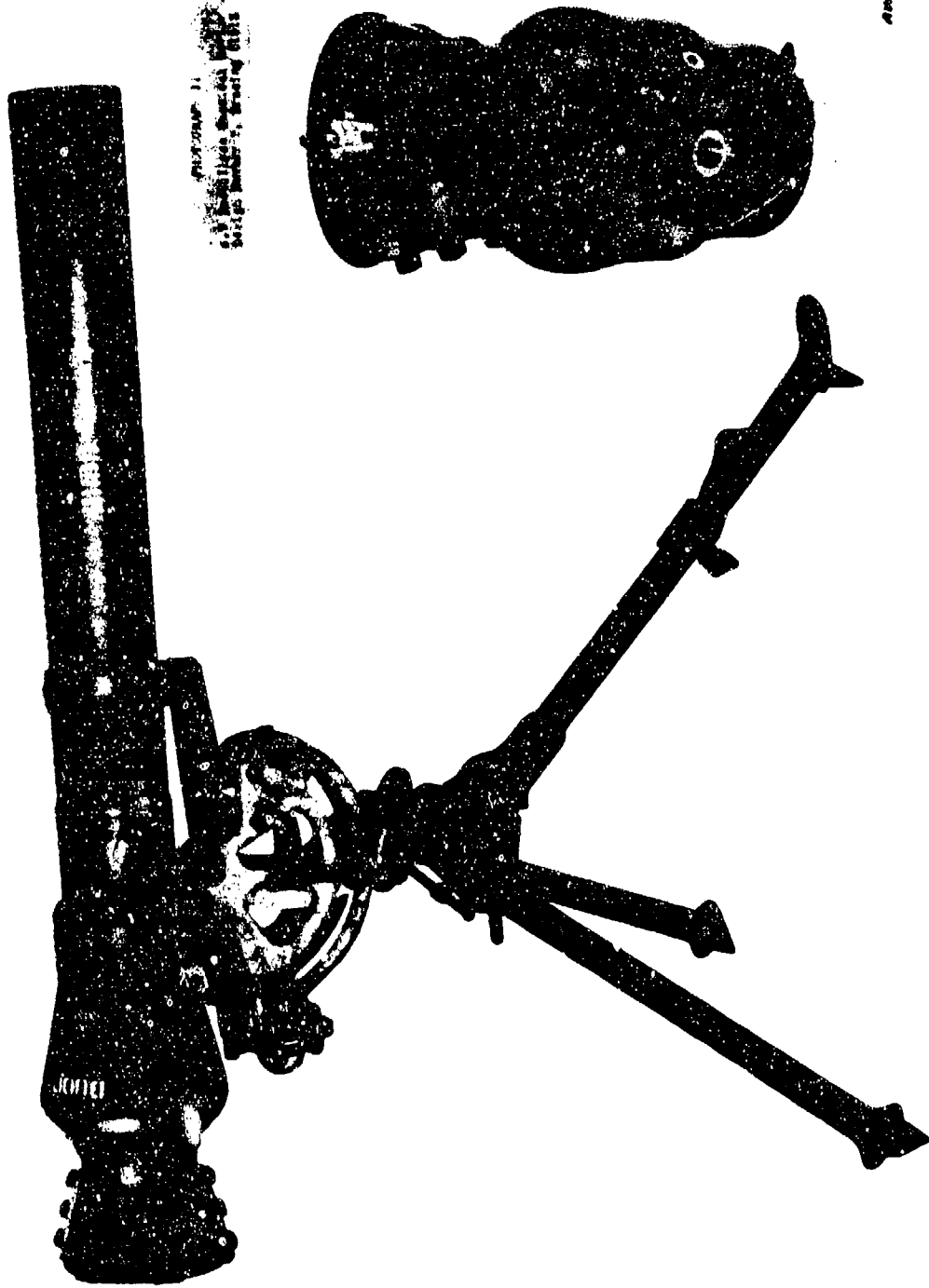


Figure 9-6. 4.2 in. Recoilless Chemical Mortar



Figure 9-7. T135 Front Nozzle Rifle

The important characteristics of this type of a repeating recoilless system are:

1. Relatively simple and compact mechanism
2. Unusually light weight (total unloaded weight approximately 300 lb)
3. Variety of mounting possibilities
4. Ease of loading for an automatic use.

The most important characteristic of the side-loading design is the feature for which it is named: Side-loading. This feature is convenient for vehicle-mounted applications. Because of its compactness, it can be enclosed completely to prevent possible jamming due to environmental and combat exposure.

The 105 mm, T237 Rifle, Figs. 9-9 through 9-11, was developed to provide a vehicle for investigation of weapon mechanism problems, sealing problems, ballistic problems, and other

concomitant problems associated with high rates of fire. It is a semiautomatic, fire chamber revolver type recoilless rifle capable of firing 5 rounds of fin-stabilized 105 mm HEAT ammunition within 12 sec. Total weight of the system is 710 lb exclusive of ammunition. Original models of the system were electrically operated so that power sources that are normally available on board full-tracked, self-propelled vehicles could be used. A gas operated option was developed along with a mechanical firing system that could be easily substituted for the electrical system.

Unique assembly and disassembly features were designed into the system so that assembly and disassembly could be accomplished in minimum time.

9-3.7 CONFIGURATION WITH PERFORATED CARTRIDGE CASE

One of the most important features of the recoilless rifle system is the use of the

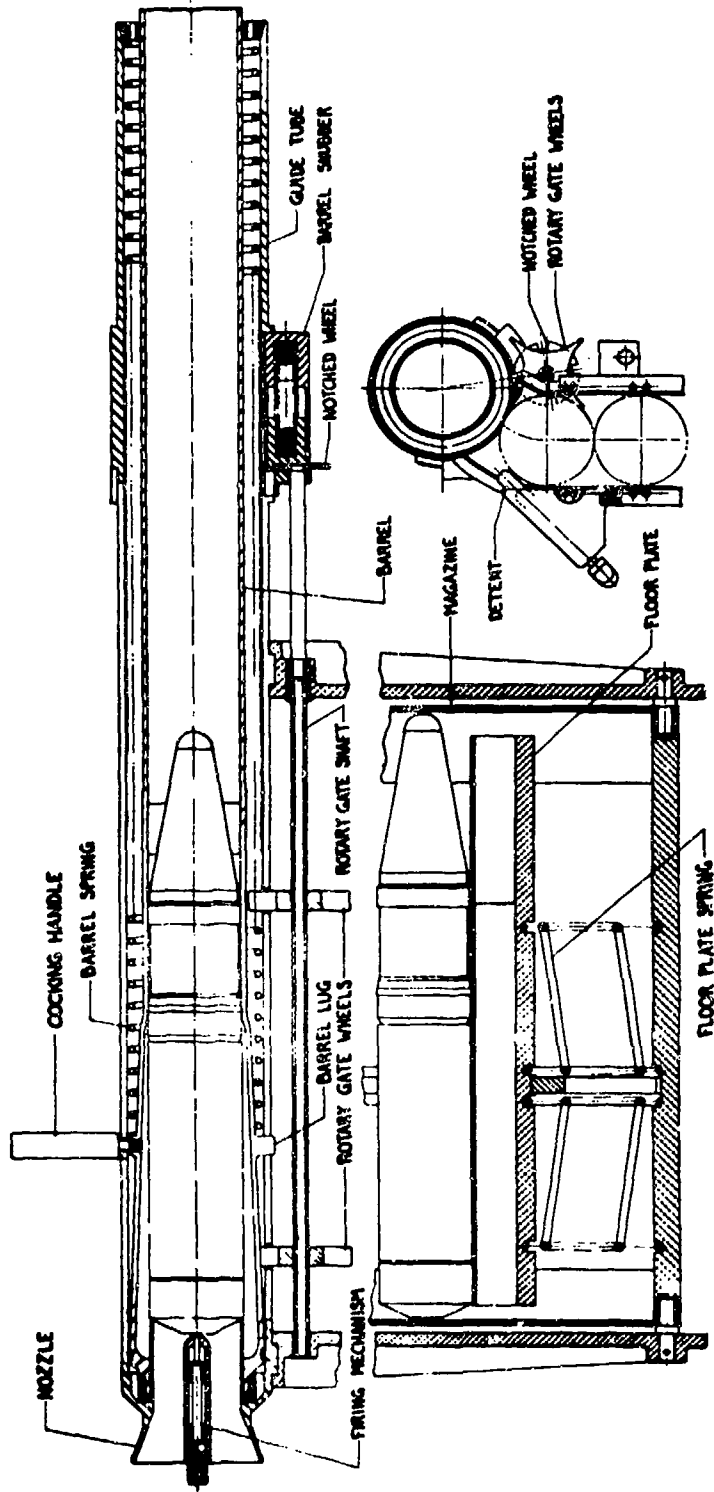


Figure 9-8. Side-loading Configuration

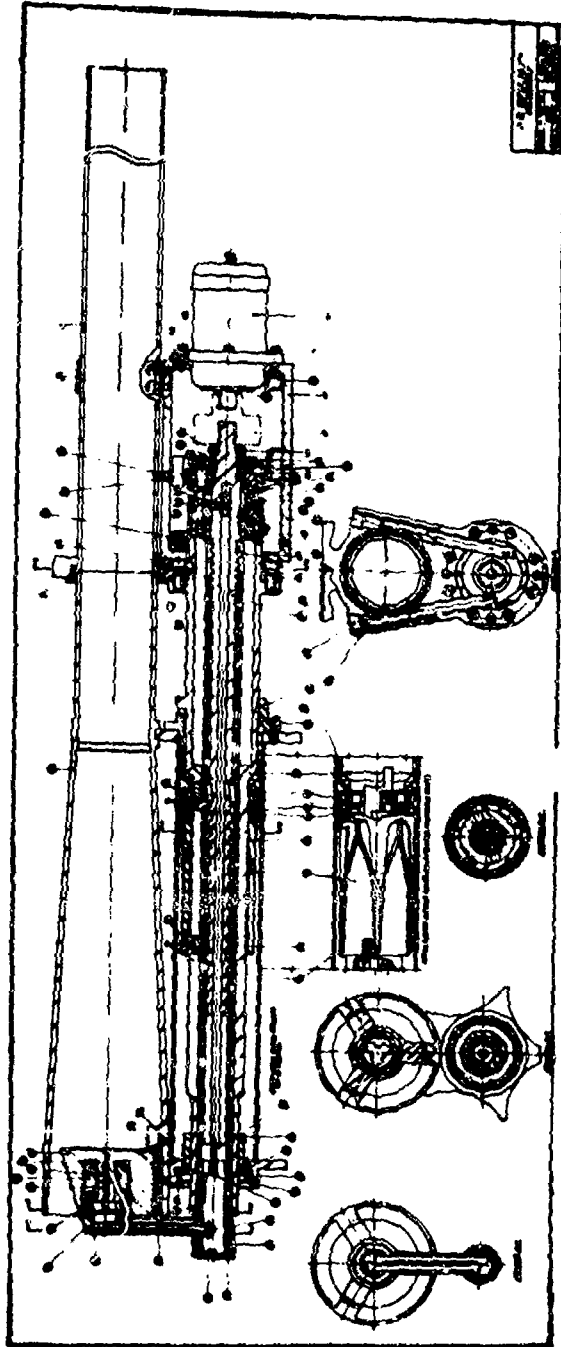


Figure 9-9. Rifle, Repeating, 105 mm, 7237. Assembly Drawing

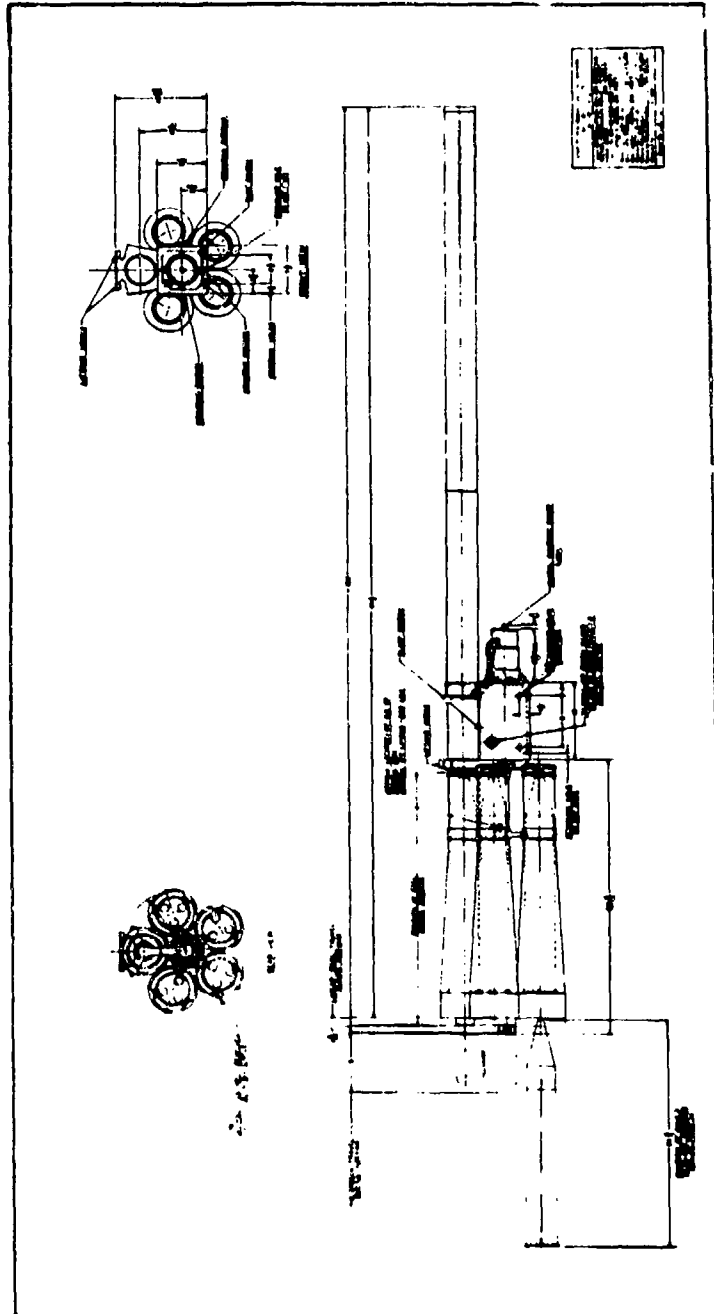


Figure 9-10. Rifle, Repeating, 105 mm, T237, Installation Drawing

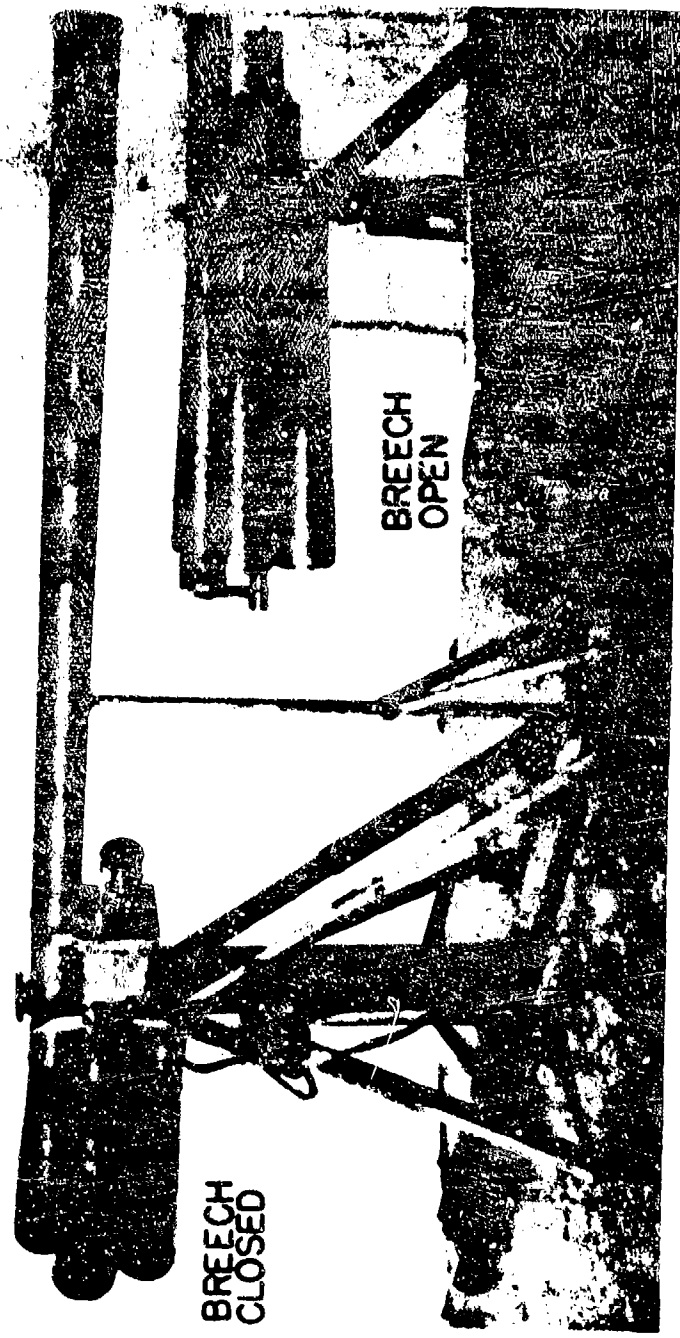


Figure 9-11. Rifle, Repeating, 105 mm, T237, on Assembly Mount

perforated cartridge case. As shown in Fig. 9-12 (Ref. 4), there are hundreds of small openings, with a thin cover that disintegrates to provide for the flow of the generated propellant gas. As the combined area of these perforations greatly exceeds the bore or throat area, there is little resistance to the flow of gas from the cartridge case. Thus, the case is made considerably smaller than the chamber. This, in turn, minimizes fluctuations in burning by insuring ignition at high loading density and combustion at correspondingly low loading density.

In order to be able to use several types of ammunition in a particular recoilless rifle or to be able to compensate for the effect of nozzle erosion and extreme ambient conditions on rifle performance, it is necessary to incorporate a recoil compensating device into the weapon system. Fig. 9-13 (Ref. 5), shows a recoil compensating ring installed in place in an M40 Rifle. The purpose of the ring is to enable the nozzle area to be adjusted until the recoil for a particular rifle-round combination is within the allowable tolerance. It is thus possible to adjust for any changes in the physical characteristics of the nozzle or type of ammunition.

Fig. 9-14 (Ref. 6) shows the use of a perforated cartridge case with a blow-out disc. The blow-out disc is one of the most important items in the central nozzle type recoilless rifle. The blow-out disc controls the amount of combustion which takes place prior to gas discharge by confining the propellant gas until the disc ruptures, and, hence, exerts considerable influence on the amount of unburned propellant loss through the nozzle during the initial stages of burning. The propellant gas generated passes through the cartridge case perforations into the annular chamber. After rupture of the blow-out disc, the gases pass from the chamber, back across the cartridge case wall, and out through the central nozzle. Blow-out discs having a thickness of 1/4 to 5/16 in.

have been made from paper-base phenolic materials for efficient use of propellant.

9-3.8 SPECIAL CONFIGURATIONS

Fig. 9-15 (Ref. 7) shows a typical configuration of a fin-stabilized projectile with the propellant attached to the boom. The propellant in this figure is pimple embossed sheet propellant in the form of circular discs with holes in the center, for the purpose of stacking on the projectile boom. The tapered stack of discs provides for proper ignition of propellant charge. The technique of attaching the propellant to the projectile also has the advantage that the metal or frangible cartridge case necessary to contain a granular form of propellant may be eliminated. This caseless charge then results in reduced round weight, greater economy in manufacturing, and elimination of case ejection after firing.

In many weapon systems it is often desirable to extend the maximum range. Fig. 9-16 (Ref. 8) shows a method of increasing the range of recoilless rifles through the use of a rocket assist. A solid propellant rocket motor is attached to the rear of the warhead compartment to provide the added energy for attaining the extra range.

One of the last series of recoilless weapon systems to be developed was the DAVY CROCKETT. As shown in Fig. 9-17, the DAVY CROCKETT weapon fired a large caliber projectile from a smaller caliber recoilless rifle. The main characteristics of this type of weapon are that the propellant gases act upon a "pusher" tube (spigot) which in turn pushes the oversize warhead that is accelerated completely outside of the gun tube. The use of a large, low pressure gun is then eliminated along with its associated problems of ballistic reproducibility.

9-4 DISADVANTAGES

The main disadvantages of a recoilless rifle

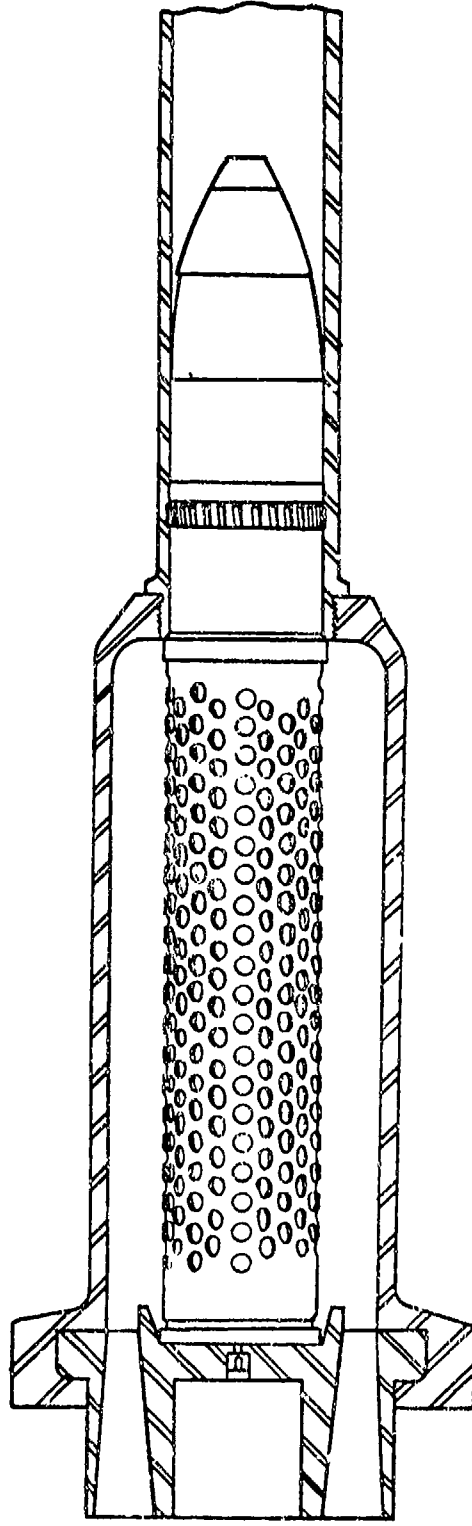


Figure 9-12. Configuration of Recoilless Rifle With Perforated Cartridge Case

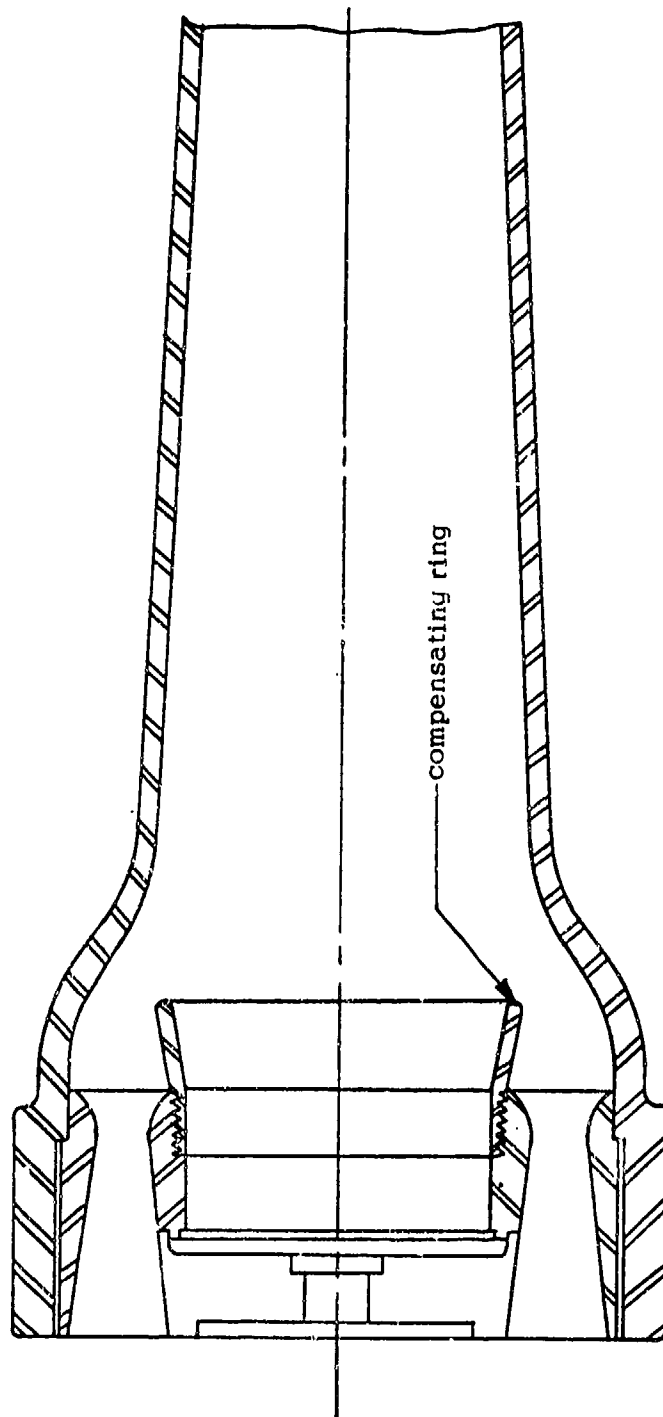


Figure 9-13. M40 Rifle With Recoil Compensating Ring in Place

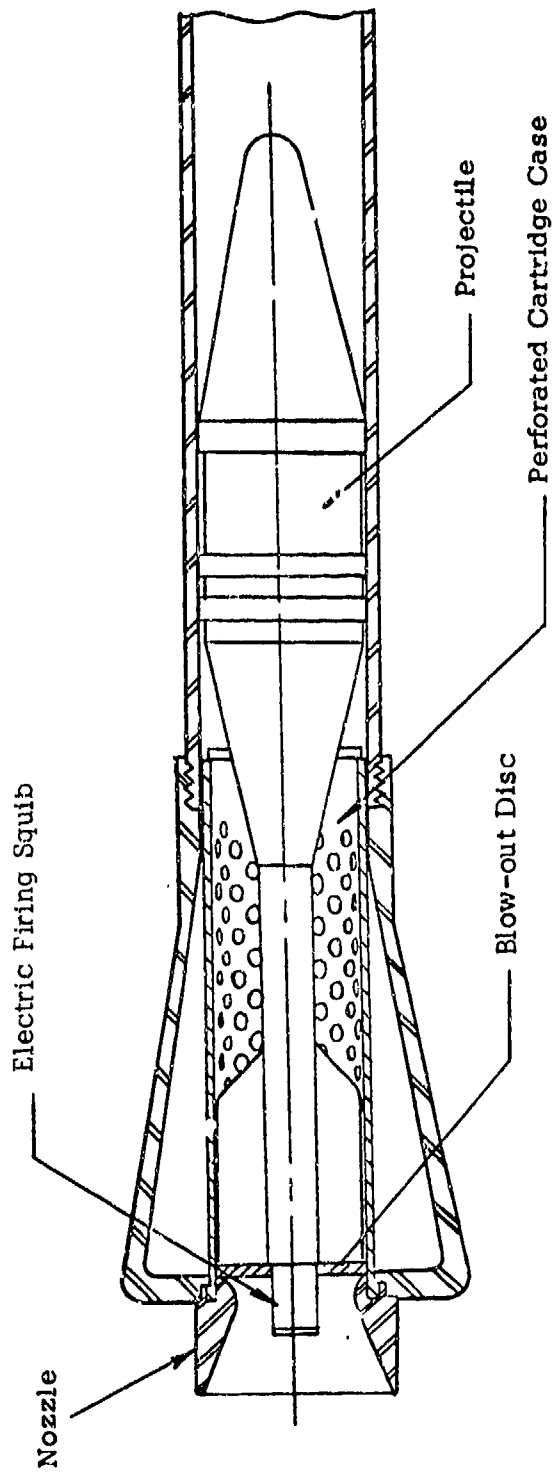


Figure 9-14. Sketch of Perforated Cartridge Case With Blow-out Disc



*Figure 9-15. Fin-stabilized Projectile With Propellant Attached, Quarter Section—
Ammunition, HEAT, 90 mm, T249E6*

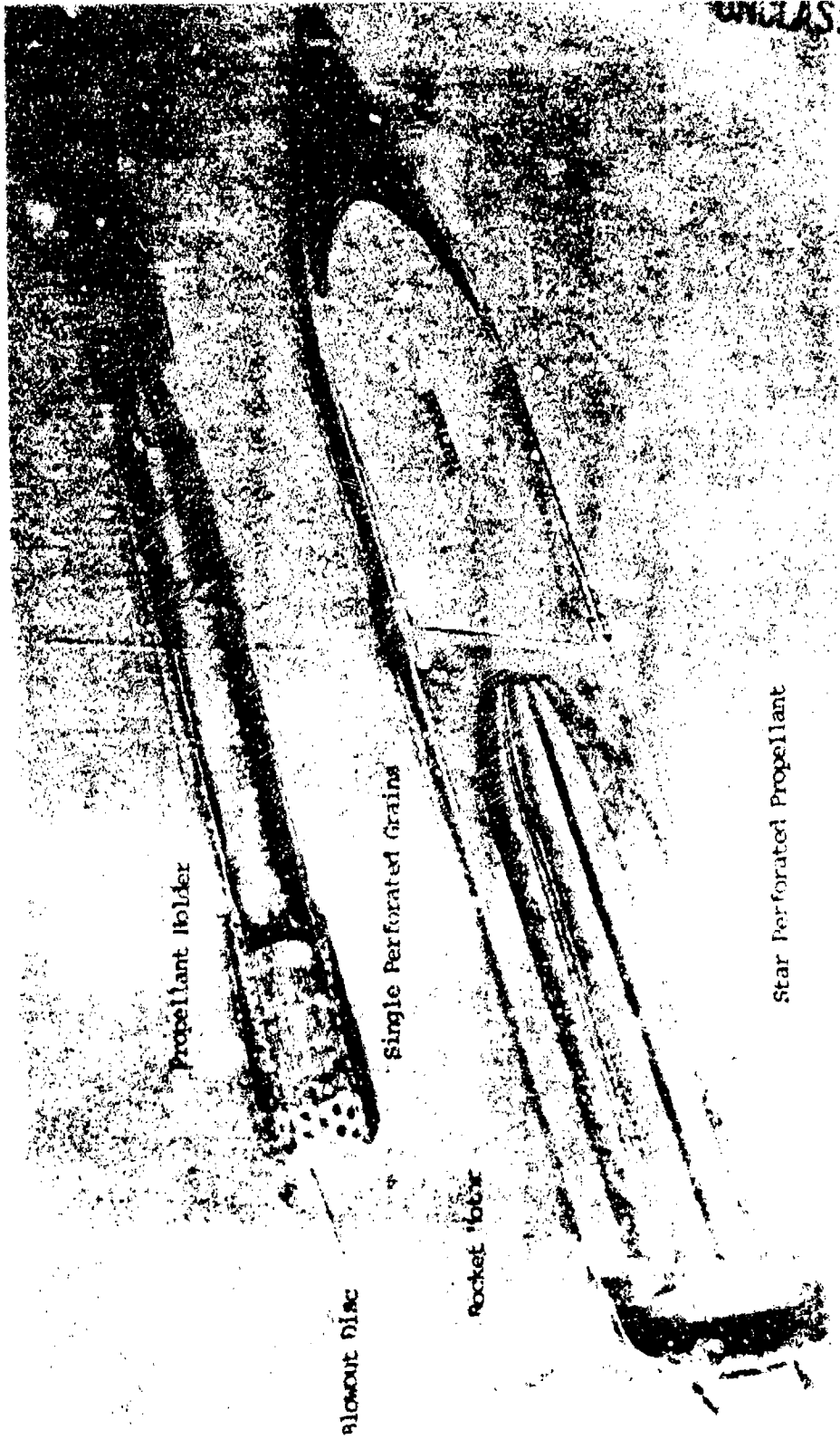


Figure 9-16. Hybrid Rocket-gun



Figure 9-17. Configuration to Fire Over-caliber Projectile, DAVY CROCKETT System, XM28



Figure 9-18. XM29 Weapon System Installed on M38A1 Vehicle

are the backblast, its associated flash, and round-to-round dispersion. Backblast is an inherent characteristic of the recoilless rifle design—the result of the escape of propellant gas to the rear of the gun. When using a recoilless rifle, it is necessary to protect both personnel and materiel for many yards to the rear of the gun. For example, the danger zone of the 57 mm M18 Rifle is a cone extending 50 ft to the rear of the weapon with a base 40 ft wide. In addition, personnel within 100 ft to the rear of the breech should not face the weapon because of the danger of flying particles thrown up by the blast action. While, in some cases, backblast may prevent the use of a recoilless rifle, altogether, many of the requirements can be met without much difficulty.

Associated with backblast are the undesirable effects of flash and smoke which serve to reveal the weapon position to the enemy. Whereas, the magnitude of backblast is determined by the projectile energy and, therefore, is incapable of considerable reduction, reductions in smoke and flash intensity have been made by the use of "smokeless" and "flashless" propellants.

Another disadvantage of a recoilless rifle is the inefficiency because of the additional propellant charge required to make the weapon recoilless. The ammunition weight and size per round are, therefore, greater for the recoilless rifle than for a closed-breech weapon of similar caliber. For example, in the case of 75 mm guns, the cartridge for the

recoilless rifle would require almost 3 lb of propellant as compared to 1 lb for a howitzer cartridge (Ref. 13). A 105 mm recoilless cartridge requires 8 lb of propellant as compared to 3 lb for the same caliber howitzer. Because of the extra propellant charge, the recoilless rifle cartridge case is longer and heavier than the closed-breech type cartridge case. However, the extra weight is offset somewhat by the fact that recoilless rifle projectiles do not have to be designed to withstand the higher acceleration forces to which a comparable howitzer projectile would be subjected during firing.

Low thermal capacity of the weapon system due to the light weight of the recoilless rifle, as compared with the heavier conventional guns of the same caliber, limits the rate of fire. Consequently, under high sustained rates of fire, the temperature of the recoilless rifle rises fairly rapidly to levels at which the yield strength of the gun tube material may fall below the safe design value and where cook-off of the cartridge may become a problem (Ref. 3).

Although initial development of recoilless rifles had as their objective in the United States giving the infantry antiarmor firepower, later objectives included adaptation to lightly armored combat vehicles for airborne forces. These objectives also lead to consideration of automatic and remote feeding, nozzle gases ducting, and salvo systems. Figs. 9-18 through 9-31 illustrate a variety of fielded and proposed configurations.

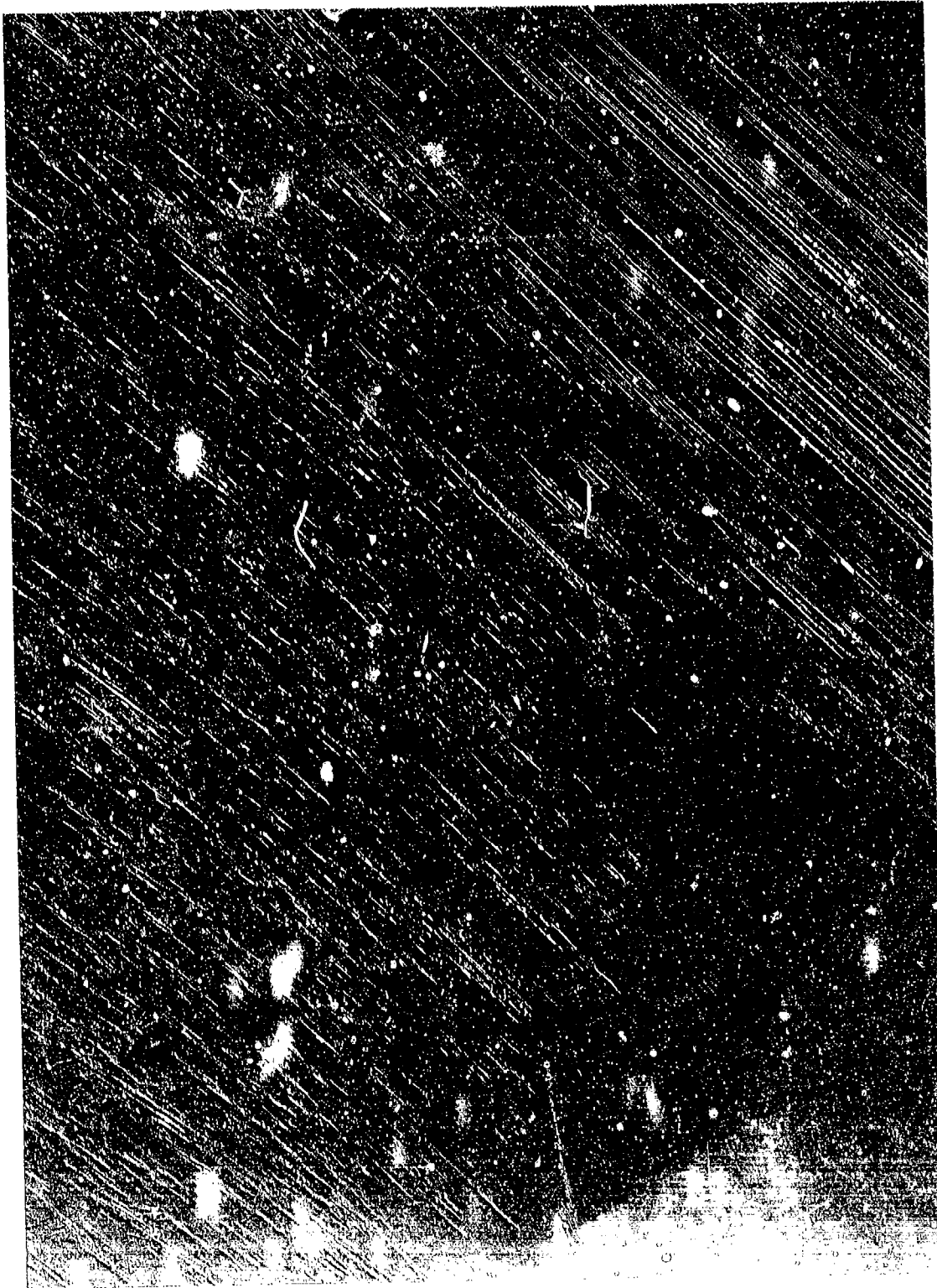


Figure 9-19. Rifle, Multiple, 106 mm Self propelled, M50

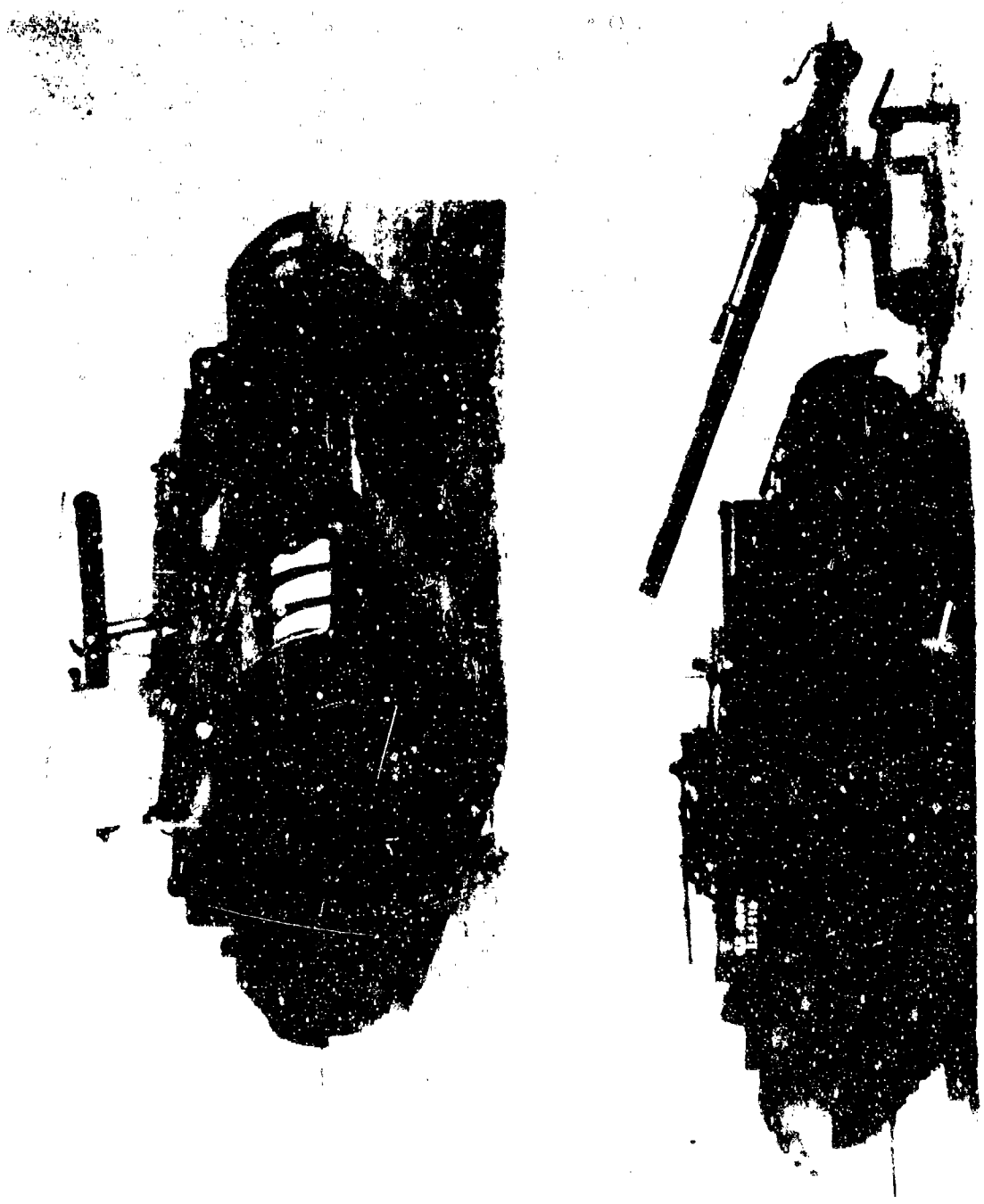


Figure 9-20. M56, Type A, M40, Recoilless Rifle



Figure 9-21. T114, Type B, Dual, M40 Recoilless Rifle

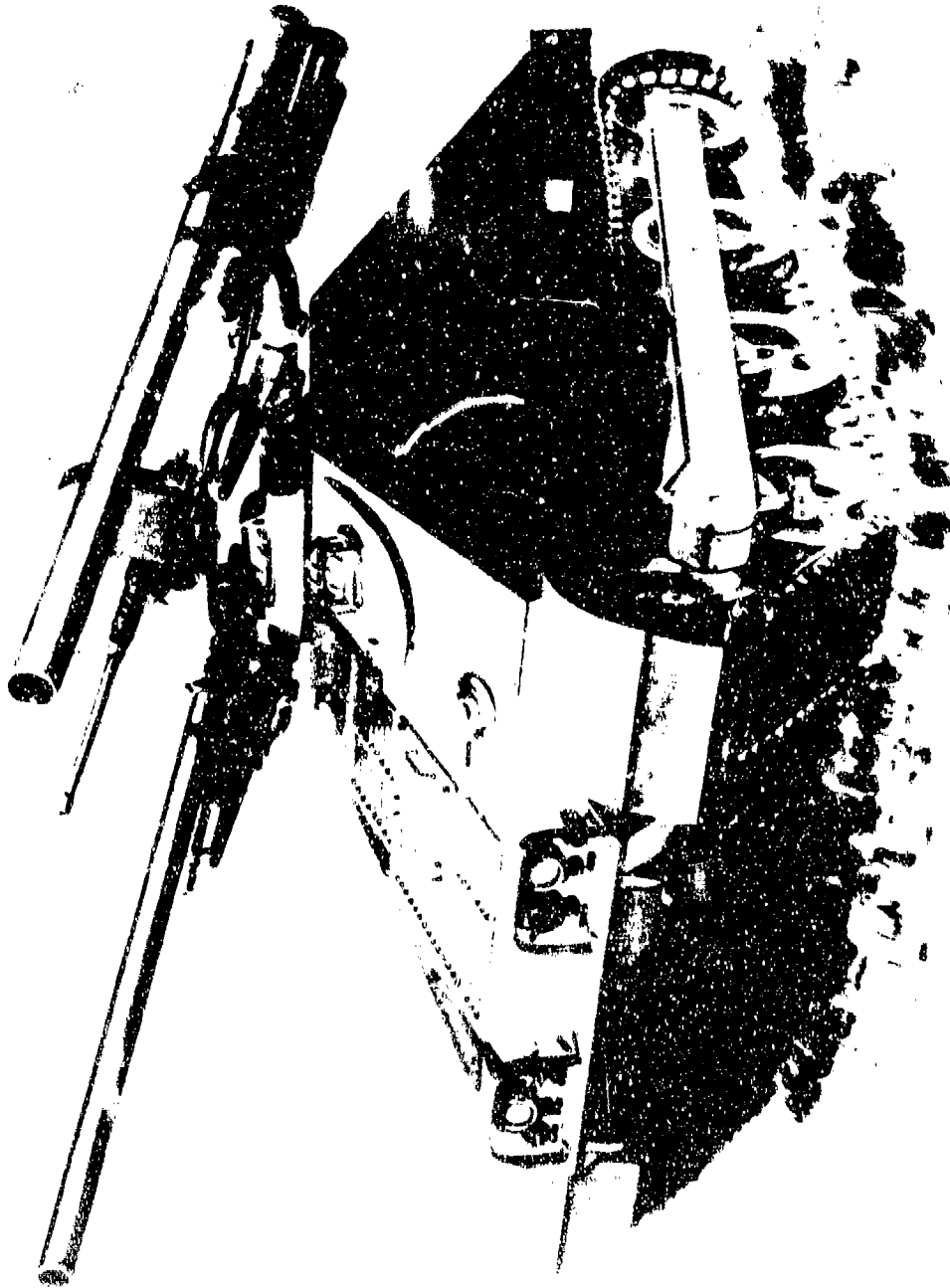


Figure 9-22. M50, Type A, Dual T237, Repeating Recillless Rifle, Revolver Type

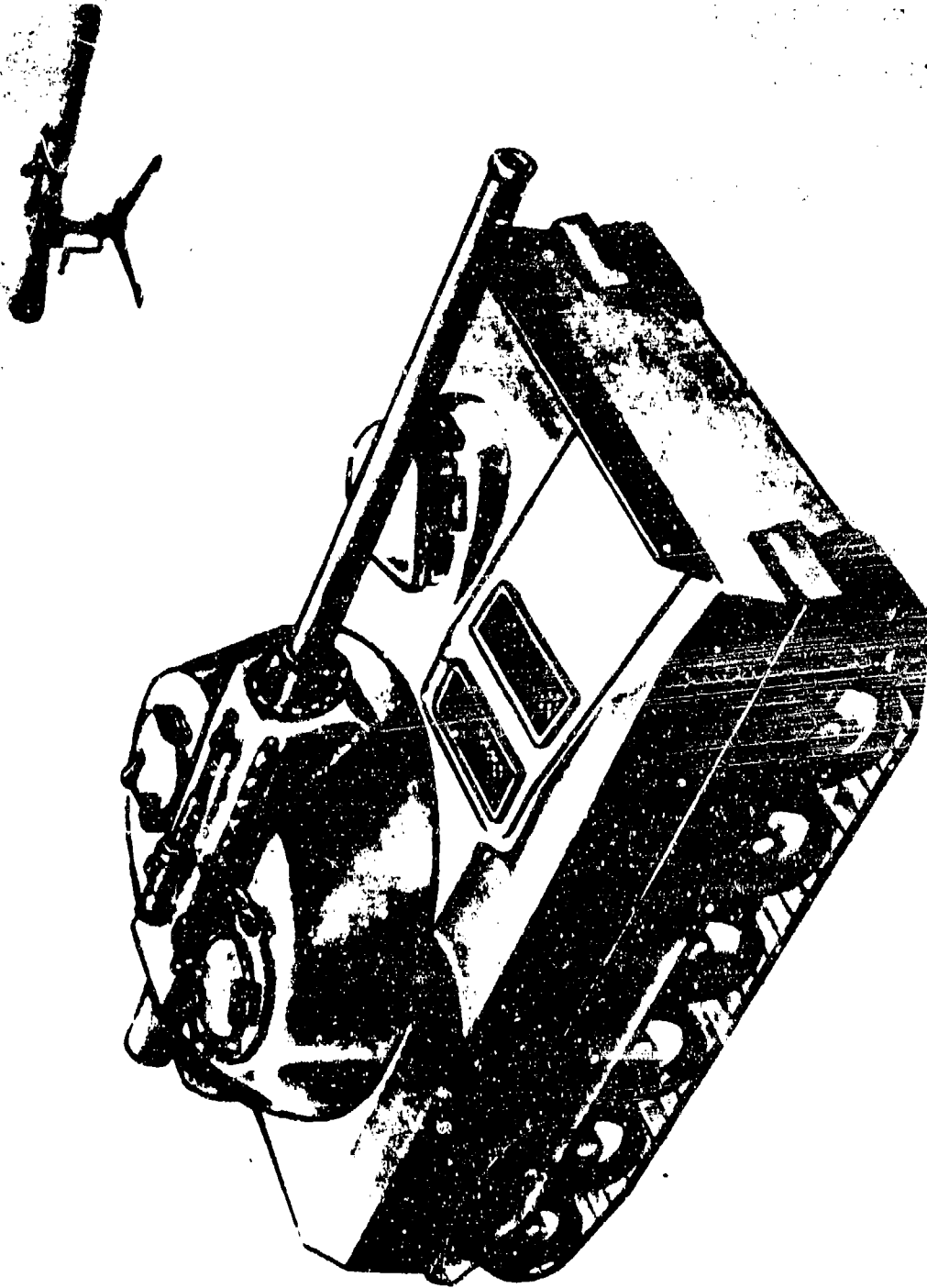


Figure 9-23. T114, Type B, Modified T237, Repeating Recoilless Rifle, Revolver Type

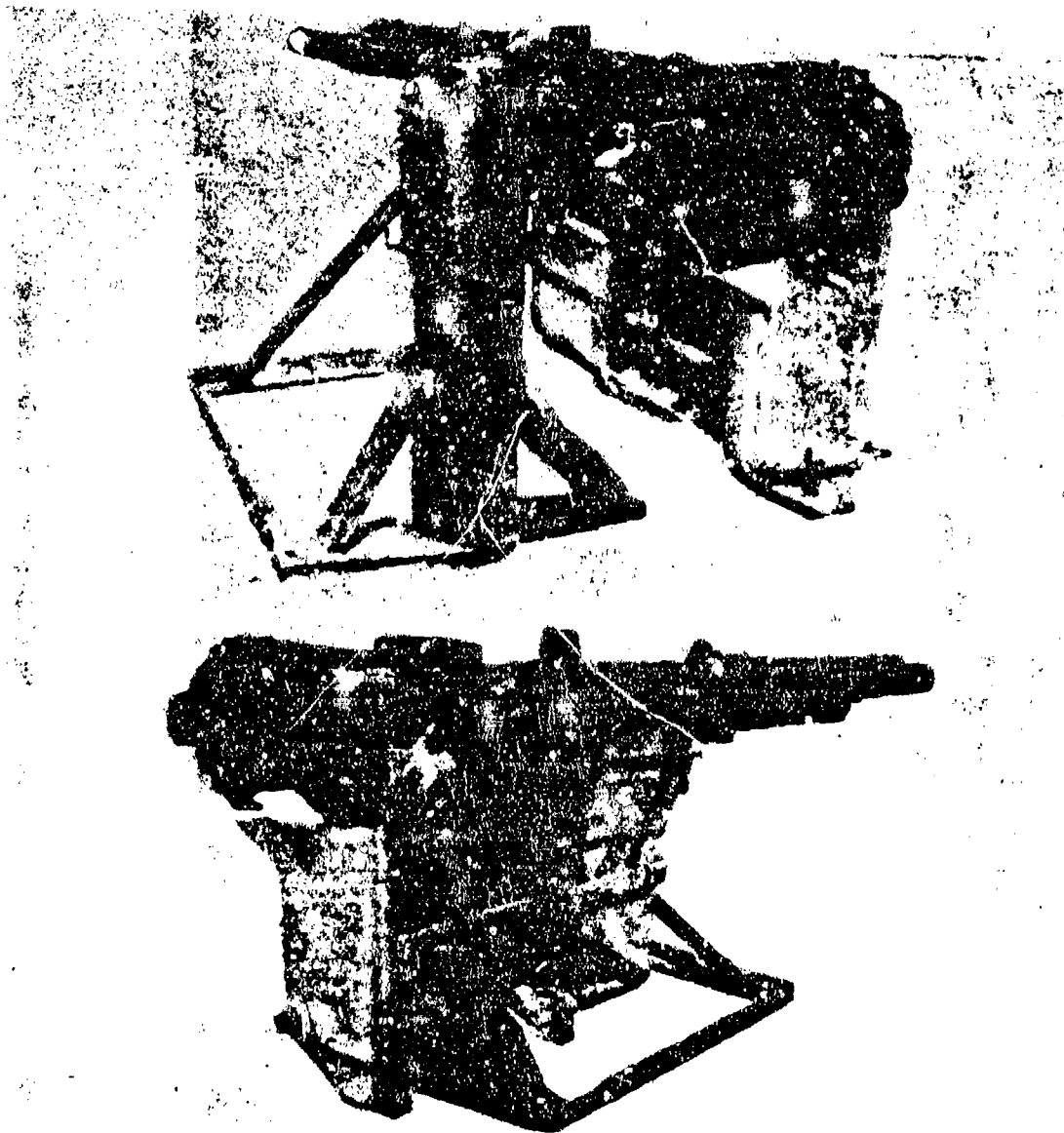


Figure 9-24. BB-1, (Mechanical Ram), Repeating Recoilless Rifle, Magazine Type



Figure 9-25. Ballistic Ram, Repeating Recoilless Rifle, Mounted on Lightweight Vehicle



Figure 9-26. M50, Type A, BB-1 (Mechanical Rsm), Repeating Recoilless Rifle, Magazine Type



Figure 9-27. M56, Type B, BB-1 (Mechanical Ram), Repeating Recoilless Rifle, Magazine Type



Figure 9-28. T114, Type B, BB-1 (Mechanical Ram,) Repeating Recoilless Rifle, Magazine Type

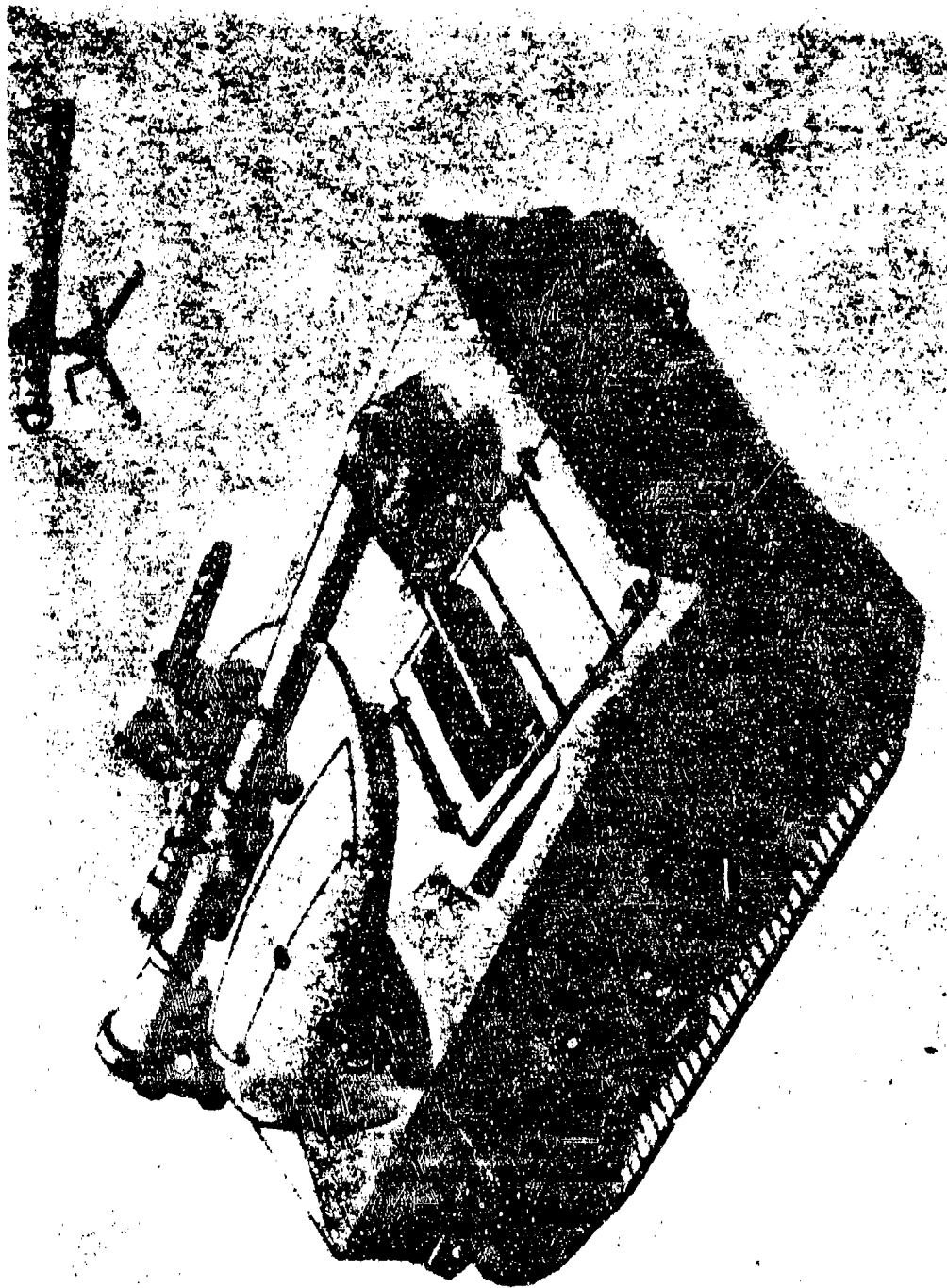


Figure 9-29. T114, Type A, Callistic Rem, Repeating Recolless Rifle, Magazine Type

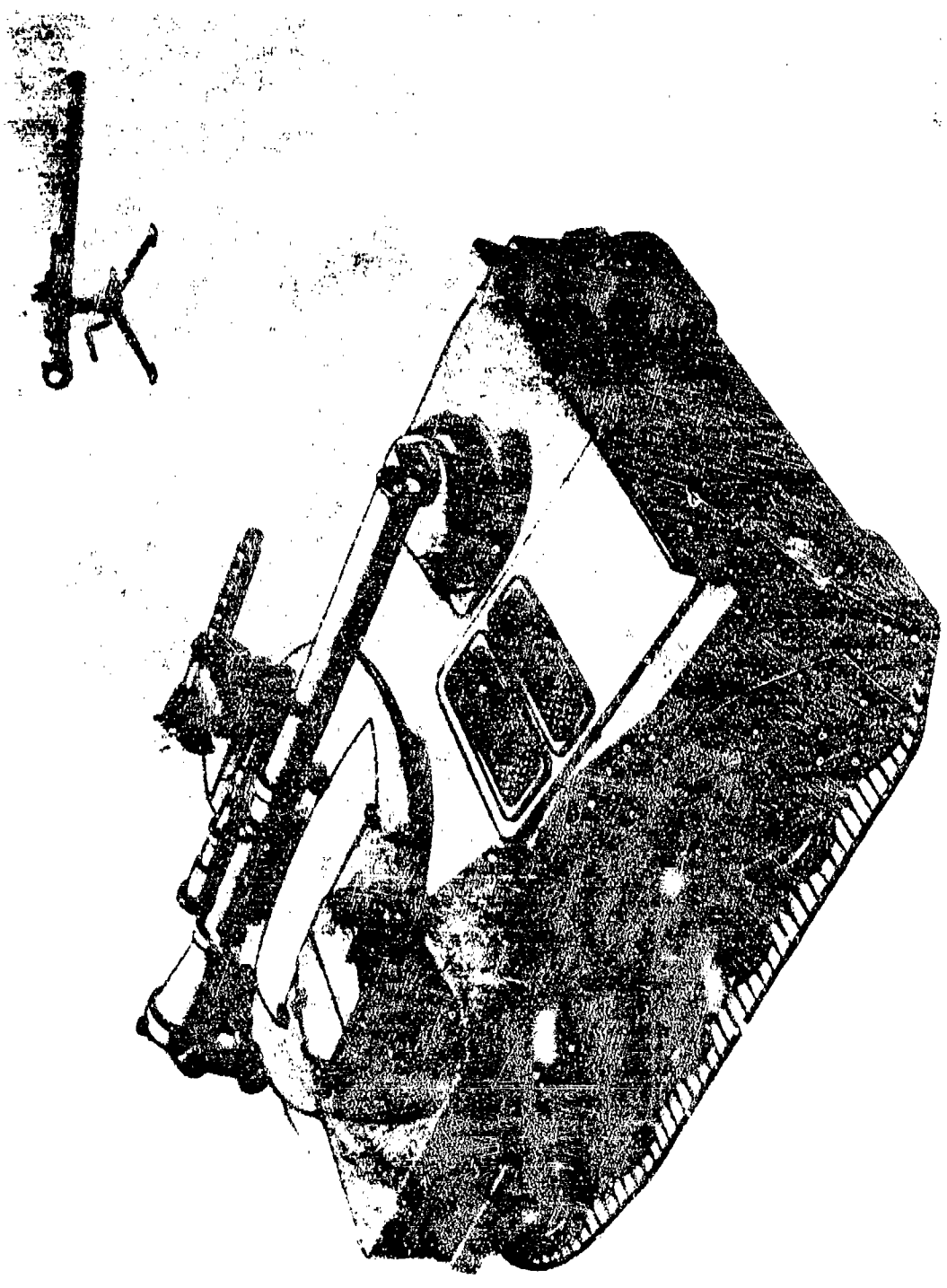


Figure 9-30 T114, Type B, Ballistic Ram, Repeating Recoilless Rifle, Magazine Type

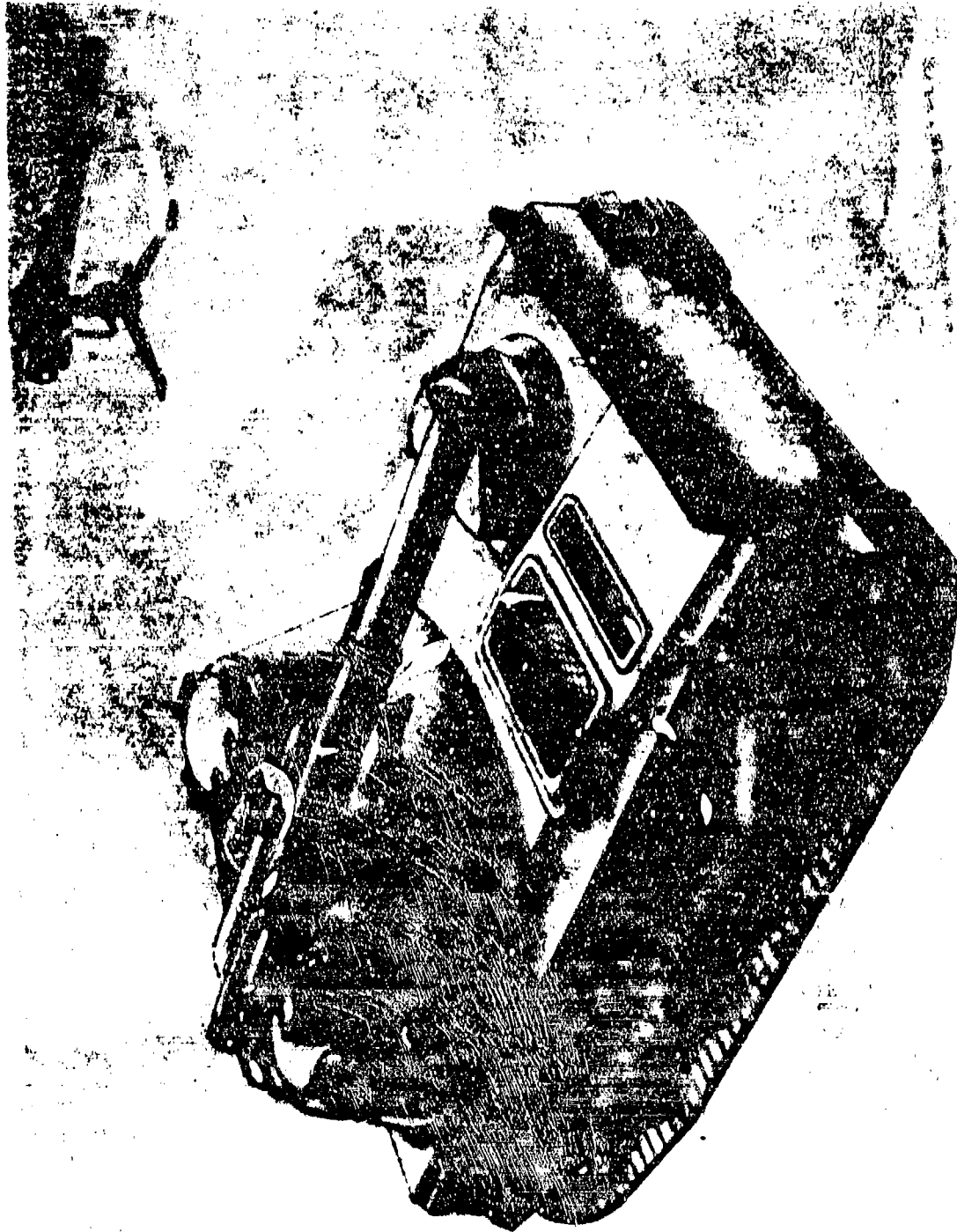


Figure 9-31. T114, Type B, Side-loading, Repeating Recoilless Rifle, Magazine Type

SECTION II

HUMAN ENGINEERING

9-5 INTRODUCTION

It is imperative that each new weapon design be studied and tested extensively in order to insure its safety and efficient functioning under the control of human operators.

From the safety standpoint, recoilless rifles have the unique requirement in that considerable attention must be devoted to the effects of backblast, noise, smoke, and flash. In addition, operational effectiveness is dependent upon other features of the weapon - such as the lack of recoil, light weight, and the psychological effects of blast, smoke, and flash. Also, the tactical and psychological advantages of placing artillery-type weapons in the hands of front-line infantry must be considered.

In order to make a concerted effort to take the capabilities of the human operator into account so as to increase the effectiveness of recoilless weapons, the Engineering Psychology Division of Frankford Arsenal (Ref. 9) divided the scope of the problem into four areas. These channels of study were

1. Analyses of the human factor aspects of previously developed systems, in order to determine whether any important steps had been omitted or whether shifts in emphasis might have produced a better weapon system.
2. Studies of the physical features of present experimental and standard weapons, bringing to bear upon them human factor data from physiology, anthropometry, and psychology.
3. Analyses of recoilless rifles and personnel functioning as a weapon system, to improve safety and efficiency.

4. Studies of the human factors evident from the first three investigations which affect the probability of a first round hit on a selected target and reduce recognition-to-hit time.

9-6 PRIMARY FACTORS

9-6.1 THE MAN USING THE WEAPON

The human engineering design considerations for the man using the weapon can be grouped into the following areas:

1. Weapon and ammunition carrying
2. Breaking-out ammunition
3. Emplacing, moving, and re-emplacing rifle
4. Loading and unloading rifle
5. Detecting and choosing targets
6. Ranging, laying of rifle, and firing.

Since recoilless rifles are infantry weapons, the problem of portability is very important. The weight of the rifle will determine whether it is capable of being carried by one or two men and how it is to be carried. A rifle weighing less than 35 lb (Ref. 14) can be efficiently carried high on the back while heavier rifles are more efficiently carried low on the back. Rifles weighing up to 70 lb are capable of being carried by one man for a short distance but will have to be carried by two men for longer distances. The type of carry employed for a specific rifle must be taken into account in the design of the weapon. For example, a two-man breech-muzzle carry, which is less fatiguing than a side-by-side carry, necessitates either per-

manent rigid handles attached to the rifle or the use of two web straps encircling the barrel and chamber of the gun.

A potentially critical situation arises with the covering and uncovering of a rifle, and breaking out the ammunition. In the case of a surprise attack, it is necessary to rapidly uncover the rifle and break out the ammunition even under conditions of inclement weather. An important consideration in this area is the ability to perform these tasks while wearing arctic clothing and mittens.

Because of the versatility of the smaller caliber recoilless rifles—capable of being fired either from the shoulder, from an integral mount or from a number of auxiliary mounts—the gun emplacement task is another important factor which must be included in human engineering design considerations. Depending upon the type of mount—integral or separate—different unfolding, locking, unscrewing, and adjusting operations may have to be performed during the emplacement of the gun. As such, all locking or adjustment knobs should be easily accessible and large enough to permit rotation, and all extension operations of bipod arms easily made under all conditions.

Of all the operations of the recoilless rifle, the loading and unloading of the rifle are the most critical of the human engineering aspects that must be considered. The loading and unloading of a rifle basically consists of unlocking and opening of the breech, inserting the round, closing of the breech, and extraction of the round. One of the essential requirements in this operation is that the handles on the breech be designed so that the assistant gunner (loader) is not required to have any part of his body pass behind the rifle when opening and closing the breech. This will depend, of course, on the proper placement and orientation of both breech and chamber handles, and the manner in which the breech opens. In order to prevent fatigue of the loader and the resulting slowdown of

round loading, it is also desirable to have the breech operations performed by horizontal pushing or pulling movements relative to the assistant gunner's chest since a man can exert more force by a push or pull than by a sidewise motion.

A specific human engineering design consideration relative to the round insertion operation is to insure that the rotating bands on the ammunition automatically engage the lands and grooves of the barrel to eliminate the delays that may result from indexing. The one aspect of the extraction process which must be considered is to allow sufficient clearance, so that the loader can make complete extraction when wearing arctic mittens, after the positive extraction of the round by the extractor device in the breechblock.

Important safety requirements necessitate that the gunner's safety indicator move automatically to the "safe" position when the breech is opened and that it be manually returned to the "fire" position after the breech is closed before the weapon can be fired. The indents of the safe and fire indicators, stamped "S" and "F", respectively, should be visible under all light conditions.

The human engineering design considerations involved during the design of a recoilless weapon may be subdivided into four areas: (1) pistol grip and trigger, (2) shoulder rests and recoil, (3) monopod handle, and (4) sight. The important design factors of the pistol grip are the trigger pull force be not more than about 7 lb per finger and that the trigger travel be not more than 0.5 in. Any travel longer than 0.5 in. causes uncertainty on the part of the gunner or may require the gunner to change his grip to exert more pressure on the trigger.

Shoulder rests should be adequately designed dimensionally for usage with both light and arctic clothing. Consideration also should be given to the possible use of canvas-covered

pads attached to areas which contact the shoulder.

For shoulder-fired recoilless rifles, a desirable design consideration in the position of the monopod handle is that the monopod and pistol grip be in the same vertical plane. This allows the gunner to brace the upper part of his left arm against his body while grasping the monopod when the weapon is fired. The result is increased steadiness of holding the rifle, with consequent better aiming.

It is important that the sighting be positioned sufficiently forward, so that when the rifle is fired from the prone position, the gunner is clear of the blast area without being extremely cramped. A second consideration is the use of a standardized sight, since variations in sights may lead to a disruption of performance when a gunner switches weapons. Sufficient head clearance also should be allowed between the sight and face shield of the rifle so that the gunner can fit his eye to the eyepiece of the sight while wearing a standard combat helmet. For further information on some of the human engineering considerations given to the first recoilless rifles, the reader is referred to Ref. 10.

9-6.2 FIELD SERVICING

Field servicing, or maintenance, is the service performed at the organizational level to keep the weapon in proper firing condition. This servicing consists of periodic inspections, cleaning and lubrication, minor adjustments, and replacement of parts that are worn, broken, or otherwise unserviceable. Because of the mobility requirements of the recoilless weapon, the amount of tools, test equipment, and supplies is limited to the organizational level. Since the maintenance skills at the organizational level are of a limited nature, the design engineer must plan appropriate preventive maintenance and servicing procedures.

All parts of the rifle should be easily

inspected for damage or traces of corrosion and then allow for ease of cleaning and lubricating. All damaged parts should be capable of replacement with a minimum amount of hand tools, i.e., removed from the weapon simply by loosening screws and nuts or by rotation of a locking knob. It should be emphasized that even the simplest of these types of operations should be capable of being performed while wearing arctic clothing.

9-6.3 MANUFACTURING PERSONNEL

The basic human engineering design considerations to be observed during the course of manufacturing of the recoilless rifle are similar but not limited to those associated with the operation and servicing of the weapon. Additional consideration must be given to the safety of the personnel loading and assembling the round of ammunition, and to the complexity of the individual assembly operations. Because of the nature of the round of ammunition, it is necessary that each assembly operation be as safe as possible, and performed under controlled conditions of environment.

In addition, each assembly and loading operation should be as simple as possible so as to avoid any possible assembly error while keeping the cost of the assembly to a minimum. The order of assembly operations also must be given special consideration, since the effect that one operation may have on another can result in errors uncontrollable by the assembly personnel. The early difficulties encountered in the original design of the fin-stabilized HEAT ammunition for the 105 mm BAT weapon are examples of some of the uncontrollable problems that can arise because the pertinent aspects and order of assembly were not considered when the design was established. For example, the necessity of positioning and retaining the propellant to the rear of the cartridge case complicated the loading process so that the loader inadvertently would introduce propel-

lant grains in the primer cavity unless he was extremely careful. This placed unnecessary responsibility on the loader for what is a normally simple operation. The most important consideration to be given here is that there should be close coordination between the design organization and the manufacturing and loading facilities during the development stage of the weapon in order to insure that the proper input of the human engineering factors is taking place.

9-7 HUMAN FACTORS ENGINEERING EVALUATION

Since the function of human engineering is to increase the efficiency of man-machine system in order to evaluate the superiority of one design over another, it is often necessary to test the design concept with the use of a mock-up and test personnel. One of the first examples of a human engineering test on a recoilless rifle was a time study of the registering of pre-engraved projectiles in the rifling (Ref. 1, Vol. IV). A time study was made of the act of chambering complete rounds, since there might be difficulty in lining up the pre-engraved rotating band with the barrel rifling. Twenty rounds of ammunition were divided into two equal lots of 10. In one of the lots, the pre-engraved rotating band was cut away completely so as to offer no obstruction to chambering. Three operators were chosen to perform the test, only one having had any previous experience with a recoilless rifle. A time study was then performed of chambering ten pre-engraved rounds and then ten plain rounds. Each chambering operation consisted of picking up the round, chambering it, closing and locking the breech, opening the breech, and extracting the round. Timing was done with stop watch by an independent observer. This pattern was repeated until fifty rounds of each lot had been chambered. It was found that the use of pre-engraved projectiles took approximately 25 percent longer to register than the plain rounds.

This result led to the eventual incorporation of automatic indexing devices in the projectiles, such as indexing buttons and springs, which reduced the time required to line up the pre-engraved rotating band with the lands and grooves of the rifling. For a round with indexing buttons, it is merely necessary to place the round in the chamber so that the projectile is started down the tube and then drive the round home with the heel of the hand. The indexing button operates by compressing into the projectile when it strikes a land, and then expanding when it hits the rifling groove. After engaging the groove, these buttons force the round to rotate so that the pre-engraved band lines up with the barrel rifling as the round is chambered and completely inserted. Thus, as a result of these tests, a slight redesign of the pre-engraved projectile enabled registering time to be the same as that of a round without the pre-engraved rotating band.

9-8 AREAS OF APPLICATION

Some areas of specific application of human engineering have been described in par. 9-6. However, at any instance of man-weapon interface—i.e., during weapon carrying, emplacing, loading, firing, maintenance, testing, manufacturing, assembly, etc.—it is necessary to insure personnel the safety while trying to attain the highest efficiency of the recoilless weapon system. For further information, the reader is referred to Ref. 10 and Ref. 14.

9-9 SPECIFIC RESPONSIBILITIES

The responsibility of the human engineering group is to insure that the design engineer has considered the human factor of the weapon system, both from the standpoint of safety and from the standpoint of operational effectiveness of the weapon. This responsibility begins with the analysis of the initial design and continues with a detailed operational and performance study of the proto-

type weapon. It coordinates the initial manufacturing and assembly operations with the design organization, and compiles the feedback of user comments on the weapon during actual field experience.

In the collection of data from these various analyses, the human engineering group is responsible for identifying specific problem

areas and identifying the specific factors that should receive highest priority. By continuously monitoring all phases of the development program, this group assures that the human engineering function is incorporated into the design of the weapon system and will not have to be compromised, "added on", or "built into" the weapon at a later date with the resulting high cost.

SECTION III

RELIABILITY

9-10 BASIC PRINCIPLES

Reliability is expressed simply as the probability of a successful operation in the mode for which it was intended. In the case of a recoilless rifle or other weapon system, this successful operation is the scoring of hits. While the design engineer keeps in mind this main purpose, he must consider such various constraints of secondary nature as cost, light weight, low silhouette, portability, and ease of maintenance and operation—all of which might affect system reliability. In designing reliability into the recoilless rifle weapon systems, the designer must remember that reliability must be considered in the practical context of the equipment being designed, i.e., in the actual environmental conditions to which the weapon system will be exposed—including operation, storage, and transportation—rather than in any abstract or theoretical sense.

Considering these primary and secondary purposes of the recoilless weapon system, it is readily seen that reliability is an important factor in the design of the system, and it is the design engineer who is in the position to make the necessary contributions for a reliable system, i.e., reliability must be designed into the equipment; it cannot be built in at a later stage in the system development. The importance of reliability is further emphasized by the fact that in producing a reliable equipment, the manufacturer will have solved simultaneously many maintainability problems. Equipment that is 100 percent reliable for its intended useful life requires no corrective maintenance. Because reliability depends to a large extent on both proper manufacturing procedures and quality control tests, the design engineer is again in the position to make major contributions to the system reliability

through proper choice of fabrication, assembly, and inspection techniques. Although the definition of reliability is straightforward, the application of reliability to the weapon has become an ever increasing problem, to the extent that reliability engineering has become a specialized field in its own right.

If the basic definition of reliability is the probability of successful operation, the reliability of the total system becomes the product of the probabilities of its individual parts to operate successfully (provided they are statistically independent). It follows from this that the more complex a system, the greater the chance of failure. By using the least number of subsystems and components necessary to accomplish the system function, i.e., by making the system as simple as performance requirements permit, it is possible to increase the reliability of the weapon system. One exception to the general rule of simplicity just described is caused by the use of redundant (parallel or back-up) subsystems.

Redundancy—providing back-up or alternate subsystems—provides a direct counter to the previously defined product rule of reliability because the higher the number of alternate subsystems, the greater the probability that one of them—and the more the system as a whole—will operate satisfactorily. At first consideration, the incorporation of redundant subsystems may seem incompatible with the ideals of light-weight and compact construction. However, with recent advances in solid-state electronics, gyroscope technology, hydraulics and other fields, light and compact components for alternate subsystems can be added without substantial increase in total system weight and envelope. The criteria for determining whether redundancy should be designed into the system are the resulting

increase in reliability; increase in weight, size, and complexity caused by addition of the backup system; and the extent to which the added component, subsystem, or system is critical to successful operation.

Another method of increasing system reliability is through the use of standard components and techniques, the reliability of which has been proven in many applications and types of operations. If a system is "designed" (implying that a new product is being developed) with relatively untried components and subsystems, the product rule of reliability will generate lower system reliability due to the lower reliability figures of the individual components. Also, when using new components, relatively little is known about their behavior in a specific environmental condition or when two or more new components are combined or used in an interacting application. The specific conditions under which a subsystem is to operate can markedly influence its reliability.

Standard components or parts are defined generally as those which are commercially available, i.e., components which do not have to be specially designed for a particular application, and which conform to a Military, Federal, or industrial Specification or Standard. Reliability history for these standard parts is available from various military, federal, commercial, and industrial trade association sources, whereas, the necessary history for a new system or component can be obtained only through the performance of accelerated life and environmental tests.

Other factors that contribute to the reliability of the system as much as those already discussed are the training of production workers to reduce human error, use of proper organization to ensure exchange of information within the design and production facilities, and adequate testing. While these areas are not primarily the concern of the design engineer, he is often the first to be aware of any problems related to them and is

often responsible for assisting in the required change in manufacturing or quality assurance procedures. Reliability also can be increased during detail design phases by proper selection of materials, protective finishes, and types of lubrication. These are discussed in pars. 9-11 and 9-12.

9-11 MATERIALS

In the selection of materials for a recoilless weapon system, several factors influence the system reliability, namely

1. Stress
2. Impact
3. Friction, wear, and abrasion
4. Corrosion resistance
5. Effects of high and low temperatures
6. Weight (portability).

In order to select the proper materials, the designer must have complete knowledge of the magnitude and nature of the operational loads, and the resulting stresses to which the weapon system will be subjected. Once the stresses have been determined for the various elements of the system, it is usually possible to select the materials that provide the necessary ultimate and fatigue strengths in order to ensure that the components will not fail under the action of prescribed loading conditions.

Impact is the second factor to be considered in the selection of materials and is one that influences the strength of the material in bending, torsion, compression, tension, and shear. Because a recoilless rifle is subjected to impact loads during transportation over various types of terrain and combat conditions, it is necessary for the designer to select materials that will provide the necessary energy absorbing properties. Since it is

difficult to ascertain the magnitude of impact loads, the designer often will include requisite impact loading factors in stress calculations to ensure that the various components will be designed adequately.

Because of the flow of hot propellant gases in recoilless rifle operations, it is important to select materials that do not exhibit high wear rates and friction at the elevated operation temperatures. These factors definitely are to be considered in the design of breech, nozzle, and gun tube since continued nozzle erosion or gun tube wear immediately would reduce the operational reliability of the system.

Recoilless rifle weapon systems are subjected to extreme variation of environmental conditions, and, in order to prevent deterioration of any component under these conditions, it is imperative to specify corrosion resistant and fungous non-nutrient materials in the design of all parts. Further, it is important to avoid the use of dissimilar metals in direct contact, since moisture can promote galvanic action resulting in serious corrosion. If it is necessary to use two dissimilar metals in contact with each other, plastic coatings may be used to provide electrical insulation, but specification of any electroplating, hot dip, or molten metal spray should be made with caution since they might be introducing new sources of galvanic action.

The mechanical behavior of materials under conditions of high and low temperature is one of the most important factors to be considered in the selection of materials for the weapon system. These conditions can cause significant changes in such material properties as creep, fatigue, tensile strength, ductility, and cause oxidation, crack formation, and surface deterioration of the material. In general, strength properties decrease and wear rates increase with increasing temperature. Because of the thermal gradients that exist within the weapon system during the course of operation, it is also necessary to consider the effects of

thermal stresses induced and avoid the use of dissimilar materials having different coefficients of expansion. The use of such dissimilar metals in contact could cause unequal expansion and set up sufficiently high stresses resulting in failure.

In the consideration of all the factors influencing the selection of materials, it is often necessary to weigh the relative significance of each of the opposing or limiting considerations over the other in order to achieve an optimum trade-off. For example, a design problem involving strength versus corrosion resistance may lead to the following considerations:

1. Pure aluminum will meet corrosion requirements for a particular component but does not meet strength requirements.
2. High strength aluminum alloys meet strength requirements but are not as corrosion resistant as pure metal.
3. Certain alloy steels have good strength and corrosion resistance properties but will introduce additional weight.
4. A combination of steel and aluminum alloy parts may meet strength and corrosion resistance requirements, but may create problems of galvanic attack between the two metals.

In order to make the proper choice from among the given alternative compromises, the designer must be able to make a quantitative comparison of these alternatives with respect to reliability and, in times of war, availability.

9-12 ENVIRONMENTAL DETERIORATION

There are three basic approaches to designing for the adverse effects of environmental conditions to which weapon systems are exposed. The first of these basic approaches is to employ effective protective

devices while using conventional components and materials in the equipment itself. In this approach, the component would be protected against climatic extremes by use of shielding, insulating, and cooling. Or, in the event of a dynamic environment generating an impulsive force, the equipment might employ some type of shock absorbing mount or support. While making use of conventional equipment, this first approach does not preclude the use of any advanced technique for protecting the equipment.

The second basic approach involves extrapolating known data on material properties, and uses known concepts and design techniques to develop components that will withstand specific environmental conditions. The third basic approach, the newest of the three, attempts to develop new methods of designing materiel (especially electronic components) and new devices based on entirely new design concepts.

Recoilless weapon systems are transported through and used over the entire spectrum of environmental factors. The process of protecting materiel against the adverse effects of moisture (including salt water), dust, sand, snow, fungus, etc., is called weatherproofing and is accomplished in a number of ways. These methods include the use of corrosion-resistant paints and finishes, sealing, potting, wholly or partly enclosing, and the proper selection of materials and components which are chosen or adapted to fit the specific needs of the design.

The various weatherproofing techniques employ:

1. Mechanical finishing for smooth, polished surfaces
2. Hot dip, electroplating, and molten metal spray processes using copper, nickel, chromium, tin, cadmium, zinc and lead plating, and aluminum and anodic coatings

3. Case hardening processes

4. Phosphate and black oxide chemical coatings

5. Numerous organic paints, including top coats and primers.

The processes furnishing the best corrosion protection involve the use of an inorganic surface treatment (chemical or electrochemical) over which an organic finish (primer and top coat) is applied. Often, some departure from the optimum corrosion protection must be made because of other required surface properties. For example, a working surface cannot be painted, but can still be given a considerable degree of corrosion protection by a chemical treatment or by electroplating.

In order to protect completely specific components of the weapon system against the effects of moisture, dust, and fungous spores, it is necessary to enclose and seal the components. Optical and gyroscopic devices and some electronic components require this type of protection since direct exposure to some of the adverse climatic effects can cause the component to become defective or inoperable. Even though a part or component of equipment is enclosed for protection, it may also be necessary to seal the enclosure in order to protect the component against "breathing". "Breathing", the inward or outward movement of air from the enclosure due to variations in ambient pressure, can cause infiltration of moisture, dust, and fungous spores into the enclosure. By use of good sealing techniques, breathing can be prevented completely to produce a hermetic seal, provided that the nature of the design is compatible to permit sealing.

Sealing techniques include impregnating the pores of the enclosure case, minimizing the cover contact area and use of gasketing materials and coatings, use of O-rings and other seal rings on rotating and sliding shafts,

and potting. Potting is a special form of hermetic sealing in which the component to be sealed is coated with a special potting compound that serves to insulate the component against certain climatic and

electrical environments. Potting finds its greatest use in the sealing of electric and electronic components that do not require replacement or maintenance and which would not be damaged during the potting process.

SECTION IV

MAINTAINABILITY

9-13 BASIC PRINCIPLES

In designing for the maintainability of a specific equipment, the design engineer must abide by a series of basic principles that are dictated by the Armed Services maintenance organizational structure. The first basic principle is that all preventive maintenance should be capable of being performed by unskilled personnel even under adverse working conditions. Secondly, in the event of equipment malfunction, the cause must be traceable, with a minimum need for special instrumentation, to a subassembly or component that can be replaced easily as a unit under combat conditions; or the malfunction should be capable of being temporarily bypassed or corrected by simple operations using simple tools. The third principle dictates that vital equipment should be so designed that it can be repaired rapidly by replacement of defective parts at the field-maintenance level, for quick return to combat units. The last principle states that complete disassembly and overhaul of the equipment need be performed only at widely separated occasions in order to avoid both the frequent long-distance shipments to remote depots and the overtaxing of depot facilities.

Maintenance pertains to actions necessary to maintain an item in serviceable condition while maintainability is a performance characteristic expressed as a probability (see MIL-STD-778 and MIL-STD-721).

9-14 ACCESSIBILITY

The importance of accessibility in maintenance is reflected in the following facts:

1. Hard-to-reach components requiring preventive maintenance or frequent replacement are more likely to be neglected

2. Inaccessible or not easily isolated equipment that needs to be energized or operating during servicing and maintenance, exposes the maintenance personnel to possible electrical shock, contact with moving parts, and other hazard

3. Ease of access reduces the probability of human error

4. Easily accessible parts and components reduce the time during which maintenance personnel and vulnerable parts of equipment being serviced would have to be exposed to undesirable environmental conditions, if maintenance must be performed under adverse conditions. The design engineer must keep these facts in mind during the course of the design process.

The problem of accessibility can be properly analyzed by asking the following series of questions:

1. What routine maintenance will be required? In answering this question, the designer has listed the components that are used during preventive maintenance or which require frequent replacement.

2. What trouble-shooting will be required at the organizational maintenance level, i.e., under combat conditions to restore the equipment rapidly to operating condition?

3. Which components, assemblies, and subassemblies will be removed and replaced as units at the organizational maintenance level and which will be adjusted at this level?

4. What trouble-shooting, removal of parts, and adjustment will occur at the field-maintenance level?

In answering this series of questions, the designer will have generated the data needed to specify the location and type of mounting for specific parts or components of equipment and controls; and the location and geometry of necessary access openings and the type of access opening covers; i.e., hinged, screw-fastened, or quick opening.

For a complete treatment of designing for accessibility in maintenance, the reader is referred to Ref. 12.

9-15 STANDARDIZATION

As pointed out in par. 9-10, the use of nonstandard components may decrease equipment reliability. Accordingly, the use of nonstandard components may also increase the required maintenance. The reasons for a possible increase in maintenance as cited in Ref. 12 are:

1. Nonstandard parts usually are stored for longer periods of time because of their low demand, a factor that tends to bring about deterioration.

2. The larger the number of different components in the equipment, the more complicated the task of maintenance personnel to install, handle, and maintain the equipment.

3. Small-quantity production of nonstandard items is characterized by lack of uniformity and makes replacement parts more difficult to obtain.

Because of the reliability and maintenance problems encountered in the use of nonstandard components, the Department of Defense Standardization Program (see Refs. 11 and

15) was prepared to guide design engineers in the application of standardization to all stages of design. This resulted in ease and rapidity of replacing and interchanging parts and components.

In addition to standardization, the designer should aim at maximum interchangeability of components and subassemblies, i.e., for different parts of the same equipment, the same components should be used wherever possible even though the functions of assemblies in which they are installed may be quite different. Maximum use of interchangeable parts leads to (1) efficient, uniform maintenance procedures; (2) fewer repair parts to support the equipment at every maintenance echelon; (3) fewer failures; and (4) lower costs. This interchangeability concept is carried out for all subassemblies and components (especially at the organizational level).

It is also important to design equipment that can be maintained and overhauled with as few tools as the end requirements permit, and with standard tools wherever possible. The use of standard tools is particularly important in the maintenance to be performed at the organization and field levels. Even at the depot level, the use of elaborate test set-ups, special jigs, and the like should be avoided. Maintenance tools should be considered as an integral part of all design phases, so that design concepts requiring heavy or elaborate maintenance and test equipment can be discarded easily in the design study. Also, by making small changes in design, it is often possible to eliminate unnecessary tools. For example, it will probably be found that reducing the variety of fasteners used on a piece of equipment will also reduce the number of hand tools required.

REFERENCES

1. *Recoilless Weapons, Volumes I to VI*, Contract No. W-36-034-ORD-7652,

W-36-034-ORD-7708, Franklin Institute, Laboratories for Research and Develop-

- ment, Philadelphia, Pa., for Ordnance Department, US Army, May 1948.
2. René R. Studler and W.J. Kroeger, *Battalion Anti-Tank Recoilless Rifles Systems*, Report No. R1273, Pitman-Dunn Laboratories, Frankford Arsenal, Philadelphia, Pa., July 1953.
 3. Robert Markgraf, *Repeating Recoilless Rifles*, Pitman-Dunn Laboratories, Frankford Arsenal, Philadelphia, Pa., March 1960.
 4. TM 9-3062, *Operation and Organization Maintenance 57 mm Rifles M18, M18A1 and T15E16, Tripod Mount M1917A2 and Weapon Tripod Mount M74*, Department of Army Technical Manual, June 1975.
 5. *Development of 105 mm Battalion Anti-tank Weapons and Interior Ballistics*, Final Report, Contract No. DA-11-022-ORD-1157, Armour Research Foundation of Illinois Institute of Technology, Chicago, Ill., December 1955.
 6. *Interim Technical Report on the Development of the 90 mm Rifle T149*, Contract No. DA-19-020-ORD-40, prepared by Arthur D. Little, Inc., for Frankford Arsenal, Cambridge, Mass., June 1, 1955.
 7. *Notes on Development Type Materiel; Cartridge, Heat, 90 mm T249E6 for Use in the 90 mm T219E4 Recoilless Rifle, Platoon Anti-Tank System (PAT)*. Report PE-6, Ordnance Project No. TA1-1461 Prepared at Frankford Arsenal under direction of Ordnance Research and Development Division, June 1958.
 8. M. Cohen, *Preliminary Design Study of a Recoilless Weapon Solution for the Missile A Requirement*, Report No. R-1488, Frankford Arsenal, Philadelphia, Pa., January 1959.
 9. *Human Engineering at Frankford Arsenal*, Human Engineering Report No. 1, MR-553, Pitman-Dunn Laboratories, Frankford Arsenal, May 1953.
 10. *Human Engineering Aspects of Recoilless Rifle Design: M18 and T66 Series*, Human Engineering Report No. 8, R1295, Pitman-Dunn Laboratories, Frankford Arsenal, Philadelphia, Pa., November 1955.
 11. AMCP 706-327, *Engineering Design Handbook, Fire Control Systems—General*.
 12. AMCP 706-134, *Engineering Design Handbook, Maintainability Guide for Design*.
 13. AMCP 706-108, *Engineering Design Handbook, Elements of Armament Engineering, Part Three, Weapon Systems and Components*.
 14. MIL-STD-1472B, *Human Engineering Design Criteria for Military Systems, Equipment and Facilities*, 31 Dec 74.
 15. Defense Standardization Manual 4120.3-M, *Standardization Policies, Procedures and Instructions*, Office of Assistant Secretary of Defense (Installations and Logistics), January 1972.

CHAPTER 10
RIFLE AND RIFLE COMPONENTS

10-0 LIST OF SYMBOLS A_b = bore area, in² P_g = propellant gas pressure, psi R = radius of projectile, in. T = rifling torque, in.-lb α = angle of rifling twist, deg ρ = polar radius of gyration of projectile,
in.

SECTION I

OVERALL DESIGN CONSIDERATIONS

10-1 GENERAL

The functions of the various rifle components are closely interdependent, and, as such, any variances in the performance of a specific component affect the overall performance uniformity of the weapon. Variations in performance also can be attributed to human and environmental interfaces as well. Items such as gunner instability, improper maintenance, or drastic changes in weather or environmental conditions may affect the system performance as much as deterioration in performance of any individual component.

In Part Two, Theoretical Analysis, of this handbook, the theoretical background was given for both interior and exterior ballistics of the recoilless rifle weapon system. With this background, it is possible to see how factors—such as lot-to-lot variations in the compositions of igniter, propellant, and primer compositions or the effects of temperature and humidity—will cause variations in the peak chamber pressure and thus, variations in the projectile muzzle velocity.

The last four chapters of this handbook describe the specific design considerations of the major components of the recoilless rifle weapon system. In these chapters, the effects of phenomena such as erosion, propellant gas leakage, projectile balloting, bias, and solid propellant loss on performance uniformity are described in detail. Upon reading the last four chapters, it is possible to understand that the weapon designer is faced with the fairly difficult task of selecting the best features of various components, given certain economic

constraints and integrating them into a weapon system that is insensitive to the factors that affect performance uniformity.

10-2 HAMMER BLOW

Most recoilless rifles use mechanical types of ignition systems to detonate the cartridge primer. Since the primer is designed to be somewhat insensitive to shock and rough handling, it is necessary to transfer a sufficient amount of energy to the firing pin for detonation of the primer to occur. In order for this operation to be reliably performed over the intended service life of the weapon, a fairly stiff hammer spring is used to accelerate the hammer prior to its impacting the firing pin. In the 120 mm HAW (heavy antitank weapon) weapon system, the hammer spring transfers 371 in.-oz of energy to the firing pin (Ref. 1). For reliable detonation of the primer to occur, it is necessary to insure that the lubrication used in the firing mechanism is not fouled by the propellant gas or fragments from the cartridge, and is not sensitive to temperature extremes.

10-3 FIRING PIN

Firing pins used to detonate percussion primers are cylindrical in shape, having a diameter of approximately 0.30 in. and a length to diameter ratio of 3 to 1. The tip of the firing pin, which stabs the primer, is hemispherical in shape with a radius of about 0.044 in. The firing pin, depending upon the type of hammer used, may be solid or have a bore on the rear of the firing pin for insertion

of the hammer mechanism. To prevent fouling of the firing mechanism, an oversized flange is placed on the forward circumference of the firing pin. This prevents passage of any products of the firing from passing by the pin into the firing mechanism.

10-4 PRIMER

The primers used in recoilless rifle ammunition are generally of the small arms, 0.30 or 0.50-cal, percussion type. For example, the primer for the 120 mm Cartridge, HEAT, XM419 uses a 0.50-cal 50M primer. The percussion primer and a supplementary FFFG black powder charge of approximately 10 grains are assembled into a metal tube and this assembly is force-fitted, cemented or threaded into the base of the cartridge or igniter tube assembly. Upon detonation, the flames of the primer and ignited FFFG powder charge vent through a flash hole in the base of the igniter tube or projectile boom to ignite the booster charge.

Since the primer functions as the link between the energy source (firing pin) and the ammunition firing, it becomes a significant key to the successful weapon operation. In order to define specific input characteristics, primers are qualified with respect to sensitivity requirements that reflect the amount of energy that the firing pin is required to deliver. Primer manufacturers customarily provide in their data sheets the 100 percent "all-fire" level of the primer. This all-fire level is the mean firing height H plus five standard deviations σ for a specific weight dropped to test the primer or $(H + 5\sigma)$ times (drop weight). Since this sensitivity data represents optimum test conditions, it is desirable to provide an added margin of input energy—usually taken as being equal to the required all-fire level. As a general rule, it is best for the designer to select the least sensitive primer available which is compatible with firing mechanism and environmental requirements.

10-5 BOOSTER

The type of charge used to ignite the main propellant charge is A1 black powder. A general rule calls for between 100 and 200 grains of powder per pound of main propellant charge. As an example, the 120 mm Cartridge, HEAT, XM419 for the HAW weapon requires a 2175-grain charge of A1 black powder for igniting a main charge of 10.7 lb of M5 Propellant. The booster charge is loaded into a cylindrical, perforated igniter tube positioned in the center of the cartridge case. Upon ignition, the booster produces a hot gas that is distributed uniformly to ignite the main propellant charge positioned around the exterior of the igniter tube. In fixed fin-stabilized ammunition, the projectile boom serves as the igniter tube, with the main propellant charge loaded around the projectile boom. Maximum loading density of the black powder booster charge usually is considered to be 0.8 g-cm^{-3} .

10-6 PROPELLANT

Both single- and double-base propellants have been used in recoilless rifle ammunition. Single-base propellants, of which M10 Propellant is an example, are those in which the principal active ingredient is nitrocellulose. Double-base propellants are those containing nitrocellulose and a liquid organic nitrate (nitroglycerin) which gelatinizes the nitrocellulose. M2 and M5 Propellants are examples of double-base propellants that were used almost exclusively in the early stages of recoilless rifle development. Except in the case of the DAVY CROCKETT weapon system, double-base propellants have not been used in the later recoilless weapons intended for repeated firings because they tend to be excessively erosive in the nozzle and bore areas. Cooler burning Propellants such as M10 and T28 (M26) were used in later recoilless rifle systems such as 90 mm MAW, 106 mm BAT, and 120 mm HAW.

Single- and double-base propellants have been used in both granular and single- or multiperforated forms. Perforated propellant grains normally have a length-to-diameter ratio of 5 to 1, with web size between 0.020 and 0.040 in. as required to meet specific performance requirements. Propellant loading densities vary between 0.4 and 0.6 g-cm⁻³. As described fully in Chapters 5 and 11, the required chamber pressure is controlled by the ballisticians' choice of propellant composition, granulation, and web. Changes in the burning characteristics can be accomplished by inhibiting certain surfaces of the propellant grain from burning. For example, a perforated grain may have its exterior surface coated with an inhibitor material that allows the grain to burn only on the surface of the perforations.

10-7 CARTRIDGE CASE

In recoilless rifle weapon systems, it is necessary to allow for the venting of the propellant gases into the chamber. To meet the requirements of the different types of chamber-nozzle configurations, several types of cartridge cases have been used. The majority of recoilless rifles use perforated steel cartridge cases with a liner inside to cover the perforation and with provisions to crimp the case to the projectile to fix the ammunition. The perforated case allows the propellant to vent radially into the chamber and rearward through the nozzle. In most cases, cost limitations have required that sidewalls of the perforated case be fabricated from rolled, perforated sheets even though the use of seamless tubing is much more desirable for strength reasons. The cartridge case base is then welded or brazed into the cartridge case. Rupture or excessive case deformation, as a result of firing, will prevent extraction of the case. To meet the strength and deformation requirements, the design results in a case with rather unfavorable weight characteristics.

The liner, which may be a Mylarfilm, serves to confine the propellant in the case and must withstand environmental and handling conditions while providing a moisture seal.

Crimping the cartridge to the projectile serves a dual purpose in recoilless rifle application: first, to "fix" the ammunition and achieve uniform alignment; and, second, to provide shot start, i.e., the force required to initiate projectile motion. Projectiles used in recoilless rifles usually have either pre-engraved or essentially no engraving bands and as a result shot start cannot occur while the band is being engraved, as is the case with artillery ammunition. Shot-start is a desirable feature in that it contributes to performance uniformity of the weapon. Too high a level of shot-start will produce excessive initial forward recoil while too low a level will produce undesirable muzzle velocity variations.

10-8 PROJECTILE

Additional design aspects must be evaluated after the projectile envelope has been established. A rotating band located on the projectile outer diameter is required in order to center the projectile in the bore, impart spin, and to provide obturation for fin-stabilized projectiles. For spinning projectiles with pre-engraved rotating bands, an additional obturator consisting of a rubber or plastic ring is needed. The rotating band may be an integral part of the projectile or it may be a separate copper material band swaged to the projectile. Plastic bands are used with fin-stabilized projectiles, and they are cemented or ejection molded into place. The height of the band is such that a minimum clearance exists between the band and bore rifling so as to minimize propellant gas leakage. The band height must take into account the degree of strain compensation present in the tube, see pars. 10-14 and 10-28.

Another design consideration is to provide

a circumferential groove in the projectile where the cartridge case is crimped in order to obtain a fixed round of ammunition. Design of the groove will depend upon the amount of shot-start force desired for separation of the projectile from the cartridge case. Two widely spaced bourrelets (bore rifling surfaces) are included on the fore and aft outer diameters of the projectile, in order to eliminate in-bore yaw (balloting) of the projectile.

For fin-stabilized projectiles, design studies will consider several possible choices, fixed versus semifixed and boattailed versus boom-tailed fins. Semifixed fins are generally used on boattailed projectiles whereas fixed fins are attached to boom type projectiles.

10-9 BREACH-CARTRIDGE RELATION

The interrelationships between the breech and the cartridge, of interest to the designer, include:

1. Installation of the round of ammunition
2. Initiation of the round
3. Retention of the case during firing
4. Proper flow configuration for recoil compensating gases
5. Adequate sealing
6. Extraction of the case after firing.

The distance between the breechblock to the seating point of the cartridge, headspace, is of major importance to the designer as it is one of the factors determining firing pin travel. Adequate sealing is essential to prevent propellant gas from entering the firing and breech mechanisms and causing erosive damage and fouling of the components. Proper clearance between the opening provided and cartridge must exist in order to assure effective chambering of the round.

10-10 CHAMBER-CARTRIDGE RELATION

Gas flow from the cartridge to nozzle is a major factor influencing the chamber-cartridge relations. Thus, in an annular nozzle recoilless rifle sufficient clearance must be provided between the cartridge and the chamber wall so as not to restrict the gas flow to the nozzle. In a central nozzle system, the annular space between the cartridge and chamber is not required since the case is frangible. Upon firing, the case ruptures and is ejected through the nozzle. However, it is often necessary to extend the chamber length to reduce solid propellant loss in this central nozzle configuration. The kidney-shaped nozzle, by minimizing propellant loss, provides the configuration with the minimum chamber volume and offers a resulting weight savings.

Radial clearance between the projectile tail fins and the cartridge case and the chamber must be provided to prevent scoring the case and/or the chamber.

10-11 TUBE-CHAMBER RELATION

Recoilless rifle ammunition using a perforated cartridge case requires support by the gun tube at the cartridge case mouth in rifles with larger than bore sized chambers. The mouth of the case is designed to minimize deformation which would prevent easy extraction of the case after firing.

The bourrelet of the projectile is designed to give a minimum clearance between the rifling lands and bourrelet diameters. Present practice, as described in par. 11-9, requires a clearance of 0.002 in. plus 0.001 times the weapon caliber in inches. The clearance between the rotating band and the rifling is held to a minimum in order to minimize propellant gas leakage past the projectile.

10-12 CHAMBER

The chamber configuration depends to a

great extent upon both the desired interior ballistics and the type of nozzle-breech. The chamber volume can be calculated, as described in Chapter 5, on the basis of a desired muzzle energy, propellant charge, and peak chamber pressure. Cylindrical and slightly forward sloping configurations have been the most widely used of the chamber contours, both having the advantage of creating a fairly even pressure distribution along the length of the cartridge case. In an attempt to improve combustion efficiency and to reduce the loss of solid propellant grains, rearward sloping and baffled chamber contours have been studied. However, these contours led to unfavorable pressure distributions across the cartridge case due to low pressure areas outside of the cartridge caused by high velocity gas flows at the narrowing chamber sections. These pressure differentials were severe enough to cause cartridge case failure, and these contours furnished no better performance than the cylindrical contour.

10-13 NOZZLES

The nozzle is one of the most important areas of design consideration since, through the careful selection of the nozzle parameters, the weapon system is made recoilless. The specific nozzle characteristics to be determined are the throat area, entrance area, entrance radius, exit area, included angle, and throat contour. The nozzle throat area is the main determining factor in the control of recoil since this area limits the rate at which the propellant gases may be discharged. However, the other nozzle characteristics also play a role in control of recoil since they determine the flow characteristics of the discharging gases.

A secondary role that the nozzle plays is as a torque compensator. Because the projectile is given a designated spin as it travels through the tube, it imparts a torque to the rifle. By properly deflecting the discharging gases in

certain types of nozzles, it is possible to apply a counter-twist to the rifle and thus neutralize any torque imparted to the weapon by the projectile. Section II of this chapter describes these nozzle design considerations in more detail and describes the effect that the various nozzle parameters have on the control of recoil.

10-14 TUBE

The length of the gun tube is limited by the allowable weapon weight. Increased projectile travel would permit a decrease in chamber pressure but would cause an increase in weapon weight. The length of the gun tube then becomes a compromise between weight and ballistic performance.

Because recoilless rifles are designed with thin walls, the tube dilates greatly during firing due to the propellant gas pressure and thermal expansion. In highly stressed rifles, this dilation becomes large enough to cause excessive clearance between the projectile and bore surface, with the result that ballooning (in-bore yaw) occurs as the projectile travels through the tube. To compensate for this phenomenon, the principle of strain compensation is incorporated. An initial interference between the projectile and bore is provided so that the clearance achieved during dilation of the bore upon firing results in the normal clearance. Because of the expansion of the bore during firing, most accessories are mounted on the tube by the use of thin metal bands.

The forcing-cone region of the tube is the interior tapered portion between the chamber and bore, including the origin of the lands. The forcing cone allows the rotating band of the projectile to be gradually engaged by the rifling and aids in centering the projectile within the bore. The rifling may be either uniform or increasing in twist. In general, the use of increasing-twist rifling causes less wear on the rifling grooves and lands, and reduces

the danger of stripping the rotating band from the projectile. However, the development of the modern progressive burning powders permits attainment of the desired muzzle velocity with lower maximum pressures so that the use of costly increasing-twist rifling is not warranted.

10-15 SUMMARY

In the preceding paragraphs of this chapter, a large number of factors which can affect weapon performance are described. Many other not so obvious factors will lower

performance the same way. For example, the booster charge in the igniter tube or tail-boom cavity is often surrounded by a primer foil liner or a nitrocellulose or cardboard capsule which is then sealed for moisture-proof protection. While not immediately obvious, it was found that certain types of lacquer coatings will inhibit the burning of the booster charge, causing improper ignition of the main propellant charge and resulting in reduced muzzle energy. Another consideration in the booster design is the combustibility of the booster inclosure. The nitrocellulose capsule provides slightly improved performance at lower temperatures.

SECTION II

NOZZLE

10-16 GENERAL

Recoilless rifles discharge about 90 percent of the propellant gases through the breech in a rearward direction in order to balance the momentum of the forward moving projectile. Since the mass of the rearward moving propellant gases is small compared to the mass of the projectile, a converging-diverging nozzle is used to give the propellant gases the high velocity necessary to make the momentum of the propellant gases equal to and opposite in direction to the momentum of the projectile.

The design of a recoilless rifle nozzle is based on four interrelated characteristics: (1) the ratio of the rifle bore area to nozzle throat area, (2) the ratio of nozzle approach area to throat area, (3) the divergence angle of the nozzle cone, and (4) the ratio of the nozzle exit area to throat area (the expansion ratio of the nozzle cone). The criteria used to determine these characteristics are based on rocket theory, with final nozzle dimensions for a specific weapon design made on the basis of empirical data obtained from balancing experiments. Empirical data have shown that the ratio of rifle bore area to nozzle throat area is approximately 1.45, provided

1. The nozzle approach area to throat area ratio is greater than or equal to 1.70
2. The divergence angle (included angle) is less than 15 deg
3. The expansion ratio of the nozzle cone is approximately 2.0.

Information on nozzle performance suggests that the elimination of recoil is feasible only over a limited range of the bore to throat area ratio. In general, a decrease in the bore to throat area ratio brings about a decrease in the rearward recoil, as would be expected. The point of zero recoil seems to occur at a bore-to-throat area ratio of 1.45, however, this value may not always be practical because the reduction in recoil obtained by enlarging the nozzle throat area will be accompanied by a decrease in muzzle velocity.

In the design of converging-diverging nozzles, it is necessary to avoid both the inclusion of any discontinuities in the contour of the nozzle and the use of largely divergent angles. Both of these design characteristics cause adverse pressure gradients in the propellant gas flow and result in a decrease in the rearward momentum of the gases being exhausted. Since the recoil of the rifle is directly dependent upon the momentum of the exhaust gases balancing the projectile momentum, it follows that retarding the gas flow will result in increased rearward recoil.

10-17 NOZZLE EROSION

Nozzle erosion is the wearing away of the nozzle inside surface caused by the impingement of high velocity gas. Nozzle erosion in recoilless rifles affects the overall rifle performance, since the cross-sectional areas of the nozzle are one of the limiting factors controlling the velocity of the propellant gas discharged. In many of the recoilless rifle systems, the erosion problem was serious enough to cause significant design difficulties and serious field maintenance problems. As a

result, studies were commissioned during various recoilless rifle programs to determine how the erosion phenomenon could be minimized.

One aspect studied was the effect of the nozzle contour on the erosion process. The general rule in nozzle design for minimizing erosion is that the nozzle contour allow the propellant gases to follow natural lines of flow while avoiding discontinuities in the direction of flow. Some of the research done on the problem was simply performed by allowing the gas flow to shape its own best nozzle shape. Examination of sectioned nozzles, eroded from an initially square entrance, showed, in most cases, a well defined circular entrance with the radius equal to the diameter of the throat (Ref. 2). More recent results have indicated that the divergent angle has a negligible effect on the erosion process and that elongating the basic circular shape (as in a kidney-shaped nozzle) also has no appreciable effect on the rate of nozzle erosion (Ref. 3).

In addition to nozzle contour, several other factors also may affect the erosion process. Studies have indicated that surface melting is the dominant mode of erosion in the nozzles of recoilless rifles. As such, the choice of nozzle material, propellant composition, and the rifle rate of fire have a definite effect on the erosion rate. Nozzle erosion tests with various pure metals and alloys, both ferrous and nonferrous, used as the nozzle material have indicated that the best metals from the standpoint of erosion resistance were pure metals such as molybdenum, tungsten, chromium, beryllium, and tantalum. Ordinary cold-rolled steels have shown the most satisfactory performance of all the steels but are much less resistant to erosion than the pure metals cited.

Another factor influencing the erosion process is the isochoric (constant volume) flame temperature of the propellant used in

the cartridge. In general, it has been shown that erosion is reduced through use of a propellant with a lower flame temperature. However, for a specific nozzle material, there is an optimum propellant for which little or no improvement will result through the use of cooler burning propellants.

The rate of erosion also is affected by the rate at which the weapon is fired. Rapid firing has an adverse effect on erosion resistance for two reasons: the time required for the nozzle material to reach its melting point is reduced, and the amount of heat capable of being conducted away from the nozzle after melting starts is reduced.

In designing for erosion resistance it probably will be necessary to make certain compromises in the nozzle design. In general, it will not be feasible to use the coolest burning propellant or the most erosion-resistant material because performance, strength, and cost requirements may dictate the use of other propellant and nozzle materials. In most cases, the nozzle purposely is designed slightly undersized so that the rifle has some rearward recoil for the initial firings. As the nozzle erodes, the point of zero recoil eventually is reached. Further erosion of the nozzle under more firings eventually causes a forward recoil condition to be reached. However, the life of the rifle nozzle has been increased by as much as 50 percent by not sizing the nozzle to give an initial zero recoil.

10-13 VARIOUS TYPES OF NOZZLES

10-18.1 CENTRAL NOZZLE

The central nozzle, as shown in Fig. 10-1, can be considered an optimum design in the sense that it is the simplest and lightest of the nozzle designs. The central nozzle concept generally requires the use of a blow-out plug or valve at the rear of the cartridge case. The blow-out plug assures retention of the propellant gases in the cartridge case and

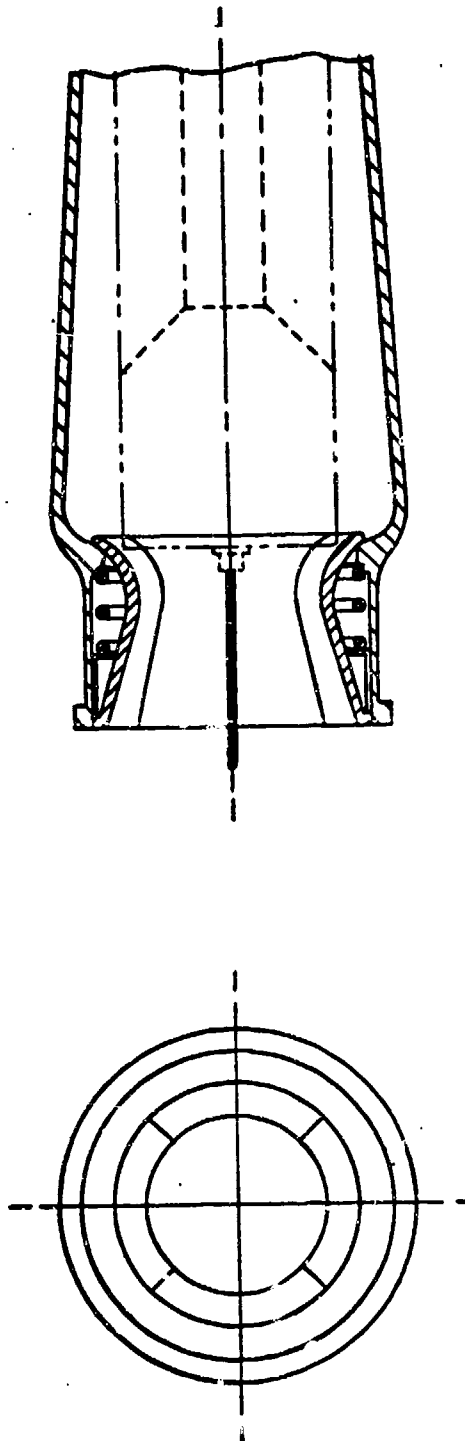


Figure 10-1. Central Nozzle

chamber until sufficient combustion has taken place. The plug then ruptures and allows the propellant gases to escape through the nozzle. While the central nozzle offers definite advantages in weight and simplicity, there are a number of disadvantages that must be considered.

One problem encountered when a spin-stabilized projectile is fired in a recoilless rifle with a central nozzle occurs because the central nozzle has complete axial symmetry about the rifle axis. As a result of this symmetry, no means are available for applying a counter torque by controlled gas discharge on the rifle to compensate for reaction to the spin of the projectile. However, vanes were placed in the central nozzle of early mortar type guns. Another problem associated with the use of the central nozzle is that it tends to lose more unburned propellant through the nozzle than other types of nozzles and, therefore, yields less uniform ballistic performance. Further more, some difficulty is encountered in providing for both a readily accessible firing mechanism and removal of the expended cartridge case. Accessibility for firing often is achieved by either attaching a firing line, commonly called a pigtail, to an electrically initiated primer or by housing a centrally located firing device in

the nozzle, such as found in the bar breech type nozzle described in par. 10-18.2. The problem of extracting the spent cartridge case is eliminated through the use of an expendable or frangible cartridge case.

General design practice with early supersonic (converging-diverging) nozzles for rockets required a nozzle contour with a well-rounded entrance section joined to truncated cones with a 14-deg total divergent angle. It was not until theoretical concepts developed in the fields of aerodynamics and jet propulsion were applied to the central nozzle recoilless rifle that it was found that an angle of 40 deg was the largest divergent angle that could be used. However, experimental work with divergent angles has shown that angles as large as 45 deg may be employed with some sacrifice in efficiency if a significant weight savings was to be gained (Ref. 3).

10-18.2 CENTRAL NOZZLE WITH BAR

As stated in par. 10-18.1, the bar breech type nozzle is a special configuration of the central orifice nozzle. The bar breech derives its name from the bar which is centered across the nozzle exit and houses the firing mechanism, as shown schematically in Fig. 10-2. The nozzle throat and exit areas are

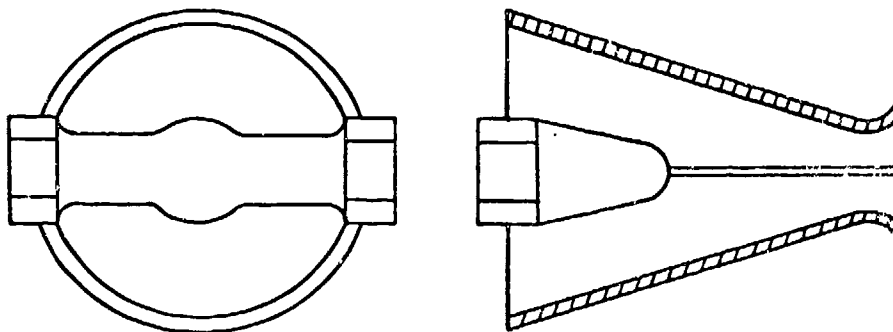


Figure 10-2. Central Nozzle With Bar

adjusted to compensate for the bar interference. The advantages are much the same as outlined for the central orifice nozzle in par. 10-18.1, i.e., simplicity and lightness in weight. The disadvantages in using the breech bar type central nozzle are fouling of the firing mechanism by the propellant gases and the erosive effects of the propellant gases on the breech bar. Another undesirable feature is that the rifle loader may have to pass his hand in back of the nozzle after the round has been chambered in order to close the breech bar. This action may be avoided by the inclusion of extended handles attached to the breech bar; however, in doing so, weight is added to the rifle.

10-18.3 CENTRAL EXPANDING NOZZLE

As stated in par. 10-18.1, one of the disadvantages in using the central nozzle design concept is the problem associated with chambering and extracting the round of ammunition. As in all recoilless rifle nozzle designs, it is necessary that the nozzle throat area be less than the bore area in order to achieve the recoilless condition. Therefore, for the rifle to be breech-loaded, provisions must be made for either enlarging the nozzle or for using a "breech door" or "breech bar" which gives the necessary opening for chambering the round and subsequently reducing the nozzle area.

The 90 mm Rifle, T234, employs a nozzle design that can be considered novel from the standpoints of design and of operation. In order to simplify and minimize chambering and extracting operations, the T234 Rifle employed a central expanding nozzle. The T234 Rifle nozzle is, itself, the breech and is segmented into eight close fitting sections which are spring-loaded to the closed condition as shown in Fig. 10-3 (Ref. 4). The insertion of a round of ammunition causes the segments to move forward and expand

radially outward to permit the larger diameter projectile to be fully inserted. What makes the use of the central expanding nozzle possible, however, is the use of a frangible cartridge case. Instead of the conventional perforated metal cartridge case, a thin "powder envelope" is used. This envelope is destroyed during the ballistic cycle, thereby eliminating the need for spent-case extraction.

10-18.4 MULTIPLE NOZZLE AND FRONT ORIFICE

The multiple nozzle, front orifice type, recoilless rifle has the distinctive feature, as shown schematically in Fig. 10-4, that the projectile covers the nozzle ports at the beginning of the ballistic cycle. There are several advantages of this design as compared with rear orifice designs. These advantages are, as described in Ref. 5:

1. A nonperforated cartridge case may be used, thus contributing to manufacturing cost savings.
2. Since the propellant charge is confined to the closed ballistic system at the beginning of the ballistic cycle, better ignition characteristics of the propellant result.
3. The loss of unburned propellant through the nozzle is negligible as a result of the closed system burning at the beginning of the ballistic cycle.
4. Nozzles of large expansion ratio can be used without lengthening the rifle.
5. The closed-chamber system will permit design variations to include automatic loading mechanisms and venting of the propellant gases through exhaust ducts.

The disadvantages in using the front orifice system are:



Figure 10-3. Central Expanding Nozzle

1. A slight increase in chamber weight.
2. An increased mount weight. Since there is an initial recoil of the rifle until the nozzles are uncovered, the rifle mount must be constructed accordingly to withstand the recoil forces.

10-18.5 ANNULAR NOZZLE

As shown in Fig. 10-5, the annular nozzle has the advantage that it is readily adaptable to most chamber and breech construction. With the annular orifice, the cartridge case is supported adequately by a solid base in the breechblock. Also, the firing mechanism is

housed within the breechblock, thus eliminating the need for any nonpermanent type of firing line or pigtail. The annular nozzle is also advantageous in that, for the same degree of expansion, the nozzle can be made shorter than for a central type nozzle. The reason is that the exit area at any distance from the throat is larger in the annular nozzle design.

Another advantage of the annular nozzle is revealed in the consideration of rifling torque compensation. In the annular nozzle design, it is possible to shape and cant the locking vanes to the breechblock so that the resulting rotational impulse of the deflected propellant gases escaping rearward balances the impulse

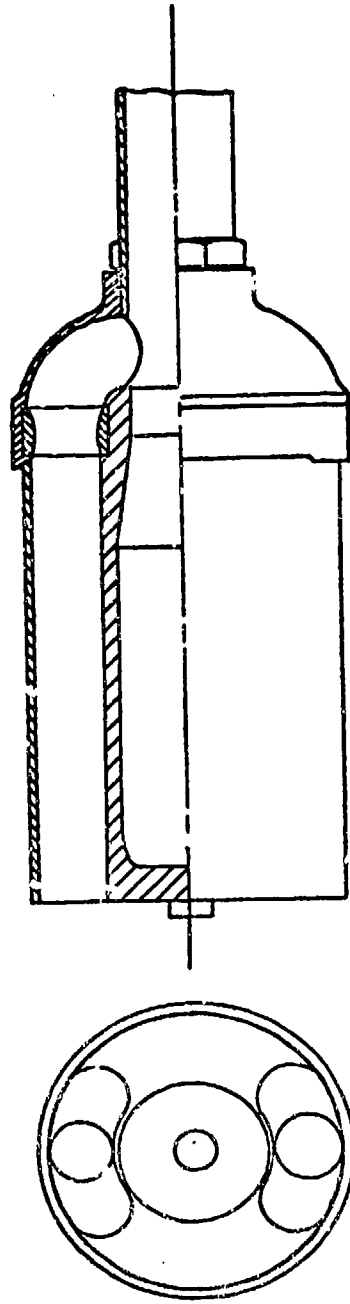


Figure 10-4. Multiple Nozzle and Front Orifice

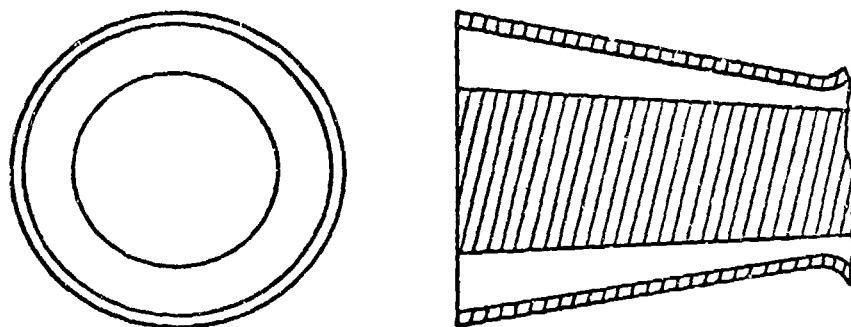


Figure 10-5. Annular Nozzle

due to the reaction of the rifle to the projectile spin.

A disadvantage of the annular nozzle is that since the locking vanes secure the breech in its closed position and deflect the discharging gases for the purpose of torque neutralization, they are subjected to the full erosive effect of the gases. The locking vanes also bear the full reaction load caused by the chamber pressure acting on the cartridge case and must be readily locked and unlocked during loading and unloading.

10-18.6 INTERRUPTED ANNULAR NOZZLE

In actual practice, all annular nozzle designs are of the interrupted type as shown in Fig. 10-6, since there must be some means of supporting the breechblock in the locked position. The interrupted annular nozzle maintains the same advantages and disadvantages described in par. 10-18.5 for the annular nozzle.

10-18.7 KIDNEY-SHAPED NOZZLE

A modification of the interrupted annular

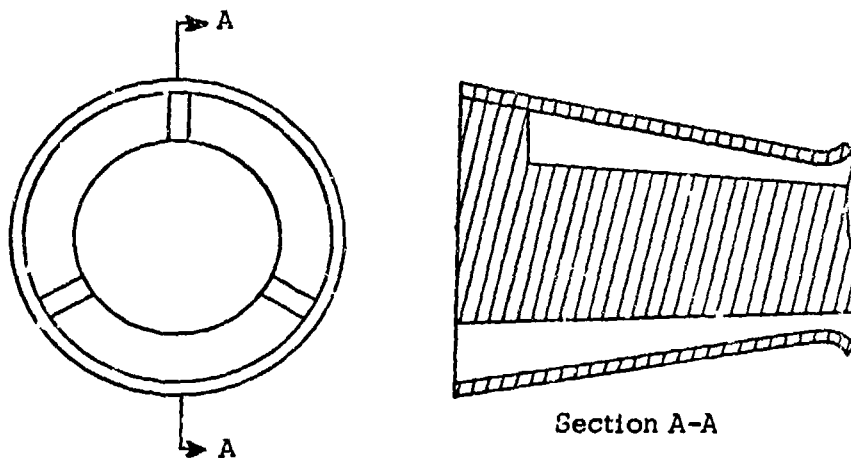


Figure 10-6. Interrupted Annular Nozzle

nozzle is the kidney-shaped nozzle that is shown schematically in Fig. 10-7. It has the advantage of complete symmetry while providing the solid center for housing the firing mechanism. The kidney-shaped nozzle easily adapts to rifling torque compensation by canting the nozzle sections or channels. The disadvantages of this nozzle are its complexity and extra weight, which make it the most costly of all the different types of nozzles to produce. It also has the tendency to develop cracks in the webs between the orifices.

Experimental ballistic data (Ref. 3) also have indicated that the kidney-shaped nozzle is slightly less efficient than the central nozzle design. In addition, the recoil compensation is

more sensitive to changes in the approach area in the kidney-shaped nozzle than in the central nozzle. Lastly, the ballistic efficiency of the kidney-shaped nozzle is slightly less than that for the central nozzle. However, because of the cartridge case support it furnishes, the kidney-shaped nozzle has found much greater use. Rifles that have used kidney-shaped nozzles are:

1. 57 mm Rifle, M18
2. 75 mm Rifle, M20
3. 105 mm Rifle, M27
4. 106 mm Rifle, M40.

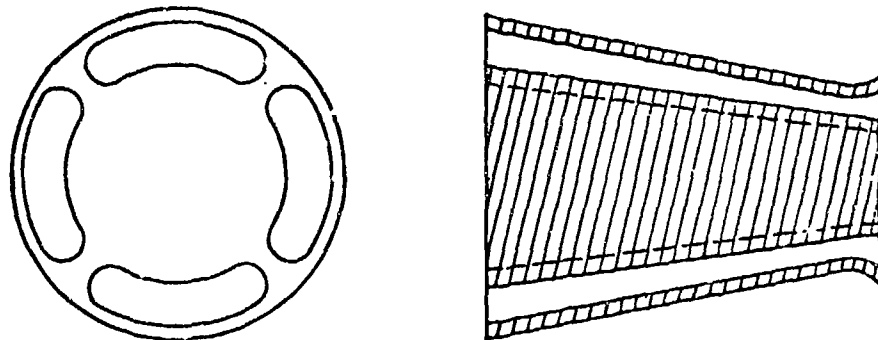


Figure 10-7. Nozzle With Kidney-Shaped Orifices

SECTION III

BREECH

10-19 GENERAL

The breech is the rear part of the recoilless rifle through which the projectile is loaded into the chamber and through which the rearward discharge of gases usually occurs. The breechblock contains the firing pin, and locates and holds the head of the cartridge case. A breechblock operating mechanism unlocks and withdraws the breechblock from the breech, swings the block clear, and returns it to the firing or closed position.

The breechblock components are a locking device, a cartridge extractor and ejector, safety devices, a percussion mechanism, and a nozzle throat adjuster. The operation of the breechblock consists of opening, extracting, and ejecting the expended or fired cartridge case from the chamber, chambering the new round of ammunition, closing the breechblock, and firing the round.

10-20 CHARACTERISTICS

The type of breech used will depend on what the requirements are for supporting the chambered round, the size of the rifle, the type of firing mechanism, and the type of ammunition. With the use of a frangible cartridge case envelope, it would be possible to incorporate the unique expanding nozzle type breech described in par. 10-22. In another rifle, the strength requirements for supporting the perforated metal cartridge case may dictate the use of an interrupted lug or interrupted-thread type breech to provide the necessary strength.

The size of the rifle also will place

limitations on the breech design. In general, a shoulder-fired rifle design necessitates the use of a lightweight breech mechanism. If the rifle is a repeating type used in an enclosed application, a front orifice rifle may be used so that the breech design is concerned only with the chambering and extracting of the ammunition.

It is necessary to determine that the critical parts of the breech and firing mechanisms have been protected from the erosive and fouling effects of leaking propellant gases. In par. 10-21, the various means of sealing or directing the flow of leaking propellant gases are discussed more fully. It is also necessary to insure that a good seal is obtained between the breech and chamber if they are joined. A leakage path between the chamber and breech will be expanded rapidly due to erosive effects and will result in a decrease in weapon performance and an increase in safety hazards.

In breech design, human engineering and safety characteristics must be considered. The breech mechanism should be easy and quick to operate. If the breech is manually operated, it must not delay the rate of fire. During continuous firing, the loader should not become unduly fatigued.

For safety, several characteristics of the breech design must be considered. Handles mounted to the breechblock should be located so that the loader does not have to pass his hands or any portion of his body behind the nozzle while locking the breech. It should be impossible for the firing mechanism to operate until the breechblock is locked

securely in place. No gas leakage paths should be present in the breech-chamber interface.

10-21 SEALING PROPELLANT GASES

In the design of the breech mechanism of a recoilless rifle, it might seem that since there is such a large escape of gases through the nozzles that there would be no concern about gas leakage. However, gas leakage can be extremely important because it can result in the erosion of locking surfaces and other important parts of the breech mechanism. This easily can be seen in the original blow-out disc type recoilless rifles designed by the British and Germans in which leaking propellant gases caused continuous malfunctions of the firing mechanisms as well as causing considerable erosion damage.

In larger conventional artillery weapons, the use of obturating pads, obturating rings, and the expansion of the cartridge case by the propellant gases are employed to form a tight seal against the walls of the chamber. In recoilless rifles, this type of gas leakage prevention cannot be used. With the use of the perforated cartridge case, the gas pressure inside and outside the cartridge case is essentially the same, and the case cannot be expected to expand in order to effect sealing. To prevent the propellant gases from reaching critical parts of the breech and firing mechanisms of recoilless rifles, annular grooves or leakage paths are designed to direct the leaking propellant gases away from critical areas by providing small expansion chambers in which the pressure of these leaking gases is reduced.

10-22 BREECH TYPES

A variety of breech mechanisms and breechblocks have been or are being used. The most widely used breechblock types are the interrupted lug and interrupted thread types. However, all the breech types and mechanisms described in the remainder of this

paragraph have been designed, built and tested for use in recoilless rifle systems.

In the interrupted thread breech, the breech recess and the breechblock are cut with a series of stepped threads so that when the breechblock is inserted and turned in the breech recess, matching sections of threads engage. The interrupted thread type of breech gives a large threaded surface or holding area which provides the necessary strength for holding the cartridge case in position during firing. The interrupted lug breech is similar to the interrupted thread type of breech except that interrupted lugs replace the threads on the breechblock and chamber.

In order to reduce the weight of the overall weapon system, several recoilless rifle weapon concepts have incorporated the cartridge case as a portion of the chamber and breech closure. This is achieved, however, by a considerable penalty in ammunition cost and weight. The 90 mm Rifle, T149 is an example of such a weapon. To hold the cartridge case in place, the breech mechanism is a rotating cam ring as shown in Fig. 10-8, the cam ring locks the round in place, cocks the firing mechanism, and actuates the extractor. The cartridge case base has two diametrically opposed projecting lugs that, upon proper chambering of the round, firmly seat in corresponding sockets in the rear of the chamber. Counterclockwise rotation of the cam ring brings two locking lugs on the ring into register with the cartridge base projections to secure the round.

In further efforts to reduce the weight of the breech mechanism and also to eliminate the manual operations for operation of the breech, one of the initial designs of the 90 mm Rifle, T234, employed a central expanding nozzle, which is itself the breech, segmented into eight close-fitting sections that are spring-loaded to the closed position. Insertion of the round of ammunition causes the segments to expand radially outward to



Figure 10-8. Rotating Cam Ring Breech Mechanism

permit insertion of the larger diameter projectile. The incorporation of such a breech mechanism was made possible in this specific case because the cartridge case was of the frangible type being destroyed during the ballistic cycle and not requiring spent case extraction.

Another type of breech mechanism studied during the 90 mm Super-PAT (platoon antitank) Program employed the idea of inserting a cylindrical bar through the nozzle of the weapon (Ref. 6). The purpose of the bar was to provide a surface that the propellant gases would strike in order to establish a condition of no-recoil. Recoil would be eliminated by varying the diameter and thus the area of the nozzle. This design was intended to simplify the mechanics of loading. Loading of the round would be accomplished by first sliding the breech bar out, inserting the loaded projectile into the chamber, and then replacing the breech bar.

10-23 BREECH ACTUATOR

The breech actuator or operating handle mechanism of the breech contains the mechanisms for performing the locking, unlocking, opening, and closing operations of the breech. In most of the early design recoilless rifles, the handles were connected directly to the breechblock. Opening of the breech consisted of first rotating the breech handle about the bore axis until the interrupted lugs or interrupted threads in the

breechblock were disengaged from their mating parts in the breech housing and then swinging the breechblock outward about some type of hinge. The 57 mm Rifle, M18, and the 75 mm Rifle, M20, are examples of rifles with this type of breech operating handle. To close the breech, these operations are performed in the reverse order. In many recoilless rifle designs, these operations also cause the cocking of the firing mechanism.

In later recoilless rifles, the breechblock operating mechanisms were designed so that the loader's hands would not have to pass behind the nozzle, as is the case when the breechblock handles are rigidly attached to the breechblock. For example, the breechblock operating handles for the 105 mm Rifle, M27, and 106 mm Rifle, M40, are connected to the breechblock by a set of cams and coupling rings which permits rotation or translation and opening of the breechblock without passing the handle behind the breech. The handles are attached at the side of the breech and are operated by only a counterclockwise rotation at the end of the handle above the rear of the breech.

Operation of the breech actuator also functions a cartridge case ejection mechanism. The extractor usually consists of a finger type projection that sits under the lip of the cartridge case base. When the breech is opened, the extractor hooks the cartridge case base and slides the case partly out of the breech so that the case can be removed easily by the loading personnel.

SECTION IV

CHAMBER

10-24 GENERAL

The section of the recoilless rifle which houses the round of ammunition is called the chamber. The chamber contains a rear opening or breech mechanism through which the projectile is loaded and a front-opening leading into the bore of the tube. After chambering of the round, the part of the projectile forward of the rotating band rests in the bore. The remainder of the round rests in the chamber with the cartridge case base supported at the breech and the cartridge case mouth supported at the forcing cone.

The function of the chamber and its relation to the cartridge case will depend upon the type of nozzle-breech design used in the rifle. If annular or kidney-shaped nozzles are used with a perforated cartridge case, it is necessary to provide a sufficient annular volume around the cartridge case to allow for the venting of the propellant gas and the resulting flow of gases to the nozzle. In the central nozzle rifle, the large annular chamber volume is not required. The contour of the chamber is either cylindrical or forward sloping, since both of these configurations give a uniform pressure distribution across the cartridge case.

10-25 SIGNIFICANCE OF CHAMBER VOLUME

The chamber volume is a major characteristic in a recoilless rifle design in that it is directly related to the pressure level and muzzle velocity and, correspondingly, to the weapon weight and length. Chapter 5, Interior

Ballistics, contains detailed analysis relating to the effect of chamber volume on performance and design of the weapon. Ref. 5, Chapter 5, indicates that the variation in peak pressure and muzzle velocity are inversely proportional to a change in chamber volume. Peak pressure varies inversely less than twice the change in chamber volume while the muzzle velocity change is only about 0.2 times that of the inverse in the chamber volume variation.

10-26 EJECTION OF PROPELLANT

In firing tests of the first recoilless rifle designs, it was learned that the amount of unburnt propellant grains ejected through the nozzle was roughly inversely proportional to the average distance the propellant grains must travel to be ejected. Thus the first attempts at the prevention of propellant loss investigated the concentration of the cartridge case perforations at the mouth end of the case so that, on the average, the propellant would travel a greater distance before being ejected. However, the resulting uneven pressure distribution on the cartridge case led to many cartridge case failures and the eventual abandonment of this approach.

Experience with standardized US recoilless rifles has shown that solid propellant loss can be maintained below ten percent when a kidney-shaped nozzle along with a perforated cartridge case is incorporated in the weapon design. The 106 mm Rifle, M40, has this type of nozzle in combination with the recoil compensating device described in par. 9-3.7 to prevent solid propellant loss. The problem with this type of nozzle arrangement is that a

large, annular area about the cartridge case must be provided so that propellant gases have an unrestricted path to the nozzle. The larger annular area increases weapon weight.

Weapons can be designed employing a central nozzle and a frangible cartridge case, as in the 90 mm, M67 Recoilless Rifle. With this combination, it is not necessary to provide a large annular area about the case since the case ruptures and is blown out of the gun upon firing. This type of recoilless weapon offers apparent promise of lower chamber weight than a rifle with a comparable kidney-shaped nozzle; but, the solid propellant loss is on the order of 30 percent of the total charge. Because of this factor, a larger chamber volume is required, the weight of which tends to counterbalance savings achieved by the use of a central nozzle and frangible case. It is, therefore, desirable to reduce the propellant loss in the central nozzle system to a level comparable with or less than that of the kidney-shaped nozzle. This not only will reduce the ammunition weight but will further reduce the weapon weight, since the chamber volume can be decreased as the propellant loss is reduced.

In principle, achievement of simultaneous nozzle-start and shot-start can provide for reduction in solid propellant loss in a central orifice recoilless rifle. Simultaneous nozzle-start shot-start occurs when a means for mutually sealing the nozzle and holding the projectile is provided in the ammunition design. Thus, when the holding member fails, gas flow out of the nozzle and projectile motion are initiated simultaneously. Furthermore, the magnitude of the start can be controlled by adjusting the force required to part the holding element. In the event simultaneous start occurs at "all burnt", propellant loss must be zero due to the corresponding closed-bomb burning resulting from start occurring at "all burnt".

Ideally, a central orifice recoilless rifle could be designed to yield a zero propellant loss by merely providing that the simultaneous start occur at or slightly below "all burnt". However, the resulting weapon will be longer and heavier than one designed for zero-start, and the advantage of reducing propellant loss to zero will be overshadowed completely by the increase in weapon weight and size.

SECTION V

TUBE

10-27 GENERAL

The tube gives the projectile direction and a rotating motion for the purpose of aerodynamic stability. The tube may be a separate member attached to the chamber or may be integral with the chamber. In either case, the tube will require the same material properties as outlined for the chamber.

Since the tube represents the largest member of the recoilless rifle, it is necessary to assure that the tube weight is a minimum while still maintaining the required strength. The minimum possible wall thickness at the point of maximum pressure must be determined (Ref. 11).

Because of the geometry of the tube and its accessibility, it would seem that the tube is an ideal member for attaching the various sighting and spotting accessories. In many of the recoilless rifle applications, this is true. However, in rifles in which the tube is made from a high-strength steel stressed to its high limit, the tube is highly strained during firing. As a result, at a specific point, the tube expands and contracts as the projectile passes this point, causing difficulties in designing the bands for mounting the various other accessories to the tube. There are many specific design considerations that need to be made in the design of the tube, and these factors are discussed in the remaining paragraphs of this section.

10-28 DESIGN CONSIDERATIONS

In the design of the recoilless rifle tube, one of the first factors considered involves the

principle of strain compensation. If a tube uses either a high strength steel stressed to its high limit or a material having a low modulus of elasticity, the tube will be highly strained during firing. The possibility arises that the projectile could be completely disengaged from the tube rifling. Use of the strain compensation principle requires that the projectile fit the tube during firing, rather than prior to firing, as described in par. 10-14 and Ref. 7.

Rifling is the term given to describe the helical grooved pattern cut in the bore throughout the gun tube. The surfaces between the grooves are called the lands. Through interaction of the projectile rotating band with the rifling, the rotation required for flight stability is imparted to the projectile. The twist of the rifling at any point is the inclination of the groove to the element of the bore through the point. The twist may be uniform, increasing, or a combination of the two, and is expressed in terms of the number of calibers of length in which the groove makes one complete turn. The exact shape of the rifling will depend on ballistic, strength, and wear factors. The rifling twist depends upon the desired rotational velocity of the projectile at the muzzle.

One of the main purposes of recoilless rifle development was to provide infantry with a lightweight, armor defeating weapon. To meet this requirement, it is necessary to use high strength materials for the tube so that the tube wall thickness and, thus, weight is minimized.

Another important tube design considera-

tion is eccentricity. Since the recoilless rifle tube wall is designed to be as thin as strength requirements allow, any deviation from the true circular path of the tube results in the loss of metal thickness at the particular point that the eccentricity occurs. Even if the tube has an eccentricity of only several thousandths of an inch, an appreciable fraction of the actual barrel strength would be lost. Consequently, all tube designs require specification of the permissible eccentricity.

Another factor of the tube design requiring consideration is the forcing cone and boresight grooves. The forcing cone is the interior tapered portion of the tube between the chamber and the bore, including the origin of the lands. The forcing cone area allows the pre-engraved rotating band of the projectile to be engaged gradually by the rifling and aids in centering the projectile within the bore.

A small but important consideration concerning the tube design is the incorporation of boresight grooves on the muzzle.

The design of some recoilless rifles requires the joining of the tube to the chamber. The factors that will determine the method by which these two rifle components are joined are the chamber and tube materials, and their wall thicknesses. Threading the tube into the chamber will depend on the ability of these components to resist distortion under application of installation torque. It is essential to provide sufficient torque to prevent the tube from rotating loose during firing. If the tube is to be brazed to the chamber, material properties need to be considered. If they are joined by brazing, it will not be necessary to maintain quite as close manufacturing tolerances since a gas tight seal between chamber and the barrel will be formed.

10-29 OTHER SUBJECTS TO BE CONSIDERED IN DESIGN

As the recoilless rifle designer endeavors to minimize the weapon weight, a problem arises with the rifle overheating during sustained rapid firing. In the recoilless rifle, this heating is more rapid than in a conventional gun due to the low heat capacity of the rifle tube. For a given weapon-round combination, a specific amount of heat is transferred to a unit area of the tube per round. The temperature rise in any section of the tube is then inversely proportional to the mass of that section. Thus, any attempt to reduce the tube weight results in a higher temperature rise per round and a faster approach to the temperature at which the yield strength of tube material rapidly decreases. Since the design stresses often approach the yield point of the tube at normal temperatures, it is possible for the yield strength to be exceeded under conditions of sustained or rapid firing.

Cook-off is the deflagration or detonation of a round of ammunition due to the autoignition of either primer or propellant and booster charges. In the case of the hand-loaded recoilless rifle, the chance of cook-off occurring is negligible since the rate of fire is not high enough to cause a sufficient increase in weapon temperature and there is no need to keep the round chambered for any length of time. In automatic recoilless rifles, cook-off becomes more of a concern but is still not likely to occur because the low heat capacity of the gun tube will limit the number of rounds that may be fired in a rapid burst. The primary danger of cook-off of a chambered round will be to the personnel and equipment in the line of fire and behind the weapon.

Ref. 8 gives an indication of the bore temperature expected after firing a recoilless rifle. For a single firing of a 57 mm Rifle,

T170, it was found that the maximum attained bore temperature occurred at the origin of the rifling and averaged about 470°F. Along the barrel, the bore temperature dropped in an almost linear manner, reaching only 160°F at the muzzle. In tests of the 106 mm BAT Weapon System, it was found that the maximum rate of fire was limited to two rapid bursts of four rounds each before the upper temperature limit of the rifle was reached (Ref. 9).

During projectile travel through the bore, the gun tube rifling offers considerable resistance to the projectile rotating band. This resistance appears in the form of a radial force acting on the rifling and is distributed uniformly around the bore. These radial forces or band pressures progress along the tube with the projectile. Although the band pressures may be large, the area of application is local and small with a very short duration, so that immediate damage is not always apparent. However, repeated application of such band pressures may ultimately damage the bore. Small, imperceptible cracks develop first and then steadily grow larger as firing continues. This progressive stress damage finally results in tube rupture or in the spalling of rifling lands. When spalling occurs, little effort from the projectile is needed to remove the spalled section from the bore. Such progressive stress damage limits the length of the service life of the gun tube to a prescribed number of firings.

Another phenomenon that is unfavorable to long tube life is erosion, the wearing away of the bore surface. Erosion is primarily a physical activity caused by the abrasive effects of the propellant gases and of the rotating band acting on the bore. The high velocity propellant gases impinge on the bore surface and sweep away some of the metal. The intense heat of the gases contributes indirectly to erosion by melting an extremely thin layer of the bore surface, thus making it

easier for gas to carry the metal away. The high heat also causes some of the propellant gas constituents to combine with the metal of the bore surface. This newly formed compound—normally a nitride and, therefore, brittle—may crack and peel-off under the action of the rotating bands and propellant gases. At the origin of rifling, the temperatures are the highest and, thus, the erosion rates are the highest. The rotating band has two contributing influences on erosion; the first induced by gas wash, the second by ordinary sliding friction. However, these influences are relatively insignificant to the damage caused by propellant gases.

A significant amount of attention was originally given to the problem of gas leakage past the pre-engraved rotating band (Ref. 10) and the erosive damage that could result. The indicated problem was not received with alarm, however, as the added clearance due to the pre-engraving amounted to only one percent of the bore area. As far as interior ballistics is concerned, this clearance area was equivalent to increasing the throat area by approximately 1.5 percent, which is of the order one would expect in variations of manufacture. Further proof was substantiated in the initial firings of the 57 mm Rifle, T15. In the first 3,000 rounds for firing of a 57 mm Rifle, T15, no evidence of erosion was found in the rifling.

As defined in par. 10-27, the tube is the means for accelerating the projectile. The use of a smooth bore definitely eliminates the problems associated with a rifled bore such as high friction, abrasion, and high resistance to the projectile. However, the use of a smooth bore requires a higher muzzle velocity in order to maintain the necessary aerodynamics for the required projectile accuracy. But, in considering the problems of gas leakage and erosion which are still present in the smooth bore rifle, the use of a smooth bore has found very limited use in US recoilless rifle weapon

systems, despite the fact that other nations use them.

Once the decision to use a rifled-bore has been made, it will be necessary to consider the rifling shape and type of rifling twist to be used in the tube. The shape of the rifling will depend upon the type of rotating band to be used. For projectiles with pre-engraved metal rotating bands, it was found, during the 57 mm Rifle, T15 program, that shallow-groove rifling will cause considerable shearing of the rotating band and give a shorter accuracy life of the tube. However, for rifles firing fin-stabilized projectiles with plastic rotating bands that are engraved during firing, shallow groove rifling is used. In the U-BAT, Super-PAT, and PAT rifle programs, for example, a shallow groove rifling with a depth of 0.006 in. is used. The use of shallow groove rifling in these applications was made possible by the use of fin-stabilized projectiles with plastic rotating bands which are fired into a rifle tube that has a slow rifling twist of 300-480 cal per turn. With this slow twist and the use of plastic bands, the stresses on the lands are considerably reduced so that a shallow groove rifling is possible.

In most recoilless rifle weapon systems, uniform rifling twist is used since it meets the desired requirements and is less expensive to manufacture than a rifle tube with multitwist rifling. However, multitwist rifling does exhibit certain advantages over uniform twist rifling. One advantage of multitwist rifling is that, through the proper selection of the rate of twist, the maximum stress on the lands and rotating band of the projectile will be less. This advantage is somewhat offset in recoilless rifles as compared with conventional guns, because they operate at lower maximum pressures and muzzle velocities. Disadvantages of multitwist rifling are: (1) higher and more concentrated pressure on the driving edge of the land and forward part of the band, (2) increased friction and abrasion, and (3) higher manufacturing costs. Weighing the apparent

advantages and disadvantages of both types of rifling twist would seem to indicate that uniform twist rifling is preferred for use in recoilless rifles. For further discussion of uniform versus multitwist rifling, the reader is directed to the material found in Refs. 11 and 12.

During firing, the rifle tube is heated and tends to droop as the temperature of the tube approaches the temperature at which the yield strength of the tube material begins to decrease. The longer and thinner the tube, the greater the droop of the tube. The extent of the temperature-caused droop also will depend on the elevation angle of the tube; the higher the elevation angle, the lower the value of the temperature at which droop begins. The rifle tube also may bow to either side due to differential heating during firing. If the rifle tube is cooled on one side by action of the wind, the bore axis will warp toward the side from which the wind blows. The amount of bowing will depend upon any warpage initially in the tube, variations in wall thickness, and the wind velocity.

As the projectile is accelerated through the rifle tube, a torque is imparted to the rifling. For uniform twist rifling, an approximate expression for the rifling torque T is given by Eq. 10-1 taken from Ref. 11.

$$T = \left(\frac{\rho^2 A_b P_g}{R} \right) \tan \alpha, \text{ in.-lb} \quad (10-1)$$

where

ρ = polar radius of gyration of projectile, in.

A_b = bore area, in²

P_g = propellant gas pressure, psi

R = radius of projectile, in.

α = angle of rifling twist, deg

SECTION VI

FIRING MECHANISM

10-30 DESIGN CHARACTERISTICS

The major components of the recoilless rifle firing mechanism are the firing pin, hammer, hammer spring, firing cable, trigger, and safeties. The firing pin is a small diameter rod with a hemispherical nose that generally is stroked under the pressure of a stiff spring to strike the primer of the chambered round of ammunition. Some designs use the stored energy in the spring to accelerate the firing pin before striking the primer. Other designs transfer all the stored energy in the spring to a hammer. The hammer is accelerated and strikes the firing pin that is positioned right in front of the primer of the chambered round.

The firing pin generally is held in place by a sear that is retracted or cammed away from the firing pin to fire the round. The sear is connected to the trigger of the rifle through the use of a push-pull type control cable. The stroking of this firing cable by the trigger mechanism provides the necessary action for releasing the sear from the firing pin.

The trigger designs for recoilless rifle use have ranged from the fairly simple sear type lever found in the 57 mm Rifle, M18, to the fairly sophisticated trigger design found in the 120 mm Rifle, XM105, which provides for the firing of the major and minor rifles from the same trigger grip. Regardless of complexity, the design considerations to be made are the ease in which the trigger is gripped and the trigger pull squeeze force required to fire the rifle. Human engineering requirements call for a trigger pull of less than 40 lb, preferably around 20 lb.

10-31 EXAMPLES

The firing mechanism operations of three recoilless rifles are discussed in this paragraph. In the 57 mm Rifle, M18, squeezing of the trigger causes the firing cable to be pulled forward (toward the muzzle). The firing cable is connected to a sear lever (see Fig. 10-9) by a safety spring. As the firing cable is pulled forward, the safety spring causes the sear lever to rotate. The forked end of the sear lever grasps the headed end of a sear which prevents the striker assembly from striking the cartridge primer. As the sear lever rotates, it retracts the sear from a hole in the striker assembly. When the sear is free from the striker assembly, a compressed firing spring drives the striker assembly (composed of a hammer and firing pin) forward to strike the primer of the chambered round (Ref. 10).

The operation of the firing mechanism of the 106 mm Rifle, M40, is similar to that just described. Pushing the firing knob in the elevating handwheel fires the rifle. The knob is connected to the firing cable by a firing transfer tang. Rotation of the tang actuates a firing cable operating lever that strokes the firing cable. At the breech end of the rifle, the firing cable is attached to a trigger that rotates as the firing cable is stroked. Attached to the trigger is a sear that prevents the firing pin from stroking. When the trigger is rotated, it causes the sear to turn and disengage from a notch in the firing pin. Accelerated by a spring, the firing pin strikes the primer of the cartridge to fire the round (Ref. 13).

The firing mechanism of the 120 mm Rifle,

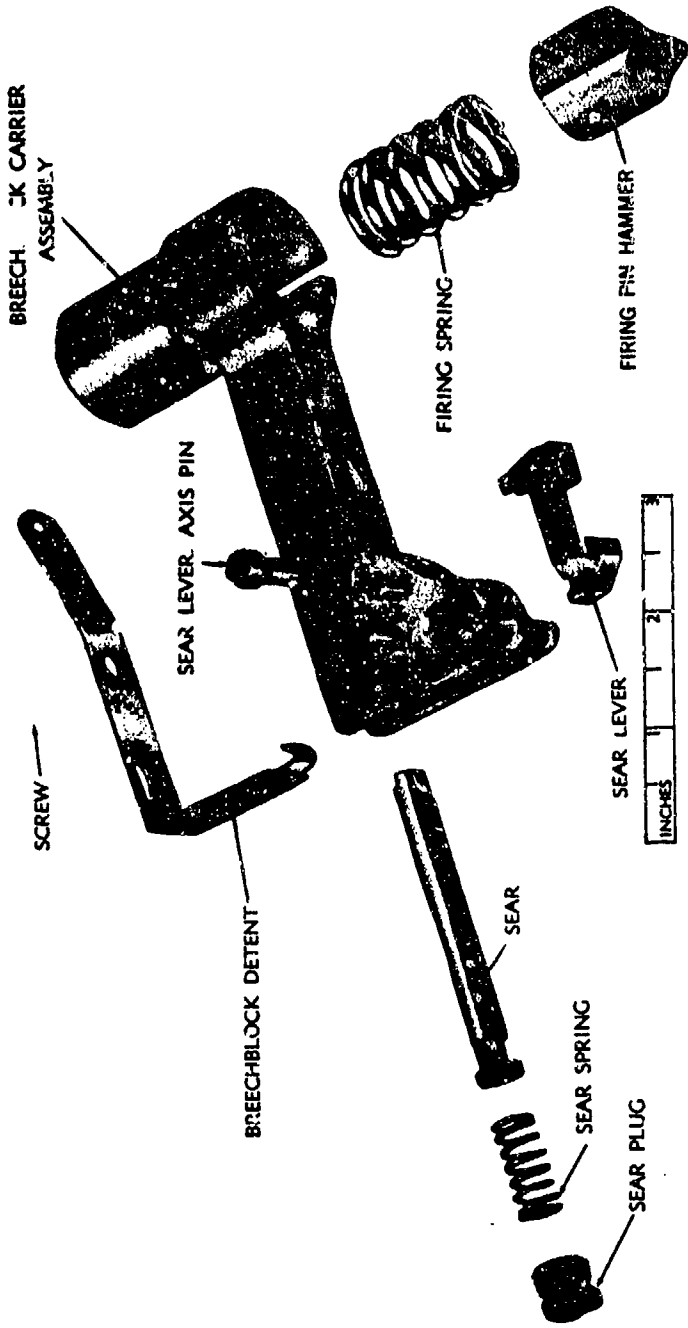


Figure 10-9. Firing Mechanism

XM105, incorporates a trigger mechanism that serves both the major caliber rifle and minor caliber spotting rifle. By twisting the trigger grip shown in Fig. 10-10, the selection of the rifle to be fired is made. Figs. 10-11 and 10-12 show the interior of the trigger mechanism with the top plate removed and indicate how the link is made to engage one or the other bell-cranks which pull the firing cables.

Operation of the trigger to fire the major caliber rifle pulls the major caliber firing cable (shown as the right cable in Figs. 10-11 and 10-12) forward. The major caliber firing cable in turn, is attached to a firing trigger (shown in Figs. 10-13 and 10-14) located at the breech. The sear is engaged by the slot in the firing trigger and is rotated by the firing trigger to a fire position when the firing cable is pulled. At the fire position, the sear releases the hammer, which then is accelerated under the action of a hammer spring to strike the firing pin which, in turn, strikes the primer of the chambered round (Ref. 14).

10-32 SAFETY DEVICES

The function of any type of safety used in recoilless rifles is to prevent the gunner from being able to fire the rifle until (1) the round has been correctly chambered, (2) the breech closed, and (3) the loader has given some type of mechanical indication that the rifle is ready

to be fired without endangering any equipment or personnel behind the rifle. In general, two types of safety devices are incorporated into the recoilless rifle design. The first safety device is generally a part of the trigger mechanism and consists of a lever or button which when depressed unlocks the trigger. This safety feature prevents firing of the weapon by any accidental contact with the trigger.

The second safety generally is located at the breech end of the rifle and is for the loader's personal safety. The safety device usually is in one of two forms. One form of the safety device consists of a simple switching type device that is connected to the firing cable. When the switch is in the "arm" position, the firing cable is free to move as the trigger is depressed by the gunner. In the "safe" position, the firing cable is locked and prevented from being stroked by any trigger motion. The loader is then able to say, by his choice of the safety position, when he feels the gun is ready to be fired. A second form of this type of safety is incorporated into the breech mechanism. When the breech is open, the firing mechanism is disconnected from the firing cable. Not until the breech has been closed and locked completely will the firing cable come into contact with the firing mechanism. This type of safety is found only if the loader can close and lock the breech from a position at the side of the rifle.

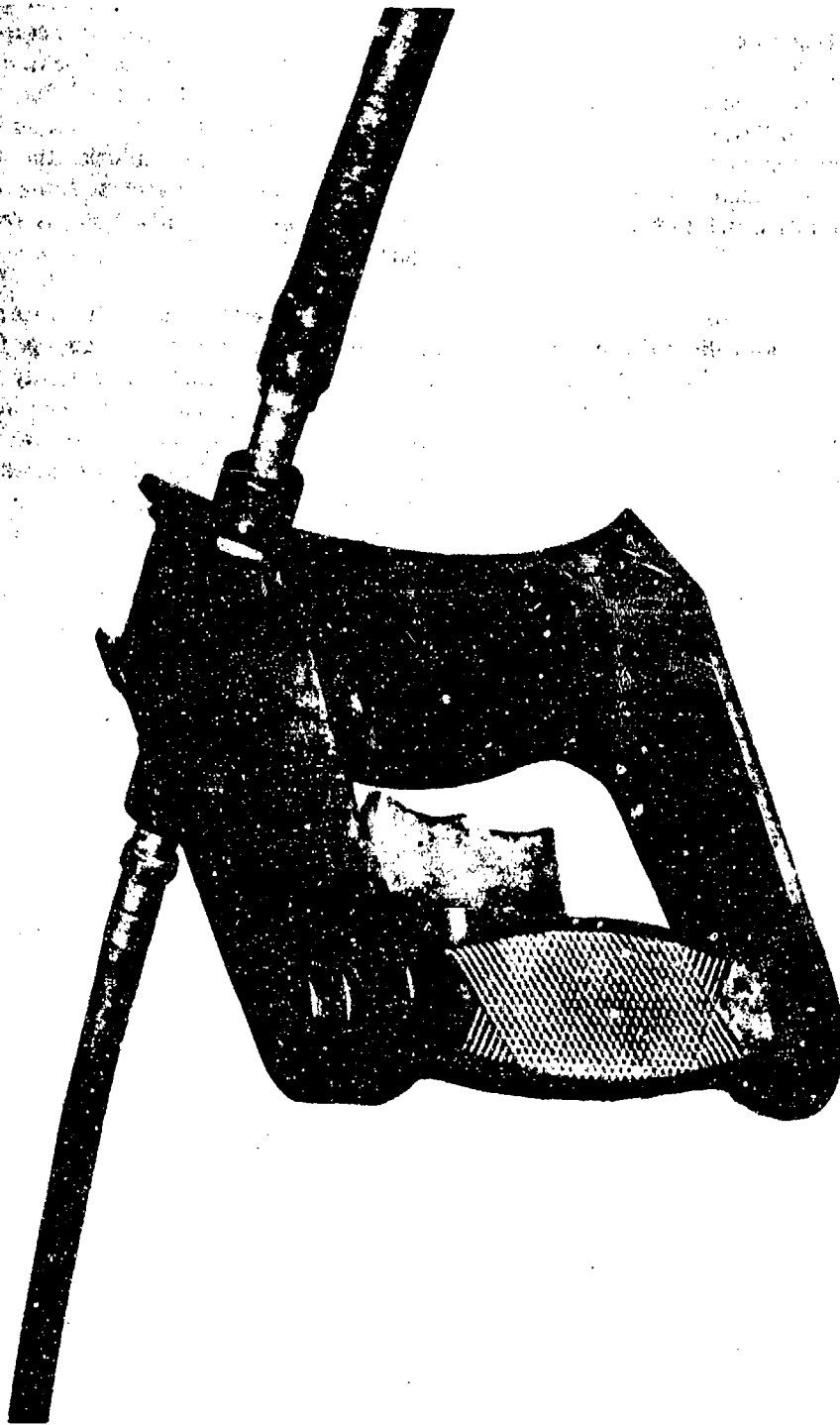


Figure 10-10. Trigger Firing Mechanism, 120 mm Recoilless Rifle, XM105

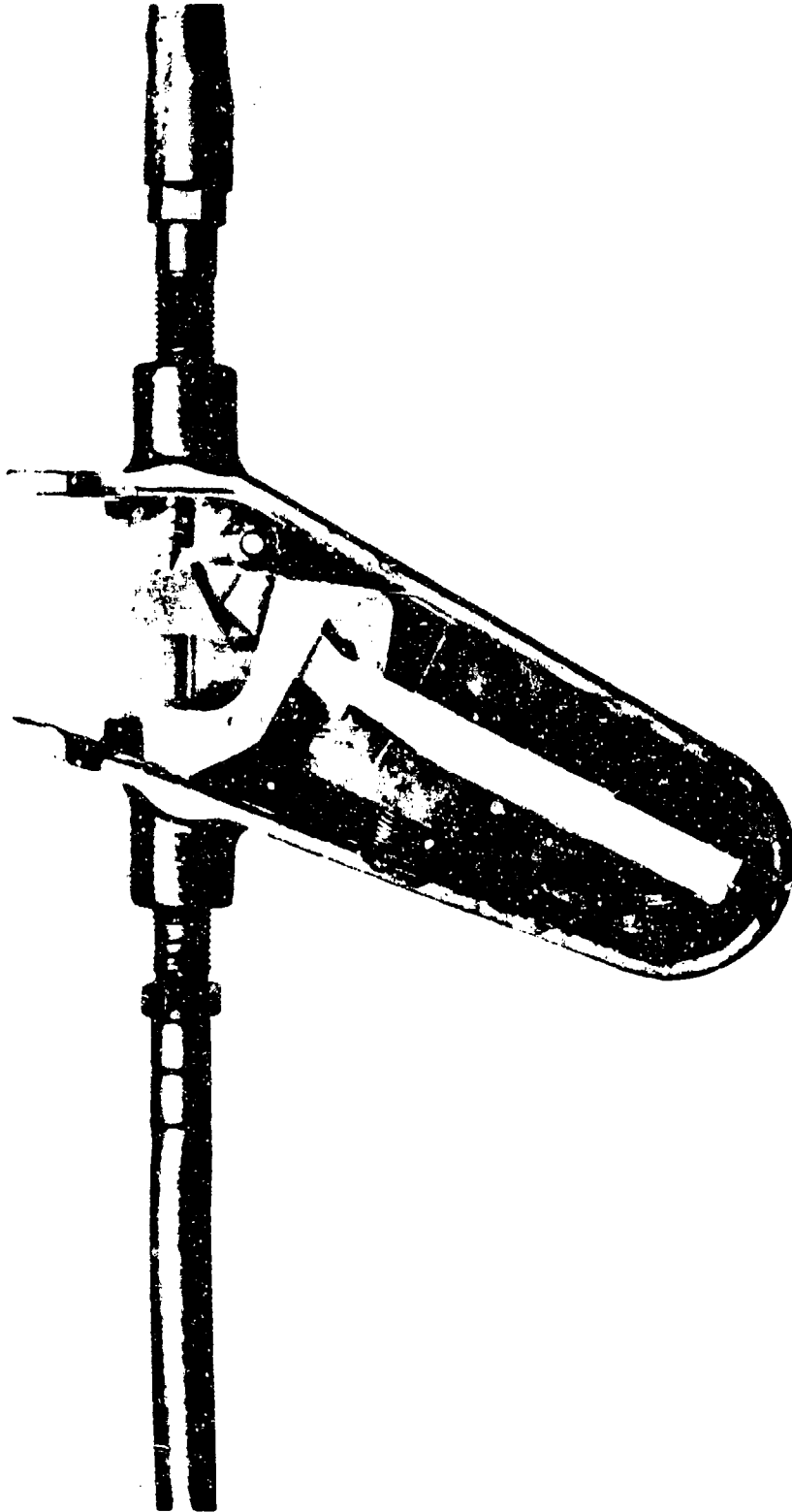


Figure 10-11. Major Level of Actuation for Firing Mechanism, 120 mm Recoilless Rifle, XM105

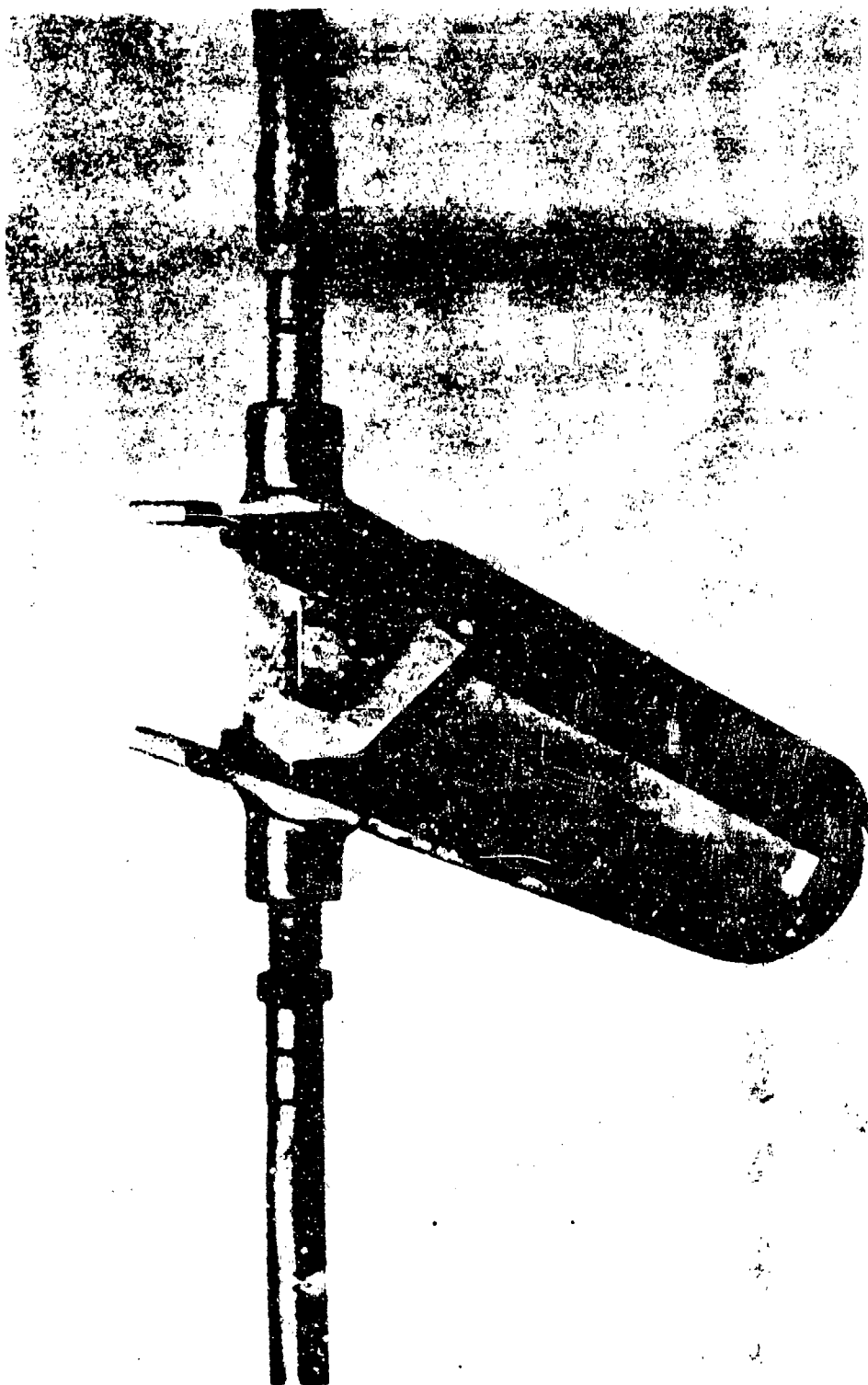


Figure 10-12. Minor Level of Actuation for Firing Mechanism, 120 mm Recoilless Rifle, XM105

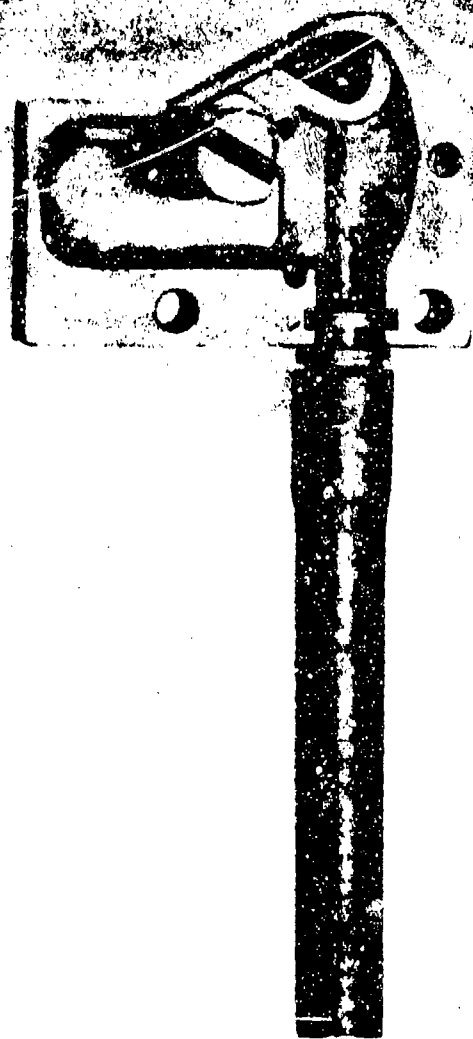


Figure 10-13. Trigger Mechanism, 120 mm Recoilless Rifle, XM105

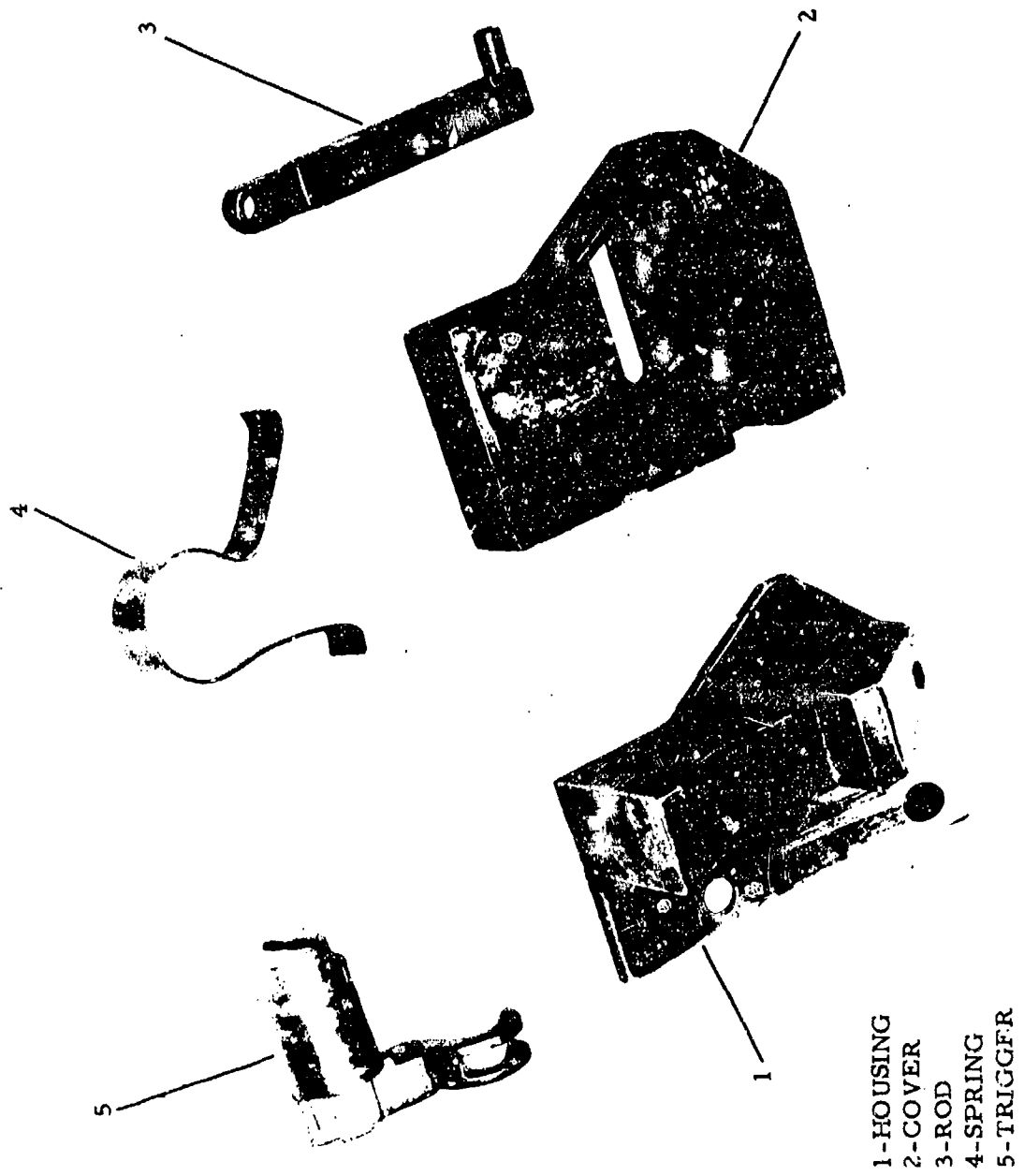


Figure 10-14. Trigger Mechanism Components, 120 mm Recoilless Rifle, XM105

REFERENCES

1. *Development of 120 mm Recoilless Heavy Antitank Weapon System (HAW)*, Final Report, Technical Memorandum M64, Frankford Arsenal, Philadelphia, Pa., 1 April 1959 through 30 June 1962.
2. *Recoilless Weapons, Volume II, Nozzles*, Contract Nos. W-36-034-ORD-7652 and W-36-034-ORD-7708, Franklin Institute, Laboratories for Research and Development, Philadelphia, Pa., for Ordnance Department, US Army, May 1948.
3. *Symposium on Nozzle Design for Recoilless Rifles*, Held at Frankford Arsenal, Philadelphia, Pa., 10 and 11 December 1951.
4. A. J. Grandy, *Nozzle Spring Design for 90 mm Recoilless Rifle, T234*, Memorandum Report M59-37-1, Frankford Arsenal, Philadelphia, Pa., July 1959.
5. *T114 Conference*, Research and Development Program, Cadillac Motor Car Division, General Motors Corporation, 28 February 1961.
6. *Recoilless Rifle Systems, Ammunition and Related Items*, Status Report No. 3, Vol. IV, Report No. R-1366, Frankford Arsenal, Philadelphia, Pa., 1 July through 30 September 1956.
7. C. W. Musser, et al., *Strain Compensated Barrels*, Report No. R-1008, Frankford Arsenal, Philadelphia, Pa., May 1951.
8. *Symposium on Recent Progress of Recoilless Rifles and Ammunition*, Held at Midwest Research Institute, Sponsored by Department of Army, 11-13 January 1954.
9. Robert Markgraf, *Repeating Recoilless Rifles*, Frankford Arsenal, Philadelphia, Pa., March 1960.
10. W. J. Kroeger and C. W. Musser, *The Design of Recoilless Infantry Weapons*, Report No. R-727, Frankford Arsenal, Philadelphia, Pa., June 1946.
11. AMCP 706-252, Engineering Design Handbook, *Guns Series, Gun Tubes*.
12. AMCP 706-108, Engineering Design Handbook, *Elements of Armament Engineering, Part Three, Weapon Systems and Components*.
13. TM 9-1000-205-12, *Operation and Organizational Maintenance Cal. .50 Spotting Rifle M8C; 106 mm Rifles M40A1 and M40A1C; 106 mm Rifle Mounts T173 and M79; and Tripod T26*, Headquarters, Department of the Army, March 1959.
14. *120 mm Rifle System, XM105E1, Heavy Antitank Weapon (F4W)* Notes on Development Type Material, PDLWS-2, Frankford Arsenal, Philadelphia, Pa., December 1962.

BIBLIOGRAPHY

W. J. Hoff, "Boundary Value Problems of the Thin-Walled Circular Cylinder," *Applied Mechanics*, December 1954.

W. J. Kroeger, *The Piping of Recoilless Gun Gases through Straight Channels and Bends*, Report R-860, Frankford Arsenal, Philadelphia, Pa., July 1948.

J. J. Donnelly and G. Schecter, *Firing Tests*

for Discharging Nozzle Gases from Recoilless Guns in Enclosed Installations, Report R-861, Frankford Arsenal, Philadelphia, Pa., July 1948.

Merrill Eig and Harvey L. Peritt, *Feasibility of Glass-Filament Wound Plastics for Use in Recoilless Rifles Such as 90 mm M67*, Technical Report 3178, Picatinny Arsenal, Dover, New Jersey, April 1965.

CHAPTER 11

AMMUNITION

11-0 LIST OF SYMBOLS

A_p	= total area of primer tube perforations, in ²	E_R	= energy required to raise surface of the propellant to its ignition temperature in time t_i , ft-lb
A_s	= surface area of propellant, in ²	F_i	= impetus of igniter material, (ft-lb)(lb) ⁻¹
a	= distance between two adjacent perforations as shown in Fig. 11-15, in.	g	= acceleration due to gravity, ft-sec ⁻²
a_1	= constant burning rate equation, in.sec ⁻¹	h	= length between perforations as shown in Fig. 11-15, in.
b	= cartridge case thickness, in.	k	= thermal conductivity of propellant, (ft-lb)(in ² -sec ⁻² K/in.) ⁻¹
b_e	= equivalent unperforated cartridge case thickness, in.	L	= length of propellant grain, in.
b_1	= constant burning rate equation, in.-sec ⁻¹ -psi ⁻ⁿ	(l/d)	= length to diameter ratio of projectile, dimensionless
C	= propellant charge weight, lb	M_o	= maximum end moment, (in.-lb)-in. ⁻¹
C_i	= igniter charge weight, lb	N_p	= number of perforations in igniter tube, dimensionless
C_2	= propellant charge burnt, lb	N_t	= weight of igniter gas produced up to time t , lb
c_p	= specific heat at constant pressure of propellant (ft-lb)(lb ⁻¹ K) ⁻¹	N'_t	= weight of igniter gas discharged from igniter tube vents up to time t , lb
$(c_p)_i$	= specific heat at constant pressure of igniter, (ft-lb)(lb ⁻¹ K) ⁻¹	n	= combustion index, dimensionless
$(c_v)_i$	= specific heat at constant volume of igniter, (ft-lb)(lb ⁻¹ K) ⁻¹	n_p	= number of perforations in propellant grain, dimensionless
D	= diameter of propellant grain, in.	P	= instantaneous space-mean igniter tube pressure, psi
E_A	= igniter gas energy made available to the propellant charge, ft-lb		

P_e	= effective pressure acting over hexagonal area, psi	t	= time, sec
P_i	= pressure acting on inside of cartridge case, psi	t_i	= ignition delay time, msec
P_o	= pressure acting on outside of cartridge case wall, psi	V	= internal volume of igniter tube, in. ³
P_p	= peak pressure, psi	V_{m}	= muzzle velocity, fps
p_c	= chamber pressure, psi	w	= propellant web, in.
Q_o	= end shear, lb-in. ⁻¹	β	= $\left[\frac{3(1 - \nu_p^2)}{r_p^2 b^2} \right]^{1/4}$, in. ⁻¹
r	= perforated cartridge case radius, in.	ΔP	= differential pressure across webs of perforated cartridge case, psi
r_R	= linear burning rate, in.-sec ⁻¹	γ_i	= specific heat ratio of igniter material, dimensionless
$(r_R)_i$	= linear burning rate igniter, in.-sec ⁻¹	ν	= Poisson's ratio, dimensionless
r_p	= perforation radius, in.	ν^*, ν_b	= constants from Ref. 1
S_i	= instantaneous igniter surface area, in. ²	ρ	= density of solid propellant, lb-in. ⁻³
T_a	= ambient temperature, °K	ρ_i	= density of igniter material, lb-in. ⁻³
T_e	= effective nozzle thrust, lb	σ_{avg}	= average stress, psi
T_i	= ignition temperature of propellant, °K	σ_{hoop}	= hoop stress, psi
T_o	= isochoric flame temperature of propellant or igniter, °K	σ_{max}	= maximum stress, psi

SECTION I

GENERAL

11-1 INTRODUCTION

The major components of a round of recoilless rifle ammunition are shown schematically in Fig. 11-1. The complete round consists of the same basic elements as other artillery ammunition; i.e., a projectile assembly, cartridge case, igniter assembly, and propellant. The projectile consists of a warhead for producing a destructive effect on the target, a fuze for initiating the warhead at the target, an aerodynamic envelope, and either a rotating band to engage the gun rifling if the projectile is spin-stabilized or fins if the projectile is fin-stabilized (or both if the fin-stabilized projectile requires slow roll at launch).

The design of a recoilless rifle projectile is similar to designs for closed breech weapons, with the exception of lower stresses due to reduced pressures, accelerations, and engraving loads. Also, the recoilless rifle cartridge case differs from the conventional case in that the wall is perforated to allow the efflux of gases to a nozzle. There are some exceptions: the 90 mm M67 System uses an unperforated case that is supported by the chamber, and the propellant gas path to the nozzle is directly rearward. Another exception is the frangible plastic envelope used in one approach to the 120 mm HAW project.

11-2 OVERALL DESIGN CONSIDERATIONS

In addition to designing recoilless rifle ammunition for its terminal effects, consideration has to be given to the overall problems associated with the assembly, loading, and packaging of the round. Because of the necessary close tolerances involved in recoilless rifle weapon systems, it is important that

the assembled round fit correctly in the rifle. In order that the rotating band of the cartridge engage the barrel rifling effectively, the correct alignment of the cartridge case and the projectile must be maintained during handling and final seating in the weapon.

During assembly of the projectile into the cartridge case, it is possible—by crimping part or all of the cartridge case mouth into a groove machined into the projectile—to maintain the necessary alignment between cartridge case and projectile, and at the same time, ensure that the cartridge case and projectile will not separate under rough handling conditions prior to and during loading operations. The length of the crimp may vary from a full crimp around the entire periphery of the case mouth (ring crimp) to small interrupted crimps made at equal intervals around the circumference of the cartridge case at a short distance from the case mouth (stab and multiple dimple crimps).

Before assembly of the projectile into the cartridge case, a rubber-base cement may be applied to the mouth of the cartridge case prior to crimping the case to the projectile. When the cartridge case is crimped to give the assembly the necessary rigidity, the rubber-base cement provides a reliable moisture seal between the case and projectile.

After assembly, painting, and marking, the complete round is packaged to withstand conditions usually found in the field. A round is packed in an individual cylindrical moisture-resistant asphalt (fiber) container which in turn is packed in a sealed metal container and then placed in a wooden box for shipping.

Some of the more difficult problems

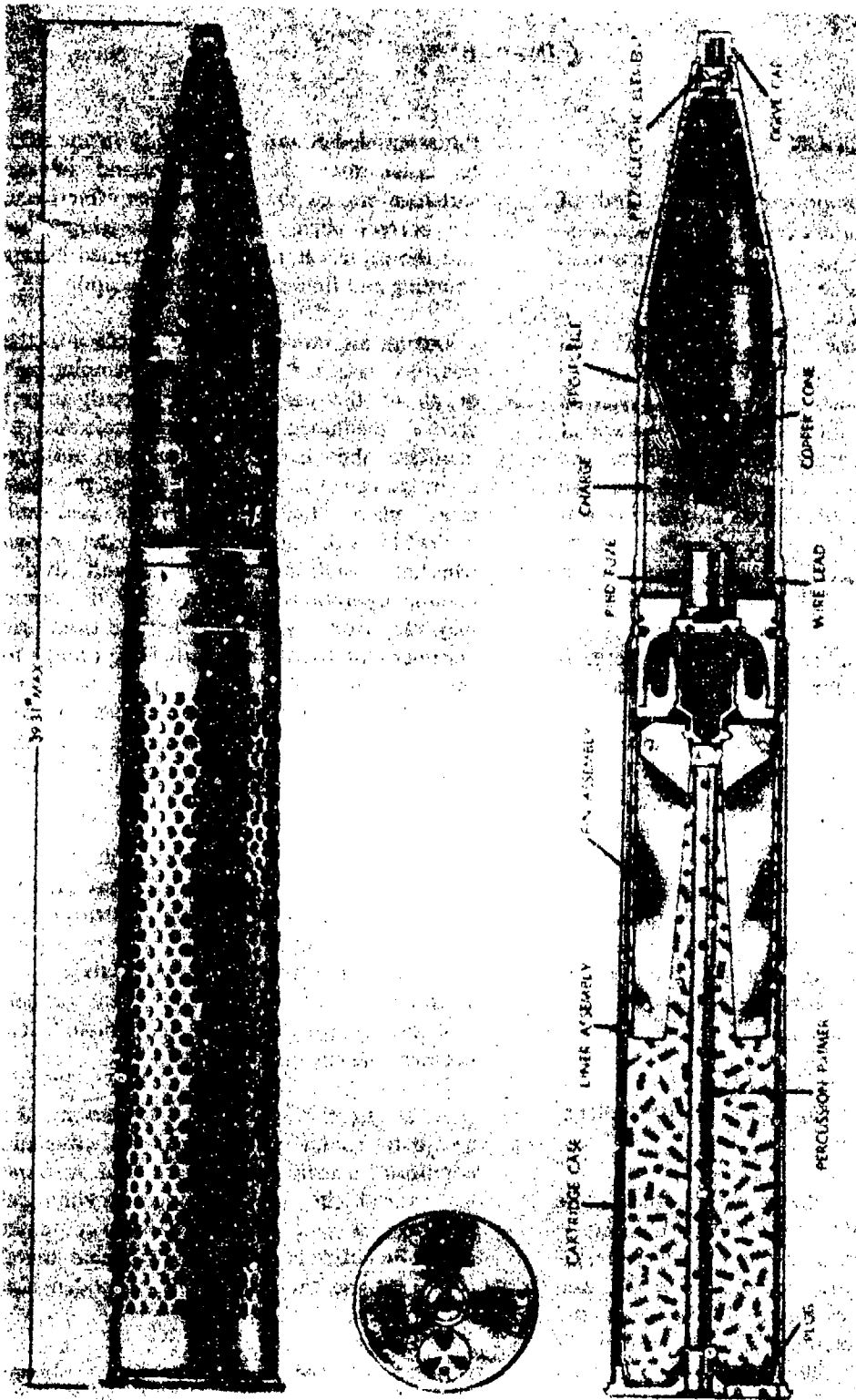


Figure 11-1. 106 mm Cartridge, HEAT, M344A1

related to loading have been encountered in the assembly of fin-stabilized HEAT ammunition. In most cases loading of the propellant is accomplished through the mouth of the cartridge case, but in most fin-stabilized projectiles, it is necessary to load the propellant through the base. Loading the propellant through a single hole in the base causes problems with packing the propellant evenly around the fins of the projectile and preventing any of the propellant grains from entering into the primer retainer of the projectile. When a base containing three holes is used, the propellant can be loaded more uniformly around the projectile fins. A more uniform flow of the propellant grains during loading of the fin-stabilized round is obtained by vibrating the complete round as the propellant flows into the cartridge case.

At times, it is desirable to be able to position the propellant in specific areas of the cartridge case because of the specific configuration of the boom of a fin-stabilized projectile or due to the position of the holes

in the primer-igniter tube. For fin-stabilized HEAT rounds, it is desirable to position the propellant at the rear of the case; whereas in spin-stabilized rounds, it may be desirable to position the propellant along the perforated section of the igniter tube. Plaster or cotton and cardboard have been used to position the propellant in the cartridge case.

Loading of the cartridge case should be performed in the shortest time possible so as to avoid the possibility of moisture absorption by the propellant. On the other hand, care must be taken to avoid damaging the cartridge case liner that retains the propellant in the cartridge case and acts as the moisture-proof barrier for the propellant.

11-3 LIST OF EXISTING CARTRIDGES WITH CHARACTERISTICS

Table 11-1 is a list of some existing recoilless rifle cartridges with pertinent design data.

TABLE 11-1
DATA FOR SOME RECOILLESS RIFLE PROJECTILES

Round	Type	Stabilization	Muzzle Velocity, fps	Maximum Range, yd	Twist, cal/rev	Complete Round Weight, lb	Projectile Weight, lb	Complete Round Length, in.	Projectile Length, in.	Cartridge Case Length, in.
<u>57 mm M13A1: 7,800 psi max. rated pressure (piezo)</u>										
M306A1	HE	Spin	1200	4930	30	5.46	2.78	17.54	6.47	12.0
M307A1	HEAT	Spin	1200	4860	30	5.43	2.75	18.78	8.07	12.0
M308A1	WP	Spin	1200	4530	30	5.43	2.75	17.54	6.43	12.0
<u>75 mm M20: 10,800 psi max. rated pressure (piezo)</u>										
M309A1	HE	Spin	990	6960	22	22.37	14.40	28.92	15.10	16.0
M310A1	HEAT-T	Spin	1000	7300	22	21.06	13.19	28.92	15.95	16.0
M311A1	WP	Spin	990	7020	22	23.20	15.10	28.92	14.54	16.0
M349	HEP-T	Spin	1400	7180	22	16.52	8.4	26.36	—	16.0
<u>90 mm M67: 7,780 psi max. rated pressure (piezo)</u>										
M371A1	HEAT	Fin	730	2200	160	9.25	6.43	28.00	28.00	16.35
<u>105 mm M27A1: 10,000 psi max. rated pressure (piezo)</u>										
M323	HE	Spin	1120		20	49.15	32.40	40.73	15.74	
M325	WP	Spin	1120		20	51.53	34.58	40.80	15.73	
M326	HEP	Spin	1265		20	40.30	24.80	38.89	17.60	
M341	HEAT	Folding Fin	1650		20	34.32	17.30	39.29		
M345B1	HEP-T	Spin	1650		20	38.00	17.54	38.00		
<u>106 mm M40A1: 11,000 psi max. rated pressure (piezo)</u>										
M344A1	HEAT	Folding Fin	1650		20	36.19	17.55	39.31		
M346B1	HEP-T	Spin	1635		20	37.93	17.54	38.10		

SECTION II

PROJECTILE

11-4 INTRODUCTION

The modern projectile used in recoilless rifle weapon systems is cylindrical in shape with a fairly long ogival nose. The projectile will have either a boattailed (tapered) or cylindrical (square) base and may be designed with fins, depending upon the type of stabilization required. The specific projectile design depends very much on its function, i.e., the type of target it is to defeat. As discussed in Chapters 3 and 5, the physical characteristics of the projectile design contribute directly to the determination of both the exterior and interior ballistics of the weapon and to the dimensions of the overall weapon system.

The relationship between the projectile characteristics (mass, diameter, and shape) and the overall weapon system is seen by considering a weapon system in which it desired to extend the projectile range. Since requirements specify the defeat of a certain target, the projectile characteristics are not changed. Thus, the only means of achieving the increased range are by increasing the chamber pressure, increasing the barrel length, or using a combination of the two. It is evident that any of these changes will result in a larger, heavier weapon, if the designer is limited to the use of specific weapon materials.

If it were possible to change the projectile characteristics while achieving the same terminal effects, it is evident that compromises would have to be made in other aspects of the weapon performance. Increasing the diameter of the projectile while maintaining a constant weight may result in a lower chamber pressure to achieve the same muzzle velocity, but will result in a shorter trajectory because of the effect of increased projectile

diameter on the exterior ballistics. From this short discussion, it can be seen that in the projectile design, it will not be possible to consider only the desired terminal effects; how the projectile can be dimensioned to achieve a minimum weight gun while still effectively defeating the specific target must be considered also.

11-5 PROJECTILE TYPES

Projectiles commonly are classified according to the type of warhead employed and the tactical use for which the projectile is intended. The various types of warheads have been described in detail in Chapter 3. Figs. 11-2 through 11-7 show simplified cross sections of various types of projectiles that are described briefly as follows:

1. High Explosive Antitank (HEAT), Figs. 11-2 and 11-3. Designed for the defeat of armor, this projectile uses a hypervelocity, shaped-charge jet formed by interaction of explosive charge and liner to penetrate tank armor. Since spin degrades penetration by "defocusing" the jet, this projectile commonly is fin-stabilized.

2. High Explosive (HE), Fig. 11-4. Designed for defeat of personnel, materiel, and field fortification through blast and fragmentation, the HE projectile consists of an explosive charge contained in a thin-wall, steel envelope. Depending upon the terminal ballistic requirements, various combinations of fragmentation and demolition effects can be obtained by proper selection of wall thicknesses and explosive charge size. Projectiles designed for fragmentation effects have thicker walls and smaller bursting charges than projectiles designed for demolition use. The standard envelope consists of a 2- to 3-caliber tangent ogive and a 2- to 3-caliber

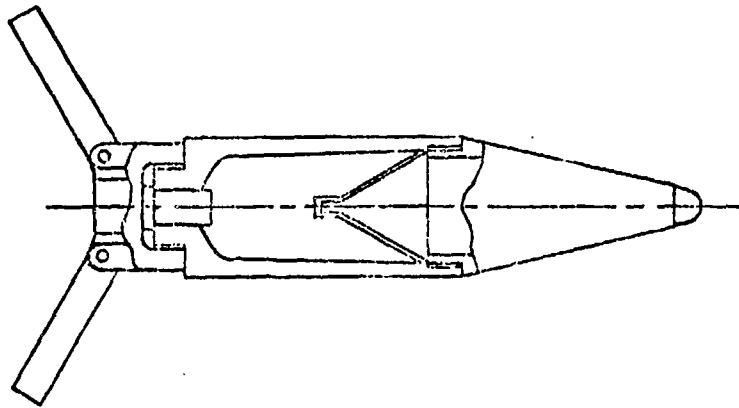


Figure 11-2. Folding Fin HEAT Projectile

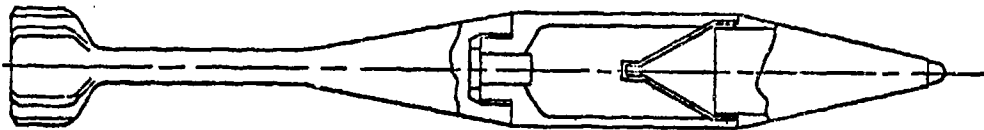


Figure 11-3. Fixed Fin HEAT Projectile

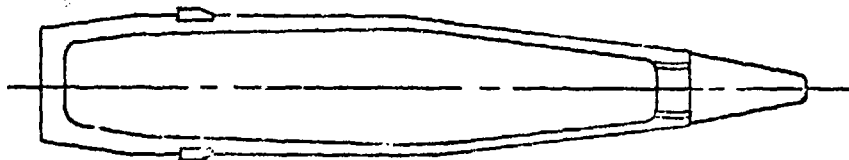


Figure 11-4. HE Projectile

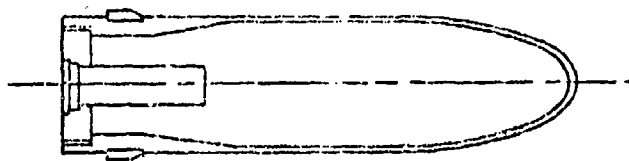


Figure 11-5. HEP Projectile

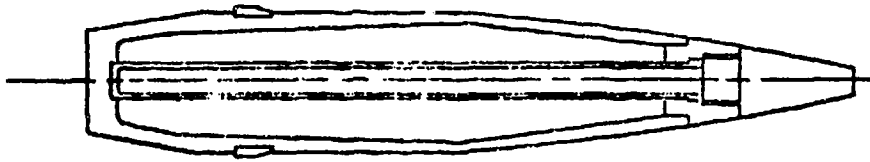


Figure 11-6. WP Projectile

cylindrical body. Depending upon the exterior ballistic requirements, the projectile may have a 0.5 caliber boattail.

3. High Explosive Plastic (HEP), Fig. 11-5. The HEP projectile is designed to defeat armor through the spalling of the rear face of the armor by action of shock waves produced by detonation of the projectile explosive charge on the armor front face. The fuze consists of an inertia type, base-detonating fuze timed to detonate the explosive after it has spread out (squashed) on the front face of the armor. The projectile design consists of a 1-caliber tangent ogive and a 2.5- to 3.5-caliber cylindrical body with a threaded base plug containing the base fuze.

4. Incendiary or White Phosphorus (WP), Fig. 11-6. Designed to provide smoke screening and incendiary effects, the WP-type projectile usually consists of HE projectile metal parts redesigned to accept a press-fit central burster tube with an enlarged mouth diameter threaded internally to accept the fuze.

5. Antipersonnel (APERS). The antipersonnel projectiles include all types of projectiles designed to release lethal subprojectiles upon actuation or detonation. Canis-

ter and beehive projectiles are examples of antipersonnel type projectiles.

The canister type projectile (Fig. 11-7) is designed for the defeat of personnel in mass attack by functioning immediately in front of the weapon to release a large number of lethal subprojectiles. The projectile consists of a cylindrical container filled with small slugs, balls, or flechettes with a thin closure crimped on the forward end. The walls are extremely thin so that they will fail due to centrifugal force upon emergence from the weapon. Longitudinal grooves are machined on the outside of the wall to assist failure of the walls. Dispersion of the payload is achieved by centrifugal force and, therefore, is a function of muzzle velocity, subprojectile masses and spin. The lethal masses appear in the form of a cone with its apex at the muzzle of the weapon.

The beehive projectile, designed for the defeat of personnel in mass attack from range zero to maximum range of the weapon through the release of flechettes at the desired range, is basically a canister projectile fuzed to function at specific ranges beyond range zero. The fuze is a mechanical time (MT) fuze that can be set for either muzzle action or time increments of 100 m.

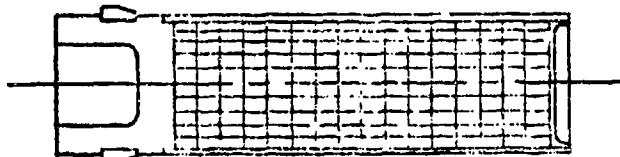


Figure 11-7. Canister Projectile

11-6 DESIGN CONSIDERATIONS

11-6.1 ENVELOPE

In the design of the projectile envelope, the designer must consider the different effects that the firing, trajectory, and impact stages of the mission have on the projectile. These considerations will involve the structural strength, aerodynamics, and the terminal ballistic effects of the projectile envelope.

1. Ability To Withstand Stress During Firing. Regardless of the function of the envelope as determined by the type of projectile, the envelope must show the ability to withstand the stresses sustained during firing (metal parts security). These stresses are a result of the propellant gas pressure acting on the base and the wall behind the projectile rotating band, and the acceleration and rotational forces acting on the entire envelope. Since the maximum rated pressures of recoilless rifles are considerably lower than for closed breech systems, the designer has greater latitude in the choice of steel and aluminum alloys, and also in the use of other materials such as plastics, reinforced plastics, and Fiberglas. A stress analysis on the envelope configuration will establish the specific strength requirements of the materials to be used and confirms the adequacy of the sections to withstand the firing stresses.

2. Aerodynamic Stability. The second area of projectile design is making the projectile aerodynamically stable in order to provide a controlled and predictable flight to the target. The method or type of stabilization—either spin or fin, or a combination of both—is based on the primary warhead type and configuration, and the effect of spin on the warhead. For spin-stabilization, twists of rifling of 1 turn in 18- to 30-calibers of travel are used.

Once the type of stabilization has been established, satisfactory aerodynamic stability can be achieved by proper mass distribution within the projectile envelope. In the absence

of aerodynamic stability, the net effect of the aerodynamic, inertia, gravitational, and gyroscopic (for spin-stabilized projectiles) forces acting on the projectile will be to increase the oscillatory motion of the projectile until it begins to tumble.

3. Terminal Ballistic Effect. The envelope, while being structurally sound and dynamically stable, also may be a contributing factor to the terminal ballistic effect and is a third consideration in projectile design. In the case of canister and beehive-type projectiles, the envelope serves only to carry the warhead from the launching weapon to the target, whereas the warhead of a high explosive type projectile contributes directly to its fragmentation effect. In the case of WP projectiles, the envelope makes a secondary contribution in that the dispersion and burning effects of the WP are controlled by the manner in which the envelope fragments upon detonation.

The optimization of all three areas of projectile design discussed in this section usually is not obtainable, and leaves the designer faced with the choice of making trade-offs to achieve the specified military characteristics.

11-6.2 REQUIRED INFORMATION

In order to prepare an initial projectile design, the designer must be supplied with the following information as determined by analysis of the specified performance requirements:

1. Warhead Type. The designer is informed of the category of primary target to be defeated in order to determine the type, configuration, and quantity of explosive or chemical charge.

2. Caliber. The caliber of a recoilless rifle is the diameter of its bore. The term caliber also may be used as a unit measurement in expressing the rifle length. Specifying the caliber of the rifle determines the projectile diameter

3. **Projectile Weight.** As determined by an overall system analysis to achieve the lightest weight system compatible with range and terminal ballistic requirements, the projectile designer will be supplied with a maximum projectile weight. This information, along with the maximum chamber pressure, will enable the designer to properly size the projectile wall thicknesses and choose materials with the necessary strength requirements.

4. **Maximum Chamber Pressure and Rifling Twist.** Specification of the maximum chamber pressure and rifling twist enables the projectile designer to perform the necessary stress analysis, to establish strength requirements, and to assure that the projectile will withstand the stresses sustained during firing.

5. **Muzzle Velocity.** In order to evaluate aerodynamically the projectile design and show that the projectile will meet minimum trajectory requirements, the designer must be provided with the muzzle velocity. Given the muzzle velocity, the designer can determine the necessary aerodynamic coefficients needed to perform trajectory and stability analyses.

11-6.3 METHOD OF STABILIZATION

The method of stabilization is based on the primary warhead type and the effect of spin on this type of warhead. As stated in par. 11-6.1, spin-stabilization is preferred because it provides the best accuracy and is the most economical round to manufacture. However, if defeat of armor is the primary purpose of the system, a HEAT warhead is then required, necessitating the use of fin-stabilization. Fin-stabilization is preferred for the HEAT warhead since the jet is affected adversely by spin. Even with flow-turned liners producing spin compensation up to approximately 30 rev per sec or with fluted designs (up to approximately 100 rev per sec), a certain amount of penetration is lost compared to a nonspinning warhead.

In recoilless systems with the exception of the original 55 mm and 75 mm systems, the HEAT projectiles are fin-stabilized to obtain maximum armor penetration for minimum caliber and weight. However, to improve accuracy even the fin-stabilized rounds are given a slow spin comparable to 1 turn in 160 to 250 calibers of travel. In imparting spin to a fin-stabilized projectile, the spin must be high enough to avoid resonance and low enough to avoid magnus effects. Generally, a spin rate between 10 to 20 revs per sec will avoid either of these conditions.

If the purpose of the system is both antiarmor and antipersonnel for which fin- and spin-stabilization, respectively, are preferred—the latter particularly for canister- and beehive-type projectiles—the designer must make a choice in favor of one or the other. Generally, spin-stabilization is chosen and the effect of spin on the fin-stabilized HEAT round minimized by designing the HEAT round without an obturating band. Thus, spin transmission to the finned round is only through friction of the obturating band on the projectile body against the rifling which is usually equal to or less than 30 revs per sec for which a flow-turned liner can provide adequate spin compensation.

11-7 METAL PARTS SECURITY—STRUCTURAL INTEGRITY WITHIN THE BALLISTIC ENVIRONMENT

11-7.1 GENERAL

Upon completion of the preliminary design layout that establishes the general configuration that satisfies the weight and material requirements, a stress analysis is conducted. This analysis establishes the strength requirements of the materials and confirms the adequacy of the section thicknesses chosen to withstand the firing stresses. Based on the results of the analysis, the envelope (section thicknesses) may have

to be redesigned to bring the stress levels into practical limits for the commonly used materials, i.e., steel and aluminum. The desired limits for steel are yield strength of 60,000 to 90,000 psi for which low to medium carbon steels can be used; the limits for aluminum are yield strengths of 40,000 to 70,000 psi for which, in order of descending preference, the following alloys can be used, 6061-T6, 2024-T3, 2014-T6, 7079-T6, and 7075-T6.

Since the maximum rated pressures of recoilless rifles are considerably lower than for closed breech systems, the designer has greater latitude in the choice of steel and aluminum alloys, and also in the use of other materials such as magnesium, plastics, reinforced plastics, and Fiberglas. In choosing materials, the designer should always keep cost in mind and use the most economical materials that will satisfy the structural, aerodynamic, and warhead requirements. For fixed-fin rounds, the fins usually are extruded aluminum. Additional material considerations are included under aerodynamic and warhead design.

11-7.2 STRESS ANALYSIS

The accepted method of stress analysis is based on thin-wall shell theory specifically adapted to the conditions of projectile design. The analysis is conducted at specific critical points based on 115% of the maximum rated pressure and minimum metal conditions to ensure an adequate factor of safety under all temperature and pressure extremes.

The critical points are:

1. The capability of the center of the base and the intersection of the wall to withstand the propellant gas pressure and the setback pressure of the filler
2. The capability of the wall immediately behind the rotating band to withstand propellant gas pressure, and the acceleration and rotation forces of the body and the filler

3. The capability of the wall immediately forward of the rotating band, the intersection of the bourrelet and the ogive, and the thin section of the ogive to withstand the forces of acceleration and rotation of the body and the filler

4. The capability of all threaded joints to withstand, in addition to the forces of acceleration and rotation, those forces due to relative distortion of the mating parts.

Although no analysis is conducted for the forces applied during the engraving of the rotating band, it is recognized that these forces exist and that temporary and/or permanent deformation of the body can occur due to band engraving. Particular attention must be paid to this during the initial metal parts security tests and if excessive deformation is evident (greater than or equal to 0.005 in.), the design must be modified to eliminate it

To avoid this body deformation problem and the associated problem in the weapon design, pre-engraved rotating bands generally are used for recoilless projectiles. However, when a pre-engraved band is used, it presents two other problems; i.e., lack of obturation (propellant gas leakage past the band) and the need for indexing the band into the rifling during loading. The first problem is of direct concern in the stress analysis in that the critical sections forward of the band are subjected to the propellant gas, a factor that must be included in the stress analysis. This problem can be alleviated by the use of a plastic or rubber obturator. However, these materials are quite sensitive to the effects of temperature extremes, and therefore, are not 100 percent reliable. Consequently, even when an obturator is used, it is good practice to assume leakage will occur, thus applying propellant gas pressure to the body sections forward of the pre-engraved rotating band and/or obturator.

The formulas, as corrected empirically, presently used in projectile design are given in

Ref. 11. The formulas will give the longitudinal, radial, and tangential stresses of each section and are combined to give the resultant stress in accordance with the Hencky-Von Mises theory of failure.

11-8 AERODYNAMIC DESIGN

Upon establishment of the design parameters including method of stabilization, the initial envelope can be designed by methods of stress and aerodynamic analyses. Detailed definition of the aerodynamic design parameters, criteria, requirements for stability, and method of analysis are given in Chapter 4.

Generally, for either spin- or fin-stabilization, satisfactory stability can be achieved by the proper distribution of the mass. For a spin-stabilized projectile the designer should attempt to maximize the axial (polar) moment of inertia and minimize the transverse moment of inertia. This usually can be achieved with a one-piece steel envelope with properly contoured walls. However, if the ratio of length to diameter (l/d) exceeds 4 to 4.5 calibers, this may not be possible and multipiece construction employing lightweight materials for the ogive and base may be required. Beyond 6 to 6.5 calibers even multipiece construction will not provide sufficient gyroscopic stability, and fin-stabilization will have to be used if the warhead requirements dictate a longer projectile. Ref. 14, even though quite old, can be used to good advantage.

11-9 OTHER DESIGN CONSIDERATIONS

Within the general design considerations discussed in par. 11-8, there are several specific considerations which deserve mention in this paragraph.

1. Joints When HE Is Used. Multipiece construction with joints exposed to the high explosive never should be used in the projectile design. Inspection costs alone would dictate against this practice, but there

is always the very real danger of an inadequately inspected projectile being loaded and fired. An in-bore detonation of the HE is too high a price to pay for the design alternative. Projectiles should not be designed with joints in a π area to be occupied by HE. Press-fit joints are used on US Army projectiles to seal WP within the projectile body; the British use threads coated with a sealant for the same purpose.

2. Bourrelet Design To Minimize Balloting. Another design consideration is the projectile-rifle relationship during the travel of the projectile through the tube. In-bore yaw (balloting) should be held to a minimum because it results in excessive yaw at muzzle exit (aerodynamic jump). Two widely spaced bourrelets (bore riding surfaces) fore and aft of the rotating band are desirable with minimum clearance between the land and bourrelet diameters. Present practice defines minimum bourrelet clearance as 0.002 in. plus 0.001 times the caliber in inches, with a minimum of 0.004 in. for 37 mm and smaller projectiles. A tolerance of plus zero minus 0.005 in. is specified for all projectiles. Thus, projectiles may be designed for a maximum clearance of 0.007 in. plus 0.001 times the caliber in inches; or for 37 mm and smaller, 0.009 in.

3. Avoidance of Abrupt Surface Irregularities. Abrupt surface irregularities also should be avoided. At any joint, the forward section always should be flush with or slightly larger than the mating part. This should be maintained under all conditions of tolerance and ovality to prevent sharp, flat, drag-producing projections into the airstream (commonly referred to as the "reverse umbrella effect").

4. Prevention of Flow Separation. Ideally, there should be no separation of the airstream over the projectile envelope during flight. If erratic flight does occur at some point in the trajectory, it is most likely due to airstream separation, or spin-yaw resonance, and/or

magnus instability. This is particularly true for fin-stabilized projectiles.

5. Boom Design for Fin-stabilization. In the design of fin-stabilized projectiles, the length of boom connecting the fin to the projectile body is limited by the gun chamber configuration. In many instances, use of the boom to contain the igniter tube requires a longer boom than necessary for projectile stability. In addition to placing the fin in a more rearward position than required for stability, and emphasizing the attendant yaw and pitch perturbation effects during launch, the tube also is subjected to bending stresses (flexure) due to unequal in-bore pressure distribution and vibrations at launch and during flight.

6. Typical Fin Design. For full caliber fixed-fins, six-bladed extruded T-section fins have been used successfully. The T-section configuration (also referred to as an end plate) is used to maximize the effectiveness of the fin by deterring the movement of air over the edge of the fin from the high pressure to the low pressure side. The end plates also add to the torsional rigidity of the fins, providing a larger bore riding surface during launch and preventing fins from entering into rifling.

In the use of folding fins, the designer should design the mechanism for opening the fins to ensure simultaneous opening of all of the blades. In the 106 mm Projectile M344, the fins are opened by the entrapped gas pressure acting on a piston geared to all fin blades.

7. Spiked Nose. If the range requirements are sufficiently short and the muzzle velocity high enough that a spiked nose configuration can be used, particular attention must be paid to spike diameter and length to avoid a dual flow condition. Dual flow is defined as the reattachment of the shock wave off the tip of the spike to the cylindrical portion of the spike. Dual flow significantly increases drag and is usually an inconsistent phenomenon from round to round. Experience indicates

dual flow generally can be avoided by the placement of a trip ring approximately 1.3 to 1.4 times the spike diameter and located approximately 1/3 caliber from the tip of the spike. A trip ring is a sharp expansion in the diameter of the spike, i.e., a ring or a flange.

8. Automatic Indexing Device. Experience with recoilless rifles has indicated that in loading a round into the weapon, difficulty often was encountered in registering the engraving of the rotating band with the lands and grooves of the rifling. Therefore, it was necessary to enter the round up to the rotating band and then slowly rotate the round until the proper location was found before the round was driven home. In order to chamber the round in one uninterrupted motion, a means for automatically indexing the projectile is needed. Automatic indexing of the projectile is accomplished by the use of two buttons located 180 deg apart on the projectile bourrelet with their center points on the centerline of the rotating band tooth helix. The buttons are machined of brass or similar material to the proper diameter in order to engage the groove in the rifling. The buttons are then crimped into holes in the bourrelet and provided with a spring or cushion that permits the buttons to compress into the projectile if they first strike a land before expanding into the rifling groove. After these buttons engage the rifling grooves, they force the round to rotate with the rifling and thereby properly register the pre-engraved rotating band into the rifling. The indexing button also may be a simple flat (leaf) spring fastened to the body in line with a given land of the rotating band so that the spring will expand into the rifling groove when loaded into the rifle.

9. Avoidance of Mass and Configurational Asymmetries. As stated previously, a slow spin is desirable for fin-stabilized projectiles to reduce the effects of asymmetry. Although initial spin can be imparted by the rifling, it is often necessary to maintain the spin throughout the flight of the round. This can be done by either beveling the leading and/or trailing

edges of fin blades or by canting the fin blades. The major difficulty in employing either of these methods in mass production is controlling the degree of bevel or cant within the closely toleranced limits required for spin control.

11-10 WARHEAD DESIGN

In general, in order to achieve a desired terminal ballistic effect, the designer is faced with the problem of packaging the largest size warhead in an envelope that is structurally adequate and aerodynamically stable. Specification of the projectile type usually dictates the warhead size, shape, and type of explosive charge or chemical filler to be used, but also will present design problems inherent with a projectile type. Detailed design parameters and criteria for terminal ballistic effects for the various types of projectiles are given in Chapter 3.

11-11 ROTATING BAND

The purpose of the rotating band is threefold: to center the projectile, impart spin, and provide obturation. However, for recoilless projectiles, a pre-engraved band normally is used for spin-stabilized projectiles, i.e., the band is machined to match the rifling in the tube. Consequently, the band provides only two of the functions and if maximum efficiency is to be obtained, a separate obturating band is required.

The pre-engraved rotating band may be machined directly from a raised projection of steel integral with the body or machined from another material which is swaged, threaded, or welded to the body prior to machining. For example, on the thin-wall HEP projectiles, the band is machined from a copper overlay welded onto the body. Clearance between the band and the rifling is held to a minimum to minimize propellant gas leakage. To facilitate engagement of the pre-engraved band into the rifling when loading the cartridge into the weapon, an indexing button

on the forward portion of the projectile body may be used. If the complete round length is short, as in the 57 mm and 75 mm systems, this is not required. However, in 106 mm or larger calibers, it generally is required.

A pre-engraved band is not used for fin-stabilized projectiles fired from rifles having a slow twist. Instead, a thin plastic band, Geon or nylon, shrunk into a shallow smooth seat is used. The forces applied to the projectile wall during engraving of the plastic band are minimal and usually can be ignored. In addition to transmitting spin, the plastic band serves as an obturator. An example of this is the M371 HEAT Cartridge for the 90 mm Recoilless Rifle.

By considering the advances being made in plastics, it may be possible for future systems to use plastic bands for spin-stabilized projectiles, thus eliminating the cost of pre-engraving and associated problems of gas leakage and indexing.

11-12 OBTURATORS

Since the pre-engraved bands do not provide obturation, it is often desirable to use an auxiliary obturating band. This band usually consists of a rubber or plastic ring located behind the rotating band. The rear edge of the obturator may be flared outward to assist the propellant gas pressure in forcing the material into the rifling. However, this generally is not required to achieve an effective seal.

Many band geometries are satisfactory, and a groove or seat may or may not be required to position the obturator while in the tube. This is left to the discretion of the designer based on test results. Of particular concern, however, is the choice of materials that will perform satisfactorily over the temperature extremes of -65° to 140° F. One hundred percent reliability under all temperature and pressure conditions rarely can be achieved.

11-13 STRAIN COMPENSATION

Because of the extremely thin walls of recoilless rifles, deformation of the rifle due to gas pressure and the attendant increase in bore diameter are of considerable concern to both the projectile and rifle designers. To compensate for the expansion of the bore, the diameter of the rear bourrelet is increased to maintain the desired fit between the projectile and the bore during travel through the tube. If an obturator is used, it also is designed for the oversize bore condition. Consequently, even when a plastic rotating band is used in lieu of a pre-engraved band, it may still be necessary to use a separate obturating band. The amount of expansion usually is determined by the rifle designer and supplied to the projectile designer. The 90 mm M67 Rifle and M371 Projectile combination is an example of a strain compensated system.

11-14 SHOT START

This is the force or chamber pressure required to start the projectile moving. A minimum shot-start pressure is required to achieve proper ignition of the propellant particularly when pre-engraved rotating bands are used. Generally, sufficient shot start can

be obtained by crimping the cartridge case tightly to the projectile. Forces of 8,000 to 10,000 lb can be obtained with a good crimp. When sufficient shot start cannot be obtained through crimping, a special tensile connection usually is made between the primer and the base of the projectile via a threaded joint. This is particularly true in fixed fin-stabilized projectiles in which the projectile boom and fin assembly are used to contain the igniter.

11-15 SPIGOTS

A spigot weapon system—whether it be mortar, closed breech, or recoilless—consists of an over-caliber warhead mounted on a full caliber type (spigot) that is inserted into the rifle barrel (muzzle loaded). The spigot may extend partially down the barrel or all the way to the chamber. The joint between the projectile base and the spigot may be either fixed or loose to permit separation (discard) of the spigot in flight. The basic purpose of the spigot is to permit the launching of large over-caliber warheads from lightweight, small, weapon systems. An example of a spigot system is the DAVY CROCKETT recoilless weapon system (see Figs. 1-13 and 1-14 in Chapter 1).

SECTION III

CARTRIDGE CASE

11-16 INTRODUCTION

Recoilless rifle cartridge cases differ from ordinary closed breech cartridge cases due to the requirement that there must be provision for rearward flow of the vented propellant gases. The two most common chamber configurations are the breechless-axial nozzle rifle and the breech loading-multiple nozzle rifle; both of which vent from the rear of the rifle. Another possible configuration is the breech loading-forward orifice rifle that may vent rearward from the sides of the chamber or even forward of the chamber itself. These three configurations are shown in Figs. 11-8, 11-9, and 11-10.

In these figures, it is shown that for the axial nozzle weapon, the rifle is usually breechless and the function of the case is that of a container and loading tool for the explosive. It is, therefore, desirable for the case to be disposed of during the firing cycle so that cartridge case ejection is not required as a separate function. Two systems—rifles incorporating combustible or frangible cartridge cases—attempt to accomplish this function. In the combustible cartridge case, the case burns and contributes to the propellant charge, whereas the frangible cartridge case disintegrates and “blows” out through the nozzle.

11-17 THE PERFORATED CARTRIDGE CASE

11-17.1 GENERAL

The main advantage of using a perforated cartridge case is the rapid radial expansion of the propellant gases into a relatively large chamber volume. Since the total perforation area greatly exceeds the bore or throat area, the case offers little resistance to the gas flow,

and enables the case to be made considerably smaller than the gun chamber. The lighter perforated cartridge case is considerably easier to handle than a comparable closed-breech cartridge case.

While the use of a perforated cartridge case results in considerable weight savings, there are several problems inherent in its use. One problem in the design of the perforated cartridge case has been the selection of case material of suitable hardness which will ensure that the case deformation resulting from firing will be small enough to allow free extraction of the case. Another problem is the selection of a material to cover the perforations in the cartridge case for use with fin-stabilized projectiles and the method by which this liner is applied to the inside of the case. The liner must be able to withstand all the environmental and handling conditions to which the case is exposed while (1) providing an adequate moisture seal for the propellant, (2) exhibiting sufficient strength to prevent the propellant grains from punching through the liner, and (3) leaving no undesirable residue in the weapon after firing.

Cartridge case perforations have been sealed with various materials. Originally, paper was used, then polyethylene and cellulose nitrate. Now, the preferred method of sealing the cartridge case perforations in fin-stabilized rounds is through the use of polyethylene terephthalate (PETP)* film. In spin-stabilized ammunition, the propellant generally is contained in a polyethylene/rayon laminated bag.

In applying a PETP liner, the PETP film is precut and preshrunk, and then placed inside of the cartridge case which has been covered with a suitable adhesive. A rubber mandrel then is inserted inside the liner and expanded so that the liner is pressed tightly against the

*Mylar (Type A), E. I. DuPont, DeNemours & Co.

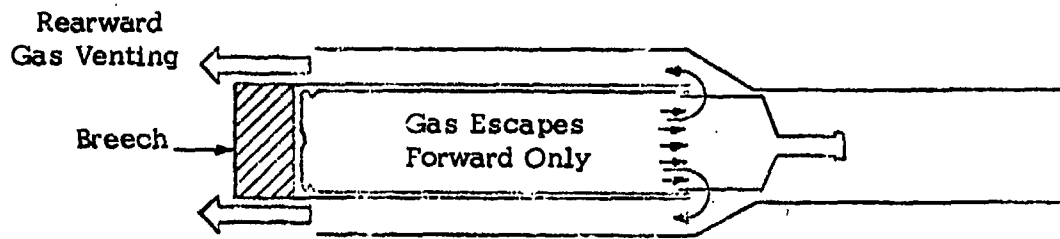


Figure 11-8. Breech Loading—Forward Orifice

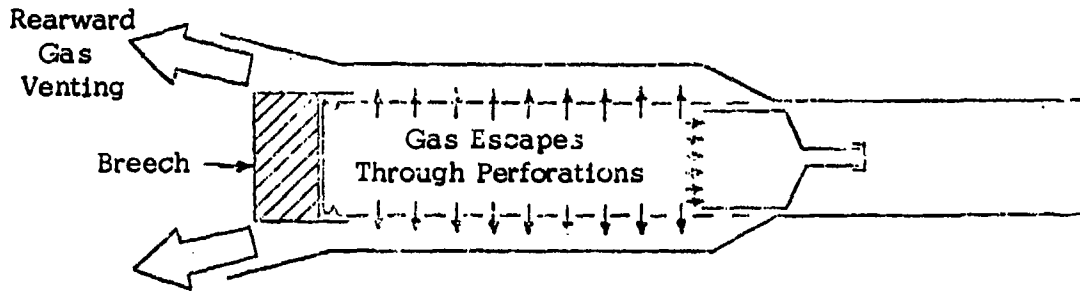


Figure 11-9. Breech Loading—Rear Orifice, Perforated Case

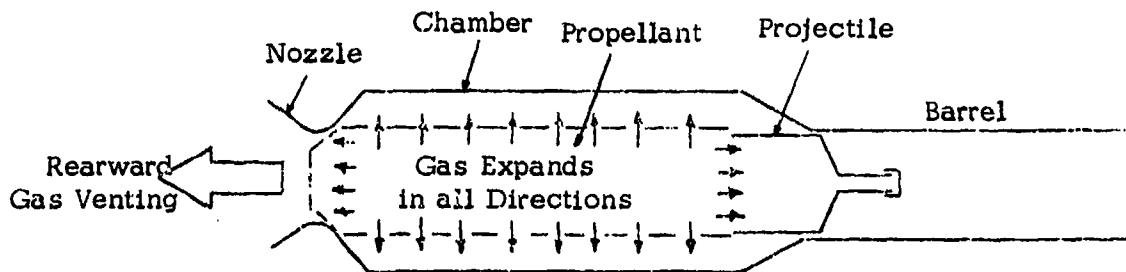


Figure 11-10. Axial Nozzle—Combustible Case

inside of the cartridge case. This procedure is described in more detail in par. 11-17.8. The resulting PETP lined case provides the necessary moisture seal while being of sufficient strength to prevent propellant grains from punching through the PETP film.

Manufacture of the perforated cartridge case has been accomplished by two different techniques. The preferred method of manufacture is to roll perforated sheet steel into a cylinder and attach it to a machined head by a copper braze. This method of manufacturing has superseded a previous, more costly method that used a drawn steel case manufactured in a manner similar to artillery cartridge cases. Prior to tapering and necking, the required number of perforations is punched out one row at a time.

11-17.2 EFFECT ON INTERIOR BALLISTICS

In the design of a perforated cartridge case, its effect on ballistic performance is of prime importance. Ballistic performance includes factors such as:

1. Rearward recoil
2. Peak chamber pressure
3. Propellant loss.

These characteristics are dependent upon the cartridge case perforation parameters, as well as those associated with the charge and chamber-nozzle configuration.

Determination of the dependence of the internal ballistic characteristics of the weapon upon the cartridge case perforation parameters is a complex problem, which in prior practice, mainly was arrived at experimentally. A specific set of numerical results is shown in par. 11-17.3 for the 57 mm M30A1B1 Case tested with the M18 Recoilless Rifle to illustrate the relative performance expected in varying the perforation parameters.

The data for Fig. 11-11 were obtained for a variation in percent perforation area and a corresponding variation of charge necessary to obtain a muzzle velocity of 1150 fps. It will be noted that as the percentage perforation increases, the charge required to maintain the 1150 fps muzzle velocity increases. This is due to the increased propellant loss and decrease in peak chamber pressure.

It also can be seen that for a 100 percent perforation area (zero strength cartridge case) the rearward recoil is minimized with a corresponding increase in the charge required. At the other extreme, approaching a zero percent perforation area (this approaches the performance of a closed-breech weapon), the charge requirement drops off sharply (increased efficiency) and the recoil increases greatly. It is to be understood that a balance between recoil and ballistic efficiency has to be chosen, with the understanding, for purpose of discussion, that an increase in charge simply indicates a decrease in efficiency.

11-17.3 EFFECT OF PERFORATION HOLE DIAMETER

Fig. 11-12 shows another set of data. In this case, both the charge and perforation hole diameter were varied while maintaining the 1150 fps muzzle velocity. In addition, the total perforation area was held constant at 50 percent. Thus, the hole spacing was increased as the hole diameter was increased, so that percentage of area effects will not be interpreted as hole-diameter effects.

The general trend of the curves in Fig. 11-12 is similar to that of the Fig. 11-11 curves with the same principles applying, except that the limitations on the extremes of hole size are more severe than those which apply to percentage perforation area. If the hole diameter approaches or exceeds the propellant grain length, the loss of unburnt propellant will be excessive. If, on the other hand, the hole diameter is reduced very

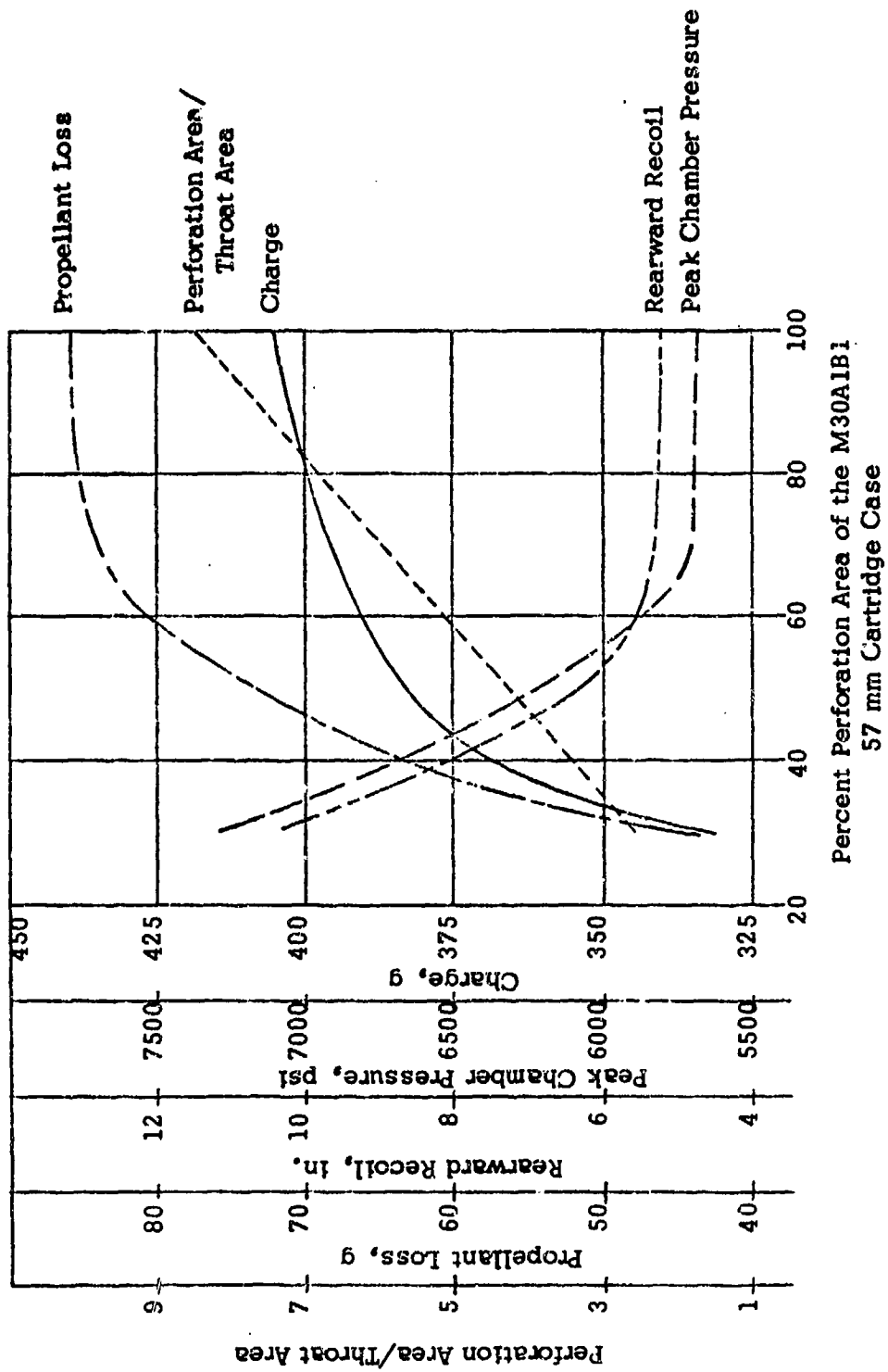


Figure 11-11. Various Ballistic Parameters as a Function of Percent Perforation of Cartridge Case, M30A1B1

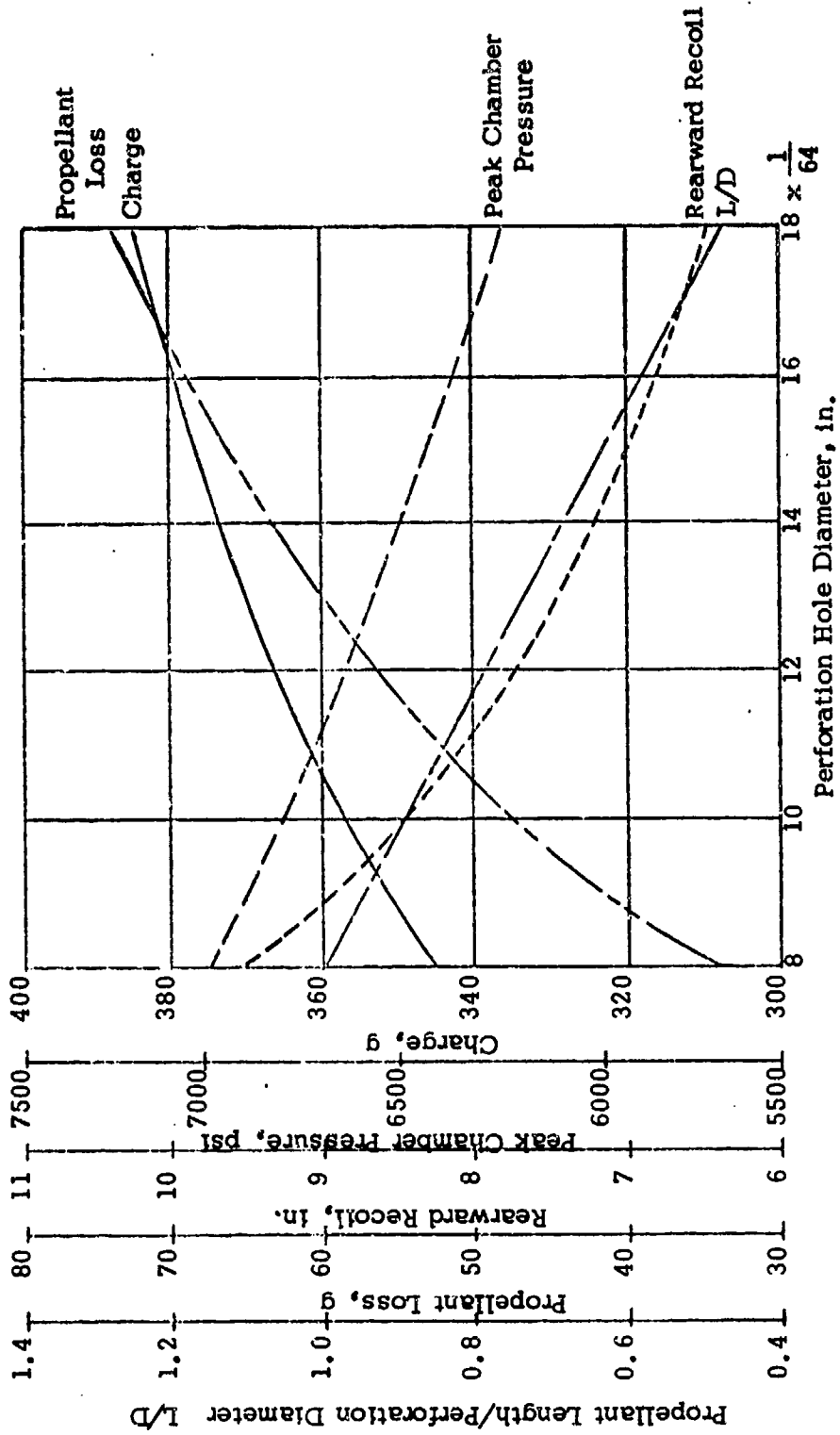


Figure 11-12. Various Ballistic Parameters as a Function of Cartridge Case Hole Diameter

greatly, the wet thickness between holes must, correspondingly, be made very small in order to maintain a constant 50 percent perforation area.

The foregoing information is presented for the purpose of indicating the trends of the experimental results which may be expected. Likewise, the results that follow indicate the trend of effects which were found by varying the arrangement of the perforations (which were assumed to be arranged in a uniform pattern).

The effects of perforation disposition were determined by comparing three types of distribution:

1. Type I. holes evenly distributed over the normally perforated section
2. Type II. holes concentrated in the breech half of the normally perforated section
3. Type III. holes concentrated in the muzzle half of the normally perforated section.

All three cases were perforated with 200 holes of 9/32 in. diameter (50 percent of the perforation area of the M30A1B1 Cartridge Case). The hole pattern for Types II and III is identical to that of the M30A1B1 Cartridge Case, except that the muzzle and the breech sections of these respective cases are not perforated.

Table 11-2(A) contains the experimental data for the three cartridge case types. The unperforated section of the Type III cases ruptured when fired; the perforated portion, on the other hand, remained intact, and showed no apparent deformation.

Judging from the amount of recoil unbalance and the pressures obtained for the various cases, there are indications that the flow of recoil-compensating gases is somewhat concentrated to the rear of the chamber,

rather than evenly distributed. For the Type III case, where the gases were forced to flow forward in the cartridge case, the perforation pattern resulted in high pressures, failure of the cartridge case, and high recoil unbalance. The test results show that the propellant losses are roughly inversely proportional to the average distance the propellant grains must travel to be ejected, and that the major portion of the flow is concentrated at the nozzle end of the case. The primer has been assumed to have negligible effects upon these tests of hole disposition, since the same type was used for all tests. However, the idea cannot be discarded entirely that, if other ignition configurations had been tried, slightly different results might have been obtained.

The actual data from Table 11-2(A) were adjusted, for ballistic variations, to a condition of equal muzzle velocity and recoil unbalance as indicated in Table 11-2(B). In adjusting both of these factors, the effective throat area was changed. These adjusted data show no large difference in the initial charge with increasing pressures when comparing case Type I to III. In making these adjustments to the data, it was assumed that the fraction of charge expelled did not change with charge or pressure level. The adjustment relations used are

$$\left. \begin{aligned} \Delta V_m / V_m &= -0.75 \Delta T_e / T_e \\ \Delta V_m / V_m &= \Delta C_2 / C_2 \\ \Delta P_p / P_p &= 1.5 \Delta T_e / T_e \\ \Delta P_p / P_p &= (\Delta C_2 / C_2) [2 + (\Delta C_2 / C_2)] \end{aligned} \right\} (11-1)$$

where

- V_m = muzzle velocity, fps
- T_e = effective nozzle thrust, lb
- C_2 = charge burnt, lb
- P_p = peak pressure, psi

TABLE 11-2

CARTRIDGE CASE DATA FOR M30A1B1

(A) Evaluation of Perforation Disposition in the M30A1B1 Case

Case Type	Charge, g	Peak Pressure, psi	Rearward Recoil, in.	Velocity, fps	Propellant Loss,	
					g	percent
I	385	6180	6.3	1150	74	19.2
II	370	7370	9.8	1146	81	21.9
III*	300	9400	35	1245	37	12.3

*Case Ruptured
 Propellant Lot PA-30191
 All cases 200 9/32-in. holes (50 percent of normal area)

(B) Evaluation of Data Adjusted to Condition of Equal Unbalance and Muzzle Velocity

Case Type	Charge, g	Peak Pressure, psi	Rearward Recoil, in.	Velocity, fps	Propellant Loss,	
					g	percent
I	385	6180	6.3	1150	74	19.2
II	380	7415	6.3	1150	83	21.9
III	390	8675	6.3	1150	48	12.3

The information obtained for the 57 mm rifle cartridge case probably may be extrapolated to other rifles within reasonable limits. However, there are other factors, such as the chamber configuration, which also have to be considered in the design and modification of a case when a particular weapon is in question. The ratio of cartridge case perforation area to nozzle throat area, for most of the cartridge-case-rifle combinations, ranges from 8 to 12. It may not be possible to reduce this ratio by 50 percent, but a 30 percent reduction of perforation area probably can be made—with no appreciable change in recoil unbalance or excessive chamber pressures—and this would permit a slight reduction in the total charge.

11-17.4 PRESSURE DIFFERENTIAL ACROSS CARTRIDGE CASE

The cartridge case must be removed from

the breech following firing. Thus, the maximum allowable deformation of the cartridge case, during the firing cycle, is determined by the very practical requirement of removing the spent case through the rifle centering ring. This deformation, in turn, depends on the differential pressure which develops across the webs of the perforated case and the strength of the case structure. The differential pressure ΔP is simply

$$\Delta P = P_i - P_o \quad (11-2)$$

where

P_o = pressure acting on outside of cartridge case (this may differ from the chamber pressure ordinarily measured at the chamber wall), psi

P_i = pressure acting on inside of cartridge case wall, psi

This is illustrated in Fig. 11-13.

Here again, as in determination of the ballistic performance of the cartridge case, it has been found necessary to use experimental data in order to arrive at definitive results. Particularly, in the case of differential pressure determination, the experimental programs had limited results due to the difficulty of instrumenting the cartridge case wall.

Experimental results were obtained for the 57 mm Recoilless Rifle, M18, with the M30 Cartridge Case. A typical pressure characteristic is shown in Fig. 11-14. This particular trace was obtained at the middle position of the case, although similar results are reported at both ends of the cartridge case.

Note that two peaks occur in the differential pressure ΔP trace. The first peak, at about 2 msec before there is any appreciable chamber (wall) pressure P_c , is probably associated with primer pressure. This peak, between 400 and 800 psi, falls off until full ignition, at which time (4-5 msec), the differential pressure rises to a maximum just prior to the maximum chamber (wall) pressure. Both pressures, P_c and ΔP , fall off rapidly thereafter, ΔP having attained a maximum value on the order of 1250 to 1500 psi and P_c a maximum of almost 7000 psi.

In view of the highly empirical nature of the results presented in this paragraph, it should be emphasized that they are presented in order to provide design guidance. At present, no more adequate model of these phenomena is available. Therefore, the cartridge case designer must initiate an experimental-analytical program geared to his specific needs.

11-17.5 STRESS ANALYSIS

The stress analysis of the perforated cartridge case is similar to that used for many other configurations, including the recoilless

rifle itself. By this, it is meant that the "full" solution may be built up, starting with the most basic "membrane solution" and adding to it the other applicable perturbations—i.e., bending effects, dynamic effects, plastic flow, etc.

In addition to this process of building a solution from the basic parts, one additional important factor must be accounted for, namely, the fact that the cartridge case is perforated. A simple, direct method that accounts for the perforations is discussed later. This is followed by a limited discussion of some analytical investigations that have been performed while developing the "full" perforated cartridge case stress analysis. These methods are

1. "Equivalent" Pressure and Elastic Constants for the Perforated Cartridge Case. In an array of closely spaced perforations, alternate rows or columns of holes generally are offset from each other so that each hole may be imagined to be in the center of a hexagonal area as shown in Fig. 11-15. Thus, the effective pressure P_e acting over the hexagonal area is really only the part of the differential pressure ΔP which acts on the ligaments (the parts of the case left intact after it is perforated).

Thus, in a method of equivalent elastic constants, the ligament material is considered as if it were "spread-out" over the case periphery; as if the "equivalent" case were unperforated. Then the equivalent P_e is adjusted to be

$$P_e = [1 - (2\pi r_p^2)/(ah)]\Delta P, \text{ psi} \quad (11-3)$$

where

ΔP = differential pressure acting on perforated cartridge cases, psi

r_p = perforation radius, in.

a, h = distances shown in Fig. 11-15, in.

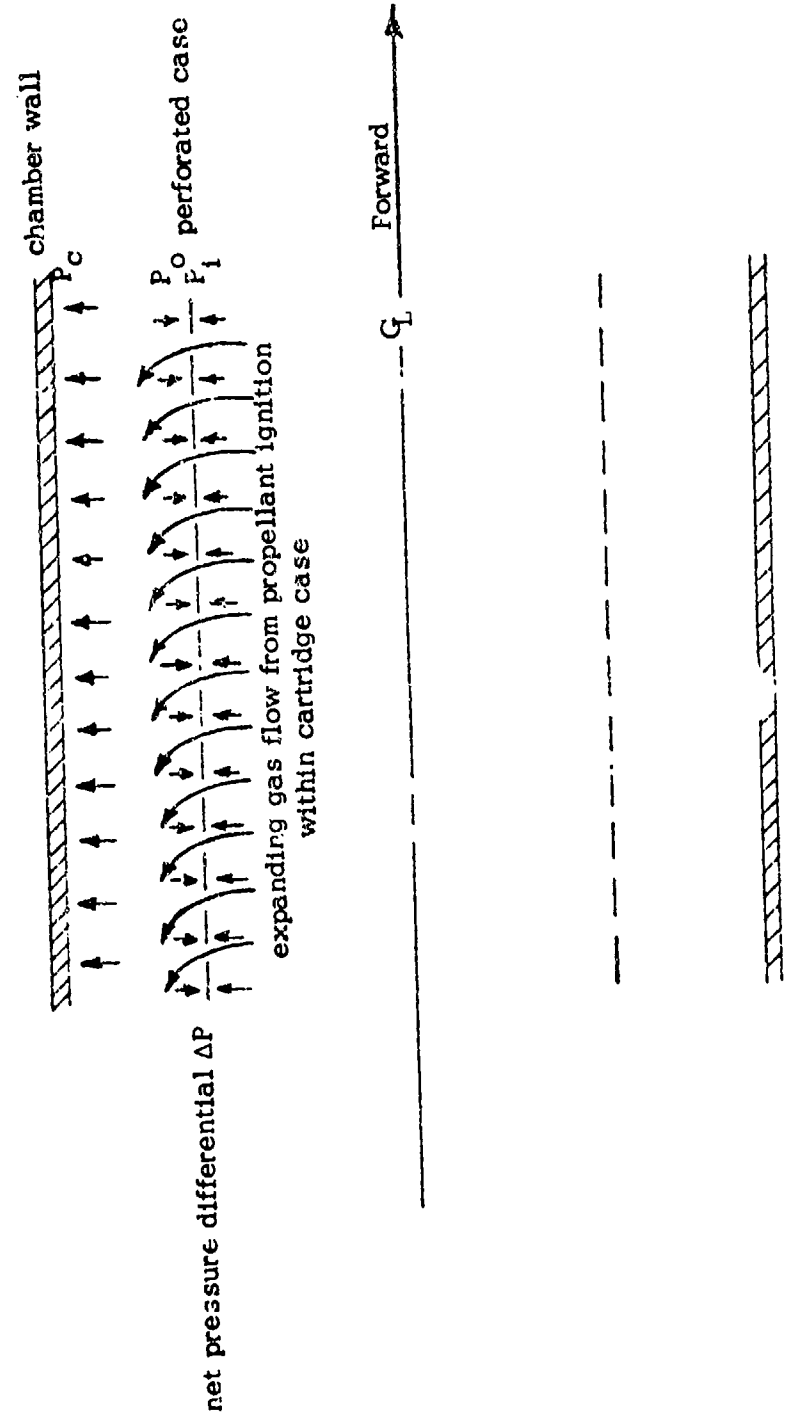


Figure 11-13. Gas Flow Through Cartridge Case

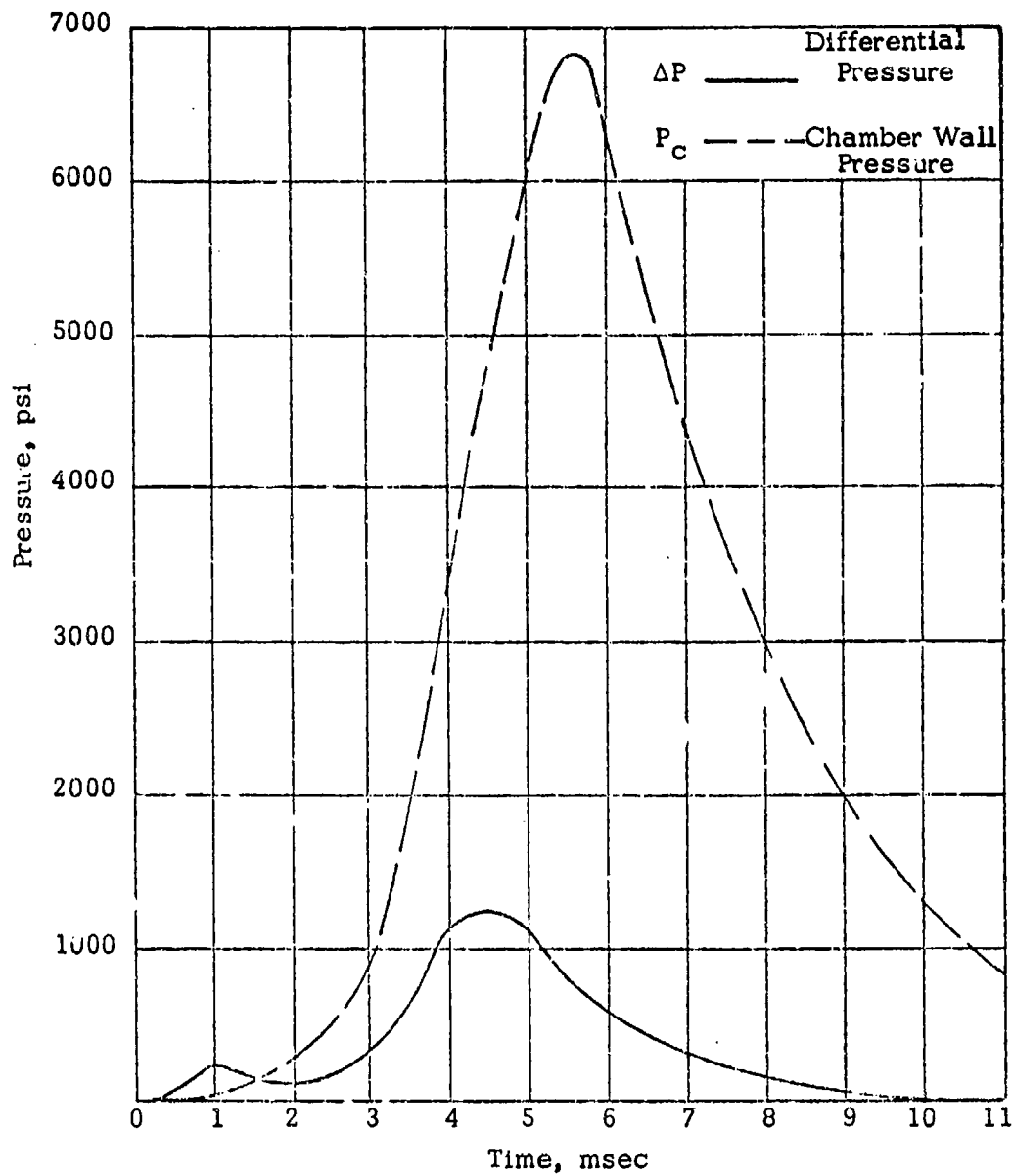


Figure 11-14. Pressure Differential Across 57 mm Cartridge Case, M30

The elastic constants of the resulting "equivalent" thin case are adjusted to obtain "equivalent" elastic constants. Material useful in this area may be found in Refs. 1, 2, 3, and 4.

In addition to the use of equivalent elastic

constants, a stress concentration factor is used sometimes to account for the variation in stress across the ligament. This variation is approximately parabolic with minimum stress occurring at the center and maximum stresses at the edges. To account for stress concentration, the nominal or average stress σ_{avg} is modified by the factor

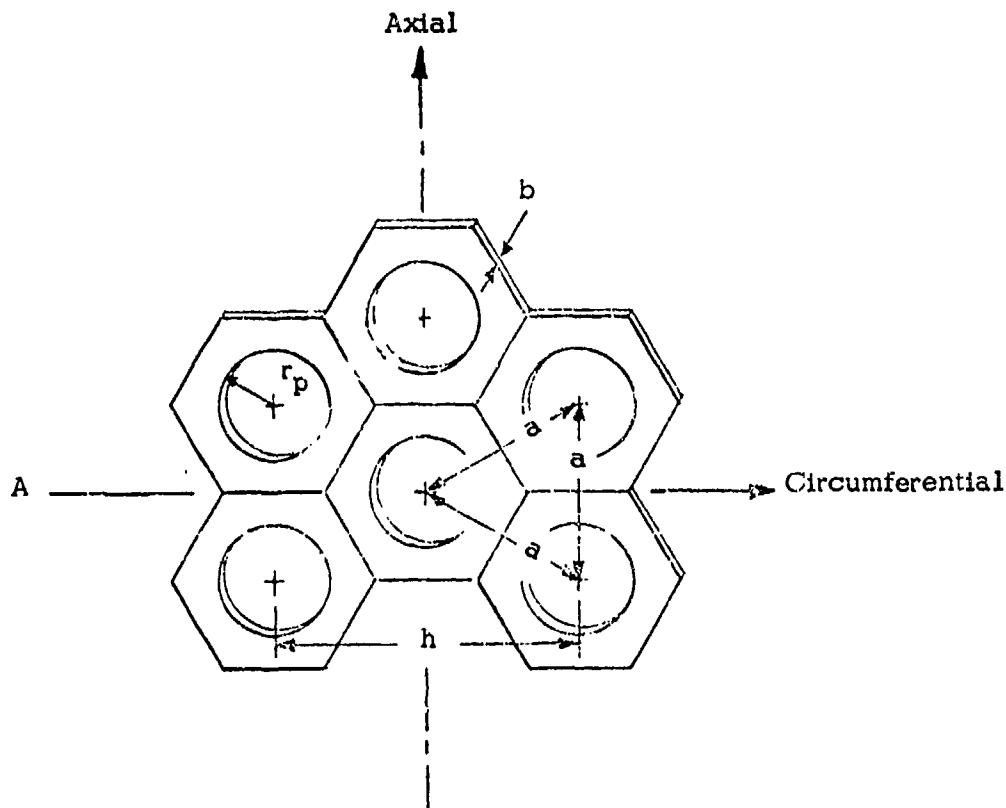


Figure 11-15. Perforation Array (Perforations in Cylindrical Cartridge Case of Radius r)

$$1 + 2[1 - (2r_p/a)]^{3/2}$$

to obtain the maximum stress σ_{max} .

$$\sigma_{max} = \sigma_{avg} \{1 + 2[1 - (2r_p/a)]^{3/2}\}, \text{ psi} \quad (11-4)$$

2. Membrane Solution (Hoop Stress). Assuming the perforated cartridge case shell to be represented by an equivalent unperforated shell, the hoop stress σ_{hoop} is given by

$$\sigma_{hoop} = P_e r / b_e, \text{ psi} \quad (11-5)$$

where

r = cartridge case radius, in.

b_e = equivalent unperforated cartridge case wall thickness, in.

$$b_e = b[1 - (2r_p/a)] \quad (11-6)$$

Eqs. 11-6 and 11-3 can be combined with Eq. 11-5 to relate the nominal or average hoop stress σ_{hoop} directly to the differential pressure ΔP .

$$\sigma_{hoop} = [\Delta P(r/b)] [a/c(a - 2r_p)] \times [1 - (2\pi r_p^2)/(ah)] \quad (11-7)$$

By use of the general expression in Eq. 11-4, the maximum hoop stress $(\sigma_{hoop})_{max}$ is given

$$\begin{aligned}
 (\sigma_{hoop})_{max} &= [\Delta P(r/h)] [a/(a - 2r_p)] \\
 &\times [1 - (2\pi r_p^2)/(ah)] \quad (11-8) \\
 &\times \{1 + 2[1 - (2r_p/a)]^{3/2}\}, \text{ psi}
 \end{aligned}$$

3. Fixed End Condition. In accounting for cartridge case restraint at either end of the cartridge case cylinder, it is frequently useful to make a further assumption, based on the apparent mechanisms involved in restraining cartridge case deformation. This assumption will frequently take the form of a "fixed" end condition, i.e., zero deformation and zero rotation at the end. This assumption is, in many cases, justified due to the relatively massive nature of the restraining portions of the rifle and of the cartridge case itself, compared with the perforated portion. In addition, the assumption is "conservative" resulting in an upper bound on longitudinal bending stresses.

If a more complex idealization of the end restraint is found justified by a particular design, it will be necessary to perform an interaction analysis between the perforated cylinder and the geometries idealized at the end in question. The number of possible combinations of configurations that may interact are endless. The reader is referred to the NASA Report TR-R-103 by Johns and Orange, *Theoretical Elastic Stress Distributions Arising from Discontinuities and Edge Loads in Several Shell-Type Structures* (Ref. 15).

For the case of fixed end restraint as shown in Fig. 11-16, however, it has been shown in Ref. 1 that the maximum end moment M_o acting on the perforated portion of the shell is given by Eq. 11-9.

$$M_o = \frac{\sqrt{3(1 - \nu_p^2)} P_e r b}{6(1 - \nu_b)(1 - \nu_p^2)}, \text{ (in. -lb) - in.}^{-1} \quad (11-9)$$

and the end shear Q_o is given by

$$Q_o = 2\beta M_o, \text{ lb-in.}^{-1} \quad (11-10)$$

where

$$\beta = [3(1 - \nu_b^2)/(r_p^2 b^2)]^{1/4}$$

where P_e is found from Eq. 11-3. ν^* is the effective Poisson ratio of a perforated plate and is discussed fully in Ref. 1. The exact definition of ν_b also is given in this reference.

4. General Perforated Cartridge Case Analysis: The preceding discussions use analyses that have been performed up to this time, in connection with stresses in perforated cartridge cases. These investigations largely have been restricted to "membrane" and "fixed-end" analysis of elastic members. It is to be emphasized that other avenues of approach exist and should be pursued in the course of cartridge case design. These additional approaches include

1. Plastic analysis. To determine extent of deformation of the pressure loaded cartridge case, in connection with removal of spent case

2. Discontinuity analysis. To obtain accurate bending stress estimates near the ends of cartridge case

3. Dynamic analysis. To account for the time dependency of cartridge case reaction to extremely short duration loading.

11-17.6 LINERS FOR THE PERFORATED CARTRIDGE CASE

In selecting a material to serve as a liner (or seal) for the recoilless rifle cartridge case, the following criteria must be considered:

1. It must leave minimum unburned residue in the gun chamber and barrel after firing, which could interfere with chambering

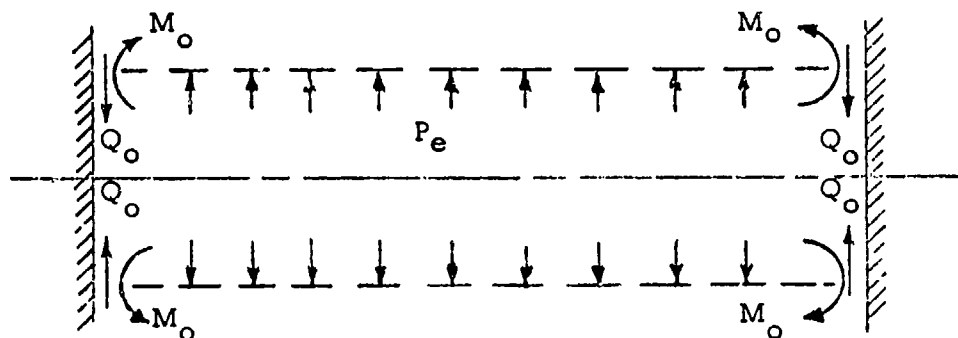


Figure 11-16. Perforated Case Force Diagram—Fixed End Conditions

of succeeding rounds or induce their premature ignition.

2. It must produce no excessive smoke, acrid fumes, or corrosive products on combustion.

3. It must have good rough-handling resistance.

4. It must not adversely affect the ballistic functioning of the ammunition.

5. It must resist ultraviolet radiation, weathering and temperature shock, and in general, show good long-term storage stability.

6. It must serve as an effective water vapor barrier.

7. It must not allow an electrical spark to be generated due to friction of propellant in motion.

Further consideration must be given to the type of propellant, i.e., single- or double-base, to be contained by the liner. The liner material must resist the tendency of nitroglycerin to migrate from double-base propellants into the liner, resulting in a nitroglycerin-starved propellant and an overly plasticized liner.

In the case of an adhesively fastened liner, the adhesive bonds and joints must resist rough handling, temperature shock, weathering, and long-term storage, and be unaffected when in contact with double-base propellant.

11-17.7 MATERIALS FOR LINERS

Two types of adhesively fastened liner material have been developed, namely,

1. Polyethylene Terephthalate (PETP)*. PETP shows good resistance to nitroglycerin migration and is therefore suitable for use with double-base as well as single-base propellants. Suitable thickness range—from the standpoint of rough-handling resistance, residue problem, and ballistic performance—is 0.003 to 0.006 in. Cartridge cases must be free of sharp burrs to prevent puncturing of the PETP film; and, to prevent electrical charge build-up, all metal parts of the complete round should be electrically connected by removing the anodizing from the threaded connections. The PETP cartridge case liner is an adhesively fastened internal liner of PETP film.

2. Cellulose Nitrate (CN). This material has poor resistance to nitroglycerin migration, and cannot be used untreated as a liner for cartridge cases containing double-base propellant, although, in principle, a thin coating of ethyl cellulose applied to the CN seal could serve as a barrier to nitroglycerin migration.

*Mylar (Type A), E. I. DuPont, DeNemours & Co.

The adhesively applied liners find their greatest application in rounds containing fixed- and folding-fin stabilized projectiles. In rounds containing spin-stabilized projectiles, the propellant is contained in a polyethylene/rayon laminated bag that is positioned around the cartridge primer.

The RS type cellulose nitrate is considered the most suitable of the commercially available lacquer types. It has the highest percentage of nitrogen, 11.8 to 12.2, as against 11.2 to 11.7 for AS type and 10.7 to 11.2 for SS type cellulose nitrate. It has higher burning rates, lower water vapor permeability, higher tensile strength, and better physical and chemical stability than the latter types. While high-viscosity CN is suitable for the production of extruded tubing, the 5- to 6-sec CN is the preferred viscosity range for dip solutions. A viscosity higher than 5-6 sec gives solutions too viscous at solid content high enough for dip application of the liner. The CN must be plasticized (e.g., with approximately 10 percent by weight of dioctyl phthalate) to make the film more pliable and distensible. In addition, plasticization of CN film serves to reduce moisture absorption and permeability of the film, and improve resistance to aging or embrittlement. An organic stabilizer, 1.0-1.5 percent by weight (e.g., diethyl-diphenylurea*) must be added to CN to improve its heat stability. Due to the extreme sensitivity of CN to ultraviolet radiation, approximately 5 percent of lampblack must be incorporated to obtain effective light stabilization.

11-17.8 APPLICATION OF LINERS

The factors that follow must be considered in the application of PETP and CN liners to recoilless rifle cartridge cases. The dip-applied CN seal is unsatisfactory because of the tendency to develop cracks around the periphery of the cartridge case perforations during long term storage. A dip-coated, shrink-fitted extruded liner of CN withstands

*Certain substituted phenols (e.g., p-methoxyphenol) are known to be more effective heat stabilizers (Ref. 10).

prolonged storage satisfactorily and is resistant to thermal shock. Dip-coating the extruded CN liner would appear to reduce the possibility of damaging the seal when chambering the round, but this has not been proven conclusively.

A completely internal liner (flat sheet cemented to the inner wall of the case) is not subject to damage by the fin portion of the fin-stabilized rounds. The cartridge case thus would act as a protective barrier for CN, and the possibility of cook-off due to contact of the liner with hot parts of the gun would be considerably less than in the case of an external CN covering. Development of an internal liner of CN was superseded by the development of the PETP liner (Ref. 6).

Another advantage offered by an adhesively sealed internal liner is a simplified and more rapid production method (Ref. 7) which eliminates the solvent hazard associated with a dip operation. The internal liner also is more economical. The time required for the application of the dipped liner is excessive due to the need for allowing drying periods of 16 hr. In addition, precautions must be taken to control atmospheric conditions and to remove dangerous solvent vapors, thus adding appreciably to the cost and limiting the ability of certain Army facilities to apply this type of liner.

Normal procedure in the case of the PETP liner is for an adhesive to be applied to the edges of the liner sheet that is pre-cut to size. The liner is cut from a roll of PETP film that previously has been shrunk approximately three percent by heating in an oven at 225°F. This eliminates shrinkage occurring when heat is applied later and prevents undue stresses from developing in the adhesive bond, which would tend to pull the liner away from the case wall. After positioning the liner in the cartridge case, a rubber covered expandable mandrel is inserted and inflated with air to 15 psi. The whole assembly is placed in an oven at 225°F for 15 min to soften the adhesive and permit it to flow. The case is then

removed from the oven and allowed to cool, after which the expander is deflated and removed.

An external PETP sleeve for recoilless rifle cartridge cases, applied by using the "shrink" characteristics of PETP at elevated temperature, is not satisfactory (Ref. 8). PETP is not combustible in the sense that cellulose nitrate is combustible, and having the metal case between it and the propellant results in the sleeves blowing off without burning, leaving undesirable residue in the weapon after firing.

It should be noted that the CN liner was developed to replace the polyethylene bag (Ref. 9) which had low resistance to rough handling and abrasion (Ref. 5).

11-18 THE FRANGIBLE CARTRIDGE CASE

11-18.1 GENERAL

The use of a frangible type cartridge case has many inherent advantages. Some of these advantages are

1. They weigh considerably less than the same caliber steel or aluminum case.
2. Their cost is relatively low because of the use of inexpensive tooling.
3. The simplicity of tooling and know-how permits their manufacture in practically any type of shop.
4. Their use eliminates an operation in the firing sequence, namely, case extraction, resulting in a higher rate of fire.
5. Finally, they eliminate fired cartridge case disposal problems.

Though having many advantages in its use, the frangible cartridge case has the disadvantage of causing gun fouling in certain applications. In breech-loaded recoilless rifles

where high rates of fire are trying to be achieved by the use of the frangible case, residue build-up on parts of the loading mechanisms has been sufficient to prevent chambering of the next round. Besides causing some amount of residue in any application, the frangible cartridge case has the disadvantage of influencing the interior ballistics of the gun by the manner in which the burning of the case can affect the propellant ignition and combustion.

11-18.2 REQUIREMENTS

The design of the frangible propellant envelope must meet the following minimum requirements:

1. Maintain chemical, physical, and dimensional stability over the temperature range of -65° to $+160^{\circ}$ F when tested as an independent item or as a complete round of ammunition for a period of 300 hr.
2. Possess sufficient mechanical strength to support itself and the propellant charge, and be capable of resisting rough handling.
3. Produce no corrosive, abrasive, or toxic effect or exhibit excessive muzzle smoke or flash when tested in complete rounds of ammunition.
4. Be chemically compatible with single-base and double-base nitrocellulose and nitroglycerin propellants and have resistance toward nitroglycerin migration at temperatures up to 180° F when tested as an assembled cartridge.
5. Be resistant to fungus, moisture and have low vapor transmission to propellant or other cartridge components.
6. Be chemically compatible with materials of the cartridge and packaging container.
7. Shall not ignite under the influence of electrostatic charge during handling.

8. Will completely disintegrate leaving minimum residue in chamber of the weapon upon firing.

9. Must not affect weapon functioning by causing an excessive build-up of pressures, velocities, and recoils thereby rendering the weapon unserviceable.

10. Have sufficient strength to withstand rough handling and resist tearing upon loading into weapon. It shall be inserted easily through the breech of the weapon without any damage occurring which would cause propellant grains to come into contact with the weapon breech and/or chamber.

11. Must be constructed of material with insulating qualities to permit a satisfactory rate of firing without cook-off occurring.

11-18.3 MATERIALS FOR FRANGIBLE CASE

Many materials have been tested for use in frangible cases, but most have had to be rejected. Kraft paper and cardboard emit smoldering particles, smoke profusely, and do not burn entirely. The same problems exist for polyethylene and Mylar in addition to their lack of desired or necessary rigidity. Further, these plastics in general retain the propellant during the combustion cycle for too short a period to influence the interior ballistic functions, and do not act as a heat sink (as do metal cases) to help in reducing gun temperature. Additionally, the high velocity plastic fragments at times damage the projectile fins.

The one material which appears to possess most of the desired characteristics is Fiberglas polyester. Considerable experimental work was conducted with this material for experimental 90 mm PAT and 120 mm HAW weapon systems.

The experimental 90 mm PAT is a breech-loaded central orifice weapon using a

spring-loaded iris-type nozzle. The nozzle is spring-loaded so that it enlarges as the ammunition is chambered, and returns to its firing position when the ammunition has passed through the nozzle area. When the frangible case was used in this weapon, residue accumulated between the segments of the iris nozzle rendering it inoperative. Thus, it was feasible to use the frangible case. Basically, the same problem existed in the 120 mm HAW weapon in which the fragments and residue were excessive enough to prevent chambering of the following round. Although these tests were considered encouraging, they were never carried to completion. It is believed, however, that a successful frangible type envelope could be developed for future systems.

11-18.4 THE DAVY CROCKETT CARTRIDGE CASE

A successful frangible envelope was designed and employed in the DAVY CROCKETT weapon system. This, however, should be considered a special or unique application and the requirements previously cited do not necessarily hold in this situation. It is a very simple application of a frangible envelope.

The DAVY CROCKETT weapon is little more than a launching tube with an integral nozzle. In this system, the frangible package contains the propellant, the ignition system, and a remote control firing cable. The system is muzzle-loaded and, therefore, the envelope is not subjected to any greater shock loading than those encountered in the standard rough handling tests. Because of the relatively high angle of elevation in normal use, any propellant envelope residue remaining after firing will drop from the weapon due to gravity. If any residue should remain in the tube, chambering of the next round will "wipe" it down into the chamber. Further, since the rate of fire of this weapon is contemplated to be relatively low, visual inspections may be made between each firing. This application uses phenolic resin, although

many other plastics adequately will meet the requirements.

11-19 THE UNPERFORATED CARTRIDGE CASE

If a recoilless rifle weapon system were developed which used an unperforated cartridge case (other than frangible), there would be several inherent advantages, namely,

1. Manufacture of the cartridge case would be easier.
2. The cartridge cases would be less costly.
3. Problems with liner materials would be eliminated.
4. Smaller diameter and less bulky chamber would be required.
5. Possibly lower strength, lighter weight cartridge case materials could be used.

One such system developed is the 90 mm, M67 with M112 Cartridge Case in which the propellant gases flow directly rearward to the nozzle. The M112 Cartridge Case is a relatively simple case. It is drawn from an aluminum disc and has a straight bore diameter with a slight external taper to facilitate extraction. A flange base is provided for extraction. The case has an anodized finish to provide erosion resistance to the hot propellant gases.

A phenolic laminated Kraft paper disc is employed in the base of the case to position the projectile in the cartridge case and serves to provide uniform ignition before rupturing and discharging through the nozzles of the weapon. The mouth of the case is crimped to the projectile to provide a specified bullet pull.

SECTION IV

IGNITER

11-20 INTRODUCTION

11-20.1 SCOPE

This section presents methods used in the design of ignition systems for recoilless rifles. A general discussion of propellant ignition is followed by special considerations and design parameters involved in ignition systems for recoilless rifles. Ignition system elements and their functions are discussed, and test and evaluation procedures outlined.

Emphasis is placed on conventional ignition systems as used in the majority of current recoilless rifles. Configurations that have been developed to satisfy requirements peculiar to nonconventional or special purpose weapons or ammunition are presented briefly for information purposes.

11-20.2 BACKGROUND

Basically, ignition of propellant is achieved by application of heat to the surface of the propellant grains. This application of heat normally is achieved by envelopment of the propellant grains in a stream of hot gas. When the surface temperature of the grain reaches a certain value T_i (ignition temperature) effective ignition occurs. The time interval during which the heat is applied and the rate of heat application are important factors in attaining this critical temperature. If the time is too short or the rate of application too slow, the ignition is unstable and effective burning may or may not take place. If it does take place, it does so after a widely variable time delay. The function of an ignition system is to produce hot gas with sufficient heat energy and action time to assure effective and uniform ignition of the propellant charge.

The propellant charge is an array of

propellant grains with air spaces between and inside the grains. The hot gas produced by the ignition system flows through these air spaces heating the surface of the grains to the ignition temperature. Ideally, the ignition system would be so designed as to initiate combustion simultaneously over the entire surface of the propellant charge. However, in practice, the igniter gas does not reach all surfaces at the same time and may never reach some areas at all. Also, the gas is cooled as it flows through the propellant charge and may not retain sufficient heat energy to ignite the more remote grains. In a closed breech weapon, if hot gases from the igniter do not reach all parts of the charge, the combustion of grains near the igniter produces additional hot gases which aid in the ignition of more remote parts of the charge. The rise in pressure accompanying this gas production further promotes combustion and increases the effectiveness of total charge ignition. The recoilless weapon, with its vented chamber and perforated cartridge case, does not function in the same manner. If the initial region of ignition is localized near the igniter tube, the gas pressure developed tends to eject the more remote propellant grains from the case before they have been ignited. A significant portion of the charge may even be ejected unburnt or partially burnt through the nozzle of the weapon. Either of these occurrences will degrade uniformity of ballistic performance. Thus, in a recoilless weapon system, simultaneity of ignition over as much of the charge as possible is far more critical than with closed breech systems; consequently, design of the ignition system becomes a matter of significance.

General design principles that have been formulated for recoilless rifle ignition systems are presented in the paragraphs that follow.

11-21 IGNITER CONFIGURATION

11-21.1 GENERAL

As shown in Fig. 11-17, a conventional recoilless rifle ignition system consists of three basic elements: primer, secondary igniter charge, and main igniter charge.

With few exceptions, primers used in recoilless ammunition are standard small arms percussion primers.

11-21.2 SECONDARY IGNITER CHARGE

The secondary igniter charge (usually FFFG black powder) acts as a booster charge for the primer. Due to the relatively large size of recoilless rifle ignition tubes, the primer often does not produce sufficient flame to assure efficient ignition of the main igniter charge along its entire length. In this case, the main igniter charge is initiated at one end and burning proceeds linearly along the ignition tube. Since the velocity of a flame front in black powder is approximately 1300 fps, burning of this type results in a measurable time delay between ignition of propellant grains at the rear of the charge and those at the front. This results in pressure gradients in the weapon chamber, ignition delays, and generally poor uniformity of ballistic performance. The use of a secondary igniter charge greatly reduces the possibility of this occurrence by increasing effective primer output. The combustion of the FFFG, which is more easily ignited and faster burning than any of the commonly used main igniter materials, rapidly produces a high velocity flame that efficiently ignites the main igniter charge.

11-21.3 MAIN IGNITER CHARGE

The main igniter charge that produces the hot gas for propellant ignition, consists usually of grade A1 black powder. Much work has been done with other igniter materials such as zirconium-lead dioxide or barium-potassium nitrate pellets. Although these

mixtures have a higher caloric output per unit weight than black powder and are generally less hygroscopic, they rarely are used in production systems due to high cost in comparison with the marginal improvement over black powder ignition. They do, however, provide a convenient means of obtaining effective ignition in cases in which physical dimensions or strength requirements of the projectile do not allow sufficient igniter tube volume to contain the necessary quantity of A1 black powder.

11-21.4 PRIMER ADAPTER AND IGNITION TUBE

The remainder of the ignition system consists of a primer adapter and a perforated ignition tube usually of aluminum or brass. The primer adapter contains the primer and secondary igniter charge and serves to fix the ignition tube to the cartridge case. In fin-stabilized ammunition, where the ignition tube is part of the projectile, the primer adapter may serve the added function of providing a shot start for the projectile. The ignition tube contains the main igniter charge and is perforated in such a pattern as to control the distribution of igniter gases to the propellant charge.

Studies have been conducted and some limited use made of systems incorporating a linear source of ignition. These systems consist of a length of PYROCORE* (small diameter lead tubing containing a core of PETN) centrally located and running the entire length of the main igniter charge with a primer affixed to the rear end. A cutaway view of this type of system is shown in Fig. 11-18. Since the velocity of flame propagation in PYROCORE is approximately 12,000 fps (10 times that of black powder), this system most nearly approximates the desired instantaneous ignition of the main igniter charge.

Also, since the main igniter charge requires a lesser degree of confinement to assure

*E. I. DuPont, DeNemours & Company, Inc. Tradename

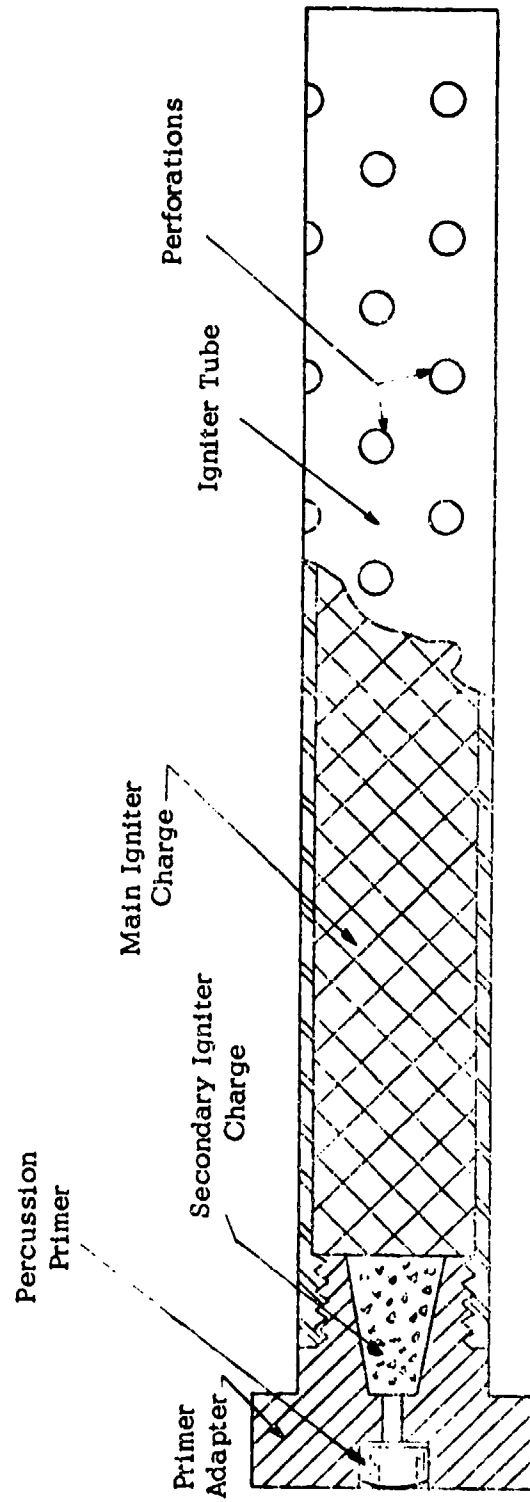


Figure 11-17. Conventional Ignition System

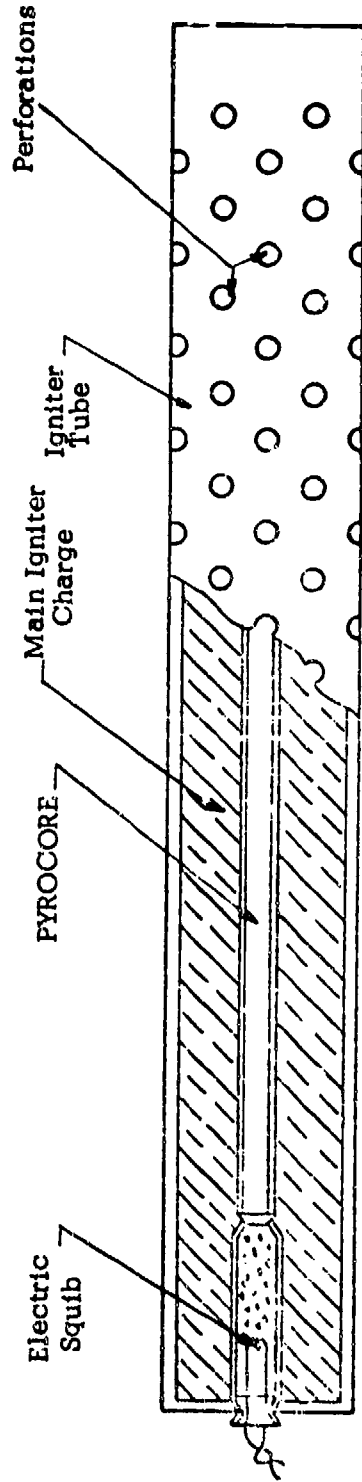


Figure 11-18. Linear (PYROCORE) Ignition System

complete combustion, the ignition tube may be designed with a greater number of perforations for better coverage of the propellant charge. However, in order to satisfactorily ignite PYROCORE, a detonation type of primer is required. Primers of this type usually are electrically or stab actuated and do not lend themselves to firing by conventional gun mechanisms. Thus, PYROCORE ignition systems normally are not used unless weapon or ammunition design is such that uniform performance cannot be easily achieved by more conventional means. For example, the DAVY CROCKETT system with its central orifice design and frangible cartridge case provides an environment in which the propellant charge had virtually no confinement. In order to support combustion under this condition, extremely rapid initiation was mandatory. Therefore, PYROCORE ignition systems were developed and standardized for this weapon system.

11-21.5 PRIMER

The two types of primers used in recoilless rifle cartridges are the small arms and artillery types. The features, advantages, and disadvantages of both types of primers are detailed in the paragraphs that follow.

11-21.5.1 Small Arms Percussion Primers

The small arms percussion primer has the feature of being one of the smallest devices available for converting mechanical energy from an appropriate source into chemical energy in the form of a deflagrating pyrotechnic reaction. The small arms primer consists of a metal primer cup into which an impact sensitive mix is loaded. After covering the mix with a paper disc, a metal anvil is pressed into the cup over the mix and paper disc. Impact by a suitably constructed hemispherical end firing pin on the primer cup will locally compress the impact sensitive mix between the indentation in the primer cup and the anvil, causing it to deflagrate.

The small size of this component makes it advantageous in serving as the link between some form of mechanical firing mechanism and the ignition of an igniter material such as black powder. Initiation of combustion by mechanical means is a key feature of the small arms primer since other initiating stimuli, such as electrical energy, frequently require more complicated initiating mechanisms and place more constraints on the weapon system. Small arms primers are also available with a variety of chemical formulations depending upon the type of brisance, corrosive effects, and temperature storage capabilities required for a specific application. While the small arms primer does not produce the large amount of high-energy gas to ignite effectively the entire propellant charge in a recoilless rifle cartridge, it is used effectively as the means for igniting a material such as black powder.

If a small arms primer is used in the initiation sequence, successful detonation of the primer must occur before any propellant ignition will take place. Although the small arms primer has attained a very high operational reliability, there have been cases in which primers have failed to function despite the application of an adequate input energy. The failures have been analyzed, and in nearly every case were found to be due to high environmental temperature, excessive exposure to high environmental temperature, and/or humidity. During installation of the small arms primer, the primer anvil is reseated farther into the primer cup in order to achieve the proper sensitivity level. Failure to reseat the primer results in the primer requiring a considerably increased firing energy for detonation. Reseating the primer anvil to a point where the priming composition separates until none is present between the cup and the top of the anvil can result in no detonation occurring regardless of the amount of firing energy applied to the primer.

11-21.5.2 Artillery-type Primers

Artillery-type primers are very similar in configuration to the igniter configuration shown in Fig. 11-17, except that no secondary igniter charge is used. The desired features or advantages of the artillery-type primer are very much like those for the igniter system of par. 11-12, in that the primer tube can be made as long as the cartridge case allows in order to radially distribute the igniter gases throughout the entire propellant charge.

The problem with using conventional artillery-type primers in recoilless rifle applications occurs in trying to ignite uniformly the propellant charge in long cartridge cases. For long artillery primers, the black powder igniter charge within the narrow primer tube tends to restrict gas flow down the length of the perforated tube. Without the presence of a secondary igniter charge to produce a higher velocity flame front, a time delay exists between the ignition of black powder closest to percussion primer and the ignition of black powder at end of primer tube. This time delay results in a corresponding uneven ignition of the propellant charge that surrounds the primer tube.

Whereas the conventional closed breech weapon can sustain a lower pressure rise during the ignition process and still have an established ignition of the propellant charge before the projectile begins to move, the recoilless rifle must have a rapid rise (3-4 msec) to peak pressure in order to sustain propellant ignition. At low pressures, the propellant gases in a recoilless rifle burn through the cartridge case liner and begin to flow through the case perforations; if ignition has not occurred throughout the propellant charge, the resultant pressure loss results in a slower low-pressure burning of the propellant which, in some cases, may generate a chamber pressure that is insufficient to expel the projectile.

11-22 BASIC DESIGN INFORMATION

In order for the most effective ignition system to be designed, pertinent characteristics of the weapon, the projectile, and the propellant charge must be defined. Most important to the designer are propellant composition, burning rate, web size, and physical dimensions of the propellant package. These factors generally are dictated by system requirements and limitations such as projectile velocity, acceleration, weapon strength, and erosion characteristics (see Chapter 5 on Interior Ballistics). Thus, the package selected on this basis may be far from optimum from a standpoint of effective ignition due to the following considerations:

1. Propellants of different compositions vary in ignition temperature and cooling effect.
2. The burning rate coefficient reflects the ability of the propellant to support combustion. Those with higher values support combustion more readily at low pressures.
3. Propellant grain size and web thickness control
 - a. Amount of free space for propagation of igniter gases
 - b. Surface area presented to the igniter gases
4. Charges having large diameter with respect to length increase ignition difficulty.

No quantitative assessment can be made of the overall effects of these factors on ignition reliability. Also, technology developed for one system cannot be applied necessarily to future developments. Thus, a complete ignition system development may be required for any specific recoilless weapon system.

11-23 DEVELOPMENT PROCEDURE

11-23.1 GENERAL

The discussion that follows is a general development procedure used successfully for recoilless weapon ignition systems. Much of the theory is qualitative in nature and serves only as a guide to relative effectiveness of ignition. Acceptance or rejection of a system must be based on the only valid measurable criteria; i.e., uniformity of ignition delay time, chamber pressure, and muzzle velocity.

It has been determined experimentally that a black powder charge of about 100 grains per pound of propellant is required for effective ignition. It is known that effective ignition becomes increasingly difficult as igniter loading density is increased, with a value of 0.03 lb/in.³ considered to be the maximum allowable. Thus, for a propellant charge of C pounds the minimum volume of igniter tube can be calculated. However, the length of the igniter is limited by the length of the projectile boom in the case of a fixed fin-stabilized round or the length of the cartridge case for a spin-stabilized round.

Also, for fin-stabilized ammunition, the igniter tube is part of the projectile in flight, and restrictions may be placed on the dimensions of the igniter tube by exterior ballistic requirements and strength requirements of the projectile. If these considerations do not permit an igniter tube of the required volume, conventional igniter design procedure cannot be followed. It then becomes necessary to investigate the feasibility of higher energy igniter materials or more sophisticated ignition systems. Alternatively, the weapon system may be re-examined and a projectile design change effected to permit increasing igniter tube volume.

11-23.2 DETERMINATION OF HOLE SIZE AND PATTERN

As mentioned previously, it is necessary

that the propellant charge be ignited simultaneously over as much of its surface as possible. Therefore, at this point, an igniter tube hole size and pattern must be determined to best achieve this condition. The equation of state for the gas inside the igniter tube is taken as

$$P[V - (C_i - N)/\rho_i] = 12(N - N')F_i, \text{ psi} \quad (11-11)$$

where

P = instantaneous space-mean internal pressure, psi

V = internal volume of igniter tube, in.³

C_i = igniter charge weight, lb

N = weight of igniter gas produced, lb

N' = weight of igniter gas discharged from igniter tube vents, lb

ρ_i = density of solid igniter material, lb-in.⁻³

F_i = impetus of igniter material, (ft-lb)-(lb)⁻¹

The weight N_t of igniter gas produced up to time t is

$$N_t = \rho_i \int_0^t (r_k)_i S_i dt, \text{ lb} \quad (11-12)$$

where

$(r_k)_i$ = burning rate (linear) of igniter material, in.-sec⁻¹

S_i = instantaneous surface area of igniter material, in.²

By use of conventional theory for isentropic flow of a perfect gas assuming sonic velocity, the weight N'_t of gas discharged from the igniter tube up to time t is represented by

$$N'_t = \int_0^t PA_p \left[\left(\frac{g\gamma_t}{F_t} \right) \left(\frac{2}{\gamma_t + 1} \right)^{(\gamma_t+1)/(\gamma_t-1)} \right]^{1/2} dt \quad (11-13)$$

where

A_p = total area of primer tube perforations, in²

γ_t = ratio of specific heats (c_p/c_v)_{*t*} for igniter gas, dimensionless

g = acceleration due to gravity, ft-sec⁻²

Simultaneous solution of Eqs. 11-11, 11-12, and 11-13 results in an expression relating internal igniter tube pressure to total perforation area for any given weight of igniter material. However, this method is extremely cumbersome and, since unknown igniter gas distribution and heat losses dictate that final ignition parameters be determined experimentally, it is unnecessarily precise. By the use of a few reasonably accurate assumptions, the perforation area can be approximated in the manner that follows.

The energy made available to the propellant by the weight flow dN'_t/dt of igniter gases from the igniter tube during the interval dt can be written $(c_p)_t T_o dN'_t$. The igniter material specific heat at constant pressure $(c_p)_t$ is used since the flow process is isenthalpic. The total energy E_A made available to the propellant during the time interval 0 to t is

$$E_A = (c_p)_t T_o \int_0^t (dN'_t/dt) dt \quad (11-14)$$

where

T_o = isochoric flame temperature of propellant gas, °K

Substituting from Eq. 11-13

$$E_A = (c_p)_t T_o \int_0^t PA_p \times \left[\frac{g\gamma_t}{F_t} \left(\frac{2}{\gamma_t + 1} \right)^{(\gamma_t+1)/(\gamma_t-1)} \right]^{1/2} dt \quad (11-15)$$

The assumption is now made that the igniter tube pressure remains constant over the relatively short ignition time t_i . Integration of Eq. 11-15 over this time results in

$$E_A = (c_p)_t T_o PA_p \left[\frac{g\gamma_t}{F_t} \left(\frac{2}{\gamma_t + 1} \right)^{(\gamma_t+1)/(\gamma_t-1)} \right]^{1/2} t_i \quad \text{ft-lb} \quad (11-16)$$

The energy required E_R to raise the surface of the propellant to its ignition temperature in time t_i is

$$E_R = [c_p \rho k t_i]^{1/2} A_s (T_i - T_a) \quad (11-17)$$

where

c_p = specific heat at constant pressure propellant, (ft-lb)-(lb-°K)⁻¹

ρ = density of propellant, lb-in.⁻³

k = thermal conductivity of propellant, (ft-lb)-(in²-sec-°K/in.)⁻¹

A_s = surface area of propellant, in²

T_i = ignition temperature of propellant, °K

T_a = ambient temperature, °K

Assume uniform distribution of igniter gases and negligible heat loss, $E_A = E_R$; therefore

$$(c_p)_t T_o PA_p \left[\frac{g\gamma_t}{F_t} \left(\frac{2}{\gamma_t + 1} \right)^{(\gamma_t+1)/(\gamma_t-1)} \right]^{1/2} t_i = (c_p \rho k t_i)^{1/2} A_s (T_i - T_a) \quad (11-18)$$

Eq. 11-18 is a general solution for ignition systems. However, in recoilless weapon systems, several of these characteristics vary slightly over the range of propellants and igniters used. Thus, the equation can be greatly simplified by insertion of average values for these characteristics. For igniter gases,

$$(c_p)_i = 620 \text{ (ft-lb)-(lb-}^\circ\text{K)}^{-1}$$

$$T_o = 2500^\circ\text{K}$$

$$\gamma_i = 1.25$$

$$F_i = 80,400 \text{ (ft-lb)-(lb)}^{-1}$$

Likewise, for a typical double-base propellant

$$c_p = 540 \text{ (ft-lb)-(lb-}^\circ\text{K)}^{-1}$$

$$T_i = 900^\circ\text{K}$$

$$T_a = 200^\circ\text{K (lowest conditioning temperature)}$$

$$\rho = 0.056 \text{ lb-in.}^{-3}$$

$$k = 7.8 \times 10^{-3} \text{ (in-sec-}^\circ\text{K)}^{-1} \text{ (ft-lb)-} \\ \text{(in.}^2\text{-sec-}^\circ\text{K/in.)}^{-1}$$

Thus, for the specific case of recoilless weapons, Eq. 11-18 reduces to

$$PA_p t_i = 0.0166 A_s \sqrt{t_i} \quad (11-19)$$

or

$$A_p = \frac{0.0166 A_s}{P \sqrt{t_i}}, \text{ in.}^2 \quad (11-20)$$

It has been determined empirically that in order to assure uniform ignition, t_i should be 2 msec or less and this value normally is used for igniter calculations. Also, internal igniter tube pressure should be held to approximately 1000 psi. This is high enough to assure uniform burning of the igniter material yet low enough to preclude any serious structural problems in igniter tube design. Substitution of these values into Eq. 11-20 results in an expression for perforation area A_p as a simple function of propellant surface area A_s .

$$A_p = 3.71 \times 10^{-4} A_s, \text{ in.}^2 \quad (11-21)$$

11-23.3 SAMPLE CALCULATIONS

The total surface area A_s of any propellant charge can be expressed in terms of physical dimensions of a single grain, charge, weight, and density.

$$A_s = \frac{4C}{\rho} \left[\frac{D + n_p w}{D^2 - n_p w^2} + \frac{1}{2L} \right], \text{ in.}^2 \quad (11-22)$$

where

C = propellant weight, lb

ρ = density of solid propellant, lb-in.⁻³

D = diameter of propellant grain, in.

w = propellant web, in.

L = length of propellant grain, in.

n_p = number of perforations in propellant grain

Perforation areas obtained using Eq. 11-21 are normally within ± 15 percent of the area actually required.

Two sample calculations are shown, and the calculated areas compared with the actual areas:

1. Example 1: 57 mm M18 Recoilless Rifle

$$C = 0.74 \text{ lb}$$

$$w = 0.021 \text{ in.}$$

$$D = 0.063 \text{ in.}$$

$$L = 0.271 \text{ in.}$$

$$n_p = 1$$

From Eq. 11-22

$$A_s = \frac{4(0.74)}{0.056} \left[\frac{0.063 + 1(0.021)}{(0.063)^2 - 1(0.021)^2} + \frac{1}{2(0.271)} \right] \\ = 1356 \text{ in.}^2$$

From Eq. 11-21

$$A_p = 3.71 \times 10^{-4}(1356) = 0.503 \text{ in}^2$$

The actual perforation area used in the M18 System is 0.60 in². Thus, the calculated area is approximately 16 percent low.

2. Example 2: 105 mm M27 Recoilless Rifle

$$C = 7.516 \text{ lb}$$

$$w = 0.038 \text{ in.}$$

$$D = 0.266 \text{ in.}$$

$$L = 0.612 \text{ in.}$$

$$n_p = 7$$

From Eq. 11-22

$$A_s = \frac{4(7.5)}{0.056} \left[\frac{(0.266) + 7(0.038)}{(0.266)^2 - 7(0.038)^2} + \frac{1}{2(0.612)} \right] \\ = 5137 \text{ in}^2$$

From Eq. 11-21

$$A_p = 3.71 \times 10^{-4}(5137) = 1.906 \text{ in}^2$$

The actual perforation used in the M27 System is 1.80 in². The calculated value is approximately 6 percent high.

11-23.4 SELECTION OF HOLE PATTERN

Once the total perforation area has been determined, the number and pattern of perforations must be selected. Ideally, a tube containing a large number of very small perforations would provide the most uniform coverage of the propellant charge. However, this results in thin, low-energy flame jets that cool rapidly and do not satisfactorily permeate the propellant charge. Experimental investigations have shown that perforations less than 7/32 in. in diameter are impractical for recoilless ignition systems.

The effect of increasing the diameter of the holes while maintaining a constant perforation area is to reduce the maximum propellant pressure in all firing temperature ranges. Increasing the hole diameter reduces the velocity and temperature of the igniter gases, resulting in nonuniform combustion of the propellant charge and a lower maximum pressure. Further increases in the hole diameter eventually result in such a low maximum pressure that "poop" shots begin to occur during low temperature firings. It has been established that, for most cases, perforations should have a diameter less than 3/8 in.

Once the hole size has been established, the number of perforations is calculated by dividing the total perforation area by the area of a single hole. To obtain uniform distributions of the igniter gases around the diameter of the charge, perforations are arranged in six rows 60 deg apart around the igniter tube diameter with each row containing an equal number of equally spaced holes.

Returning to Example 2 of par. 11-23.3 for the 105 mm system, the calculated total perforation area is 1.906 in². Therefore, if a hole diameter of 7/32 in. is assumed (area = 0.038 in²), the number of perforations in the igniter tube $N_p = 1.906/0.038 = 50.2 \approx 50$. Thus, for this example, an initial design of six rows of eight or nine 7/32-in. diameter holes is indicated. The design as finalized contained six rows of eight 7/32-in. diameter perforations.

11-23.5 PRELIMINARY BALLISTIC TESTING

For preliminary ballistic testing, igniter tubes of the previously selected geometry are sectioned and provided with a transparent window for observation of primer function. The tubes are loaded with the estimated charge of inert, simulated black powder (100 grains per pound of propellant) and a live

primer and secondary igniter (1 grain per 100 grains of black powder). Internal thermocouples are placed at several points along the length of the tube for measurement of flame temperature as a function of time. The primers are then fired and high-speed motion pictures taken. Analysis of these films in conjunction with the temperature records permits selection of the primer-secondary igniter combination that most efficiently envelopes the main igniter charge in flame. This study also serves as a basis for refinement of primer adapter design.

When a primer-secondary igniter combination has been chosen, igniter tubes are then loaded with the estimated charge of A1 black powder. These tubes are loaded into sectioned cartridge cases containing inert propellant grains of the proper size and configuration. The igniter tubes are fired, and high-speed motion pictures again are taken and analyzed. The analysis considers the following characteristics:

1. Time from primer initiation to first appearance of flame jets, and variance in time of appearance of flame jets along the length of igniter tube
2. Length of propagation of flame jets through propellant, and variance in this length
3. Variance in time of propagation of flame jets to most remote propellant grains
4. Lateral flame coverage of propellant grains located between igniter tube flash holes
5. Duration of flame jets.

By use of these characteristics, modifications in igniter charge and igniter tube design are studied to optimize flame coverage of the propellant charge.

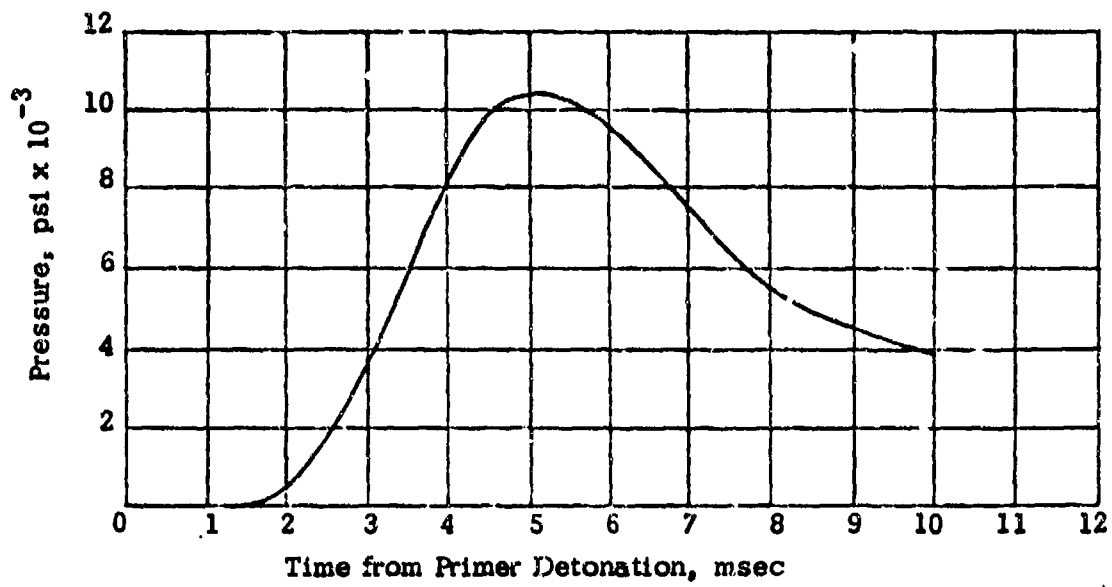
Once a preliminary propellant-ignition package has been selected, several complete rounds are loaded and fired. Firings are

conducted in a test weapon instrumented for measurement of chamber pressure as a function of time. These pressure-time records are as vital a factor in ignition system development as in prototype weapon design. Fig. 11-19 shows pressure-time records from two identical rounds fired during early phases of one development program. The curve of Fig. 11-19(A) is typical of normal ignition in a recoilless rifle. Fig. 11-19(B) represents a round in which adequate ignition was not achieved. Notice that the time to reach maximum pressure in Fig. 11-19(A) is much shorter than in Fig. 11-19(B). In addition, the unevenness of this portion of the curve in Fig. 11-19(B) indicates localized pressures which, as mentioned previously, are not conducive to good ignition. Some ignition delay is to be expected due to primer delay and time required for flame propagation. Within reasonable limits ($t_i \leq 2$ msec), the absolute magnitude of delay time is relatively unimportant. Most significant is consistency in both delay time and in the shape of that portion of the pressure curve within this time. The inconsistency of these parameters in the example given required redesign of the ignition system.

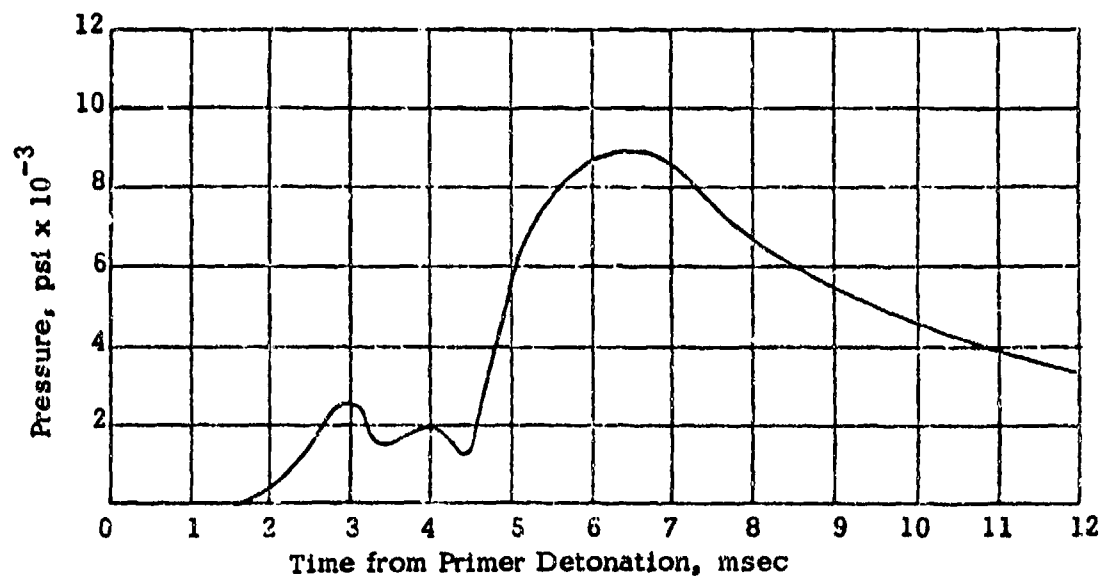
After the initial firings are completed, the pressure records are analyzed in conjunction with records of projectile velocity. The velocity data are also important since nonuniform round-to-round velocity indicates incomplete or erratic burning of the propellant charge which most likely stems from inadequate and/or nonuniform ignition. Further refinements of the propellant-ignition package, if required, are made at this point.

11-23.6 FINAL ENGINEERING TESTING

After preliminary tests have been completed and a prototype propellant-ignition system selected, full scale uniformity firings are initiated. Large samples of ammunition are conditioned at several temperatures ranging from -65° to $+160^{\circ}$ F and fired from



(A) P-T Record, Normal Ignition



(B) P-T Record, Poor Ignition

Figure 11-19. P-T Curves for Good and Poor Ignition

a completely instrumented weapon. Measurements of velocity, chamber pressure, and weapon recoil are subjected to extensive statistical analysis to assure reliability of future performance. Also, these firings are monitored for general function, misfires,

hangfires, or other indication of ignition system inconsistency. If any difficulties are encountered in these firings, they are resolved by reversion to the preliminary ballistic test procedure for further refinement of system characteristics.

SECTION V

THE FUZE

11-24 GENERAL

A fuze is a device for igniting, detonating, or releasing the charge of a warhead either upon impact, at a certain predetermined time, at a specific distance from the target, or under other desired circumstances. Essentially, the fuze must initiate detonation at the optimum time while assuring that detonation does not occur prematurely. Therefore, the fuze must insure the safety of the round during normal handling while taking advantage of the forces or effects available during and after launch to activate and prepare the fuze for firing.

Since the function of HEAT, HE, and HEP projectiles is the same for both recoilless rifle and closed breech weapons, the same type of fuze is used in both type of rounds.

11-25 TYPE OF FUZING

The discussion that follows is a general survey of the types of fuzing associated with various types of rounds. A detailed discussion of the principles of operation and the problems of the design and development of these fuzes is contained in Ref. 13.

1. High Explosive Antitank (HEAT). Projectiles of this type contain a shaped charge of high explosive to effect the penetration of armor by means of the "Munroe" effect. Superquick (SQ) fuze action is required with these rounds to preserve the proper standoff distance required for the shaped charge effect. The period of time from impact until

detonation of bursting charge is on the order of 100 μ sec. Nose type contact fuzing generally is employed to achieve this action. One such fuze employs an explosive element in the nose with a provision for its detonation products to be "spit back" through a tube to the base of the shaped charge. Another means that has been employed to accomplish this result is to place a piezoelectric transducer in the nose and use the voltage generated upon impact to initiate an electric detonator in the base of the shaped charge.

2. High Explosive Plastic (HEP). Projectiles of this type use a base-detonating (BD) fuze with a functioning delay to allow time for the plastic filler to flatten against the target prior to initiation.

3. High Explosive (HE), Smoke, and Target Practice (TP). These rounds are generally contact fuzed with a point-detonating (PD) fuze. Some HE rounds have been fuzed with settable mechanical time (MT) fuzes equipped with a point-detonating element. This combination provides for an airburst capability if desired.

11-26 SAFE-ARM SEPARATION

An important function of the fuze safing system is to ensure that the detonating pin or arm is locked in position during handling and gun firing. After firing setback, this safe-arm subsystem arms (unlocks) the firing pin when the desired safe separation distance has been achieved between the gun and projectile.

SECTION VI

PROPELLANT

11-27 INTRODUCTION

During the firing of a gun, a mass is accelerated to a desired velocity and given direction by the expansion of a gas in the chamber behind the projectile. In order to accelerate the projectile to velocities of greater than 1000 fps in the length of the gun barrel, a source of energy is required, capable of generating sufficient pressure within less than 20 msec; the time available to accelerate a projectile. Also, the energy source must be readily manufactured, easy to transport, and capable of being safely applied. Because the time cycle involved is quite small, there is not sufficient time for the completion of slow processes such as heat transfer. Solid chemical propellants meet these energy requirements while also furnishing the gaseous products to propel the projectile.

A gun can be fundamentally described as a heat engine. When the propellant charge is ignited, gases are generated by the burning of the surface of each propellant grain and a rapid pressure increase occurs in the gun chamber. As the projectile begins to move due to this pressure increase, the chamber volume increases, resulting in a decrease in the chamber pressure. However, the burning rate of the propellant surfaces is high enough so that the net effect is a rapid increase in chamber pressure until a maximum is reached when the projectile is at a relatively short distance from the start of the gun barrel rifling. As the projectile travels beyond this point, the pressure drops until at muzzle exit, the pressure is, depending upon propellant and gun design, 10 to 30 percent of the maximum pressure.

While pressure acts to drive the projectile forward, a rearward force, recoil, also acts to move the gun backward. In recoilless rifles,

these recoil forces are countered by the rearward discharge of gases through a nozzle at the breech. Conditions can thus be controlled so that there can be a balance of recoil and projectile momentums. Since about half of the generated propellant gas is discharged from the chamber, only the other half remains to increase the pressure in the gun which means that the required propellant weight for a recoilless rifle may exceed that for a comparable closed breech rifle by a factor of as much as three to one.

The purpose of propellant design for a specific gun is to select both the correct chemical formulation of propellant material and the correct granulation, i.e., specification of the individual grain configuration, which will give rise to the pressure-time history required to achieve the specified muzzle velocity while not exceeding the structural limitations of the weapon. Whereas these limitations constitute one set of design problems, consideration also must be given to cartridge case volume, nozzle erosion, reduction of flash and smoke, and ballistic uniformity. It may not be possible to satisfy all of these considerations; therefore, a certain amount of compromise is necessary.

Cartridge case volume may place limitations on the amount of propellant charge that can be used so that a propellant with a higher level of available energy per unit weight or a propellant configuration with a higher loading density may have to be used. The rate of burning of the propellant must be controlled so that the rate of gas evolution does not develop peak pressures exceeding structural limitations on the rifle. Burnt propellant should leave little or no residue that could corrode the rifle bore, create smoke, or reduce weapon efficiency.

It is also desirable to use a cooler burning propellant in order to decrease nozzle erosion and produce combustion gases that are as cool as possible at the muzzle in order to reduce flash and thus prevent exposure of the gun position by night. By the same token, it is desirable that the combustion be smokeless to prevent obscuration of the target and revealing of the gun position by day.

To ensure ballistic uniformity, the propellant grain should be capable of complete and uniform ignition, and be uniform in size and shape. Also, the propellant should be capable of being stored for periods of time up to the rated useful life without decomposition or deterioration which would result in nonuniform or erratic ballistic behavior.

11-28 HISTORY

In the early stages of recoilless weapon development, double-base propellants (M2 and M5), both single- and multiperforated grains, were used depending on the system caliber and bore length. As the weapon development progressed, however, double-base propellants were found to be excessively erosive in the nozzle areas for weapons intended to be used for repeated fire. This condition seriously curtailed weapon life. Improved ignition systems and a change to a single-base propellant (M10) increased weapon life threefold.

Subsequent to adoption of M10 Propellant, a program was initiated to develop an improved propellant with respect to chemical stability, pressure-temperature relationship, and loading density for the 106 mm Recoilless Rifle, M40A1. Three propellants were developed for study to satisfy this requirement—T18, T25, and T28. Results of this study were:

1. T18 Propellant was not acceptable as a substitute because of loading density problems.

2. Both T25 and T28 Propellants possessed excellent storage life.

3. Use of either T25 or T28 Propellants resulted in 50 percent lower velocities and pressures, depending upon temperature, than the M10 Propellant when tested in the 106 mm Recoilless Rifle.

4. The T28 Propellant met the requirements of the 106 mm ammunition while generating a 1,600 psi lower peak pressure level when using the same charge amount as used with the M10 Propellant. The T28 Propellant was given the M26 nomenclature and recommended for standardization for other recoilless rifles and guns as applicable (see Ref. 2).

Although T28 Propellant is recommended for use in recoilless rifles, highly specialized systems, such as the DAVY CROCKETT, have used double-base propellants despite their highly erosive characteristics. These propellants were employed because of their superior ignitability and because higher impetus propellants were required to meet system requirements. Also, the concept of employment of nuclear systems did not anticipate large numbers of rounds being fired.

11-29 BASIC CHARACTERISTICS

11-29.1 PROPELLANT COMPOSITIONS

On a composition basis, propellants are divided into the following three groups:

1. Single-base Propellants. Nitrocellulose is the principal active ingredient of a single-base propellant. It may contain a stabilizer (usually possessing plasticizing properties) or any other material in a low state of oxidation. Inhibiting or accelerating materials such as metals or metallic salts also may be included. M10 Propellant is an example of a single-base propellant.

2. Double-base Propellants. "Double-base" generally defines propellant compositions containing nitrocellulose and nitroglycerin. A better definition of a double-base propellant is one containing nitrocellulose and a liquid organic nitrate that gelatinizes the nitrocellulose. It also may contain additives similar to the single-base compositions. Nitroglycerin propellants have not been used extensively in the United States as standard propellants because their high combustion temperature makes them quite corrosive, reducing the service life of the gun. Furthermore, they may possibly be in short supply in an emergency. M2 Propellant is an example of double-base propellant.

3 Triple-base Propellants. These propellants have three basic active ingredients—nitrocellulose, nitroglycerin, and nitroguanidine—in addition to such other additives as may be necessary. M15 Propellant is an example of a triple-base propellant.

11-29.2 IMPETUS

Impetus is a measure of the energy available in a propellant composition expressed in foot-pounds of energy per pound of propellant. The impetus is proportional to the number of moles of gas released per pound of propellant and to the flame temperature of the gas. A high impetus propellant would require fewer pounds of charge to achieve a given muzzle energy than a propellant with a lower impetus.

11-29.3 FLAME TEMPERATURE

Flame temperature or more accurately isochoric flame temperature is the temperature at which the gas is evolved from the solid propellant when combustion is at constant volume. While a high impetus is desirable for efficiency, a high flame temperature is undesirable because of resulting increased erosive and muzzle flash characteristics.

11-29.4 WEB THICKNESS

The web thickness of a propellant grain is the minimum burning thickness or the minimum thickness of the grain between any two boundary surfaces.

The relationship between percentage change in web thickness and percentage change in peak pressure is a reciprocal proportion. For example, a 4 percent decrease in web thickness of the single-perforated M10 Propellant grain used in the 57 mm M18 Recoilless Rifle System results in a 10 percent increase in peak pressure. Decreasing the web thickness also causes the peak pressure to be reached in a shorter time and, therefore, at an earlier point in the projectile travel. Increasing the web thickness has the opposite effect and results in a longer rise time to peak pressure.

11-29.5 BURNING RATE

The rate at which the burning surface recedes along the normal to the propellant surface is known as the linear burning rate. It is a characteristic of the propellant and, for a given composition, depends only on the initial propellant temperature and the chamber pressure. Empirically, the linear burning rate r_b is given by Eq. 11-23.

$$r_b = a_1 + b_1 p_c^n, \text{ in. -sec}^{-1} \quad (11-23)$$

where

a_1, b_1 = constants dependent upon propellant and initial temperature

p_c = chamber pressure, psi

n = combustion index, dimensionless

For a given propellant shape, a propellant composition with a higher burning rate results in a shorter time to consume the propellant charge; therefore, peak pressure is reached in

a shorter rise time and at an earlier point in projectile travel.

11-29.5 PROPELLANT SHAPE

The basic grain shapes are

1. Cylindrical, with one or more perforations running completely through the grain from end to end
2. Cords or ribbons
3. Thin, flat grains in a variety of shapes: diamond, square, hexagonal, circular, circular-perforated, etc.
4. Smoothly spherical (such as ball powder) rolled, rough-spherical.

In general, the combustion of propellant grains progresses evenly from the surface where ignition occurs, through subsequent layers of the explosive as each layer reaches the ignition temperature. Thus, propellants burn only on their exposed surfaces. For a given gun design, optimum ballistic performance is obtained by the correct rate of gas production and total burning time. The burn rate and burn time are determined by selecting a propellant composition with the required burning rate and then specifying the web and proper grain geometry. Selection of the grain geometry has a definite effect on rifle performance. As discussed in par. 11-31, a grain shape whose surface area decreases during firing will attain a maximum gas pressure earlier than a grain geometry whose surface area increases burning rate.

In addition to granular propellants, other propellants were investigated for use in recoilless systems. Some of those investigated were cord, sheet, ball, and plateau. Generally speaking, except for sheet propellant, these studies were not carried to completion and did not show promise in the weapons studied.

Sheet propellant, however, was investigated

extensively to improve temperature coefficients of ballistic performance for recoilless rifle ammunition. The principal configurations studied were stacked circular discs and "scroll" assemblies. Scroll configuration study was abandoned because of its excessive erosive burning characteristics. The disc propellant configuration appeared very promising and was selected for use in ammunition for the 90 mm shoulder-fired PAT M67 System. This ammunition passed all phases of the Engineering Tests and most phases of the Standardization Test; however, a serious problem developed when this round was subjected to the arctic tests. The propellant in the arctic environment became brittle and caused excessive ballistic performance dispersion, particularly erratic high pressures. This condition necessitated a switch to granular-type propellant, and M26 Propellant was established for use in this system.

11-30 CHEMICAL AND PHYSICAL CHARACTERISTICS

The potential thermal energy of a propellant when fired in a gun is partially converted from chemical energy into the kinetic energy of the projectile. The proportion of the total available energy that can be used by the projectile is limited by the length of projectile travel in the barrel, maximum pressure, expansion ratio, friction, and heat conduction energy losses. Given a maximum pressure limit, the ballisticians attempt to maximize the projectile muzzle velocity—while staying below pressure limit—through the proper choice of propellant composition, geometry, and web thickness.

The web and propellant weight combination that produces the maximum velocity at a specified pressure is the optimum charge. Table 11-3 lists chemical compositions and combustion characteristics of various propellants used in recoilless rifle systems. Curves of burning rate versus pressure can be found in the Chemical Propulsion Information Agency/*M2 Solid Propellant Manual*.

TABLE 11-3
COMPOSITION OF SEVERAL PROPELLANTS

Propellant Specification	M2	M6	M10		T181		T26		M26 (T26)		T31	T32	T33
			FA-PD-123	FA-PD-125	FA-PD-126	PA-PD-329	OAC-PD-134						
Nitrocellulose (NC)	77.45	81.95	98	72.00	73.25	67.25	30.00	25.00	30.95	35.80	21.30	35.45	
% Nitrogen	13.15	13.15	13.15	13.15	13.15	13.15	12.20	13.15	12.20	13.35	12.20	13.35	
Nitroglycerin (NG)	18.50	15.00		18.75	20.00	25.00	43.00		35.00				35.00
Barium Nitrate	1.40	1.40		0.75	0.75	0.75							
Potassium Nitrate	0.75	0.75		0.70	0.70	0.70							
Potassium Sulfate			1.00										
Diphenylamine (DPA)			1.00										
Ethyl Centralite	0.60	0.60		6.50	5.00	6.00	2.00		7.95				7.95
Graphite	0.30	0.30	0.10**	0.30	0.30	0.30							
Carbon Black													
Ethyl Alcohol (Residual)			1.50	1.20	1.20	1.20	0.20*		0.30				0.30
Water (Residual)			0.50	0.30	0.30	0.30	0.50		0.50				0.50
Isochoric Flame Temp., °K	3319	3245	3000	2938	3071	3061	3674		3100				3135
Force F, ft-lb/lb x 10 ⁻¹	360	362	339	346	353	356	367		366				368
Unoxidized Carbon, %			4	3.4	1.8	2.2	0		3.0				2.6
Combustibles, %			64.5	59.1	56.1	57.3	36.9		58.5				58.1
Heat of Explosion Q, cal/g	1060	1047	936	910	962	962	1222		957				971
Gas Volume V, moles/g	0.03900	0.03935	0.04388	0.04219	0.04133	0.04157	0.03788		0.04245				0.04222
Ratio of Specific Heats γ	1.2238	1.2258	1.2342	1.2421	1.2373	1.2383	1.2174		1.2415				1.2410
Isochoric Flame Temp., °K	2712	2647	2431	2365	2482	2488	3018		2495				2526
Convulsion, in ³ per lb			27.7E	28.13	28.56	28.77	26.86		29.15				28.04
Specific Gravity			1.67	1.63	1.62	1.52	1.62		1.62				1.62

* Added

** Glaze Added

† Obsolete

11-01 PROGRESSIVE AND REGRESSIVE BURNING

The different propellant geometries available can be divided into two groups according to the change in the burning surface area as burning proceeds in the propellant grain. In solid propellant grains, such as cords or strips, the burning surface area continually decreases during combustion. Propellant grains that have a continually decreasing burning surface area are termed regressive types of grains or are said to exhibit regressive burning. Multiperforated grains are examples of propellant grains which exhibit an increase in burning surface area during combustion and are termed progressive grains. Within these two classifications there are degrees of regressiveness or progressiveness. For example, a single-perforated grain is only slightly regressive, showing an almost constant burning surface, compared to a spherical or cubical

shape which is highly regressive.

Since the amount of gas evolved depends upon the amount of surface area being consumed, it is apparent that the choice of regressive or progressive propellant will have the effect of determining at what point in projectile travel peak chamber pressure will occur. A regressive grain will produce maximum pressure earlier in the projectile travel, and the maximum pressure will be higher than a progressive grain of the same composition.

Sometimes it is even of further advantage to be able to control the shape of the pressure-travel curve through changing the type of burning for a specific propellant geometry by inhibiting the burning of some of the grain surfaces. As an example, a single-perforated grain can be coated on the outside surface to inhibit burning so that only a progressive burning occurs from the inside.

REFERENCES

1. Armour Research Foundation Reports in Connection with Project No. LO37, *Interior Ballistics and Ignition Study on Expendable and Non-Expendable Perforated Cartridge Cases*, Interim Report No. 1 and Final Report.
2. G. Horvay, "The Plane Stress Problem of Perforated Plates", *J. Applied Mechanics*, Sept. 1952.
3. I. Malkin, "Notes on a Theoretical Basis for Design of Tube Sheets of Triangular Layout", *Trans. ASME*, April 1952.
4. J. W. Dally and A. J. Durelli, "Stresses in Perforated Panels", *Product Engineering*, March 1952.
5. F. Einberg and A. J. Tuckerman, *Cellulose Nitrate Seal for the Recoilless Cartridge Case*, Frankford Arsenal Report R-1134, May 1953.
6. *Chemical Studies for Recoilless Ammunition Cases*, United Shoe Machinery Corp., Beverly, Mass., Final Report, Phase I, Contract DA-19-020-ORD-1847, Task III (Project TS4-4018), 25 June 1954.
7. *Lining Studies for Recoilless Rifle Shell Cases, Part II--Production Studies*, United Shoe Machinery Corp., Beverly, Mass., Contract DA-19-020-ORD-1847, Task III (Project TS4-4018), Sept. 1955.
8. *Development of Cartridge Case Liners for Recoilless Ammunition*, Emhart Manufacturing Company, Hartford, Conn., Final Report, Contract DA-19-059-ORD-1093, 13 November 1952 to 15 September 1966.

9. A. S. Tuckerman and J. Nazia, *Liner for the Recoilless Rifle Cartridge Case*, Frankford Arsenal Report R-697, January 1946.
10. G. P. Sollott and F. Einberg, *Investigation of Heat Stabilizers for Nitrocellulose*, Frankford Arsenal Report R-1918, August 1959.
11. AMCP 706-247, *Engineering Design Handbook, Ammunition Series, Section 4, Design for Projection*.
12. O. C. Zienkiewicz, *Finite Element Method*, McGraw-Hill Book Co., Inc., 1951.
13. AMCP 706-210, *Engineering Design Handbook, Fuels*.
14. R. M. Wood, *Theoretical and Practical Considerations Regarding the Stability of Fin-Stabilized Ammunition*, presented at Picatinny Arsenal 1st Jan 1955 (unpublished BRL report).
15. Johns and Orange, *Theoretical Elastic Stress Distributions Arising from Discontinuities and Edge Loads in Several Shell-type Structures*, NASA Report TR-R-103.

BIBLIOGRAPHY

G. P. Sollott and L. Berger, *Polyethylene Terephthalate Seal for the Recoilless Rifle Cartridge Case*, Frankford Arsenal Report R-1409, October 1957.

J. VanHorn and F. Einberg, *Extruded, Shrink-Fitted Cellulose Nitrate Seal for Recoilless Cartridge Cases*, Frankford Arsenal Report R-1233, November 1954.

N. C. Bauman, *Development of M26 Propellant for 1.7 mm Recoilless Rifle M40A1*, Picatinny Arsenal Report No. DR-TR 3-61.

Development of 105 mm Battalion At-Range Weapons and Interior Ballistics for the Design of Recoilless Rifles, Summary Report, Vol I ARF Project No. LO34, ORD Project No. TS4-4020, Contract No. DA-11-022-CRD 1157, July 1, 1954.

Major General Thomas J. Hayes, *Elements of Ordnance*, John Wiley & Sons, Inc., 1938.

AMCP 706-106, -107, -108, *Engineering Design Handbook, Elements of Armament Engineering, Parts One, Two, and Three*.

J. Corner, *Theory of the Interior Ballistics of Guns*, John Wiley & Sons, Inc., 1950.

AMCP 706-244, *Engineering Design Handbook, Ammunition Series, Section 1, Artillery Ammunition - General*.

Recoilless Rifle Technical Information Index, 1944-1958 Publications Bulletin, Frankford Arsenal PB8, September 1959 and Supplement 1.1 (1958-1962) 1962.

Nomenclature and Definitions in the Ammunition Area, MIL-STD-444, 6 February 1959.

Statistical Aids, Interim Pamphlet Number 9030, Materiel Test Procedures TFCP 700-700, U. S. Army Test and Evaluation Command.

AMCP 706-150, *Engineering Design Handbook, Ballistic Series, Interior Ballistics of Guns*.

AD-827 080, Jacob M. Swotinsky, *In-Tube Burning Rocket for the Advanced, Light Antitank Weapon*, Technical Report 3665, Picatinny Arsenal, January 1968.

AD-819 373L, *Product Improvement Test of Cartridge, HEAT-FS, MS344A1, 106 mm*.



AD-674 649, *Effect of Loading Rate and Winding Sequence on Fatigue and Rupture of Pressurized Filament-Wound, Glass-Reinforced Plastic Cylinders*, Technical Report 3693, Picatinny Arsenal, August 1968.

AD-24698, *Development of an Improved Propellant Igniter System for 57 mm Rifle M18*, Picatinny Arsenal, Technical Report No. 1946, 30 July 1953.

AD-493 265, *Examination of Unfired, Separate Loading Propelling Charge Assembly for 105 mm Recoilless Gun L. G. 41*, Picatinny Arsenal, Technical Report 1439, 23 August 1944.

AD-489 321, Vincent W. Puleo, *Conversion of 57 mm, M306A1, Target Practice Cartridges to HE Cartridges*, Picatinny Arsenal, Technical Report No. 3438, August 1966.

AD-18671, *Cartridge, Semi-Fixed, HEP-T, T81E17 for 105 mm Howitzer M2A1 and M4 and Cartridge HEP-T, M326 for 105 mm Recoilless Rifle M27*, Picatinny Arsenal, 1 October 1952.

AD-471 372, *Cartridge, HEAT-T, T43 for 105 mm Recoilless Gun T19*, Picatinny Arsenal, 5 May 1950.

AD-471 730, *Cartridge, HE, T-42 for 105 mm Recoilless Gun T19*.

AD-431 530, William J. Gaston, *Malfunction Investigation of Cartridge, 106 mm HEAT, M344A1, with Fuze PIBD, M509*, Picatinny Arsenal, Technical Report No. 3144, February 1964.

AD-422 747, *Encyclopedia of Explosives and Related Items*, Picatinny Arsenal.

CHAPTER 12

MOUNTS

SECTION I

INTRODUCTION

12-1 GENERAL

The recoilless rifle mount is that part of the weapon system which provides a firm base during firing, and mobility or portability during transport. Since recoilless weapons exert little or no recoil force, mounts are needed for holding and positioning only. Therefore, any simple structure of sufficient stability such as a tripod, or an appropriately configured saddle to hold it on the gunner's shoulder, is adequate to support a weapon of this type.

The first consideration given to the design of a mount is the specific application. Mount design depends on whether the weapon is to be fired from a vehicle, ground, shoulder, or a combination of these. The weight distribution and configuration of the weapon dictates whether or not the rifle can be shoulder-fired. For the shoulder-fired rifle, the mount must provide for firing from either an upright or prone position and, typically, consists of an adjustable monopod located under the barrel and a folding bipod. In firing from the prone position, the bipod is in the unfolded position, providing a fixed three point support with the monopod as shown in Fig. 12-1. In the upright firing position, the bipod is folded underneath the weapon and serves as the shoulder rest.

If the rifle is to be fired from a ground mount only, it can be mounted on a simple tripod. If the rifle weighs more than 80 lb the

maximum allowed by Ref. 1 for a 2- to 3-ft lift off the ground, it will be necessary that the mount be a separate piece of equipment which provides quick mounting and removal of the rifle from the mount. A requirement for mobility over short distances also may dictate the incorporation of a wheel or wheels in the base legs of the mounts. Many of the medium-caliber recoilless rifles have a requirement for both ground and vehicular mounting so that the mount will need to be strong enough to sustain the accelerations induced by vehicular travel. In vehicular or towed mounts, the vertical transportation forces can be estimated for one of four conditions involving transportation over level but rough terrain.

Load factors for a mount on a sprung chassis are:

1. 3.0 g's for maximum speeds of less than 30 mph
2. 5.0 g's for maximum speeds of 30 mph or more

Load factors for a mount on an unsprung chassis are:

1. 5.0 g's for maximum speeds of less than 30 mph
2. 12.0 g's for maximum speeds of 30 mph or more

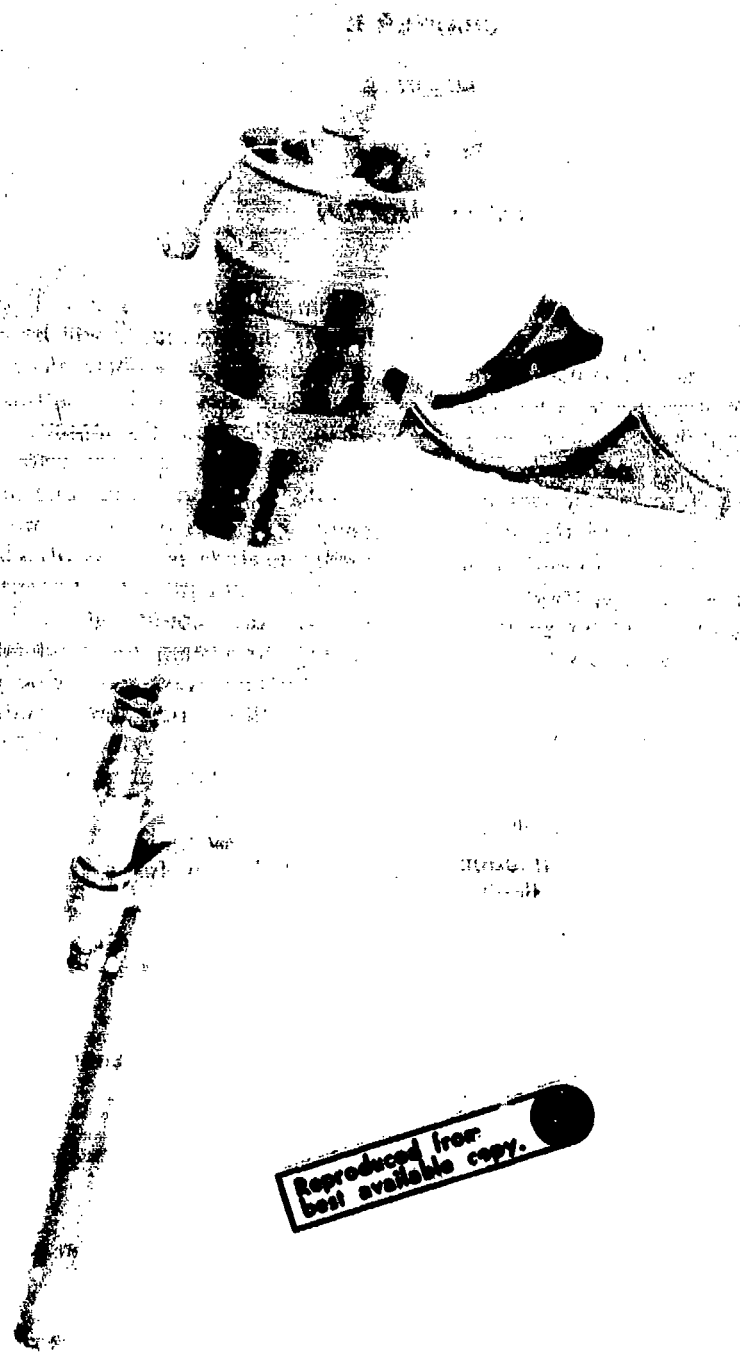


Figure 12-1. Prone Firing Position (Rifle, 57 mm, T66)

Reproduced from
best available copy.

12-2 SPECIFIC EXAMPLES

12-2.1 M79 MOUNT

As shown in Fig. 12-2 (Ref. 1), the 106 mm rifle mount consists of a wheel-barrow-tripod-type base assembly, an elevating and firing assembly, and a traversing assembly. The M79 Mount provides a stable base for using the 106 mm M40A1 Rifle with cal .50 Spotting Rifle M8C on the ground and as a means of mounting the rifle on the body of 1/4-ton 4 X 4 utility trucks (Ref. 2).

The elevating and firing assembly houses the controls and mechanisms used to support, elevate, depress, and fire the 106 mm rifle. The elevating handle is the control for elevating and depressing the rifle. Fine elevation adjustments are made by the firing and vernier elevating shaft knob which is in the center of the elevating handle and also

serves as the control for firing both the major-caliber and spotting rifles. The elevating cradle assembly incorporates a support and locking yoke for mounting the 106 mm rifle. Installed in the elevating cradle are a firing transfer housing and tang which serve to actuate the firing cable operating levers for firing both 106 mm and spotting rifles.

The traversing assembly houses the controls and mechanisms used to traverse the rifles and supports the elevating and firing assembly. The traversing handle serves as the control for traversing the rifles. In the center of the traversing handwheel is the free traverse shifting shaft knob that is used to disengage the traversing drive from internal gearing to permit free traversing of the rifles.

The elevating and traversing base assembly provides a stable base for ground mounting the rifles. The adjustable base left and right

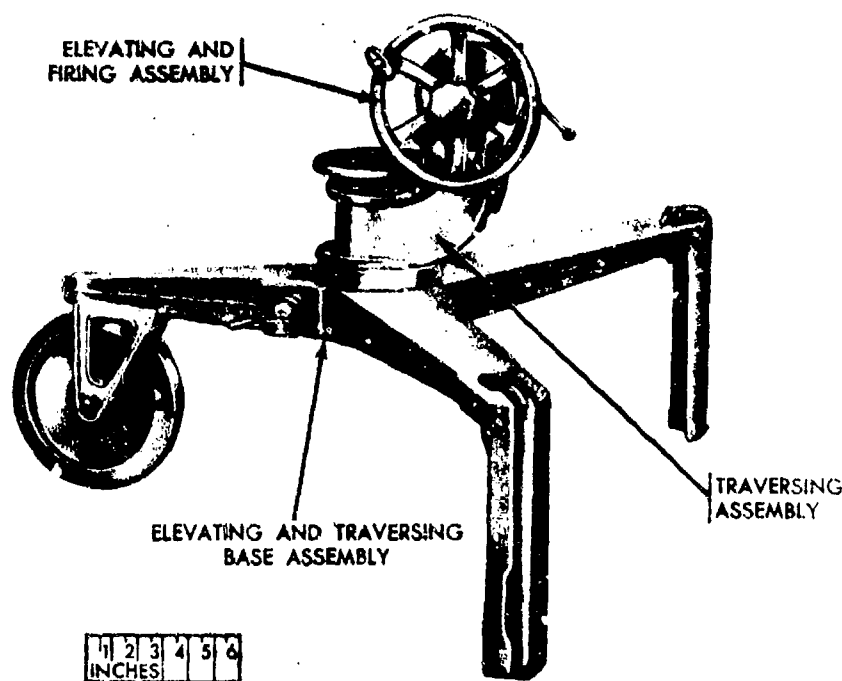


Figure 12-2. 106 mm Rifle Mount, M79

arms are basically identical, each having a base handle and base locking clamp for locking the mount to trucks. The handles also are used for lifting the rear of the mount by two men and moving the mount in a "wheelbarrow" manner on the wheel assembled in the base front arm. A base locking lever incorporated into the base front arm serves to lock the base left and right arms in either the open position for ground firing, installation on trucks, or "wheelbarrow" positions.

12-2.2 T173 MOUNT

The T173 Mount and Tripod T26 is used to provide a stable base for using the 106 mm M40A1C Rifle on the ground. As shown in Fig. 12-3 (Ref. 2), the Rifle Mount T173 consists of an elevating and firing assembly, a traversing assembly, and an adapter assembly. The elevating and firing assembly, and traversing assembly are identical to the

respective assemblies of the 106 mm Rifle Mount M79 described in par. 12-2.1. The differences between the T173 and M79 Mounts are in the base assembly.

The T173 Mount incorporates an adapter assembly (see Fig. 12-3) which consists principally of an adapter plate, three adapter latches, a collar assembly, and a capstan assembly. This adapter assembly is designed to mount and lock Rifle Mount T173 to Tripod T26. The T26 Tripod is a simple aluminum tripod composed of two folding legs and one fixed leg as does the M79 Mount. Folding leg release buttons, incorporated in each folding leg, serve to lock and unlock the folding leg key, permitting the folding legs to be locked in an open position for operation and in a folded position for stowing. Whereas the M79 Mount with front base wheel enables the 106 mm M40A1 Rifle to be wheelbarrowed by two or more men for short



Figure 12-3. 106 mm Rifle Mount, T173 Removed from Tripod, T26

distances over even terrain, the T173 Mount requires the removal of the 106 mm M40A1C Rifle for moving because of the total system weight of 400 lb.

12-2.3 XM124 MOUNT

The XM124 Mount configuration described here contains a unique Joystick System that provides rigid joystick for free traverse and elevation, parallelogram suspension of the rifle, adjustable friction drag, and provision for placement of gunner adjacent to the traverse axis. This mount concept was developed and ultimately rejected for the 120 mm Heavy Antitank Weapon System, XM105F1 (HAW) and is described here for design and conceptual information.

The XM124 Mount is a variable ratio ground-vehicular mount and is designed for engaging stationary as well as moving targets, with the necessary freedom of movement and aiming accuracy. As shown in Fig. 12-4 (Ref. 3), the XM124 Mount provided for direct control of the weapon attitude through the use of a joystick control. The down-range pointing joystick provided either a direct control ratio of 1:1, which is desirable for moving targets, or a variable ratio between 9:1 and 36:1 for use on distant fixed targets.

The 1:1 ratio is obtained by releasing the brake and locking the release shaft assembly in place to form a rigid system. The joystick control would be then centered and fixed relative to the rifle. When the brake is released, the rifle could be moved in free traverse and elevation.

The mount is designed as shown in Fig. 12-5 so that the joystick control lever is operated by the left hand, with the gunner on the left side of the rifle and adjacent to the traverse axis. The gunner's right hand is on a

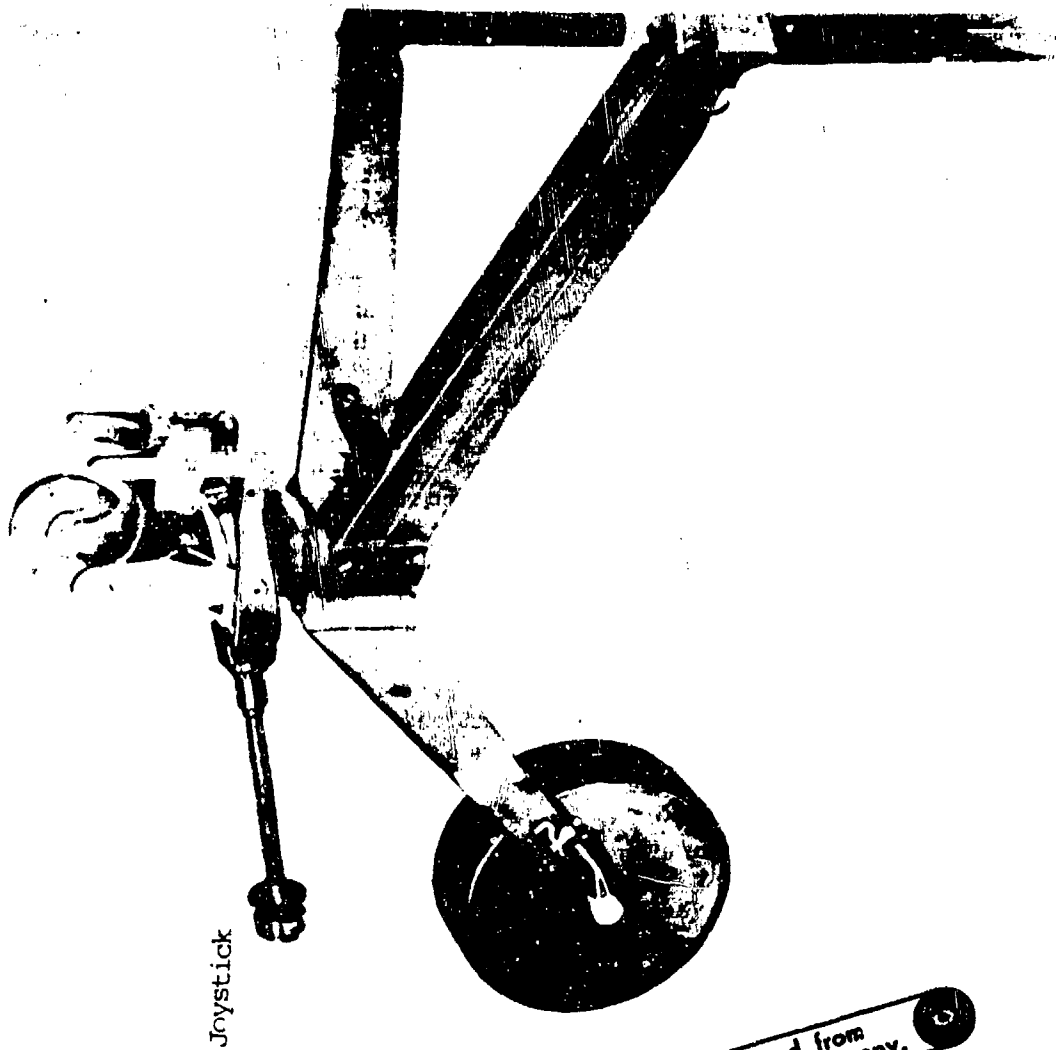
trigger mechanism which also serves as a control handle when the mount is in free traverse. This position of the gunner permits maximum sweep of the rifle without operator discomfort.

The base legs of the XM124 Mount are very similar to those of the M79 Mount. With the wheeled front base leg, the XM124 is also capable of being "wheelbarrowed". Vehicle mounting of the XM124 Mount is also similar to the M79 Mount.

12-2.4 T234 MOUNT

Fig. 12-6 (Ref. 4) shows the integral shoulder mount and accessory package designed for the 9C mm T234 Recoilless Rifle. The original design of this mounting assembly—containing the monopod, bipod, face shield, firing mechanism, and sight bracket—specified that the assembly be made from one molded plastic housing. Because of strength requirements, the design of the assembly was modified to consist partly of magnesium and partly of Fiberglass or entirely of magnesium.

The entire assembly slipped onto the muzzle end of the rifle and was locked in position with a snap ring. A glass laminate material padded with a heat-resistant filler and covered with an abrasion and tear-resistant glass cloth was selected for the face shield and the shoulder pad. This sandwich construction provided good thermal insulation to protect the gunner from a hot rifle tube. As a result of the inability of this accessory package to meet shock requirements and maintain proper sight alignment, this design was dropped in favor of a simple folding bipod mount, which when folded, served as the shoulder mount on later configurations of the T234 Recoilless Rifle.



Joystick

Reproduced from
best available copy.

Figure 12-4. Mount, XM124



Figure 12-5. Two-hand Control (Tracking Handle and Trigger Handle) Vehicle Mounted

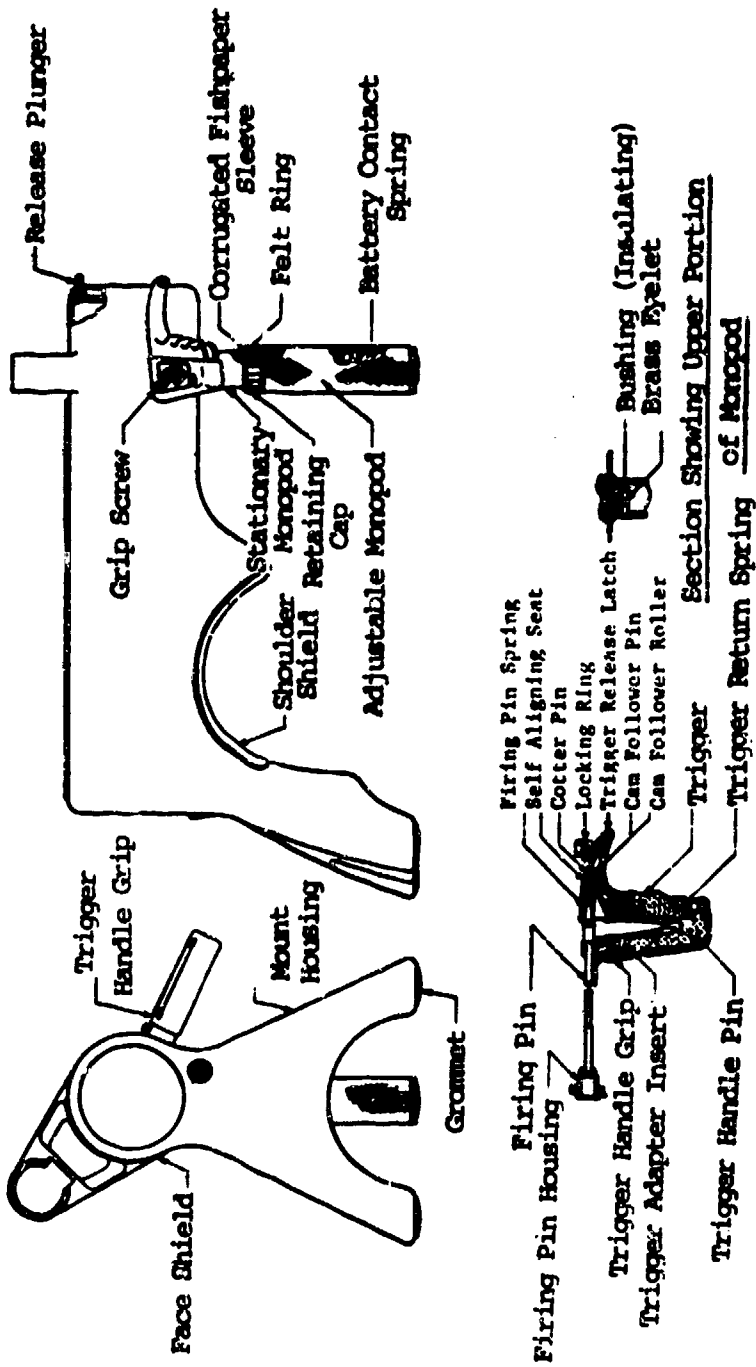


Figure 12-6. Integral Accessory Package for 90 mm Recoilless Rifle, T234

SECTION II

ACCESSORY MOUNTING EQUIPMENT

12-3 GENERAL

In a complete recoilless rifle system, the various accessory items that must be fastened or connected to the rifle include such accessories as ground mount, vehicular mount, optical sight, spotting rifle, heat shield, various handles, and firing mechanism. Among these, the optical sight and the spotting rifle deserve particular attention in that they must be precisely positioned on the major-caliber rifle, and their positions must be accurately retained throughout field use of the weapon. This presents a problem as the expansion and contraction of the rifle chamber and tube are considerably greater than those of conventional weapons of comparable caliber. The absence of recoil allows the weight of the recoilless rifle to be reduced to a level where the material and wall thickness of the chamber and tube are the determining factors. When the rifle tube wall section is made as light as permissible for a given material, the change in diameter upon firing occurs quite early and is quite large. It can be shown that the strain in a thin-walled tube is approximately equal to the yield-point stress in tension divided by the modulus of elasticity of tube material. It can be seen from this, that a 5-in. diameter tube will undergo a diametral expansion of about 0.025 in., 0.028 in., or 0.038 in. when the tube material is steel, aluminum, or titanium, respectively.

For a tube that expands and contracts to this extent, it is not advisable to have enlarged portions or projections to act as fastening pads integrally machined with the tube. Not only does this make the machining more

difficult, but the stress concentration pattern, the asymmetric constriction to the motion of the projectile, and the deflection of the tube upon firing are highly objectionable. For example, any increase in thickness on one side will, by lowering the stress and strain levels at that side, cause the barrel to deflect or bow when subjected to internal pressure. Since this occurs almost instantaneously (in milliseconds), it sets up transverse vibrations in the barrel and seriously affects accuracy.

Fastening pads to a barrel that undergoes expansion and contraction has proven to be fruitless. Welding of mounting pads to a high-strength alloy steel gun tube is also inadvisable because the stresses set up and the changes inflicted upon the grain structure of the steel would severely damage the tube wall. Finally, hydrogen brazing rarely lasts for more than one shot, and the various cements that have been tried also fail rapidly.

12-4 MOUNTING METHODS

12-4.1 MODERATELY STRESSED WEAPONS

One means that has proven successful for moderately-stressed weapons is to install a thin band around the barrel (see mounting bands on the 75 mm M20 Rifle). The band must, however, have an expansion capability equal to or greater than (by an adequate amount of interference fit) the expansion of the barrel on firing. If steel is to be used as the material for the expansion device, it should have a yield-point strength at least equal to that of the steel barrel, otherwise the

fastening device will become loose upon repeated firings. By employing a high-strength material with a lower modulus of elasticity, such as titanium or high-strength aluminum, a fastening band can be installed around the barrel and will not become loose. Any band, however, should not be massive enough to materially constrict the expansion of the barrel upon which it is placed, since this will cause stress concentrations in the barrel wall and disturb the projectile travel. A band thickness of 25 to 50 percent of the barrel wall thickness and a band width of 0.75 in. to 1.00 in. should be more than adequate to hold one end of an accessory mounting bracket. However, no appreciable longitudinal or circumferential load is to be applied on the band since this may cause it to be displaced relative to the barrel due to vibrations of the barrel. Hence, without keying to the barrel, the band cannot be relied upon for accurate positioning.

This method of fastening is not used for the higher performance weapons with larger expansion of the barrel.

12-4.2 HIGHLY STRESSED WEAPONS

The HAW 120 mm XM105E1 is an example of a highly stressed recoilless rifle. The barrel is designed to employ the strain compensation principle (described in Chapter 10) with a 200,000 psi yield-strength material that permits the barrel wall thickness to be less than 0.25 in. In order to provide the necessary mounting surfaces while allowing for the radial expansion caused by the high strain in the barrel during firings, the accessory sleeve as shown in Fig. 12-7 (Ref. 3) was adopted for use on the HAW weapon system.

The use of the accessory sleeve allows the XM90 Spotting Rifle to be located as close as possible to the centerline of the major rifle so as to provide the smallest turning moment

resulting from recoil of the spotting weapon. The brackets which mount the spotting rifle fulfill two functions—recoil is transferred to the main weapon, and a means of biasing is provided for best trajectory matching. Biasing adjustment is made through the linear adjustment mechanism located in the forward bracket of the accessory sleeve. This mechanism provides for both azimuth and elevation correction. The rear bracket of the accessory sleeve provides the thrust (recoil) support for the spotting rifle.

With the use of the accessory sleeve on the HAW weapon system, the optical fire control components as well as the gunner's eye are protected from the radial shock at the moment of firing. The sight bracket is mounted with bolts on a pad located on the rear side of the accessory sleeve, under the thrust bearing bracket. The telescope mount is attached to this sight bracket which is located as close as practical to the center of rotation of the mount to provide the smallest possible dislocation during target tracking.

12-5 MOUNTING REQUIREMENTS

12-5.1 GROUND AND VEHICULAR MOUNTS

The general requirements for a ground and vehicular mount are that the mount be light while sufficiently rugged to withstand the vibration and shocks induced during transport by vehicle. Light weight of the mount is required since the weapon system should be easily mounted for transportability by the vehicle and conveniently removable from the vehicle for quick ground emplacement. Figs. 12-2 and 12-4 show the ground and vehicular mounts for the Battalion Antitank Weapon (BAT) and the Joystick System considered for the HAW weapon systems, respectively. Vehicle installation of the XM124 Mount for the HAW weapon is shown in Fig. 12-8.



- 1 - Accessory Sleeve
- 2 - Tracking Handle
- 3 - Retainer
- 4 - Nut
- 5 - Bushing

Figure 12.7. Accessory Sleeve Mounting Bracket for M103 120mm Rifle, XM106



*Figure 12-8. Ground and Vehicular Mounted 120 mm Recoilless Rifle System, XM105 HAW -
Jeep Mounted - Traveling Position*

12-5.2 TELESCOPE MOUNT

The telescope mount is an independent unit which is attached to a supporting bracket of the major-caliber weapon and holds the fire control telescope. The mount is required to securely hold and position the telescope for ease of use by gunner, while incorporating provisions for making azimuth and elevation adjustments to ensure proper boresighting and boresight retention of the telescope with respect to the weapon. For the case of the mount holding an elbow telescope, the mount will be required to have a device for making adjustments in the cant of the telescope.

The exploded view of the M110 Telescope Mount for attaching the M103 Telescope to the 90 mm MAW M67 Rifle, as shown in Fig. 12-9 (Ref. 5), is typical of the mount design for straight-tube telescopes. The M110 Telescope Mount features a spring-loaded latch in a gimbal tube which seats the telescope quickly and accurately in the mount. Rotation of either azimuth or elevation boresight worm screws actuates the respective wedge gear which then tilts the telescope supporting gimbal tube to the desired orientation. Fig. 12-10 shows a telescope mounted to the major-caliber weapon.

12-5.3 SPOTTING RIFLE MOUNT

As discussed in par. 12-4.2, the mounts for the spotting rifle must fulfill the requirements of transferring the spotting rifle recoil to the major-caliber weapon and providing for biasing adjustment. Another consideration in mounting the spotting rifle was locating the spotting rifle as close as possible to the centerline of the major rifle so as to minimize the turning moment caused by the spotting rifle recoil.

The exact location and type of mounting for the spotting rifle will depend on the type of spotting rifle used for the specific application. For the larger, ground-fired recoilless rifles, such as the BAT and HAW weapons, the spotting rifle is mounted on the top of the major-caliber weapon using two brackets as described in par. 12-4.2. Shoulder-fired recoilless rifles require the use of the lighter and smaller spotting pistol. Fig. 12-11 (Ref. 6) shows the type of mount used for the XM14 Spotting Rifle in the 90 mm MAW weapon system. As seen in Fig. 12-11, the front and rear brackets provide for both the necessary transfer of recoil to the major-caliber weapon and the biasing adjustment mechanism.



Figure 12-9. Exploded View of Telescope Mount, M110

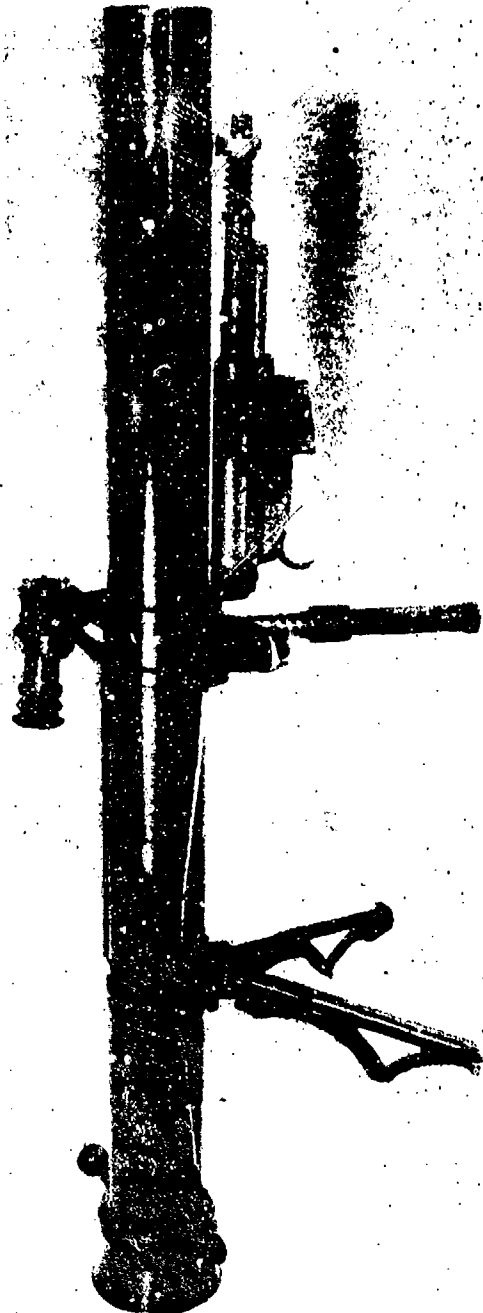


Figure 12-10. Rifle, Facelless, 90 mm, M67 With 10 mm Pistol, Sporting, XM14 and Telescops

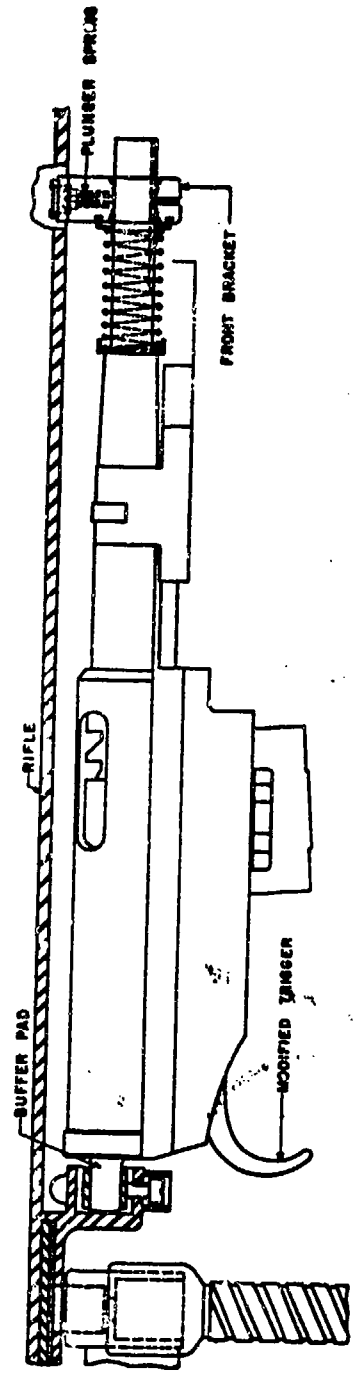


Figure 12-11. Spotting Pistol, XM14 Mounted on 90 mm Rifle, M67

REFERENCES

1. MIL-STD-1472B, *Human Engineering Design Criteria for Military System, Equipment and Facilities*, 31 Dec 1974.
2. TM 9-1000-205-12, *Operation and Organizational Maintenance 0.50-Cal. Spotting Rifle M8C; 106 mm Rifles M40A1 and M40A1C; 106 mm Rifle Mounts T173 and M79; and Tripod T26*, Headquarters, Department of the Army, Washington, DC, 5 March 1959.
3. *Development of 120 mm Recoilless Heavy Antitank Weapon System (HAW)*, Final Report, Technical Memorandum M64, Frankford Arsenal, Philadelphia, Pa., 1 April 1959 through 30 June 1962.
- 3A. 120 mm Rifle System XM105E1, Heavy Antitank Weapon (HAW), Notes in Development Type Material, Report POL WS-2, Frankford Arsenal, December 1952.
4. *Recoilless Rifle Systems, Ammunition and Related Items*, Status Report No. 1, Vol. IV, Report No. R-1316, Frankford Arsenal, Philadelphia, Pa., 1 January through 31 March 1956.
5. *Recoilless Rifle Systems, Ammunition and Related Items*, Status Report No. 1, Vol. VIII, Report No. R-1553A, Frankford Arsenal, Philadelphia, Pa., 1 January through 31 March 1960.
6. *Recoilless Rifle Systems, Ammunition and Related Items*, Status Report No. 4, Vol. VI, Report No. R-1499, Frankford Arsenal, Philadelphia, Pa., 1 October through 31 December 1958.

CHAPTER 13

FIRE CONTROL

13-1 GENERAL

Recoilless rifle weapon systems use optical sighting equipment to establish the rate of fire to the target or, when the spotting rifle is incorporated as part of the weapon, to direct the spotting round to the target. AMCP 706-327, *Fire Control Systems—General* (Ref. 1) contains information relating to optical fire control components and sights. The spotting rifle as a fire control adjunct is discussed in this chapter and the reader is referred to Ref. 1 for information relating to the optical components.

Several recoilless rifle systems use a subcaliber rifle, called the spotting rifle, as the method of fire control. The spotting rifle is mounted on the major caliber gun so that the barrel axes of the two rifles are parallel. In operation, the spotting rifle is fired at the target and the point of impact of the spotting projectile observed visually by a flash of light and puff of smoke caused from the detonation of the incendiary or spotter mix contained in the spotting projectile. The spotting projectile often provides a visual trace that enables the observer to follow the trajectory of the projectile to the target. In the event the projectile misses the target, the position of impact becomes a landmark for correcting the aim. The lay of the rifle weapon system is changed successively until a spotting round impacts on the target. At this time, the firing sequence of the spotting rifle ends and the major caliber weapon is then fired.

Matching of the trajectory, at selected

ranges, of the major caliber projectile by the spotting round is the principle upon which the spotting rifle functions as a fire control device. Thus, if the spotting projectile hits the target, the major caliber projectile also can be made to hit the target provided: (1) the lay of the weapon was not altered after the spotting round hit the target, (2) the major caliber weapon is fired before the target moves to different position, and (3) the trajectories of the two projectiles follow a known relationship. This relationship is referred to as matching and pertains to a correspondance between projectiles at some point at a given range. The basic problem associated with the matching process is caused by the inherent difference in the exterior ballistic characteristics of the major and spotting projectiles.

Matching of the projectile trajectories requires that the following relation be met (Ref. 2):

$$\frac{C_{D1}}{W/S_1} = \frac{C_{D2}}{W/S_2} \quad (13-1)$$

(Major Caliber Projectile) (Spotting Projectile)

where

C_D = drag coefficient, dimensionless

W/S = sectional density, lb-in⁻²

W = weight of projectile, lb

S = projectile cross-sectional area, in²

In practice, it is impossible to meet the requirement of Eq. 13-1 exactly and,

consequently, a mismatch in trajectory results. In order to compensate for the mismatch, a horizontal bias compensating for wind and differential spinning effects or a vertical bias adjustment for difference in projectile drag is introduced between the spotting and major caliber rifles. The muzzle velocity of the subcaliber ammunition is also adjusted (usually increased) in order to correct for the projectile's mismatch. Ideally, a spotting projectile should be designed with the same ballistic coefficient as that of the main round in order that the two trajectories be matched over the desired range. The maximum practical ballistic coefficient (see Chapter 4) of the spotting projectile is less than that of the major caliber ammunition. This coefficient can be maximized by improved streamlining, by increasing W/g through use of higher density materials, and by minimizing the caliber of the spotting projectile.

The DAVY CROCKETT Recoilless Rifle System, as a result of their unique configuration, presented the following listed problems relating to the spotting rifle design.

1. The spotting rifle must be positioned sufficiently far from the bore axis to clear the warhead at the muzzle. In these weapons, the warhead is greater than bore size, see Fig. 1-14 for example.
2. These weapons are not direct fire as is the case in other recoilless rifles but are fired at high angles of elevation similar to mortars.
3. The XM29 version of the DAVY CROCKETT is zone fired, i.e., two sets of semifixed ammunition are provided, each for a different range.

The spotting rifle selected for the XM29 Weapon was the 37 mm XM77E1. Two sets of ammunition, M415 and M446, were provided for this spotting rifle; one round to be used in conjunction with the short range major

caliber ammunition and the other with the long range. For the XM28 Weapon, a 20 mm spotting rifle using the M101 Spotter Round was standardized. A fin-stabilized spotting projectile was provided in the two 37 mm and 20 mm spotting rounds.

These spotting rifles and associated ammunition selected produced a net circular probable error (CPE) within established requirements.

13-2 TYPICAL DESIGNS

13-2.1 106 mm RIFLE, M40 WITH CAL .50 SPOTTING RIFLE, M8C

The cal .50 Spotting Rifle, M8C is mounted above the 106 mm Rifle, M40 with its barrel axis parallel to that of the barrel of the recoilless rifle. This spotting rifle is a gas-operated, semiautomatic, magazine-fed, percussion-fired weapon using special cal .50 spotter-tracer ammunition. In the gas operated rifle, a port is provided in the side of the barrel. A portion of the high pressure propellant gases behind the projectile is tapped off through the hole and passes through an orifice into a gas cylinder when the spotter-tracer projectile has passed the port. A thrust is generated as a result of these gases acting on an operating rod. This thrust is applied through a mechanism to provide the energy required for performing the automatic functions necessary for sustained firing. These functions include unlocking the bolt (device which holds the cartridge in place during firing and retracts the cartridge case after firing), retracting the bolt, and operating the other elements of the gun mechanism.

The gas-operating mechanism of the cal .50 Spotting Rifle, M8C is an impingement type of mechanism and consists of a simple gas cylinder, operating rod, and a bolt of rectangular cross section which is carried by an inertia slide. The inertia slide is a cylindrical metal block surrounding the bolt

on the top and sides. The operating rod impinges directly on the slide which, through a series of springs, transfers the inertia of the operating rod to the bolt for performing the operations of chambering and extracting the round of ammunition. One feature of the Spotting Rifle, M8C is the incorporation of a needle-valve type gas regulator in the gas cylinder assembly. This valve can be adjusted manually to control the operation of the weapon. Adjustment of the operating power was provided in order to correct for differences in effective rigidity of the various types of DAT weapon system mounts and the normal variances between the different lots of spotting rifle ammunition (Ref. 3).

The cal .50 Spotting Rifle, M8C has the following characteristics and design data (Ref. 3):

Weight	:	26 lb
Length (overall)	:	49.441 in.
Barrel Length	:	32.00 in.
Muzzle Velocity	:	1723 fps.

13-2.2 120 mm RIFLE, XM105 WITH SPOTTING RIFLE, XM90E1

The Spotting Rifle, XM90E1 for the HAW weapon system is a 15 mm (cal .60) gas-operated rifle similar to the cal .50 Spotting Rifle, M8C for the 106 mm Rifle, M40. In order to match the trajectory of the 120 mm projectile, ballistic calculations indicated that the smallest spotting bullet which could be used was a cal .60 (15 mm). As a result, it was necessary to develop the larger Spotting Rifle, XM90E1 instead of using the standardized Spotting Rifle, M8C. The Spotting Rifle, XM90E1 operates in much the same manner as the Spotting Rifle, M8C. The major exception to the operational similarity is in the gas system of the Rifle, XM90E1, which is designed to close the gas

port after 0.9 in. of operating rod travel and use gas expansion to complete the stroke (Ref. 3). In contrast, the Rifle M8C uses the complete open gas impingement and expansion method for stroking the operating rod. The Spotting Rifle, XM90E1 also incorporates a charging mechanism that uses the mechanism advantage of the charging handle in conjunction with a roller cocking system to bring the peak charging effort to 34 lb (reduced from a reasonable value of 65 lb).

The Spotting Rifle, XM90E1 has the following characteristics and design data (Ref. 3):

Weight	:	37.0 lb
Length	:	54.6 in.
Barrel Length	:	32.0 in.
Muzzle Velocity	:	1800 fps.

13-3 TYPES OF SPOTTER-TRACER ROUNDS

During World War II, the Germans developed an experimental cal .30 observing bullet containing white phosphorus to produce smoke and flash. While not widely used during the War, the round was later tested in the US and proved to function fairly well. The smoke puff was well defined, but the flash was small and of extremely short duration. The design of the impact mechanism was complicated and did not prove to be completely reliable on various types of terrain. In view of this and the potential hazard of handling white phosphorus, the bullet was rendered undesirable for further study.

Studies were then concentrated upon the use of red phosphorus, an allotropic form of phosphorus which can be handled as a dry powder. Early in these studies, it was found that the size and duration of flash was

dependent upon the red phosphorus content of the composition.

A cal .30 bullet would be useful for only a very short range because of the restricted volume. As a result, effort was concentrated on the cal .50 size which could contain approximately twice the red phosphorus content of a cal .30 bullet. Development of the cal .50 bullet eventually led to the design of a Spotter-Tracer Projectile, M48A1, employed in the 106 mm Recoilless Rifle System, M40A1 (BAT). This was the standardized projectile from which the 10 mm and the 15 mm experimental spotter-tracer rounds were scaled. The current cal .50 spotter-tracer cartridge has been changed to M48A2 since the BAT system development.

The most investigated areas have been in the spotter composition and the fuze design. These studies are described in pars. 13-5 and 13-6.

13-4 EVALUATION OF TARGET DISPLAY

From an examination of the many field variables involved, it is apparent that smoke and flash provide valuable information to the gunner. Since smoke provides the gunner with desirable supplementary information, the spotting round should produce visible smoke on impact.

Flash perception is governed by the Bunsen-Roscoe Law (Ref. 2) which states that the product of intensity of a point source of light and time is a constant for the production of a given quality of perception. The flash duration is a very weak function of intensity above 1 millilambert, averaging about 0.04 sec. This means that the spot can be made more detectable by increasing either the duration or the intensity or both up to about 40 msec. Above 40 msec, duration is no longer an effective variable, and intensity alone determines the visual perception.

13-5 COMPOSITIONS

Spotting compositions (Ref. 2) for small-caliber ammunition contain red phosphorus as the principal flash and smoke producing fuel in combination with barium nitrate, an oxidizing compound. White phosphorus is used widely in large chemical projectiles and other smoke producing devices, and is probably the most efficient material for producing dense white smoke. However, the low melting and ignition temperatures, 44°C, of white phosphorus create serious hazards in handling and, wherever possible, red phosphorus is used instead. Red phosphorus, which is an allotropic form of white phosphorus, has a melting temperature of 590°C and, depending on purity, an ignition temperature which varies from 200° to 280°C. Red phosphorus can be handled and loaded as a dry powder, burns more slowly than white phosphorus in air, requires an oxidizer to burn efficiently, and gives a longer flash duration when used in a composition. Red phosphorus has a slightly higher density than white phosphorus and, on the basis of an equivalent weight in an explosive composition, produces an equal quantity of smoke. For example, the 32-grain charge of spotter composition IM-144 used in the Spotter-Tracer, M48A1, contains 50 percent red phosphorus (or 16 grains) which produces a smoke puff approximately equal to that of 16 grains of white phosphorus exploded in the air. White phosphorus projectiles normally require a fuze mechanism and a charge of high explosive in order to burst the projectile and permit the white phosphorus to react with the air.

Because of the restricted volume in small-caliber spotting rounds, it is efficient to use a composition such as the standard composition IM-144, which burns with violence under confinement, thus requiring no separate charge to burst the metal container upon initiation. However, preparation, handling, and loading of the red phosphorus

compositions must be done under strict rules of safety. Because red phosphorus compositions of the IM-144 type are sensitive to impact and friction; zinc stearate, aluminum stearate, or graphite may be added to the formula for the purpose of reducing friction during loading.

In the course of development of the spotting cartridge for the HAW weapon system, a number of tests were performed with such pyrophoric metal powders as magnesium, titanium, and zirconium, in place of red phosphorus (Ref. 3). These incendiary mixes—of which IM-942, IM-943, and IM-982 are prime examples—resulted in brighter flash but less smoke in comparison with the more generally used composition IM-444. These mixtures also required the use of a detonator to insure proper initiation. However, even with the poor smoke display, it was felt that because these mixes were less hazardous to handle, they also should be considered for use in the HAW weapon system.

13-6 IGNITION

Ignition of a spotting projectile is designed to occur when the nose of the projectile strikes an object. The force of impact operates a mechanism in the projectile which initiates the explosive train that in turn bursts the projectile and expels the pyrotechnic material. The fuzing mechanism must be fast enough to function before the projectile buries into soft earth to preclude obscuration of flash and smoke. At a range of 1,000 yd, the Spotter, M48A2 penetrates ordinary field earth about 3 to 6 in. before exploding.

The most common projectile design for impact initiation employs a thin, relatively weak metal nose that is crushed easily by impact to ignite a friction-and-impact-sensitive composition contained within the nose of the projectile. For projectiles containing

incendiaries, where impacting against the earth is not required, the thin metal nose design is satisfactory and relatively easy to manufacture.

The problem associated with most spotting projectiles is the failure to achieve an acceptable level of reliable performance against the diverse set of conditions under which the projectile must ignite. Spotting projectiles must function against a variety of terrain including earth, sand, snow, and hard concrete or macadam road surfaces—even by a grazing impact. On the other hand, the spotting round must not function prematurely when fired in heavy rain or when fired through tall field grass. In order to maintain this high reliability, a number of different kinds of fuzing have been investigated. These fuze designs are air-gap, stab-pin, dynamite-filled, and designs for operation by projectile spin decay and electrical ignition.

The simplest of the fuzing concepts is the air-gap design. As shown in Fig. 13-1 (Ref. 2), the air-gap Spotting Projectile, M48A1 is believed to function in one or more of the three following ways: (1) crush-up by straight or graze impact with hard surfaces; (2) by the open nose scooping up softer earth, sand, bits of stones, etc., which are forces against the incendiary composition; and (3) instantaneous high compression of small column of air trapped in the air-gap hole causing crush-up of the incendiary composition. Two other unconfirmed theories of operation of the air-gap fuzing concept are that the incendiary composition is detonated by either a shock-wave created at the point of impact or the adiabatic heating of the column of air in front by sudden compression. The purpose of the aluminum container for the red phosphorus spotting composition IM-144 is that (1) it acts as a cover to prevent functioning of the incendiary composition IM-163A by drops of rain and tall grass, and (2) aluminum is chemically compatible with the red phosphorus whereas copper is not.

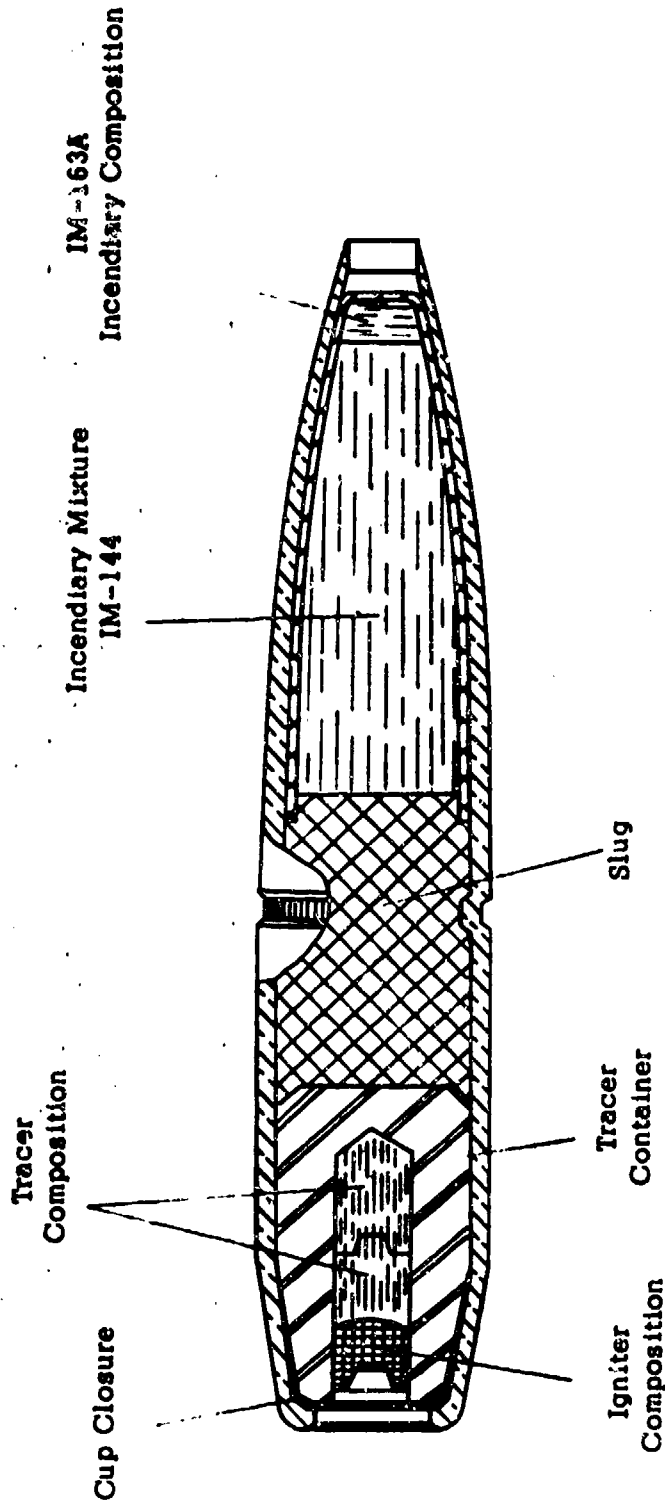


Figure 13-1. Bullet, Spotter-tracer, Cal .50, M48A2

A second type of fuze investigated as a possible alternative to the air-gap type was the stab-pin fuze. The stab-pin fuze for the cal .50 experimental Projectile, T140E12, (shown in Fig. 13-2, Ref. 2) is the simplest in design of the mechanically operated types of fuzes. The operating sequence of the stab-pin fuze follows: centrifugal force caused by projectile spin opens the firing pin retaining ring; on impact, the pin is driven into the stab sensitive primer that ignites the spotting pyrotechnic charge. During development testing of the BAT weapon system, it was found that the stab-pin type fuze did not give better overall function than the air-gap design that was adopted and standardized in the Spotter Projectile, M48A1 (prior to the introduction of the current M49A2 version).

During the U-BAT Weapon System development program, a number of different fuze types were tested for the cal .50 Spotter-Tracer Bullet. The electrically initiated fuze was based on the principle of using some of the chemical energy of the burning tracer mixer to charge a barium titanite crystal and then discharging this energy on an electrically sensitive primer to ignite the spotting mixture. In the actual design, the burning spotter mixture heated the barium titanite crystal above its Curie temperature (120°C) and thus charged the crystal. The crystal was connected to a 6200 pF storage capacitor by a 0.003 in. air gap. Upon impact of the spotter projectile, the storage capacitor was brought in contact with the primer and its

electrical energy discharged to cause primer detonation. It was found that the condenser would attain enough energy to denote the primer after 500 yd of projectile flight.

The use of the principle of spin decay in the fuzing mechanism was studied extensively and resulted in several proposed graze and arming systems. These fuzes incorporated or led to desirable features such as detonator safety through the use of an explosive train interrupter, greater mass concentration toward the ogive by placing the spotter charge between the fuze and tracer, and loading of the spotter charge as a capsulated unit. A typical spin decay fuze consisted of a metal block (graze mass) that contained a stab-sensitive primer. The graze mass initially is held in place by an antitwist spring. The action of the centrifugal force causes the antitwist springs to move radially outward and release the graze mass upon being subjected to a specified spin rate. Upon decay or spin, a drive spring is able to push the graze mass with the stab primer right up against the firing pin so that even a grazing action would cause the firing pin to stab the primer.

One of the last types of fuzes tested during the U-BAT Program was the dynamite-filled fuze. While the display tests were performed satisfactorily, it was found that the nitroglycerin in the various materials studied deteriorated under storage conditions. As a result, this configuration was not used in production projectiles.

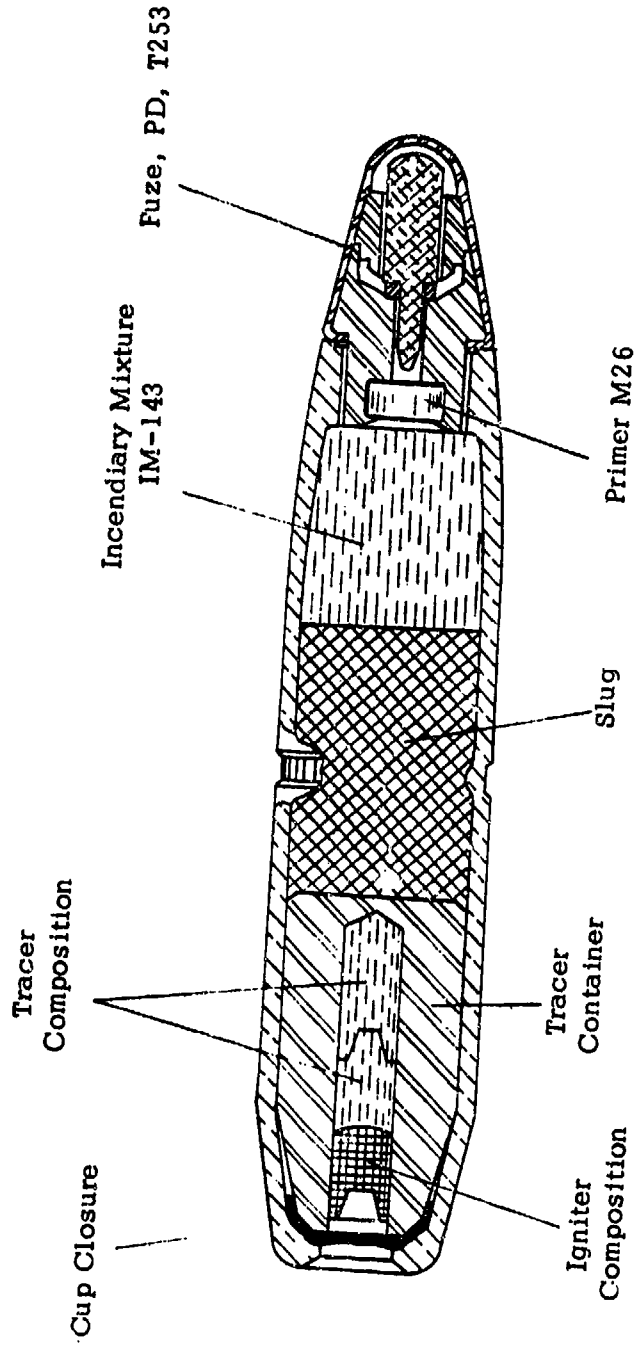


Figure 13-2. Design of Cal .50 Bullet, T140E12

REFERENCES

1. AMCP 706-327, Engineering Design Handbook, *Fire Control Systems--General*.
2. *Recoilless Rifle Handbook* (Unpublished), Frankford Arsenal, Philadelphia, Pa.
3. *Development of 120 mm Recoilless Weapon System, XM89*, Memorandum Report M59-14-5, Frankford Arsenal, Philadelphia, Pa., Quarterly Progress Report No. 4, 1 January 1960 through 31 March 1960.

BIBLIOGRAPHY

Symposium on Recent Progress of Recoilless Rifles and Ammunition. Held at Midwest Research Institute, 11-13 January 1954, Sponsored by the Department of Army, 390 pp.

D. Walters, *A Spotting Rifle for the 90 mm Gun Mounted on the T42 Tank*, Report

R-1123, Pitman-Dunn Laboratories, Frankford Arsenal, Philadelphia, Pa., April 1953.

E. D. Crane, B. Werbel and G. Weingarten, *Development of Pyrotechnic Spotting and Ejection Charges for Use in Davy Crockett 37 mm Spotting Round*, Report TM 1431, Picatinny Arsenal, Dover, New Jersey, March 1965, 24 pp.

INDEX

A

Accessory mounting, 12-9
 Accuracy, 4-5
 Aerodynamic coefficients, 4-5, 4-9, 4-11;
 4-17, 4-22, 4-25
 Aerodynamic drag, *See*: Aerodynamic force,
 drag
 Aerodynamic force, 4-7
 drag, 4-7, 4-21
 lift, 4-7
 magnus, 4-7, 4-18, 4-19
 normal, 4-7
 Aerodynamic jump, 4-15, 4-18
 Aerodynamic moment, 4-7
 damping, 4-8
 magnus, 4-8
 roll damping, 4-8
 static, 4-7
 Aircraft tables, *See*: Slacci tables
 "All-burnt" condition, 5-59, 10-24
 Ammunition design, 11-1, 10-4
 Approximate methods (interior ballistics),
 5-11
 design tables, 5-14, 5-17
 graphs, 5-19
 piezometric efficiency, 5-12, 5-13
 similarity, 5-29
 thermodynamic efficiency, 5-11, 5-13

B

Ballistic efficiency, 5-12, 5-13
 Ballistic parameters, 5-9
 determination, 2-13
 Ballistic parameters, variation analysis,
 5-31
 flow factor, 5-32
 propellant regressiveness, 5-33
 quickness factor, 5-33
 Ballistic
 exterior, *See*: Exterior ballistics
 interior, *See*: Interior ballistics
 terminal, *See*: Terminal Ballistics
 Barrel, *See*: Tube

BAT (Battalion AntiTank Weapon), 1-11,
 1-12, 1-14, 1-15, 1-26, 1-28, 1-30, 1-38,
 1-42, 1-44, 1-45, 1-46, 2-9, 6-21, 9-39,
 10-4, 10-27, 10-28, 12-10, 12-13, 13-7
 Blast
 damage, 6-43, 1-18, 5-48, 6-51, 9-23
 measurement, 8-26
 Blowout disc, 2-3
 Bore area, 2-3
 Boresight grooves, 10-26
 Bore-size nozzle, 6-39
 Bore, smooth, 1-13
 Bourrelet, 1-13, 1-14, 10-6, 11-12, 11-13
 Breakwire system, 8-7
 Breech, 10-6, 10-19
 actuator, 10-22
 design, "blockback" principle, 1-37
 self-ejecting, 1-37, 1-44
 Breechblock, interrupted thread, 1-9, 10-20

C

Cannon, *See*: Rifle
 Cartridge case, 11-17, 10-5, 11-51
 combustible, 1-41, 11-7
 frangible, 10-24, 11-3, 11-17, 11-31
 perforated, 1-7, 1-9, 2-4, 2-5, 9-10, 10-23,
 11-17, 11-28
 Case liner, 2-3, 11-28
 Chamber, 10-23, 10-6
 pressure, 2-13, 2-14, 10-23
 volume, 2-3, 10-23
 Chamber, tapered, 1-9
 Coil detector, *See*: Solenoid detector
 Conservation of momentum, *See*: Momentum
 balance
 Constant air temperature (interior ballistic
 solution), 5-47
 Convergent-divergent nozzle, *See*: Nozzle, de
 Laval
 Cook-off, 10-26
 Copper crusher gage, 8-17
 Critical pressure, 6-9
 ratio, *See*: Critical pressure

INDEX (Cont'd)

D

Danger zone, 2-6, 2-8, 6-51
 Data, 1-4, 9-41
 DAVY CROCKET, 1-32, 1-33, 1-45, 2-9,
 9-15, 10-4, 11-32, 11-39, 11-52, 13-2
 de Laval nozzle, *See*: Nozzle, de Laval
 Definitions, 2-3
 Design, 5-11, 9-1, 9-45, *See also*: the specific
 parts; e.g., rifle, ammunition, mounts,
 firing mechanism
 data, 5-9
 examples, 2-17, 5-13, 5-18, 5-29, 5-48,
 5-55, 5-60, 11-43
 Digital computer (interior ballistics solution),
 5-57
 Directional coefficient, 6-48
 Disadvantages, 9-15
 Droop, 10-28
 Ducting (nozzle blast), 6-51

E

Error sources (hitting target), 7-5
 Example systems, *See*: Systems, examples
 Exhaust velocity, 6-11
 Expansion ratio, nozzle, *See*: Nozzle ex-
 pansion ratio
 Exterior ballistics, 4-1

F

Field servicing, 9-39
 Fins
 fixed, 4-17
 folded, 4-18
 Fire control, 2-9, 7-7, 7-8, 7-11, 13-1
See also: Spotting rifle
 Firing mechanism, 10-29
 Flash
See: Nozzle flash,
 suppression, 1-39, 5-85, 6-49
 Flow
 rate, 6-10, 6-12
 separation, 6-18
 Flow spoilers, 5-85
 Force, *See*: Aerodynamic force
 Forcing cone, 10-26

Fragment

patterns, 3-18
 size, 3-16
 speed, 3-16, 3-19
 Fragmentation, 3-15
 Functional diagram, 2-5, 2-6
 Fuze, 1-44, 11-49

G

Gas

flow, 2-5, 2-7
 leakage, 10-27
 pressure, internal, 1-38, 5-7, 10-23
 temperature, 5-7

Gun

expansion ratio, 2-4
 pressure, *See*: Gas pressure
 requirements, 2-13
 volume, 2-13
 weight, 5-86, 10-24, 10-25
 Gun chamber, *See*: Chamber
 Gun tube, *See*: Tube

H

HAW (Heavy Antitank Weapon), 1-30, 2-17,
 10-3, 10-4, 11-3, 11-32, 12-10, 12-13
 Heat transfer, 1-38, 5-61
 Heating, 1-18, 10-26
 History, 1-3
 Hit probability, 2-9, 7-5
 Human engineering, 9-1, 9-37, 10-19

I

Igniter, 1-39, 11-35
 theory, 11-41
 Indexing, automatic, 11-14
 Instrumentation, *See*: Measurement tech-
 niques
 Interior ballistic basic equations, 5-29, 5-35
 "all burnt" condition, 5-59
 burning, 5-37, 5-42
 energy, 5-41, 5-43
 motion, 5-35, 5-42
 propellant gas, 5-35, 5-41, 5-43
 Interior ballistic equations, heat transfer, 5-61

INDEX (Cont'd)

Interior ballistic equations (cont'd)
 solution, 5-62
 Interior ballistic equations (all burnt)
 solution, 5-59
 Interior ballistic equations solution, 5-45
 constant average temperature, 5-47
 numerical integration (digital computer),
 5-57
 Interior ballistics, 1-39, 1-40, 5-1, 11-19
 parameters, 5-8
 Intermediate flash, 6-49

J

Jet

See: Nozzle jet
 See: Warhead jet

Jump (gun), 7-5

See also: Aerodynamic jump

K

Kill probability, 2-9, 7-23
 types, 7-23

L

Liner

See: Case Liner
 See: Warhead liner

Loading density, 2-4

M

Maintainability, 9-1, 9-49
 Matching (spotting rifle), 7-9, 13-1
 Materials, 9-44
 MAW (Medium Antitank Weapon), 1-20
 Measurement techniques, (exterior ballistics)
 spin, 8-25
 yaw, 8-24
 Measurement techniques (interior ballistics),
 8-1
 acceleration, 8-22
 pressure, 8-17
 recoil, 8-23
 strain, 8-21

temperature, 8-24

velocity, 8-5

Moby-Dick See: Projectile, T171

Momentum

balance, 2-5, 6-5, 9-2

conservation, 2-5, 6-5, 9-2

ratio, 6-21, 6-22, 6-25

Mott equation, 3-15

Mount design, 12-1

Muzzle

energy, 2-11, 2-12, 2-14

flash, 5-48, 5-85

momentum, 2-12

velocity, 7-18, 7-25, 8-5, 10-23

N

Nozzle, 1-9, 1-42, 2-4, 2-5, 5-7, 5-41, 5-81,
 10-7, 10-9, 10-23

blast, See: Blast damage

damage, 6-31

design, 6-15, 6-23, 6-27, 6-36

efficiency, 6-6, 6-18

entrance area, 2-4, 6-27, 6-29

erosion, 1-18, 1-42, 2-4, 6-23, 6-26, 6-31

6-37, 6-39, 6-41, 9-2, 10-9

chemical, 6-31

melting, 6-31

resistance, 6-32

exit, 2-4

expansion

angle, 2-4, 6-24, 6-46

ratio, 2-4, 6-13, 6-6, 6-9, 6-22, 6-25

flash, 6-43, 6-44, 6-49, 9-23

jet, 6-44,

life, 6-26, 6-31

surface temperature, 6-35

throat area, 2-4, 6-23, 6-25

thrust, 6-13, 6-17, 6-24, 6-25

Nozzle brake, 6-39

Nozzle, types,

annular, 1-9, 10-14, 10-23

central, 2-13, 6-28, 10-10, 10-23, 10-24

de Laval, 6-9, 6-12, 10-9, 10-12

kidney-shaped, 10-16, 10-23

multiple, 10-13

supersonic: See: Nozzle de Laval

INDEX (Cont'd)

O

Obturation, 1-13, 4-17, 11-15
 ONTOS, 1-14, 1-28
 Optimization, *See*: Parameter optimization

P

Parameter optimization (interior ballistics),
 5-51
 length, 5-55
 weight, 5-51
 PAT (Platoon AntiTank recoilless rifle), 1-19,
 1-20, 1-22, 1-45, 10-28, 11-32
 Photography, high speed, 8-13
 Piezoelectric gage, 8-18
 Piezometric efficiency, 2-4, 2-15, 5-12, 5-13,
 6-45, 9-1
 Pressure gradient (interior ballistics), 5-83
 Pressure joint, *See*: Self-sealing joint
 Primary flash, 6-49
 Projectile, 10-5
 envelope, 11-10
 travel, 2-4
 types, 11-6, 11-7
 caseless, 1-38
 Projectiles, specific,
 HE, 1-19
 HEAT, 1-9, 1-11, 1-14, 1-15, 1-17, 1-19,
 1-44, 9-39
 M54, 1-17
 M63, 1-17
 M323, 1-15
 M325 WP, 1-15
 M326 HEP, 1-15
 M344, 1-14, 1-15
 M371 HEAT, 1-20, 1-21
 RA (Rocket Assisted), 1-20
 T115 HE, 1-18
 T118, 1-13
 T119E10, 1-13
 T119, 1-14
 T119, E11, 1-14, 7-10
 T119 HEAT, 1-14, 1-15, 7-10
 T131, 1-18, 1-20
 T138, 1-14
 T138E57 HEAT, 1-15
 T139 HEP, 1-11, 7-10

T139 WP, 1-11
 T139E36 HEP, *See*: M326 HEP
 T171 ("Moby Dick"), 1-14, 1-44
 T184, 1-13
 T184 HEAT, 1-11, 1-15
 T188 HEAT, 1-18
 T249 HEAT, 1-19
 T249E6 HEAT, 1-20
 T261 WP, 1-15
 T263 HE, 1-15
 T268 HE, 1-11 7-10
 T273 HEP RA, 1-20
 T274 HEAT RA, 1-20
 WP, 1-19

Propellant, 1-40, 11-51, 11-55
 additives, 5-85
 burning, 5-7, 5-83
 ejection, 10-23
 loss, unburnt, 5-81
 requirements, 2-13
 Propellant force, *See*: Propellant impetus
 Propellant impetus, 2-4, 11-53
 Propellant weight coefficient, 5-13, 5-14
 PYROCORE, 11-39

R

Radar, doppler, 8-11
 Recoil cancellation, 6-1, 9-1
 theory, 6-21
 Recoil compensators, 6-41
 Recoil, dimensionless, *See*: Momentum ratio
 Recording equipment, 8-28
 Reliability, 9-1, 9-43
 Repeating rifle, 1-26
 Rifle components design, 10-1
 Rifle design, 10-1
 Rifles, specific,
 ARF, *See*: T41
 EIK, 1-6, 1-35
 M18, *See*: T15
 M20, *See*: T21
 M27, *See*: T19
 M28, *See*: XM63
 M29, *See*: XM64
 M40, 1-14, 1-15, 1-26, 6-21, 7-8, 7-12,
 10-17, 10-23, 13-2
 M40A1: *See*: T170E3

INDEX (Cont'd)

Rifles, specific, (cont'd)

M67, *See*: T219E4T15(M18): 1-4, 1-7, 1-8, 1-9, 1-11, 1-17,
1-18, 5-81, 6-21, 6-27, 6-28, 6-30,
6-39, 6-49, 7-8, 7-11, 9-23, 10-17,
10-27, 10-28, 10-29, 11-19, 11-24

T-16, 1-4, 1-9

T17, 1-4, 1-9

T18, 1-5, 1-11

T19(M27), 1-5, 1-9, 1-11, 1-12, 1-14, 1-38,
6-49, 7-8, 7-11, 10-17T21(M20), 1-4, 1-9, 1-10, 1-11, 6-41, 6-49,
7-8, 7-11, 9-2, 10-17, 12-9

T21E4, 1-9

T41 (ARF), 1-5, 6-28

T62, 1-4, 1-17

T62E1, 1-17

T66, 1-4, 1-13, 1-17

T66E2, 5-78

T118, 1-14

T135, 1-6, 1-15, 1-16, 6-21

T135-7, 1-5

T136, 1-12, 1-13, 1-14, 1-15, 1-26, 1-28

T136E1, 1-13, 1-26

T136E2, 1-6, 1-13, 1-26

T137, 1-6, 1-14

T149, 1-5, 1-19, 1-15, 10-20

T170, 1-14, 1-15, 1-26, 6-41, 10-27

T170E3 (M40A1), 1-6, 1-15, 11-52,
12-3

T184, 1-5, 1-14, 1-19, 1-20

T189, 1-22, 1-24, 1-25, 1-26

T190, 1-4, 1-18

T191, 1-18

T192, 1-4

T192E4 (M67), 1-5, 1-11, 1-20, 1-21,
7-8, 7-12, 10-24, 11-3, 11-33, 12-13

T219 PAT, 1-20, 1-22

T230E1, 1-36

T230E2, 1-36

T234, 1-5, 1-22, 1-23, 1-30, 12-5

T234E, 1-5, 1-22, 1-23, 1-30, 12-5

T237, 1-6, 1-22, 1-26, 1-27, 9-10

T246, 1-30

XM28, *See*: XM63XM29, *See*: XM64

XM63, 1-6, 1-32, 1-34

XM64, 1-32, 1-35, 13-2

XM89, 1-30

XM105, 1-31, 10-29, 13-3

XM105E1, 1-6, 12-10

Rifling, 10-25, 10-28

Rocket motor, 2-4

Rotating band, pre-engraved, 1-7, 1-9, 1-18,
1-19, 11-15Round, *See*: Projectile

S

Safety, 9-37, 10-19, 10-31

Sealing, 10-20

Secondary flash, 6-49

Self-sealing joint, 1-9

Shaped charge, 3-7, 3-8, 3-9

Shock wave, 6-43

Siacci tables, functions, and method, 4-30

Side loading, 9-10

Sky screen, 8-11

Solenoid detector, 8-10

Solutions, approximate, *See*: Approximate
Methods

Spigot configuration, 1-32, 1-35, 11-6

Spin, 3-8, 4-5

slow, 4-18

stabilization, *See*: Stabilization, spinSpotting rifle, 1-16, 2-9, 2-16, 7-7, 7-9, 7-11,
12-3, 12-10, 12-13, 13-1, 13-2

T43, 1-16, 1-26, 1-28

T46, 1-16

T46E1, 1-16

T46E2, 1-16

See also: Fire control

Stability, 4-13, 4-5

dynamic, 4-15, 4-18

gyroscopic, 4-13, 4-16

magnus, 4-16, 4-19

projectile, 4-5, 4-13

static, 4-13, 4-17

Stabilization

fin, 4-17, 11-11, 11-14, 11-36

spin, 4-13, 7-11, 10-12, 11-11

Standoff, 3-7, 3-9, 3-10

Straight-pipe nozzle, *See*: Bore-size nozzle

INDEX (Cont'd)

Strain

compensation, 10-25, 11-16
 gage, 8-18

Super-PAT, *See*: PAT

Supersonic nozzle, *See*: Nozzle, de Laval

System

design, 2-1, 9-1
 effectiveness, 7-1, 9-37
 examples, 9-23
 integration, 2-1
 requirements, 2-9, 2-10

T

Target

area, 7-25
 hard, 7-25

Taylor-Macoll equation, 4-23

Temperature, gun, 1-38, 5-61

multiple-shot solution, 5-64

single-shot solution, 5-64

theory vs experiment, 5-67

Terminal ballistics, 3-1, 3-3

Test weapon, 2-15

Theoretical analyses, 3-1

Thermodynamic constants, 5-7

Thermodynamic efficiency, 5-11, 5-13

Throat area, 2-13, 6-9

Thrust, *See*: Nozzle thrust

Thrust coefficient, *See*: Nozzle thrust

Trade-off, 2-3, 2-9, 2-13, 4-17, 9-45

Trajectory calculations, 4-5

flat, 4-28

particle, 4-27

Tube, 10-25, 10-6, 10-7

U

U-BAT (Ultimate Battalion AntiTank

Weapon), *See*: BAT

User, 9-37

V

Velocity measurement, *See*: Measurement
 techniques, velocity

W

Wall thickness, 3-15

Warhead

jet, 3-7, 3-9, 3-10, 3-13

liner, 3-9, 3-12

Warheads, 3-7, 3-15, 3-23, 3-3, 7-23, 11-7,

11-15, 11-49

AP, 3-3

HE, 3-4, 3-5, 3-15, 11-7, 11-9

HEAT, 3-4, 3-7, 7-23, 11-7, 11-11

HEP, 3-4, 3-23, 7-23

Weapon system

T165, 1-26, 1-29

T166, 1-26

(AMCRD-TT)

AMCP 706-238

FOR THE COMMANDER:

OFFICIAL:



C. J. HAROLD
LTC, GS
Adjutant General

ROBERT L. KIRWAN
Brigadier General, USA
Chief of Staff

DISTRIBUTION:
Special

ENGINEERING DESIGN HANDBOOKS

Available to DA activities from Letterhead Army Depot, AFPH: AMXLE-AYD, Chambersburg, PA 17201. All other requesters--ROR, Navy, Air Force, Marine Corps, nonilitary Government agencies, contractors, private industry, individuals, universities, and others--must purchase handbooks from National Technical Information Service, Department of Commerce, Springfield, VA 22151. See Preface for further details and AIC policy regarding requisitioning of classified documents.

No. ANCP 706-	Title	No. ANCP 706-	Title
100	Design Guidance for Producibility	205	Timing Systems and Components
104	Value Engineering	210	Fuses
106	Elements of Armament Engineering, Part One, Sources of Energy	211(C)	Fuses, Proximity, Electrical, Part One (U)
107	Elements of Armament Engineering, Part Two, Ballistics	212(S)	Fuses, Proximity, Electrical, Part Two (U)
108	Elements of Armament Engineering, Part Three, Weapon Systems and Components	213(S)	Fuses, Proximity, Electrical, Part Three (U)
109	Tables of the Cumulative Binomial Probabilities	214(S)	Fuses, Proximity, Electrical, Part Four (U)
110	Experimental Statistics, Section 1, Basic Concepts and Analysis of Measurement Data	215(C)	Fuses, Proximity, Electrical, Part Five (U)
111	Experimental Statistics, Section 2, Analysis of Enumerative and Classificatory Data	217	Harassing Weapon Systems Against RF Energy
112	Experimental Statistics, Section 3, Design and Analysis of Comparative Experiments	237	Mortar Weapon Systems
113	Experimental Statistics, Section 4, Special Topics	238	Recoilless Rifle Weapon Systems
114	Experimental Statistics, Section 5, Tables	239	Small Arms Weapon Systems
115	Environmental Series, Part One, Basic Environmental Concepts	240(C)	Grenades (U)
116	Environmental Series, Part Two, Natural Environmental Factors	242	Design for Control of Projectile Flight Characteristics (Replaces -246)
117	Environmental Series, Part Three, Induced Environmental Factors	244	Ammunition, Section 1, Artillery Ammunition--General, with Table of Contents, Glossary, and Index for Series
118	Environmental Series, Part Four, Life Cycle Environments	245(C)	Ammunition, Section 2, Design for Terminal Effects (U)
119	Environmental Series, Part Five, Glossary of Environmental Terms	246	Ammunition, Section 3, Design for Control of Flight Characteristics (Replaced by -247)
120	Criteria for Environmental Control of Mobile Systems	247	Ammunition, Section 4, Design for Projection
121	Packaging and Pack Engineering	248	Ammunition, Section 5, Inspection Aspects of Artillery Ammunition Design
123	Hydraulic Fluids	249	Ammunition, Section 6, Manufacture of Metallic Components of Artillery Ammunition
124	Reliable Military Electronics	259	Gun--General
125	Electrical Wire and Cable	251	Muzzle Devices
127	Infrared Military Systems, Part One	252	Gun Tubes
128(S)	Infrared Military Systems, Part Two (U)	253	Breech Mechanism Design
130	Design for Air Transport and Airdrop Material	255	Spectral Characteristics of Muzzle Flash
132	Maintainance Engineering Techniques (MET)	260	Automatic Weapons
133	Maintainability Engineering Theory and Practice (METAP)	269	Propellant Actuated Devices
134	Maintainability Guide for Design	280	Design of Aerodynamically Stabilized Free Rockets
135	Inventions, Patents, and Related Matters	281(S&D)	Weapon System Effectiveness (U)
136	Servo-mechanisms, Section 1, Theory and Signal Converters	282	Propulsion and Propellants (Replaced by -285) Structures
138	Servo-mechanisms, Section 2, Amplification	286	Warheads--General (U)
139	Servo-mechanisms, Section 3, Power Elements and System Design	290(C)	Surface-to-Air Missiles, Part One, System Integration
140	Trajectories, Differential Effects, and Data for Projection	291	Surface-to-Air Missiles, Part Two, Weapon Control
150	Interior Ballistics of Guns	293	Surface-to-Air Missiles, Part Three, Computers
158	Fundamentals of Ballistic Impact Dynamics, Part One	294(C)	Surface-to-Air Missiles, Part Four, Missile Armament (U)
159(S)	Fundamentals of Ballistic Impact Dynamics, Part Two (U)	295(C)	Surface-to-Air Missiles, Part Five, Countermeasures (U)
160(C)	Elements of Terminal Ballistics, Part One, Kill Mechanisms and Vulnerability (U)	296	Surface-to-Air Missiles, Part Six, Structures and Power Sources
161(C)	Elements of Terminal Ballistics, Part Two, Collection and Analysis of Data Concerning Targets (U)	297(C)	Surface-to-Air Missiles, Part Seven, Sample Problem (U)
162(S&D)	Elements of Terminal Ballistics, Part Three, Application to Missile and Space Targets (U)	300	Fabric Design
163(S)	Basic Target Vulnerability (U)	312	Rotational Molding of Plastic Powders
164	Liquid-Filled Projectile Design	313	Short Fiber Plastic Base Composites
170(S)	Armor and Its Applications (U)	327	Fire Control Systems--General
175	Solid Propellants, Part One	329	Fire Control Computing Systems
176	Solid Propellants, Part Two	331	Compressing Elements
177	Properties of Explosives of Military Interest	335(S&D)	Design Engineers' Nuclear Effects Manual (DENEM), Volume I, Functions and Weapon Systems (U)
178	Properties of Explosives of Military Interest, Section 2 (Replaced by -177)	336(S&D)	Design Engineers' Nuclear Effects Manual (DENEM), Volume II, Electronic Systems and Logical Systems (U)
179	Explosive Trains	337(S&D)	Design Engineers' Nuclear Effects Manual (DENEM), Volume III, Nuclear Environment (U)
180	Principles of Explosive Behavior	340	Design Engineers' Nuclear Effects Manual (DENEM), Volume IV, Nuclear Effects (U)
181	Explosions in Air, Part One	341	Carriages and Mounts--General
182(S&D)	Explosions in Air, Part Two (U)	342	Cradles
185	Military Pyrotechnics, Part One, Theory and Application	343	Recoil Systems
186	Military Pyrotechnics, Part Two, Safety, Procedures and Glossary	344	Top Carriages
187	Military Pyrotechnics, Part Three, Properties of Materials Used in Pyrotechnic Compositions	345	Bottom Carriages
188	Military Pyrotechnics, Part Four, Design of Ammunition for Pyrotechnic Effects	346	Equilibrators
189	Military Pyrotechnics, Part Five, Bibliography	347	Elevating Mechanisms
190	Army Weapon System Analysis	350	Traversing Mechanisms
191	System Analysis and Cost-Effectiveness	355	Wheeled Amphibians
192	Computer Aided Design of Mechanical Systems, Part One	356	The Automotive Assembly
193	Computer Aided Design of Mechanical Systems, Part Two	357	Automotive Suspensions
195	Development Guide for Reliability, Part One, Intro. Section, Background, and Planning for Army Materiel Requirements	360	Automotive Bodies and Hulls
196	Development Guide for Reliability, Part Two, Design for Reliability	361	Military Vehicle Electrical Systems
197	Development Guide for Reliability, Part Three, Reliability Prediction	362	Military Vehicle Power Plant Cooling
198	Development Guide for Reliability, Part Four, Reliability Measurement	363	Electromagnetic Compatibility (EMC)
199	Development Guide for Reliability, Part Five, Contracting for Reliability	411(S)	Vulnerability of Communication-Electronic and Electro-Optical Systems (Except Guided Missiles) to Electronic Warfare, Part One, Introduction and General Approach to Electronic Warfare Vulnerability (U)
200	Development Guide for Reliability, Part Six, Mathematical Appendix and Glossary	412(C)	Vulnerability of Communication-Electronic and Electro-Optical Systems (Except Guided Missiles) to Electronic Warfare, Part Two, Electronic Warfare Vulnerability of Tactical Communications (U)
201	Helicopter Engineering, Part One, Preliminary Design	413(S)	Vulnerability of Communication-Electronic and Electro-Optical Systems (Except Guided Missiles) to Electronic Warfare, Part Three, Electronic Warfare Vulnerability of Ground-Based and Airborne Surveillance and Target Acquisition Radars (U)
202	Helicopter Engineering, Part Two, Detail Design	414(S)	Vulnerability of Communication-Electronic and Electro-Optical Systems (Except Guided Missiles) to Electronic Warfare, Part Four, Electronic Warfare Vulnerability of Avionics (U)
203	Helicopter Engineering, Part Three, Qualification Assurance	415(S)	Vulnerability of Communication-Electronic and Electro-Optical Systems (Except Guided Missiles) to Electronic Warfare, Part Five, Optical/Electronic Warfare Vulnerability of Electro-Optical Systems (U)
204	Helicopter Performance Testing	416(S)	Vulnerability of Communication-Electronic and Electro-Optical Systems (Except Guided Missiles) to Electronic Warfare, Part Six, Electronic Warfare Vulnerability of Satellite Communications (U)
		445	Sabot Technology Engineering
		470	Metric Conversion Guide for Military Applications

*CURRENT REVISION--not available
 *REVISION UNDER PREPARATION
 *OBSOLETE--out of stock